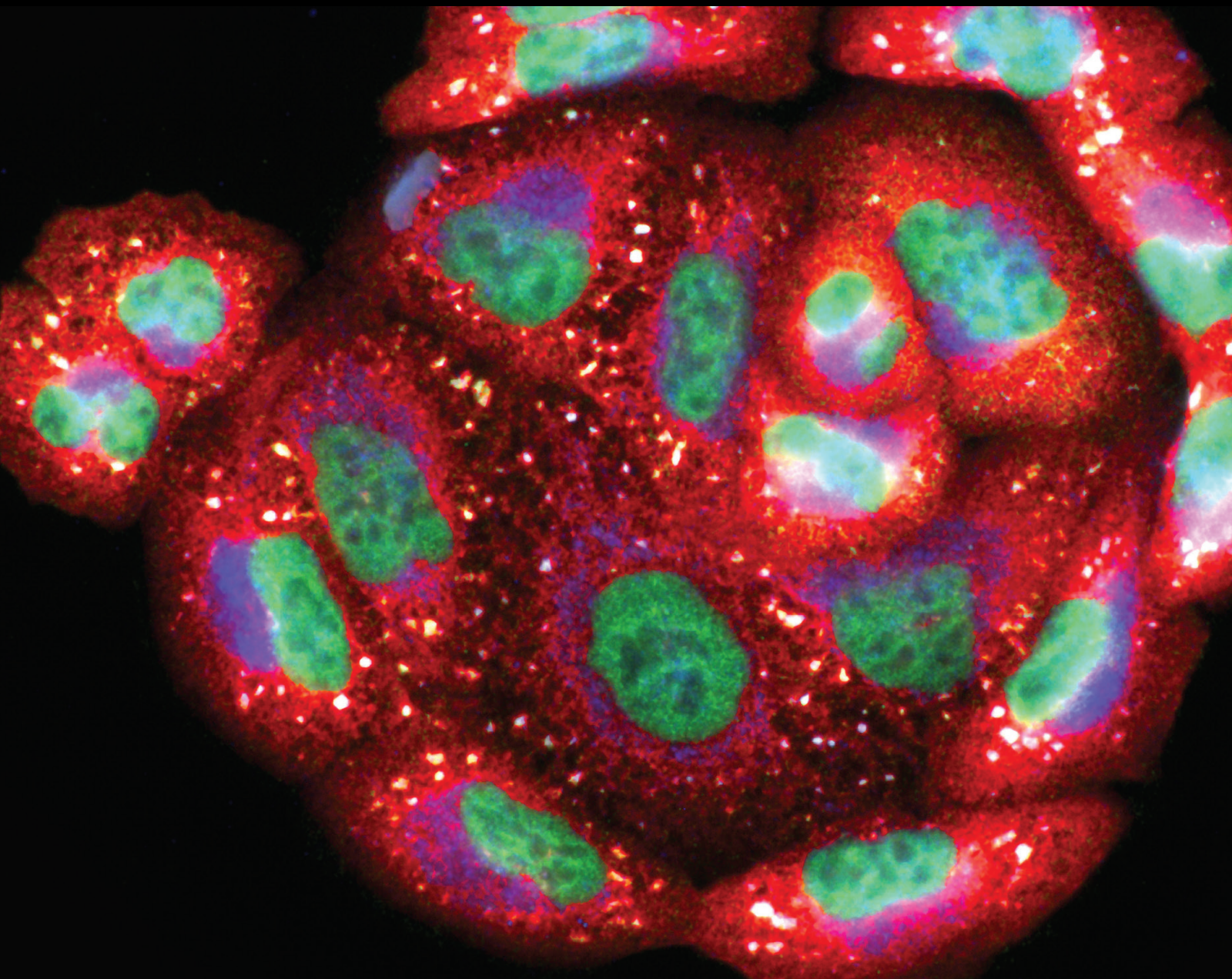# Effects of Plant-Based Compounds on Cellular and Molecular Mechanisms of Oxidative Stress

Lead Guest Editor: Márcio Carocho
Guest Editors: Patricia Morales, Yang Ye, and Marina Soković

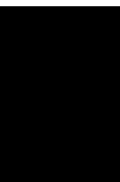# Effects of Plant-Based Compounds on Cellular and Molecular Mechanisms of Oxidative Stress

Effects of Plant-Based Compounds on Cellular and Molecular Mechanisms of Oxidative Stress

Lead Guest Editor: Márcio Carocho
Guest Editors: Patricia Morales, Yang Ye, and Marina Soković

Tim Hofer (iD), Norway
John D. Horowitz, Australia
Silvana Hrelia (iD), Italy
Dragan Hrncic, Serbia
Zebo Huang (iD), China
Zhao Huang (iD), China
Tarique Hussain (iD), Pakistan
Stephan Immenschuh (iD), Germany
Norsharina Ismail, Malaysia
Franco J. L (iD), Brazil
Sedat Kacar (iD), USA
Andleeb Khan (iD), Saudi Arabia
Kum Kum Khanna, Australia
Neelam Khaper (iD), Canada
Ramoji Kosuru (iD), USA
Demetrios Kouretas (iD), Greece
Andrey V. Kozlov (iD), Austria
Chan-Yen Kuo, Taiwan
Gaocai Li (iD), China
Guoping Li (iD), USA
Jin-Long Li (iD), China
Qiangqiang Li (iD), China
Xin-Feng Li (iD), China
Jialiang Liang (iD), China
Adam Lightfoot, United Kingdom
Christopher Horst Lillig (iD), Germany
Paloma B. Liton (iD), USA
Ana Lloret (iD), Spain
Lorenzo Loffredo (iD), Italy
Camilo López-Alarcón (iD), Chile
Daniel Lopez-Malo (iD), Spain
Massimo Lucarini (iD), Italy
Hai-Chun Ma, China
Nageswara Madamanchi (iD), USA
Kenneth Maiese (iD), USA
Marco Malaguti (iD), Italy
Steven McAnulty, USA
Antonio Desmond McCarthy (iD), Argentina
Sonia Medina-Escudero (iD), Spain
Pedro Mena (iD), Italy
Víctor M. Mendoza-Núñez (iD), Mexico
Lidija Milkovic (iD), Croatia
Alexandra Miller, USA
Sara Missaglia (iD), Italy

Premysl Mladenka (iD), Czech Republic
Sandra Moreno (iD), Italy
Trevor A. Mori (iD), Australia
Fabiana Morroni (iD), Italy
Ange Mouithys-Mickalad, Belgium
Iordanis Mourouzis (iD), Greece
Ryoji Nagai (iD), Japan
Amit Kumar Nayak (iD), India
Abderrahim Nemmar (iD), United Arab Emirates
Xing Niu (iD), China
Cristina Nocella, Italy
Susana Novella (iD), Spain
Hassan Obied (iD), Australia
Pál Pacher, USA
Pasquale Pagliaro (iD), Italy
Dilipkumar Pal (iD), India
Valentina Pallottini (iD), Italy
Swapnil Pandey (iD), USA
Mayur Parmar (iD), USA
Vassilis Paschalis (iD), Greece
Keshav Raj Paudel, Australia
Ilaria Peluso (iD), Italy
Tiziana Persichini (iD), Italy
Shazib Pervaiz (iD), Singapore
Abdul Rehman Phull, Republic of Korea
Vincent Pialoux (iD), France
Alessandro Poggi (iD), Italy
Zsolt Radak (iD), Hungary
Dario C. Ramirez (iD), Argentina
Erika Ramos-Tovar (iD), Mexico
Sid D. Ray (iD), USA
Muneeb Rehman (iD), Saudi Arabia
Hamid Reza Rezvani (iD), France
Alessandra Ricelli, Italy
Francisco J. Romero (iD), Spain
Joan Roselló-Catafau, Spain
Subhadeep Roy (iD), India
Josep V. Rubert (iD), The Netherlands
Sumbal Saba (iD), Brazil
Kunihiro Sakuma, Japan
Gabriele Saretzki (iD), United Kingdom
Luciano Saso (iD), Italy
Nadja Schroder (iD), Brazil

Anwen Shao, China
Iman Sherif, Egypt
Salah A Sheweita, Saudi Arabia
Xiaolei Shi, China
Manjari Singh, India
Giulia Sita, Italy
Ramachandran Srinivasan, India
Adrian Sturza, Romania
Kuo-hui Su, United Kingdom
Eisa Tahmasbpour Marzouni, Iran
Hailiang Tang, China
Carla Tatone, Italy
Shane Thomas, Australia
Carlo Gabriele Tocchetti, Italy
Angela Trovato Salinaro, Italy
Rosa Tundis, Italy
Kai Wang, China
Min-qi Wang, China
Natalie Ward, Australia
Grzegorz Wegrzyn, Poland
Philip Wenzel, Germany
Guangzhen Wu, China
Jianbo Xiao, Spain
Qiongming Xu, China
Liang-Jun Yan, USA
Guillermo Zalba, Spain
Jia Zhang, China
Junmin Zhang, China
Junli Zhao, USA
Chen-he Zhou, China
Yong Zhou, China
Mario Zoratti, Italy

Contents

Review Article

Effects of Traditional Chinese Medication-Based Bioactive Compounds on Cellular and Molecular Mechanisms of Oxidative Stress

Bo Liang ⬤,[1] **Yong-Chun Zhu,**[1] **Jia Lu,**[1,2] **and Ning Gu** ⬤[2]

[1]*Nanjing University of Chinese Medicine, Nanjing, China*
[2]*Nanjing Hospital of Chinese Medicine Affiliated to Nanjing University of Chinese Medicine, Nanjing, China*

Correspondence should be addressed to Ning Gu; guning@njucm.edu.cn

The oxidative stress reaction is the imbalance between oxidation and antioxidation in the body, resulting in excessive production of oxygen free radicals in the body that cannot be removed, leading to excessive oxidation of the body, and causing damage to cells and tissues. A large number of studies have shown that oxidative stress is involved in the pathological process of many diseases, so inhibiting oxidative stress, that is, antioxidation, is of great significance for the treatment of diseases. Studies have shown that many traditional Chinese medications contain antioxidant active bioactive compounds, but the mechanisms of those compounds are different and complicated. Therefore, by summarizing the literature on antioxidant activity of traditional Chinese medication-based bioactive compounds in recent years, our review systematically elaborates the main antioxidant bioactive compounds contained in traditional Chinese medication and their mechanisms, so as to provide references for the subsequent research.

1. Introduction

Oxidative stress is the imbalance between oxidation and antioxidation in the body, which leads to the excessive production of oxygen free radicals that cannot be removed, resulting in excessive oxidation and thereby causing damage to cells and tissues [1–3]. Free radicals are also produced in a normal physiological state, but there are two kinds of antioxidant systems in our body: enzyme antioxidant system and nonenzymatic antioxidant system [4]. They clear free radicals produced by normal metabolism in the body to maintain the dynamic balance of free radical production and clearance and protect the body from oxidative damage. When the body is damaged exogenously or endogenously, the oxidation capacity of the body is enhanced, producing excessive free radicals and releasing a large number of reactive oxygen species (ROS). However, the reduction of antioxidant capacity makes the accumulation of excessive free radicals in the body cannot be removed, thus causing oxidative damage to the body and the occurrence of diseases [4]. Modern studies have

shown that many traditional Chinese medications (TCM) and their bioactive compounds are rich in antioxidants, mainly including flavonoids, phenols, terpenes, polysaccharides, saponins, alkaloids, vitamins, and trace elements [5, 6]. Through their direct or indirect effects on the body's antioxidant system, they achieve the purpose of eliminating excessive free radicals and thus protect the body [6]. Here, we summarize these recent advances in the field of TCM-based bioactive compounds as they apply to oxidative stress. In addition, current barriers for further research are also discussed. Due to the ongoing research in this field, we believe that stronger evidence to support the application of TCM-based bioactive compounds for oxidative stress will emerge in the near future.

2. TCM-Based Bioactive Compounds and Oxidative Stress

2.1. Polyphenols. Many TCM contain polyphenols, and their antioxidant mechanism is mainly related to the hydrogen

donor of their phenolic hydroxyl groups, which can bind to free radicals and terminate the chain reaction of free radicals [7–9].

As natural polyphenolic phytochemicals that exist primarily in tea, tea polyphenols have been shown to have many clinical applications [10, 11]. Tea polyphenols could protect tri-ortho-cresyl phosphate-induced ovarian damage via inhibiting oxidative stress [12] and ameliorate hepatic oxidative stress though reducing hepatic inflammation and NLRP3 inflammasome activation caused by a moderate dose of perfluorodecanoic acid [13]. Additionally, it can not only regulate the antioxidant enzyme system in the body and play an efficient scavenging effect on free radicals by activating the Nrf2/Keap1 pathway [9, 14] but also inhibit the oxidase system in the body, such as inhibiting the production of NADPH oxidase, to reduce the production of ROS in vascular endothelium and protect the heart [9, 15]. Additionally, tea polyphenols could protect PC12 cells against methamphetamine-induced reactive oxide species production through increasing the antioxidant capacities and expressions of the phosphorylation of ataxia telangiectasia mutant and checkpoint kinase 2 [16]. Tea polyphenols decrease intracellular reactive oxygen species accumulation via activating NFE2L2 and MAPK pathways in bovine mammary epithelial cells exposed to hydrogen peroxides [17]. Fresh tea leaf is unusually rich in polyphenols known as catechins which may constitute up to 30% of the dry leaf weight [18]. Catechins are ROS scavengers and metal ion chelators, whereas their indirect antioxidant activities comprise induction of antioxidant enzymes, inhibition of prooxidant enzymes, and production of the phase II detoxification enzymes and antioxidant enzymes [19]. In a paralleled, crossover, and randomized controlled study, single-dose consumption of green tea catechins influences oxidative stress biomarkers, which could be beneficial for oxidative metabolism at rest and during exercise, possibly through the catechol-O-methyltransferase mechanism [20].

Salvianolic acid is another activity of phenolic acids. Salvianolic acid A/B/C are bioactive polyphenols extracted from *Radix Salviae* (Danshen), which possesses a variety of pharmacological activities. Salvianolic acid A effectively protects the kidney against oxidative stress in 5/6 nephrectomized rats by activating the Akt/GSK-3β/Nrf2 signaling pathway and inhibiting the NF-κB signaling pathway [21]. Salvianolic acid A ameliorates oxidation in ischemia-reperfusion-induced injury, and these protective effects may partially occur via activation of Nrf2/HO-1 and Akt/mTORC1 signaling pathways [22, 23]. Salvianolic acid A prevents Ang II-induced oxidative stress by inhibiting the activation of the Akt pathway in the macrophages [24]. Salvianolic acid B abolishes oxidative stress in the hippocampus by inhibiting NLRP3 inflammasome activation [25]. Salvianolic acid B protects the endothelial cells against oxidative stress injury by inhibiting endothelial permeability and MAPK and NF-κB signaling pathways [26]. Salvianolic acid B relieves oxidative stress via inhibiting the transforming growth factor-β1 pathway in lipopolysaccharide-induced acute lung injury rats [27]. Salvianolic acid B protects against subarachnoid hemorrhage-triggered oxidative damage by upregulating the Nrf2 antiox-idant signaling pathway, which may be modulated by SIRT1 activation [28]. Furthermore, salvianolic acid C protects the hepatocytes from acetaminophen-induced oxidative stress damage by mitigating mitochondrial oxidative stress through inhibition of the Keap1/Nrf2/HO-1 signaling axis [29]. Salvianolic acid C effectively attenuates lipopolysaccharide-induced oxidative stress via the TLR4/NF-κB pathway [30].

The antioxidative effect of resveratrol *in vivo* is not to scavenge ROC directly but to play a role as a gene regulator [31–33]. Resveratrol inhibits NADPH oxidase-mediated production of ROS by downregulating the expression and activity of the oxidase [31]. Resveratrol can activate SIRT1 [34]. Studies have shown that among the established SIRT1 targets, FoxO transcription factors contribute to the antioxidative effects of resveratrol by upregulating antioxidative enzymes and eNOS [31, 34, 35]. SIRT1 inhibits the production of ROS in mitochondria through proliferator-activated receptor-coactivator-1α deacetylation and nitric oxide-dependent mechanism [36]. Resveratrol results in relieving oxidative stress, which may be largely associated with the alleviation of metabolic disturbances [37]. In addition, resveratrol upregulated the activities of some antioxidant enzymes by activating Nrf2 [31, 38]. Resveratrol also has effects on nonenzymatic antioxidants [31]. For example, resveratrol can upregulate γ-glutamylcysteine synthetase by activating Nrf2 [38], thus increasing the content of glutathione in endothelial cells [39].

Polyphenols include also flavonoids, which are a series of compounds with C6-C3-C6 as the basic carbon frame [40, 41]. Their antioxidant and anti-inflammatory activities are mainly due to their ability to prevent or inhibit reactions related to oxygen free radicals, mediate or increase the activity of antioxidant enzymes, and thus scavenging ROS [2]. They can improve the antioxidant status by weakening the activity of the NF-κB pathway and inhibiting the expression of a variety of inflammatory cytokines and chemokines, such as monocyte chemoattractant protein-1, nitric oxide synthase, cyclooxygenase, lipoxygenase, cell adhesion molecules, tumor necrosis factor, and interleukin [2, 42].

Baicalein, a widely distributed natural flavonoid [43], downregulates protein kinase R-like ER kinase and upregulates Nrf2 to significantly alleviate oxidative stress [44–47]. Moreover, baicalein exerts a protective effect under oxidative stress through regulating the KLF4/MARCH5/Drp1 pathway [48, 49], stabilizing carboxyl terminus of Hsc70-interacting protein activity to promote receptor-interacting serine/-threonine kinase 1/3 ubiquitination and degradation [50], and regulating PARP-1/AIF [51] and NF-κB pathways [47, 52].

Baicalin, also extracted from *Scutellariae Radix* (Huangqin) [53, 54], alleviates intestinal oxidative damage by inhibiting NF-κB and increasing mTOR signaling to modulate downstream oxidative responses after deoxynivalenol challenge [55, 56]. Baicalin inactivates succinate dehydrogenase to suppress ROS production and protects glutamine synthetase protein stability against oxidative stress [57]. Baicalin treatment inhibits the NF-κB and p38 MAPK signaling pathways, thereby achieving its antioxidant effect in a dose-dependent manner in atherosclerosis [58]. Baicalin also

protects against LPS-induced injury by decreasing oxidative stress [59] and represses C/EBPβ via redox homeostasis [60].

Luteolin is a common flavonoid that is abundantly present in various edible plants; it is known to exhibit beneficial effects [61]. Luteolin effectively alleviates oxidative stress injury induced by hydrogen peroxide through P38 MAPK/NF-κB activation [42, 62–64]. Luteolin activates the Nrf2 pathway and increases the antioxidant defense capacities of ochratoxin A-treated cells [65]. Luteolin exhibits antioxidative property in lipopolysaccharide-stimulated murine macrophages through transforming growth factor beta-activated kinase 1 TAK1 inhibition and Nrf2 activation [66]. Luteolin also enhances the antioxidative process in intracerebral hemorrhage and testicular injury by activating the p62-Keap1-Nrf2 [67] or Nrf2/HO-1 pathway [68]. Moreover, p21 upregulation and mTOR signaling inhibition are involved in the antioxidant effect of luteolin [69].

The antioxidation of quercetin is mainly the result of the joint action of the catechol group on the B ring and the free hydroxyl group (OH-) on the A ring [70, 71]. In addition, quercetin has a 3-OH group, which is an effective inhibitor of lipid oxidation and can effectively reduce the abnormal production of ROS [42, 70]. Quercetin attenuates d-galactose-induced aging-related oxidative alterations through NF-κB [72], reverses lipopolysaccharide or 1,2-dimethylhydrazine-mediated oxidative stress via targeting the MAPK/Nrf2/Keap1 signaling pathway [73, 74], and improves d-galactosamine-induced cellular damage by inhibiting oxidative stress via inhibiting HMGB1 [75] and SIRT1/ER stress [76].

Silymarin can increase the activity of antioxidant enzymes, such as superoxide dismutase and catalase, so it can scavenge free radicals efficiently. Silymarin can also inhibit lipid peroxidation, so it can protect the integrity of the structure and function of hepatocytes from various oxidative damage [77, 78].

Puerarin prominently alleviated oxidative stress through TLR4/NLRP3 inflammasome activation [79], Nrf2 pathway [80, 81], and antioxidant enzymes [80] by significantly downregulating HIF-1α and upregulating TIMP-3 and BCL-2 [82]. Moreover, puerarin may inhibit MAPK and active STAT3 to enhance the antioxidant capacity [83].

2.2. Saponins.
The main saponins in TCM are steroidal saponins and triterpenoid saponins. The contents of steroidal saponins were more in *Anemarrhenae Rhizoma* (Zhimu), *Asparagi Radix* (Tiandong), *Ophiopogonis Radix* (Maidong), and *Paris polyphylla* (Chonglou), and the contents of triterpenoid saponins in *Panax ginseng C.A. Mey* (Renshen), *Acanthopanax senticosus* (*Rupr. Maxim.*) *Harms* (Ciwujia), and *Cimicifugae Rhizoma* (Shengma) were higher.

The levels of malondialdehyde and lactate dehydrogenase can be reduced by timosaponin, which improves superoxide dismutase and nitric oxide [84]. The research showed that timosaponin could protect PC12 cells by reducing the level of ROS induced by hydrogen peroxide [85]. Timosaponin may have the effect of protecting INS-1 pancreatic β cells through reducing IL-1β production by inhibiting the NLRP3 inflammasome in macrophages and restoring the insulin

secretion ability and cell viability by reducing oxidative stress [86]. Timosaponin can also reduce the activity of NF-κB to inhibit the production of inflammatory factors and reduce the inflammatory response [84].

Ginsenoside, a potential treatment candidate for the attenuation of aging-related disease [87], produces antidepressant-like effects on chronic unpredictable mild stress-exposed rats involving protection against oxidative stress and thus the neuronal deterioration resulting from inflammatory responses [88]. Ginsenoside not only upregulates GPX4 to reduce oxidative stress and thereby alleviates 6-hydroxydopamine-induced neuronal damage [89] but also effectively attenuates D-galactose-induced oxidative stress via restoring the upstream PI3K/AKT signaling pathway [90]. Besides, ginsenoside significantly ameliorates oxidative stress through regulating SIRT1 [91]. In cardiomyocytes, ginsenoside decreases oxidative stress via activating the antioxidant signal pathway of AMPK [92, 93], PERK/Nrf2/HMOX1 [94], and Nrf2 pathways [95, 96].

2.3. Polysaccharides.
Polysaccharides are a kind of compound composed of more than 10 glycosyl groups bound by glycosidic bonds, which is one of the four basic substances of life [97]. Polysaccharides have the characteristic of antioxidant stress. Several antioxidant mechanisms of polysaccharides include direct scavenging of ROS, enhancement of antioxidant enzyme activity, and binding of polysaccharide molecules with metal ions necessary for ROS to inhibit the production of free radicals [98–100].

Astragalus polysaccharides extracted from the dried rhizome of *Astragalus membranaceus* (Huangqi) can improve the activity of antioxidant enzymes and reduce oxidative stress indices [97, 101–103]; it alleviates hydrogen peroxide-triggered oxidative injury via elevating the expression of KLF2 via the MEK/ERK pathway [104] and alleviates tilmicosin-induced toxicity by inhibiting oxidative damage and modulating the expressions of HSP70, NF-κB, and Nrf2/HO-1 pathway [105]. Astragalus polysaccharides can also effectively alleviate oxidative stress-mediated osteoporosis, which may be related to its regulation of the FoxO3a/Wnt2/β-catenin pathway [106]. Astragalus polysaccharides combined with matrine exert a synergistic protective effect against oxidative stress, which might be associated with regulating TFF3 expression [107].

Lycium barbarum polysaccharides from *Goji berries* or *Lycium barbarum L.* (Gouqi) could protect retinal ganglion cells from CoCl$_2$-induced apoptosis by reducing mitochondrial membrane potential and ROC [108]. And Lycium barbarum polysaccharides present antioxidant effects with utility [109, 110], resulting from direct reduction of ROS, restoration of endogenous antioxidant enzymes, and downregulation of p-eIF2α, GRP78, and CHOP [97, 101, 110, 111].

Ziziphus jujuba polysaccharides from Ziziphus jujuba Mill (Zao) contain four fractions (one neutral polysaccharide fraction named ZJPN and three acidic polysaccharide fractions named ZJPa1, ZJPa2, and ZJPa3 separately), and their superoxide anion scavenging ability is stronger than hydroxyl radicals [112]. In addition, the acidic

TABLE 1: TCM-based bioactive compounds and oxidative stress.

Bioactive compounds	Cellular and molecular mechanisms	References
Polyphenols		
Tea polyphenols	Reduce inflammation and NLRP3 inflammasome activation, regulate the antioxidant enzyme system and play an efficient scavenging effect on free radicals by activating the Nrf2/Keap1 pathway, inhibit the oxidase system, increase the antioxidant capacities and expressions of p-ATM and p-Chk2, and activate NFE2L2 and MAPK pathways.	[9, 12–17]
Salvianolic acid	Regulate Akt, Keap1/Nrf2/HO-1, TLR4/NF-κB, and MAPK signaling pathways, inhibit NLRP3 inflammasome activation, inhibit endothelial permeability, and inhibit transforming growth factor-β1 pathway.	[21–30]
Resveratrol	Inhibit NADPH oxidase-mediated production, activate SIRT1, upregulate antioxidative enzymes and eNOS, alleviate metabolic disturbances, upregulate the activities of some antioxidant enzymes by activating Nrf2, and upregulate γ-glutamylcysteine synthetase by activating Nrf2.	[31, 34–39]
Baicalein	Downregulate PERK and upregulate Nrf2; regulate KLF4-MARCH5-Drp1, PARP-1/AIF, and NF-κB pathways; and stabilize CHIP activity to promote RIPK1/RIPK3 ubiquitination and degradation.	[44–52]
Baicalin	Inhibit NF-κB and p38 MAPK signaling pathways and increase mTOR signaling, inactivate succinate dehydrogenase to suppress ROS production, and repress C/EBPβ via redox homeostasis.	[55–60]
Luteolin	Activate P38 MAPK/NF-κB, Nrf2, and p21 pathways; inhibit mTOR signaling.	[42, 62–69]
Quercetin	Attenuate oxidative alterations through NF-κB and MAPK/Nrf2/Keap1 signaling pathways; inhibit HMGB1 and SIRT1/ER stress.	[72–76]
Silymarin	Increase the activity of antioxidant enzymes; inhibit lipid peroxidation.	[77, 78]
Puerarin	Alleviate oxidative stress through TLR4/NLRP3 inflammasome activation, Nrf2 pathway, and antioxidant enzymes by downregulating HIF-1α and upregulating TIMP-3 and BCL-2; inhibit MAPK and active STAT3.	[79–83]
Saponins		
Timosaponin	Reduce MDA and LDH, improve SOD and NO, reduce ROS, reduce IL-1β production by inhibiting the NLRP3 inflammasome, and reduce the activity of NF-κB.	[84–86]
Ginsenoside	Upregulate GPX4; restore the PI3K/AKT signaling pathway; regulate SIRT1; and activate AMPK, PERK/Nrf2/HMOX1, and Nrf2 pathways.	[88–96]
Polysaccharides		
Astragalus polysaccharides	Improve the activity of antioxidant enzymes and reduce oxidative stress indices; alleviate oxidative injury via elevating the expression of KLF2 via the MEK/ERK pathway; inhibit oxidative damage and modulate the expressions of HSP70, NF-κB, and Nrf2/HO-1 pathway; and regulate FoxO3a/Wnt2/β-catenin pathway.	[97, 101–106]
Lycium barbarum polysaccharides	Reduce mitochondrial membrane potential and ROC, reduce ROS, restore endogenous antioxidant enzymes, and downregulate p-eIF2α, GRP78, and CHOP.	[97, 101, 108–111]
Ziziphus jujuba polysaccharides	Strong superoxide anion scavenging ability; outstanding chelation to ferrous ions.	[101, 112]
Angelica polysaccharides	Increase SOD, reduce MDA, and overenhance the phosphorylation of Akt/hTERT; upregulate mir-126, which could activate the PI3K/AKT and mTOR signal pathways.	[113–115]
Cordyceps polysaccharides	Good ability of scavenging DPPH and ABTS free radicals.	[101]

polysaccharide fractions show outstanding chelation to ferrous ions [101].

Other polysaccharides such as Angelica polysaccharides can increase the activity of superoxide dismutase, reduce the level of malondialdehyde, and overenhance the phosphorylation of Akt/hTERT to mitigate the harm of the peroxidation of low-density lipoprotein [113, 114]. Further, Angelica polysaccharides can upregulate miR-126, which could activate the PI3K/AKT and mTOR signal pathways, to attenuate cellular oxidative response damage [115].

Cordyceps (Dongchongxiacao) is a genus of ascomycete fungi that has been used for TCM [116]. The polysaccharides contained in *Cordyceps* have a good ability to scavenge DPPH and ABTS free radicals [101, 117].

3. Conclusions

Many TCM-based bioactive compounds are rich in antioxidants and have good development prospects. However, different bioactive compounds have different targets for inhibiting oxidative stress (see Table 1), and the side effects

of various bioactive compounds have not been fully studied. Therefore, we need to further explore the antioxidant mechanisms of TCM and in-depth study the side effects of related bioactive compounds to provide protection for the treatment of related diseases.

Data Availability

The data used to support the findings of this study are included within the article.

Conflicts of Interest

The authors declare that there is no conflict of interest regarding the publication of this paper.

Acknowledgments

References

[1] H. Sies, "Oxidative stress: a concept in redox biology and medicine," *Redox Biology.*, vol. 4, pp. 180–183, 2015.

[2] S. Das, I. Mitra, S. Batuta, M. Niharul Alam, K. Roy, and N. A. Begum, "Design, synthesis and exploring the quantitative structure-activity relationship of some antioxidant flavonoid analogues," *Bioorganic and Medicinal Chemistry Letters*, vol. 24, no. 21, pp. 5050–5054, 2014.

[3] E. Zaplatic, M. Bule, S. Z. A. Shah, M. S. Uddin, and K. Niaz, "Molecular mechanisms underlying protective role of quercetin in attenuating Alzheimer's disease," *Life Sciences*, vol. 224, pp. 109–119, 2019.

[4] S. Janciauskiene, "The beneficial effects of antioxidants in health and diseases," *Chronic Obstructive Pulmonary Diseases*, vol. 7, no. 3, pp. 182–202, 2020.

[5] Y. Zhong, M. C. Menon, Y. Deng, Y. Chen, and J. C. He, "Recent advances in traditional Chinese medicine for kidney disease," *American Journal of Kidney Diseases*, vol. 66, no. 3, pp. 513–522, 2015.

[6] B. Liang, Y. Zhou, L. Fu, and H. L. Liao, "Antiarrhythmic mechanisms of Chinese herbal medicine Dingji Fumai decoction," *Evidence-Based Complementary and Alternative Medicine*, vol. 2020, Article ID 9185707, 9 pages, 2020.

[7] H. S. Oz, "Chronic inflammatory diseases and green tea polyphenols," *Nutrients*, vol. 9, no. 6, p. 561, 2017.

[8] E. Roh, J.-E. Kim, J. Y. Kwon et al., "Molecular mechanisms of green tea polyphenols with protective effects against skin photoaging," *Critical Reviews in Food Science and Nutrition*, vol. 57, no. 8, pp. 1631–1637, 2017.

[9] L. Xing, H. Zhang, R. Qi, R. Tsao, and Y. Mine, "Recent advances in the understanding of the health benefits and molecular mechanisms associated with green tea polyphe-

nols," *Journal of Agricultural and Food Chemistry*, vol. 67, no. 4, pp. 1029–1043, 2019.

[10] S.-T. Wang, W.-Q. Cui, D. Pan, M. Jiang, B. Chang, and L.-X. Sang, "Tea polyphenols and their chemopreventive and therapeutic effects on colorectal cancer," *World Journal of Gastroenterology*, vol. 26, no. 6, pp. 562–597, 2020.

[11] M. Alagawany, M. E. Abd el-Hack, M. Saeed et al., "Nutritional applications and beneficial health applications of green tea and l-theanine in some animal species: a review," *Journal of Animal Physiology and Animal Nutrition*, vol. 104, no. 1, pp. 245–256, 2020.

[12] S. Yang, S. Shao, B. Huang et al., "Tea polyphenols alleviate tri-ortho-cresyl phosphate-induced autophagy of mouse ovarian granulosa cells," *Environmental Toxicology*, vol. 35, no. 4, pp. 478–486, 2020.

[13] D. Wang, Q. Gao, T. Wang et al., "Green tea polyphenols and epigallocatechin-3-gallate protect against perfluorodecanoic acid induced liver damage and inflammation in mice by inhibiting NLRP3 inflammasome activation," *Food Research International*, vol. 127, p. 108628, 2020.

[14] M. C. Jaramillo and D. D. Zhang, "The emerging role of the Nrf2-Keap1 signaling pathway in cancer," *Genes and Development*, vol. 27, no. 20, pp. 2179–2191, 2013.

[15] H.-S. Kim, M. J. Quon, and J.-a. Kim, "New insights into the mechanisms of polyphenols beyond antioxidant properties; lessons from the green tea polyphenol, epigallocatechin 3-gallate," *Redox Biology*, vol. 2, pp. 187–195, 2014.

[16] Q. Ru, Q. Xiong, X. Tian et al., "Tea polyphenols attenuate methamphetamine-induced neuronal damage in PC12 cells by alleviating oxidative stress and promoting DNA repair," *Frontiers in Physiology*, vol. 10, p. 1450, 2019.

[17] Y. Ma, L. Zhao, M. Gao, and J. J. Loor, "Tea polyphenols protect bovine mammary epithelial cells from hydrogen peroxide-induced oxidative damage in vitro1," *Journal of Animal Science*, vol. 96, no. 10, pp. 4159–4172, 2018.

[18] H. N. Graham, "Green tea composition, consumption, and polyphenol chemistry," *Preventive Medicine*, vol. 21, no. 3, pp. 334–350, 1992.

[19] J. Bernatoniene and D. Kopustinskiene, "The Role of Catechins in Cellular Responses to Oxidative Stress," *Molecules*, vol. 23, no. 4, p. 965, 2018.

[20] M. Sugita, M. P. Kapoor, A. Nishimura, and T. Okubo, "Influence of green tea catechins on oxidative stress metabolites at rest and during exercise in healthy humans," *Nutrition*, vol. 32, no. 3, pp. 321–331, 2016.

[21] H.-F. Zhang, J.-H. Wang, Y.-L. Wang et al., "Salvianolic Acid A Protects the Kidney against Oxidative Stress by Activating the Akt/GSK-3β/Nrf2 Signaling Pathway and Inhibiting the NF-κB Signaling Pathway in 5/6 Nephrectomized Rats," *Oxidative Medicine and Cellular Longevity*, vol. 2019, Article ID 2853534, 16 pages, 2019.

[22] G. Zu, T. Zhou, N. Che, and X. Zhang, "Salvianolic acid A protects against oxidative stress and apoptosis induced by intestinal ischemia-reperfusion injury through activation of Nrf2/HO-1 pathways," *Cellular Physiology and Biochemistry.*, vol. 49, no. 6, pp. 2320–2332, 2018.

[23] H. Zhang, Y.-y. Liu, Q. Jiang et al., "Salvianolic acid A protects RPE cells against oxidative stress through activation of Nrf2/HO-1 signaling," *Free Radical Biology and Medicine*, vol. 69, pp. 219–228, 2014.

[24] L. Li, T. Xu, Y. du et al., "Salvianolic acid A attenuates cell apoptosis, oxidative stress, Akt and NF-κB activation in angiotensin-II induced murine peritoneal macrophages," *Current Pharmaceutical Biotechnology*, vol. 17, no. 3, pp. 283–290, 2016.

[25] Q. Huang, X. Ye, L. Wang, and J. Pan, "Salvianolic acid B abolished chronic mild stress-induced depression through suppressing oxidative stress and neuro-inflammation via regulating NLRP3 inflammasome activation," *Journal of Food Biochemistry*, vol. 43, no. 3, article e12742, 2019.

[26] Q. Liu, X. Shi, L. Tang et al., "Salvianolic acid B attenuates experimental pulmonary inflammation by protecting endothelial cells against oxidative stress injury," *European Journal of Pharmacology*, vol. 840, pp. 9–19, 2018.

[27] D.-H. Zhao, Y.-J. Wu, S.-T. Liu, and R.-Y. Liu, "Salvianolic acid B attenuates lipopolysaccharide-induced acute lung injury in rats through inhibition of apoptosis, oxidative stress and inflammation," *Experimental and Therapeutic Medicine*, vol. 14, no. 1, pp. 759–764, 2017.

[28] X. Zhang, Q. Wu, Y. Lu et al., "Cerebroprotection by salvianolic acid B after experimental subarachnoid hemorrhage occurs via Nrf2- and SIRT1-dependent pathways," *Free Radical Biology and Medicine*, vol. 124, pp. 504–516, 2018.

[29] C.-T. Wu, J.-S. Deng, W.-C. Huang, P.-C. Shieh, M.-I. Chung, and G.-J. Huang, "Salvianolic acid C against acetaminophen-induced acute liver injury by attenuating inflammation, oxidative stress, and apoptosis through inhibition of the Keap1/Nrf2/HO-1 signaling," *Oxidative Medicine and Cellular Longevity*, vol. 2019, Article ID 9056845, 13 pages, 2019.

[30] Y. Duan, W. An, H. Wu, and Y. Wu, "Salvianolic acid C attenuates LPS-induced inflammation and apoptosis in human periodontal ligament stem cells via toll-like receptors 4 (TLR4)/nuclear factor kappa B (NF-κB) pathway," *Medical Science Monitor*, vol. 25, pp. 9499–9508, 2019.

[31] N. Xia, A. Daiber, U. Förstermann, and H. Li, "Antioxidant effects of resveratrol in the cardiovascular system," *British Journal of Pharmacology*, vol. 174, no. 12, pp. 1633–1646, 2017.

[32] H. Li, N. Xia, and U. Förstermann, "Cardiovascular effects and molecular targets of resveratrol," *Nitric Oxide: Biology and Chemistry*, vol. 26, no. 2, pp. 102–110, 2012.

[33] N. Xia, U. Forstermann, and H. Li, "Resveratrol as a gene regulator in the vasculature," *Current Pharmaceutical Biotechnology*, vol. 15, no. 4, pp. 401–408, 2014.

[34] C.-P. Hsu, P. Zhai, T. Yamamoto et al., "Silent information regulator 1 protects the heart from ischemia/reperfusion," *Circulation*, vol. 122, no. 21, pp. 2170–2182, 2010.

[35] K. Hasegawa, S. Wakino, K. Yoshioka et al., "Sirt1 protects against oxidative stress-induced renal tubular cell apoptosis by the bidirectional regulation of catalase expression," *Biochemical and Biophysical Research Communications*, vol. 372, no. 1, pp. 51–56, 2008.

[36] C. Beauloye, L. Bertrand, S. Horman, and L. Hue, "AMPK activation, a preventive therapeutic target in the transition from cardiac injury to heart failure," *Cardiovascular Research*, vol. 90, no. 2, pp. 224–233, 2011.

[37] K. Szkudelska, M. Okulicz, I. Hertig, and T. Szkudelski, "Resveratrol ameliorates inflammatory and oxidative stress in type 2 diabetic Goto-Kakizaki rats," *Biomedicine and Pharmacotherapy*, vol. 125, p. 110026, 2020.

[38] Z. Ungvari, Z. Bagi, A. Feher et al., "Resveratrol confers endothelial protection via activation of the antioxidant transcription factor Nrf2," *American Journal of Physiology Heart and Circulatory Physiology*, vol. 299, no. 1, pp. H18–H24, 2010.

[39] Z. Ungvari, N. Labinskyy, P. Mukhopadhyay et al., "Resveratrol attenuates mitochondrial oxidative stress in coronary arterial endothelial cells," *American Journal of Physiology Heart and Circulatory Physiology*, vol. 297, no. 5, pp. H1876–H1881, 2009.

[40] T.-Y. Wang, Q. Li, and K.-S. Bi, "Bioactive flavonoids in medicinal plants: structure, activity and biological fate," *Asian Journal of Pharmaceutical Sciences*, vol. 13, no. 1, pp. 12–23, 2018.

[41] M. Rodriguez-Canales, E. Martinez-Galero, A. D. Nava-Torres et al., "Anti-Inflammatory and Antioxidant Activities of the Methanolic Extract of Cyrtocarpa procera Bark Reduces the Severity of Ulcerative Colitis in a Chemically Induced Colitis Model," *Mediators of Inflammation*, vol. 2020, Article ID 5062506, 11 pages, 2020.

[42] M. M. Fardoun, D. Maaliki, N. Halabi et al., "Flavonoids in adipose tissue inflammation and atherosclerosis: one arrow, two targets," *Clinical Science*, vol. 134, no. 12, pp. 1403–1432, 2020.

[43] L. Avila-Carrasco, P. Majano, J. A. Sánchez-Toméro et al., "Natural plants compounds as modulators of epithelial-to-mesenchymal transition," *Frontiers in Pharmacology*, vol. 10, p. 715, 2019.

[44] Y. Dong, Y. Xing, J. Sun, W. Sun, Y. Xu, and C. Quan, "Baicalein alleviates liver oxidative stress and apoptosis induced by high-level glucose through the activation of the PERK/Nrf2 signaling pathway," *Molecules*, vol. 25, no. 3, p. 599, 2020.

[45] J. Ma, S. Li, L. Zhu et al., "Baicalein protects human vitiligo melanocytes from oxidative stress through activation of NF-E2-related factor2 (Nrf2) signaling pathway," *Free Radical Biology and Medicine*, vol. 129, pp. 492–503, 2018.

[46] J. Y. Jeong, H.-J. Cha, E. O. Choi et al., "Activation of the Nrf2/HO-1 signaling pathway contributes to the protective effects of baicalein against oxidative stress-induced DNA damage and apoptosis in HEI193 Schwann cells," *International Journal of Medical Sciences*, vol. 16, no. 1, pp. 145–155, 2019.

[47] Y. Yuan, W. Men, X. Shan et al., "Baicalein exerts neuroprotective effect against ischaemic/reperfusion injury via alteration of NF-kB and LOX and AMPK/Nrf2 pathway," *Inflammopharmacology*, vol. 28, no. 5, pp. 1327–1341, 2020.

[48] Q. Li, Z. Yu, D. Xiao et al., "Baicalein inhibits mitochondrial apoptosis induced by oxidative stress in cardiomyocytes by stabilizing MARCH5 expression," *Journal of Cellular and Molecular Medicine*, vol. 24, no. 2, pp. 2040–2051, 2020.

[49] Z. Yu, Q. Li, Y. Wang, and P. Li, "A potent protective effect of baicalein on liver injury by regulating mitochondria-related apoptosis," *Apoptosis*, vol. 25, no. 5-6, pp. 412–425, 2020.

[50] Y. Wang, L. Li, G. Liu et al., "Baicalein protects cardiomyocytes from oxidative stress induced programmed necrosis by stabilizing carboxyl terminus of Hsc70-interacting protein," *International Journal of Cardiology*, vol. 311, pp. 83–90, 2020.

[51] W.-H. Li, Y.-L. Yang, X. Cheng et al., "Baicalein attenuates caspase-independent cells death via inhibiting PARP-1 activation and AIF nuclear translocation in cerebral ischemia/reperfusion rats," *Apoptosis*, vol. 25, no. 5-6, pp. 354–369, 2020.

[52] J.-J. Yan, G. H. du, X.-M. Qin, and L. Gao, "Baicalein attenuates the neuroinflammation in LPS-activated BV-2 microglial cells through suppression of pro-inflammatory cytokines, COX2/NF-κB expressions and regulation of metabolic abnormality," *International Immunopharmacology*, vol. 79, p. 106092, 2020.

[53] P. Cheng, T. Wang, W. Li et al., "Baicalin alleviates lipopolysaccharide-induced liver inflammation in chicken by suppressing TLR4-mediated NF-κB pathway," *Frontiers in Pharmacology*, vol. 8, p. 547, 2017.

[54] H. Chen, Y. He, S. Chen, S. Qi, and J. Shen, "Therapeutic targets of oxidative/nitrosative stress and neuroinflammation in ischemic stroke: applications for natural product efficacy with omics and systemic biology," *Pharmacological Research*, vol. 158, p. 104877, 2020.

[55] P. Liao, Y. Li, M. Li et al., "Baicalin alleviates deoxynivalenol-induced intestinal inflammation and oxidative stress damage by inhibiting NF-κB and increasing mTOR signaling pathways in piglets," *Food and Chemical Toxicology*, vol. 140, p. 111326, 2020.

[56] A. Zha, Z. Cui, M. Qi et al., "Dietary baicalin zinc supplementation alleviates oxidative stress and enhances nutrition absorption in deoxynivalenol challenged pigs," *Current Drug Metabolism*, vol. 21, no. 8, pp. 614–625, 2020.

[57] X. Song, Z. Gong, K. Liu, J. Kou, B. Liu, and K. Liu, "Baicalin combats glutamate excitotoxicity via protecting glutamine synthetase from ROS-induced 20S proteasomal degradation," *Redox Biology*, vol. 34, p. 101559, 2020.

[58] Y. Wu, F. Wang, L. Fan et al., "Baicalin alleviates atherosclerosis by relieving oxidative stress and inflammatory responses via inactivating the NF-κB and p38 MAPK signaling pathways," *Biomedicine and Pharmacotherapy*, vol. 97, pp. 1673–1679, 2018.

[59] J. Ma, R. Wang, H. Yan, R. Xu, A. Xu, and J. Zhang, "Protective effects of Baicalin on lipopolysaccharide-induced injury in Caenorhabditis elegans," *Pharmacology*, vol. 105, no. 1-2, pp. 109–117, 2020.

[60] K. Lei, Y. Shen, Y. He et al., "Baicalin Represses C/EBPβ via Its Antioxidative Effect in Parkinson's Disease," *Oxidative Medicine and Cellular Longevity*, vol. 2020, Article ID 8951907, 14 pages, 2020.

[61] T. Boeing, P. de Souza, S. Speca et al., "Luteolin prevents irinotecan-induced intestinal mucositis in mice through antioxidant and anti-inflammatory properties," *British Journal of Pharmacology.*, vol. 177, no. 10, pp. 2393–2408, 2020.

[62] H. I. Chen, W.-S. Hu, M.-Y. Hung et al., "Protective effects of luteolin against oxidative stress and mitochondrial dysfunction in endothelial cells," *Nutrition, Metabolism, and Cardiovascular Diseases*, vol. 30, no. 6, pp. 1032–1043, 2020.

[63] W. Wu, D. Li, Y. Zong et al., "Luteolin inhibits inflammatory responses via p38/MK2/TTP-mediated mRNA stability," *Molecules*, vol. 18, no. 7, pp. 8083–8094, 2013.

[64] M. Vatarescu, S. Bechor, Y. Haim et al., "Adipose tissue supports normalization of macrophage and liver lipid handling in obesity reversal," *The Journal of Endocrinology*, vol. 233, no. 3, pp. 293–305, 2017.

[65] M. Liu, C. Cheng, X. Li et al., "Luteolin alleviates ochratoxin A induced oxidative stress by regulating Nrf2 and HIF-1α pathways in NRK-52E rat kidney cells," *Food and Chemical Toxicology*, vol. 141, p. 111436, 2020.

[66] Y.-C. Cho, J. Park, and S. Cho, "Anti-inflammatory and antioxidative effects of luteolin-7-O-glucuronide in LPS-stimulated murine macrophages through TAK1 inhibition and Nrf2 activation," *International Journal of Molecular Sciences*, vol. 21, no. 6, p. 2007, 2020.

[67] X. Tan, Y. Yang, J. Xu et al., "Luteolin exerts neuroprotection via modulation of the p62/Keap1/Nrf2 pathway in intracerebral hemorrhage," *Frontiers in Pharmacology*, vol. 10, p. 1551, 2020.

[68] W. A. al-Megrin, S. Alomar, A. F. Alkhuriji et al., "Luteolin protects against testicular injury induced by lead acetate by activating the Nrf2/HO-1 pathway," *IUBMB Life*, vol. 72, no. 8, pp. 1787–1798, 2020.

[69] K. Iida, T. Naiki, A. Naiki-Ito et al., "Luteolin suppresses bladder cancer growth via regulation of mechanistic target of rapamycin pathway," *Cancer Science*, vol. 111, no. 4, pp. 1165–1179, 2020.

[70] J. Mlcek, T. Jurikova, S. Skrovankova, and J. Sochor, "Quercetin and its anti-allergic immune response," *Molecules*, vol. 21, no. 5, p. 623, 2016.

[71] L. Xiao, G. Luo, Y. Tang, and P. Yao, "Quercetin and iron metabolism: what we know and what we need to know," *Food and Chemical Toxicology*, vol. 114, pp. 190–203, 2018.

[72] A. H. el-Far, M. A. Lebda, A. E. Noreldin et al., "Quercetin attenuates pancreatic and renal D-galactose-induced aging-related oxidative alterations in rats," *International Journal of Molecular Sciences*, vol. 21, no. 12, p. 4348, 2020.

[73] L. Sun, G. Xu, Y. Dong, M. Li, L. Yang, and W. Lu, "Quercetin protects against lipopolysaccharide-induced intestinal oxidative stress in broiler chickens through activation of Nrf2 pathway," *Molecules*, vol. 25, no. 5, p. 1053, 2020.

[74] S. G. Darband, S. Sadighparvar, B. Yousefi et al., "Quercetin attenuated oxidative DNA damage through NRF2 signaling pathway in rats with DMH induced colon carcinogenesis," *Life Sciences*, vol. 253, p. 117584, 2020.

[75] P. Fang, J. Liang, X. Jiang et al., "Quercetin attenuates d-GaLN-induced L02 cell damage by suppressing oxidative stress and mitochondrial apoptosis via inhibition of HMGB1," *Frontiers in Pharmacology*, vol. 11, p. 608, 2020.

[76] T. Hu, J.-J. Shi, J. Fang, Q. Wang, Y.-B. Chen, and S.-J. Zhang, "Quercetin ameliorates diabetic encephalopathy through SIRT1/ER stress pathway in db/db mice," *Aging*, vol. 12, no. 8, pp. 7015–7029, 2020.

[77] S. Clichici, D. Olteanu, A. Filip, A.-L. Nagy, A. Oros, and P. A. Mircea, "Beneficial effects of silymarin after the discontinuation of CCl4-induced liver fibrosis," *Journal of Medicinal Food*, vol. 19, no. 8, pp. 789–797, 2016.

[78] A. Tajmohammadi, B. M. Razavi, and H. Hosseinzadeh, "Silybum marianum(milk thistle) and its main constituent, silymarin, as a potential therapeutic plant in metabolic syndrome: a review," *Phytotherapy Research*, vol. 32, no. 10, pp. 1933–1949, 2018.

[79] L. Guan, C. Li, Y. Zhang et al., "Puerarin ameliorates retinal ganglion cell damage induced by retinal ischemia/reperfusion through inhibiting the activation of TLR4/NLRP3 inflammasome," *Life Sciences*, vol. 256, p. 117935, 2020.

[80] Y.-D. Jeon, J.-H. Lee, Y.-M. Lee, and D.-K. Kim, "Puerarin inhibits inflammation and oxidative stress in dextran sulfate sodium- induced colitis mice model," *Biomedicine and Pharmacotherapy*, vol. 124, p. 109847, 2020.

[81] M. Li, D. Yuan, Y. Liu, H. Jin, and B. Tan, "Dietary Puerarin supplementation alleviates oxidative stress in the small intestines of Diquat-challenged piglets," *Animals*, vol. 10, no. 4, p. 631, 2020.

[82] M. Waqas, H. Qamar, J. Zhang et al., "Puerarin enhance vascular proliferation and halt apoptosis in thiram-induced avian tibial dyschondroplasia by regulating HIF-1α, TIMP-3 and BCL-2 expressions," *Ecotoxicology and Environmental Safety*, vol. 190, p. 110126, 2020.

[83] Q. Song, Y. Zhao, Q. Li, X. Han, and J. Duan, "Puerarin protects against iron overload-induced retinal injury through regulation of iron-handling proteins," *Biomedicine and Pharmacotherapy*, vol. 122, p. 109690, 2020.

[84] Y.-L. Yuan, B.-Q. Lin, C.-F. Zhang et al., "Timosaponin B-II ameliorates palmitate-induced insulin resistance and inflammation via via IRS-1/PI3K/Akt and IKK/NF-κB Pathways," *The American Journal of Chinese Medicine*, vol. 44, no. 4, pp. 755–769, 2016.

[85] Q. Xie, H. Zhao, N. Li, L. Su, X. Xu, and Z. Hong, "Protective effects of timosaponin BII on oxidative stress damage in PC12 cells based on metabolomics," *Biomedical Chromatography*, vol. 32, no. 10, p. e4321, 2018.

[86] K. Shi, J. Zhu, D. Chen et al., "Lipidomics analysis of timosaponin BII in INS-1 cells induced by glycolipid toxicity and its relationship with inflammation," *Chemistry & Biodiversity*, vol. 17, no. 4, article e1900684, 2020.

[87] J. Hou, Y. Yun, J. Xue, B. Jeon, and S. Kim, "Doxorubicin-induced normal breast epithelial cellular aging and its related breast cancer growth through mitochondrial autophagy and oxidative stress mitigated by ginsenoside Rh2," *Phytotherapy Research*, vol. 34, no. 7, pp. 1659–1669, 2020.

[88] Y. Li, L. Wang, P. Wang et al., "Ginsenoside-Rg1 rescues stress-induced depression-like behaviors via suppression of oxidative stress and neural inflammation in rats," *Oxidative Medicine and Cellular Longevity*, vol. 2020, Article ID 2325391, 15 pages, 2020.

[89] G. H. Lee, W. J. Lee, J. Hur, E. Kim, H. G. Lee, and H. G. Seo, "Ginsenoside Re mitigates 6-hydroxydopamine-induced oxidative stress through upregulation of GPX4," *Molecules*, vol. 25, no. 1, p. 188, 2020.

[90] W. Li, J.-Q. Wang, Y.-D. Zhou et al., "Rare ginsenoside 20(R)-Rg3 inhibits D-galactose-induced liver and kidney injury by regulating oxidative stress-induced apoptosis," *The American Journal of Chinese Medicine*, vol. 48, no. 5, pp. 1141–1157, 2020.

[91] B. Cheng, W. Gao, X. Wu et al., "Ginsenoside Rg2 ameliorates high-fat diet-induced metabolic disease through SIRT1," *Journal of Agricultural and Food Chemistry*, vol. 68, no. 14, pp. 4215–4226, 2020.

[92] S.-H. Hong, H.-J. Hwang, J. W. Kim et al., "Ginsenoside compound-Mc1 attenuates oxidative stress and apoptosis in cardiomyocytes through an AMP-activated protein kinase-dependent mechanism," *Journal of Ginseng Research*, vol. 44, no. 4, pp. 664–671, 2020.

[93] H.-J. Fan, Z.-B. Tan, Y.-T. Wu et al., "The role of ginsenoside Rb1, a potential natural glutathione reductase agonist, in preventing oxidative stress-induced apoptosis of H9C2 cells," *Journal of Ginseng Research*, vol. 44, no. 2, pp. 258–266, 2020.

[94] J. Sun, X. Yu, H. Huangpu, and F. Yao, "Ginsenoside Rb3 protects cardiomyocytes against hypoxia/reoxygenation injury *via* activating the antioxidation signaling pathway of

PERK/Nrf2/HMOX1," *Biomedicine and Pharmacotherapy*, vol. 109, pp. 254–261, 2019.

[95] Q. Li, Y. Xiang, Y. Chen, Y. Tang, and Y. Zhang, "Ginsenoside Rg1 protects cardiomyocytes against hypoxia/reoxygenation injury via activation of Nrf2/HO-1 signaling and inhibition of JNK," *Cellular Physiology and Biochemistry*, vol. 44, no. 1, pp. 21–37, 2018.

[96] Y. Gao, S. Chu, Z. Zhang, and N. Chen, "Hepataprotective effects of ginsenoside Rg1 - a review," *Journal of Ethnopharmacology*, vol. 206, pp. 178–183, 2017.

[97] H. Wang, Y. M. Liu, Z. M. Qi et al., "An overview on natural polysaccharides with antioxidant properties," *Current Medicinal Chemistry*, vol. 20, no. 23, pp. 2899–2913, 2013.

[98] X. Wang, J. Wang, J. Zhang, B. Zhao, J. Yao, and Y. Wang, "Structure-antioxidant relationships of sulfated galactomannan from guar gum," *International Journal of Biological Macromolecules*, vol. 46, no. 1, pp. 59–66, 2010.

[99] H. Qi, Q. Zhang, T. Zhao, R. Hu, K. Zhang, and Z. Li, "In vitro antioxidant activity of acetylated and benzoylated derivatives of polysaccharide extracted from *Ulva pertusa* (Chlorophyta)," *Bioorganic and Medicinal Chemistry Letters*, vol. 16, no. 9, pp. 2441–2445, 2006.

[100] W. Pasanphan, G. R. Buettner, and S. Chirachanchai, "Chitosan gallate as a novel potential polysaccharide antioxidant: an EPR study," *Carbohydrate Research*, vol. 345, no. 1, pp. 132–140, 2010.

[101] R. Jiao, Y. Liu, H. Gao, J. Xiao, and K. F. So, "The anti-oxidant and antitumor properties of plant polysaccharides," *The American Journal of Chinese Medicine*, vol. 44, no. 3, pp. 463–488, 2016.

[102] A. Awad, S. R. Khalil, B. M. Hendam, R. M. Abd el-Aziz, M. M. M. Metwally, and T. S. Imam, "Protective potency of Astragalus polysaccharides against tilmicosin- induced cardiac injury via targeting oxidative stress and cell apoptosis-encoding pathways in rat," *Environmental Science and Pollution Research International*, vol. 27, no. 17, pp. 20861–20875, 2020.

[103] Q. Sun, X. Wu, H. Wang et al., "Protective effects of Astragalus polysaccharides on oxidative stress in high glucose-induced or SOD2-silenced H9C2 cells based on PCR array analysis," *Diabetes, Metabolic Syndrome and Obesity*, vol. 12, pp. 2209–2220, 2019.

[104] D. Li, Y. Liu, R. Xu et al., "Retracted article: Astragalus polysaccharide alleviates H2O2-triggered oxidative injury in human umbilical vein endothelial cells via promoting KLF2," *Artificial Cells, Nanomedicine, and Biotechnology*, vol. 47, no. 1, pp. 2188–2195, 2019.

[105] M. R. Farag, W. M. Elhady, S. Y. A. Ahmed, H. S. A. Taha, and M. Alagawany, "Astragalus polysaccharides alleviate tilmicosin-induced toxicity in rats by inhibiting oxidative damage and modulating the expressions of HSP70, NF-kB and Nrf2/HO-1 pathway," *Research in Veterinary Science*, vol. 124, pp. 137–148, 2019.

[106] L. Ou, P. Wei, M. Li, and F. Gao, "Inhibitory effect of Astragalus polysaccharide on osteoporosis in ovariectomized rats by regulating FoxO3a/Wnt signaling pathway," *Acta Cirurgica Brasileira*, vol. 34, no. 5, article e201900502, 2019.

[107] X. Yan, Q.-G. Lu, L. Zeng et al., "Synergistic protection of astragalus polysaccharides and matrine against ulcerative colitis and associated lung injury in rats," *World Journal of Gastroenterology*, vol. 26, no. 1, pp. 55–69, 2020.

[108] L. Liu, X.-Y. Sha, Y.-N. Wu, M. T. Chen, and J. X. Zhong, "*Lycium barbarum* Polysaccharides protects retinal ganglion cells against oxidative stress injury," *Neural Regeneration Research*, vol. 15, no. 8, pp. 1526–1531, 2020.

[109] C. Pop, C. Berce, S. Ghibu et al., "Effects of Lycium barbarum L. polysaccharides on inflammation and oxidative stress markers in a pressure overload-induced heart failure rat model," *Molecules*, vol. 25, no. 3, p. 466, 2020.

[110] F.-L. Yang, Y.-X. Wei, B.-Y. Liao et al., "Effects of Lycium barbarum polysaccharide on endoplasmic reticulum stress and oxidative stress in obese mice," *Frontiers in Pharmacology*, vol. 11, p. 742, 2020.

[111] H. Amagase, B. Sun, and C. Borek, "_Lycium barbarum_ (goji) juice improves in vivo antioxidant biomarkers in serum of healthy adults," *Nutrition Research*, vol. 29, no. 1, pp. 19–25, 2009.

[112] S. C. Chang, B. Y. Hsu, and B. H. Chen, "Structural characterization of polysaccharides from _Zizyphus jujuba_ and evaluation of antioxidant activity," *International Journal of Biological Macromolecules*, vol. 47, no. 4, pp. 445–453, 2010.

[113] P. Ji, Y. Wei, W. Xue et al., "Characterization and antioxidative activities of polysaccharide in Chinese Angelica and its processed products," *International Journal of Biological Macromolecules*, vol. 67, pp. 195–200, 2014.

[114] P. Lai and Y. Liu, "Angelica sinensispolysaccharides inhibit endothelial progenitor cell senescence through the reduction of oxidative stress and activation of the Akt/hTERT pathway," *Pharmaceutical Biology*, vol. 53, no. 12, pp. 1842–1849, 2015.

[115] X. Zhang, H. Xue, P. Zhou et al., "_Angelica_ polysaccharide alleviates oxidative response damage in HaCaT cells through up-regulation of miR-126," *Experimental and Molecular Pathology*, vol. 110, p. 104281, 2019.

[116] S. Y. Yoon, S. Park, and Y. Park, "The anticancer properties of Cordycepin and their underlying mechanisms," *International Journal of Molecular Sciences*, vol. 19, no. 10, p. 3027, 2018.

[117] B.-J. Ke and C.-L. Lee, "Using submerged fermentation to fast increase N6-(2-hydroxyethyl)-adenosine, adenosine and polysaccharide productions of Cordyceps cicadae NTTU 868," *AMB Express*, vol. 9, no. 1, p. 198, 2019.

Research Article

Protective Effect of Degraded *Porphyra yezoensis* Polysaccharides on the Oxidative Damage of Renal Epithelial Cells and on the Adhesion and Endocytosis of Nanocalcium Oxalate Crystals

Qian-Long Peng,[1] Chuang-Ye Li,[1] Yao-Wang Zhao (ID),[1] Xin-Yuan Sun,[2] Hong Liu,[2] and Jian-Ming Ouyang (ID)[2]

[1]*Department of Urology, Hunan Children's Hospital, Changsha 410007, China*
[2]*Institute of Biomineralization and Lithiasis Research, Jinan University, Guangzhou 510632, China*

Correspondence should be addressed to Yao-Wang Zhao; yw508@sina.com and Jian-Ming Ouyang; toyjm@jnu.edu.cn

The protective effects of *Porphyra yezoensis* polysaccharides (PYPs) with molecular weights of 576.2 (PYP1), 105.4 (PYP2), 22.47 (PYP3), and 3.89 kDa (PYP4) on the oxidative damage of human kidney proximal tubular epithelial (HK-2) cells and the differences in adherence and endocytosis of HK-2 cells to calcium oxalate monohydrate crystals before and after protection were investigated. Results showed that PYPs can effectively reduce the oxidative damage of oxalic acid to HK-2 cells. Under the preprotection of PYPs, cell viability increased, cell morphology improved, reactive oxygen species levels decreased, mitochondrial membrane potential increased, S phase cell arrest was inhibited, the cell apoptosis rate decreased, phosphatidylserine exposure reduced, the number of crystals adhered to the cell surface reduced, but the ability of cells to endocytose crystals enhanced. The lower the molecular weight, the better the protective effect of PYP. The results in this article indicated that PYPs can reduce the risk of kidney stone formation by protecting renal epithelial cells from oxidative damage and reducing calcium oxalate crystal adhesion, and PYP4 with the lowest molecular weight may be a potential drug for preventing kidney stone formation.

1. Introduction

A kidney stone is a complex multifactorial disease and one of the common causes of renal damage. Exposure of renal epithelial cells to high oxalic acid can induce oxidative stress of cells and generate reactive oxygen species (ROS), thereby causing oxidative damage to renal epithelial cells and inducing the formation of kidney stones [1, 2]. Therefore, finding low-cost and effective drugs to reduce the damage of renal epithelial cells caused by oxalic acid is important to prevent kidney stones.

Studies over the past decades have shown that antioxidants in diet may help prevent or delay oxidative damage, thereby reducing the risk of various diseases caused by oxidative damage [3]. Seaweed polysaccharides are natural biological compounds that are beneficial to human health due to

their effective antioxidant properties and free radical scavenging properties [4–6]. Presa et al. [7] obtained six kinds of sulfated polysaccharides from green seaweed *Udotea flabellum*, which can protect cells from oxidative damage caused by $FeSO_4$, $CuSO_4$, and ascorbate.

The factors that affect the activity of polysaccharides include the acid group content, polysaccharide structure, polysaccharide conformation, and molecular weight (Mw) of polysaccharides [8]. Di Lorenzo et al. [9] showed that polysaccharides from *Opuntia ficus* can repair wounds and accelerate skin regeneration, and polysaccharides with low Mw have strong repair activity. Sun et al. [10] proved that low-Mw polysaccharides from *Porphyridium cruentum* (6.53 kDa) have better antitumor and immunoregulatory activities than high-Mw polysaccharides (903.3 kDa). Zhao et al. [11] showed that tea polysaccharides (TPS0, TPS1,

TPS2, and TPS3) with Mws of 10.88, 8.16, 4.82, and 2.3 kDa, respectively, could inhibit the adhesion of calcium oxalate monohydrate (COM) to human renal proximal tubular (HK-2) cells, and TPS2 with moderate Mw had the best protective effect. In addition, TPS with lower molecular weight have a better ability to increase the percentage of the dihydrate crystalline phase in CaOx crystals and reduce the size of CaOx monohydrate crystals [12].

The *Porphyra yezoensis* polysaccharide (PYP) is a low-cost, rich-source polysaccharide with high sulfuric acid groups and has good antioxidant capacity. PYP has a typical *Porphyran* structure and a backbone of alternating $(1 \rightarrow 3)$-linked β-D-galactose units and $(1 \rightarrow 4)$-linked 3,6-anhydro-α-L-galactose or $(1 \rightarrow 4)$-linked α-L-galactose 6-sulfate units [13]. Qian et al. [14] showed that plasma triglycerides, total cholesterol, and plasma low-density lipoprotein cholesterol in rats after oral administration of PYP were significantly reduced, indicating that PYP had a hypolipidemic activity. Fu et al. [15] proved that PYP has an immunoregulatory activity. PYP regulates the immune system by activating the NF-κB signaling pathway, promotes differentiation and activation of regulatory T cells (Tregs), and regulates the balance of T helper (Th)1/Th2 cells to maintain immune homeostasis. Chen and Xue [16] demonstrated that PYPs can inhibit the proliferation of SGC-7901 tumor cells, induce tumor cell apoptosis, and have antitumor effects on SGC-7901 mice, which can be used for cancer prevention and treatment.

In previous studies [13], we degraded the original PYP with Mw = 4669 kDa, obtained a series of degraded polysaccharides with low Mw, and characterized their chemical structures. This PYP has a repair effect on oxidatively damaged HK-2 cells, and the polysaccharide with the lowest Mw (4.02 kDa) has the best repair effect. In addition, we also studied the differences in toxicity and calcification of hydroxyapatite (HAP) on A7R5 cells before and after PYP protection [17]. PYPs could effectively reduce the cytotoxicity of HAP and inhibit the osteogenic transformation of the A7R5 cells. PYP protection inhibited cell necrosis and decreased alkaline phosphatase activity and expressions of bone/chondrocyte phenotype genes.

The repair of damaged cells by polysaccharides is equivalent to the treatment of diseases, whereas the preprotection of cells from oxidative damage is equivalent to the active prevention of diseases. Therefore, the preprotection of cells with exogenous antioxidants is more important to human health than repairing damaged cells. Kidney stones not only cause great harm to human beings but also lead to serious economic losses. Using scientific methods to prevent the occurrence of kidney stones or reduce their recurrence rate will be less than the cost of treatment and will reduce the pain of patients. Therefore, clinically, the scientific significance of preventing kidney stones is greater than that of treatment. PYPs also have a protective effect from calcium oxalate crystals [18]. PYP protection reduced the crystal toxicity, prevented the destruction of the cytoskeleton, reduced the expression of osteopontin and transmembrane protein (CD44), and finally inhibited the adhesion and endocytosis of HK-2 cells to nano-COM.

Besides calcium oxalate crystals, oxalic acid is also one of the most common foreign toxic substances that lead to stone formation. But the protective effect of degraded PYPs on HK-2 cells from cytotoxicity of oxalic acid has not been studied. In this study, normal HK-2 cells were preprotected by PYPs with different Mws, and then we studied the resistance of the protected cells to oxidative damage of oxalic acid and the ability to inhibit crystal adhesion and promote crystal endocytosis. We aimed to provide insight into preventing kidney stone formation and delaying its recurrence.

2. Materials and Methods

2.1. Materials and Apparatus

2.1.1. Materials. Natural *P. yezoensis* polysaccharide (PYP0) was provided by Shaanxi Ciyuan Biotechnology Co., Ltd. The polysaccharide content was 95%. Four different molecular weights of degraded polysaccharides PYP1 (576.2 kDa), PYP2 (105.4 kDa), PYP3 (22.47 kDa), and PYP4 (3.89 kDa) were obtained by the H_2O_2 oxidative degradation method [13]. The polysaccharide structure was characterized by ^{1}H NMR, ^{13}C NMR, FT-IR, and GC-MS spectral analysis. PYP has a typical *Porphyran* structure and has a backbone of alternating $(1 \rightarrow 3)$-linked β-D-galactose units and $(1 \rightarrow 4)$-linked 3,6-anhydro-α-L-galactose or $(1 \rightarrow 4)$-linked α-L-galactose 6-sulfate units. The contents of the sulfate group ($-OSO_3H$) of PYPs are 17.51% to 17.86%, and the contents of $-COOH$ are 1.42% to 1.70% [13].

Calcium oxalate monohydrate (COM) crystals have a size of about 100 nm. Human proximal tubular epithelial (HK-2) cells were purchased from the Shanghai Cell Bank of the Chinese Academy of Sciences (Shanghai, China). The following materials were also purchased for the study: fetal bovine serum and cell culture medium (DMEM) (Gibco, USA); penicillin and streptomycin (Beijing Pubo Biotechnology Co., Ltd., Beijing, China); cell proliferation assay kit (CCK-8), JC-1 (5,5,6,6-tetrachloro-1,1′,3,3′-tetraethyl-imidacarbocyanine iodide) dye, Annexin V-FITC/PI cell apoptosis and necrosis double dye kits, 4′,6-diamidino-2-phenylindole (DAPI), fluorescein isothiocyanate (FITC), LysoTracker Red, and reactive oxygen species (ROS) kit (Shanghai Beyotime Bio-Tech Co., Ltd., Shanghai, China); and cell culture plates of 6, 12, and 96 wells (NEST, China). Conventional reagents such as oxalic acid and anhydrous ethanol are analytically pure (Guangzhou Chemical Reagent Factory, China).

2.1.2. Apparatus. The apparatus used in the study include the following: microplate reader (Safire2, Tecan, Männedorf, Switzerland); X-L type environmental scanning electron microscope (SEM, Philips, Eindhoven, Netherlands); X-ray powder diffractometer (D/MAX2400, Japan); inverted fluorescence microscope (Leica DMRA2, Germany); optical microscope (Olympus, CKX41, Japan); flow cytometer (FACSAria, BD Corporation, CA, USA); and confocal laser scanning microscope (LSM510 Meta Duo Scan, Zeiss, Germany).

2.2. Experimental Methods

2.2.1. Cell Culture and Grouping.
HK-2 cells were cultured in DMEM containing 10% fetal bovine serum in a 5% CO_2 humidified environment at 37°C. Upon reaching a mono-layer of 80%–90% confluence, cells were gently blown after trypsinization to form a cell suspension for subsequent cell experiments. The cell suspension (1×10^5 cells/mL) was inoculated per well in 96-well plates and incubated for 24 h. The cells were divided into three groups: (1) control group, where only the serum-free DMEM culture medium was added; (2) protection group, where the serum-free medium containing PYPs with concentrations of 20, 40, 60, 80, and 100 μg/mL was added, and the culture medium was aspirated after 12 h. The cells were then treated with 2.8 mmol/L of oxalate dissolved in PBS and incubated for 3.5 h; and (3) injured group, in which 2.8 mmol/L of oxalate dissolved in PBS was added and incubated for 3.5 h.

2.2.2. Cell Viability Detection.
The density of seeded cells and experimental grouping were the same as those in Section 2.2.1. After the treatment time was reached, 10 μL of CCK-8 reagent was added to each well and incubated for 1.5 h in the dark. Absorbance (A) was measured at 450 nm according to the CCK-8 kit instruction. Cell viability was determined using the following equation:

$$\text{Cell viability (\%)} = \frac{A(\text{treatment group})}{A(\text{control group})} \times 100. \quad (1)$$

2.2.3. Cell Morphology Observation by Hematoxylin-Eosin (HE) Staining.
The cell suspension (1×10^5 cells/mL, 2 mL) was inoculated per well in 6-well plates and incubated for 24 h. The cells were divided into three groups: (1) control group, where only the serum-free DMEM culture medium was added; (2) protection group, where the serum-free medium containing PYPs with concentrations of 100 μg/mL was added, and the culture medium was aspirated after 12 h. The cells were then treated with 2.8 mmol/L of oxalate dissolved in PBS and incubated for 3.5 h; and (3) injured group, in which 2.8 mmol/L of oxalate dissolved in PBS was added and incubated for 3.5 h. After the treatment time was reached, cells were fixed with 4% paraformaldehyde for 15 min and stained with hematoxylin and eosin according to the manufacturer's instructions. Morphological changes of the cells were observed under a microscope.

2.2.4. Changes in Intracellular Reactive Oxygen Species (ROS) Levels.
We followed the methods of Huang et al. [17]. The density of seeded cells and experimental grouping were the same as those in Section 2.2.3. After the treatment time was reached, 500 μL of DCFH-DA diluted with the serum-free medium was added. The samples were stained with DCFH-DA for 30 min, the cells were qualitatively observed under a fluorescence microscope, and the fluorescence intensity was quantitatively detected by a microplate reader.

2.2.5. Measurement of Mitochondrial Membrane Potential ($\Delta\Psi m$).
We followed the methods of Huang et al. [17]. The density of seeded cells and experimental grouping were the same as those in Section 2.2.3. After the treatment time was reached, the cells were stained with JC-1 for 1 h in the dark, and the cells were qualitatively observed under a fluorescence microscope. In the same operation as above, the cells were digested with 0.25% trypsin (moderate digestion), and the cell deposits were centrifuged at 1000 rpm for 5 min. The samples were detected by flow cytometry according to the requirements of the JC-1 kit.

2.2.6. Cell Cycle Detection.
The density of seeded cells and experimental grouping were the same as those in Section 2.2.3. After the treatment time was reached, the cells were washed twice with PBS and digested with 0.25% trypsin; then, 10% fetal bovine serum DMEM was used to terminate digestion, and the cells were centrifuged at 1000 rpm for 5 min. The collected cells were washed twice with PBS, then fixed using 70% ethanol for 24 h at 4°C. Ethanol was removed by centrifugation, and the cells were washed twice with PBS. Cells were then resuspended in 200 μL propidium iodide (PI) and kept at 37°C for 15 min. The cell cycle was analyzed by the flow cytometer.

2.2.7. Apoptosis and Necrosis Detection.
We followed the methods of Huang et al. [17]. The density of seeded cells and experimental grouping were the same as those in Section 2.2.3. After the treatment time was reached, the cells were washed twice with PBS and digested with 0.25% trypsin; then, 10% fetal bovine serum DMEM was used to terminate digestion, and the cells were centrifuged at 1000 rpm for 5 min. Then, 200 μL of the binding buffer was added and mixed thoroughly into the cells. The cells were stained with 5 μL of Annexin V-FITC, incubated in the dark at room temperature for 10 min, and then centrifuged. The supernatant was removed. Afterward, 200 μL of the binding buffer was added and mixed thoroughly into the cells. Then, 5 μL of PI was added to stain the cells. After the treatment was administered, the cells were detected through flow cytometry.

2.2.8. Phosphatidylserine (PS) Exposure Assay.
The density of seeded cells and experimental grouping were the same as those in Section 2.2.3. After the treatment time was reached, the cells were washed twice with PBS and digested with 0.25% trypsin; then, 10% fetal bovine serum DMEM was used to terminate digestion, and the cells were centrifuged at 1000 rpm for 5 min. 200 μL of the binding buffer was added and mixed thoroughly, stained with 5 μL of Annexin V-FITC for 30 min at 4°C in the dark, and then detected through flow cytometry.

2.2.9. Preparation of Fluorescence-Labeled COM.
A mixture of 0.05 g of COM and 5 mL of APTES in 50 mL of anhydrous ethanol was refluxed with continuous stirring under nitrogen for 3 h. Next, 0.025 g of FITC was added to the mixture for a reaction time of 6 h at 74°C. The FITC-tagged COM was then collected through centrifugation, washed several times with anhydrous ethanol and distilled water to ensure that no free FITC remained, and dried.

2.2.10. Quantitative Analysis of Internalized COM Crystals.
We followed the methods of Huang et al. [17]. The density

of seeded cells and experimental grouping were the same as those in Section 2.2.3. Cells in groups were exposed to a serum-free medium containing $200 \mu g/mL$ FITC-labeled COM crystals for 24 h. After reaching the incubation times, the cells were treated with ethylenediaminetetraacetic acid (EDTA) (5 mM) for 5 min to remove the adherent COM, and the percentages of cells with internalized crystals and the fluorescence intensity were measured by flow cytometry.

2.2.11. Observation of COM Localization in Lysosomes. We followed the methods of Huang et al. [17]. The density of seeded cells and experimental grouping were the same as those in Section 2.2.3. Cells in groups were exposed to a serum-free medium containing $200 \mu g/mL$ FITC-labeled COM crystals for 24 h. After reaching the incubation times, the cells were stained with 70 nM LysoTracker Red to label lysosomes for 2 h and then fixed with paraformaldehyde for 30 min, and the cell nucleus was stained with DAPI. The crystal distribution was observed by a confocal laser scanning microscope.

2.2.12. Quantitative Analysis of Adherent COM Crystals. We followed the methods of Huang et al. [17]. The density of seeded cells and experimental grouping were the same as those in Section 2.2.3. Cells in groups were exposed to a serum-free medium containing $200 \mu g/mL$ FITC-labeled COM crystals for 1 h in 4°C that inhibited endocytosis of cells to COM [19]. The cells were washed twice with cold PBS to eliminate unbound crystals, followed by trypsinization, and the percentage of cells with adherent crystals was measured by a flow cytometer.

2.2.13. SEM Observation of Adhered Crystals on the Cell Surface. The density of seeded cells and experimental grouping were the same as those in Section 2.2.3. Cells in groups were exposed to a serum-free medium containing $200 \mu g/mL$ COM crystals for 1 h. After reaching the adhesion time, the cells were washed with PBS and fixed in 2.5% glutaraldehyde at 4°C for 24 h, dehydrated in gradient ethanol (30%, 50%, 70%, 90%, and 100%, respectively), dried under the critical point of CO_2, and treated with gold sputtering. The crystal adhesion was observed by SEM.

2.2.14. Statistical Analysis. Experimental data were expressed as the mean ± standard deviation ($\bar{x} \pm SD$). The experimental results were analyzed statistically using SPSS 13.0 software (SPSS Inc., Chicago, IL, USA). The differences in the means between the experimental groups and the control group were analyzed using one-way ANOVA, followed by the Tukey post hoc test. If $p < 0.05$, there was significant difference; if $p < 0.01$, the difference was extremely significant; if $p > 0.05$, there was no significant difference.

3. Results

3.1. PYP Preprotection Reduces Oxalic Acid Damage to HK-2 Cells. Four kinds of PYPs were used to preprotect HK-2 cells. The oxidative damage of oxalic acid to HK-2 cells before and after PYPs preprotected cells was detected by the CCK-8 method (Figure 1). The cell viability of the injured group
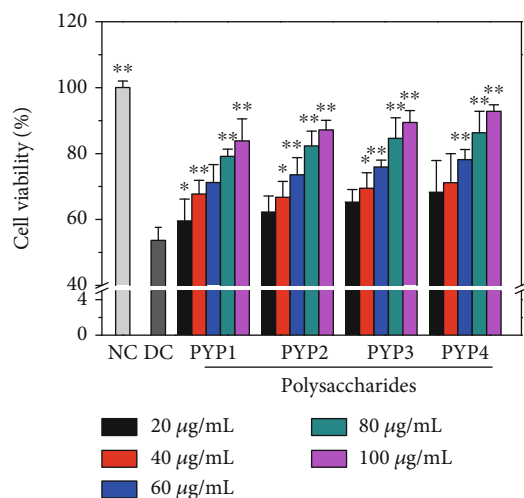
Figure 1: Cell viability change of HK-2 cells before and after PYP protection. NC: normal control; DC: damaged control. Oxalate damage concentration: 2.8 mmol/L; damage time: 3.5 h; protective time: 12 h. Compared with the DC group, $*p < 0.05$, $**p < 0.01$.

(53.68%) was significantly lower than that of the control group (100%), whereas the cell viability of the protection group was higher than that of the injured group, indicating that the preprotection of the four PYPs could improve the ability of HK-2 cells to resist oxidative damage caused by oxalic acid.

As the Mw of PYP decreased or the concentration of polysaccharides increased, the viability of cells increased; that is, the low-Mw PYP4 had a good preprotective effect. At a concentration of $100 \mu g/mL$, the cell viability after 12 h preprotection by PYP1, PYP2, PYP3, and PYP4 was 83.88%, 87.21%, 89.43%, and 92.84%, respectively.

3.2. PYP Preprotection Improves Cell Morphology. Hematoxylin-eosin staining was used to observe the morphological changes of damaged HK-2 cells before and after PYP protection (Figure 2). Normal HK-2 cells were tightly connected, large, and plump. The morphology of HK-2 cells in the injured group was irregular and disordered, the cell volume was reduced, the cell density was reduced, and the cells had the tendency to apoptosis. HK-2 cells preprotected by PYPs were less damaged by oxalic acid, resulting in the increase in the number of normal cells and decrease in the number of apoptotic cells (indicated by arrows in Figure 2), of which PYP4 had the best protective effect, indicating that PYP4 with low Mw had the best protective ability for HK-2 cells.

3.3. PYP Preprotection Reduces Intracellular ROS. Figure 3 shows the changes in the ROS of cells after protecting PYPs. Compared with the normal group, HK-2 cells in the injured group have the strongest fluorescence intensity, indicating that the ROS level was the highest. However, the fluorescence intensity of ROS in the cells preprotected by PYPs decreased to different degrees, indicating that PYPs can reduce the generation of ROS in the cells, thereby reducing the oxidative damage of the cells, and PYP4 with the lowest Mw had the most significant degree of reduction.
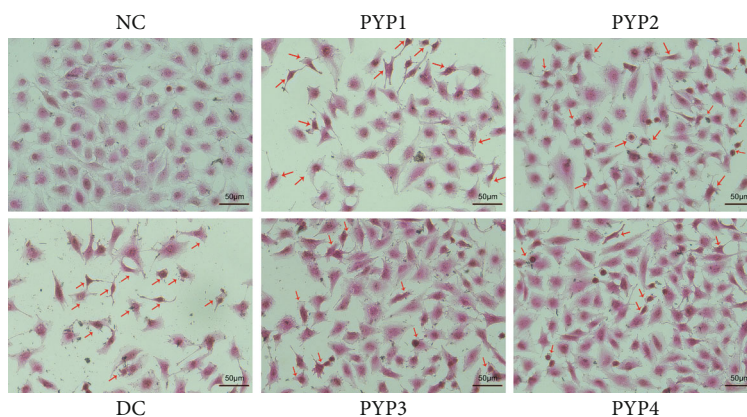
FIGURE 2: Morphological changes of HK-2 cells before and after PYP protection. $c(PYP) = 100 \mu g/mL$; oxalate damage concentration: 2.8 mmol/L; damage time: 3.5 h; protective time: 12 h. The red arrow indicates apoptotic cells.

(a)

(b)
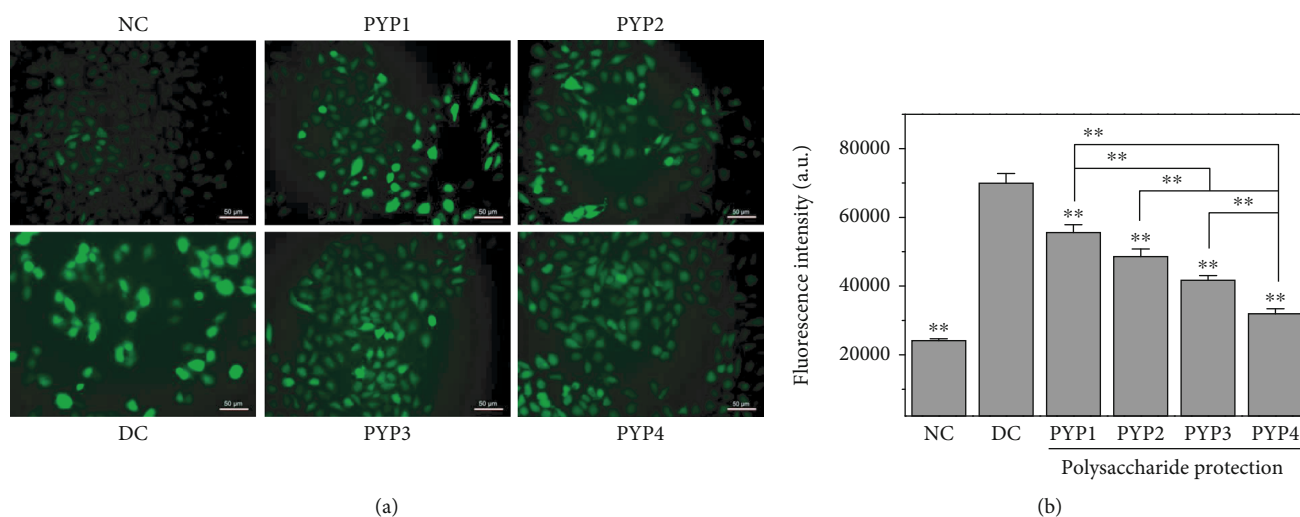
FIGURE 3: ROS changes in HK-2 cells before and after PYP protection. (a) Fluorescence microscopy images. (b) Quantitative fluorescence intensity of ROS. NC: normal control. DC: damaged control. Oxalate damage concentration: 2.8 mmol/L; damage time: 3.5 h; $c(PYP) = 100 \mu g/mL$; protective time: 12 h. Compared with the DC group, $^*p < 0.05$, $^{**}p < 0.01$.

3.4. PYP Preprotection Inhibits Decline in Mitochondrial Membrane Potential ($\Delta\Psi m$).

The fluorescent probe JC-1 is a cationic lipophilic dye that can freely pass through the cell membrane. At high $\Delta\Psi m$ (normal cells), the fluorescent probe JC-1 molecules accumulated in the mitochondrial matrix to form polymers (J-aggregates), which produced red fluorescence (Figure 4(a)). When cells are damaged, $\Delta\Psi m$ decreased, and JC-1 was primarily in a monomer form (JC-1-monomer), producing green fluorescence.

Figure 4(a) is the change of $\Delta\Psi m$ quantitatively detected by flow cytometry. Compared with the normal group of cells (4.43%), the red fluorescence of the injured cells was weaker, and the green fluorescence was stronger, indicating that $\Delta\Psi m$ decreased remarkably (51.07%). After the protection of PYPs, the red fluorescence of the cells increased, the green fluorescence decreased, $\Delta\Psi m$ decreased in different degrees, and the decreased value of $\Delta\Psi m$ decreased (18.05%–45.85%) (Figure 4(c)), indicating that the degree of cell damage was reduced.

3.5. S Phase Cells Decreased and G1 Phase Cells Increased after PYP Preprotection.

The stagnation of the cell cycle reflects the degree of DNA damage. The greater the degree of DNA damage, the greater the cell damage. After the normal HK-2 cells were damaged by oxalic acid, the number of cells in the S phase increased (Figure 5(b)), and the number of cells in the G1 phase decreased (Figure 5(c)), indicating that oxalic acid-damaged HK-2 cells were arrested in the S phase. After PYP preprotection, S phase cells decreased and G1 phase cells increased, among which the number of G1 phase cells preprotected by PYP4 increased more, indicating that PYP4 had a better protective effect.

3.6. PYP Preprotection Inhibits Cell Apoptosis.

Figure 6 shows apoptosis and necrosis of cells before and after PYP preprotection. The result was quantitatively detected by the Annexin V/PI double staining method. Compared with the control group (apoptotic cells (3.36%)), the number of apoptotic cells (32.36%) in the oxalic acid-damaged group was

(a)

(b)

(c)
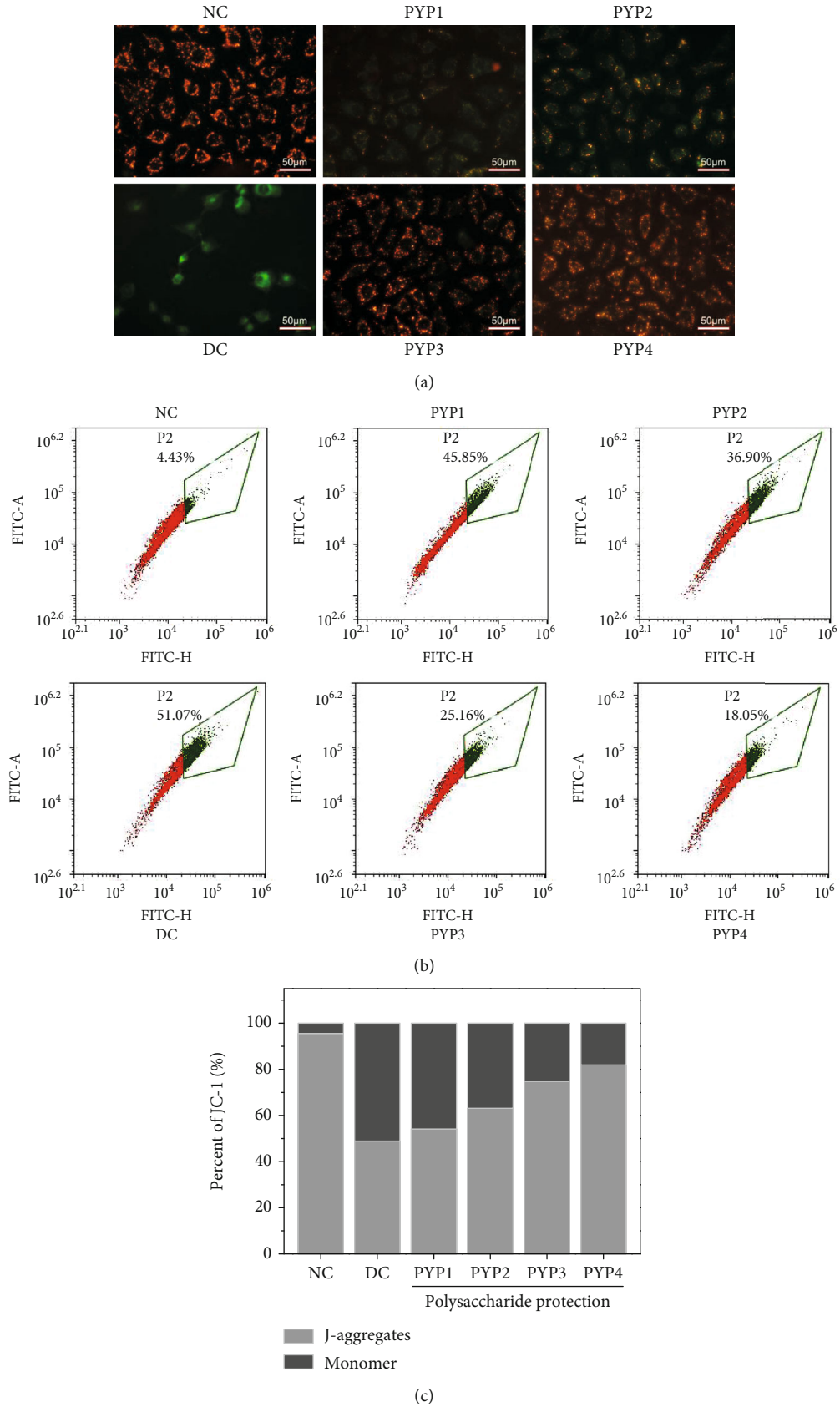
FIGURE 4: $\Delta\Psi$m changes in HK-2 cells before and after PYP protection. (a) Fluorescence microscopy images. (b) Flow cytometric data of $\Delta\Psi$m. (c) Quantitative results. Experimental conditions and statistical significance are the same as in Figure 3.

(a)

(b)

(c)
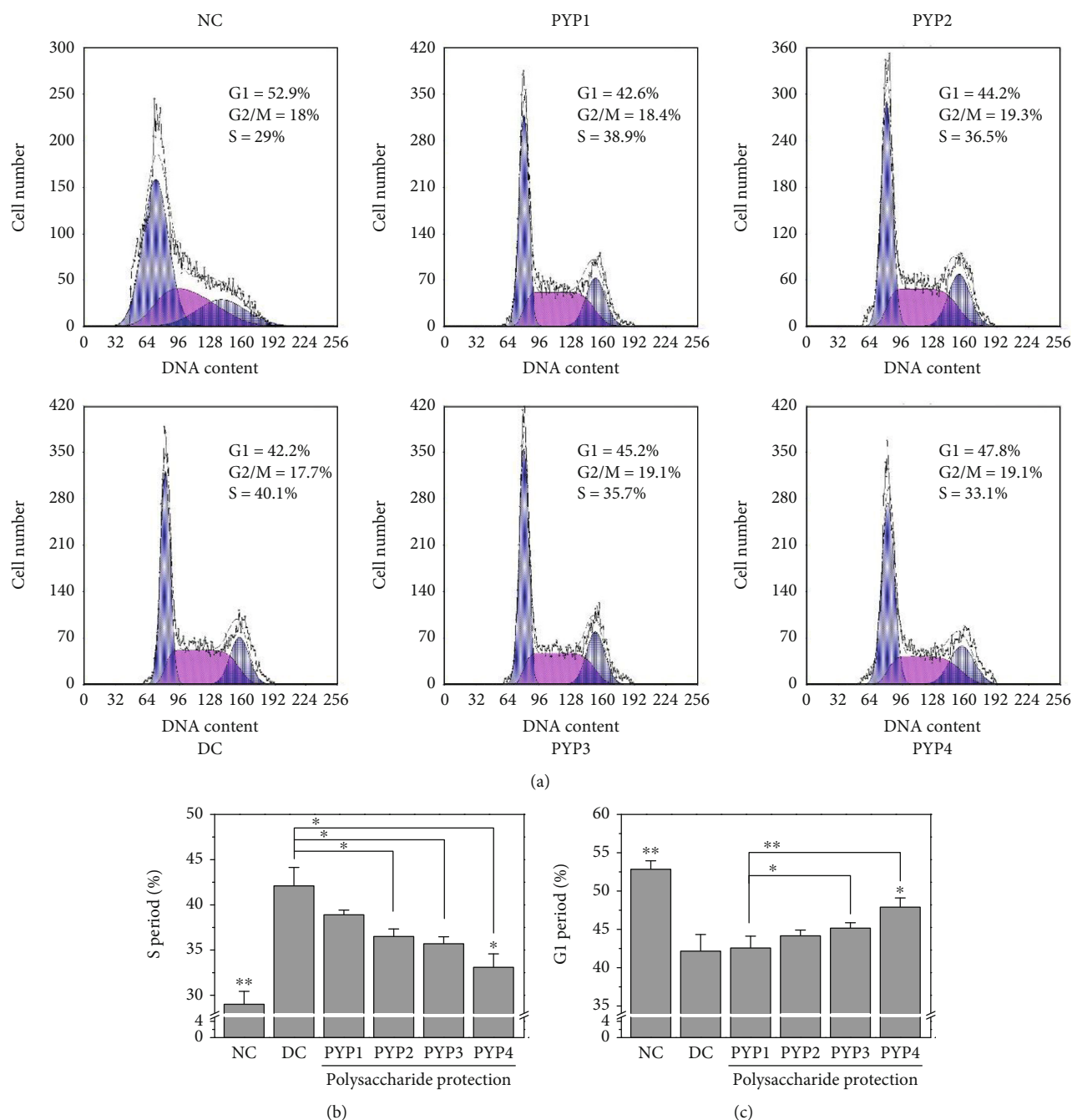
FIGURE 5: Cell cycle progressions of HK-2 cells before and after PYP protection. (a) Flow cytometric data of the cell cycle. (b) Quantitative result of the S phase. (c) Quantitative result of the G1 phase. Experimental conditions and statistical significance are the same as in Figure 3.

significantly increased. After PYP protection, PYPs can effectively reduce the number of apoptotic cells (7.31%–23.52%), of which PYP4 had a better inhibitory effect (7.31%).

3.7. PYP Preprotection Inhibits Phosphatidylserine (PS) Exposure.
Under normal circumstances, PS is located inside the renal tubular epithelial cell membrane, but after the cell membrane is damaged, part of the PS will migrate to the outside of the cell membrane. As shown in Figure 7, the amount of PS exposure on the surface of HK-2 cells in the normal group was lower (4.77%), whereas the amount of PS exposure

(42.17%) in the cells damaged by oxalic acid was significantly increased. After preprotection by PYPs, the amount of PS exposure decreased (19.68%–3.95%), and the protective effect of PYP4 was more significant.

3.8. PYP Preprotection Promotes Endocytosis of COM Crystals by Cells.
After using DAPI and LysoTracker Red to label the nucleus and lysosome, respectively, the nucleus and lysosome showed blue fluorescence and red fluorescence, respectively. The distribution of green fluorescence-labeled COM crystals in cell lysosomes can be observed by a confocal microscope.

(a)

(b)
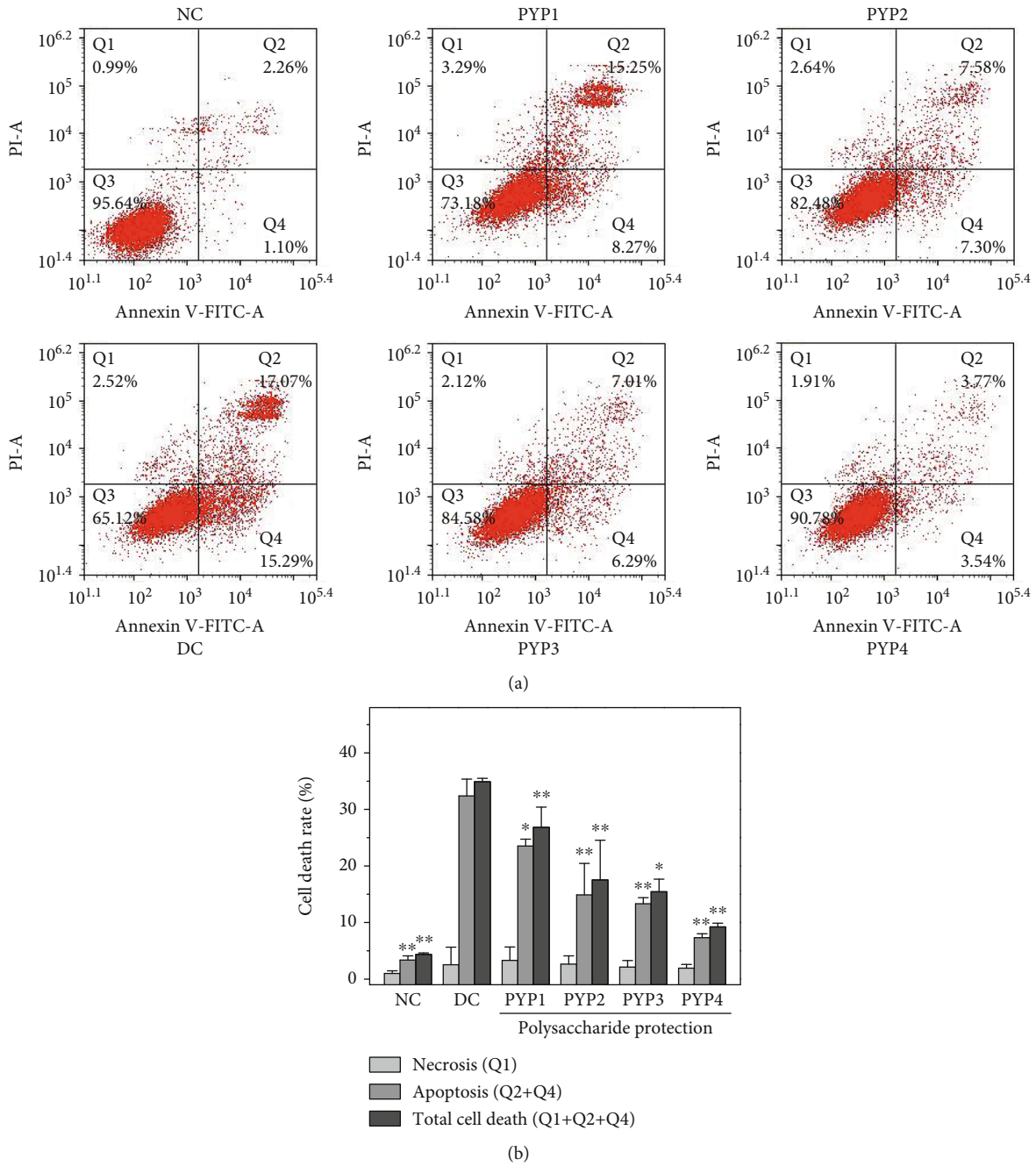
FIGURE 6: Cell apoptosis and necrosis of HK-2 cells before and after PYP protection. (a) Flow cytometric data of cell apoptosis and necrosis. (b) Quantitative results. Experimental conditions and statistical significance are the same as in Figure 3.

As shown in Figure 8, the COM crystal with green fluorescence overlaps with the lysosome with red fluorescence, which indicated that the nano-COM crystal has entered the lysosome. A large number of COM crystals overlapped in normal cells indicating that more crystals were endocytosed by normal cells. However, the number of overlapping COM crystals in the injured group decreased, indicating that the damaged cell lysozyme has a reduced ability to internalize COM crystals. After the cells were preprotected by PYPs, the number of crystals entering the lysosome increased compared with the injured group, and as the Mw of PYP

decreased, the number of crystals entering the lysosome gradually increased.

Flow cytometry was used to quantitatively detect the difference in endocytosis of nano-COM crystals by cells before and after PYP preprotection (Figure 9(a)). After incubating FITC-labeled COM crystals with a size of approximately 100 nm with HK-2 cells at 37°C for 24 h, EDTA was used to remove the crystals adhered to the cell surface. The cells with FITC signals detected were the cells that endocytosed crystals [20, 21]. The proportion of cells endocytosing crystals in the oxalic acid-damaged group (19.47%) was significantly lower

(a)

(b)
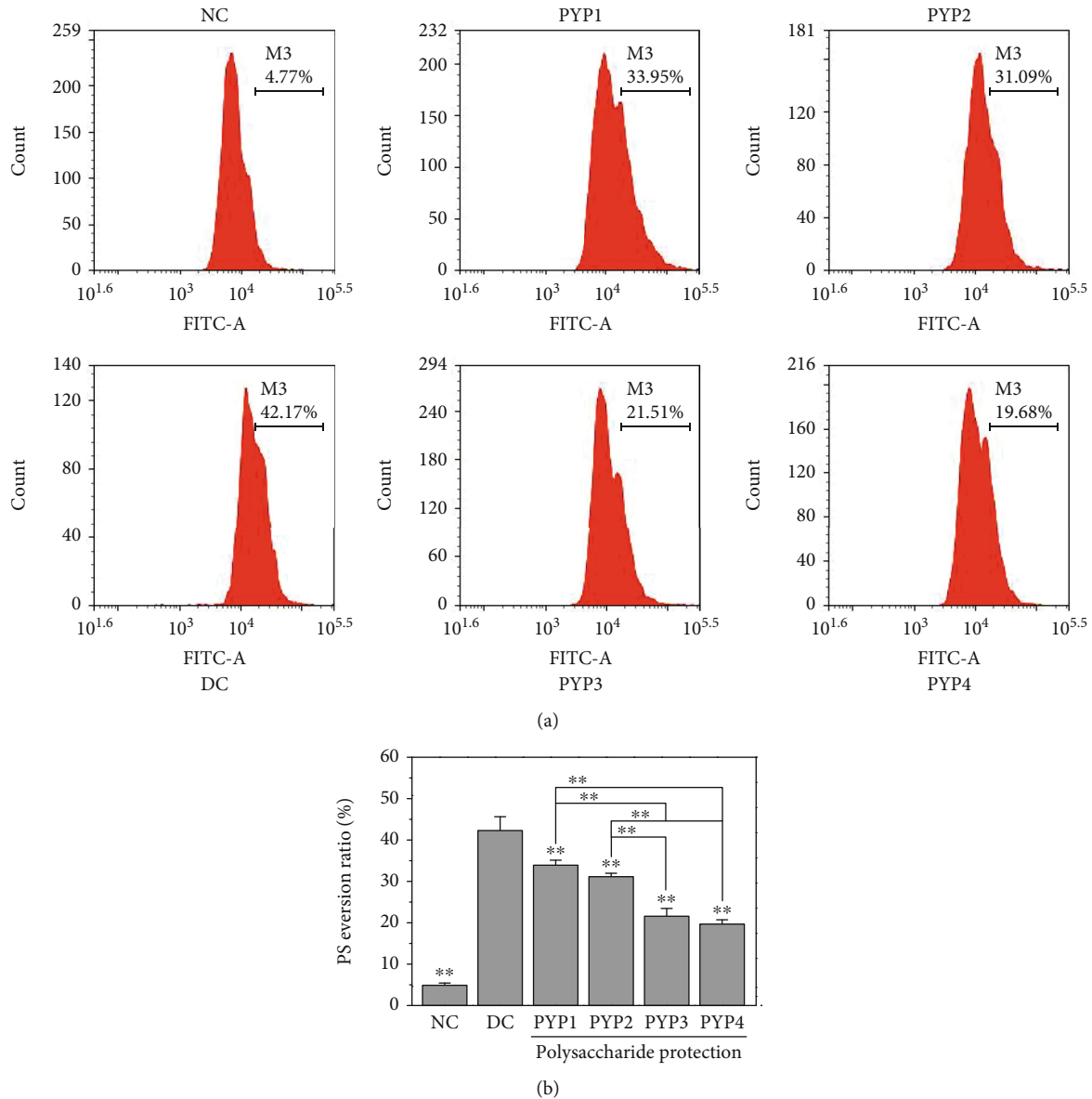
FIGURE 7: PS exposure of HK-2 cells before and after PYP protection. (a) Flow cytometric data of PS exposure. (b) Quantitative results. Experimental conditions and statistical significance are the same as in Figure 3.

than that in the normal control group (41.06%). The cell proportion of endocytic crystals after PYP preprotection was between the control and injured groups (23.34%–33.48%) (Figure 9(b)), and the lower the Mw, the larger the cell proportion of endocytic crystals.

3.9. PYP Preprotection Inhibits COM Adhesion on the Cell Surface. A scanning electron microscope was used to observe the adhesion of HK-2 cells to COM crystals before and after PYP protection (Figure 10). The normal control group had plump cell morphology, smooth cell surface, and fewer amounts of adhered crystals. However, in the injured group, the cell morphology changed evidently, the cell surface became rough, and the amount of adherent crystals on the cell surface increased remarkably. The cells preprotected by PYPs were less damaged; the amount of crystals adhering

to the cell surface was between the cells of the control and damaged groups, and as the Mw of PYP decreased, the amount of crystals gradually decreased; i.e., PYP4 with the lowest Mw had the best protective effect on the cells.

Flow cytometry was used to quantitatively detect the difference in cell adhesion to nano-COM crystals before and after PYP preprotection (Figure 11). The nano-COM crystals were incubated with cells at 4°C. At this temperature, the endocytosis behavior of cells was inhibited, but crystal adhesion was unaffected [20, 21]. The percentage of cells adhering to the crystals was measured by flow cytometry, and cells presenting FITC signals were regarded as cells with adherent crystals (Figure 11(a)). The percentage of cells adhering to crystals in the normal group was 11.05%, which was significantly lower than that in the injured group (51.05%). However, the percentage of cells adhering to crystals in the PYP
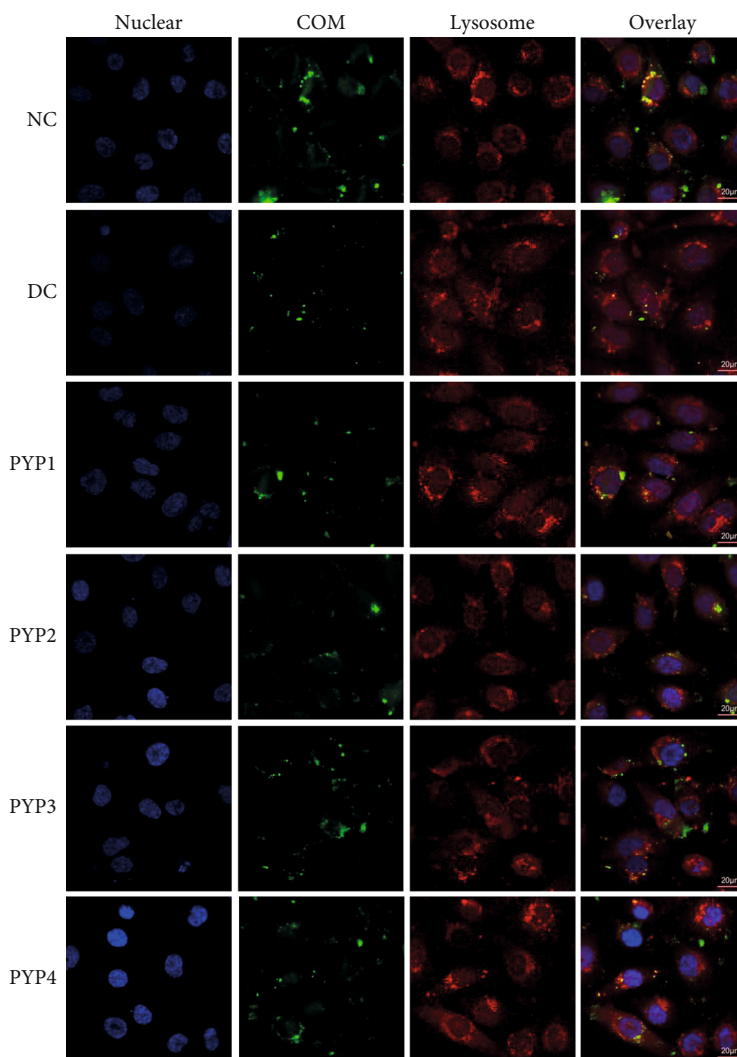
Figure 8: Observation of the accumulation of nano-COM in HK-2 cell lysosomes before and after PYP protection by confocal microscopy. COM concentration: 200 μg/mL; endocytosis time: 24 h. Use DAPI and LysoTracker Red to label the nucleus (blue) and lysosome (red), respectively. Other experimental conditions are the same as in Figure 3.

protection group was 22.71%–44.76% (Figure 11(b)), and the percentage of cells adhering to crystals in the PYP4 protection group was the lowest (22.71%).

4. Discussion

4.1. PYPs Preprotect HK-2 Cells from Oxidative Damage. The damage of renal epithelial cells is the main reason for kidney stone formation, and the addition of exogenous antioxidants may reduce the oxidative damage of cells. Antioxidants such as vitamin E [22] and seaweed polysaccharides [23] can effectively protect kidney cells from oxidative stress mediated by oxalic acid in vitro. PYP is a polysaccharide with high sulfate content and strong antioxidant capacity. As such, we evaluated the protective effects of PYPs with different Mws on oxalic acid-induced oxidative damage of HK-2 cells. The cell viability test results and cell morphology observation showed that PYP preprotection could reduce the damage of oxalic acid to cells (Figures 1 and 2).

The excessive production of ROS is the main mechanism that causes cell damage. Oxalic acid causes toxicity to cells, leading to the generation of ROS in cells (Figure 3). The production of ROS can cause oxidative stress in cells, leading to the dysfunction of normal cells. ROS primarily occurs in the mitochondria of cells; thus, ROS is the direct cause of the decrease in $\Delta\Psi$m. Excessive ROS can increase the permeability of the mitochondrial membrane and depolarize the mitochondria, resulting in the decrease of $\Delta\Psi$m. Our results indicated that cells preprotected by PYPs have reduced ROS production and decreased $\Delta\Psi$m, thereby reducing oxidative damage caused by oxalic acid.

Oxidative stress can also lead to DNA damage, thereby causing cell cycle retention [24]. Cells in the oxalic acid-treated group experienced S phase retention (Figure 5(b)). The specific inhibition caused DNA damage, leading cells to enter the death procedure [25]. Therefore, mitochondrial dysfunction and DNA damage activate apoptosis, leading to cell apoptosis (Figure 6). The cells protected

(a)

(b)
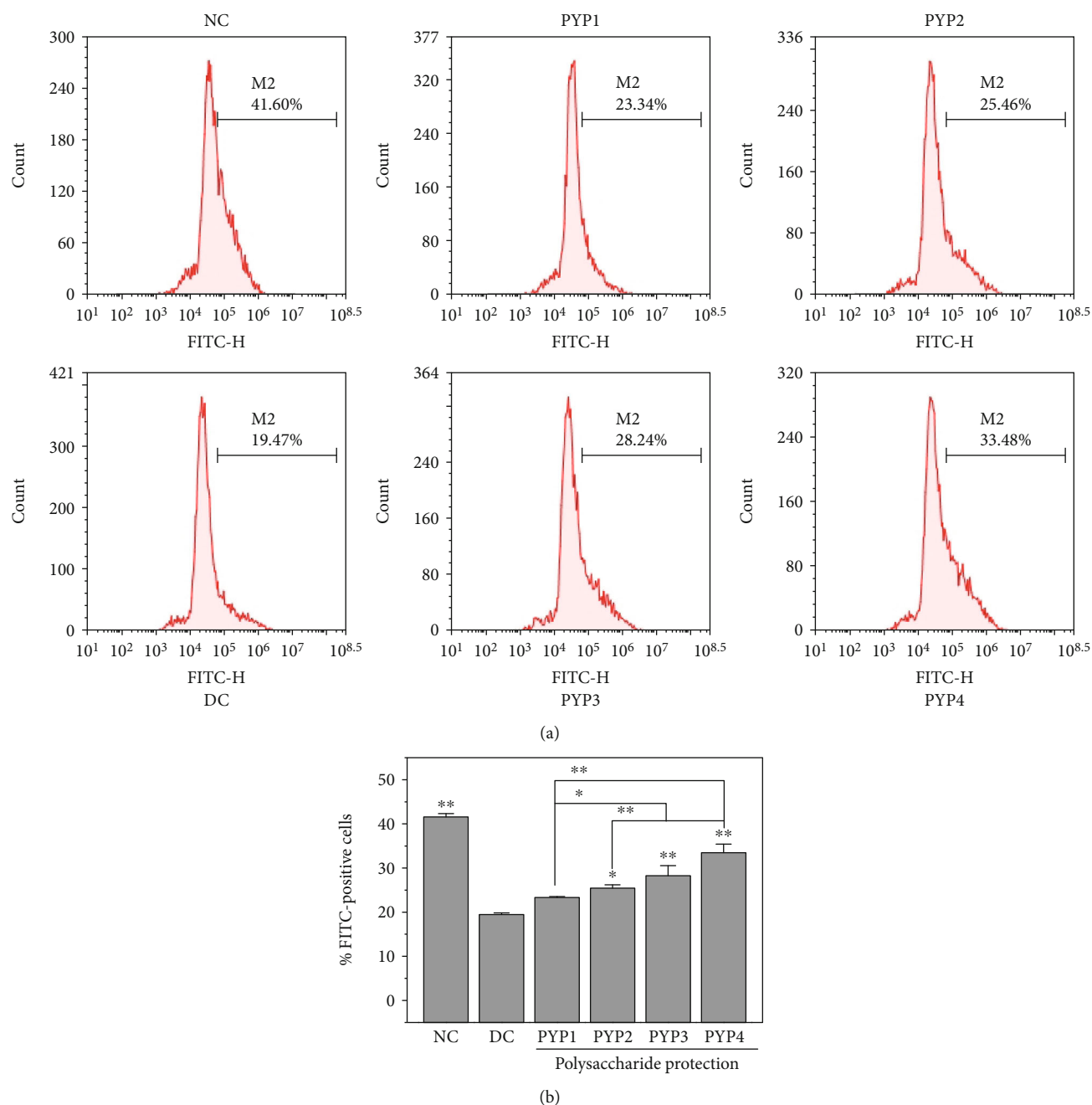
FIGURE 9: Flow cytometry analysis of internalized COM crystals by HK-2 cells before and after PYP protection. (a) Flow cytometric data. (b) Quantitative results. COM concentration: 200 μg/mL; endocytosis time: 24 h. Use DAPI and LysoTracker Red to label the nucleus (blue) and lysosome (red), respectively. Compared with the DC group, $^*p < 0.05$, $^{**}p < 0.01$.

by PYPs gradually reduced the number of S phase cells and the number of apoptosis. This result is consistent with previous studies, and similar results were obtained in SRA01/04 cells treated with *Lycium barbarum* polysaccharides [26].

Based on the abovementioned research results, we propose the following causes of the protective effect of PYPs on HK-2 cells (Figure 12): oxalic acid can cause oxidative damage of cells and intracellular ROS generation and lead to mitochondrial dysfunction and S phase cell cycle retention, thereby inducing cell apoptosis. However, after PYPs

preprotect the cells, PYPs effectively improved the ability of HK-2 cells to resist the oxidative damage mediated by oxalic acid and reduced the generation of ROS in the cells, the damage to the mitochondria, and the number of cells staying in the S phase and apoptotic cells.

The protective effect of PYPs on HK-2 cells enhances the ability of cells to resist exogenous damage and inhibits changes in cell morphology, apoptosis, and PS eversion, which can increase the resistance of cells to adhered crystals and reduce the risk of crystal aggregation on the cell surface, thereby inhibiting the formation of kidney stones.
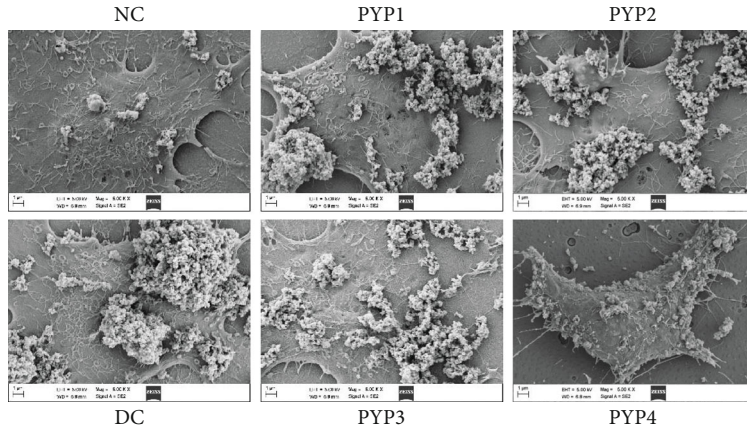
FIGURE 10: SEM observation of the nano-COM crystals adhered to the surface of HK-2 cells before and after PYP protection. COM concentration: 200 μg/mL; adhesion time: 1 h.

(a)

(b)
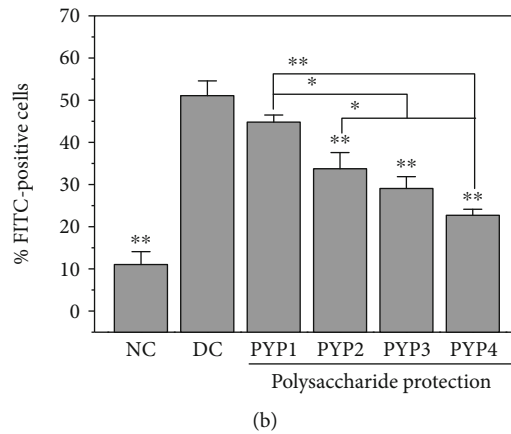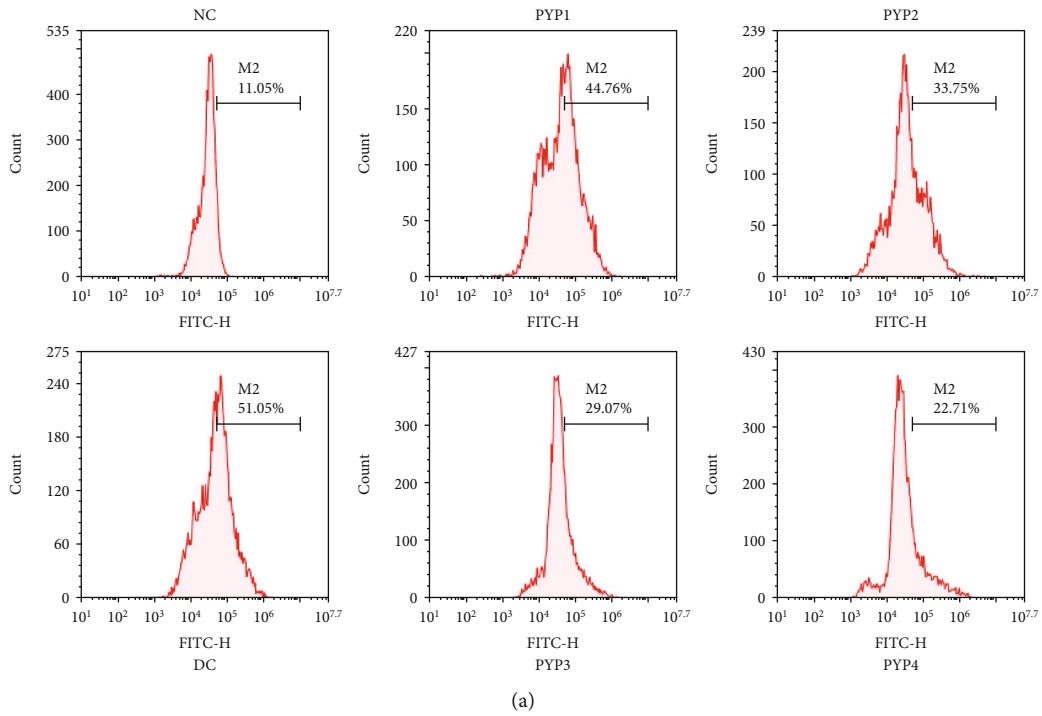
FIGURE 11: Flow cytometry quantitative analysis of adherent COM crystals on HK-2 cells before and after PYP protection. (a) Flow cytometric data. (b) Quantitative results. COM concentration: 200 μg/mL; adhesion time: 1 h. Compared with the DC group, $^{*}p < 0.05$, $^{**}p < 0.01$.
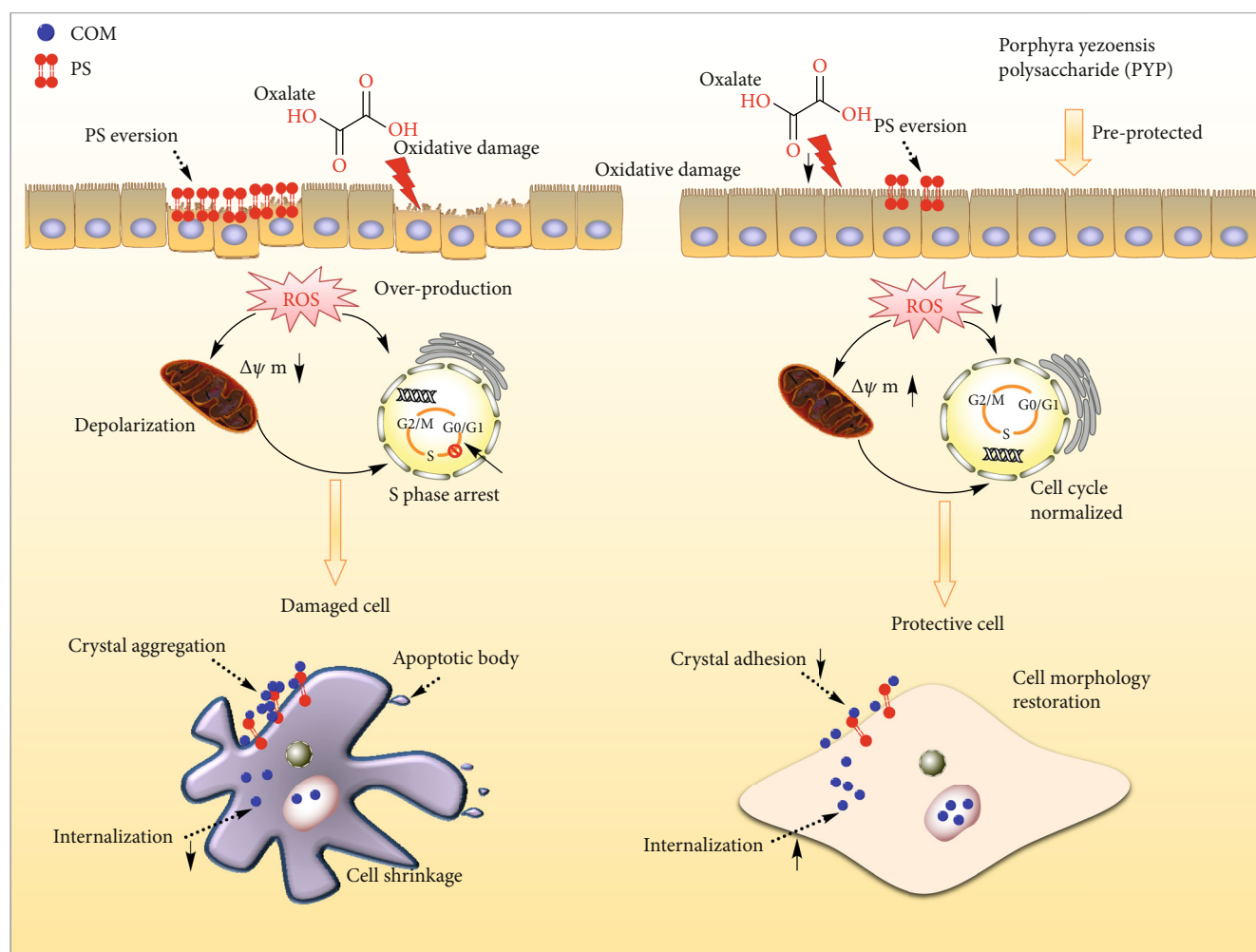
FIGURE 12: Mechanism diagram of protection of HK-2 cells by PYPs with different molecular weights.

4.2. PYP Protection Reduces Adhesion to COM Crystals on Cells and Promotes Crystal Endocytosis. Normal renal tubular epithelial cells have a complete structure and function, and few active sites are found on the cell surface, which adhere to urine microcrystals; thus, such cells can resist the adhesion of urine microcrystals. Cell damage is the primary condition for crystal adhesion [27, 28]. The mechanism diagram of protection of HK-2 cells by PYPs with different molecular weights is shown in Figure 12. Our results indicated that oxalic acid can cause damage to cells, destroy the tight junctions between cells (Figure 2), change the polarity of the cell membrane surface, migrate cell membrane components (such as PS) to the cell surface (Figure 7), and induce a large number of negatively charged crystal adhesion molecules such as osteopontin [29], hyaluronic acid, and CD44 on the cell surface [30]. These negatively charged macromolecules can adhere to positively charged surfaces of COM crystals, thereby promoting the adhesion of crystals to cells (Figures 10 and 11). The crystals adhering to the cell surface can further damage the cells and increase the adhesion of the crystals. However, the cells preprotected by PYPs have effectively improved their ability to resist oxidative damage; the degree of cell damage is reduced, and the adhesion sites on

the cell surface are reduced, thereby reducing the adhesion of cells to crystals (Figure 11).

However, cells can reduce the damage caused by the adhered crystals through endocytosis [31]. As the endocytosed crystals enter the lysosomes (Figure 8), the crystals dissolve in the acidic environment inside the lysosomes and are expelled from the body [32]. Moreover, as the endocytosed crystals in cells depend on the integrity of the cell membrane structure and function, the endocytosis of damaged cells will be weakened, and crystals entering the lysosomes will be decreased (Figure 9). However, the ability of PYP-protected cells to engulf crystals is enhanced, and the number of crystals entering the lysosomes is increased.

The protection of renal epithelial cells with PYPs can not only reduce the adhesion of crystals on the cell surface but also improve the ability of cells to engulf crystals. These aspects can reduce the risk of adhesion and aggregation of crystals on the cell surface, thereby reducing the risk of kidney stone formation.

4.3. PYP with Low Mw Has Good Protective Ability on Cells. The biological activity of polysaccharides is affected by their structural characteristics, including the Mw and functional

group content of polysaccharides [33]. Only when the Mw of polysaccharides is within a certain range can it exert the best biological activity, and for polysaccharides with different properties, the Mw range for exerting the best activity is different. Under normal circumstances, degraded polysaccharides can better exert their biological activities. Xing et al. [34] confirmed that the scavenging effect of low-Mw chitosan (9 kDa) on hydroxyl radicals is stronger than that of high-Mw chitosan (760 kDa). Zhao et al. [35] demonstrated that low Mw of sulfated polysaccharides from *Laminaria japonica* has a strong antioxidant effect, which has a protective effect on liver injury induced by CCl_4 and D-GalN in mice.

The results showed that PYP with low Mw has a strong ability to inhibit HK-2 cells from oxidative damage; thus, PYP4 shows the strongest ability to inhibit COM crystal adhesion and promote endocytosis of COM crystals. The inhibition of HK-2 cells may be related to the following factors: polysaccharides with larger Mw and steric hindrance, overlapping polysaccharide chains, stronger intramolecular hydrogen bond force, tighter structure, and weaker ability to contact with cells, thereby preventing the active groups from exerting their effect [36]. However, the Mw of polysaccharides decreases; polysaccharides have a higher degree of freedom, increased solubility in vivo, and more exposed acidic groups ($-OSO_3^-$) and can easily enter the cells to react directly with free radicals, thereby increasing the antioxidant capacity of cells. Some studies have also shown that low-Mw polysaccharides have more terminal hydroxyl groups, which are conducive to scavenging free radicals [37]. Therefore, PYP4 with the lowest Mw shows the strongest biological activity.

5. Conclusions

Four PYPs with Mws of 576.2, 105.4, 22.47, and 3.89 kDa can protect HK-2 cells from oxidative damage by oxalic acid, and the lower the Mw, the stronger the protective ability of polysaccharides. Under the protection of PYPs, cell vitality increased; cell morphology improved; the ROS level decreased; mitochondrial membrane potential increased; S phase cell arrest was inhibited; and the apoptotic cell rate, PS exposure, and the amount of COM crystals adhering to the cell surface decreased, whereas the amount of endocytosed crystals increased. These results indicated that PYP4 could reduce the risk of calcium oxalate kidney stone formation and might be a potential drug for preventing kidney stones.

Data Availability

All the data supporting the results were shown in the paper and can be available from the corresponding authors.

Conflicts of Interest

The authors declare that they have no competing interests.

References

[1] S. R. Khan, "Renal tubular damage/dysfunction: key to the formation of kidney stones," *Urological Research*, vol. 34, no. 2, pp. 86–91, 2006.

[2] S. L. Yu, X. G. Gan, J. M. Huang et al., "Oxalate impairs aminophospholipid translocase activity in renal epithelial cells via oxidative stress: implications for calcium oxalate urolithiasis," *The Journal of Urology*, vol. 186, no. 3, pp. 1114–1120, 2011.

[3] L. Badimon, P. Chagas, and G. Chiva-Blanch, "Diet and cardiovascular disease: effects of foods and nutrients in classical and emerging cardiovascular risk factors," *Current Medicinal Chemistry*, vol. 26, no. 19, pp. 3639–3651, 2019.

[4] G. Huang, X. Chen, and H. Huang, "Chemical modifications and biological activities of polysaccharides," *Current Drug Targets*, vol. 17, no. 15, pp. 1799–1803, 2016.

[5] E. Gómez-Ordóñez, A. Jiménez-Escrig, and P. Rupérez, "Bioactivity of sulfated polysaccharides from the edible red seaweed _Mastocarpus stellatus_," *Bioactive Carbohydrates and Dietary Fibre*, vol. 3, no. 1, pp. 29–40, 2014.

[6] L. S. Costa, G. P. Fidelis, S. L. Cordeiro et al., "Biological activities of sulfated polysaccharides from tropical seaweeds," *Biomedicine & Pharmacotherapy*, vol. 64, no. 1, pp. 21–28, 2010.

[7] F. B. Presa, M. L. M. Marques, R. L. S. Viana, L. T. D. B. Nobre, L. S. Costa, and H. A. O. Rocha, "The protective role of sulfated polysaccharides from green seaweed Udotea flabellum in cells exposed to oxidative damage," *Marine Drugs*, vol. 16, no. 4, p. 135, 2018.

[8] A. Neira-Carrillo, F. Luengo-Ponce, P. Vásquez-Quitral et al., "Sulfonated polymethylsiloxane as an additive for selective calcium oxalate crystallization," *European Journal of Inorganic Chemistry*, vol. 2015, no. 7, pp. 1167–1177, 2015.

[9] F. di Lorenzo, A. Silipo, A. Molinaro et al., "The polysaccharide and low molecular weight components of _Opuntia ficus indica_ cladodes: Structure and skin repairing properties," *Carbohydrate Polymers*, vol. 157, pp. 128–136, 2017.

[10] L. Sun, L. Wang, and Y. Zhou, "Immunomodulation and antitumor activities of different-molecular-weight polysaccharides from *Porphyridium cruentum*," *Carbohydrate Polymers*, vol. 87, no. 2, pp. 1206–1210, 2012.

[11] Y.-W. Zhao, L. Liu, C.-Y. Li, H. Zhang, X.-Y. Sun, and J.-M. Ouyang, "Preprotection of Tea Polysaccharides with Different Molecular Weights Can Reduce the Adhesion between Renal Epithelial Cells and Nano-Calcium Oxalate Crystals," *Oxidative Medicine and Cellular Longevity*, vol. 2020, Article ID 1817635, 13 pages, 2020.

[12] H. Liu, X. Y. Sun, F. X. Wang, and J. M. Ouyang, "Regulation on calcium oxalate crystallization and protection on HK-2 cells of tea polysaccharides with different molecular weights," *Oxidative Medicine and Cellular Longevity*, vol. 2020, Article ID 5057123, 14 pages, 2020.

[13] X. Y. Sun, H. Zhang, J. Liu, J. M. Ouyang, and J.-M. Ouyang, "Repair activity and crystal adhesion inhibition of polysaccharides with different molecular weights from red algaePorphyra

yezoensisagainst oxalate-induced oxidative damage in renal epithelial cells," *Food & Function*, vol. 10, no. 7, pp. 3851–3867, 2019.

[14] L. Qian, Y. Zhou, and J. X. Ma, "Hypolipidemic effect of the polysaccharides from _Porphyra yezoensis_," *International Journal of Biological Macromolecules*, vol. 68, pp. 48-49, 2014.

[15] L. Fu, Y. Qian, C. Wang, M. Xie, J. Huang, and Y. Wang, "Two polysaccharides from Porphyra modulate immune homeostasis by NF-κB-dependent immunocyte differentiation," *Food & Function*, vol. 10, no. 4, pp. 2083–2093, 2019.

[16] Y. Chen and Y. Xue, "Optimization of microwave assisted extraction, chemical characterization and antitumor activities of polysaccharides from Porphyra haitanensis," *Carbohydrate Polymers*, vol. 206, pp. 179–186, 2019.

[17] L. H. Huang, H. Liu, J. Y. Chen et al., "Seaweed Porphyra yezoensis polysaccharides with different molecular weights inhibit hydroxyapatite damage and osteoblast differentiation of A7R5 cells," *Food & Function*, vol. 11, no. 4, pp. 3393–3409, 2020.

[18] H. Zhang, X. Y. Sun, X. W. Chen, and J. M. Ouyang, "Degraded Porphyra yezoensis polysaccharide protects HK-2 cells and reduces nano-COM crystal toxicity, adhesion and endocytosis," *Journal of Materials Chemistry B*, vol. 8, no. 32, pp. 7233–7252, 2020.

[19] J. L. Owens, H. S. Cheung, and D. J. McCarty, "Endocytosis precedes dissolution of basic calcium phosphate crystals by murine macrophages," *Calcified Tissue International*, vol. 38, no. 3, pp. 170–174, 1986.

[20] C. Y. Rao, X. Y. Sun, and J. M. Ouyang, "Effects of physical properties of nano-sized hydroxyapatite crystals on cellular toxicity in renal epithelial cells," *Materials Science & Engineering. C, Materials for Biological Applications*, vol. 103, p. 109807, 2019.

[21] L. H. Huang, J. Han, J. M. Ouyang, and B. S. Gui, "Shape-dependent adhesion and endocytosis of hydroxyapatite nanoparticles on A7R5 aortic smooth muscle cells," *Journal of Cellular Physiology*, vol. 235, no. 1, pp. 465–479, 2019.

[22] S. Thamilselvan, S. R. Khan, and M. Menon, "Oxalate and calcium oxalate mediated free radical toxicity in renal epithelial cells: effect of antioxidants," *Urological Research*, vol. 31, no. 1, pp. 3–9, 2003.

[23] P. Bhadja, J. Lunagariya, and J.-M. Ouyang, "Seaweed sulphated polysaccharide as an inhibitor of calcium oxalate renal stone formation," *Journal of Functional Foods*, vol. 27, pp. 685–694, 2016.

[24] H. Turkez, M. I. Yousef, E. Sönmez et al., "Evaluation of cytotoxic, oxidative stress and genotoxic responses of hydroxyapatite nanoparticles on human blood cells," *Journal of Applied Toxicology*, vol. 34, no. 4, pp. 373–379, 2014.

[25] P. Nurse, "A long twentieth century of the cell cycle and beyond," *Cell*, vol. 100, no. 1, pp. 71–78, 2000.

[26] B. Qi, Q. Ji, Y. Wen et al., "Lycium barbarum polysaccharides protect human lens epithelial cells against oxidative stress-induced apoptosis and senescence," *PLoS One*, vol. 9, no. 10, article e110275, 2014.

[27] H. Ozturk, A. Cetinkaya, T. S. Firat, B. K. Tekce, S. E. Duzcu, and H. Ozturk, "Protective effect of pentoxifylline on oxidative renal cell injury associated with renal crystal formation in a hyperoxaluric rat model," *Urolithiasis*, vol. 47, no. 5, pp. 415–424, 2019.

[28] Y. W. Zhao, C. Y. L. Da Guo, C. Y. Li, and J. M. Ouyang, "Comparison of the adhesion of calcium oxalate monohydrate to HK-2 cells before and after repair using tea polysaccharides," *International Journal of Nanomedicine*, vol. Volume 14, pp. 4277–4292, 2019.

[29] A. P. Evan, F. L. Coe, S. R. Rittling et al., "Apatite plaque particles in inner medulla of kidneys of calcium oxalate stone formers: osteopontin localization," *Kidney International*, vol. 68, no. 1, pp. 145–154, 2005.

[30] B. Wang, G. He, G. Xu, J. M. Wen, and X. Yu, "miRNA-34a inhibits cell adhesion by targeting CD44 in human renal epithelial cells: implications for renal stone disease," *Urolithiasis*, vol. 48, pp. 109–116, 2019.

[31] J. C. Lieske, R. Norris, H. Swift, and F. G. Toback, "Adhesion, internalization and metabolism of calcium oxalate monohydrate crystals by renal epithelial cells," *Kidney International*, vol. 52, no. 5, pp. 1291–1301, 1997.

[32] S. Chaiyarit, N. Singhto, and V. Thongboonkerd, "Calcium oxalate monohydrate crystals internalized into renal tubular cells are degraded and dissolved by endolysosomes," *Chemico-Biological Interactions*, vol. 246, pp. 30–35, 2016.

[33] G. Jiao, G. Yu, J. Zhang, and H. S. Ewart, "Chemical structures and bioactivities of sulfated polysaccharides from marine algae," *Marine Drugs*, vol. 9, no. 2, pp. 196–223, 2011.

[34] R. E. Xing, S. Liu, Z. Y. Guo et al., "Relevance of molecular weight of chitosan and its derivatives and their antioxidant activities in vitro," *Bioorganic & Medicinal Chemistry*, vol. 13, no. 5, pp. 1573–1577, 2005.

[35] X. Zhao, C. H. Xue, Z. J. Li, Y. P. Cai, H. Y. Liu, and H. T. Qi, "Antioxidant and hepatoprotective activities of low molecular weight sulfated polysaccharide from Laminaria japonica," *Journal of Applied Phycology*, vol. 16, no. 2, pp. 111–115, 2004.

[36] J. H. Cheng, C. L. Tsai, Y. Y. Lien, M. S. Lee, and S. C. Sheu, "High molecular weight of polysaccharides from Hericium erinaceus against amyloid beta-induced neurotoxicity," *BMC Complementary and Alternative Medicine*, vol. 16, no. 1, p. 170, 2016.

[37] G. Chen, F. Bu, X. Chen, C. Li, S. Wang, and J. Kan, "Ultrasonic extraction, structural characterization, physicochemical properties and antioxidant activities of polysaccharides from bamboo shoots (Chimonobambusa quadrangularis) processing by-products," *International Journal of Biological Macromolecules*, vol. 112, pp. 656–666, 2018.

Review Article

Pleiotropic Effects of Eugenol: The Good, the Bad, and the Unknown

Oana M. Aburel [ID],[1,2] **Ioana Z. Pavel** [ID],[3,4] **Maria D. Dănilă** [ID],[1,2] **Theia Lelcu** [ID],[1,2] **Alexandra Roi** [ID],[5,6] **Rodica Lighezan** [ID],[7,8] **Danina M. Muntean** [ID],[1,2] and **Laura C. Rusu** [ID][5,6]

[1]*Department of Functional Sciences-Pathophysiology, Faculty of Medicine, "Victor Babes" University of Medicine and Pharmacy, Eftimie Murgu Sq. No. 2, 300041 Timișoara, Romania*
[2]*Center for Translational Research and Systems Medicine, Faculty of Medicine, "Victor Babeș" University of Medicine and Pharmacy, Eftimie Murgu Sq. No. 2, 300041 Timișoara, Romania*
[3]*Department II-Pharmacognosy, Faculty of Pharmacy, "Victor Babeș" University of Medicine and Pharmacy, Eftimie Murgu Sq. No. 2, 300041 Timișoara, Romania*
[4]*Pharmaco-Toxicological Evaluations Research Center, Faculty of Pharmacy, "Victor Babeș" University of Medicine and Pharmacy, Eftimie Murgu Sq. No. 2, 300041 Timișoara, Romania*
[5]*Department-Oral Pathology, Faculty of Dentistry, "Victor Babeș" University of Medicine and Pharmacy, Eftimie Murgu Sq. No. 2, 300041 Timișoara, Romania*
[6]*Multidisciplinary Center for Research, Evaluation, Diagnosis and Therapies in Oral Medicine, Faculty of Dentistry, "Victor Babeș" University of Medicine and Pharmacy, Eftimie Murgu Sq. No. 2, 300041 Timișoara, Romania*
[7]*Department of Infectious Diseases-Parasitology, Faculty of Medicine, "Victor Babes" University of Medicine and Pharmacy, Eftimie Murgu Sq. No. 2, 300041 Timișoara, Romania*
[8]*Center for Diagnostic and Study of Parasitic Diseases, Faculty of Medicine, "Victor Babeș" University of Medicine and Pharmacy, Eftimie Murgu Sq. No. 2, 300041 Timișoara, Romania*

Correspondence should be addressed to Rodica Lighezan; lighezan.rodica@umft.ro
and Danina M. Muntean; daninamuntean@umft.ro

Oana M. Aburel and Ioana Z. Pavel contributed equally to this work.

Received 31 July 2020; Revised 21 January 2021; Accepted 11 February 2021; Published 2 March 2021

Academic Editor: M rcio Carocho

Phytocompounds and medicinal herbs were used in traditional ancient medicine and are nowadays increasingly screened in both experimental and clinical settings due to their beneficial effects in several major pathologies. Similar to the drug industry, phytotherapy is interested in using nanobased delivery systems to view the identification and characterization of the cellular and molecular therapeutic targets of plant components. Eugenol, the major phenolic constituent of clove essential oil, is a particularly versatile phytochemical with a vast range of therapeutic properties, among which the anti-inflammatory, antioxidant, and anticarcinogenic effects have been systematically addressed. In the past decade, with the emerging understanding of the role of mitochondria as critical organelles in the pathophysiology of noncommunicable diseases, research regarding the role of phytochemicals as modulators of bioenergetics and metabolism is on a rise. Here, we present a brief overview of the major pharmacological properties of eugenol, with special emphasis on its applications in dental medicine, and provide preliminary data regarding its effects, alone, and included in polyurethane nanostructures, on mitochondrial bioenergetics, and glycolysis in human HaCaT keratinocytes.

1. Introduction

Eugenol (4-allyl-2-methoxyphenol) is the major volatile, biologically active component of clove oil, classically obtained from the dried flower buds of *Eugenia caryophyllata* Thunb. (Myrtaceae) [1]. This phytochemical has emerged from ancient times as a versatile molecule with a plethora of applications in drug, food and cosmetic industries, and agriculture [2]. In medicine, eugenol is best known for its original use in dentistry as cavity filling cement with local antiseptic and analgesic effects [3, 4]. However, the compound has been systematically investigated for numerous other pharmacological activities, such as anti-infective (antimicrobial, antihelmintic, antiviral, antifungal, antiparasitic, and insecticidal) [5, 6], anti-inflammatory, antioxidant [7, 8], and anticarcinogenic, when administered alone or in synergistic association with conventional therapies [9–11].

Modulation of multiple intracellular signaling pathways is the hallmark of most phytochemicals, and a tremendous amount of research is currently aimed at providing their thorough characterization. This is particularly true for their counteracting effects against oxidative stress and low-grade chronic inflammation, the major interconnected pathomechanisms of noncommunicable diseases (cardiometabolic, renal, liver pathologies, and cancer), and ageing [12]. Eugenol has elicited dose-dependent radical scavenging and anti-inflammatory activities in various *in vitro* experiments and animal models of chronic diseases [13], as well as antiproliferative and cytotoxic effects on several cancer cell lines and tumors [14, 15].

Phytochemicals present the advantages of low toxicity and high tolerability but there is an unmet need to both prevent their early metabolization and direct them towards the subcellular specific domains of action. Nowadays, an increasing amount of research is aimed at enhancing bioavailability and providing targeted delivery of natural compounds (recently reviewed in refs. [16, 17]). In the past decade, several natural product-based nanoformulations using polyurethane structures have been prepared, yielding promising results [18–23].

After oral administration in humans, eugenol is rapidly absorbed, metabolized, and almost completely excreted into urine as sulphate or glucuronide conjugates [24]. To overcome these disadvantages, a previous study reported the encapsulation of eugenol in polyurethane nanostructures with good thermal stability and encapsulation efficiency that can be further used for *in vitro* and *in vivo* testing [25].

Despite the fact that prolongation of the circulating lifetime and/or cellular entry may be facilitated by nanocarriers, the effects of these particles on various organelles require a thorough characterization. This is particularly true for mitochondria, organelles that are currently viewed as integrative hubs for energetics, redox control, and in/out signaling of almost all cells; indeed, it is mitochondrial dysfunction that triggers oxidative stress, potentiates inflammation in the setting of chronic pathologies [26], and influences all steps of oncogenesis, including cancer progression [27, 28].

The present paper is double-aimed (i) to provide a brief overview of eugenol pleiotropic cellular effects with a particular emphasis on its controversial role in dental medicine and (ii) to present preliminary data regarding the effects of eugenol, alone, and in polyurethane nanoformulations, on mitochondrial bioenergetics, and glycolysis in HaCaT human keratinocytes.

2. Overview of the Eugenol Use in Dental Medicine

Eugenol belongs to the phenol propanoid class ($C_{10}H_{12}O_2$) and is, probably, the compound with the longest history of use in dental medicine in association with other materials, the most popular being a zinc oxide-eugenol (ZOE) paste. ZOE is obtained by mixing the zinc oxide powder with the liquid eugenol resulting in a zinc eugenolate chelate matrix. Owing to advantages such as low cost, good sealing, and easy handling, ZOE formulations have been widely used since the beginning of the last century as temporary restorative or impression materials, cements, bases, and liners and have also been incorporated in various endodontic sealers [29–31].

After filling a dentinal cavity with ZOE temporary cements, low amounts of eugenol slowly diffuse through the dentin tubules and exert anti-inflammatory, immunemodulatory [32], antinociceptive effects on the dental pulp, and sensitive teeth [29, 33, 34] together with antibacterial and anticariogenic activities [35, 36]. The anti-inflammatory effect of eugenol has been widely reported by several studies, being ascribed to the following mechanisms: (i) inhibition of the synthesis of inflammatory mediators by interference with the arachidonic acid metabolism [37], particularly via the cyclooxygenase pathway (decreased prostaglandins and thromboxanes) and less via the lipooxygenase pathway (decreased leukotrienes) [38–40], (ii) inhibition of neutrophil chemotaxis and decreased superoxide generation [41], and (iii) reduction of pain via inhibition of the periapical/intradental nerve activity [42, 43]. More recently, the beneficial role of eugenol-based paste on preventing alveolar osteitis and promoting superior wound healing was reported in a study that included 270 patients having the third molars extracted [44].

At variance to their protective effects, ZOE-based materials were also reported to elicit local cytotoxicity, in particular pulpal chronic inflammation, degeneration, and even necrosis either when placed in direct contact with vital tissues or via diffusion across dentinal tubules. Among the presumed mechanisms, an increase in cell membrane permeability/injury (due to their lipophilicity), alteration of ionic homeostasis, oxidation by peroxidases (with subsequent formation of cytotoxic metabolites), and generation of reactive oxygen species (ROS) was mostly reported [42, 45].

There is a huge amount of research demonstrating the cytotoxicity of various ZOE cements on human primary/permanent cell lines and animal cell lines/models. Several conclusions can be drawn from these studies. First, the results of the cytotoxicity studies in animal-based cell models are different from the ones obtained in human cells, even for the same tested material. Thus, the Chinese hamster lung fibroblasts [46] or mouse fibroblasts [47, 48] are more sensitive to eugenol's toxic effects as compared to primary or immortalized human cell lines; accordingly, human cells

should be used for the clinical relevance of these studies. Second, all ZOE-based root canal sealers dissolve when exposed to an aqueous environment for extended periods and may cause mild to severe cytotoxic reactions [49] with the highest toxic effect being recorded for the freshly mixed material [50]; thus, the time-dependent evolution of cytotoxicity should be equally addressed. Third, all sealing materials will trigger periapical inflammation when present in the apical tissues; therefore, confining the filling to the root canal (i.e., avoiding overfilling) is critical for preventing/reducing chronic inflammation [51]. In this regard, Hong et al. deliberately overfilled root canals of monkey incisors with two ZOE-based sealers and reported mild to severe irritation of the periapical tissues that persisted over the 6-month period of experimental follow-up [52].

Last but not least, an important yet rather less addressed issue in the literature, is the dose titration. Jeng et al. investigated the dose-dependency of cytotoxicity and reported that eugenol was toxic to primary oral mucosal fibroblasts in high concentrations ($\geq$3 mmol/L), and cell death was associated with intracellular depletion of glutathione and ATP, respectively. At variance, a protective effect was described at lower concentrations (<1 mmol/L) presumably via the inhibition of xanthine oxidase activity and lipid peroxidation [53]. Comparable results with respect to total cell death were obtained when human diploid fibroblasts were incubated with high doses of eugenol (4 mM) [54]. Cytotoxicity of eugenol against normal human pulp fibroblasts was also demonstrated in terms of reduction of cell growth/survival and impairment of reparative processes, such as synthesis collagen and expression bone sialoprotein [55].

The group of Sagakami reported that eugenol elicited indiscriminate toxicity towards both normal human oral cells (cultured pulp cells, periodontal ligament fibroblasts, and gingival fibroblasts) and oral squamous cell carcinoma cell lines; specifically, eugenol induced rapid (after 4 h of incubation) nonapoptotic cell death with very low tumor specificity (IC 50 for normal cells was very close to the one for tumor cells) as compared to classic chemoterapeutic drugs [56]. These authors also reported a hormetic effect in cultured periodontal ligament fibroblasts (but interestingly, not in gingival fibroblasts) with an anti-inflammatory activity at lower doses that was lost when eugenol was applied in a higher dose [57]. Of note, a similar hormetic response (antioxidant at low doses, no effect, or prooxidant at high doses) was previously reported in the literature for another natural polyphenol, resveratrol [58].

Cytotoxic effects for ZOE and eugenol were reported not only for primary human oral cells but also towards immortalized human cells (dental pulp stem cells and oral keratinocytes), albeit in the latter case, zinc (and not eugenol) was considered to be responsible for most of the cytotoxicity [32, 56, 59]. Moreover, despite early ZOE toxicity, it was eugenol that downregulated the expression of the mRNA genes responsible for the synthesis of proinflammatory cytokines (IL-1, IL-6, and IL-8) in inflamed human dental pulp stem cells (but not in mouse bone marrow monocytes) [32].

A word of caution is in order in pediatric dentistry regarding eugenol genotoxicity. Escobar-Garcia et al.

reported DNA damage in human pulp fibroblasts from primary teeth, when eugenol was applied in the lowest concentrations (0.06–5.1 μM), an effect that, paradoxically, disappeared at higher concentrations (320 to 818 μM) [60]. More recently, the same group reported that eugenol in low concentration (13 μM) elicited an anti-inflammatory effect on cultured dental pulp fibroblasts exposed to lipopolysaccharide (LPS) that consisted in the inhibition of the gene expression of TNF-α (but not of IL-1β) and of the NF-κB signaling pathway; unexpectedly, a proinflammatory effect was found for eugenol in non-LPS-exposed fibroblasts (i.e., in the absence of the induced inflammation) [61]. In a recent elegant study, Jeanneau et al. confirmed the anti-inflammatory properties of eugenol when applied alone on LPS-stimulated human periodontal fibroblasts assessed by its ability to inhibit the secretion of proinflammatory cytokines, IL-6 and TNF-α; however, the effects were not recapitulated when a ZOE cement was used. Moreover, neither eugenol alone nor the cement-based eugenol could decrease monocyte adhesion and migration as compared to a hydrocortisone-based cement. The authors concluded that the hydrocortisone (but not eugenol)-containing root sealers are able to modulate the initial steps of inflammation [62].

In isolated cases, eugenol was demonstrated to act as a contact allergen capable to trigger allergic responses, most frequently, by delayed hypersensitivity reactions (contact stomatitis), and rarely by type I hypersensitivity reactions (contact urticaria or even anaphylactic shock) [63–66].

Other disadvantages of eugenol/ZOE were published, such as inhibition of the polymerization of methacrylate monomers and resins, low mechanical strength, and limited durability (degradation occurs through hydrolysis) that might cause secondary fractures and reduction of the bond strength of posts luted to root canals [59, 67–70].

However, there is no general consensus in the literature regarding the "ugly" side of eugenol. Accordingly, in the past decade, several groups reported that ZOE is a suitable base material for composite resin restoration that did not affect (or even positively impacted) the composite polymerization measured by their microhardness [29, 71] and the bond strength [72]. Moreover, recent systematic reviews were not able to show evidence for the superiority of one sealing material over another with respect to biocompatibility and fracture resistance of endodontically treated teeth; also, only moderate evidence for the lack of a reinforcing effect for ZOE-based sealers was reported [73, 74]. The beneficial vs. deleterious effects of eugenol and ZOE are summarized in Table 1.

At variance from the conflicting results regarding the indications and contraindications of eugenol in dental medicine, there is a relative consensus in the literature on its beneficial effects in the setting of inflammation and cancer in both cell lines and animal models, as briefly described in the following subchapters.

3. Protective Cellular Effects of Eugenol: A Bird's Eye View

The link between inflammation and cancer was firstly proposed by the visionary German pathologist and anthropologist

TABLE 1: The "good" vs. the "bad" side of eugenol and ZOE-based materials in dentistry.

Type of material	Type of study	Beneficial effects	Deleterious effects	Ref.
Eugenol	In vivo	(i) Anti-inflammatory properties (ii) Antinociceptive activity	—	[33]
Eugenol	In vitro	(i) Antimicrobial activity against the periodontal pathogens	—	[35]
Eugenol	In vitro	(i) Antibacterial activity against oral pathogens (ii) Cario-protective action (iii) Antifungal activity (iv) Cytotoxic action against several cancer cells (v) Antimutagenic action	—	[36]
Eugenol	In vitro	—	(i) Suppresses polymerization (ii) Reduces the mechanical properties of composite resins but to a distance of less than 100 nm	[29]
Eugenol	In vivo	(i) Promoted wound healing (ii) Anti-inflammatory action (iii) Analgesic action	—	[44]
Eugenol	In vitro	(i) No DNA strand break activity	(i) Cytotoxic effects to oral mucosal fibroblasts (ii) Decrease of cellular ATP level (iii) Inhibition of lipid peroxidation	[53]
Eugenol	In vitro	(i) Concentration-dependent effect on cellular growth	(i) Decreased cell survival (ii) Decreased collagen synthesis	[55]
Eugenol	In vitro	(i) Apoptosis of oral SCC cells line	(i) Low tumor-specificity	[56]
Eugenol	In vitro		(i) Toxic effects on dental pulp fibroblasts (even at very low concentrations)	[60]
Eugenol	In vivo		(i) Hypersensitivity response of oral mucosa (ii) Cytotoxic effects	[63]
Eugenol	In vitro		(i) Retardation of the resin dental materials polymerization	[67]
ZOE	In vitro	(i) Anti-inflammatory effect (ii) Immunomodulatory effects	(i) Decrease in cell viability (ii) Cytotoxic effect in high concentrations	[32]
ZOE	In vivo	(i) Anaesthetic action (ii) Inhibition of intradental nerve activity	—	[43]
ZOE	In vitro	(i) Good mechanical properties as a base under composite materials	—	[71]
ZOE	In vivo In vitro	(i) Anti-inflammatory effects (ii) Inhibition of synthesis of cyclooxygenase derivatives	—	[39]
ZOE	In vitro	—	(i) Increased cytotoxicity and apoptosis of human periodontal ligament fibroblasts	[46]
ZOE	In vitro	—	(i) High cytotoxicity for fibroblasts cell lines	[47]
ZOE	In vitro	—	(i) Cytotoxic activity (ii) Inhibition of the metabolic activity	[48]
ZOE	In vitro	—	(i) High cytotoxicity on human periodontal ligament cells and V79 cells	[49]
ZOE	In vitro	—	(i) Cytotoxic activity on human periodontal ligament fibroblasts and L929 cells	[50]
ZOE	In vitro	—	(i) Negative effects on microtensile bond strength of adhesives to dentin	[59]
ZOE (Endomethasone)	In vitro	—	(i) Decrease in bond strength to the root dentin	[68]
ZOE (Endomethasone)	In vivo	—	(i) Periapical inflammation with granulomatous reaction around the sealer particles	[51]

TABLE 1: Continued.

Type of material	Type of study	Beneficial effects	Deleterious effects	Ref.
ZOE + hydrocortisone (Endomethasone N)	*In vitro*	(i) Decreased cell migration and secretion of IL-6 and TNF-α by human periodontal ligament cells	—	[62]

Rudolf Virchow, and the importance of preventing and/or reversing inflammation for the cancer control is nowadays widely recognized [75]. Eugenol exerts protective anti-inflammatory, antioxidant, and anticarcinogenic effects, as shown by several studies described below and summarized in Table 2.

3.1. Anti-Inflammatory and Antioxidant Activities of Eugenol. Inflammation is the natural response of our body against a variety of aggressors (physical or chemical agents, pathogens, injured cells, immune complexes, etc.) that exerts protective effects in the acute phase and becomes deleterious in the chronic one.

Oxidative stress is classically defined as the overproduction of reactive oxygen species (ROS) and/or decreased antioxidant defense [8] and, together with inflammation, are responsible for extensive cellular damage in the vast majority of chronic noncommunicable pathologies, such as cardiovascular [76, 77], metabolic [78], renal [79], neurodegenerative [80] diseases, cancer [81], and ageing [12].

Important, a bidirectional relationship between inflammation and oxidative stress occurs in that inflammation that arises as a defense reaction in response to ROS-mediated local tissue injury may become a source of supplementary oxyradicals. Moreover, both conditions share as a common denominator the fact that in the long run they become the major systemic pathomechanisms of the abovementioned chronic diseases [82]. The major sources of ROS are mitochondria, the NADPH oxidases, xanthine oxidase, uncoupled eNOS, and, more recently, monoamine oxidases (MAOs) [83]. The antioxidant enzymes are mainly represented by superoxide dismutases, catalase, glutathione peroxidases, thioredoxin peroxidases, and heme oxygenase-1. Any impairment of the fragile equilibrium of pro- vs. antioxidant systems is responsible for the occurrence of oxidative stress [84] that may further trigger/potentiate the inflammatory reaction. The close link between the redox status and inflammation has been systematically documented by reports on aggravated inflammatory response when either the ROS-producing enzymes were overexpressed or the antioxidant enzymes were knocked-down (reviewed in ref. [77]).

Two excellent summative reviews on the anti-inflammatory/antioxidant activity of phenylpropanoids and eugenol, respectively, were recently published [7, 85]. While the former review mainly summarized the papers reporting a decrease in the expression of various inflammatory mediators (TNF-α, NF-κB, COX-2, IL-1?, IL-4, IL-5, IL-6, iNOS, and NO) in both *in vitro* and *in vivo* models and also, of those associated with an increase in the antioxidant enzymes (superoxide dismutase, glutathione peroxidase, catalase, and glutathione peroxidase) [7], the latter addressed the effects of eugenol on the arachidonic acid- (AA-) derived mediators

of inflammation. Thus, these authors reported the inhibitory effect of eugenol on prostaglandins and leukotrienes production and reduction in edema formation in several animal models of inflammation. Moreover, in human platelets, eugenol inhibited the AA and platelet-activating factor- (PAF-) induced aggregation. It has been also shown that eugenol and sodium eugenol acetate produced an inhibition in AA-induced thromboxane B_2 and PGE_2 formation in a concentration-dependent manner. A structurally similar compound, methyl-eugenol was evaluated in cerebral ischemic models and reported to increase superoxide dismutase and catalase activity, inhibit NO production, decrease the proinflammatory cytokines (TNF-α, IL-1β, and IL-6), and increase the anti-inflammatory ones (IL-10 and TGF-β), thus, indicating a potential role in the treatment of ischemia-related inflammatory diseases [85].

Leukocyte recruitment to tissue is of paramount importance in the inflammatory process. In this regard, eugenol was proven to mitigate leukocyte rolling, adhesion, and migration to the inflammatory site [86]. These results are supported by other studies performed on LPS-treated mice in which eugenol reduced lung infiltration with neutrophils/macrophages [87] and mitigated the release of inflammatory cytokines (TNF-α, IL-1β, and IL-6) [88] and the activation of NF-κB [87]. Moreover, in a murine model of ovalbumin-induced allergic asthma, eugenol inhibited eosinophil lung tissue infiltration and reduced the levels of both ovalbumin-specific IgE as well as IL-4 and IL-5, the key cytokines in allergic pathologies, thereby suppressing the generation of a Th2-type immune response [89].

Recently, oral administration of eugenol in rats fed a high-fat diet (1 month) was reported to significantly decrease both total serum cholesterol and LDL cholesterol. Moreover, it mitigated inflammation and steatosis in liver sections, decreased the activities of the hepatic enzymes alanine aminotransferase and alkaline phosphatase, and increased the ones of the antioxidant enzymes superoxide dismutase and catalase in hypercholesterolemic rats. These observations further support the pleiotropic effects of the compound and delineate new avenues for research in fatty liver disease therapy [90]. Also, the anti-inflammatory and antioxidant effects of eugenol in association with cinnamaldehyde on peripheral blood mononuclear cells (PBMCs) harvested from patients with rheumatoid arthritis have been reported [91].

In recent years, the inflammatory response has been also related to the occurrence of mitochondrial dysfunction. In particular, mitochondrial DNA but also cardiolipin and N-formyl peptides are released as a result of cellular stress/damage and have been reported to induce systemic inflammation [26]. In the presence of severe inflammation, mitochondrial dysfunction was described to be associated with cell death

TABLE 2: Overview of the anti-inflammatory, antioxidant, and anticarcinogenic effects of eugenol.

Eugenol properties	Parameters/tumor type	Biological effects	Ref.
Anti-inflammatory	Histological quantification of liver inflammatory foci/microscopic field	Decrease of the liver inflammatory cell infiltration	[90]
Anti-inflammatory	Cytokine levels	Decrease of the TNF-α and IL-6 level in the culture supernatant of RA-PBMCs	[91]
Anti-inflammatory	Mouse skin expression of COX-2 cytokine levels	Decrease of skin COX-2 expression and serum TNF-α, IL-6, and PGE2 level in TPA-treated mice	[95]
Anti-inflammatory	Leukocyte migration	Decrease of the number and adherence of leukocytes	[86]
Anti-inflammatory	Cytokine levels	Inhibition of lung infiltration with eosinophils decrease of IL-4 and IL-5 levels	[89]
Anti-inflammatory	Cytokine levels	Inhibition of TNF-α, IL-1β, and IL-6 release	[88]
Anti-inflammatory	Inflammatory cells cytokine level NF-κB activation	Inhibition of lung infiltration with neutrophils/macrophages; reduction of TNF-α release and of NF-κB activation	[76]
Anti-inflammatory	Inflammation-related gene expression (NF-κB, IL-1β, and TNF-α)	Inhibition of NF-κB and TNF-α gene expression	[61]
Antioxidant	Antioxidant enzyme (SOD and CAT) activity	Increase of serum SOD and CAT activity	[90]
Antioxidant	Intracellular ROS production and reduced glutathione level antioxidant enzyme (SOD, CAT, and GPx) activity	Decrease of ROS generation and increase of reduced glutathione level in RA-PBMC increase of SOD, CAT, and GPx activity in RA-PBMC culture	[91]
Antioxidant	Cutaneous glutathione level and glutathione reductase, CAT, and GPx activity	Increase of cutaneous glutathione level and glutathione reductase, CAT, and GPx activity in TPA-treated mice	[95]
Anticarcinogenic	MCF-7 human breast cancer cells	Inhibition of human breast cancer cell proliferation	[102]
Anticarcinogenic	Mouse skin cancer	Reduction in tumor size and incidence	[95]
Anticarcinogenic	Mouse skin cancer	Restriction of skin carcinogenesis at the dysplastic stage	[96]
Anticarcinogenic	Rat gastric cancer	Inhibition of gastric carcinoma development through NF-κB suppression	[99]
		Apoptosis stimulation through modulation of Bcl-2 proteins, Apaf-1, caspases, and cytochrome c inhibition of invasion and angiogenesis by MMP activity and VEGF and TIMP-2 expression modulation	[98]
Anticarcinogenic	HSC-2 human oral squamous cell carcinoma cell line	Nonapoptotic cell death through oxidative stress and reduction of ATP utilization	[108]
Anticarcinogenic	Human melanoma cells B16 xenograft mouse model	Tumor size reduction and delay in tumor growth; prevention of metastasis	[97]
Anticarcinogenic	Human breast cancer cells	Proliferation inhibition and apoptosis stimulation through down-regulation of survivin and the E2F1 transcription factor	[103]
Anticarcinogenic	A549 human lung adenocarcinoma cells	Inhibition of cell proliferation, migration, and invasion through modulation of MMP activity and the PI3K/Akt pathway	[100]
Anticarcinogenic	HCT-15 and HT-29 human colorectal adenocarcinoma cells	Apoptosis stimulation through the reduction of $\Delta\Psi$m with oxidative stress and DNA fragmentation	[106]
Anticarcinogenic	HL-60 human promyelocytic leukemia cells	Apoptosis stimulation through oxidative stress, MPT, and cytochrome c release, reduction of Bcl-2 level and DNA fragmentation	[107]

Table 2: Continued.

Eugenol properties	Parameters/tumor type	Biological effects	Ref.
Anticarcinogenic	Human KB oral squamous carcinoma cells and DU-145 androgen-insensitive prostate cancer cells	Cell growth inhibition and apoptosis stimulation	[104]
Anticarcinogenic	MDA-MB-231, MCF-7 (breast cancer lines), SIHA (cervix cancer lines), SK-Mel-28, and A2058 (melanoma lines)	Apoptosis stimulation through cell cycle deregulation and DNA damage, ROS overproduction, disruption of the cytoplasmic membrane, mitochondrial failure, PCNA downregulation	[105]

RA-PBMCs: PBMCs isolated from rheumatoid arthritis patients; TPA: 12-O-tetradecanoylphorbol-13-acetate; MAPK: mitogen-activated protein kinases; SOD: superoxide dismutase; CAT: catalase; GPx: glutathione peroxidase; PARP: polyadenosinediphosphate-ribose polymerase; MPT: mitochondrial permeability transition; PCNA: proliferation cell nuclear antigen; $\Delta\Psi m$: mitochondrial membrane potential.

via necrosis; conversely, in the setting of moderate inflammation, the intrinsic, mitochondrial-dependent apoptotic way of death will prevail. Interestingly, eugenol has been reported to induce early (less than 1 h exposure) mitochondrial collapse and vacuolization, followed by nonapoptotic cell death in human normal oral cells. Thus, at variance from the classic proapoptotic effect in cancer cells, eugenol might activate pyroptosis (inflammatory cell necrosis) or paraptosis (associated with mitochondria enlargement and cytoplasmic vacuolization) as cell death pathways in normal cells [92].

Therefore, targeting both chronic inflammation and oxidative stress (mainly, mitochondrial-derived) represent a promising therapeutic strategy in various pathologies. Both effects have also been described in relation to the anticarcinogenic effects of eugenol as detailed below.

3.2. Anticarcinogenic Activity of Eugenol. Phytochemicals are biologically active plant compounds with preventive and/or curative anticancer properties that display low toxicity and reduced side effects as compared to standard therapies. Assessing their beneficial effects as an adjunctive therapy in cancer currently represents one of the most active field of research [93]. Cancer treatment requires the inhibition of aberrant cell proliferation and destruction of malignant cells. In this respect, eugenol has been reported to elicit proapoptotic effects in several (but not all) tumor/cell lines.

Accordingly, a study performed in primary melanoma cell lines established from patients' tissues described an antiproliferative activity for the dimeric forms (biphenyls) of eugenol which was mild for dehydrodieugenol, higher for its O,O'-methylated form (O,O'-dimethyl-dehydrodieugenol), and markedly pronounced for the racemic mixture of the brominated biphenyl (6,6′-dibromo-dehydrodieugenol) (S7) [94].

In a murine model of skin cancer, Kaur et al. found that treatment with eugenol did not influence tumor development, but succeeded to decrease the tumor size [95]. The anticarcinogenic effect of eugenol was accompanied by antiinflammatory properties, as shown by the reduction of several inflammatory markers such as cyclooxygenase-2 (COX-2), nitric oxide synthase (iNOS), cytokine levels (IL-6), tumor necrosis factor-alpha (TNF-α), and prostaglandin E2 [95]. Moreover, in a mouse skin cancer model, eugenol displayed chemopreventive properties, reducing the incidence and size of skin tumors and improving animal survival

rates through apoptosis stimulation, cellular proliferation inhibition, and restriction of skin carcinogenesis at the dysplastic stage via c-Myc and H-ras oncogene downregulation and p53 tumor suppressor gene expression upregulation [96]. The tumor-suppressive effects of eugenol in skin cancers has been described to occur in relation to human melanoma and was associated with tumor size reduction, delay in tumor growth, and prevention of metastasis [97].

In a rat model of chemically-induced gastric cancer, treatment with eugenol decreased tumor incidence to 16.66%. Eugenol treatment triggered apoptosis via the mitochondrial pathway through the modulation of Bcl-2 proteins, apoptotic protease activating factor 1 (Apaf-1), caspases and cytochrome c, and limited angiogenesis by modifying the activity of the matrix metalloproteinases (MMP), vascular endothelial factor (VEGF), and tissue inhibitor of metalloproteinase-2 (TIMP-2) [98, 99]. Similarly, in a human lung adenocarcinoma cell line, reduction of the MMP-2 (along with phosphate-Akt) expression was demonstrated after eugenol administration, leading to inhibition of cell viability and impaired cell migration and invasion [100].

Moreover, in several human breast cancer cell lines, the epoxide forms of eugenol, lupeol, and lutein have been reported to induce apoptosis [101], while methyl-eugenol inhibited cancer cell proliferation [102]. These effects were recapitulated in the case of eugenol as well, via the downregulation of the breast cancer oncogene E2F1 and its antiapoptosis target survivin and upregulation of the cell cycle arrest-inducing protein p21^{WAF1}, respectively [103]. Indeed, the proapoptotic effect of eugenol was confirmed not only in the case of breast cancer but also in human oral squamous carcinoma cells [104] and human cervix cancer and melanoma lines, respectively [105]. Treatment with this compound led to cell cycle deregulation and DNA damage via cytoplasmic membrane disruption, ROS overproduction, mitochondrial membrane potential decrease, and the downregulation of proliferating cell nuclear antigen, an essential factor in DNA replication and repair [105]. Excessive ROS generation, dissipation of the mitochondrial membrane potential, and DNA fragmentation have also been reported by other studies as mechanisms of eugenol-induced apoptosis. Thus, in a human colorectal adenocarcinoma cell line, these effects were accompanied by p53 and caspase-3 activation [106], while in a human promyelocytic leukemia cell line, the reduction of the antiapoptotic Bcl-2 protein level

and the release of cytochrome c into the cytosol were recorded [107]. However, it must be noted that eugenol was reported to also induce nonapoptotic cell death through oxidative stress and reduction of ATP utilization in a human oral squamous cell carcinoma line [108].

The anticarcinogenic (chemopreventive-antioxidant and cytotoxic, prooxidant, and proapoptotic) effects of eugenol were the topic of a recent excellent review [109].

3.3. Modulation of Mitochondrial Metabolism by Eugenol. Mitochondrial dysfunction is currently accepted as the central pathomechanism of cancer. Therefore, targeting mitochondrial metabolic pathways has emerged as a valuable strategy to inhibit tumor growth. The mitochondria-targeted drugs or phytochemicals induce selectively disruption of cancerous mitochondria (and subsequent death of malignant cells) via several mechanisms, such as inhibition of respiratory function and ATP depletion, induction of the mitochondrial permeability transition, and, the previously mentioned, mitochondrial DNA damage [110].

Eugenol's effect on mitochondrial respiration can be traced back to the late 70s when Cotmore et al. firstly reported in isolated rat liver mitochondria a dose-dependent inhibition, particularly of the nicotinamide adenine dinucleotide- (NAD-) supported respiration (using glutamate as substrate) together with the uncoupling of the oxidative phosphorylation from the electron transport [111]. Several years later, Usta et al. provided further insights into the effects of the compound on mitochondrial function in the same *in vitro* model. In brief, these authors demonstrated that eugenol dose-dependently elicited the (i) inhibition of NADH oxidase (complex I of the electron transport system), (ii) reduction of mitochondrial membrane potential ($\Delta\Psi m$), and (iii) stimulation of the ATPase activity of F1F0-ATP-ase (complex V) with subsequent ATP depletion in rat liver mitochondria [112].

Eugenol is a weak lipophilic acid (i.e., it might permeate the mitochondrial membranes and release a H^+ into the matrix) and also an analogue of dinitrophenol (a classical mitochondrial uncoupler). Together with complex I inhibition, these properties might be responsible for the dissipation of the proton gradient across the inner membrane (normally used by the ATP synthase to generate ATP); subsequently, the enzyme will work in the reverse mode and become an energy-dissipating structure [113]. Of note, eugenol had no effect on succinate dehydrogenase (complex II of the electron transport system) activity in isolated rat mitochondria. More recently, the same group reported the chemosensitivity of a human breast cancer cell line MCF-7 to eugenol. The compound elicited a dose-dependent: (i) decrease in cellular viability and proliferation (EC_{50}: 0.9 mM), (ii) decrease in ATP level and mitochondrial membrane potential, (iii) increase in reactive oxygen species generation, (iv) release of cytochrome-c and lactate dehydrogenase, and (v) nonapoptotic Bcl-2 independent toxicity [114]. The last finding is in line with the results from the group of Sakagami, which confirmed the nonapoptotic cell death in three human normal oral cell types (gingival fibroblast, periodontal ligament fibroblast, and pulp cell) yet with no effect on ATP utilization (except for periodontal fibroblasts). Importantly, Sakagami

et al. also reported that eugenol (2 mM) elicited a rapid suppression (after 20 min incubation) of the tricarboxylic acids cycle in all three cell lines mentioned above, whereas the intracellular concentration of glycolytic metabolites slightly increased [92]. In an elegant study, Yan et al. further provided mechanistic insights into the signal transduction underlying the anticarcinogenic effect of eugenol in MCF10A human breast epithelial cells transfected with the H-ras oncogene (MCF10A-ras). These authors reported that eugenol (200 μM) suppressed cell growth and inhibited oxidative phosphorylation and fatty acids oxidation via the downregulation of the c-Myc/PGC-1β/ERRα pathway. Of note, the latter was upregulated in the breast cancer MCF10A-ras cells but not in the untransformed MCF10A cells [115].

In line with these observations, we aimed to investigate the effect of eugenol, free, or encapsulated in polyurethane nanoformulations [25], on both mitochondrial bioenergetics and glycolysis in SCC-4 human squamous cell carcinoma cells by means of the extracellular flux analyzer Seahorse XF24e (Agilent Technologies Inc.). This automatic platform provides a simultaneous measurement of oxygen consumption rate (OCR) as an indicator of mitochondrial respiration, and the extracellular acidification rate (ECAR) as an indirect measurement of anaerobic glycolysis, according to a previously described method [116]. In brief, cellular metabolic activity was challenged with the classic modulators of the mitochondrial electron transport chain: the first automatic injection was performed using oligomycin (1 μg/ml), the inhibitor of the mitochondrial ATP synthase; FCCP (3 μM), a classic uncoupler, was further injected, followed by antimycin A (5 μM), the inhibitor of mitochondrial complex III. OCR was reported in units of pmoles/min and ECAR in mpH/min. SCC-4 human squamous carcinoma cells were incubated for 24 h with eugenol (free or incorporated in polyurethane structures), and we found that free eugenol (50 μM) induced a decrease of OCR parameters (i.e., inhibition of mitochondrial respiration) coupled with an increase of ECAR (i.e., stimulation of glycolysis); surprisingly, opposite effects were recorded for eugenol nanoformulations, i.e., an increase in basal and maximal respiration (OCR) plus a decrease in glycolysis (ECAR) [116]. The effects of free eugenol are in line with the abovepresented literature data, yet the paradoxical effect of nanostructures requires further investigations.

We further recapitulated the experiments using the normal HaCaT human keratinocytes incubated with 50 μM free eugenol (EU), polyurethane particles alone (P), and EU encapsulated in polyurethane structures (EU + P) for 24, 48, and 72 h. First, the cytotoxic effect of the compounds on HaCaT cells was assessed at 24 h—Figure 1(a), 48 h—Figure 1(b), and 72 h—Figure 1(c), respectively. Cytotoxicity was evaluated by means of the MTT assay, as previously described [117]. HaCaT cells were seeded in 96-well culture plates (1×10^4 cells/well) and allowed to attach. Next, the medium was replaced and cells were incubated for 24, 48, and 72 h, respectively, with the tested compounds. Cells were randomized into 5 groups: control group—untreated cells (CTRL); DMSO group—cells treated with 50 μM DMSO used to prepare the free EU stock solution (DMSO); group treated with 50 μM free EU (EU); group treated with 50 μM

(a)

(b)

(c)
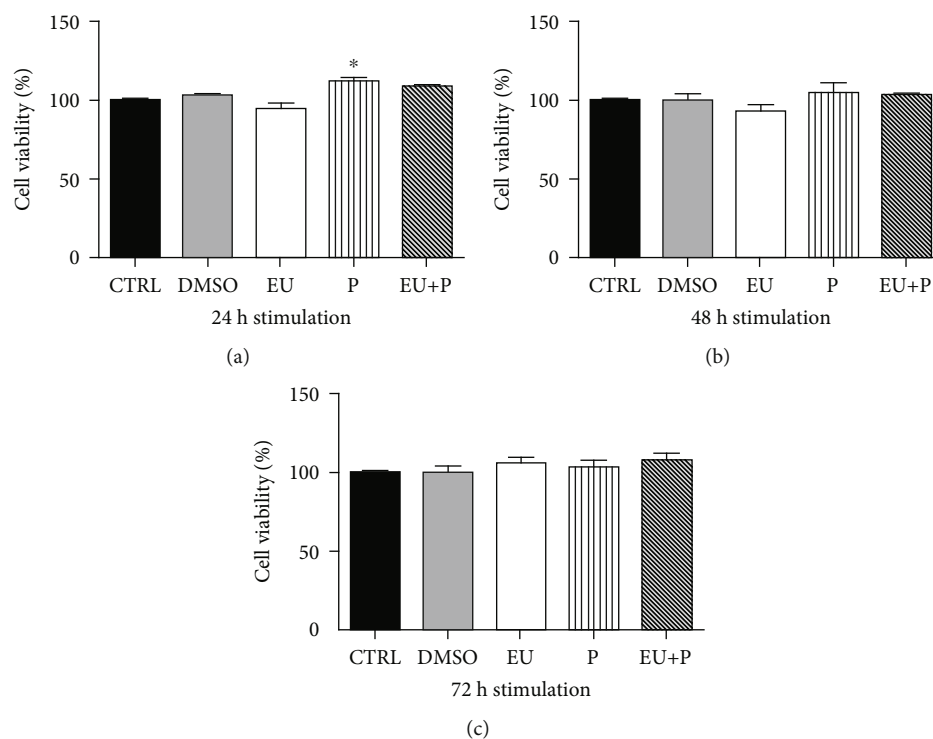
Figure 1: The time-dependency of HaCaT cell viability. (EU: free eugenol; P: polyurethane nanostructure alone; EU + P: eugenol included as nanoformulation). Data are presented as mean ± SD. Experiments were performed in triplicate ($^*p < 0.05$ vs. Ctrl).
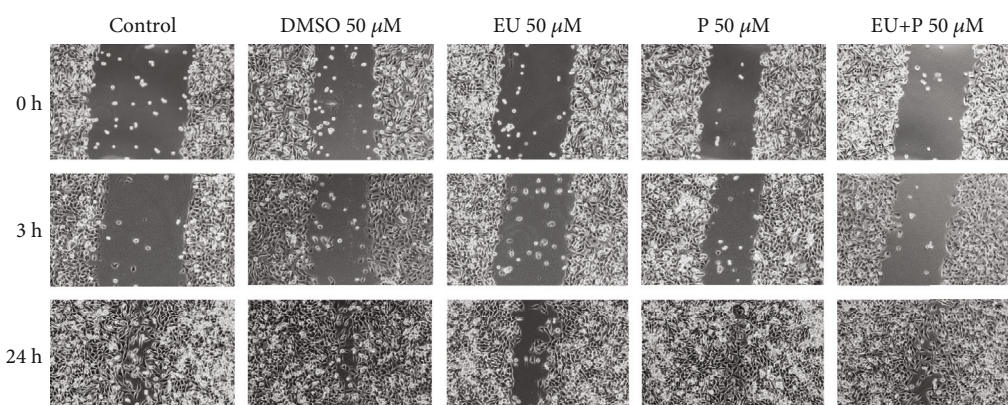
Figure 2: The effects of compounds ($50\,\mu$M) on HaCaT cell migration. (EU: free eugenol, P: polyurethane nanostructure alone, EU + P: eugenol included as nanoformulation). Pictures were taken at 0, 3, and 24 h poststimulation (10× magnification).

polyurethane structures which were used to encapsulate EU (P); and group treated with $50\,\mu$M encapsulated EU (EU + P). A volume of $10\,\mu$L of $5\,$mg/mL MTT solution from the MTT toxicology assay kit (Sigma-Aldrich) was added in each well. In the presence of NADPH-dependent cellular oxidoreductases, MTT precipitated as the insoluble formazan (during 4 h). The reduced MTT was measured spectrophotometrically at 570 nm, using a microplate reader (xMarkMicroplate Spectrophotometer, Bio-Rad). All experiments were performed in triplicate.

At 24 h poststimulation, EU elicited a discrete, nonsignificant cytotoxic effect, whereas the polyurethane structures (P, EU + P) provoked an unexpected mild increase in cell viability (Figure 1(a)). Similar results were obtained at 48 h of stim-

ulation (Figure 1(b)), while at 72 h, the EU group also showed a trend for an increase in cell viability vs. CTRL (Figure 1(c)).

We further evaluated the effect of the compound ($50\,\mu$M) on HaCaT cell migration using the scratch assay, as previously described [118]. To this aim, 2×10^5 cells/well were cultured in 12-well plates for 48 h prior to the experiment. Scratches were drawn in well-defined zones of the cells monolayer (at a confluence of 90%) using a sterile pipette tip. The detached cells were removed by washing with PBS before stimulation, and afterward, the cells were incubated with the compounds. Images of the cells were taken at the starting point of the experiment, and after 3 and 24 h, respectively, using the inverted microscope Olympus IX73 and the cellSense Dimension software. Figure 2 shows that P and EU
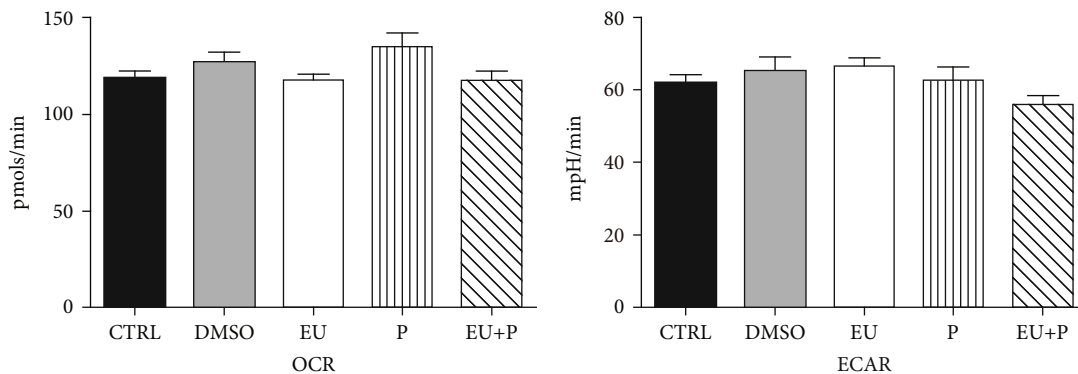
FIGURE 3: The effects of 24 h incubation of HaCaT cells on OCR and ECAR. Data are presented as mean ± SD. Experiments were performed in triplicate.
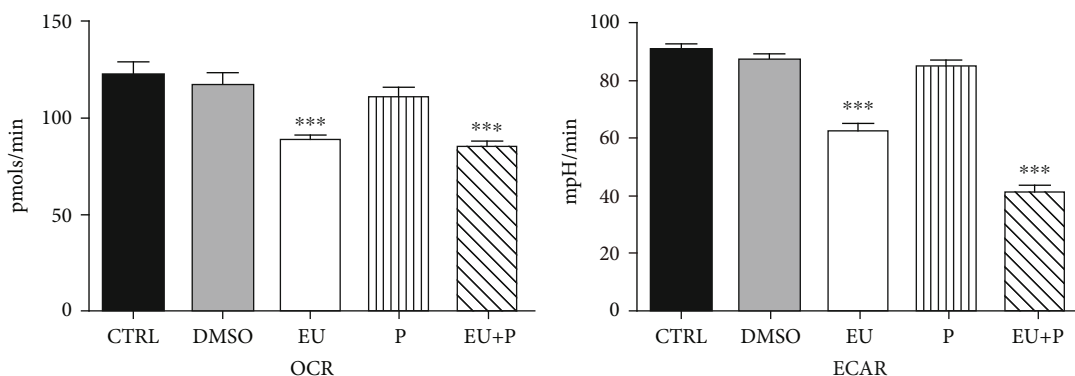
FIGURE 4: The effects of 48 h incubation of HaCaT cells on OCR and ECAR. Data are presented as mean ± SD. Experiments were performed in triplicate (***$p < 0.001$ vs. Ctrl).
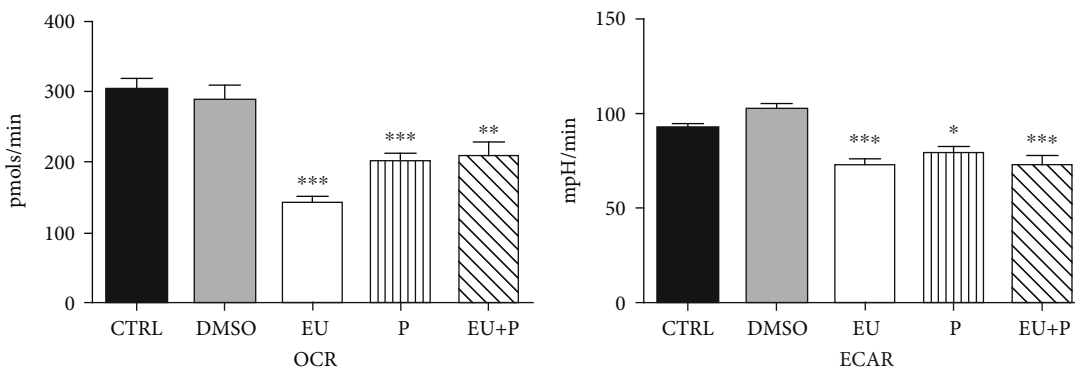
FIGURE 5: The effects of 72 h incubation of HaCaT cells on OCR and ECAR. Data are presented as mean ± SD. Experiments were performed in triplicate (*$p < 0.05$; **$p < 0.01$; ***$p < 0.001$ vs. Ctrl).

+ P groups exhibited a promigratory effect upon HaCaT cells at 24 h poststimulation vs. the control group. EU alone elicited at 24 h stimulation a mild reduction of cellular migration as compared to P/EU + P groups.

Finally, we evaluated the bioenergetic profile of HaCaT human keratinocytes treated with the compounds (50 μM) at 24 h—Figure 3, 48 h—Figure 4, and 72 h—Figure 5 using the Seahorse extracellular flux analyzer, as previously described.

No significant effect on OCR and ECAR was observed after 24 h of treatment (Figure 3). At variance, a significant metabolic inhibition was noticed for the two other periods of exposure (Figures 4 and 5). Thus, in the EU and EU + P groups, both OCR and ECAR significantly decreased at 48 h of incubation (Figure 4). Surprisingly, at 72 h, not only EU and EU + P but also P, the polyurethane particles *per se*, induced a significant inhibitory effect on both metabolic pathways, oxidative phosphorylation, and glycolysis (Figure 5).

The polyurethane nanostructures represent a safe formulation as previously reported [25], since they neither elicited a cytotoxic effect on HaCaT cells regardless of the incubation

period (Figures 1(a)–1(c), P group) nor interfered with their migration (Figure 2, P group). However, the nanoformulations significantly depressed the cellular metabolism at 72 h (Figure 5, P group).

4. Conclusions

Eugenol is a versatile molecule that has successfully survived the test of time in dental medicine. Nowadays, it has emerged as a promising phytochemical in the armamentarium of adjunctive anticancer therapeutics via the modulation of chronic inflammation, oxidative stress, and mitochondrial dysfunction, the major pathomechanisms of noncommunicable diseases. The current understanding of the signaling pathways responsible for eugenol interaction with cellular metabolism is far from being elucidated. Further studies aimed at characterizing its effects on bioenergetics and mitochondrial metabolism in both normal and malignant cell lines are fully warranted.

Conflicts of Interest

The authors declare no conflict of interest.

Authors' Contributions

Oana M. Abure and Ioana Z. Pavel contributed equally to this work.

Acknowledgments

References

[1] M. Raja, "Versatile and synergistic potential of eugenol: a review," *Pharmaceutica Analytica Acta*, vol. 6, no. 5, 2015.

[2] G. P. Kamatou, I. Vermaak, and A. M. Viljoen, "Eugenol–from the remote Maluku Islands to the international market place: a review of a remarkable and versatile molecule," *Molecules*, vol. 17, no. 6, pp. 6953–6981, 2012.

[3] R. S. Najjar, N. M. Alamoudi, A. A. El-Housseiny, A. A. Al Tuwirqi, and H. J. Sabbagh, "A comparison of calcium hydroxide/iodoform paste and zinc oxide eugenol as root filling materials for pulpectomy in primary teeth: a systematic review and meta-analysis," *Clinical and Experimental Dental Research*, vol. 5, no. 3, pp. 294–310, 2019.

[4] A. Brezhnev, P. Neelakantan, R. Tanaka, S. Brezhnev, G. Fokas, and J. P. Matinlinna, "Antibacterial additives in epoxy resin-based root canal sealers: a focused review," *Dentistry journal*, vol. 7, no. 3, p. 72, 2019.

[5] M. R. Pichika, K.-K. Mak, M. B. Kamal et al., "A comprehensive review on eugenol's antimicrobial properties and industry applications: a transformation from ethnomedicine to industry," *Pharmacognosy Reviews*, vol. 13, no. 25, pp. 1–9, 2019.

[6] A. Marchese, R. Barbieri, E. Coppo et al., "Antimicrobial activity of eugenol and essential oils containing eugenol: a mechanistic viewpoint," *Critical Reviews in Microbiology*, vol. 43, no. 6, pp. 668–689, 2017.

[7] J. N. Barboza, C. da Silva Maia Bezerra Filho, R. O. Silva, J. V. R. Medeiros, and D. P. de Sousa, "An overview on the anti-inflammatory potential and antioxidant profile of eugenol," *Oxidative Medicine and Cellular Longevity*, vol. 2018, Article ID 3957262, 9 pages, 2018.

[8] D. M. Muntean, A. Sturza, M. D. Danila, C. Borza, O. M. Duicu, and C. Mornos, "The role of mitochondrial reactive oxygen species in cardiovascular injury and protective strategies," *Oxidative Medicine and Cellular Longevity*, vol. 2016, Article ID 8254942, 2016.

[9] A. Hussain, K. Brahmbhatt, A. Priyani, M. Ahmed, T. A. Rizvi, and C. Sharma, "Eugenol enhances the chemotherapeutic potential of gemcitabine and induces anticarcinogenic and anti-inflammatory activity in human cervical cancer cells," *Cancer Biotherapy & Radiopharmaceuticals*, vol. 26, no. 5, pp. 519–527, 2011.

[10] M. L. Abdullah, M. M. Hafez, A. Al-Hoshani, and O. Al-Shabanah, "Anti-metastatic and anti-proliferative activity of eugenol against triple negative and HER2 positive breast cancer cells," *BMC complementary and alternative medicine*, vol. 18, no. 1, p. 321, 2018.

[11] S. S. Islam, I. Al-Sharif, A. Sultan, A. Al-Mazrou, A. Remmal, and A. Aboussekhra, "Eugenol potentiates cisplatin anticancer activity through inhibition of ALDH-positive breast cancer stem cells and the NF-κB signaling pathway," *Molecular Carcinogenesis*, vol. 57, no. 3, pp. 333–346, 2018.

[12] L. Zuo, E. R. Prather, M. Stetskiv et al., "Inflammaging and oxidative stress in human diseases: from molecular mechanisms to novel treatments," *International Journal of Molecular Sciences*, vol. 20, no. 18, p. 4472, 2019.

[13] S. Fujisawa and Y. Murakami, "Eugenol and its role in chronic diseases," *Advances in Experimental Medicine and Biology*, vol. 929, pp. 45–66, 2016.

[14] S. K. Jaganathan and E. Supriyanto, "Antiproliferative and molecular mechanism of eugenol-induced apoptosis in cancer cells," *Molecules*, vol. 17, no. 6, pp. 6290–6304, 2012.

[15] R. Pezzani, B. Salehi, S. Vitalini et al., "Synergistic effects of plant derivatives and conventional chemotherapeutic agents: an update on the cancer perspective," *Medicina*, vol. 55, no. 4, p. 110, 2019.

[16] L. Biasutto, A. Mattarei, M. La Spina et al., "Strategies to target bioactive molecules to subcellular compartments. Focus on natural compounds," *European Journal of Medicinal Chemistry*, vol. 181, p. 111557, 2019.

[17] J. K. Patra, G. Das, L. F. Fraceto et al., "Nano based drug delivery systems: recent developments and future prospects," *Journal of nanobiotechnology*, vol. 16, no. 1, p. 71, 2018.

[18] F. Borcan, A. Chirita-Emandi, N. I. Andreescu et al., "Synthesis and preliminary characterization of polyurethane nanoparticles with ginger extract as a possible cardiovascular

protector," *International Journal of Nanomedicine*, vol. 14, pp. 3691–3703, 2019.

[19] F. Borcan, M. Preda, L. C. Borcan et al., "Comparative characterization of birch bark extracts encapsulated inside polyurethane microstructures," *Materiale Plastice*, vol. 55, no. 3, pp. 385–388, 2018.

[20] F. Borcan, C. M. Soica, S. Ganta, M. M. Amiji, C. A. Dehelean, and M. F. Munteanu, "Synthesis and preliminary in vivo evaluations of polyurethane microstructures for transdermal drug delivery," *Chemistry Central Journal*, vol. 6, no. 1, p. 87, 2012.

[21] L. C. Borcan, Z. Dudas, A. Len, J. Fuzi, F. Borcan, and M. C. Tomescu, "Synthesis and characterization of a polyurethane carrier used for a prolonged transmembrane transfer of a chili pepper extract," *International Journal of Nanomedicine*, vol. 13, pp. 7155–7166, 2018.

[22] C. Danciu, F. Borcan, C. Soica et al., "Polyurethane microstructures–a good or bad in vitro partner for the isoflavone genistein?," *Natural Product Communications*, vol. 10, no. 6, pp. 951–954, 2015.

[23] A. Heghes, C. M. Soica, S. Ardelean et al., "Influence of emulsifiers on the characteristics of polyurethane structures used as drug carrier," *Chemistry Central Journal*, vol. 7, no. 1, p. 66, 2013.

[24] I. U. Fischer, G. E. von Unruh, and H. J. Dengler, "The metabolism of eugenol in man," *Xenobiotica*, vol. 20, no. 2, pp. 209–222, 2008.

[25] Z. Popa, L. Rusu, R. Susan et al., "Obtaining and characterization of a polyurethane carrier used for eugenol as a possible remedy in oral therapies," *Materiale Plastice*, vol. 55, no. 1, pp. 9–13, 2018.

[26] A. Picca, A. M. S. Lezza, C. Leeuwenburgh et al., "Fueling inflamm-aging through mitochondrial dysfunction: mechanisms and molecular targets," *International Journal of Molecular Sciences*, vol. 18, no. 5, p. 933, 2017.

[27] C. C. Hsu, L. M. Tseng, and H. C. Lee, "Role of mitochondrial dysfunction in cancer progression," *Experimental Biology and Medicine*, vol. 241, no. 12, pp. 1281–1295, 2016.

[28] P. E. Porporato, N. Filigheddu, J. M. B. Pedro, G. Kroemer, and L. Galluzzi, "Mitochondrial metabolism and cancer," *Cell Research*, vol. 28, no. 3, pp. 265–280, 2018.

[29] L. H. He, D. G. Purton, and M. V. Swain, "A suitable base material for composite resin restorations: zinc oxide eugenol," *Journal of Dentistry*, vol. 38, no. 4, pp. 290–295, 2010.

[30] T. Koch, A. Peutzfeldt, V. Malinovskii, S. Flury, R. Haner, and A. Lussi, "Temporary zinc oxide-eugenol cement: eugenol quantity in dentin and bond strength of resin composite," *European Journal of Oral Sciences*, vol. 121, no. 4, pp. 363–369, 2013.

[31] W. Qu, W. Bai, Y. H. Liang, and X. J. Gao, "Influence of warm vertical compaction technique on physical properties of root canal sealers," *Journal of Endodontics*, vol. 42, no. 12, pp. 1829–1833, 2016.

[32] J. H. Lee, H. H. Lee, H. W. Kim, J. W. Yu, K. N. Kim, and K. M. Kim, "Immunomodulatory/anti-inflammatory effect of ZOE-based dental materials," *Dental Materials*, vol. 33, no. 1, pp. e1–e12, 2017.

[33] A. N. Daniel, S. M. Sartoretto, G. Schmidt, S. M. Caparroz-Assef, C. A. Bersani-Amado, and R. K. N. Cuman, "Anti-inflammatory and antinociceptive activities A of eugenol

essential oil in experimental animal models," *Revista Brasileira de Farmacognosia*, vol. 19, no. 1b, pp. 212–217, 2009.

[34] M. R. Diaz and J. M. Sembrano, "A comparative study of the efficacy of garlic and eugenol as palliative agents against dental pain of pulpal origin," *The Journal of the Philippine Dental Association*, vol. 35, no. 1, pp. 3–10, 1985.

[35] L. Cai and C. D. Wu, "Compounds from Syzygium aromaticum possessing growth inhibitory activity against oral pathogens," *Journal of Natural Products*, vol. 59, no. 10, pp. 987–990, 1996.

[36] B. Kouidhi, T. Zmantar, and A. Bakhrouf, "Anticariogenic and cytotoxic activity of clove essential oil (Eugenia caryophyllata) against a large number of oral pathogens," *Annales de Microbiologie*, vol. 60, no. 4, pp. 599–604, 2010.

[37] D. Thompson and T. Eling, "Mechanism of inhibition of prostaglandin H synthase by eugenol and other phenolic peroxidase substrates," *Molecular Pharmacology*, vol. 36, no. 5, pp. 809–817, 1989.

[38] F. E. Dewhirst, "Structure-activity relationships for inhibition of prostaglandin cyclooxygenase by phenolic compounds," *Prostaglandins*, vol. 20, no. 2, pp. 209–222, 1980.

[39] S. Hashimoto, K. Uchiyama, M. Maeda, K. Ishitsuka, K. Furumoto, and Y. Nakamura, "In vivo and in vitro effects of zinc oxide-eugenol (ZOE) on biosynthesis of cyclooxygenase products in rat dental pulp," *Journal of Dental Research*, vol. 67, no. 8, pp. 1092–1096, 1988.

[40] K. C. Srivastava and U. Justesen, "Inhibition of platelet aggregation and reduced formation of thromboxane and lipoxygenase products in platelets by oil of cloves," *Prostaglandins, Leukotrienes, and Medicine*, vol. 29, no. 1, pp. 11–18, 1987.

[41] Y. Azuma, N. Ozasa, Y. Ueda, and N. Takagi, "Pharmacological studies on the anti-inflammatory action of phenolic compounds," *Journal of Dental Research*, vol. 65, no. 1, pp. 53–56, 1986.

[42] K. Markowitz, M. Moynihan, M. Liu, and S. Kim, "Biologic properties of eugenol and zinc oxide-eugenol: a clinically oriented review," *Oral Surgery, Oral Medicine, and Oral Pathology*, vol. 73, no. 6, pp. 729–737, 1992.

[43] H. Trowbridge, L. Edwall, and P. Panopoulos, "Effect of zinc oxide-eugenol and calcium hydroxide on intradental nerve activity," *Journal of Endodontics*, vol. 8, no. 9, pp. 403–406, 1982.

[44] J. S. Jesudasan, P. U. Wahab, and M. R. Sekhar, "Effectiveness of 0.2% chlorhexidine gel and a eugenol-based paste on post-operative alveolar osteitis in patients having third molars extracted: a randomised controlled clinical trial," *The British Journal of Oral & Maxillofacial Surgery*, vol. 53, no. 9, pp. 826–830, 2015.

[45] D. Thompson, K. Norbeck, L. I. Olsson, D. Constantin-Teodosiu, J. Van der Zee, and P. Moldeus, "Peroxidase-catalyzed oxidation of eugenol: formation of a cytotoxic metabolite(s)," *The Journal of Biological Chemistry*, vol. 264, no. 2, pp. 1016–1021, 1989.

[46] G. Szczurko, M. Pawinska, E. Luczaj-Cepowicz, A. Kierklo, G. Marczuk-Kolada, and A. Holownia, "Effect of root canal sealers on human periodontal ligament fibroblast viability: ex vivo study," *Odontology*, vol. 106, no. 3, pp. 245–256, 2018.

[47] J. S. Kwon, R. P. Illeperuma, J. Kim, K. M. Kim, and K. N. Kim, "Cytotoxicity evaluation of zinc oxide-eugenol and non-eugenol cements using different fibroblast cell lines,"

Acta Odontologica Scandinavica, vol. 72, no. 1, pp. 64–70, 2013.

[48] T. Schwarze, G. Leyhausen, and W. Geurtsen, "Long-term cytocompatibility of various endodontic sealers using a new root canal model," *Journal of Endodontics*, vol. 28, no. 11, pp. 749–753, 2002.

[49] F. M. Huang, K. W. Tai, M. Y. Chou, and Y. C. Chang, "Cytotoxicity of resin-, zinc oxide-eugenol-, and calcium hydroxide-based root canal sealers on human periodontal ligament cells and permanent V79 cells," *International Endodontic Journal*, vol. 35, no. 2, pp. 153–158, 2002.

[50] K. Araki, H. Suda, and L. S. Spangberg, "Indirect longitudinal cytotoxicity of root canal sealers on L929 cells and human periodontal ligament fibroblasts," *Journal of Endodontics*, vol. 20, no. 2, pp. 67–70, 1994.

[51] M. Bernath and J. Szabo, "Tissue reaction initiated by different sealers," *International Endodontic Journal*, vol. 36, no. 4, pp. 256–261, 2003.

[52] Y. C. Hong, J. T. Wang, C. Y. Hong, W. E. Brown, and L. C. Chow, "The periapical tissue reactions to a calcium phosphate cement in the teeth of monkeys," *Journal of Biomedical Materials Research*, vol. 25, no. 4, pp. 485–498, 1991.

[53] J. H. Jeng, L. J. Hahn, F. J. Lu, Y. J. Wang, and M. Y. Kuo, "Eugenol triggers different pathobiological effects on human oral mucosal fibroblasts," *Journal of Dental Research*, vol. 73, no. 5, pp. 1050–1055, 1994.

[54] L. Lindqvist and P. Otteskog, "Eugenol: liberation from dental materials and effect on human diploid fibroblast cells," *Scandinavian Journal of Dental Research*, vol. 88, no. 6, pp. 552–556, 1980.

[55] M. Anpo, K. Shirayama, and T. Tsutsui, "Cytotoxic effect of eugenol on the expression of molecular markers related to the osteogenic differentiation of human dental pulp cells," *Odontology*, vol. 99, no. 2, pp. 188–192, 2011.

[56] T. Koh, M. Machino, Y. Murakami, N. Umemura, and H. Sakagami, "Cytotoxicity of dental compounds towards human oral squamous cell carcinoma and normal oral cells," *In Vivo*, vol. 27, no. 1, pp. 85–95, 2013.

[57] T. Koh, Y. Murakami, S. Tanaka, M. Machino, and H. Sakagami, "Re-evaluation of anti-inflammatory potential of eugenol in IL-1β-stimulated gingival fibroblast and pulp cells," *In Vivo*, vol. 27, no. 2, pp. 269–273, 2013.

[58] G. Scapagnini, S. Davinelli, T. Kaneko et al., "Dose response biology of resveratrol in obesity," *Journal of Cell Communication and Signaling*, vol. 8, no. 4, pp. 385–391, 2014.

[59] K. T. Pinto, R. Stanislawczuk, A. D. Loguercio, R. H. M. Grande, and R. J. Baue, "Effect of exposure time of zinc oxide eugenol restoration on microtensile bond strength of adhesives to dentin," *Rev Port Estomatol Med Dent Cir Maxilofac*, vol. 55, pp. 83–88, 2014.

[60] M. Escobar-Garcia, K. Rodriguez-Contreras, S. Ruiz-Rodriguez, M. Pierdant-Perez, B. Cerda-Cristerna, and A. Pozos-Guillen, "Eugenol toxicity in human dental pulp fibroblasts of primary teeth," *The Journal of Clinical Pediatric Dentistry*, vol. 40, no. 4, pp. 312–318, 2016.

[61] A. Martinez-Herrera, A. Pozos-Guillen, S. Ruiz-Rodriguez, A. Garrocho-Rangel, A. Vertiz-Hernandez, and D. M. Escobar-Garcia, "Effect of 4-allyl-1-hydroxy-2-methoxybenzene (eugenol) on inflammatory and apoptosis processes in dental pulp fibroblasts," *Mediators of Inflammation*, vol. 2016, Article ID 9371403, 2016.

[62] C. Jeanneau, T. Giraud, J. L. Milan, and I. About, "Investigating unset endodontic sealers' eugenol and hydrocortisone roles in modulating the initial steps of inflammation," *Clinical Oral Investigations*, vol. 24, no. 2, pp. 639–647, 2020.

[63] N. Sarrami, M. N. Pemberton, M. H. Thornhill, and E. D. Theaker, "Adverse reactions associated with the use of eugenol in dentistry," *British Dental Journal*, vol. 193, no. 5, pp. 257–259, 2002.

[64] P. Tammannavar, C. Pushpalatha, S. Jain, and S. V. Sowmya, "An unexpected positive hypersensitive reaction to eugenol," *Case Reports*, vol. 2013, no. sep18 1, p. bcr2013009464, 2013.

[65] W. A. Wiltshire, M. R. Ferreira, and A. J. Ligthelm, "Allergies to dental materials," *Quintessence International*, vol. 27, no. 8, pp. 513–520, 1996.

[66] T. Bui, K. F. Mose, and F. Andersen, "Eugenol allergy mimicking burning mouth syndrome," *Contact Dermatitis*, vol. 80, no. 1, pp. 54-55, 2019.

[67] S. Fujisawa and Y. Kadoma, "Action of eugenol as a retarder against polymerization of methyl methacrylate by benzoyl peroxide," *Biomaterials*, vol. 18, no. 9, pp. 701–703, 1997.

[68] D. Cecchin, A. P. Farina, M. A. Souza, B. Carlini-Junior, and C. C. Ferraz, "Effect of root canal sealers on bond strength of fibreglass posts cemented with self-adhesive resin cements," *International Endodontic Journal*, vol. 44, no. 4, pp. 314–320, 2011.

[69] A. S. Altmann, V. C. Leitune, and F. M. Collares, "Influence of eugenol-based sealers on push-out bond strength of fiber post luted with resin cement: systematic review and meta-analysis," *Journal of Endodontics*, vol. 41, no. 9, pp. 1418–1423, 2015.

[70] P. Saxena, S. K. Gupta, and V. Newaskar, "Biocompatibility of root-end filling materials: recent update," *Restorative Dentistry & Endodontics*, vol. 38, no. 3, pp. 119–127, 2013.

[71] R. Itskovich, I. Lewinstein, and U. Zilberman, "The influence of zinc oxide eugenol (ZOE) and glass ionomer (GI) base materials on the microhardness of various composite and GI restorative materials," *The Open Dentistry Journal*, vol. 8, no. 1, pp. 13–19, 2014.

[72] E. J. Souza-Junior, V. C. Bueno, C. T. Dias, and L. A. Paulillo, "Effect of endodontic sealer and resin luting strategies on pull-out bond strength of glass fiber posts to dentin," *Acta odontologica latinoamericana : AOL*, vol. 23, no. 3, pp. 216–221, 2010.

[73] D. A. Fonseca, A. B. Paula, C. M. Marto et al., "Biocompatibility of root canal sealers: a systematic review of in vitro and in vivo studies," *Materials*, vol. 12, no. 24, p. 4113, 2019.

[74] E. Uzunoglu-Ozyurek, S. Kucukkaya Eren, and S. Karahan, "Effect of root canal sealers on the fracture resistance of endodontically treated teeth: a systematic review of in vitro studies," *Clinical Oral Investigations*, vol. 22, no. 7, pp. 2475–2485, 2018.

[75] J. Todoric, L. Antonucci, and M. Karin, "Targeting inflammation in cancer prevention and therapy," *Cancer Prevention Research*, vol. 9, no. 12, pp. 895–905, 2016.

[76] R. D'Oria, R. Schipani, A. Leonardini et al., "The role of oxidative stress in cardiac disease: from physiological response to injury factor," *Oxidative Medicine and Cellular Longevity*, vol. 2020, Article ID 5732956, 29 pages, 2020.

[77] S. Steven, K. Frenis, M. Oelze et al., "Vascular inflammation and oxidative stress: major triggers for cardiovascular disease," *Oxidative Medicine and Cellular Longevity*, vol. 2019, Article ID 7092151, 26 pages, 2019.

[78] S. Le Lay, G. Simard, M. C. Martinez, and R. Andriantsitohaina, "Oxidative stress and metabolic pathologies: from an adipocentric point of view," *Oxidative Medicine and Cellular Longevity*, vol. 2014, Article ID 908539, 18 pages, 2014.

[79] J. Pedraza-Chaverri, L. G. Sanchez-Lozada, H. Osorio-Alonso, E. Tapia, and A. Scholze, "New pathogenic concepts and therapeutic approaches to oxidative stress in chronic kidney disease," *Oxidative Medicine and Cellular Longevity*, vol. 2016, Article ID 6043601, 21 pages, 2016.

[80] A. Singh, R. Kukreti, L. Saso, and S. Kukreti, "Oxidative stress: a key modulator in neurodegenerative diseases," *Molecules*, vol. 24, no. 8, p. 1583, 2019.

[81] S. Reuter, S. C. Gupta, M. M. Chaturvedi, and B. B. Aggarwal, "Oxidative stress, inflammation, and cancer: how are they linked?," *Free Radical Biology & Medicine*, vol. 49, no. 11, pp. 1603–1616, 2010.

[82] P. S. Tucker, A. T. Scanlan, and V. J. Dalbo, "Chronic kidney disease influences multiple systems: describing the relationship between oxidative stress, inflammation, kidney damage, and concomitant disease," *Oxidative Medicine and Cellular Longevity*, vol. 2015, Article ID 806358, 8 pages, 2015.

[83] A. Sturza, C. M. Popoiu, M. Ionica et al., "Monoamine oxidase-related vascular oxidative stress in diseases associated with inflammatory burden," *Oxidative Medicine and Cellular Longevity*, vol. 2019, Article ID 8954201, 8 pages, 2019.

[84] G. Savoiu-Balint, C. Borza, C. Cristescu et al., "Endogenous and exogenous antioxidant protection for endothelial dysfunction," *Rev Chim (Bucharest)*, vol. 62, no. 6, pp. 680–683, 2011.

[85] R. de Cássia da Silveira e Sá, L. Andrade, R. dos Reis Barreto de Oliveira, and D. de Sousa, "A review on anti-inflammatory activity of phenylpropanoids found in essential oils," *Molecules*, vol. 19, no. 2, pp. 1459–1480, 2014.

[86] C. F. Estevao-Silva, R. Kummer, F. C. Fachini-Queiroz, and R. Grespan, "Anethole and eugenol reduce in vitro and in vivo leukocyte migration induced by fMLP, LTB4, and carrageenan," *Journal of Natural Medicines*, vol. 68, no. 3, pp. 567–575, 2014.

[87] C. B. Magalhaes, D. R. Riva, L. J. DePaula et al., "In vivo anti-inflammatory action of eugenol on lipopolysaccharide-induced lung injury," *Journal of Applied Physiology*, vol. 108, no. 4, pp. 845–851, 2010.

[88] C. B. Magalhaes, N. V. Casquilho, M. N. Machado et al., "The anti-inflammatory and anti-oxidative actions of eugenol improve lipopolysaccharide-induced lung injury," *Respiratory Physiology & Neurobiology*, vol. 259, pp. 30–36, 2019.

[89] C. Pan and Z. Dong, "Antiasthmatic effects of Eugenol in a mouse model of allergic asthma by regulation of vitamin D3 upregulated protein 1/NF-κB pathway," *Inflammation*, vol. 38, no. 4, pp. 1385–1393, 2015.

[90] A. A. Harb, Y. K. Bustanji, I. M. Almasri, and S. S. Abdalla, "Eugenol reduces LDL cholesterol and hepatic steatosis in hypercholesterolemic rats by modulating TRPV1 receptor," *Scientific Reports*, vol. 9, no. 1, p. 14003, 2019.

[91] S. Mateen, M. T. Rehman, S. Shahzad et al., "Anti-oxidant and anti-inflammatory effects of cinnamaldehyde and eugenol on mononuclear cells of rheumatoid arthritis patients," *European Journal of Pharmacology*, vol. 852, pp. 14–24, 2019.

[92] H. Sakagami, M. Sugimoto, Y. Kanda et al., "Changes in metabolic profiles of human oral cells by benzylidene ascorbates and eugenol," *Medicines*, vol. 5, no. 4, p. 116, 2018.

[93] M. H. Farzaei, R. Bahramsoltani, and R. Rahimi, "Phytochemicals as adjunctive with conventional anticancer therapies," *Current Pharmaceutical Design*, vol. 22, no. 27, pp. 4201–4218, 2016.

[94] M. Pisano, G. Pagnan, M. Loi et al., "Antiproliferative and pro-apoptotic activity of eugenol-related biphenyls on malignant melanoma cells," *Molecular Cancer*, vol. 6, no. 1, pp. 8–8, 2007.

[95] G. Kaur, M. Athar, and M. S. Alam, "Eugenol precludes cutaneous chemical carcinogenesis in mouse by preventing oxidative stress and inflammation and by inducing apoptosis," *Molecular Carcinogenesis*, vol. 49, no. 3, pp. 290–301, 2010.

[96] D. Pal, S. Banerjee, S. Mukherjee, A. Roy, C. K. Panda, and S. Das, "Eugenol restricts DMBA croton oil induced skin carcinogenesis in mice: downregulation of c-Myc and H-ras, and activation of p53 dependent apoptotic pathway," *Journal of Dermatological Science*, vol. 59, no. 1, pp. 31–39, 2010.

[97] R. Ghosh, N. Nadiminty, J. E. Fitzpatrick, W. L. Alworth, T. J. Slaga, and A. P. Kumar, "Eugenol causes melanoma growth suppression through inhibition of E2F1 transcriptional activity∗," *Journal of Biological Chemistry*, vol. 280, no. 7, pp. 5812–5819, 2005.

[98] P. Manikandan, R. S. Murugan, R. V. Priyadarsini, G. Vinothini, and S. Nagini, "Eugenol induces apoptosis and inhibits invasion and angiogenesis in a rat model of gastric carcinogenesis induced by MNNG," *Life Sciences*, vol. 86, no. 25-26, pp. 936–941, 2010.

[99] P. Manikandan, G. Vinothini, R. Vidya Priyadarsini, D. Prathiba, and S. Nagini, "Eugenol inhibits cell proliferation via NF-κB suppression in a rat model of gastric carcinogenesis induced by MNNG," *Investigational New Drugs*, vol. 29, no. 1, pp. 110–117, 2011.

[100] L. Fangjun and Y. Zhijia, "Tumor suppressive roles of eugenol in human lung cancer cells," *Thoracic Cancer*, vol. 9, no. 1, pp. 25–29, 2018.

[101] M. Behbahani, "Evaluation of in vitro anticancer activity of Ocimum basilicum, Alhagi maurorum, Calendula officinalis and their parasite Cuscuta campestris," *PLoS ONE*, vol. 9, no. 12, p. e116049, 2014.

[102] J. P. Noudogbessi, M. Gary-Bobo, A. Adomou et al., "Comparative chemical study and cytotoxic activity of Uvariodendron angustifolium essential oils from Benin," *Natural Product Communications*, vol. 9, no. 2, pp. 261–264, 2014.

[103] I. Al-Sharif, A. Remmal, and A. Aboussekhra, "Eugenol triggers apoptosis in breast cancer cells through E2F1/survivin down-regulation," *BMC cancer*, vol. 13, no. 1, p. 600, 2013.

[104] A. Carrasco, C. Espinoza, V. Cardile et al., "Eugenol and its synthetic analogues inhibit cell growth of human cancer cells (part I)," *Journal of the Brazilian Chemical Society*, vol. 19, no. 3, pp. 543–548, 2008.

[105] P. L. de Sá Júnior, D. A. D. Câmara, A. S. Costa et al., "Apoptotic effect of eugenol envolves G2/M phase abrogation accompanied by mitochondrial damage and clastogenic effect on cancer cell _in vitro_," *Phytomedicine*, vol. 23, no. 7, pp. 725–735, 2016.

[106] S. K. Jaganathan, A. Mazumdar, D. Mondhe, and M. Mandal, "Apoptotic effect of eugenol in human colon cancer cell

lines," *Cell Biology International*, vol. 35, no. 6, pp. 607–615, 2011.

[107] C. B. Yoo, K. T. Han, K. S. Cho et al., "Eugenol isolated from the essential oil of _Eugenia caryophyllata_ induces a reactive oxygen species-mediated apoptosis in HL-60 human promyelocytic leukemia cells," *Cancer Letters*, vol. 225, no. 1, pp. 41–52, 2005.

[108] T. Koh, Y. Murakami, S. Tanaka et al., "Changes of metabolic profiles in an oral squamous cell carcinoma cell line induced by eugenol," *In Vivo*, vol. 27, no. 2, pp. 233–243, 2013.

[109] D. P. Bezerra, G. C. G. Militao, M. C. de Morais, and D. P. de Sousa, "The dual antioxidant/prooxidant effect of eugenol and its action in cancer development and treatment," *Nutrients*, vol. 9, no. 12, p. 1367, 2017.

[110] M. T. Jeena, S. Kim, S. Jin, and J. H. Ryu, "Recent progress in mitochondria-targeted drug and drug-free agents for cancer therapy," *Cancers*, vol. 12, no. 1, p. 4, 2020.

[111] J. M. Cotmore, A. Burke, N. H. Lee, and I. M. Shapiro, "Respiratory inhibition of isolated rat liver mitochondria by eugenol," *Archives of Oral Biology*, vol. 24, no. 8, pp. 565–568, 1979.

[112] J. Usta, S. Kreydiyyeh, K. Bajakian, and H. Nakkash-Chmaisse, "In vitro effect of eugenol and cinnamaldehyde on membrane potential and respiratory chain complexes in isolated rat liver mitochondria," *Food and Chemical Toxicology*, vol. 40, no. 7, pp. 935–940, 2002.

[113] G. Lippe, G. Coluccino, M. Zancani, W. Baratta, and P. Crusiz, "Mitochondrial F-ATP synthase and its transition into an energy-dissipating molecular machine," *Oxidative Medicine and Cellular Longevity*, vol. 2019, Article ID 8743257, 10 pages, 2019.

[114] R. al Wafai, W. el-Rabih, M. Katerji et al., "Chemosensitivity of MCF-7 cells to eugenol: release of cytochrome-c and lactate dehydrogenase," *Scientific Reports*, vol. 7, no. 1, p. ???, 2017.

[115] X. Yan, G. Zhang, F. Bie et al., "Eugenol inhibits oxidative phosphorylation and fatty acid oxidation via downregulation of c-Myc/PGC-1β/ERRα signaling pathway in MCF10A-ras cells," *Scientific reports*, vol. 7, no. 1, p. 12920, 2017.

[116] O. M. Duicu, I. Z. Pavel, F. Borcan et al., "Characterization of the eugenol effects on the bioenergetic profile of SCC-4 human squamous cell carcinoma cell line," *Rev Chim*, vol. 69, no. 9, pp. 2567–2570, 2018.

[117] M. Mioc, I. Z. Pavel, R. Ghiulai et al., "The cytotoxic effects of betulin-conjugated gold nanoparticles as stable formulations in normal and melanoma cells," *Frontiers in Pharmacology*, vol. 9, p. 429, 2018.

[118] D. E. Coricovac, E. A. Moacă, I. Pinzaru et al., "Biocompatible colloidal suspensions based on magnetic iron oxide nanoparticles: synthesis, Characterization and Toxicological Profile," *Frontiers in Pharmacology*, vol. 8, p. 154, 2017.

Research Article

Gymnema inodorum (Lour.) Decne. Extract Alleviates Oxidative Stress and Inflammatory Mediators Produced by RAW264.7 Macrophages

Benjawan Dunkhunthod,[1] Chutima Talabnin,[2] Mark Murphy,[3] Kanjana Thumanu,[4] Patcharawan Sittisart,[5] and Griangsak Eumkeb ✆[1]

[1]*School of Preclinical Sciences, Institute of Science, Suranaree University of Technology, Nakhon Ratchasima 30000, Thailand*
[2]*School of Chemistry, Institute of Science, Suranaree University of Technology, Nakhon Ratchasima 30000, Thailand*
[3]*School of Biomolecular Science, Liverpool John Moores University, Liverpool L3 3AF, UK*
[4]*Synchrotron Light Research Institute (Public Organization), Nakhon Ratchasima 30000, Thailand*
[5]*Division of Environmental Science, Faculty of Liberal Arts and Science, Sisaket Rajabhat University, Sisaket 33000, Thailand*

Correspondence should be addressed to Griangsak Eumkeb; griang@sut.ac.th

Gymnema inodorum (Lour.) Decne. (*G. inodorum*) is widely used in Northern Thai cuisine as local vegetables and commercial herb tea products. In the present study, *G. inodorum* extract (GIE) was evaluated for its antioxidant and anti-inflammatory effects in LPS plus IFN-γ-induced RAW264.7 cells. Major compounds in GIE were evaluated using GC-MS and found 16 volatile compounds presenting in the extract. GIE exhibited antioxidant activity by scavenging the intracellular reactive oxygen species (ROS) production and increasing superoxide dismutase 2 (SOD2) mRNA expression in LPS plus IFN-γ-induced RAW264.7 cells. GIE showed anti-inflammatory activity through suppressing nitric oxide (NO), proinflammatory cytokine production interleukin 6 (IL-6) and also downregulation of the expression of cyclooxygenase-2 (COX-2), inducible nitric oxide synthase (iNOS), and IL-6 mRNA levels in LPS plus IFN-γ-induced RAW264.7 cells. Mechanism studies showed that GIE suppressed the NF-κB p65 nuclear translocation and slightly decreased the phosphorylation of NF-κB p65 (p-NF-κB p65) protein. Our studies applied the synchrotron radiation-based FTIR microspectroscopy (SR-FTIR), supported by multivariate analysis, to identify the FTIR spectral changes based on macromolecule alterations occurring in RAW264.7 cells. SR-FTIR results demonstrated that the presence of LPS plus IFN-γ in RAW264.7 cells associated with the increase of amide I/amide II ratio (contributing to the alteration of secondary protein structure) and lipid content, whereas glycogen and other carbohydrate content were decreased. These findings lead us to believe that GIE may prevent oxidative damage by scavenging intracellular ROS production and activating the antioxidant gene, SOD2, expression. Therefore, it is possible that the antioxidant properties of GIE could modulate the inflammation process by regulating the ROS levels, which lead to the suppression of proinflammatory cytokines and genes. Therefore, GIE could be developed into a novel antioxidant and anti-inflammatory agent to treat and prevent diseases related to oxidative stress and inflammation.

1. Introduction

Inflammation is the immune system's response to harmful stimuli, such as infection and tissue injury [1]. Macrophages are a diverse group of white blood cells known for eliminating pathogens through phagocytosis. Macrophages play a central role in promoting inflammatory lesions, which cause pathological tissue damage in various inflammatory diseases [2]. It is well known that interferon-gamma (IFN-γ) or lipopolysaccharide (LPS) is sufficient to induce classically activated macrophages [3]. The nuclear factor kappa light chain enhancer of activated B cells (NF-κB) is an important

transcription factor playing crucial roles in the inflammatory response [4]. In response to inflammatory stimuli, the nuclear localization signal of cytosolic NF-κB into the nucleus binds to a consensus sequence in the promoters of target genes including proinflammatory cytokines, chemokines, adhesion proteins, and inducible enzymes (COX-2 and iNOS) [5]. Due to the response with the existence of cellular stimuli, activated macrophages produce high levels of proinflammatory cytokines, including IL-6, interleukin 1β (IL-1β), TNF-α, and prostaglandin (PGE$_2$) [6]. These cytokines are involved in the process of pathological pain. During inflammation, free radical molecules such as NO and reactive oxygen intermediates (ROI) are also generated by inflammatory cells. Free radicals are involved in an imbalance of the redox system and damaging cells and tissues [7]. The link between oxidative stress and inflammation has extensively been demonstrated that the mechanism by which continued oxidative stress can lead to chronic inflammation. This mechanism leads to various inflammatory diseases such as diabetes, cardiovascular diseases, cancer, degenerative diseases, ischemia, and anemia [8]. Currently, the available drug in treating inflammatory disorders is often not successful, lacking availability, high cost, and causes of undesirable side effects [9, 10]. Based on these, the necessity for exploring a better anti-inflammatory therapeutic agent is always in need.

Herbs' use as traditional medicine has a long history in treating various diseases, including inflammatory diseases. It is currently well known that many bioactive compounds derived from natural products play an essential role in a wide range of therapeutic effects [11]. The World Health Organization (WHO) recognizes the vital role of traditional medicines and continues to support the integration of conventional medicine into each country's health system [12].

G. inodorum is one of the local Thai vegetables belonging to the family Asclepiadaceae. It is found ubiquitously in Southeastern Asia, including Thailand, especially in the northern region. In Thailand, its local name is "Phak chin da" or "Phak chiang da." It has been known to have therapeutic effects in curing certain diseases, including diabetes mellitus, rheumatic arthritis, and gout. The literature survey reported that the leaves of G. inodorum had many phytochemical compounds such as phenolics, flavonoids, terpenoids, and glycoside [13, 14]. Moreover, its antioxidant, antiadipogenesis, antidiabetic, and hypoglycemic effects were also reported [14–16]. Therefore, the phytochemical constituents presented in G. inodorum may contribute to its biological activity. Numerous studies exhibited that the phytochemical compounds, especially flavonoids and phenolic content, had contributed to the redox-modulating properties of natural compounds, which had also been shown to modulate the inflammatory response virtually [15–17]. Along this line, it is possible that G. inodorum may exert a beneficial effect on alleviating intracellular ROS and inflammation. However, to the best of our knowledge, this plant's antioxidant and anti-inflammatory activities have not earlier been reported, especially for the research study in cell-based assays.

Fourier-transform infrared spectroscopy (FTIR) is an analytical technique widely applied for studying the vibrational fingerprint for organic compounds [17]. This tech-

nique was previously applied to study biomedical research to investigate biomolecule profiles (lipid, protein, nucleic acids, and carbohydrate) in various biological samples without the need for probe molecules [18–20]. Synchrotron light is exceptionally bright. When a synchrotron light (SR) source, FTIR spectroscopy, and microscopy are combined together, it is called "Synchrotron radiation-based FTIR microspectroscopy (SR-FTIR)." This technique takes advantage of synchrotron light brightness, making it possible to record high-quality spectra and explore the biochemical changes within biological samples' microstructures without destruction's inherent structures of its [21].

The present study is aimed at investigating the anti-inflammatory and the antioxidant effect of GIE on LPS plus IFN-γ-induced RAW264.7 cells. The SR-FTIR was applied to detect biomolecule changes in RAW264.7 cells induced by LPS plus IFN-γ and their response to GIE treatment.

2. Materials and Methods

2.1. Preparation of GIE. G. inodorum (dried leaves) was purchased from commercial products (Chiangda organic company garden, Chiangmai, Thailand). The voucher specimens were deposited at the botanical garden of Suranaree University of Technology (SUT) Herbarium and authenticated by Dr. Santi Wattatana, a lecturer and a plant biologist at the Institute of Science, SUT, Thailand. The plant extractions were conducted following the method of Tiamyom et al. [14]. Briefly, the dried powder of G. inodorum was soaked in 95% ethanol with a ratio of 1 : 3 (g : mL) at room temperature for 7 days. The pooled extract was filtered through Whatman No. 1 filter paper. The ethanolic extract was concentrated using a vacuum rotary evaporator at 50°C and lyophilized to obtain the powder of GIE. The crude extract was stored at -20°C till use in subsequent experiments. GIE was dissolved in dimethyl sulfoxide (DMSO) and diluted to 0.1% (v/v) in the cell culture medium.

2.2. Identification of Phytochemical Constituents of GIE Gas Chromatography-Mass Spectrometry (GC-MS) Analysis. GC-MS analysis of GIE was performed using a Bruker 450-GC/Bruker 320-MS equipped with Rtx-5MS fused silica capillary column (30 m length × 250 μm diameter × 0.25 μm film thickness). For GC-MS detection, an electron ionization system was operated in the electron impact mode with ionization energy of 70 eV. The injector temperature was maintained at 250°C, and the ion-source temperature was 200°C. The oven temperature was programmed from 110°C (2 min), with an increase of 10°C/min to 200°C (3 min), then 5°C/min to 280°C, ending with a 20 min isothermal at 280°C. The MS scan range was 45-500 atomic mass units (amu), and helium was used as the carrier gas with a flow rate of 1.0 mL/min. The chemical components were identified by matching their mass spectra with those recorded in the NIST mass spectral library 2008.

2.3. Ferric Reducing/Antioxidant Power (FRAP) Assay. The ferric reducing capacity of GIE was determined by using the colorimetric method as described by Rupasinghe et al. [22]. Briefly, 20 μL of each of the samples and 180 μL of

FRAP reagent (300 mM acetate buffer (pH 3.6), 10 mM 2, 4, 6-tripyridyl-s-triazine (TPTZ), and 20 mM $FeCl_3 \bullet 6H_2O$ solution) were mixed in a 96-well plate for 6 min. The absorbance was recorded at 595 nm using a microplate reader (Bio-Rad Laboratories, Inc., Hercules, CA, USA). The different concentrations of Trolox (Cat. No. 238813, Sigma-Aldrich, St. Louis, USA) and vitamin C (Cat. No. 95210, Fluka Chemie GmbH, Buchs, Switzerland) were used to develop the standard calibration curve. FRAP values were expressed as a milligram of Trolox equivalent antioxidant capacity (TREA) or vitamin C equivalent antioxidant capacity (VCEA) per gram of dry extract.

2.4. 2,2-Diphenyl-1-Picryl-Hydrazyl (DPPH) Radical-Scavenging Activity Assay. The ability of GIE to scavenge the DPPH radical was estimated according to the method of Yang et al. [23]. Briefly, an aliquot of 100 μL of the sample at different concentrations was added to 100 μL of 0.2 mM DPPH solution (Cat. No. D9132, Sigma-Aldrich, St. Louis, USA) in a 96-well plate. The reaction mixture was kept in the dark for 15 min, and the absorbance was measured at 517 nm using a microplate reader (Bio-Rad Laboratories, Inc., Hercules, CA, USA). The positive standards (Trolox and vitamin C) were prepared using the same procedure. A lesser absorbance rate demonstrated higher radical scavenging activity. The percentage inhibition of free radical was calculated using the following equation: %Inhibition = $[(A_{control} - A_{sample})/A_{control}] \times 100$. The sample concentration providing 50% inhibition (IC_{50}) was determined from a dose-response curve using linear regression analysis.

2.5. Cell Culture. The murine macrophage cell line RAW264.7 (CLS Cell Lines Service GmbH., Eppelheim, Germany) was cultured in RPMI-1640 medium (Cat. No. 1IVG1-31800022) supplemented with 10% heat-inactivated fetal bovine serum (FBS, Cat. No. 1IVG7-10270-106) and 100 U/mL penicillin-streptomycin (Cat. No. 1IVG7-15140-122) (GIBCO, Grand Island, NY, USA). Cells were maintained at 37°C in 95% humidified with 5% of the CO_2 atmosphere.

2.6. Measurement of Cell Proliferation by the 3-(4,5-Dimethylthiazol-2-yl)-2,5-Diphenyl-Tetrazolium Bromide (MTT) Assay. The effect of GIE on cell viability was evaluated by using a tetrazolium dye colorimetric assay as described by Tiamyom et al. [14] and Dunkhunthod et al. [24]. Briefly, RAW264.7 cells were seeded in a 96-well plate (2×10^4 cells/well) and cultured for 24 h. Cells were treated with different concentrations of GIE for 24 h. Following treatment, the culture medium was removed, the MTT solution (0.5 mg/mL) (Cat. No. M6494, Invitrogen, Carlsbad, CA, USA) was added and further incubated at 37°C for 4 h. Subsequently, 150 μL DMSO was added to dissolve formazan crystal formed by viable cells, and absorbance was measured at 540 nm with a microplate spectrophotometer (Bio-Rad Laboratories, Inc., Hercules, CA, USA).

2.7. Detection of Intracellular ROS by $2',7'$-Dichlorofluorescein-Diacetate (DCFH-DA) Assay. Relative changes of intracellular ROS in RAW264.7 cells were monitored using the fluorescent probe DCFH-DA (Cat. No.

D6883, Sigma-Aldrich, St. Louis, USA) as previously described by Sittisart and Chitsomboon [25]. Briefly, RAW264.7 cells were seeded onto a 96-well black plate at 2.0×10^4 cells/well and cultured for 24 h. After removing the medium, the cells were pretreated with GIE at the concentration of 50, 100, 200, or 300 μg/mL or a selective ROS scavenger, N-acetyl-cysteine 3 mM (NAC, Cat. No. A9165, Sigma-Aldrich, St. Louis, USA) for 3 h prior to exposing them to 1 μg/mL lipopolysaccharide (LPS) (LPS from *Escherichia coli* O111:B4, Cat. No. L2630, Sigma-Aldrich, St. Louis, USA) plus 10 ng/mL IFN-γ (Cat. No. 200-16, Shenandoah Biotechnology Inc., Warwick, PA, USA) for 24 h. After removing the medium and washing the cells with PBS twice, 20 μM DCFH-DA in Hank's Balanced Salt Solution (HBSS, Cat. No. TFS-CB-14175095, GIBCO, Grand Island, NY, USA) was then added, and the cells were incubated for 30 min at 37°C. The cells were washed twice with phosphate-buffered saline (PBS), and fluorescence intensity was measured using a Gemini EM fluorescence microplate reader (Molecular Devices, Sunnyvale, CA, USA) with an excitation wavelength of 485 nm and an emission wavelength of 535 nm. Data were expressed as the percentage of $2'$-$7'$-dichlorofluorescein (DCF) fluorescence intensity that was calculated according to the following formula: DCF fluorescence intensity (%) = (DCF fluorescence intensity$_{test group}$/DCF fluorescence intensity$_{control group}$) $\times 100$.

2.8. Cell Treatment. The RAW 264.7 cells (6×10^5 cells/well) were seeded in a 6-well plate and cultured for 24 h. The cells were pretreated with GIE at the concentration of 50, 100, 200, or 300 μg/mL or 1 μM dexamethasone (DEX, Cat. No. API-04, G Bioscience, St. Louis, MO, USA) or 300 μg/mL of vitamin E (Vit.E, Cat. No. 95240, Fluka Chemie GmbH, Buchs, Switzerland) for 3 h prior to exposing them to 1 μg/mL LPS plus 10 ng/mL IFN-γ for 24 h.

2.9. Observation of Morphological Changes by Hematoxylin Staining. The phenotype feature of RAW264.7 cells was observed by staining with hematoxylin solution described by Dunkhunthod et al. [24] and visualized under the inverted fluorescence microscope (Olympus Corporation, Shinjuku, TYO, Japan).

2.10. Determination of NO by Griess Reagents. After treatment, the culture supernatants were collected for analysis of NO using Griess reagents. The accumulation of nitrite in culture supernatants as an indicator of NO production by RAW264.7 cells was evaluated using Griess reagent (Cat. No. 109023, Merck KGaA, Darmstadt, Germany) as described by Sittisart and Chitsomboon [25]. The amount of nitrite in the samples was calculated using the linear sodium nitrite calibration curves at a concentration range of 2.5-100 μM.

2.11. Determination of Proinflammatory Cytokines (IL-6 and TNF-α) and Anti-inflammatory Cytokines (IL-10) by ELISA. After treatment, the supernatants containing antigens were collected. The levels of IL-6, TNF-α, and IL-10 were quantified by DuoSet® ELISA Kits (IL-6; Cat. No. DY406-05, TNF-α; Cat. No. DY410-05, and IL-10; Cat. No. DY417-05,

R & D systems Inc., Minneapolis, MN, USA) according to the manufacturer's instructions. The *optical density* of each well was measured at 450 nm with a microplate reader (Bio-Rad Laboratories, Inc., Hercules, CA, USA). The number of cytokines in the samples was calculated using standard cytokine linear calibration curves at indicated concentration ranges.

2.12. Detection of mRNA Expression by Quantitative Real-Time Polymerase Chain Reaction (qRT-PCR). To determine the level of mRNA expression of inflammatory genes (iNOS and COX-2) and antiantioxidant genes, including SOD2, glutathione S-transferase pi 1 (GSTP1), NAD(P)H quinone dehydrogenase 1 (NQO1), cysteine ligase catalytic subunit (GCLC), and glutamate-cysteine ligase regulatory subunit (GCLM) in RAW264.7 macrophage cells after treating with GIE. Total RNA was isolated using TRIzol reagent (Cat. No. 15-596-026, Invitrogen, Carlsbad, CA, USA), and 2 μg of total RNA was reverse transcribed to single-stranded cDNA using the SuperScript VILO cDNA Synthesis Kit (Cat. No. 11754-050, Invitrogen™, California, USA) at 42°C for 1 h. qPCR was performed in a LightCycler® 480 Real-Time PCR System (Roche Diagnostics, Mannheim, Germany) using SYBR green master mix. The PCR was performed in a final volume of 20 μL containing 1 μL of primer mixture (10 μM), 10 μL of 2X SYBR Green Master Mix (Cat. No. 04707516001, Roche Diagnostics, Mannheim, Germany), 5 μL of cDNA template (5 μg), and 4 μL of nuclease-free distilled water. Real-time PCR cycles included initial denaturation at 95°C for 5 min, 95°C for 10 s, annealing at 60°C for 20 s, and extension at 72°C for 30 s through 40 cycles. The specificity of each of the PCR products was confirmed by melting curve analysis. The fold change in mRNA expression was calculated by comparing the GAPDH normalized threshold cycle numbers (Ct) in the untreated- and GIE treated-LPS plus IFN-γ-induced cells compared to the uninduced cells using the $2^{-\Delta\Delta Ct}$ method. Triplicate wells were run for each experiment, and two independent experiments were performed. The primer sequences designed for qRT-PCR analysis are listed in Table 1.

2.13. Western Blotting Analysis. The expression of NF-κB p65 and p-NF-κB p65 in RAW264.7 macrophage cells after treating with GIE for 24 h was examined. After incubation, the cells were washed three times with PBS and placed in 150 μL of ice-cold lysis buffer (1 mL RIPA buffer supplemented with 2 mM phenylmethylsulfonyl fluoride (PMSF), 2 μM leupeptin, and 1 μM E-64) for 20 min. The disrupted cells were then transferred to microcentrifuge tubes and centrifuged at 14,000 g at 4°C for 30 min. The supernatant was collected, and the protein concentration of cell lysate was estimated by the Lowry method [26]. Thirty micrograms of cellular proteins were separated by sodium dodecyl sulfate-polyacrylamide gel electrophoresis (SDS-PAGE) using 10% polyacrylamide gels (125 volts, 120 min). The proteins in the gel were transferred onto a nitrocellulose membrane (Amersham, Pittsburgh, PA, USA) at 80 volts for 1 h. The membrane was blocked with 5% bovine serum albumin (BSA) in 0.1% Tween 20 in a PBS buffer (0.1% PBST) at room temperature for 1 h. The membranes were then incubated

with a 1 : 1,000 dilution of the mouse monoclonal anti-NF-κB p65 antibody (F-6, Cat. No. sc-8008), anti-p-NF-κB p65 (27.Ser 536, Cat. No. sc136548), and α-tubulin (B-7, Cat. No. sc-5286) (Santa Cruz Biotechnology, Inc., Dallas, TX, USA) at 4°C overnight. After extensive washing with 0.1% PBST, the membranes were incubated with a 1 : 5,000 dilution of the secondary antibody mouse IgGκ light chain binding protein conjugated to horseradish peroxidase (m-IgGκ BP-HRP, Cat. No. sc-516102, Santa Cruz Biotechnology, Inc., Dallas, TX, USA) at room temperature for 1 h. The membranes were washed three times for 5 min each time, with 0.1% PBST. The membranes were incubated for 3 min in SuperSignal™ West Pico Chemiluminescent Substrate (Cat. No. 34079, Thermo Scientific, Waltham, MA, USA) and exposed to film. The relative expression of NF-κB p65 and p-NF-κB p65 proteins was quantified densitometrical using the software image J. The α-tubulin was used as a housekeeping protein.

2.14. Immunofluorescence Staining. As a marker of NF-κB activation, the NF-κB p65 subunit's nuclear translocation was visualized in RAW264.7 cells by immunofluorescence microscopy. Cells were seeded at a density of 6×10^4 cells/well in an 8-well cell culture slide. After 24 h of incubation, cells were pretreated with 300 μg/mL GIE or 1 μM of DEX for 3 h. Then, cells were coincubated with 1 μg/mL LPS +10 ng/mL IFN-γ for another 24 h. After incubation, cells were fixed with 4% paraformaldehyde for 15 min and then permeabilized with 0.1%Triton-X100 for 10 min at room temperature. After washing with PBS, the samples were blocked in 0.1% PBST containing 4% BSA and then incubated overnight at 4°C with the mouse monoclonal anti-NF-κB p65 antibody (F-6, Cat. No. sc-8008, Santa Cruz Biotechnology, Inc., Dallas, TX, USA) diluted 1 : 200 in 0.1% PBST containing 1% BSA. After washing with 0.1% PBST, each reaction was followed by incubation for 1 h with anti-mouse conjugated to Alexa 488-conjugated goat anti-mouse IgG (Cat. No. ab150113, Abcam, Cambridge, UK) diluted 1 : 250 in 0.1% PBST containing 1% BSA. After washing with 0.1% PBST, the cells were incubated with 10 mg/mL Hoechst 33258 diluted 1 : 2000 in 0.1% PBST (Cat. No. H3569, Invitrogen, Waltham, MA, USA) for 10 min at room temperature and then washed with 0.1% PBST. Slides were mounted with Bio Mount HM mounting medium (Cat. No. 05-BMHM100, Bio-Optica Milano S.p.a., Milano, Italy). Images of the fixed RAW264.7 cells were taken with confocal microscopy (Nikon, Melville, NY, USA).

2.15. Detection of Biomolecule Changing by SR-FTIR Microspectroscopy. FTIR experiments were conducted using a spectroscopy facility at the Synchrotron Light Research Institute (Public Organization), Nakhon Ratchasima, Thailand. Sample preparation was performed, as previously described by Dunkhunthod et al. [24]. FTIR spectra were acquired in transmission mode with a Vertex 70 FTIR spectrometer coupled with an IR microscope Hyperion 2000 (Bruker Optics, Ettlingen, Germany), using synchrotron radiation as an IR source. The microscope was equipped with a 64×64 element MCT, FPA detector, which allowed

TABLE 1: Oligomeric nucleotide primer sequence of qRT-PCR.

Gene	Forward primer (5$'$-3$'$)	Reverse primer (5$'$-3$'$)
iNOS	CAGCACAGGAAATGTTTCAGC	TAGCCAGCGTACCGGATGA
COX-2	TTTGGTCTGGTGCCTGGTC	CTGCTGGTTTGGAATAGTTGCTC
IL-6	CTGCAAGAGACTTCCATCCAG	AGTGGTATAGACAGGTCTGTTGG
TNF-α	CAGGCGGTGCCTATGTCTC	CGATCACCCCGAAGTTCAGTAG
SOD2	TTAACGCGCAGATCATGCA	GGTGGCGTTGAGATTGTTCA
GSTP1	TGGGCATCTGAAGCCTTTTG	GATCTGGTCACCCACGATGAA
NQO1	TTCTGTGGCTTCCAGGTCTT	AGGCTGCTTGGAGCAAAATA
GCLC	GATGATGCCAACGAGTCTGA	GACAGCGGAATGAGGAAGTC
GCLM	CTGACATTGAAGCCCAGGAT	GTTCCAGACAACAGCAGGTC
GAPDH	AACGACCCCTTCATTGAC	TCCACGACATACTCAGCAC

simultaneous spectral data acquisition with a 36× objective. The measurements were performed using an aperture size of 10 μm × 10 μm with a spectral resolution of 4 cm^{-1}, with 64 scans coadded. FTIR spectrum was recorded within a spectral range of 4000-600 cm^{-1} using OPUS software (Bruker Optics Ltd., Ettlingen, Germany).

Unsupervised explorative multivariate data analysis by Principal Component Analysis (PCA) was conducted using variables within a spectral range of 3,000-2,800 cm^{-1} and 1,800-950 cm^{-1}. Data manipulations were processed following the method of Tiamyom et al. [14] with slight modification. Briefly, the data were preprocessed by taking the second derivative using the Savitzky-Golay algorithm (with 15 points of smoothing), followed by normalization with extended multiplicative signal correction (EMSC) (Unscrambler® X software version 10.5, CAMO Software AS, Oslo, Norway). The outcome of the analysis could be presented as 2D score plots and loading plots. The integrated peak areas of the second derivative FTIR spectra were calculated using OPUS 7.2 software (Bruker Optics, Ettlingen, Germany) in the lipid regions (3000-2800 cm^{-1}), nucleic acids regions (1257-1204 cm^{-1} and 1125-1074 cm^{-1}), and glycogen and other carbohydrates regions (1181-1164 cm^{-1} and 1063-1032 cm^{-1}). The band area ratio of amide I to amide II was obtained by calculating the ratio of the amide I (1670-1627 cm^{-1}) area to the area under the amide II (1558-1505 cm^{-1}) regions.

2.16. Statistical Analysis. All data are expressed as the means ± S.D. from at least three independent experiments. The statistical significances (Statistical Package for the Social Sciences, version 19) were determined by performing a one-way analysis of variance (ANOVA). Tukey's test was used as a *post hoc* test. $p < 0.05$ was considered as statistically significant difference, which was indicated by the different superscript letters.

3. Results and Discussion

3.1. GC-MS Analysis of Volatile Oil Constituents of GIE. In this study, the phytochemical constituents of GIE were analyzed. GC-MS analysis in GIE reported about 16 compounds (as shown in Table 2). The major prevailing compounds were

linolenic acid (24.91%), n-Hexadecanoic acid (Palmitic acid) (16.98%), and Methylparaben (11.58%). Besides, it also presented the other chemical compounds, which are known to exhibit important pharmacological activity, in particular, anti-inflammatory and antioxidant activities such as phytol [27, 28], squalene [29], γ-tocopherol, dl-α-tocopherol [30, 31], and stigmasterol [32, 33].

Phytol, diterpene alcohol, has been reported to have remarkable anti-inflammatory activity by reducing carrageenan-induced paw edema and inhibiting the recruitment of total leukocytes and neutrophils, a decrease in IL-1β and TNF-α levels and oxidative stress [27]. Jeong [28] also reported that phytol suppressed H_2O_2-induced inflammation, as indicated by the reduced expression of the mRNA levels of TNF-α, IL-6, IL-8, and COX-2. Squalene, a natural lipid belonging to the terpenoid family, significantly inhibited the secretion of proinflammatory cytokines (TNF-α, IL-1β, IL-6, and IFN-γ), proinflammatory enzymes (iNOS, COX-2, and myeloperoxidase (MPO)), and enhanced expression levels of anti-inflammatory enzymes (heme oxygenase-1 (HO-1)) and transcription factors (Nrf2 and PPARγ) in overactivation of neutrophils, monocytes, and macrophages [29]. γ-Tocopherol and dl-α-tocopherol exhibited anti-inflammatory activity *in vitro* and *in vivo*, whereas the combination of γ- and α-tocopherols seems to be more potent than supplementation with α-tocopherols alone [30]. These results provide evidence that GIE is a source of antioxidants and anti-inflammatory agents, which could have beneficial effects on treating inflammation-related diseases. However, further studies are needed to clarify pharmacological properties.

3.2. Antioxidant Capacity of GIE. Antioxidants can act via several pathways. Therefore, to investigate the antioxidant activity of the GIE, we estimated their reducing antioxidant power and free radical scavenging by using the FRAP and DPPH radical scavenging assays, respectively. Trolox and vitamin C were used as standard antioxidant compounds. As shown in Table 3, GIE exhibited antioxidant activity due to its ability to reduce ferric ion (Fe^{3+}) to ferrous ion (Fe^{2+}) by 24.00 ± 0.69 μg VCEA/mg of dry extract and 28.06 ± 0.78 μg TREA/mg of dry extract. GIE at a concentration of 406.59 ± 0.11 μg/mL displayed the ability to scavenge DPPH

TABLE 2: GC-MS analysis of GIE.

No.	Peak name	Formula	Molecular weight (g/mol)	RT (min)	%Area
1	2,3-Dihydrobenzofuran	C_8H_8O	120.15	4.74	3.76
2	2-Methoxy-5-vinylphenol	$C_9H_{10}O_2$	150.17	5.89	1.42
3	Methylparaben	$C_8H_8O_3$	152.15	7.71	11.58
4	Tetradecanoic acid	$C_{14}H_{28}O_2$	228.37	11.09	2.86
5	n-Hexadecanoic acid	$C_{16}H_{32}O_2$	256.43	14.06	16.98
6	Phytol	$C_{20}H_{40}O$	128.17	16.73	5.96
7	Linolenic acid	$C_{18}H_{30}O_2$	278.43	17.42	24.91
8	Octadecanoic acid	$C_{18}H_{36}O_2$	284.48	17.70	2.04
9	Glycerol beta-palmitate	$C_{19}H_{38}O_4$	330.50	23.60	5.54
10	Beta-Monolinolein	$C_{21}H_{38}O_4$	354.52	26.36	6.31
11	9,12,15-Octadecatrienal	$C_{18}H_{30}O$	262.43	26.51	9.50
12	Squalene	$C_{30}H_{50}$	410.72	28.27	0.93
13	γ-Tocopherol	$C_{28}H_{48}O_2$	416.68	31.37	1.80
14	dl-α-Tocopherol	$C_{29}H_{50}O_2$	430.72	33.04	2.33
15	Stigmasterol	$C_{29}H_{48}O$	412.69	35.67	2.50
16	Olean-12-ene-3,28-diol, (3beta)-	$C_{30}H_{50}O_2$	442.73	46.98	1.57

TABLE 3: The FRAP and DPPH scavenging activities of GIE and standard compounds.

Sample	FRAP values (μg VCEA/mg of dry extract)	(μg TREA/mg of dry extract)	DPPH scavenging activity (IC$_{50}$) μg/mL
GIE	24.00 ± 0.69	28.06 ± 0.78	406.59 ± 0.11[c]
Vitamin C	—	—	44.57 ± 0.59[a]
Trolox	—	—	67.19 ± 4.82[b]

Values are mean ± S.D. ($n = 3$) and are representative of three independent experiments with similar results. One-way ANOVA performed the comparison, and Tukey was used as a *post hoc* test. The degree of significance was denoted with different letters for the comparison between sample groups. $p < 0.05$ was considered as statistically significant.

radical at 50% (IC$_{50}$). In contrast, the positive antioxidant controls, vitamin C, and Trolox exhibited the IC$_{50}$ values of approximately $44.57 \pm 0.59\,\mu$g/mL and $67.19 \pm 4.82\,\mu$g/mL, respectively.

Based on GC-MS analysis (Table 2), GIE contained many bioactive compounds such as phytol, squalene, γ-tocopherol, dl-α-tocopherol, and stigmasterol, which were reported to have antioxidant activity. Previous studies demonstrated that the phytochemical screening of GIE indicated the presence of phenolic, flavonoids, terpenoids, and glycoside [14, 15]. Numerous studies have shown that plant products' antioxidant capacity is related to their phenolic and flavonoid contents [34–36]. The synergistic effect of some substances present in GIE had been reported the antioxidant activity. Previous studies showed that the combination of squalene and α-tocopherol displayed a synergistic effect by reducing the rate of oxidation in a crocin bleaching assay where squalene might act as a competitive compound to α-tocopherol [37]. The sunflower seed oil containing total polyphenols and α-tocopherol had a positive K_a/K_c ratio of rate constants

for antioxidant and crocin value antioxidant activity. It is possible that the synergistic effect occurs between α-tocopherol and total polyphenols [38]. Besides, the presence of α-, β-, γ-tocopherol in sunflower seed oil may contribute to the oil resistance to oxidation [38, 39]. Therefore, the presence of squalene, α-tocopherol, γ-tocopherol, and phenolic in GIE may provide synergistic effects on antioxidant activity. However, it is also essential to further confirm whether the antioxidant activity of the combination of α-tocopherol plus squalene or other volatile compounds in GIE is synergistic. Moreover, the synergistic action of such compounds from plants had been calculated by the combination index (CI) [40–42].

3.3. Cytotoxic Effects of GIE on RAW264.7 Cells. The cytotoxicity of GIE was evaluated by MTT assay. The RAW264.7 cells were treated with various concentrations of the GIE, ranging from 100 to $500\,\mu$g/mL for 24 h. As shown in Figure 1(a), the results demonstrated that GIE at the concentration ranges of 100-400 μg/mL did not show a toxic effect on RAW264.7 cells ($p > 0.05$). At the highest tested concentration ($500\,\mu$g/mL), the number of living RAW264.7 cells decreased by up to 71.50% compared to the control group. Based on these results, the nontoxic concentration ranges of GIE (50, 100, 200, and 300 μg/mL) were selected for treating cells in further investigation.

3.4. GIE Attenuated the Intracellular ROS Generation and Increased SOD2 mRNA Expression in LPS plus IFN-γ-Induced RAW264.7 Cells. ROS generated by inflammatory cells also stimulates pathways that lead to the amplification of inflammation. ROS-induced kinase activation leads to the activation of transcription factors, which triggers the generation of proinflammatory cytokines and chemokine. Therefore, it is possible that the inflammation would be controlled by suppressing intracellular ROS production.
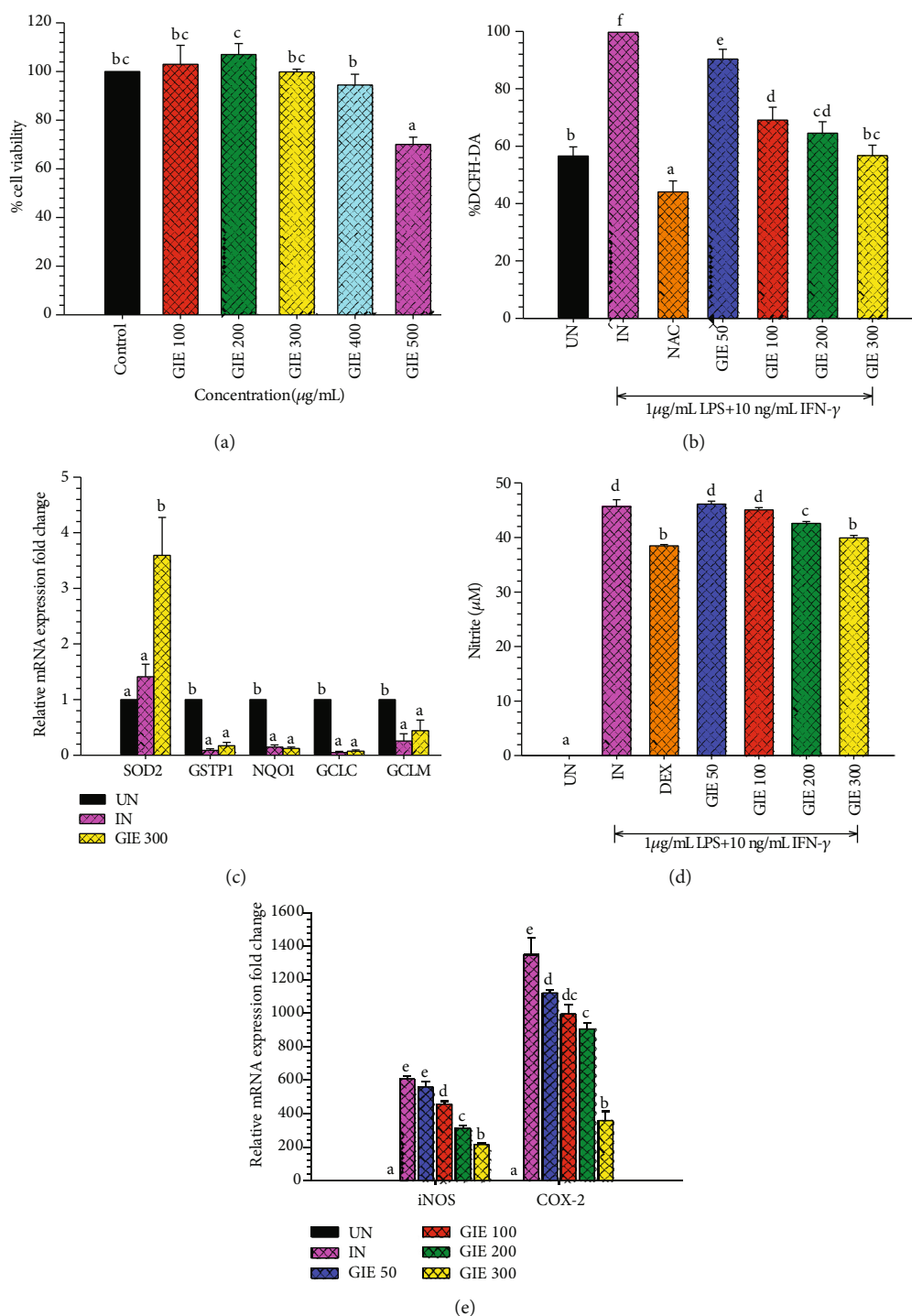
Figure 1: (a) Cytotoxic effects of GIE on RAW264.7 cells. Cells were treated with different concentrations of GIE (100-500 μg/mL) for 24 h. MTT assay was used to determine cell viability. Values are expressed as a percentage of the control. (b) GIE attenuated the intracellular ROS production in LPS plus IFN-γ-induced RAW264.7 cells. The intracellular ROS levels are expressed as a percentage of the control. (c) The effects of GIE on antioxidant mRNA expression in LPS plus IFN-γ-induced RAW264.7 cells. (d) GIE suppressed NO production in LPS plus IFN-γ-induced RAW264.7 cells. Nitrite concentration was determined from a sodium nitrite standard curve, and the results are expressed as a concentration (μM) of nitrite in a culture medium. (e) The effects of GIE on COX-2 and iNOS mRNA expression in LPS plus IFN-γ-induced RAW264.7 cells. The data represent the mean ± S.D. of two independent experiments. Cells were pretreated with GIE, NAC, or DEX for 3 h and then coincubated with LPS plus IFN-γ for 24 h. UN: uninduced cells; IN: untreated LPS plus IFN-γ-induced cells; NAC: cells were pretreated with NAC at 3 mM; DEX: cells were pretreated with DEX at 1 μM; GIE (50, 100, 200, and 300): cells were pretreated with GIE at concentrations range of 50, 100, 200, and 300 μg/mL, respectively. One-way ANOVA performed the comparison, and Tukey was used as a *post hoc* test. The degree of significance was denoted with different letters for the comparison between sample groups. $p < 0.05$ was considered as statistically significant.

Antioxidants are proved that help to protect cells and tissue from damage caused by free radical molecules [43]. According to FRAP and DPPH results, the possibility of GIE to scavenge intracellular ROS formation was further evaluated using the cell-base assay, DCFH-DA model. LPS and IFN-γ were chosen as an inflammatory inducing molecule, which can trigger the generation of a series of inflammatory mediators and reactive oxygen. NAC, as a nutritional supplement, was applied as the positive antioxidant control. The cells were pretreated with various concentrations of GIE (50, 100, 200, and 300 μg/mL) for 3 h and then coincubated with LPS plus IFN-γ for another 24 h. As shown in Figure 1(b), while LPS plus IFN-γ increased ROS formation in RAW264.7 cells (by 1.76-fold compared to uninduced cells), pretreated cells with GIE significantly reduced ROS generation in a concentration-dependent manner. Surprisingly, the highest concentration of GIE showed the efficacy of decreasing the intracellular ROS level to $56.72 \pm 3.62\%$, which was a similar level of the basal intracellular ROS production ($56.56 \pm 3.18\%$) in uninduced cells (UN). As expected, the positive antioxidant compound, NAC, possessed a potent free radical scavenging activity by decreasing the intracellular ROS level to $44.07 \pm 3.82\%$ compared to untreated LPS plus IFN-γ-induced cells. These results lead us to believe that GIE could inhibit ROS production by scavenging free radicals in cells, which is confirmed by the results of the FRAP and DPPH assay (Table 3). Our study was in agreement with other studies, which reported that *G. inodorum* displayed the antioxidant activity measuring by various *in vitro* antioxidant assays [13, 44]. However, this is the first report of the study, proving the antioxidant effect of this plant in the cell-based assay. Next, the inhibitory effect of GIE on oxidative stress was investigated by measuring antioxidant enzyme mRNA expression in RAW264.7 cells induced by LPS plus IFN-γ. Following stimulation of the cells by LPS plus IFN-γ, SOD2 mRNA expression exhibited a slight increase, along with a significant decrease in GSTP1, NQO1, GCLC, and GCLM mRNA expression (Figure 1(c)). Treatment by 300 μg/mL GIE achieved a statistically significant increase in SOD2 mRNA expression in LPS plus IFN-γ-induced cells ($p < 0.05$). However, with concentrations of 300 μg/mL, there was no statistically significant difference in the mRNA expression of GSTP1, NQO1, GCLC, and GCLM compared to LPS plus IFN-γ-induced cells (IN) ($p > 0.05$). These results provide evidence that GIE inhibited ROS production by upregulating the expression of SOD2 mRNA levels in LPS plus IFN-γ-induced RAW264.7 cells.

ROS is considered to be a causal factor in inflammatory responses. Higher levels of ROS can cause toxicity or act as signaling molecules. The cellular levels of ROS are controlled by low molecular mass antioxidants and antioxidant enzymes. SOD2 is one of the primary cellular antioxidant enzymes, which catalyze the dismutation of superoxide anion (O_2^-) to oxygen and hydrogen peroxide (H_2O_2) [45]. SOD2 was actively expressed via the NF-κB pathway during the progression of inflammatory conditions. The intracellular SOD2 has a protective role by suppressing the nucleotide-binding oligomerization domain, leucine-rich repeat, and pyrin domain-containing (NLRP) inflammasome-caspase-

1-IL-1β axis under inflammatory conditions [46]. Superoxide dismutase (SOD) also acts as an anti-inflammatory due to its inhibitory effects on the release of lipid peroxidation-derived prostaglandins, thromboxane, and leukotrienes [47]. Therefore, GIE elevated the levels of SOD2 can be an effective therapeutic strategy in oxidative stress and inflammation.

3.5. GIE Suppressed the Production of NO and Attenuated iNOS and COX-2 mRNA Expression in LPS plus IFN-γ-Induced RAW264.7 Cells. NO is a reactive nitrogen species (RNS), which also plays essential biology roles, similar to ROS. NO is synthesized by activating macrophages involved in an immune and inflammatory response. Inhibition of NO production was usually used as the necessary pharmacological treatment of inflammation-related diseases. Therefore, in this study, we investigated whether GIE could modulate NO production in LPS plus IFN-γ-induced RAW264.7 cells and measured for NO production using the Griess assay. The anti-inflammatory agent, dexamethasone (DEX), was used as the reference drug. As shown in Figure 1(d), the results showed that LPS plus IFN-γ induced significantly increased NO production ($p < 0.05$), reaching $45.68 \pm 1.26 \mu$M in untreated LPS plus IFN-γ-induced cells (IN). GIE reduced NO production in a dose-dependent manner. Moreover, the extract at concentrations of 200 and 300 μg/mL significantly suppressed NO production compared to untreated LPS plus IFN-γ-induced cells (IN) ($p < 0.05$). The highest concentration of GIE at 300 μg/mL exhibited the NO suppression (12.62% of NO inhibition), approximately the same efficiency as the reference drug, DEX (15.80% of NO inhibition).

In the inflammatory response, NO and PGE$_2$ are synthesized by iNOS and COX-2, respectively [48]. To confirm if the suppression of NO production by GIE was related to change in iNOS as well as COX-2 mRNA levels, qRT-PCR was performed. Figure 1(e) showed that iNOS and COX-2 mRNA expression was increased in LPS plus IFN-γ-induced cells (IN). At the same time, pretreated GIE significantly decreased the expression of iNOS and COX-2 mRNA levels in a concentration-dependent manner ($p < 0.05$). The present study indicates that the suppressive effect of GIE on NO production is mediated through the inhibition of iNOS mRNA expression. Therefore, iNOS reduction leads to the lower of PGE$_2$ and COX-2 expression in activated macrophages with LPS. There is no doubt that LPS and IFN-γ also efficiently enhance COX-2 expression in RAW264.7 cells [49]. Our results demonstrate that GIE can exhibit anti-inflammatory activity by attenuating COX-2 mRNA expression. Thus, GIE might play essential roles in ameliorating inflammation by suppressing NO production and downregulation of iNOS and COX-2 mRNA expression.

3.6. GIE Suppressed Proinflammatory Cytokines (IL-6 and TNF-α), Proinflammatory mRNA Expression, and Slightly Increased Anti-inflammatory Cytokines (IL-10) in LPS plus IFN-γ-Induced RAW264.7 Cells. Inflammation is mediated by cytokines released from immune cells in response to pathogens' molecular components, such as the LPS of gram-negative bacteria. TNF-α in inflammatory processes is an essential proinflammatory mediator, leading to other

(a)

(b)

(c)

(d)

(e)
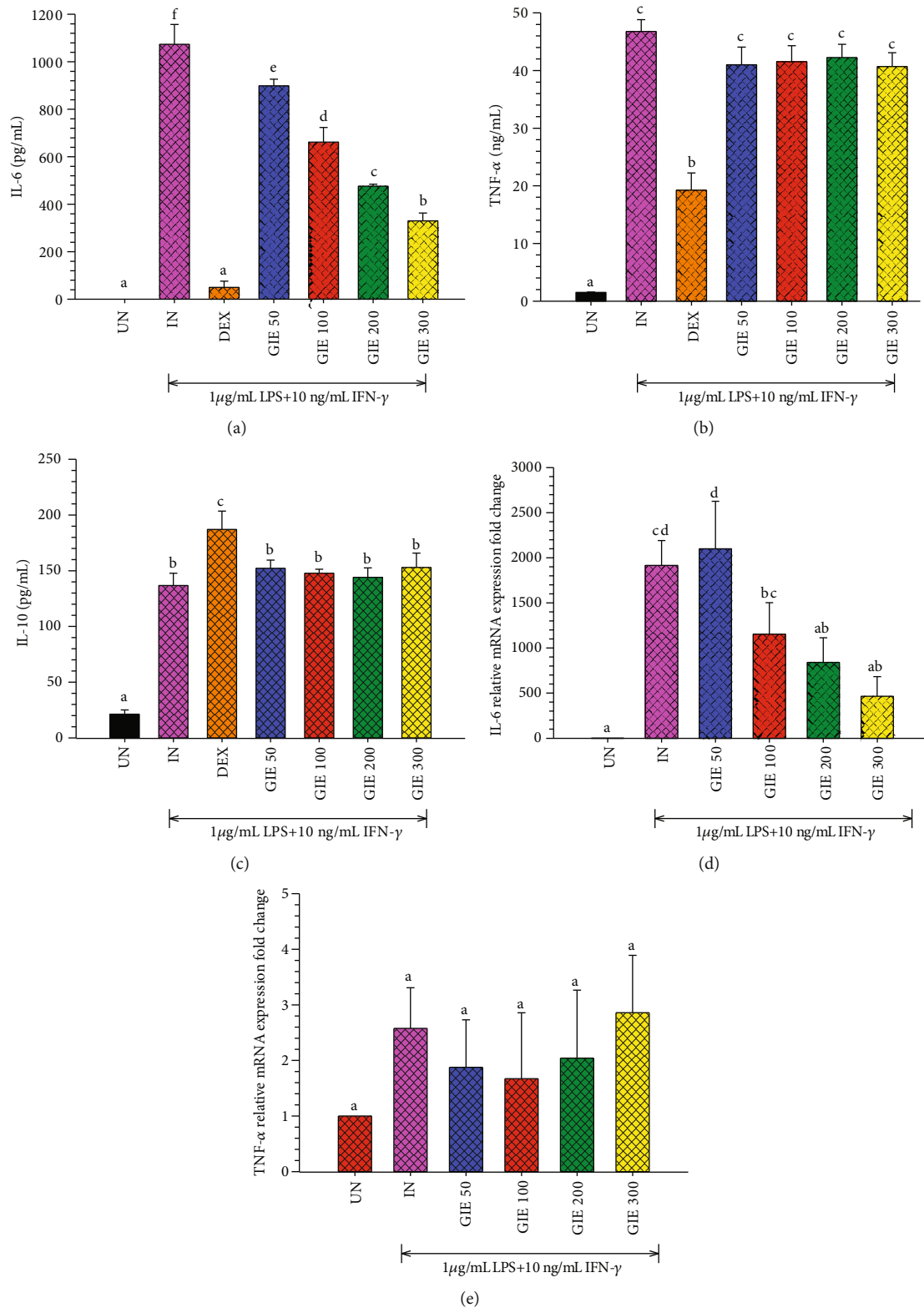
Figure 2: GIE suppressed the secretion of (a) proinflammatory cytokines IL-6, (b) TNF-α, and slightly increased (c) anti-inflammatory cytokines IL-10 secretion in LPS plus IFN-γ-induced RAW264.7 cells. The effects of GIE on (d) IL-6 and (e) TNF-α mRNA expression. Cells were pretreated with GIE or DEX for 3 h and then coincubated with LPS plus IFN-γ for 24 h. UN: uninduced cells; IN: untreated LPS plus IFN-γ-induced cells; DEX: cells were pretreated with DEX at 1 μM; GIE (50, 100, 200, and 300): cells were pretreated with GIE at concentrations range of 50, 100, 200, and 300 μg/mL, respectively. The data represent the mean ± S.D. of two independent experiments. One-way ANOVA performed the comparison, and Tukey was used as a *post hoc* test. The degree of significance was denoted with different letters for the comparison between sample groups. $p < 0.05$ was considered as statistically significant.
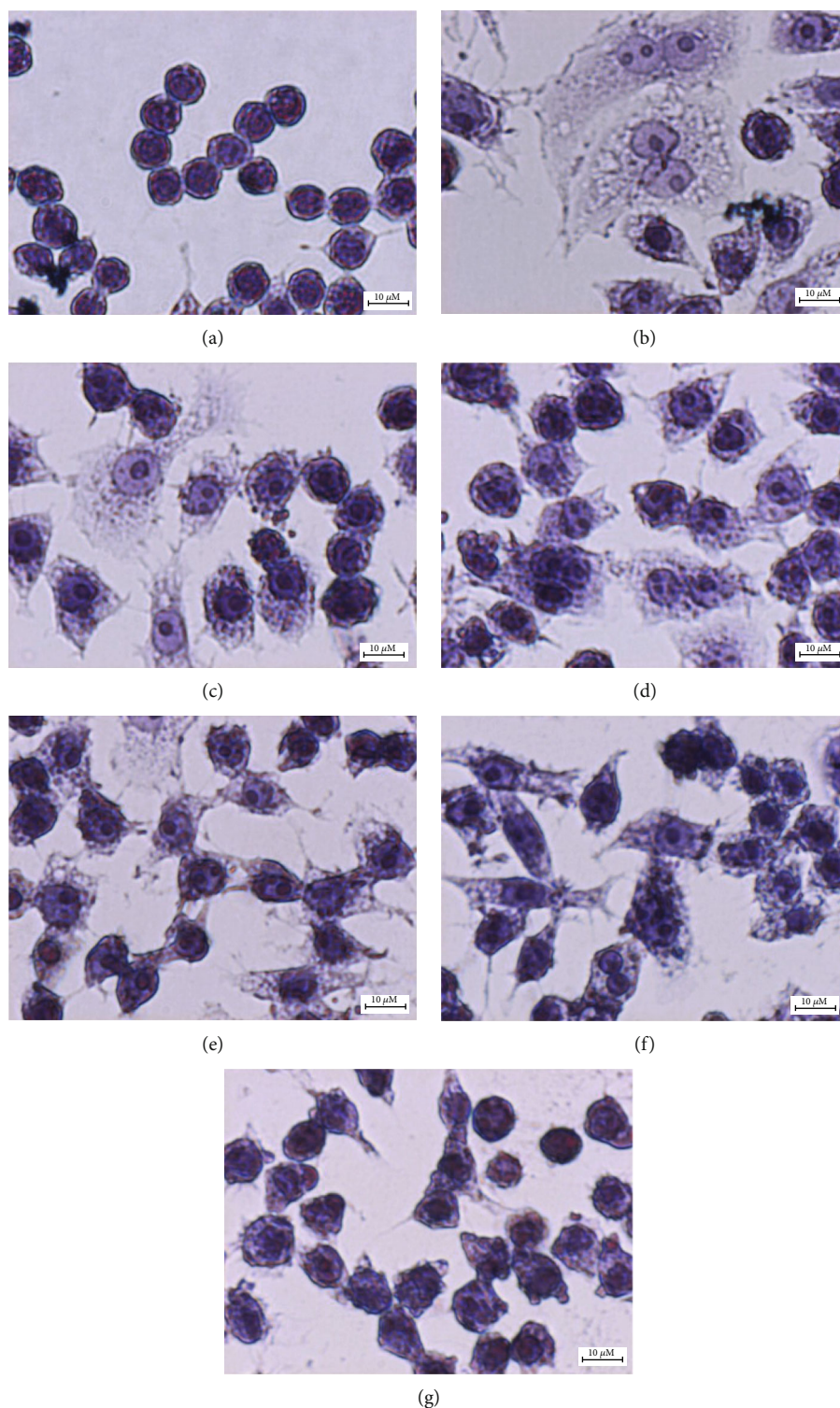
Figure 3: Effects of GIE on the morphology of LPS plus IFN-γ-induced RAW264.7 cells. Cells were stained with hematoxylin staining: (a) uninduced RAW264.7 cells, (b) untreated LPS plus IFN-γ-induced cells, (c) cells were pretreated with DEX at 1μM, (d), (e), (f), and (g) cells were pretreated with GIE at concentrations range of 50, 100, 200, and 300μg/mL, respectively (original magnification at ×600, scale bar; 10μm).

inflammatory molecular expressions as IL-6 and COX-2. However, IL-10 is a key anti-inflammatory cytokine with immunomodulatory effects, causing the inhibition of another proinflammatory cytokine such as TNF-α [50]. In order to confirm the anti-inflammatory activity of the GIE, the effects of the extract on proinflammatory cytokine (IL-6 and TNF-α) and anti-inflammatory cytokine (IL-10) production were evaluated in LPS plus IFN-γ-induced RAW264.7 cells by
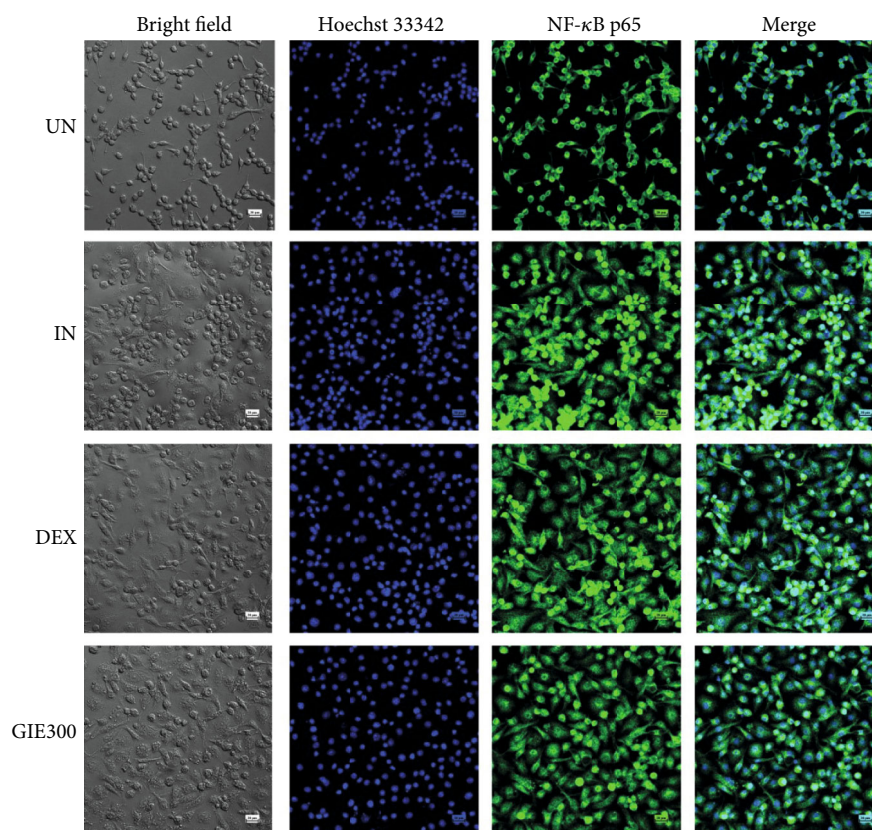
FIGURE 4: Effects of GIE on the nuclear translocation of NF-κB p65 in LPS plus IFN-γ-induced RAW264.7 cells at 24 h. Cells were pretreated with GIE or DEX for 3 h and then coincubated with LPS plus IFN-γ for 24 h. The nuclear translocation of NF-κB p65 was detected using an immunofluorescence assay and visualized under confocal microscopy. The figure represents the cell morphology (bright field), the nuclear translocation of NF-κB p65 (green fluorescence), nucleus (blue fluorescence), and costaining (overlay green and blue fluorescence). Scale bar, 20 μm. UN: uninduced cells; IN: untreated LPS plus IFN-γ-induced cells; DEX: cells were pretreated with DEX at 1 μM; GIE300: cells were pretreated with GIE 300 μg/mL.

using ELISA. The results indicated that GIE at all tested-concentration significantly suppressed LPS plus IFN-γ-induced IL-6 production ($p < 0.05$; Figure 2(a)) and slightly decreased TNF-α production compared to untreated LPS plus IFN-γ-induced cells (IN) (Figure 2(b)). As expected, DEX (a reference drug) could also inhibit LPS plus IFN-γ-induced IL-6 and TNF-α production by 95.38% and 58.88%, respectively. Surprisingly, LPS plus IFN-γ induced the secretion of IL-10 about 6.5-fold compared to uninduced cells. DEX significantly increased the secretion of IL-10 level by almost 36.78% compared to untreated LPS plus IFN-γ-induced cells ($p < 0.05$; Figure 2(c)). While pretreated-GIE only showed a slight increase in IL-10 levels (around 5-10%) but no significant difference compared to untreated LPS plus IFN-γ-induced cells ($p > 0.05$). qRT-PCR was performed to investigate whether suppression of TNF-α and IL-6 production by GIE was related to a change in mRNA levels for both proinflammatory cytokines. Increasing concentrations of GIE produced a decrease in the order of IL-6 mRNA levels in LPS plus IFN-γ-induced cells (Figure 2(d)). However, GIE slightly decreased TNF-α mRNA levels compared to LPS plus IFN-γ-induced cells (Figure 2(e)). The profile of IL-6 and TNF-α suppression by GIE suggests that GIE acts more potent on IL-6 than TNF-α.

Base on GC-MS analysis, the volatile oil compounds presenting in GIE, including phytol, squalene, γ-tocopherol, dl-α-tocopherol, and stigmasterol, have been reported to have anti-inflammatory and antioxidant activities. Therefore, the anti-inflammatory effects of the GIE could simply rely on volatile oil components that may exert synergistic effects. This is the first study concerning the inhibitory activity against proinflammatory cytokines (IL-6 and TNF-α) in LPS plus IFN-γ-induced RAW264.7 cells. The secretion of proinflammatory cytokines, TNF-α and IL-6, is an important factor in upregulating the inflammatory process. The high levels of TNF-α and IL-6 play a critical role in acute and chronic inflammatory diseases; both cytokines are prime targets for intervention by anti-inflammatory therapeutic agents. Therefore, the development of anti-inflammatory substances, which can modulate proinflammatory mediators' production, is an efficient way to manage inflammatory conditions. These results provide evidence that GIE could be a source of anti-inflammatory agents, which may have a beneficial effect on treating inflammation-associated diseases.

3.7. Effects of GIE on the Morphology of LPS plus IFN-γ-Induced RAW264.7 Cells. The morphological alteration in LPS plus IFN-γ-induced RAW264.7 cells in the presence or

(a)

(b)
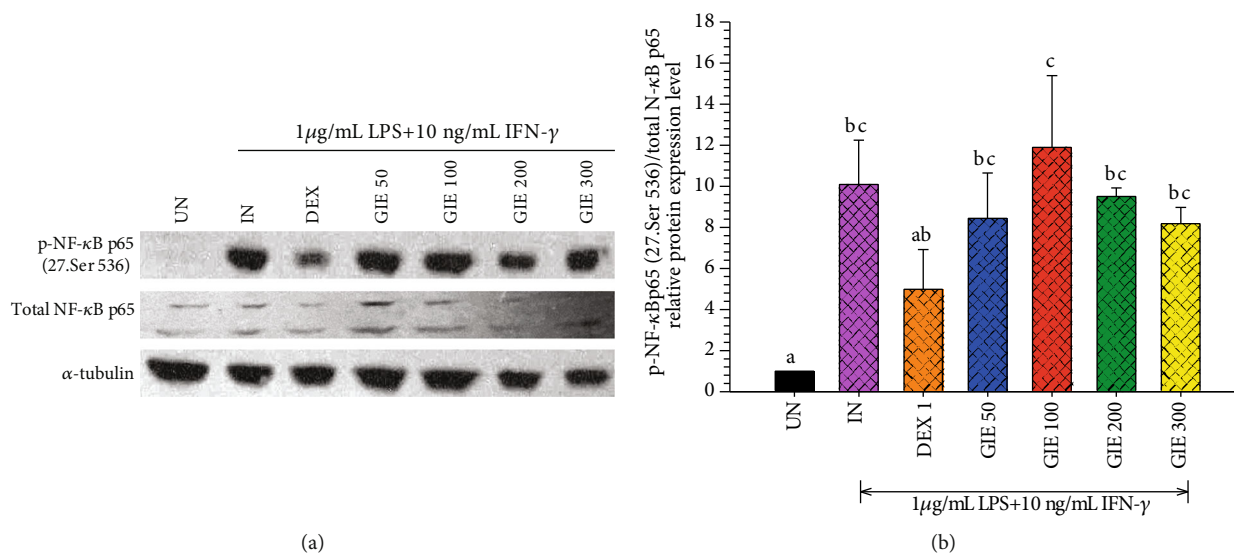
FIGURE 5: Effects of GIE on phosphorylation of NF-κB p65 induced by LPS plus IFN-γ in RAW264.7 cells. Cells were pretreated with GIE or DEX for 3 h and then coincubated with LPS plus IFN-γ for 24 h. The protein expression was analyzed by Western blotting. (a) The cellular proteins were used to detect the phosphorylated NF-κB p65 and total form of NF-κB with α-tubulin as a housekeeping control protein. (b) Mean densitometric values are expressed as bar charts. The data represent the mean ± S.D. of three independent experiments. One-way ANOVA performed the comparison, and Tukey was used as a *post hoc* test. The degree of significance was denoted with different letters for the comparison between sample groups. $p < 0.05$ was considered as statistically significant. UN: uninduced cells; IN: untreated LPS plus IFN-γ-induced cells; DEX: cells were pretreated with DEX at 1 μM; GIE300: cells were pretreated with GIE 300 μg/mL.

absence of GIE were also observed (as seen in Figures 3(a)–3(g)). The results demonstrated that LPS and IFN-γ caused cell morphology to change into a pseudopodia formation, spreading, and pancake-like shape within 24 h of stimulation (Figure 3(b)). The phenotypic polarization of macrophages allows the macrophage to engulf lipids, dead cells, other substances perceived as danger signals and secrete a large number of inflammatory molecules [51, 52]. In contrast, uninduced cells (UN) displayed a circular shape, a common form of RAW264.7 cells (Figure 3(a)). The pretreatment with GIE decreased the degree of cell spreading and pseudopodia formation, which was obviously observed in cells after pretreated with GIE 300 μg/mL (Figure 3(g)). Our results are in substantial agreement with a previous study of Kang et al. that the cotreatment of LPS with the crude methanol extract of *Citrus aurantium* L. reduces the level of cell spreading and pseudopodia formation by suppressing cell differentiation [53].

3.8. Effects of GIE on NF-κB p65 Nuclear Translocation and p-NFκB p65 (27.Ser 536) Protein Expression in LPS plus IFN-γ-Induced RAW264.7 Cells. Given that LPS plus IFN-γ-induced inflammation is through Toll-like receptor (TLR) signaling, NF-κB is activated and translocate into the nucleus to regulate the induced transcription of proinflammatory genes [54]. As a marker of NF-κB activation, the nuclear translocation of the NF-κB p65 was visualized in LPS plus IFN-γ-induced RAW264.7 cells by immunofluorescence confocal microscopy. As shown in Figure 4, LPS plus IFN-γ-induced RAW264.7 cells (IN) showed marked NF-κB p65 staining in the nuclei, while uninduced cells (UN) showed weaker nuclear NF-κB expression but stronger staining in the cyto-

plasm. GIE treatment (GIE300) attenuated LPS plus IFN-γ-induced nuclear translocation of NF-κB p65. Based on these findings, GIE can decrease the nuclear translocation of NF-κB, thus further inhibiting the expression of target inflammatory genes.

To further investigate whether GIE can regulate NF-κB signaling in LPS plus IFN-γ-induced RAW264.7 cells, the phosphorylation of NF-κB p65 was detected by Western blotting. Stimulation of the uninduced cells by LPS plus IFN-γ (IN) exhibited significantly higher phosphorylation of NF-κB p65 than uninduced cells (UN) ($p < 0.05$; Figures 5(a) and 5(b)). Pretreatment with 1 μM DEX or GIE showed a trend to reduce the phosphorylation of NF-κB p65 proteins, but no significant difference compared to LPS plus IFN-γ-induced cells (IN) ($p > 0.05$). This result suggests that GIE exhibits a slight inhibitory effect on the phosphorylation of NF-κB p65 to exert its anti-inflammatory effects.

In oxidative stress and anti-inflammation, enhancement of antioxidant gene expression plays an essential role in cell protection. It has been reported that superoxide dismutase (SOD) can modulate ROS-dependent signaling pathways during inflammatory responses [55]. The activation of Nrf2 antioxidant pathway prevents LPS-induced transcriptional upregulation of proinflammatory cytokines [56]. This research found that GIE increased the antioxidant gene expression, SOD2, and reduced NO and ROS production. Therefore, it is possible that the antioxidant properties of GIE could modulate the inflammation process caused by regulating the ROS levels.

3.9. Vitamin E Exhibited Anti-inflammatory Activities by Suppressing iNOS, COX-2, and IL-6 mRNA Expression in

(a)

(b)

(c)

(d)
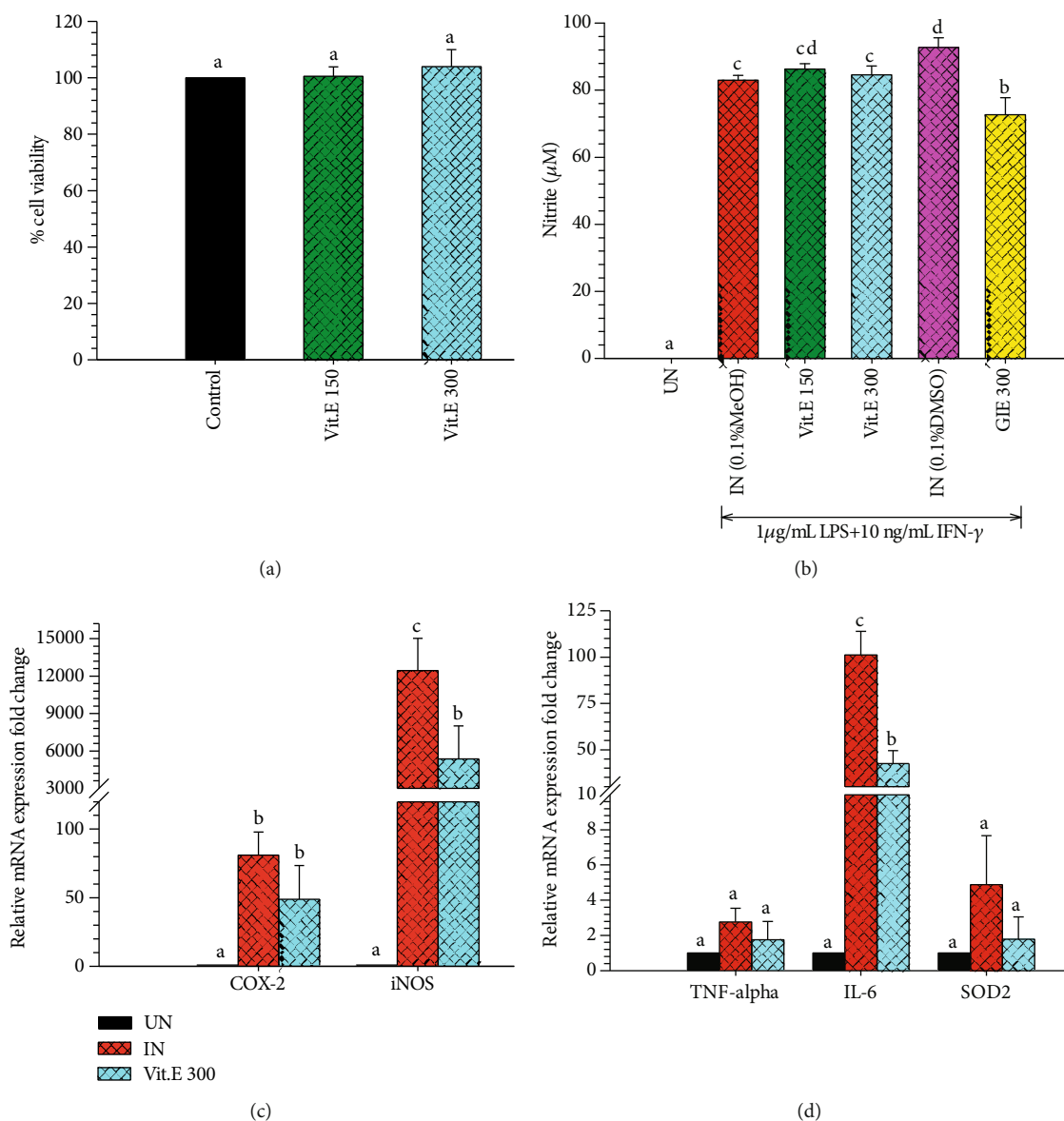
FIGURE 6: (a) Cytotoxic effects of Vit.E on RAW264.7 cells for 24 h. MTT assay was used to determine cell viability. Values are expressed as a percentage of the control. (b) The effect of Vit.E compared to GIE on NO production in LPS plus IFN-γ-induced RAW264.7 cells. Nitrite concentration was determined from a sodium nitrite standard curve, and the results are expressed as a concentration (μM) of nitrite in a culture medium. The data represent the mean ± S.D. of three independent experiments. (c) The effects of Vit.E on COX-2 and iNOS mRNA expression in LPS plus IFN-γ-induced RAW264.7 cells. (d) The effects of Vit.E on TNF-α, IL-6, and SOD2 mRNA expression in LPS plus IFN-γ-induced RAW264.7 cells. The data represent the mean ± S.D. of two independent experiments. Cells were pretreated with GIE or DEX for 3 h and then coincubated with LPS plus IFN-γ for 24 h. UN: uninduced cells; IN: untreated LPS plus IFN-γ-induced cells; DEX: cells were pretreated with DEX at 1 μM; GIE 300: cells were pretreated with GIE 300 μg/mL; Vit.E (150 and 300): cells were pretreated with Vit.E 150 and 300 μg/mL, respectively. One-way ANOVA performed the comparison, and Tukey was used as a *post hoc* test. The degree of significance was denoted with different letters for the comparison between sample groups. $p < 0.05$ was considered as statistically significant.

LPS plus IFN-γ-Induced RAW264.7 Cells. GIE has been reported to have antioxidant and anti-inflammatory activities in LPS plus IFN-γ-induced RAW264.7 cells in this research. Based on GC-MS analysis, we found that GIE consisted of many volatile oil compounds, including phytol, squalene, γ-tocopherol, dl-α-tocopherol, and stigmasterol. The antioxidant and anti-inflammatory activities of these

active constituents have been demonstrated in several studies. Therefore, it is essential to confirm whether the active ingredients contributed to the antioxidant and anti-inflammatory abilities of GIE. The dl-alpha-tocopherol or Vit.E was *chosen* to elucidate the anti-inflammation and anti-oxidative activities in LPS plus IFN-γ-induced RAW264.7 cells. The cytotoxicity of Vit.E was evaluated. The results

TABLE 4: Band assignments of major absorptions in FTIR spectra in 3000-950 cm^{-1} regions.

Band position of 2nd derivative spectra (cm^{-1})	Assignments
2962	CH$_3$ stretching (antisymmetric) due to the methyl terminal of membrane phospholipids
2923	CH$_2$ antisymmetric stretching of methylene group of membrane phospholipids
2875	CH$_3$ symmetric stretching: lipids and proteins
2852	CH$_2$ symmetric stretching: mainly lipids
1655	Amide I: C=O (80%) and C–N (10%) stretching, N–H (10%) bending vibrations: proteins α-helix
1544	Amide II: N–H (60%) bending and C–N (40%) stretching vibrations: proteins α-helix
1515	CO$_2$ antisymmetric stretching
1463	CH$_2$ bending vibrations: mainly lipids with little contributions from proteins
1452	CH$_2$ bending vibrations: mainly lipids with little contributions from proteins
1394	COO$^-$ symmetric stretching: fatty acids and amino acids
1243	PO$_2^{2-}$ asymmetric stretching vibrations: RNA, DNA, and phospholipids
1176	C–O vibrations from glycogen and other carbohydrates
1087	PO$_2^{2-}$ asymmetric stretching vibrations: RNA, DNA, and phospholipids
1047	C–O vibrations from glycogen and other carbohydrates
963	C–C/C–O is stretching of deoxyribose vibration

exhibited that Vit.E at 150 and 300 μg/mL did not reduce the cell viability compared to RAW264.7 cells (Figure 6(a)). Then, the noncytotoxic concentration of Vit.E at 300 μg/mL was chosen to perform subsequent experiments. Vit.E did not suppress NO production induced by LPS plus IFN-γ in RAW264.7 cells (Figure 6(b)). The results indicated that Vit.E showed a significantly suppressed iNOS and IL-6 mRNA expression lower than untreated LPS plus IFN-γ-induced cells (IN) ($p < 0.05$; Figures 6(c) and 6(d)), whereas COX-2, TNF-α, and SOD2 were lower than IN but no significant difference ($p > 0.05$; Figures 6(c) and 6(d)). Therefore, these results imply that Vit.E exhibits the inhibitory effect on the inflammatory gene expression, which is related to the anti-inflammatory effects of GIE. As mentioned above, GIE consists of many volatile oils; therefore, the antioxidant and anti-inflammatory activities of it may cause by other chemical compositions found in this plant. Moreover, phenolic, flavonoids, terpenoids, and glycoside in GIE were reported in previous studies [14, 15]. The presence of flavonoids had been reported to be associated with the antioxidant and anti-inflammatory activities of several plant extracts [25, 57, 58]. Thus, it is possible that phenolic and flavonoid compounds in GIE could provide substantial antioxidant and anti-inflammatory activities. In order to compare the inhibitory effect of Vit.E and GIE, GIE at 300 μg/mL contains Vit.E approximately 6.99 μg/mL. The results indicated that GIE at 300 μg/mL had inhibitory effect on COX-2 (73.48% inhibition, Figure 1(e)), iNOS (64.58% inhibition, Figure 1(e)), and IL-6 (75.72% inhibition, Figure 2(d)) mRNA levels higher than Vit.E alone at 300 μg/mL, which inhibited COX-2 (40.74% inhibition, Figure 6(c)), iNOS (56.86% inhibition, Figure 6(c)), and IL-6 (58.42% inhibition, Figure 6(d)). These results imply that the anti-inflammatory effect of GIE on these cells may have synergistic activities that cause by the combination of compounds presenting in GIE.

3.10. SR-FTIR Detected Biomolecule Alterations in RAW264.7 Cells.

SR-FTIR was applied to detect the effects of GIE on biomolecule alterations such as lipids, proteins, nucleic acids, and carbohydrates based on their specific vibrational fingerprints. The detailed spectral band assignments of samples are given in Table 4. As shown in Figure 7(a), the representative FTIR spectra acquired in the 3800-900 cm^{-1} from four individuals of sample groups, including uninduced RAW264.7 cells, untreated LPS plus IFN-γ-induced RAW264.7 cells, 1 μM of DEX-, and 300 μg/mL GIE-treated LPS plus IFN-γ-induced RAW264.7 cells. The second derivative analysis in spectral regions ranges from 3,000 to 2800 cm^{-1} for lipid regions and 1800 to 950 cm^{-1} for protein regions, nucleic acid, and other carbohydrate regions (as shown in Figures 7(b) and 7(c)) respectively. The 2nd spectral revealed the prominent differences between the average spectra belonging to the different groups. The spectral differences were clearly observed mainly in lipid regions centered at 2962 cm^{-1}, 2923 cm^{-1}, and 2852 cm^{-1}, protein regions centered at 1655 cm^{-1} and 1544 cm^{-1}, nucleic acid and other carbohydrates regions centered at 1243 cm^{-1}, 1176 cm^{-1}, 1087 cm^{-1}, and 1047 cm^{-1}. The integral area of 2nd derivative FTIR spectral regions in each region was calculated to analyze the differences between lipid regions (2972-2951 cm^{-1}, 2934-2910 cm^{-1}, 2878-2870 cm^{-1}, and 2856-2843 cm^{-1}), nucleic acids (1257-1204 cm^{-1} and 1125-1074 cm^{-1}), glycogen, and other carbohydrates (1181-1164 cm^{-1} and 1063-1032 cm^{-1}) as shown in Figure 8(a). The level of lipid content was significantly increased in all test groups compared to the uninduced group ($p < 0.05$), whereas the highest level of lipid was found in DEX- and GIE-treated groups. This increase in lipid content might be due to the changing of the cell membrane and lipid accumulation in RAW264.7 cells. According to the results of cell morphological changes stained by hematoxylin staining, the

(a)

(b)

(c)
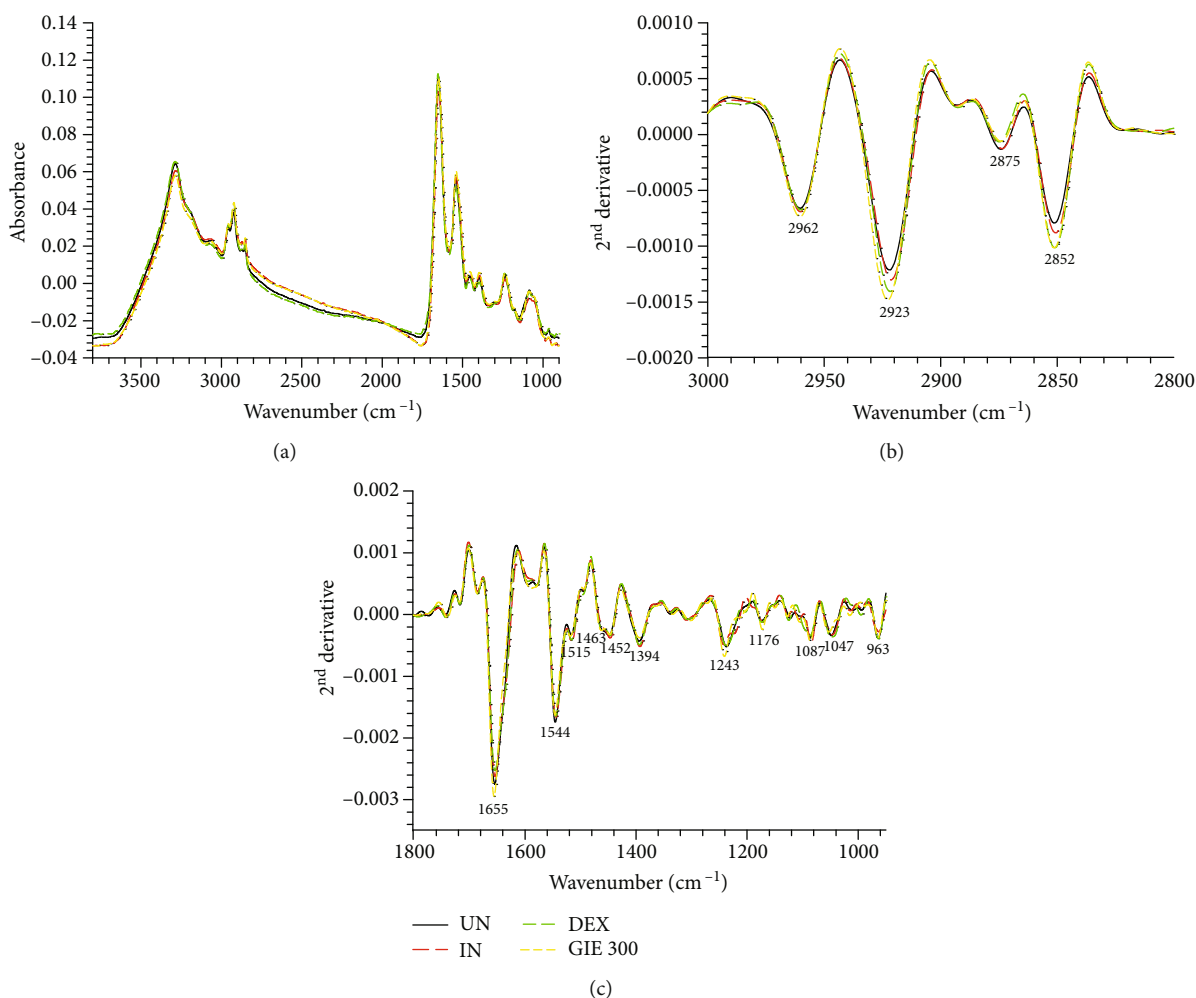
FIGURE 7: FTIR spectra obtained using SR-FTIR and processed with a second derivative. (a) Average original FTIR spectra (3800-900 cm^{-1}), (b) average the second derivative spectra of lipid regions (3000-2800 cm^{-1}), and (c) average the 2nd derivative spectra of protein and nucleic acid and other carbohydrate regions (1800-950 cm^{-1}). The data obtained from uninduced cells (UN, $n = 70$), untreated LPS plus IFN-γ-induced cells (IN, $n = 70$), 1 μM of DEX-treated cells (DEX, $n = 70$), and 300 μg/mL of GIE-treated LPS plus IFN-γ-induced cells (GIE300, $n = 70$).

phenotypic changes of RAW264.7 cells are induced by LPS and IFN-γ (Figures 3(b)–3(g)). The increasing lipid content may be related to the inflammatory phenotype of macrophages in which they are able to engulf lipids, dead cells, and other substances perceived as danger signals via phagocytosis [52]. All ingested lipids are then processed by acid lipases within the lysosomes, leading to free fatty acids and cholesterol generation [59]. Nevertheless, our data indicated that nucleic acid content seemed to increase in the DEX-treated cells and decrease in GIE-treated cells. However, the differences were not statistically significant from both uninduced cells and untreated LPS plus IFN-γ-induced cells ($p > 0.05$). According to these findings, the present data showed that the selected GIE concentration did not affect the cells' nucleic acids, consistent with the cytotoxic effect of GIE obtained from MTT assay. These results are confirmed by the study of Machana et al. [60], which reported the DNA content in apoptotic cell death, by contrast, to increase during necrotic cell death. As shown in Figure 8(a), the glycogen and other carbohydrate content

of the untreated LPS plus IFN-γ-induced cells were significantly decreased compared to the uninduced cells ($p < 0.05$). Upon DEX and GIE treatment, the glycogen and other carbohydrate contents were increased compared to the untreated LPS plus IFN-γ-induced cells. The band area ratio of amide I (1670-1627 cm^{-1})/amide II regions (1558-1505 cm^{-1}) was calculated to obtain information about changes in protein composition and structure (Figure 8(b)). There was a significant increase in the ratio of amide I to amide II bands in untreated LPS plus IFN-γ-induced RAW264.7 cells compared to the uninduced RAW264.7 cells ($p < 0.05$), revealing an alteration in the structures of proteins. In comparison, the GIE treating group showed a significant decrease in amide I/amide II ratio compared to untreated LPS plus IFN-γ-induced RAW264.7 cells ($p < 0.05$). According to amide I and amide II profiles depending on the protein structural composition, the changing of amide I/amide II ratio suggests that there are some alterations in protein structure and conformation in LPS plus IFN-γ-induced RAW264.7 cells [18].
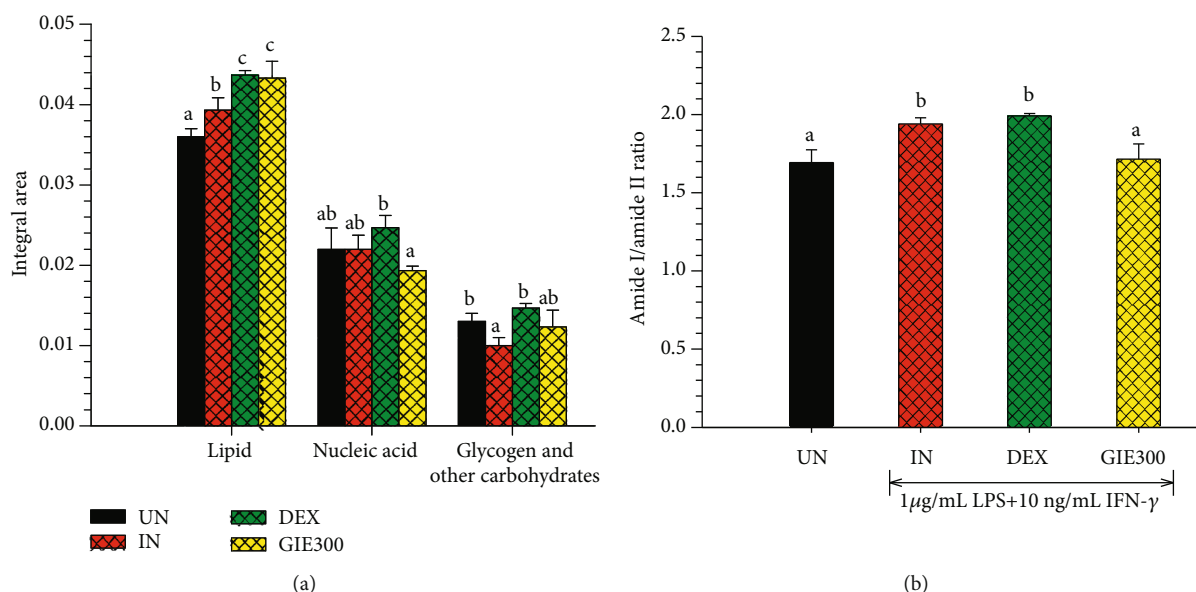
FIGURE 8: Bar graph shows (a) integrated areas of remarkable lipid, nucleic acid, glycogen, and other carbohydrate regions and (b) the amide I/amide II ratio of 2nd derivative spectra. Data are represented as means ± S.D. for three replicates. The data obtained from uninduced cells (UN, $n = 70$), untreated LPS plus IFN-γ-induced cells (IN, $n = 70$), 1 μM of DEX-treated cells (DEX, $n = 70$), and 300 μg/mL of GIE-treated LPS plus IFN-γ-induced cells (GIE300, $n = 70$). One-way ANOVA performed the comparison, and Tukey was used as a *post hoc* test. The degree of significance was denoted with different letters for the comparison between sample groups. $p < 0.05$ was considered as statistically significant.

Based on the spectral differences, the PCA analysis was applied to confirm any possible discrepancies between four sample groups in spectral ranges of 3000-2800 cm^{-1} and 1800-950 cm^{-1}. Four clusters of spectra were distinctly visualized in two-dimensional score plots, including PC1 vs. PC2, PC1 vs. PC3, and PC1 vs. PC4 score plot as shown in Figures 9(a)–9(c), respectively. PCA loading plots were used to indicate the contribution of variables between sample groups (as shown in Figures 9(d) and 9(e)). The PCA analysis obviously illustrated that the clusters of untreated LPS plus IFN-γ-induced RAW264.7 cells (IN) and DEX-treated cells (DEX) were separated from the cluster of GIE-treated cells (GIE300) along PC1 (33%). They were also separated from the group of uninduced RAW264.7 cells (UN) along with the PC2 score (9%) as shown in Figure 9(a). The amide I band from protein at 1629 cm^{-1} and 1623 cm^{-1} (assigned to the β-sheet structure) were heavily loaded for negative PC1 and positive PC2 loading, respectively (Figure 9(d)), which were responsible for discriminating the untreated LPS plus IFN-γ-induced RAW264.7 cells and DEX-treated cells, respectively. These data indicated that the amide I protein of the untreated LPS plus IFN-γ-induced RAW264.7 cells and DEX-treated cells were higher than the uninduced and GIE-treated cells. The cluster of DEX-treated cells was discriminated from uninduced and untreated LPS plus IFN-γ-induced RAW264.7 cells along PC3 (8%) (Figure 9(b)) in correlation with the positive loading centered at 2960 cm^{-1}, 2925 cm^{-1}, and 2854 cm^{-1}, assigned to the C-H stretching vibration of lipid in the cells (Figure 9(e)). Moreover, the cluster of uninduced and DEX-treated cells could be distinguished from untreated LPS plus IFN-γ-induced

RAW264.7 cells by their having positive PC4 scores (5%) (Figure 9(c)), which were associated with the negative loading plot centered at 1232 cm^{-1}, 1201 cm^{-1}, and 998 cm^{-1}, attributing to C–C from nucleic acid and C–O from a glycoprotein and other carbohydrates. This data displayed that the glycogen and other carbohydrates in uninduced and DEX-treated cells were higher than untreated LPS plus IFN-γ-induced RAW264.7 cells. These results provide evidence that PCA analysis has corresponded to the integrated peak areas obtained from 2nd derivative spectra (Figures 8(a) and 8(b)).

4. Conclusions

To our knowledge, the present study is the first report of the antioxidant and anti-inflammatory effects of GIE in LPS plus IFN-γ-induced RAW264.7 cells. GIE exerted an antioxidative effect based on its ROS scavenging properties and elevating the antioxidant gene expressions. GIE possesses anti-inflammatory effects by suppressing both proinflammatory mediators and gene expression in LPS plus IFN-γ-induced RAW264.7 cells. The data from SR-FTIR spectroscopy exhibited that LPS plus IFN-γ could affect the biochemical profile of RAW264.7 cells. SR-FTIR analysis was able to evaluate the effect of GIE on the changing of macromolecules, including lipid, protein structure, nucleic acid, glycogen, and other carbohydrates. These findings provide evidence that GIE has significant antioxidant and anti-inflammatory properties and could serve as a potent compound of those activities that warrant further research and development.

(a)

(b)

(c)

UN • DEX •
IN • GIE300 •

(d)
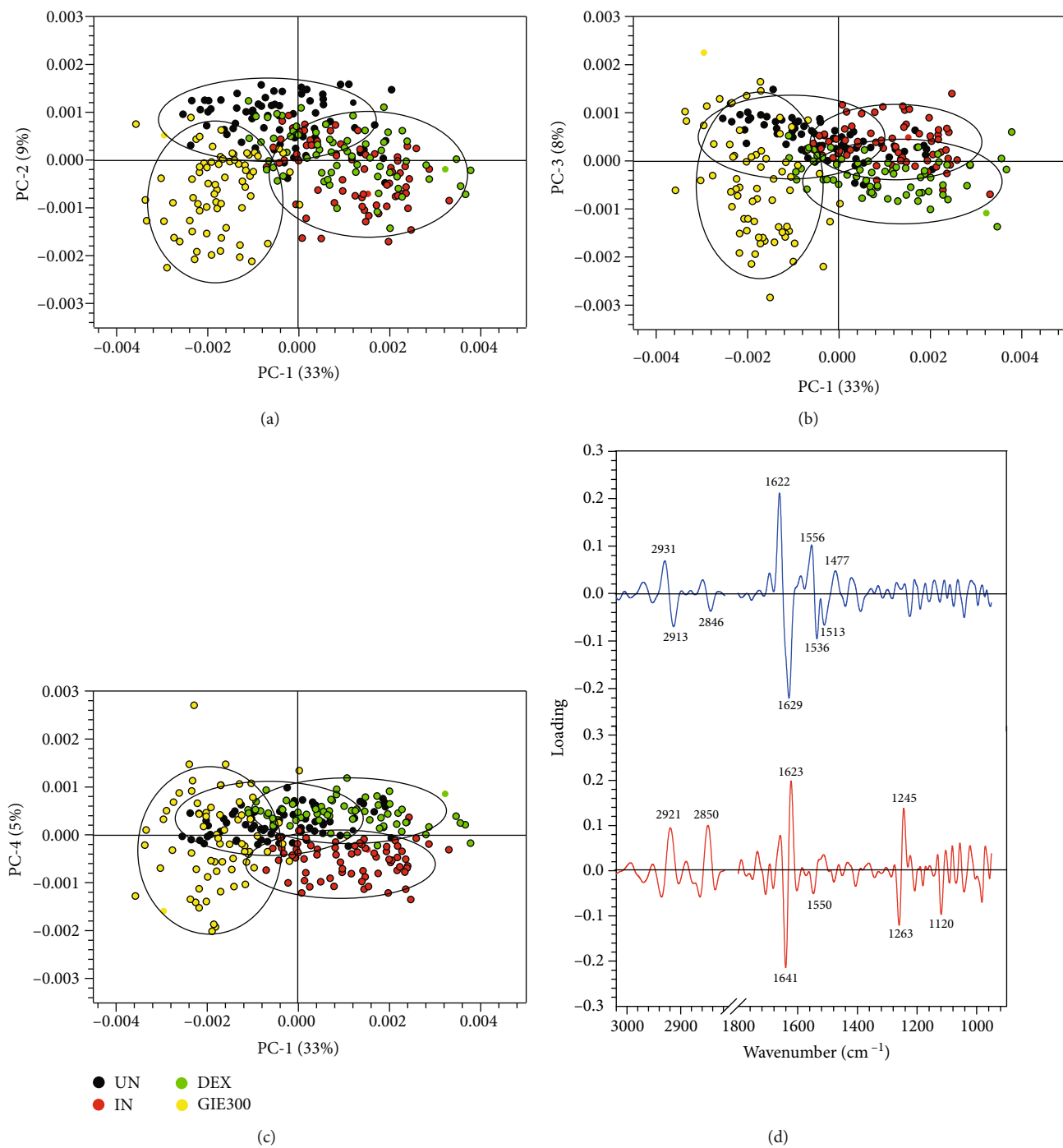
FIGURE 9: Continued.

(e)
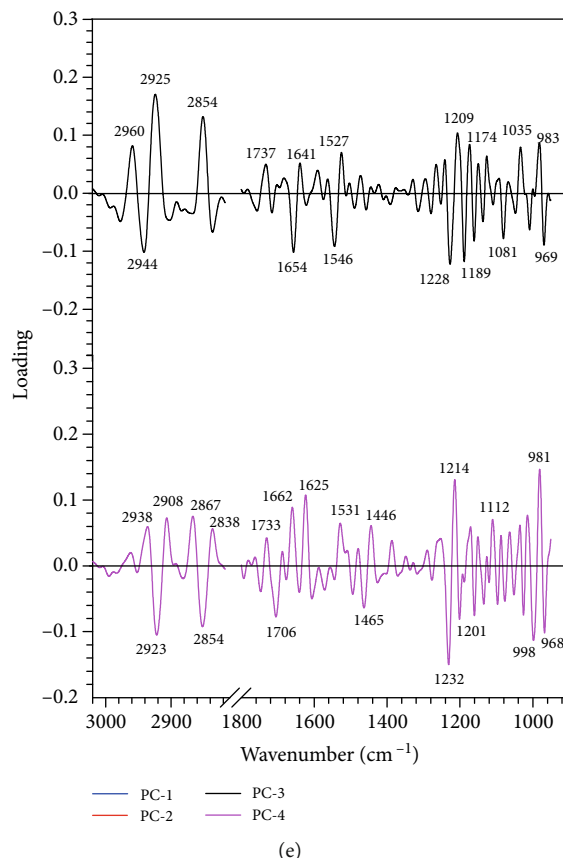
FIGURE 9: PCA analysis of the FTIR spectra of uninduced cells (UN, $n = 70$), untreated LPS plus IFN-γ-induced cells (IN, $n = 70$), 1 μM of DEX-treated cells (DEX, $n = 70$), and 300 μg/mL of GIE-treated LPS plus IFN-γ-induced cells (GIE300, $n = 70$) in the spectral range of 3000-2800 cm^{-1} and 1800-950 cm^{-1} regions. PCA 2D score plot of (a) PC1 versus PC2, (b) PC1 versus PC3, and (c) PC1 versus PC4. PCA loading plot of (d) PC1 and PC2 and (e) PC3 and PC4.

Data Availability

The datasets used and analyzed during this study are available from the corresponding author on reasonable request.

Conflicts of Interest

The authors declare that there are no conflicts of interest regarding the publication of this manuscript.

Authors' Contributions

B.D. performed experiments and data analysis and drafted the manuscript. C.T. designed the study and revised the manuscript. M.M. contributed and designed the experiments and critical discussion. K.T. performed the SR-FTIR microspectroscopy. P.S. investigated ROS by DCFH-DA, proinflammatory cytokines (IL-6 and TNF-α), and anti-inflammatory cytokines (IL-10) by ELISA. G.E. supervised, coordinated, and improved quality and proofread the manuscript. All authors have read and approved the submission.

Acknowledgments

References

[1] S. Watanabe, M. Alexander, A. V. Misharin, and G. R. S. Budinger, "The role of macrophages in the resolution of inflammation," *The Journal of Clinical Investigation*, vol. 129, no. 7, pp. 2619–2628, 2019.

[2] D. L. Laskin, V. R. Sunil, C. R. Gardner, and J. D. Laskin, "Macrophages and tissue injury: agents of defense or destruction?," *Annual Review of Pharmacology and Toxicology*, vol. 51, no. 1, pp. 267–288, 2011.

[3] F. O. Martinez and S. Gordon, "The M1 and M2 paradigm of macrophage activation: time for reassessment," *F1000Prime Reports*, vol. 6, 2014.

[4] J. B. Calixto, M. F. Otuki, and A. R. Santos, "Anti-inflammatory compounds of plant origin. Part I. Action on arachidonic acid pathway, nitric oxide and nuclear factor κ B (NF-κB)," *Planta Medica*, vol. 69, no. 11, pp. 973–983, 2003.

[5] A. D. Politis, K. Ozato, J. E. Coligan, and S. N. Vogel, "Regulation of IFN-gamma-induced nuclear expression of IFN

consensus sequence binding protein in murine peritoneal macrophages," *The Journal of Immunology*, vol. 152, no. 5, pp. 2270–2278, 1994.

[6] J.-M. Zhang and J. An, "Cytokines, inflammation and pain," *International Anesthesiology Clinics*, vol. 45, no. 2, pp. 27–37, 2007.

[7] S. Reuter, S. C. Gupta, M. M. Chaturvedi, and B. B. Aggarwal, "Oxidative stress, inflammation, and cancer: how are they linked?," *Free Radical Biology and Medicine*, vol. 49, no. 11, pp. 1603–1616, 2010.

[8] P. Arulselvan, M. T. Fard, W. S. Tan et al., "Role of antioxidants and natural products in inflammation," *Oxidative Medicine and Cellular Longevity*, vol. 2016, Article ID 5276130, 15 pages, 2016.

[9] R. E. Sevinsky, D. W. Stewart, and S. Harirforoosh, "Nonsteroidal anti-inflammatory drugs: is there a link between cardiovascular and renal adverse effects?," *Journal of Integrative Nephrology and Andrology*, vol. 4, no. 1, p. 1, 2017.

[10] S. Wongrakpanich, A. Wongrakpanich, K. Melhado, and J. Rangaswami, "A comprehensive review of non-steroidal anti-inflammatory drug use in the elderly," *Aging and Disease*, vol. 9, no. 1, pp. 143–150, 2018.

[11] T. Charoonratana, T. Songsak, C. Monton et al., "Quantitative analysis and formulation development of a traditional Thai antihypertensive herbal recipe," *Phytochemistry Reviews*, vol. 13, no. 2, pp. 511–524, 2014.

[12] World Health Organization, *WHO Medicines Strategy 2004-2007: Countries at the Core*, World Health Organization, 2004.

[13] A. Chanwitheesuk, A. Teerawutgulrag, and N. Rakariyatham, "Screening of antioxidant activity and antioxidant compounds of some edible plants of Thailand," *Food Chemistry*, vol. 92, no. 3, pp. 491–497, 2005.

[14] K. Tiamyom, K. Sirichaiwetchakoon, T. Hengpratom et al., "The effects of Cordyceps sinensis (Berk.) Sacc. and Gymnema inodorum (Lour.) Decne. Extracts on adipogenesis and lipase activity in vitro," *Evidence-based Complementary and Alternative Medicine*, vol. 2019, Article ID 5370473, 13 pages, 2019.

[15] C. Chaiyasut, P. Kesika, K. Chaiyasut, P. Sittiyuno, S. Peerajan, and B. S. Sivamaruthi, "Total phenolic content and free radical scavenging activity of representative medicinal plants of Thailand," *Asian Journal of Pharmaceutical and Clinical Research*, vol. 10, no. 11, pp. 137–141, 2017.

[16] K. Shimizu, M. Ozeki, A. Iino, S. Nakajyo, N. Urakawa, and M. Atsuchi, "Structure-activity relationships of triterpenoid derivatives extracted from *Gymnema inodorum* leaves on glucose absorption," *Japanese Journal of Pharmacology*, vol. 86, no. 2, pp. 223–229, 2001.

[17] S. Sabbatini, C. Conti, G. Orilisi, and E. Giorgini, "Infrared spectroscopy as a new tool for studying single living cells: is there a niche?," *Biomedical Spectroscopy and Imaging*, vol. 6, no. 3-4, pp. 85–99, 2017.

[18] O. Bozkurt, S. Haman Bayari, M. Severcan, C. Krafft, J. Popp, and F. Severcan, "Structural alterations in rat liver proteins due to streptozotocin-induced diabetes and the recovery effect of selenium: Fourier transform infrared microspectroscopy and neural network study," *Journal of Biomedical Optics*, vol. 17, no. 7, article 076023, 2012.

[19] S. Siriwong, Y. Teethaisong, K. Thumanu, B. Dunkhunthod, and G. Eumkeb, "The synergy and mode of action of quercetin plus amoxicillin against amoxicillin-resistant Staphylococcus

[20] P. Pocasap, N. Weerapreeyakul, and K. Thumanu, "Alyssin and iberin in cruciferous vegetables exert anticancer activity in HepG2 by increasing intracellular reactive oxygen species and tubulin depolymerization," *Biomolecules & Therapeutics*, vol. 27, no. 6, pp. 540–552, 2019.

[21] P. Yu, "Synchrotron IR microspectroscopy for protein structure analysis: potential and questions," *Spectroscopy*, vol. 20, no. 5,6, pp. 229–251, 2006.

[22] H. V. Rupasinghe, L. Wang, G. M. Huber, and N. L. Pitts, "Effect of baking on dietary fibre and phenolics of muffins incorporated with apple skin powder," *Food Chemistry*, vol. 107, no. 3, pp. 1217–1224, 2007.

[23] H. Yang, Y. Dong, H. Du, H. Shi, Y. Peng, and X. Li, "Antioxidant compounds from propolis collected in Anhui, China," *Molecules*, vol. 16, no. 4, pp. 3444–3455, 2011.

[24] B. Dunkhunthod, K. Thumanu, and G. Eumkeb, "Application of FTIR microspectroscopy for monitoring and discrimination of the anti-adipogenesis activity of baicalein in 3T3-L1 adipocytes," *Vibrational Spectroscopy*, vol. 89, pp. 92–101, 2017.

[25] P. Sittisart and B. Chitsomboon, "Intracellular ROS scavenging activity and downregulation of inflammatory mediators in RAW264.7 macrophage by fresh leaf extracts of Pseuderanthemum palatiferum," *Evidence-based Complementary and Alternative Medicine*, vol. 2014, Article ID 309095, 11 pages, 2014.

[26] O. H. Lowry, N. J. Rosebrough, A. L. Farr, and R. J. Randall, "Protein measurement with the Folin phenol reagent," *Journal of Biological Chemistry*, vol. 193, no. 1, pp. 265–275, 1951.

[27] R. O. Silva, F. B. M. Sousa, S. R. Damasceno et al., "Phytol, a diterpene alcohol, inhibits the inflammatory response by reducing cytokine production and oxidative stress," *Fundamental & Clinical Pharmacology*, vol. 28, no. 4, pp. 455–464, 2014.

[28] S. H. Jeong, "Inhibitory effect of phytol on cellular senescence," *Biomedical Dermatology*, vol. 2, no. 1, 2018.

[29] A. Cárdeno, M. Aparicio-Soto, S. Montserrat-de la Paz, B. Bermudez, F. J. Muriana, and C. Alarcón-de-la-Lastra, "Squalene targets pro- and anti-inflammatory mediators and pathways to modulate over-activation of neutrophils, monocytes and macrophages," *Journal of Functional Foods*, vol. 14, pp. 779–790, 2015.

[30] E. Reiter, Q. Jiang, and S. Christen, "Anti-inflammatory properties of α\- and γ-tocopherol," *Molecular Aspects of Medicine*, vol. 28, no. 5-6, pp. 668–691, 2007.

[31] P. Mathur, Z. Ding, T. Saldeen, and J. L. Mehta, "Tocopherols in the prevention and treatment of atherosclerosis and related cardiovascular disease," *Clinical Cardiology*, vol. 38, no. 9, pp. 570–576, 2015.

[32] V. Jimenez-Suarez, A. Nieto-Camacho, M. Jiménez-Estrada, and B. Alvarado Sanchez, "Anti-inflammatory, free radical scavenging and alpha-glucosidase inhibitory activities of Hamelia patens and its chemical constituents," *Pharmaceutical Biology*, vol. 54, no. 9, pp. 1822–1830, 2016.

[33] M. Zeb, S. Khan, T. Rahman, M. Sajid, and S. Seloni, "Isolation and biological activity of β-sitosterol and stigmasterol from the roots of Indigofera heterantha," *Pharmacy & Pharmacology International Journal*, vol. 5, no. 5, p. 139, 2017.

[34] M. R. Loizzo, R. Tundis, M. Bonesi et al., "Radical scavenging, antioxidant and metal chelating activities of *Annona cherimola* Mill. (cherimoya) peel and pulp in relation to their total

phenolic and total flavonoid contents," *Journal of Food Composition and Analysis*, vol. 25, no. 2, pp. 179–184, 2012.

[35] M. El Jemli, R. Kamal, I. Marmouzi, A. Zerrouki, Y. Cherrah, and K. Alaoui, "Radical-scavenging activity and ferric reducing ability of Juniperus thurifera (L.), J. oxycedrus (L.), J. phoenicea (L.) and Tetraclinis articulata (L.)," *Advances in Pharmacological Sciences*, vol. 2016, Article ID 6392656, 6 pages, 2016.

[36] J. S. Youn, Y.-J. Kim, H. J. Na et al., "Antioxidant activity and contents of leaf extracts obtained from Dendropanax morbifera LEV are dependent on the collecting season and extraction conditions," *Food Science and Biotechnology*, vol. 28, no. 1, pp. 201–207, 2019.

[37] E. Finotti, M. D'Ambrosio, F. Paoletti, V. Vivanti, and G. Quaglia, "Synergistic effects of α-tocopherol, β-sitosterol and squalene on antioxidant activity assayed by crocin bleaching method," *Nahrung (Weinheim)*, vol. 44, no. 5, pp. 373-374, 2000.

[38] G. Perretti, E. Finotti, S. Adamuccio, R. Della Sera, and L. Montanari, "Composition of organic and conventionally produced sunflower seed oil," *Journal of the American Oil Chemists' Society*, vol. 81, no. 12, pp. 1119–1123, 2004.

[39] N. V. Yanishlieva, A. Kamal-Eldin, E. M. Marinova, and A. G. Toneva, "Kinetics of antioxidant action of α- and γ-toco-pherols in sunflower and soybean triacylglycerols," *European Journal of Lipid Science and Technology*, vol. 104, no. 5, pp. 262–270, 2002.

[40] T.-C. Chou, "Theoretical basis, experimental design, and computerized simulation of synergism and antagonism in drug combination studies," *Pharmacological Reviews*, vol. 58, no. 3, pp. 621–681, 2006.

[41] K.-R. Kwon, M. B. Alam, J.-H. Park, T.-H. Kim, and S.-H. Lee, "Attenuation of UVB-induced photo-aging by polyphenolic-rich Spatholobus suberectus stem extract via modulation of MAPK/AP-1/MMPs signaling in human keratinocytes," *Nutrients*, vol. 11, no. 6, p. 1341, 2019.

[42] H.-U. Son, E.-K. Yoon, C.-Y. Yoo et al., "Effects of synergistic inhibition on α-glucosidase by phytoalexins in soybeans," *Biomolecules*, vol. 9, no. 12, p. 828, 2019.

[43] M. Allegra, *Antioxidant and Anti-Inflammatory Properties of Plants Extract*, Multidisciplinary Digital Publishing Institute, 2019.

[44] S. Nanasombat, K. Yansodthee, and I. Jongjaited, "Evaluation of antidiabetic, antioxidant and other phytochemical properties of Thai fruits, vegetables and some local food plants," *Walailak Journal of Science and Technology (WJST)*, vol. 16, no. 11, pp. 851–866, 2018.

[45] B. Halliwell and J. M. Gutteridge, "Role of free radicals and catalytic metal ions in human disease: an overview," in *Methods in Enzymology*, pp. 1–85, Elsevier, 1990.

[46] Y. Yoon, T. J. Kim, J. M. Lee, and D. Y. Kim, "SOD2 is upregulated in periodontitis to reduce further inflammation progression," *Oral Diseases*, vol. 24, no. 8, pp. 1572–1580, 2018.

[47] P. Kirkham and I. Rahman, "Oxidative stress in asthma and COPD: antioxidants as a therapeutic strategy," *Pharmacology & Therapeutics*, vol. 111, no. 2, pp. 476–494, 2006.

[48] E. Karpuzoglu and S. A. Ahmed, "Estrogen regulation of nitric oxide and inducible nitric oxide synthase (iNOS) in immune cells: implications for immunity, autoimmune diseases, and apoptosis," *Nitric Oxide*, vol. 15, no. 3, pp. 177–186, 2006.

[49] S. I. Jang, Y.-J. Kim, W.-Y. Lee et al., "Scoparone from Artemisia capillaris inhibits the release of inflammatory mediators in RAW 264.7 cells upon stimulation cells by interferon-γ plus LPS," *Archives of Pharmacal Research*, vol. 28, no. 2, pp. 203–208, 2005.

[50] R. Sundaram, P. Shanthi, and P. Sachdanandam, "Tangeretin, a polymethoxylated flavone, modulates lipid homeostasis and decreases oxidative stress by inhibiting NF-κB activation and proinflammatory cytokines in cardiac tissue of streptozotocin-induced diabetic rats," *Journal of Functional Foods*, vol. 16, pp. 315–333, 2015.

[51] F. Y. McWhorter, T. Wang, P. Nguyen, T. Chung, and W. F. Liu, "Modulation of macrophage phenotype by cell shape," *Proceedings of the National Academy of Sciences*, vol. 110, no. 43, pp. 17253–17258, 2013.

[52] I. Tabas and K. E. Bornfeldt, "Macrophage phenotype and function in different stages of atherosclerosis," *Circulation Research*, vol. 118, no. 4, pp. 653–667, 2016.

[53] S.-R. Kang, D.-Y. Han, K.-I. Park et al., "Suppressive effect on lipopolysaccharide-induced proinflammatory mediators by Citrus aurantium L. in macrophage RAW 264.7 cells via NF-B signal pathway," *Evidence-based Complementary and Alternative Medicine*, vol. 2011, Article ID 248592, 12 pages, 2011.

[54] P. P. Tak and G. S. Firestein, "NF-κB: a key role in inflammatory diseases," *The Journal of Clinical Investigation*, vol. 107, no. 1, pp. 7–11, 2001.

[55] J. A. Lee, H. Y. Song, S. M. Ju et al., "Differential regulation of inducible nitric oxide synthase and cyclooxygenase-2 expression by superoxide dismutase in lipopolysaccharide stimulated RAW 264.7 cells," *Experimental & Molecular Medicine*, vol. 41, no. 9, pp. 629–637, 2009.

[56] J.-F. Luo, X.-Y. Shen, C. K. Lio et al., "Activation of Nrf2/HO-1 pathway by nardochinoid C inhibits inflammation and oxidative stress in lipopolysaccharide-stimulated macrophages," *Frontiers in Pharmacology*, vol. 9, p. 911, 2018.

[57] C.-l. Lu, W. Zhu, M. Wang, X.-j. Xu, and C.-j. Lu, "Antioxidant and anti-inflammatory activities of phenolic-enriched extracts of Smilax glabra," *Evidence-based Complementary and Alternative Medicine*, vol. 2014, Article ID 910438, 8 pages, 2014.

[58] J. C. Ruiz-Ruiz, A. J. Matus-Basto, P. Acereto-Escoffié, and M. R. Segura-Campos, "Antioxidant and anti-inflammatory activities of phenolic compounds isolated from Melipona beecheii honey," *Food and Agricultural Immunology*, vol. 28, no. 6, pp. 1424–1437, 2017.

[59] S. C.-C. Huang, B. Everts, Y. Ivanova et al., "Cell-intrinsic lysosomal lipolysis is essential for alternative activation of macrophages," *Nature Immunology*, vol. 15, no. 9, pp. 846–855, 2014.

[60] S. Machana, N. Weerapreeyakul, S. Barusrux, K. Thumanu, and W. Tanthanuch, "FTIR microspectroscopy discriminates anticancer action on human leukemic cells by extracts of *Pinus kesiya*; *Cratoxylum formosum* ssp. *pruniflorum* and melphalan," *Talanta*, vol. 93, pp. 371–382, 2012.

Review Article

Vhavenda Herbal Remedies as Sources of Antihypertensive Drugs: Ethnobotanical and Ethnopharmacological Studies

Gundo Mudau [ID], Samuel Odeyemi [ID], and John Dewar

Department of Life and Consumer Sciences, College of Agriculture and Environmental Sciences, University of South Africa, Johannesburg 1709, South Africa

Correspondence should be addressed to Samuel Odeyemi; odeyesw@unisa.ac.za

Hypertension is a dominant risk factor for the development of cardiovascular, kidney, and eye diseases. In Africa, it increasingly leads to hospitalisation and a strain on the public health system. However, rather than modern medicine, African traditional healers are the first choice for most South Africans. Therefore, this study is aimed at gathering information on herbal remedies traditionally used for the treatment of high blood pressure in Vhavenda, South Africa, and comparing this information with reports in the literature regarding plants used to manage high blood pressure. An ethnobotanical survey was carried out in Vhembe district and its environs with 53 herbalists and indigenous people aged between 36 and 66 years from January to October 2019 using a semistructured questionnaire. The plants were collected with each respondent; they were authenticated and kept in herbarium. A total of 51 different plants were mentioned as being most commonly used for hypertension treatment. Of these, 44 plants were identified, with those from the Fabaceae family followed by plants from the Celastraceae family being commonly mentioned. Of these, the *Elaeodendron transvaalense*, *Tabernaemontana elegans*, *Elephantorrhiza elephantina*, and *Aloe vossii* were commonly cited species. According to the literature data, most of the identified plants are yet to be scientifically investigated for the treatment of hypertension, whereas only preliminary investigations have been carried out on other plants, suggesting that these preliminary investigations may have highlight promising antihypertensive activities *in vitro* that are indicative of their potential as antihypertensive drugs. Therefore, there is a need to scientifically investigate the antihypertensive potentials of these plants as a potential source of antihypertensive treatment and compounds.

1. Introduction

Hypertension is increasing at an alarming rate as a major public health concern after infection with the human immunodeficiency virus (HIV) and tuberculosis (TB). It is becoming one of the common cardiovascular diseases and a major health concern worldwide [1]. The two types of hypertension viz systolic and diastolic, graded as to patient blood pressure (BP): grade I or mild (BP 140–159/90–99 mmHg), grade II or moderate (BP 160–179/100–109 mmHg), and grades III and IV or severe (BP>180–210/110–120 mmHg) [2]. The exact causes of high blood pressure are unknown, but several risk factors such as family history, smoking, extensive use of alcohol, being overweight or obese, high sodium intake, high sugar intake, or lack of physical activity have been linked to

the development of hypertension [3]. The incidence of hypertension has been reported mainly in individuals over 50 years in age, although there have been a few reports involving younger patients [4]. There are also reports that suggest that other conditions such as kidney failure, insulin resistance, atherosclerosis, cardiovascular diseases, and nervous system problems cause or exacerbate high blood pressure [5, 6]. There are different treatment regimens for hypertension, but these are associated with side effects, and hence, there is still a need for alternative treatment modalities. In this regard, different societies have their own systems in place to maintain and restore well-being, including traditional medicine that are of great importance as research has shown that their therapeutic properties are associated with secondary plant metabolites which treat the disease

effectively with fewer or no side effects compared to the use of synthetic drugs [7].

A recent report suggests that more than three quarters of the world population depends on traditional medicine [8]. In Africa, the use of traditional medicine is popular due to trust and belief in its efficacy and dissatisfaction shown towards modern medicine [9]. Traditional medicine was in existence in Africa long before western medicine, and it is believed to link with "ubuntu," connecting the patient to the land and to embrace nature [10]. Thus, traditional medicine is an integral and important part of the African heritage with this system developed by the society and passed on from one generation to the next in various forms [11, 12].

In Africa, traditional healers are believed to heal the physical and psychospiritual unwellness of an individual, reflecting a holistic approach to healing and treatments [9, 13]. This has led to a dependence on traditional healers such that they provide health services to over 80% of the population in rural communities due to their accessibility and affordability, and they have become the first choice for treatment for many people [14–16]. The relatively small number of health facilities and the associated delays in processing and treatment have influenced rural communities in their choice of traditional medicine rather than modern health care [10, 17]. In Thailand, the government has developed a healing system called "traditional Thai medicine" involving a health policy designed to reduce the use of expensive modern medicines that is linked to a scientific approach of 4-year curricula for training programs that culminate in a bachelor's degree [18]. Zimbabwe has also taken the initiative where they have their own Traditional Medical Practitioner Act which integrates traditional and modern medicines [19]. The South African government is attempting to close the gap between modern medicine and traditional medicine by providing complementary and alternative health services [20, 21]. In 2007, the South African government passed the Traditional Health Practitioner Act No. 22 so that in May 2014, sections of this Act provided more autonomy to the Traditional Health Practitioner Council of South Africa [22–24]. In light of these developments, this study is aimed at documenting indigenous knowledge on the herbal remedies used by the people of Vhembe District, Thulamela, South Africa, for the treatment of hypertension.

2. Methods

2.1. Ethnobotanical Survey

2.1.1. The Study Area and Population. Vhembe is one of the five districts in the Limpopo Province, South Africa (SA), located in the far northern part of South Africa sharing borders with Zimbabwe and Mozambique. It covers a surface area of $25,596 \, km^2$ with a population of 1,393,949 in 2016 (Figure 1), is a predominantly rural, cultural hub, and is a catalyst for agricultural and tourism development [25, 26]. The Vhembe district consists of three ethnics groups with Thohoyandou as the capital. It is the former Tsonga homeland of Gazankulu with Hlanganani and Malamulele. It has a population of 800,000 Venda-speaking, 400,000 Tsonga-speak-

ing, and 27,000 Northern Sotho-speaking citizens [27]. Interviews with participants in this study were conducted at Thulamela municipality, Thohoyandou town which has a population of 618,462 and a growth rate of 0.62% (2001-2011) [27]. The study area falls into the category of villages with a high prevalence of hypertension.

2.1.2. Ethics Approval. Consent to enter Tshififi village was obtained from the headman of the Tshikalange Tribal Authority. This allowed the proposed study to proceed within the jurisdiction of Tshififi and nearby areas. In practice, the respondents were each provided with a consent form that was approved by the University of South Africa's Ethics Committee (REC Reference No. 2018/CAES/146) before the study was explained to them. Each respondent who agreed to participate in the study then signed the consent form before the interviews were conducted in the knowledge that their anonymity was assured. Collected plant samples were authenticated at the Horticulture center, University of South Africa, Science Campus, and the voucher specimen was deposited.

2.1.3. Data Collection. Since high blood pressure is a common health problem in the study area, the traditional healers were not asked for information on their diagnostic criteria. The survey was conducted during January and October 2019 and involved conducting face-to-face interviews with each respondent—in the local dialect where the respondent answered 12 open-end questions so that the researcher could collate demographic details of the traditional healers as well as the plants that they used to manage hypertension. The demographic information about each respondent included their age, gender, educational background, and locality. The information about the plants includes the vernacular names of the plants, parts used, methods of preparation of the recipes, route of administration, dosage, duration of treatment, and the management of other diseases for which the plants are used. The study relied on the recommendations of the headman, who identified the traditional healers and other qualified respondents.

2.1.4. Plant Collection and Identification. A good rapport was established between the researcher and the respondents and with their assistance; plant species were collected during several visits over the course of the study. The selected respondents were those often-assisting traditional healers in plant collection from their natural habitat. A broad approach was used to correctly identify collected plant materials. This involved (i) comparison against samples in the Unisa Herbarium, (ii) against data from the literature, and (iii) consultation with botanists from within the Unisa College of Agriculture and Environmental Science (CAES) laboratories, the Unisa Department of Life and Consumer Sciences, and the Unisa Horticulture Centre. Consulted data bases included the PlantZAfrica database (http://pza.sanbi.org/), SANBI infobases (https://www.sanbi.org/resources/infobases/), and Vhenda inventory [28]. The voucher specimens of all the collected plant species were deposited in the Herbarium at the University of South Africa, Science Campus.
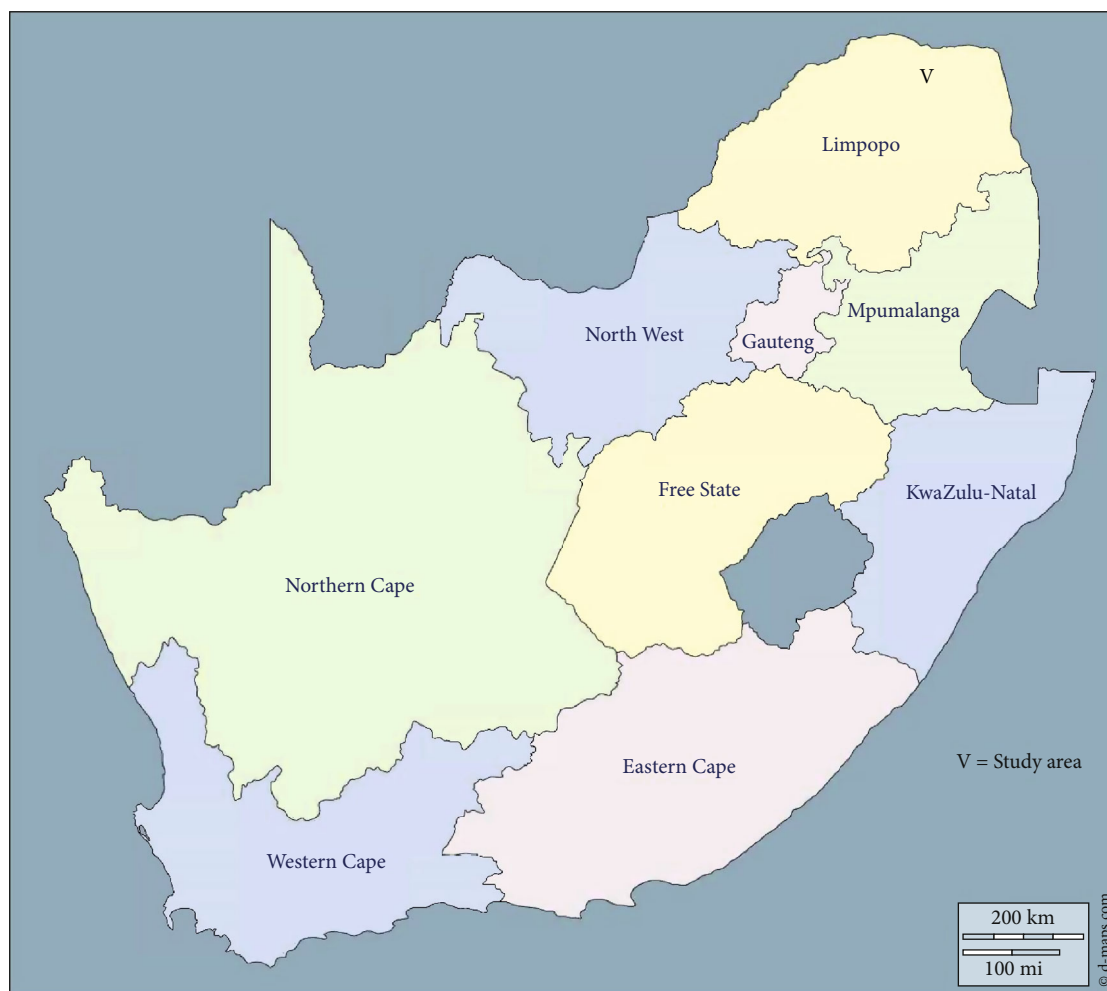
Figure 1: Study area: Vhembe district located in Limpopo province, South Africa.

2.1.5. Data Processing and Analysis. Data acquired from the questionnaire were uploaded onto a Microsoft Excel (365) spreadsheet and analyzed using both descriptive and inferential statistics. Percentages were used to analyse the respondents' sociodemographic data, and the relative frequency of citation (RFC) was used to determine the relative use of the plants.

(1) Relative Frequency of Citation (RFC). This was calculated using the formula:

$$RFC = \frac{Fc}{N}, \tag{1}$$

where Fc is the number of respondents who cited a species and N is the total number of the respondents. The RFC was used to determine the importance of a particular plant species ($0 < RFC < 1$).

2.2. Literature Review. ScienceDirect, PubMed, and Google Scholar databases were used to compare the literature reporting on medicinal plants showing antihypertensive activity against the data obtained in the survey. This was carried out using keywords (antihypertensive plants, ethnobotanical survey, medicinal plants, ethnomedicine, ethnobotany, herbal medicine, and treatment of hypertension). To obtain information on plants used in South Africa, the word "South Africa" was inserted and combined with the different keywords as indicated earlier.

3. Results

3.1. Ethnobotanical Survey

3.1.1. Demographic Information of the Participants and Their Knowledge of Hypertension. A total of 60 respondents were approached to participate in this study, and of these, 53 agreed to participate including 23 traditional healers. As shown in the sociodemographic data of the participants (Table 1), the participants were based across 11 villages, 47.2% of the participants were males and 52.8% were females. All of the participants spoke Tshivenda, and most worship the ancestors (92.5%). The majority of the participants (43.4%) were within the age range of 56 to 66 years suggesting that the older age groups are the custodians of traditional knowledge. About forty percent (39.6%) of the participants

TABLE 1: The sociodemographic information of the respondents.

Biodata	Sex		Religion		Age group (years)				Level of education				Income level	
	Females	Males	Ancestor worshipers	Christianity	36-45	46-55	56-66	>66	No formal education	Primary education	Secondary education	Tertiary education	Pensioners	Client based
Traditional healers	12	11	20	1	3	9	10	1	4	11	13	1	6	17
Other respondents	16	14	29	3	4	12	13	1	2	10	12	-	-	-
Percentage	52.8	47.2	92.5	7.5	13.2	39.6	43.4	3.8	11.3	39.6	47.2	1.9	26.1	73.9

had primary education, 47.2% secondary education, 1.9% tertiary education, and 11.3% had no formal education. None of the participants in this study was employed, and with the exception of one healer who used eight plant species and another who used 12 plant species, all of the participants used up to six plant species to treat hypertension. All the traditional healers that participated in this survey got their trainings through family knowledge particularly from ancestors.

3.1.2. Diversity of Plants Used for the Treatment of Hypertension.
The information on the medicinal plants used for traditional management of hypertension is presented in Table 2. A total of 51 plants species belonging to 30 families were reported as part of the hypertension treatment program in this study. The family distribution is shown in Figure 2. Members of the Fabaceae family were most commonly mentioned (10 times) followed by members of the Celastraceae family (3 times). Most of the plant parts used in the treatment decoction involved the roots, leaves, stems, and/or a combination of these parts (Figure 3). A decoction was prepared by drying, crushing, and soaked the plant part in water before a teacup of decoction was orally administered two or three times a day, while the majority (49%) of the respondents use the roots followed by the leaves with 40% usage (Figure 3).

3.1.3. Frequently Collected Plant Species.
The RFC value of each reported medicinal plant species was calculated and summarized (Table 2). The plants with 50% or more citations (RFC ≥ 0.5) were considered to be relatively important plants. In total, 3 plants were cited frequently by the respondents: Mukuvhazwivhi/Mulumanamana (*Elaeodendron transvaalense*), Muhatu (*Tabernaemontana elegans*), and Gumululo (*Elephantorrhiza elephantina*) with RFC values of 0.71, 0.52, and 0.52, respectively.

3.2. Analysis of Literature Review.
From the review of literature, 62 families comprising to 139 plant species were reportedly used for the treatment of hypertension and related symptoms (Suppl. Table 1). The Asteraceae ($n = 16$) is the most commonly reported family, followed by the Fabaceae ($n = 9$), Rutaceae ($n = 8$), Anacardiaceae ($n = 7$), and Lamiaceae ($n = 7$) with the indicated number of plant species, respectively. The plants that were frequently cited in the literature are *Psidium guajava* L., *Catharanthus roseus* (L.), *Citrullus lanatus* (Thunb.), *Agave americana* (L.), *Hypoxis hemerocallidea* (Fisch.), *Musa acuminata*, *Clausena anisata* (Willd.), and *Ruta graveolens*.

3.2.1. Comparative Analysis of the Ethnobotanical Survey with Literature Data.
Comparing the antihypertensive plants in the ethnobotanical research with data from the literature revealed that 14% have been reported from the medicinal plants in the survey as antihypertensives. Furthermore, there are similarities between the ethnobotanical survey and data from the literature in terms of the most frequently cited families. The Fabaceae is the dominantly represented family whereas the most frequently reported plant is the *C. sativa* both in the survey and literature data. In contrast, 88% of the plant species identified in the present survey have not

been reported previously in South Africa as antihypertensive plants. These newly reported plants include *Elaeodendron transvaalense*, *Tabernaemontana elegans*, and *Elephantorrhiza elephantina*.

3.2.2. Plant-Derived Compounds Reported for Antihypertensive Activity.
A quick summary obtained from the literatures clearly identified different classes of compounds. Some of these compounds have been evaluated for their antihypertensive activities using *in vitro* or *in vivo* assays belonging to different classes such as phenolics, flavonoids, glycosides, alkaloids, saponins, tannins, triterpenes, and peptides (Suppl. Table 1). Phenolics ($n = 44$) are the most commonly reported group of compounds identified with antihypertensive activities, followed by flavonoids ($n = 31$) and alkaloids ($n = 27$).

3.2.3. Reported Mechanisms of the Herbal Remedies and Extracts towards the Alleviation of Hypertension.
In the literature, most of the plants used for the management of hypertension carry out their antihypertensive activity through the inhibition of angiotensin-converting enzyme (ACE), reduction of oxidative stress, vasorelaxation via the nitric oxide-guanylyl cyclase pathway, and a prostaglandin-mediated mechanism as well as anti-inflammatory activities. Other reported mechanisms include the activation of the ATP-sensitive potassium channel, lowering of systolic blood pressure, EDRF-dependent or -independent pathways, endothelium-dependent vasorelaxation, a $\beta 1$ agonist effect and direct vasoconstrictive effect, lowering left ventricular systolic pressure, reduction of systemic blood pressure and heart rate, inhibition of oxytocin-induced contraction, nitric oxide and angiotensin II-like activities, redox-sensitive phosphorylation of eNOS via the PI3-kinase pathway, and inhibition of Na+ and K+ reabsorption. Supplementary Table 1 shows that 24 plants inhibit ACE only, and 38 plants possess both antioxidant and anti-inflammatory activities, while 59 plant species have not been investigated for their mechanism of action.

4. Discussion

4.1. Demographic Information.
As there were more females than males interviewed in the current survey, the predominance of women in relation to men can probably be ascribed to the involvement of men in other fields of work or the interview period such as when men were not at home. This is in agreement with the findings of a comparable study conducted in the Western Cape, South Africa [1], that reported a higher proportion of female over male respondents. The higher number of females to males in this study is similar to previous reports [1, 102, 103], but some authors also provided contrasting reports by suggesting that parents usually prefer to transfer indigenous knowledge to boys [104]. It will be fair to say that not all the respondents are traditional healers, so women being traditionally caretakers of the family's health may have impacted their knowledge on medicinal plants that exceed those of men. However, the predominance of women to men as the custodian of traditional

TABLE 2: Ethnobotanical information of plants used by traditional healers to treat hypertension.

Family	Local name	Botanical name	Part(s) used/collected	Voucher number	Mode of preparation	Route of administration	RFC	Plant growth form	Relevant reported disease treated or use
Anacardiaceae	Muadaba/Mulivhadza	Lannea schweinfurthii Engl.	Roots	GVM-017	Ground	Drinking	0.33	Tree	High blood pressure, snake bite, diarrhoea, fever, and malaria [29]
Anacardiaceae	Munungumaswi	Ozoroa reticulata (baker f.) R. & A. Fern. subsp.	Roots	GVM-024	Ground	Drinking	0.09	Shrub	Diarrhoea, stomach pain, vaginal and oral candidiasis, malaria, aphrodisiac, and cholera [30]
Annonaceae	Muvhulavhusiku	Xylopia odoratissima Welw. Ex Oliv.	Roots	GVM-039	Ground	Drinking	0.09	Tree	Infertility, stomach ache, diabetes, abdominal ulcers, fever, epilepsy, and angina [31, 32]
Apocynaceace	Munadzi	Rauvolfia caffra Sond	Leaves	GVM-030	Ground	Drinking	0.24	Tree	Tumour, sexually transmitted infections, anxiety, psychosis, schizophrenia, insanity, insomnia, and epilepsy [33–36]
Apocynaceae	Muhatu	Tabernaemontana elegans Stapf	Roots	GVM-034	Ground & fresh leaves soaked	Drinking & added to soft porridge	0.52	Tree	Cancer, chest pain, tuberculosis, venereal diseases, wounds, and menorrhagia [37, 38]
Asphodelaceae	Tshikhopha/Tshikopa	Aloe vossii Reynolds	Leaves	GVM-002	Ground	Drinking	0.47	Shrub	No record
Asteraceae	Mushidzhi	Bidens Pilosa L.	Leaves	GVM-004	Ground	Drinking	0.09	Shrub	Fever, malaria, inflammation, hyperemesis gravidarum (morning sickness), wounds, intestinal worms, otitis, dysentery/bacillary dysentery, constipation, Colics, and cancer [39–41]
Brassicaceae	Muobadali	Capparis tomentosa Lam.	Roots	GVM-009	Ground	Drinking	0.28	Shrub	Headache, mental disorder, snake bites, chest pains, impotency, and barrenness [42, 43]
Cactaceae	Mudoro	Opuntia ficus-indica (L.) Mill.	Bark	GVM-022	Ground	Drinking	0.09	Shrub	Weight control, diabetes, hypertension, asthma, ulcers, rheumatic pain, wounds, and fatigue [44, 45]
Canellaceae	Mulanga	Warburgia salutaris (G.Bertol.) Chiov.	Leaves	GVM-037	Ground	Drinking	0.09	Tree	Bronchial infections, oral thrush, cystitis, coughs, colds, tuberculosis, influenza, sinus, and other respiratory complaints [46–48]
Cannabaceae	Mbanzhe	Cannabis sativa L.	Leaves and stem	GVM-008	Ground	Drinking	0.18	Tree	Sprue syndrome, sterility, impotency, diarrhoea, indigestion, epilepsy, insanity, colic pain, and diabetes [49, 50]

Table 2: Continued.

Family	Local name	Botanical name	Part(s) used/collected	Voucher number	Mode of preparation	Route of administration	RFC	Plant growth form	Relevant reported disease treated or use
Celastraceae	Malambamapikwa	Elachyptera parvifolia (Oliv.) N. Hallé	Roots	GVM-013	Ground	Drinking	0.09	Shrub	Limited data
Celastraceae	Mukuvhazwivhi/Mulumanamana	Elaeodendron transvaalense R.H.Archer	Bark	GVM-014	Ground& fresh leaves soaked	Drinking	0.71	Shrub	Diabetes, coughs, diarrhoea, stomach ailments, herpes, and sexually associated diseases [51–53].
Celastraceae	Mukwatikwati	Mystroxylon aethiopicum (Thunb.) Loes.	Bark and root	GVM-040	Ground	Drinking	0.09	Tree	Haemorrhagic diarrhoea, infectious diseases, and magic [28, 54]
Chrysobalanaceae	Muvhula	Parinari curatellifolia planch. ex Benth	Roots	GVM-026	Ground	Drinking	0.24	Tree	Hypertension, diabetes and liver-related illnesses [55, 56]
Combretaceae	Mufhatelathundu	Combretum zeyheri Sond.	Roots	GVM-010	Ground	Drinking	0.09	Tree	Tumours or diarrhoea, hypertension, and even cancer [57]
Cucurbitaceae	Nyapiringuhule	Momordica boivinii Baill.	Roots	GVM-020	Ground	Drinking	0.09	Shrub	Spiritual ailments, stomach problem [58, 59]
Ebenaceae	Mukwatikwati	Euclea linearis Zeyh. Ex Hiern	Roots	GVM-016	Ground	Drinking	0.09	Shrub	Malaria [60]
Euphorbiaceae	Masunungule	Croton gratissimus Burch.	Leaves	GVM-011	Ground	Drinking	0.09	Tree	Coughs, chest complaints, coughs, fever, sexually transmitted diseases, skin care, and perfumery [61, 62]
Fabaceae	Muangaila	Millettia stuhlmannii Taub.	Roots	GVM-019	Ground	Drinking	0.09	Tree	Stomachache and protection of homesteads and properties [63]
Fabaceae	Muvhambangoma	Albizia versicolor Oliv	Leaves and roots	GVM-001	Ground	Drinking	0.09	Tree	Venereal diseases, coughs, joint pains, tapeworms, fever, diarrhoea, and sores [64–66]
Fabaceae	Mufhulu	Burkea africana Hook.	Leaves	GVM-007	Ground	Drinking	0.09	Tree	Headache, migraine, dizziness, pain, inflammation, thrush, tooth ache, heavy menstruation, abdominal pain, inflammation, and pneumonia [67, 68]
Fabaceae	Gumululo	Elephantorrhiza elephantina (Burch.) Skeels	Leaves and roots	GVM-015	Ground & fresh leaves soaked	Drinking	0.52	Shrub	Dysentery, diarrhoea, coughing, pneumonia, chest complaints, heart conditions, hypertension, stomach ailments, syphilis, infertility in women, waist pain in infants, fever, haemorrhoids, aphrodisiac, and emetic to mitigate the anger of the ancestors [69, 70]

Table 2: Continued.

Family	Local name	Botanical name	Part(s) used/collected	Voucher number	Mode of preparation	Route of administration	RFC	Plant growth form	Relevant reported disease treated or use
Fabaceae	Muhataha	*Pterocarpus rotundifolius* (Sond.) Druce	Roots	GVM-028	Ground	Drinking	0.09	Tree	Anemia, venereal, kidney diseases, and fertility in cows [14, 71]
Fabaceae	Mutsheketsheke	*Senna didymobotrya* (Fresen). H.S Irwin & Barneby	Aerial parts	GVM-041	Ground	Drinking	0.19	Shrub	Fever, enteric problems, anthelmintic, and antifungal [72, 73]
Fabaceae	muḓuwaḓuwane	*Senna italica* Mill.	Leaf and root	GVM-042	Ground	Drinking	0.19	Shrub	Laxative, purgative, constipation, rheumatic, and intestinal disorders [74]
Fabaceae	Muyekeyeke	*Senna obtusifolia* (L.) H.S.Irwin & Barneby	Root	GVM-043	Ground	Drinking	0.19	Herb	Laxatives, treatment of scorpion stings, gingivitis, dysentery, diarrhoea, tremors, and for dark brown urine [75, 76]
Fabaceae	Mutsheketsheke	*Senna occidentalis* (L.) Link	Roots	GVM-032	Ground	Drinking	0.19	Shrub	Laxative, analgesic, expectorant, diuretic, anthelmintic, tuberculosis, gonorrhoea, urinary tract diseases, and liver diseases [77]
Fabaceae	Mukundulela	*Vigna vexillata* (L.) A.Rich.	Leaves	GVM-036	Ground	Drinking	0.09	Shrub	Food, cancer, cardiovascular diseases, and diabetes [78]
Hyacinthaceae	Tshiganama	*Drimia sanguinea* (Schinz) Jessop	Bulb	GVM-012	Ground	Drinking	0.09	Shrub	Candidiasis, common warts, condylomata acuminate, genital warts, syphilis, and yaws [79]
Icacinaceae	Galange	*Pyrenacantha kaurabassana* Baill.	Roots	GVM-029	Ground	Drinking	0.09	Shrub	Ulcers, diarrhoea, herpes, and HIV [80, 81]
Lamiaceae	Mukwatikwati	*Volkameria glabra* (E. Mey.) Mabb. & Y.W. Yuan	Leaf and root	GVM-044	Ground	Drinking	0.09	Tree	Limited information
Loganiaceae	Mukongovhoti	*Strychnos potatorum* L.f.	Leaves and roots	GVM-033	Ground	Drinking	0.24	Shrub	Inflammation, anemia, jaundice, gonorrhea, leucorrhoea, gastropathy, bronchitis, chronic diarrhoea, dysentery, strangury, renal and vesicle calculi, diabetes, burning sensation, dipsia, conjunctivitis, scleritis, ulcers, and some eye diseases [82, 83]

TABLE 2: Continued.

Family	Local name	Botanical name	Part(s) used/collected	Voucher number	Mode of preparation	Route of administration	RFC	Plant growth form	Relevant reported disease treated or use
Meliaceae	Museranga	*Melia azedarach* L.	Leaves	GVM-018	Ground	Drinking	0.09	Tree	Antidiarrhoeal, deobstruent, diuretic, anthelmintic, and constipating [84]
Moringaceae	Muringa	*Moringa oleifera* Lam.	Leaves	GVM-021	Ground	Drinking & added to soft porridge	0.33	Tree	Diabetes, tuberculosis, fever, stomach aches, ear infections, skin infections, lithiasis, hypertension, microbial, fungal viral infections, hepatotoxicity, inflammation, and fever. [85, 86]
Ochnaceae	Mutavhatsindi	*Brackenridgea zanguebarica* Oliv.	Roots	GVM-005	Ground	Drinking	0.09	Tree	Cause sterility in adults, warding off evil spirits, and protection from lightning strikes [87, 88]
Olacaeae	Tshitanzwatanzwa	*Ximenia americana* L.	Roots	GVM-038	Ground	Drinking	0.09	Shrub	Antiseptic, measles, jaundice, and headaches [89]
Phyllanthaceae	Munzere	*Bridelia micrantha* (Hochst.) Baill.	Bark	GVM-006	Ground	Drinking	0.24	Tree	Gastrointestinal ailments, painful joints, retained placenta, diabetes mellitus, syphilis, prehepatic jaundice, tape worm abdominal pain, conjunctivitis, headache, scabies, bloody diarrhoea, dysentery, emetic, wound infection, coughs, threadworms, tonic for children, sore eyes, epigastric pain, relief of headache, purgative diarrhoea, and worms [90, 91]
Rhamnaceae	Munie	*Berchemia discolor* (Klotzsch) Hemsl.	Leaves	GVM-003	Ground	Drinking	0.24	Tree	Malaria [92]
Rubiaceae	Sulesule	*Paederia bojeriana* (A.Rich. Ex DC.) Drake	Leaves	GVM-025	Ground & fresh leaves soaked	Drinking	0.09	Tree	No record
Rubiaceae	Mutondo	*Pterocarpus angolensis* DC	Leaves	GVM-027	Ground	Drinking	0.24	Tree	Diarrhoea, heavy menstruation, nose bleeding, headache, stomachache, schistosomiasis, sores, and skin problems [93, 94]
Santalaceae	Mupeta	*Osyris lanceolata* Hochst. & Steud.	Roots	GVM-023	Ground & fresh leaves soaked	Drinking	0.28	Shrub	Candidiasis, venereal diseases, styptic effects on wounds, menorrhagia, and infertility [95, 96]

TABLE 2: Continued.

Family	Local name	Botanical name	Part(s) used/collected	Voucher number	Mode of preparation	Route of administration	RFC	Plant growth form	Relevant reported disease treated or use
Tropaeolaceae	Bopa	*Tropaeolum majus* L.	Leaves	GVM-035	Ground	Drinking	0.09	Tree	Antidepressant, hypertension, constipation, asthma inflammation, and urinary tract infection [97–99]
Vitaceae	Mutumbulambudzana	*Rhoicissus tridentata* (L.f.) Wild & R.B. Drumm.	Roots	GVM-031	Ground	Drinking	0.09	Shrub	Helminths (worms) & inflammation, miscarriages, and diarrhoea [100, 101]
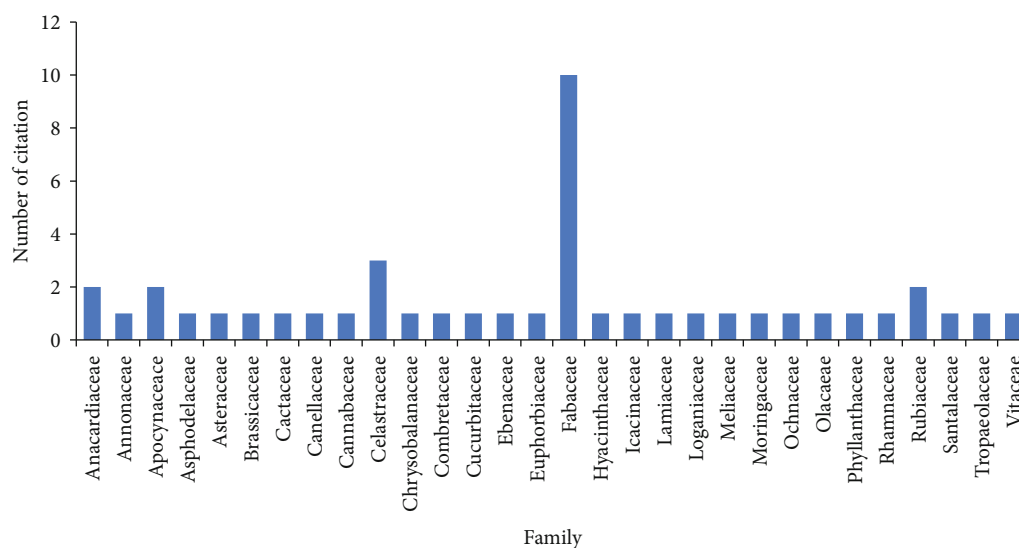
FIGURE 2: Distribution of use by traditional healers of plant families for the treatment of hypertension in the Vhembe district.
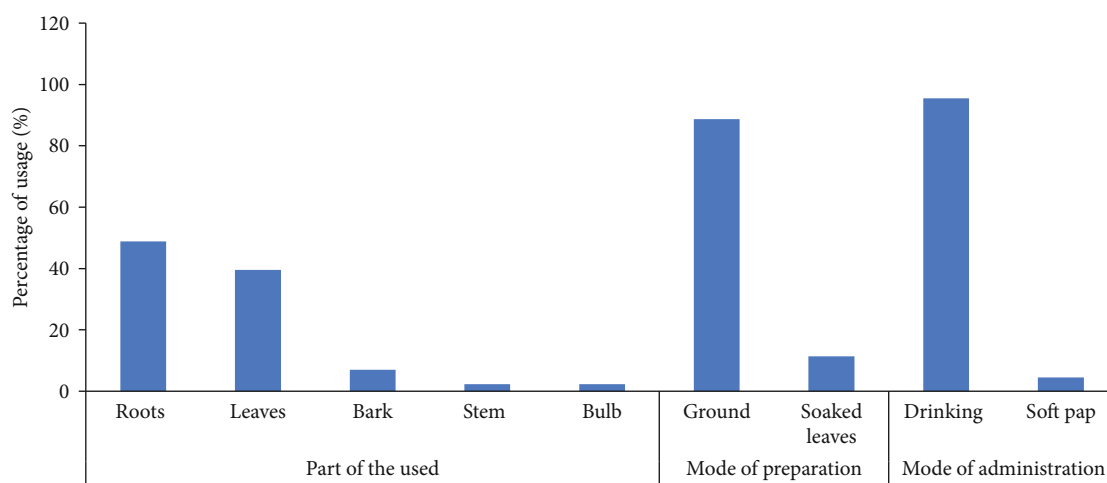
FIGURE 3: Plant parts as well as mode of preparation and administration of plants for use in treating hypertension.

knowledge varies according to the population under investigation in terms of their sociocultural characteristics. The higher percentage of ages between 55 and 66 years corroborates with previous reports suggesting that mainly adults and older people practice traditional medicine [103, 105, 106]. This study clearly shows the persistent gap in knowledge of herbal practice between the younger and older generations, suggesting the urgent need for documentation of this invaluable knowledge. Interestingly, the high education level of the informants and traditional healers in this study is enough to encourage the documentation of this knowledge or practice. This contrasts with reports that most traditional practitioners in Nigeria involved in maternal healthcare have no formal education [107].

4.2. Medicinal Plants Used in the Treatment of Hypertension. Most of the respondents in the present ethnobotanical survey mentioned medicinal plants belonging to the Fabaceae, Celastraceae, and Rubiaceae families. In other reports on the medicinal plants used for the treatment of hypertension, members of these families are often reported alongside with the Asteraceae and Rutaceae for use in the phytotherapy of various diseases including hypertension [50, 108–110]. In this study, the regular mention of the Fabaceae family is in agreement with previous reports on the plants used to manage hypertension [111–113]. This study also confirmed that the Fabaceae family is one of the plant families that is highly represented in the study area. The higher percentage usage of the roots and leaves is not uncommon and has been reported to be the preparation of herbal recipes in many other traditional medicines [114]. The reported findings in this study on the high frequency of leaves' use could be related to their visibility and ease of collection. The preparation of the leaves and roots in ground form for drinking is in agreement with surveys carried out in Ethiopia [115], Nigeria [116], Cameroon [117], and South Africa [108] suggesting that this is a common practice in traditional medicine. Most traditional healers may consider medicines that are milled in a mortar

to a powder to be more efficient, as the powdered form of the plant material enhances the extraction of the active ingredients. Improved extraction efficiency from a powder may be due to a specific increase in the surface area of powdered particles that improves extraction of the medicinally important plant compounds. The predominance of trees to shrubs and herbs is similar to the survey in Botswana [118] and contrasts with the results of a survey in parts of the Eastern Cape province of South Africa where the commonly used plant is a herb [119]. To the best of our knowledge, *Elaeodendron transvaalense* and *Tabernaemontana elegans* frequently used in this study have never been reported in an ethnobotanical survey or investigated for the treatment of hypertension. However, *Elephantorrhiza elephantina* is part of the treatment regimen used by the Bapedi people for treating hypertension [120]. *Elaeodendron transvaalense* is also used in traditional medicine by the Vhavenda people of South Africa in the treatment of stomach ailments, cancer, diarrhoea, coughs, herpes, skin infections, inflammations, rashes, HIV/AIDS, and other sexually transmitted diseases. A report has indicated the extraction from *E. transvaalense* of three triterpenoids lup-20(30)-ene-3α,29-diol, lup-20(29)-ene-30-hydroxy-3-one, and Ψ–taraxastanonol together with some polyphenols [52]. Extracts of the plant *Tabernaemontana elegans* are used as to wash wounds, treat heart and pulmonary diseases, chest pains, and cancer, and have been reported to contain monoterpene bisindole alkaloids, such as tabernaemontanine, dregamine, 16-epidregamine, tabernaelegantine C, tabernaelegantinine B, voacangine, and vobasine. In addition, the alkaloids from *T. elegans* have been reported to induce apoptosis in colon carcinoma cells and show antimicrobial activity [38, 121, 122].

4.3. Antihypertensive Herbal Medicine Preparations and Route of Administration.

This current study on plants used to treat hypertension reports mainly on single herbal preparations. Although there are reports on monocomponent recipes in traditional medicine, multiherbal preparations have also been reported [50, 108, 120]. Furthermore, the reported medicinal plants reported here are commonly used in the management of other disease conditions such as diabetes, cancer, sexually transmitted infections, tuberculosis, fever, skin infection, and sexual problems [2, 50, 114, 115, 117, 118, 121, 123]. In this study, the preparation of the medicinal recipes was by decoction and administered orally.

4.4. Analysis of the Literature Data Compared with the Survey.

A review of the literature for plants used to treat hypertension in South Africa identified a large number of medicinal species ($n = 139$), and some of these plants have also been reported elsewhere for the treatment of hypertension. In South Africa, the most frequently cited plants are *Psidium guajava*, *Catharanthus roseus*, *Citrullus lanatus*, *Agave americana*, *Hypoxis hemerocallidea*, *Musa acuminata*, *Clausena anisata*, *Ruta graveolens*, *Lantana camara*, *Trichilia emetica*, *Leonotis leonurus*, *Ballota africana*, *Momordica charantia*, and *Cannabis sativa* [124–129]. For instance, *Psidium guajava* with the highest citation is also commonly used in other parts of the world such as India, Mexico, Nige-

ria, and Spain for the management of hypertension [124, 125, 129]. Comparison of the survey results with the literature data shows that the majority of the medicinal plants reported from the survey have not been previously reported for the treatment of hypertension. Although they appear in the inventory of plants used by the people of Vhenda, these plants have not been identified as antihypertensives [28]. This study indicates the multipurpose usage of medicinal plants and the dominance of the Fabaceae family of plants as an essential component of traditional medicine. With more than 490 species, the Fabaceae family is the second largest family of medicinal plants currently being used in traditional medicine. The family has been reported to show different medicinal potentials including antioxidant, antidiabetic, antibacterial, cytotoxic, and antihypertensive properties [130, 131]. In parallel to the data reported in the current study, the possible mechanisms for the antihypertensive properties of the Fabaceae family may involve the PI3-kinase/PKB/Akt pathway, inhibition of ACE and/or antioxidant properties [130].

4.4.1. Plant Species in the Survey Previously Investigated for Their Antihypertensive Properties.

The antihypertensive activity of *Opuntia ficus*–indica Mill. was reported among Zulu medicinal plants where the aqueous leaf extract inhibited the activity of ACE *in vitro* [132]. Other investigations on *O. ficus*–indica have indicated antihypercholesterolemic, antihyperlipidemic, anti-inflammatory, and antioxidant activities perhaps due to the presence of phenolics and flavonoid compounds [133]. *R. caffra*, also known as quinine tree, is a fast-growing tree predominantly found in Africa. It is traditionally used for the treatment of hypertension, cough, stomach ailments, wounds, and diarrhoea [36]. Antihypertensive activity associated with this plant was shown by a reduction in the systolic and diastolic blood pressure in spontaneously hypertensive rats [134]. The high blood pressure lowering effect has been linked to the presence of reserpine [135]. The cultivation for food of *Cannabis sativa* L. also known as hemp has been limited due to the presence of the psychoactive compound (tetrahydrocannabinol). However, a peptide isolated from the hemp seed has been reported to show antioxidant and antihypertensive activities through the inhibition of ACE [136].

4.4.2. Toxicity Report.

One of the traditional healers confirmed the warning that there is a need to carefully consider the use of Senna plant seeds in traditional remedies as the seeds of *Senna occidentalis* could be lethal [137]. The oral administration to rats of *Elephantorrhiza elephantina* extract was reported to lead to a decrease in their respiratory rate [123]. However, a report [52] confirmed that the use of *Elaeodendron transvaalense* showed few side effects. A report indicated that the extracts of *D. sanguinea* induced cardiac glycoside poisoning in sheep [138]. Foetidin, isolated from member of the Cucurbitaceae, has been reported to be toxic to certain cell lines [52]. Crude methanol and dichloromethane extracts of *S. didymobotrya* roots were reported to be toxic after a period of 14 days, killing 80% of mice at

a dose of 5000 mg/kg body weight with an LD_{50} of 1927 mg/kg [103].

5. Conclusion

Traditional knowledge is sacred and is jealously guided. As a result, the Vhavenda people of South Africa have developed their own traditional way of treating hypertension. The present survey documented medicinal plants belonging to 30 families that are used for the treatment of hypertension and other diseases. Since the traditional healers in the study area use combinations of plants to treat hypertension, the efficacy of the treatment may be due to an ability to treat a broad spectrum of conditions such as bacterial infection, malaria, oxidative stress, and inflammation. This efficacy, together with the beneficial interaction between the healer and patient, may result in a psychosomatic improvement in the patient that combines to reduce blood pressure. However, according to the literature review, most of these plants have not been reported or investigated for their antihypertensive activity. This study will assist in the identification of useful plants. Also, these plants need to be investigated and their bioactive compounds isolated, to contribute to the discovery of new, effective, and affordable antihypertensive drugs.

Data Availability

All the data used to support the findings of this study are included within the articles, and the plant samples are available at the University of South Africa, Florida Campus.

Conflicts of Interest

The authors declare that they have no conflicts of interest.

Supplementary Materials

Supplementary Table 1: ethnopharmacological details of reported medicinal plants used by traditional healers in South Africa. (Supplementary Materials)

References

[1] D. Davids, D. Gibson, and Q. Johnson, "Ethnobotanical survey of medicinal plants used to manage high blood pressure and type 2 diabetes mellitus in Bitterfontein, Western Cape Province, South Africa," Journal of Ethnopharmacology, vol. 194, pp. 755–766, 2016.

[2] K. Malik, M. Ahmad, R. W. Bussmann et al., "Ethnobotany of anti-hypertensive plants used in northern Pakistan," Frontiers in Pharmacology, vol. 9, p. 789, 2018.

[3] M. Eddouks, M. Maghrani, A. Lemhadri, M.-L. Ouahidi, and H. Jouad, "Ethnopharmacological survey of medicinal plants used for the treatment of diabetes mellitus, hypertension and cardiac diseases in the south-east region of Morocco (Tafilalet).," Journal of Ethnopharmacology, vol. 82, no. 2–3, pp. 97–103, 2002.

[4] S. R. Tee, X. Y. Teoh, W. A. Aiman, A. Aiful, C. S. Har, and Z. F. Tan, "The prevalence of hypertension and its associated risk factors in two rural communities in Penang, Malaysia," International e-Journal of Medical Science and Education, vol. 4, no. 2, pp. 27–40, 2010.

[5] M. E. Hall, J. M. do Carmo, A. A. da Silva, L. A. Juncos, Z. Wang, and J. E. Hall, "Obesity, hypertension, and chronic kidney disease," International Journal of Nephrology and Renovascular Disease, vol. 7, pp. 75–88, 2014.

[6] J. R. Petrie, T. J. Guzik, and R. M. Touyz, "Diabetes, hypertension, and cardiovascular disease: clinical insights and vascular mechanisms," The Canadian Journal of Cardiology, vol. 34, no. 5, pp. 575–584, 2018.

[7] D. Van Rooyen, B. Pretorius, N. M. Tembani, and W. ten Ham, Curationis, vol. 38, no. 2, 2015DENOSA, 2015.

[8] O. Oyebode, N. Kandala, P. J. Chilton, and R. J. Lilford, "Use of traditional medicine in middle-income countries: a WHO-SAGE study," Health Policy and Planning, vol. 31, no. 8, pp. 984–991, 2016.

[9] M. Ashu Agbor and S. Naidoo, "Ethnomedicinal plants used by traditional healers to treat oral health problems in Cameroon," Evidence-Based Complementary and Alternative Medicine, vol. 2015, Article ID 649832, 10 pages, 2015.

[10] A. M. Agbor and S. Naidoo, "A review of the role of African traditional medicine in the management of oral diseases," African Journal of Traditional, Complementary and Alternative Medicines, vol. 13, no. 2, pp. 133–142, 2016.

[11] B. Güler, E. Manav, and E. Uğurlu, "Medicinal plants used by traditional healers in Bozüyük (Bilecik–Turkey)," Journal of Ethnopharmacology, vol. 173, pp. 39–47, 2015.

[12] V. Nanadagopalan, M. J. Gritto, and A. Doss, "An ethnobotanical survey of medicinal plants used by local traditional healers of Thiruvengimalai, Tiruchirapalli district, Tamil Nadu, southern India," Asian Journal of Pharmaceutical Science & Technology, vol. 5, no. 3, pp. 156–159, 2015.

[13] M. G. Hewson, "Integrating indigenous knowledge with science teaching," in Embracing Indigenous Knowledge in Science and Medical Teaching, pp. 119–131, Springer, 2015.

[14] T. E. Tshikalange, B. C. Mophuting, J. Mahore, S. Winterboer, and N. Lall, "An ethnobotanical study of medicinal plants used in villages under Jongilanga Tribal Council, Mpumalanga, South Africa," African Journal of Traditional, Complementary and Alternative Medicines, vol. 13, no. 6, pp. 83–89, 2016.

[15] C. C. Asuzu, T. Elumelu-Kupoluyi, M. C. Asuzu, O. B. Campbell, E. O. Akin-Odanye, and D. Lounsbury, "A pilot study of cancer patients' use of traditional healers in the Radiotherapy Department, University College Hospital, Ibadan, Nigeria," Psycho-Oncology, vol. 26, no. 3, pp. 369–376, 2017.

[16] C. M. Audet, J. Salato, M. Blevins et al., "Occupational hazards of traditional healers: repeated unprotected blood exposures risk infectious disease transmission," Tropical Medicine & International Health, vol. 21, no. 11, pp. 1476–1480, 2016.

[17] K. C. Chinsembu, "Ethnobotanical study of medicinal flora utilised by traditional healers in the management of sexually transmitted infections in Sesheke District, Western Province, Zambia," Revista Brasileira de Farmacognosia, vol. 26, no. 2, pp. 268–274, 2016.

[18] K. Maneenoon, C. Khuniad, Y. Teanuan et al., "Ethnomedicinal plants used by traditional healers in Phatthalung Province, Peninsular Thailand," Journal of Ethnobiology and Ethnomedicine, vol. 11, no. 1, p. 43, 2015.

[19] T. Ngarivhume, C. I. E. A. van't Klooster, J. T. V. M. de Jong, and J. H. Van der Westhuizen, "Medicinal plants used by

traditional healers for the treatment of malaria in the Chipinge district in Zimbabwe," *Journal of Ethnopharmacology*, vol. 159, pp. 224–237, 2015.

[20] C. W. Musyimi, V. N. Mutiso, E. S. Nandoya, and D. M. Ndetei, "Forming a joint dialogue among faith healers, traditional healers and formal health workers in mental health in a Kenyan setting: towards common grounds," *Journal of Ethnobiology and Ethnomedicine*, vol. 12, no. 1, p. 4, 2016.

[21] O. Esan, J. Appiah-Poku, C. Othieno et al., "A survey of traditional and faith healers providing mental health care in three sub-Saharan African countries," *Social Psychiatry and Psychiatric Epidemiology*, vol. 54, no. 3, pp. 395–403, 2019.

[22] Government Gazette No 30660, *Traditional Health Practitioners Act 22 of 2007*, Department of Health, Government Printing Works, 2008.

[23] G. Louw and A. Duvenhage, "Are there 200,000 and more traditional healers practicing in South Africa?," *Australasian Medical Journal*, vol. 9, no. 12, pp. 498–505, 2016.

[24] B. Tshehla, "Traditional health practitioners and the authority to issue medical certificates," *South African Medical Journal*, vol. 105, no. 4, p. 279, 2015.

[25] S. A. Motadi, X. G. Mbhenyane, H. V. Mbhatsani, N. S. Mabapa, and R. L. Mamabolo, "Prevalence of iron and zinc deficiencies among preschool children ages 3 to 5 y in Vhembe district, Limpopo province, South Africa," *Nutrition*, vol. 31, no. 3, pp. 452–458, 2015.

[26] Municipalities of South Africa, "Vhembe District Municipality (DC34)," *Municipalities of South Africa*, 2017, 2019, https://municipalities.co.za/services/129/vhembe-district-municipality.

[27] Statistics South Africa, "Local Municipality | Statistics South Africa," 2011, 2019, http://www.statssa.gov.za/?page_id=993&id=thulamela-municipality.

[28] K. Magwede, B.-E. van Wyk, and A. E. van Wyk, "An inventory of Vhavenḓa useful plants," *South African Journal of Botany*, vol. 122, pp. 57–89, 2019.

[29] A. Maroyi, "Review of ethnomedicinal, phytochemical and pharmacological properties of Lannea schweinfurthii (Engl.) Engl.," *Molecules*, vol. 24, no. 4, p. 732, 2019.

[30] S. M. Maregesi, O. D. Ngassapa, L. Pieters, and A. J. Vlietinck, "Ethnopharmacological survey of the Bunda district, Tanzania: plants used to treat infectious diseases," *Journal of Ethnopharmacology*, vol. 113, no. 3, pp. 457–470, 2007.

[31] N. A. F. Fernandes, L. I. N. Canelo, D. I. M. D. de Mendonça, and A. J. G. de Mendonça, "Acetylcholinesterase inhibitory activity of extracts from Angolan medicinal plants," *International Journal of Pharmacognosy and Phytochemical Research*, vol. 7, no. 4, pp. 768–776, 2015.

[32] S. Suzana Augustino, J. B. Hall, F. B. S. Makonda, and R. C. Ishengoma, "Medicinal resources of the Miombo woodlands of Urumwa, Tanzania: plants and its uses," *Journal of Medicinal Plants Research*, vol. 5, no. 27, pp. 6352–6372, 2011.

[33] A. M. A. G. Nasser and W. E. Court, "Stem bark alkaloids of rauvolfia caffra," *Journal of Ethnopharmacology*, vol. 11, no. 1, pp. 99–117, 1984.

[34] S. Bindu, K. B. Rameshkumar, B. Kumar, A. Singh, and C. Anilkumar, "Distribution of reserpine in Rauvolfia species from India – HPTLC and LC–MS studies," *Industrial Crops and Products*, vol. 62, pp. 430–436, 2014.

[35] T. E. Tshikalange, J. J. M. Meyer, and A. A. Hussein, "Antimicrobial activity, toxicity and the isolation of a bioactive compound from plants used to treat sexually transmitted diseases," *Journal of Ethnopharmacology*, vol. 96, no. 3, pp. 515–519, 2005.

[36] T. K. Milugo, L. K. Omosa, J. O. Ochanda et al., "Antagonistic effect of alkaloids and saponins on bioactivity in the quinine tree (Rauvolfia caffra sond.): further evidence to support biotechnology in traditional medicinal plants," *BMC Complementary and Alternative Medicine*, vol. 13, no. 1, p. 285, 2013.

[37] C. Pallant and V. Steenkamp, "In-vitro bioactivity of Venda medicinal plants used in the treatment of respiratory conditions," *Human & Experimental Toxicology*, vol. 27, no. 11, pp. 859–866, 2008.

[38] T. A. Mansoor, P. M. Borralho, S. Dewanjee, S. Mulhovo, C. M. P. Rodrigues, and M. J. U. Ferreira, "Monoterpene bisindole alkaloids, from the African medicinal plant Tabernaemontana elegans, induce apoptosis in HCT116 human colon carcinoma cells," *Journal of Ethnopharmacology*, vol. 149, no. 2, pp. 463–470, 2013.

[39] A. P. Bartolome, I. M. Villaseñor, and W.-C. Yang, "Bidens pilosa L. (Asteraceae): botanical properties, traditional uses, phytochemistry, and pharmacology," *Evidence-Based Complementary and Alternative Medicine*, vol. 2013, Article ID 340215, 51 pages, 2013.

[40] T. V. N. Thien, V. H. T. Huynh, L. K. T. Vo et al., "Two new compounds and α-glucosidase inhibitors from the leaves of Bidens pilosa L.," *Phytochemistry Letters*, vol. 20, pp. 119–122, 2017.

[41] F. Oliveira, V. Andrade-Neto, A. Krettli, and M. G. Brandão, "New evidences of antimalarial activity of Bidens pilosa roots extract correlated with polyacetylene and flavonoids," *Journal of Ethnopharmacology*, vol. 93, no. 1, pp. 39–42, 2004.

[42] O. Akoto, I. V. Oppong, I. Addae-Mensah, R. Waibel, and H. Achenbach, "Isolation and characterization of dipeptide derivative and phytosterol from Capparis tomentosa Lam," *Scientific Research and Essay*, vol. 3, no. 8, pp. 355–358, 2008.

[43] G. H. Tekulu, T. Hiluf, H. Brhanu, E. M. Araya, H. Bitew, and T. Haile, "Anti-inflammatory and anti-nociceptive property of Capparis tomentosa Lam. root extracts," *Journal of Ethnopharmacology*, vol. 253, p. 112654, 2020.

[44] E. Salehi, Z. Emam-Djomeh, G. Askari, and M. Fathi, "Opuntia ficus indica fruit gum: extraction, characterization, antioxidant activity and functional properties," *Carbohydrate Polymers*, vol. 206, pp. 565–572, 2019.

[45] U. Osuna-Martínez, J. Reyes-Esparza, and L. Rodríguez-Fragoso, "Cactus (Opuntia ficus-indica): a review on its antioxidants properties and potential pharmacological use in chronic diseases," *Natural Products Chemistry & Research*, vol. 2, no. 6, 2014.

[46] G. P. Khumalo, N. J. Sadgrove, S. Van Vuuren, and B.-E. Van Wyk, "Antimicrobial activity of volatile and non-volatile isolated compounds and extracts from the bark and leaves of Warburgia salutaris (Canellaceae) against skin and respiratory pathogens," *South African Journal of Botany*, vol. 122, pp. 547–550, 2019.

[47] E. L. Kotina, B.-E. Van Wyk, and P. M. Tilney, "Anatomy of the leaf and bark of Warburgia salutaris (Canellaceae), an important medicinal plant from South Africa," *South African Journal of Botany*, vol. 94, pp. 177–181, 2014.

[48] T. Rabe and J. van Staden, "Isolation of an antibacterial sesquiterpenoid from Warburgia salutaris," *Journal of Ethnopharmacology*, vol. 73, no. 1–2, pp. 171–174, 2000.

[49] E. B. Russo, "Cannabis and epilepsy: an ancient treatment returns to the fore," *Epilepsy & Behavior*, vol. 70, Part B, pp. 292–297, 2017.

[50] S. Odeyemi and G. Bradley, "Medicinal plants used for the traditional management of diabetes in the Eastern Cape, South Africa: pharmacology and toxicology," *Molecules*, vol. 23, 2018.

[51] M. S. S. Deutschländer, M. van de Venter, S. Roux, J. Louw, and N. Lall, "Hypoglycaemic activity of four plant extracts traditionally used in South Africa for diabetes," *Journal of Ethnopharmacology*, vol. 124, no. 3, pp. 619–624, 2009.

[52] T. E. Tshikalange and A. Hussein, "Cytotoxicity activity of isolated compounds from Elaeodendron transvaalense ethanol extract," *Journal of Medicinal Plants Research*, vol. 4, no. 16, pp. 1695–1697, 2010.

[53] G. P. Khumalo, N. J. Sadgrove, S. F. Van Vuuren, and B.-E. Van Wyk, "Antimicrobial lupenol triterpenes and a polyphenol from Elaeodendron transvaalense, a popular southern African medicinal bark," *South African Journal of Botany*, vol. 122, pp. 518–521, 2019.

[54] H. J. de Boer, A. Kool, A. Broberg, W. R. Mziray, I. Hedberg, and J. J. Levenfors, "Anti-fungal and anti-bacterial activity of some herbal remedies from Tanzania," *Journal of Ethnopharmacology*, vol. 96, no. 3, pp. 461–469, 2005.

[55] M. T. Olaleye, A. E. Amobonye, K. Komolafe, and A. C. Akinmoladun, "Protective effects of Parinari curatellifolia flavonoids against acetaminophen-induced hepatic necrosis in rats," *Saudi Journal of Biological Sciences*, vol. 21, no. 5, pp. 486–492, 2014.

[56] S. Ogbonnia, "Extracts of Mobola plum (Parinari curatellifolia Planch ex Benth, Chrysobalanaceae) seeds and multiple therapeutic activities," in *Nuts and Seeds in Health and Disease Prevention*, pp. 767–774, Academic Press, 2011.

[57] P. Fyhrquist, L. Mwasumbi, C.-A. Hæggström, H. Vuorela, R. Hiltunen, and P. Vuorela, "Ethnobotanical and antimicrobial investigation on some species of Terminalia and Combretum (Combretaceae) growing in Tanzania," *Journal of Ethnopharmacology*, vol. 79, no. 2, pp. 169–177, 2002.

[58] F. Tamiru, L. Adane, and B. Bekele, "Phytochemical screening of root extract of Momordica boivinii and isolation of two steroids," *Research Journal of Phytochemistry*, vol. 12, no. 1, pp. 21–34, 2018.

[59] M. Pakia, J. A. Cooke, and J. van Staden, "The ethnobotany of the Midzichenda tribes of the coastal forest areas in Kenya: 2. Medicinal plant uses," *South African Journal of Botany*, vol. 69, no. 3, pp. 382–395, 2003.

[60] K. C. Chinsembu, "Plants as antimalarial agents in sub-Saharan Africa," *Acta Tropica*, vol. 152, pp. 32–48, 2015.

[61] S. F. van Vuuren and A. M. Viljoen, "In vitro evidence of phyto-synergy for plant part combinations of Croton gratissimus (Euphorbiaceae) used in African traditional healing," *Journal of Ethnopharmacology*, vol. 119, no. 3, pp. 700–704, 2008.

[62] N. J. Sadgrove, L. G. Madeley, and B.-E. Van Wyk, "Volatiles from African species of Croton (Euphorbiaceae), including new diterpenes in essential oil from Croton gratissimus," *Heliyon*, vol. 5, no. 10, article e02677, 2019.

[63] M. Tshisikhawe, N. M. Siaga, and R. B. Bhat, "Population dynamics of Millettia stuhlmannii Taub. in Ha-Makhuvha, Vhembe district of Limpopo Province, South Africa," *Phyton*, vol. 80, pp. 127–132, 2011.

[64] K. C. Chinsembu, A. Hijarunguru, and A. Mbangu, "Ethnomedicinal plants used by traditional healers in the management of HIV/AIDS opportunistic diseases in Rundu, Kavango East Region, Namibia," *South African Journal of Botany*, vol. 100, pp. 33–42, 2015.

[65] N. C. Dlova and M. A. Ollengo, "Traditional and ethnobotanical dermatology practices in Africa," *Clinics in Dermatology*, vol. 36, no. 3, pp. 353–362, 2018.

[66] G. M. Rukunga and P. G. Waterman, "Triterpenes of Albizia versicolor and Albizia schimperana stem barks," *Fitoterapia*, vol. 72, no. 2, pp. 188–190, 2001.

[67] J. P. Dzoyem and J. N. Eloff, "Anti-inflammatory, anticholinesterase and antioxidant activity of leaf extracts of twelve plants used traditionally to alleviate pain and inflammation in South Africa," *Journal of Ethnopharmacology*, vol. 160, pp. 194–201, 2015.

[68] E. Mathisen, D. Diallo, Ø. M. Andersen, and K. E. Malterud, "Antioxidants from the bark ofBurkea africana, an African medicinal plant," *Phytotherapy Research*, vol. 16, no. 2, pp. 148–153, 2002.

[69] O. O. Olaokun, A. E. Alaba, K. Ligege, and N. M. Mkolo, "Phytochemical content, antidiabetes, anti-inflammatory antioxidant and cytotoxic activity of leaf extracts of Elephantorrhiza elephantina (Burch.) Skeels," *South African Journal of Botany*, vol. 128, pp. 319–325, 2020.

[70] V. Maphosa, P. Masika, and B. Moyo, "Investigation of the anti-inflammatory and antinociceptive activities of *Elephantorrhiza elephantina* (Burch.) Skeels root extract in male rats," *African Journal of Biotechnology*, vol. 8, no. 24, 2009.

[71] N. Lall, A. Blom van Staden, S. Rademan et al., "Antityrosinase and anti-acne potential of plants traditionally used in the Jongilanga community in Mpumalanga," *South African Journal of Botany*, vol. 126, pp. 241–249, 2019.

[72] T. Anthoney Swamy, M. C. Ngule, K. Jackie, A. Edwin, and M. E. Ngule, "Evaluation of in vitro antibacterial activity in Senna didymobotrya roots methanolic-aqua extract and the selected fractions against selected pathogenic microorganisms," *International Journal of Current Microbiology and Applied Sciences*, vol. 3, no. 5, pp. 362–376, 2014.

[73] J. K. Mworia, C. M. Kibiti, M. P. Ngugi, and J. N. Ngeranwa, "Antipyretic potential of dichloromethane leaf extract of Eucalyptus globulus (Labill) and Senna didymobotrya (Fresenius) in rats models," *Heliyon*, vol. 5, no. 12, article e02924, 2019.

[74] Y. Dabai, A. Kawo, and R. M. Aliyu, "Phytochemical screening and antibacterial activity of the leaf and root extracts of Senna italica," *African Journal of Pharmacy and Pharmacology*, vol. 6, no. 12, 2012.

[75] I. Y. Sudi, D. M. Ksgbiya, E. K. Muluh, and A. Clement, "Nutritional and phytochemical screening of Senna obtusifolia indigenous to Mubi, Nigeria," *Advances in Applied Science Research*, vol. 2, no. 3, pp. 432–437, 2011.

[76] J. H. Doughari, A. M. El-Mahmood, and I. Tyoyina, "Antimicrobial activity of leaf extracts of Senna obtusifolia (L)," *African Journal of Pharmacy and Pharmacology*, vol. 2, no. 1, pp. 7–13, 2008.

[77] A. V. F. F. Teles, R. A. Fock, and S. L. Górniak, "Effects of long-term administration of Senna occidentalis seeds on the hematopoietic tissue of rats," *Toxicon*, vol. 108, pp. 73–79, 2015.

[78] K. Sowndhararajan, P. Siddhuraju, and S. Manian, "Antioxidant and free radical scavenging capacity of the underutilized

legume, Vigna vexillata (L.) A. Rich," *Journal of Food Composition and Analysis*, vol. 24, no. 2, pp. 160–165, 2011.

[79] J. A. Asong, P. T. Ndhlovu, N. S. Khosana, A. O. Aremu, and W. Otang-Mbeng, "Medicinal plants used for skin-related diseases among the Batswanas in Ngaka Modiri Molema District Municipality, South Africa," *South African Journal of Botany*, vol. 126, pp. 11–20, 2019.

[80] L. Boudesocque-Delaye, D. Agostinho, C. Bodet et al., "Antibacterial polyketide heterodimers from *Pyrenacantha kaurabassana* tubers," *Journal of Natural Products*, vol. 78, no. 4, pp. 597–603, 2015.

[81] J. J. Omolo, V. Maharaj, D. Naidoo et al., "Bioassay-guided investigation of the Tanzanian plant *Pyrenacantha kaurabassana* for potential anti-HIV-active compounds," *Journal of Natural Products*, vol. 75, no. 10, pp. 1712–1716, 2012.

[82] P. B. Mallikharjuna, L. N. Rajanna, Y. N. Seetharam, and G. K. Sharanabasappa, "Phytochemical studies of Strychnos potatorum L.f.- a medicinal plant," *E-Journal of Chemistry*, vol. 4, no. 4, pp. 510–518, 2007.

[83] E. Sanmugapriya and S. Venkataraman, "Studies on hepatoprotective and antioxidant actions of Strychnos potatorum Linn. seeds on CCl4-induced acute hepatic injury in experimental rats," *Journal of Ethnopharmacology*, vol. 105, no. 1–2, pp. 154–160, 2006.

[84] D. Sharma and Y. P. S. Dr, "Preliminary and pharmacological profile of Melia azedarach L.: an overview," *Journal of Applied Pharmaceutical Science*, vol. 3, no. 12, pp. 133–138, 2013.

[85] S. Suresh, A. S. Chhipa, M. Gupta et al., "Phytochemical analysis and pharmacological evaluation of methanolic leaf extract of Moringa oleifera Lam. in ovalbumin induced allergic asthma," *South African Journal of Botany*, vol. 130, pp. 484–493, 2020.

[86] I. Ngom, B. D. Ngom, J. Sackey, and S. Khamlich, "Biosynthesis of Zinc Oxide Nanoparticles Using Extracts of *Moringa Oleifera*: Structural & Optical Properties," *Materials Today: Proceedings*, 2020.

[87] S. E. Drewes and N. A. Hudson, "Brackenin, a dimeric dihydrochalcone from Brackenridgea zanguebarica," *Phytochemistry*, vol. 22, no. 12, pp. 2823–2825, 1983.

[88] S. E. Drewes, N. A. Hudson, R. B. Bates, and G. S. Linz, "Medicinal plants of Southern Africa. Part 1. Dimeric chalcone-based pigments from Brackenridgea zanguebarica," *Journal of the Chemical Society, Perkin Transactions 1*, pp. 2809–2813, 1987.

[89] G. F. Sousa Carvalho, L. K. Marques, H. G. Sousa et al., "Phytochemical study, molecular docking, genotoxicity and therapeutic efficacy of the aqueous extract of the stem bark of Ximenia americana L. in the treatment of experimental COPD in rats," *Journal of Ethnopharmacology*, vol. 247, p. 112259, 2020.

[90] T. A. Ngueyem, G. Brusotti, G. Caccialanza, and P. V. Finzi, "The genus Bridelia: a phytochemical and ethnopharmacological review," *Journal of Ethnopharmacology*, vol. 124, no. 3, pp. 339–349, 2009.

[91] E. Green, L. C. Obi, A. Samie, P. O. Bessong, and R. N. Ndip, "Characterization of n-Hexane sub-fraction of Bridelia micrantha (Berth) and its antimycobacterium activity," *BMC Complementary and Alternative Medicine*, vol. 11, no. 1, p. 28, 2011.

[92] Y.-W. Chin, L. K. Mdee, Z. H. Mbwambo et al., "Prenylated flavonoids from the root bark of Berchemia discolor, a Tanza-

[93] A. Samie, A. Housein, N. Lall, and J. J. M. Meyer, "Crude extracts of, and purified compounds from, *Pterocarpus angolensis*, and the essential oil of *Lippia javanica*: their in-vitro cytotoxicities and activities against selected bacteria and *Entamoeba histolytica*," *Annals of Tropical Medicine and Parasitology*, vol. 103, no. 5, pp. 427–439, 2013.

[94] A. Maroyi, "Traditional use of medicinal plants in south-central Zimbabwe: review and perspectives," *Journal of Ethnobiology and Ethnomedicine*, vol. 9, no. 1, p. 31, 2013.

[95] R. B. Mulaudzi, A. R. Ndhlala, M. G. Kulkarni, J. F. Finnie, and J. Van Staden, "Antimicrobial properties and phenolic contents of medicinal plants used by the Venda people for conditions related to venereal diseases," *Journal of Ethnopharmacology*, vol. 135, no. 2, pp. 330–337, 2011.

[96] N. A. Masevhe, L. J. McGaw, and J. N. Eloff, "The traditional use of plants to manage candidiasis and related infections in Venda, South Africa," *Journal of Ethnopharmacology*, vol. 168, pp. 364–372, 2015.

[97] A. C. Melo, S. C. A. Costa, A. F. Castro et al., "Hydroethanolic extract of Tropaeolum majus promotes anxiolytic effects on rats," *Revista Brasileira de Farmacognosia*, vol. 28, no. 5, pp. 589–593, 2018.

[98] C. Gomes, E. L. B. Lourenço, É. B. Liuti et al., "Evaluation of subchronic toxicity of the hydroethanolic extract of Tropaeolum majus in Wistar rats," *Journal of Ethnopharmacology*, vol. 142, no. 2, pp. 481–487, 2012.

[99] S. Valsalam, P. Agastian, M. V. Arasu et al., "Rapid biosynthesis and characterization of silver nanoparticles from the leaf extract of Tropaeolum majus L. and its enhanced in-vitro antibacterial, antifungal, antioxidant and anticancer properties," *Journal of Photochemistry and Photobiology B: Biology*, vol. 191, pp. 65–74, 2019.

[100] E. Green, A. Samie, C. L. Obi, P. O. Bessong, and R. N. Ndip, "Inhibitory properties of selected South African medicinal plants against Mycobacterium tuberculosis," *Journal of Ethnopharmacology*, vol. 130, no. 1, pp. 151–157, 2010.

[101] F. O. Orech and J. G. Schwarz, "Ethno-phytotherapeutic remedies used in meat, milk, and blood products by the Maasai people of Kenya," *South African Journal of Botany*, vol. 108, pp. 278–280, 2017.

[102] V. Urso, M. A. Signorini, M. Tonini, and P. Bruschi, "Wild medicinal and food plants used by communities living in Mopane woodlands of southern Angola: results of an ethnobotanical field investigation," *Journal of Ethnopharmacology*, vol. 177, pp. 126–139, 2016.

[103] R. Korir, C. Mutai, C. Kiiyukia, and C. Bii, "Antimicrobial activity and safety of two medicinal plants traditionally used in Bomet District of Kenya," *Research Journal of Medicinal Plant*, vol. 6, no. 5, pp. 370–382, 2012.

[104] S. Suleman, T. Beyene Tufa, D. Kebebe et al., "Treatment of malaria and related symptoms using traditional herbal medicine in Ethiopia," *Journal of Ethnopharmacology*, vol. 213, pp. 262–279, 2018.

[105] I. P. Dike, O. O. Obembe, and F. E. Adebiyi, "Ethnobotanical survey for potential anti-malarial plants in south-western Nigeria," *Journal of Ethnopharmacology*, vol. 144, no. 3, pp. 618–626, 2012.

[106] M. S. Traore, M. A. Baldé, M. S. T. Diallo et al., "Ethnobotanical survey on medicinal plants used by Guinean traditional

healers in the treatment of malaria," *Journal of Ethnopharmacology*, vol. 150, no. 3, pp. 1145–1153, 2013.

[107] S. Kankara, M. Ibrahim, M. Mustafa, and R. Go, "Ethnobotanical survey of medicinal plants used for traditional maternal healthcare in Katsina State, Nigeria," *South African Journal of Botany*, vol. 97, pp. 165–175, 2015.

[108] N. I. Mongalo and T. J. Makhafola, "Ethnobotanical knowledge of the lay people of Blouberg area (Pedi tribe), Limpopo Province, South Africa," *Journal of Ethnobiology and Ethnomedicine*, vol. 14, no. 1, p. 46, 2018.

[109] M. H. Yetein, L. G. Houessou, T. O. Lougbégnon, O. Teka, and B. Tente, "Ethnobotanical study of medicinal plants used for the treatment of malaria in plateau of Allada, Benin (West Africa)," *Journal of Ethnopharmacology*, vol. 146, no. 1, pp. 154–163, 2013.

[110] R. Muganga, L. Angenot, M. Tits, and M. Frédérich, "Antiplasmodial and cytotoxic activities of Rwandan medicinal plants used in the treatment of malaria," *Journal of Ethnopharmacology*, vol. 128, no. 1, pp. 52–57, 2010.

[111] S. D. Karou, T. Tchacondo, M. A. Djikpo Tchibozo et al., "Ethnobotanical study of medicinal plants used in the management of diabetes mellitus and hypertension in the central region of Togo," *Pharmaceutical Biology*, vol. 49, no. 12, pp. 1286–1297, 2011.

[112] H. E. Gbekley, S. I. D. Karou, G. Katawa et al., "Ethnobotanical survey of medicinal plants used in the management of hypertension in the maritime region of Togo," *African Journal of Traditional, Complementary and Alternative Medicines*, vol. 15, no. 1, pp. 85–97, 2018.

[113] F. Balogun and A. Ashafa, "A review of plants used in south African traditional medicine for the management and treatment of hypertension," *Planta Medica*, vol. 85, no. 4, pp. 312–334, 2019.

[114] A. A. Adeyemi, A. A. Gbolade, J. O. Moody, O. O. Ogbole, and M. T. Fasanya, "Traditional anti-fever Phytotherapies in Sagamu and Remo north districts in Ogun state, Nigeria," *Journal of Herbs Spices & Medicinal Plants*, vol. 16, no. 3–4, pp. 203–218, 2010.

[115] F. Mesfin, S. Demissew, and T. Teklehaymanot, "An ethnobotanical study of medicinal plants in Wonago Woreda, SNNPR, Ethiopia," *Journal of Ethnobiology and Ethnomedicine*, vol. 5, no. 1, p. 28, 2009.

[116] A. Gbolade, "Ethnobotanical study of plants used in treating hypertension in Edo state of Nigeria," *Journal of Ethnopharmacology*, vol. 144, no. 1, pp. 1–10, 2012.

[117] D. J. Simbo, "An ethnobotanical survey of medicinal plants in Babungo, Northwest Region, Cameroon," *Journal of Ethnobiology and Ethnomedicine*, vol. 6, no. 1, p. 8, 2010.

[118] D. Motlhanka and G. P. Nthoiwa, "Ethnobotanical survey of medicinal plants of Tswapong north, in eastern Botswana: a case of plants from Mosweu and Seolwane villages," *European Journal of Medicinal Plants*, vol. 3, no. 1, pp. 10–24, 2013.

[119] O. S. Olorunnisola, G. Bradley, and A. J. Afolayan, "Ethnobotanical information on plants used for the management of cardiovascular diseases in Nkonkobe Municipality, South Africa," *Journal of Medicinal Plants Research*, vol. 5, no. 17, pp. 4256–4260, 2011.

[120] S. S. Semenya and M. J. Potgieter, "Kirkia wilmsii: a Bapedi treatment for hypertension," *South African Journal of Botany*, vol. 100, pp. 228–232, 2015.

[121] C. A. Pallant, A. D. Cromarty, and V. Steenkamp, "Effect of an alkaloidal fraction of Tabernaemontana elegans (Stapf.) on selected micro-organisms," *Journal of Ethnopharmacology*, vol. 140, no. 2, pp. 398–404, 2012.

[122] A. Paterna, S. E. Gomes, P. M. Borralho, S. Mulhovo, C. M. P. Rodrigues, and M.-J. U. Ferreira, "Vobasinyl-Iboga Alkaloids from Tabernaemontana elegans: Cell Cycle Arrest and Apoptosis-Inducing Activity in HCT116 Colon Cancer Cells," *Journal of Natural Products*, vol. 79, no. 10, pp. 2624–2634, 2016.

[123] A. S. Odeyemi, G. Bradley, and S. Semenya, "Medicinal uses, phytochemistry and pharmacological properties of Elaeodendron transvaalense," *Nutrients*, vol. 11, no. 3, p. 545, 2019.

[124] E. Díaz-de-Cerio, V. Verardo, A. M. Gómez-Caravaca, A. Fernández-Gutiérrez, and A. Segura-Carretero, "Health effects of Psidium guajava L. leaves: an overview of the last decade," *International Journal of Molecular Sciences*, vol. 18, no. 4, 2017.

[125] R. M. P. Gutiérrez, S. Mitchell, and R. V. Solis, "Psidium guajava: a review of its traditional uses, phytochemistry and pharmacology," *Journal of Ethnopharmacology*, vol. 117, no. 1, pp. 1–27, 2008.

[126] R. B. Singh, S. S. Rastogi, N. K. Singh, S. Ghosh, S. Gupta, and M. A. Niaz, "Can guava fruit intake decrease blood pressure and blood lipids?," *Journal of Human Hypertension*, vol. 7, no. 1, pp. 33–38, 1993.

[127] E. Irondi, S. Agboola, G. Oboh, A. Boligon, M. Athayde, and F. Shode, "Guava leaves polyphenolics-rich extract inhibits vital enzymes implicated in gout and hypertension in vitro," *Journal of Intercultural Ethnopharmacology*, vol. 5, no. 2, pp. 122–130, 2016.

[128] J. Mensah, R. Okoli, A. Turay, and E. Ogie-Odia, "Phytochemical analysis of medicinal plants used for the management of hypertension by Esan people of Edo state, Nigeria," *Ethnobotanical Leaflets*, vol. 2009, no. 10, p. 7, 2009.

[129] A. O. Ademiluyi, G. Oboh, O. B. Ogunsuyi, and F. M. Oloruntoba, "A comparative study on antihypertensive and antioxidant properties of phenolic extracts from fruit and leaf of some guava (Psidium guajava L.) varieties," *Comparative Clinical Pathology*, vol. 25, no. 2, pp. 363–374, 2016.

[130] B. Huisamen, C. George, S. Genade, and D. Dietrich, "Cardioprotective and anti-hypertensive effects of Prosopis glandulosa in rat models of pre-diabetes: cardiovascular topics," *Cardiovascular Journal Of Africa*, vol. 24, no. 2, p. 10, 2013.

[131] J. P. Dzoyem, L. J. McGaw, and J. N. Eloff, "In vitro antibacterial, antioxidant and cytotoxic activity of acetone leaf extracts of nine under-investigated Fabaceae tree species leads to potentially useful extracts in animal health and productivity," *BMC Complementary and Alternative Medicine*, vol. 14, no. 1, p. 147, 2014.

[132] S. Ramesar, H. Baijnath, T. Govender, and I. Mackraj, "Angiotensin I-converting enzyme inhibitor activity of nutritive plants in KwaZulu-Natal," *Journal of Medicinal Food*, vol. 11, no. 2, pp. 331–336, 2008.

[133] N. el Imane Harrat, S. Louala, F. Bensalah, F. Affane, H. Chekkal, and M. Lamri-Senhadji, "Anti-hypertensive, anti-diabetic, hypocholesterolemic and antioxidant properties of prickly pear nopalitos in type 2 diabetic rats fed a high-fat diet," *Nutrition & Food Science*, vol. 49, no. 3, pp. 476–490, 2019.

[134] S. Mlala, O. Oyedeji, and B. Nkeh-Chungag, *Chemical Constituents and Biological Studies of Tagetes Minuta L. and Rauvolfia Caffra Sond*, University of Fort Hare, 2015.

[135] J. Kennedy and M. Thorley, "Pharmacognosy, phytochemistry, medicinal plants (2nd ed.)," *Carbohydrate Polymers*, vol. 42, no. 4, pp. 428-429, 2000.

[136] A. T. Girgih, R. He, S. Malomo, M. Offengenden, J. Wu, and R. E. Aluko, "Structural and functional characterization of hemp seed (Cannabis sativa L.) protein-derived antioxidant and antihypertensive peptides," *Journal of Functional Foods*, vol. 6, pp. 384–394, 2014.

[137] R. Mao, P. Xia, Z. He et al., "Identification of seeds based on molecular markers and secondary metabolites in Senna obtusifolia and Senna occidentalis," *Botanical Studies*, vol. 58, no. 1, p. 43, 2017.

[138] R. A. Schultz, T. S. Kellerman, and H. Van den Berg, "The role of fluorescence polarization immuno-assay in the diagnosis of plant-induced cardiac glycoside poisoning livestock in South Africa," *The Onderstepoort Journal of Veterinary Research*, vol. 72, no. 3, pp. 189–201, 2005.

Research Article

Fermented Wheat Germ Extract as a Redox Modulator: Alleviating Endotoxin-Triggered Oxidative Stress in Primary Cultured Rat Hepatocytes

Máté Mackei [ID],[1] **Júlia Vörösházi** [ID],[1] **Csilla Sebők** [ID],[1] **Zsuzsanna Neogrády** [ID],[1] **Gábor Mátis** [ID],[1] **and Ákos Jerzsele** [ID][2]

[1]*Division of Biochemistry, Department of Physiology and Biochemistry, University of Veterinary Medicine, István utca 2, H-1078 Budapest, Hungary*
[2]*Department of Pharmacology and Toxicology, University of Veterinary Medicine, István utca 2, H-1078 Budapest, Hungary*

Correspondence should be addressed to Máté Mackei; mackei.mate@univet.hu

Bioactive compounds such as benzoquinone derivates presented in fermented wheat germ extract (FWGE) have several positive effects on overall health status of humans and animals alike. Since available data regarding the antioxidant activity of FWGE are limited, the aim of our study was to investigate its effects on the cellular redox homeostasis applying primary hepatocyte cell cultures of rat origin. Cultures were challenged to lipopolysaccharide (LPS) treatment for 2 or 8 hours to trigger inflammatory response. Further, culture media were concomitantly supplemented with or without FWGE (Immunovet®, 0.1% and 1%). In order to monitor the metabolic activity of the cell cultures, CCK-8 test was applied, while reactive oxygen species (ROS) production was measured using Amplex Red method. Malondialdehyde concentration of culture media as a specific marker of lipid peroxidation and the activity of glutathione peroxidase in cell lysates were also determined to monitor the redox status of the cultures. Based on our findings, it can be concluded that FWGE did not show cytotoxic effects in any applied concentration in cell cultures. Furthermore, FWGE efficiently decreased cellular ROS production and lipid peroxidation rate in case of LPS-induced inflammatory response. However, without LPS treatment, higher concentration of FWGE increased the rate of both ROS and malondialdehyde synthesis. This observation may refer to the prooxidant activity of high dose FWGE, which is an important beneficial effect regarding tumor cells. However, in case of noninflamed hepatocytes, considering the results of glutathione peroxidase activity, the application of the product did not result in severe oxidative distress. In accordance with the abovementioned findings, FWGE as a redox modulator, applied in the appropriate concentration, can serve as a promising candidate in the supplementary therapy of patients suffering from various inflammatory diseases, decreasing the free radical generation, thus avoiding the occurrence of cytotoxic effects.

1. Introduction

Based on its various beneficial biological effects, fermented wheat germ extract (FWGE) is successfully used in human medicine, mainly in the supportive therapy of people suffering from cancer. Bioactive compounds—most importantly different benzoquinone derivates—found in FWGE provide significant anticancer effects by influencing several cellular molecular mechanisms [1]. The FWGE stimulates the immune response against tumor cells by decreasing the

MHC-I expression in the cell membrane and rendering cancer cells more effectively be recognized by natural killer (NK) cells [1]. In addition, FWGE increases tumor necrosis factor α (TNFα) production by macrophages, leading to improved immune response towards tumor cells, inhibition of angiogenesis, and increased apoptosis of the target cells [2]. Furthermore, FWGE is also able to increase interleukin 1α (IL-1α), IL-2, IL-5, and IL-6 levels [3], which are considered to be among the main regulatory molecules of the inflammatory response. Beyond its immunomodulatory effects, FWGE can

enhance oxidative stress in tumor cells, inducing cell destruction caused by the produced free radicals [4]. Moreover, it has the ability to affect the carbohydrate and nucleotide metabolism of cancer cells. As an example, by the inhibition of hexokinase enzyme, it is able to decrease cellular ATP production and hinder the synthesis of pentoses, which are necessary for cell division [5]. Besides, FWGE impedes the activity of ribonucleotide reductase enzyme, directly decelerating the production of nucleotides needed for the DNA synthesis [6]. As a result of all the mentioned effects, FWGE is able to effectively decrease the proliferation of several malignant tumor types and to increase the apoptosis of these cells. These findings were initially confirmed in studies on HT-29 colorectal adenocarcinoma and HL-60 leukaemia cell lines [2]. By virtue of the efficient antitumor activity of FWGE, slower tumor growth rate has been detected, resulting in longer life expectancy. The FWGE-triggered improvement of the general health condition and the successful prevention of cancer-associated cachexia can also contribute to the better prognosis [7]. The decreased velocity of tumor growth and metastasis formation was described in case of numerous forms of tumors, such as in melanoma, in neuroblastoma, and in different cervical, testicular, or thyroid cancer types [6].

With the modulation of cellular and humoral immune response, FWGE can serve as a considerable effector not just in point of its immunomodulatory activity towards the neoplastic cells but also as a result of its general immunostimulatory effects [6]. Significant enhancement of the immune response was detected in FWGE treated, beforehand immunosuppressed mice, mainly resulting from the effective induction of differentiation and blast transformation of lymphocytes [8]. Beyond these results, FWGE is capable to be used in different immune-mediated diseases and to resolve the immunosuppressive effects caused by cyclophosphamide treatment [6, 9]. Considerable anti-inflammatory activity of FWGE was also detected based on the inhibition of cyclooxygenase (COX) enzymes, successfully supporting the action of nonsteroidal anti-inflammatory drugs (NSAIDs) [7].

Regarding the potential antioxidant effects of FWGE, containing high concentration of bioactive free radical scavenger molecules, only limited data are available. It was reported to decrease the amount of reactive oxygen species (ROS) such as superoxide anion radicals [10]. However, further research is required concerning the antioxidant activity of FWGE.

Following its application in human medicine, FWGE was also introduced to veterinary practice for companion animals, and based on its immunostimulatory, anti-inflammatory, and suggested antioxidant effects, it can serve as a proper candidate for maintaining and improving the general health status of the patients [11]. The application of FWGE can be of high importance in case of elderly, debilitated animals, suffering in various chronic diseases [12]. Furthermore, applying FWGE in companion animals affected by neoplastic diseases may also be promising, based on its antitumor activity and its ability to improve general health condition. In addition, FWGE can be also effectively used as a natural growth promoter in chicken [11] and turkey [12], contributing to improved productivity and health conditions of farm animals. In accordance with its antimicrobial activity, FWGE is proved to be efficient to treat mycoplasma infection [13] and to mitigate the spreading of Salmonella Typhimurium in chicken; further, the efficiency of different applied vaccines can be also enhanced by dint of FWGE's immunostimulatory effects [14].

In spite of the above described effects—such as antitumor, immunostimulatory, anti-inflammatory, and antimicrobial activity—only limited data are available about the possible effects of FWGE on the antioxidant status of eukaryotic cells. Hence, in this present study, we aimed to investigate the effects of FWGE (Immunovet®) on the redox homeostasis as well as on the oxidative status of the liver. The investigations were carried out using primary hepatocyte cultures of rat origin, which model can be a proper tool to observe the exact molecular mechanisms on the cellular level. This *in vitro* study—applying rat as a widely used and accepted model animal in the research—can serve with relevant and valuable information about FWGE-induced alterations in farm and companion animals, moreover in humans.

2. Materials and Methods

All reagents used in the study were purchased from Sigma-Aldrich (Darmstadt, Germany), except when otherwise specified. Animal procedures described hereinafter were performed in strict accordance with the national and international law along with institutional guidelines and were confirmed by the Local Animal Welfare Committee of the University of Veterinary Medicine, Budapest, and by the Government Office of Pest County, Food Chain Safety, Plant Protection, and Soil Conservation Directorate, Budapest, Hungary.

2.1. Cell Isolation and Culturing Conditions. Isolation and culturing of primary rat hepatocytes were carried out based on our formerly developed and published method [15]. Briefly, hepatocyte isolation was performed using 8-week-old Wistar rats (approx. 200-250 g). Animals were kept and fed according to the actual Hungarian and European animal welfare laws. After carbon dioxide narcosis, median laparotomy was performed followed by the cannulation of the vena portae and the thoracic section of the vena cava caudalis. The liver was flushed and exsanguinated through the portal system, using different buffers and multistep perfusion. In order to recirculate the buffers, the effusing amount of the solutions was collected via the vena cava caudalis.

To perfuse the liver, 300 mL ethylene glycol tetraacetic acid (EGTA, 0.5 mM) containing Hanks' Balanced Salt Solution (HBSS) buffer, 200 mL EGTA-free HBSS buffer, and finally, 130 mL EGTA-free HBSS buffer, supplemented with 50 mg type IV collagenase (Serva, Duisburg, Germany), and 2.5 mM $CaCl_2$ and $MgCl_2$ were used.

During the liver perfusion, all of the applied buffers were warmed up to 40°C and oxygenated with Carbogen (95% O_2, 5% CO_2); the velocity was set to 30 mL/min. The collagenase containing buffer was recirculated until the complete disintegration of the liver parenchyma. After excision of the liver

and disruption of the capsule, cell suspension was filtered using sterile gauze sheets. Cell suspension was placed for 50 min into 25 mg/mL bovine serum albumin (BSA) containing ice-cold HBSS in order to avoid undesired cluster formation.

Hepatocytes were isolated using low speed multistep differential centrifugation (3 times, $100 \times g$, 2 min), and the gained pellets were resuspended in Williams' Medium E supplemented with 50 mg/mL gentamycin, 2 mM glutamine, 20 IU/L insulin, $4 \mu g/L$ dexamethasone, 0.22% $NaHCO_3$, and in the first 24 h of culturing with 5% foetal bovine serum (FBS).

After resuspendation, viability of hepatocytes was tested by trypan blue exclusion test, always exceeding 90%. The number of the cells was determined by cell counting in Bürker's chamber to further adjust the appropriate cell concentrations to 10^6 cells/mL. Hepatocytes were seeded onto 96- and 6-well Greiner Advanced TC cell culture dishes (Greiner Bio-One Hungary Kft., Mosonmagyaróvár, Hungary) previously coated with collagen type I ($10 \mu g/cm2$), using $200 \mu L$/well seeding volume in the 96-well plates and 2 mL/well in the 6-well plates. Cultures were incubated at 37°C and 100% relative air humidity. Cell culture media were changed after 4 h, and confluent monolayer cell cultures were gained after 24 h incubation (Figure 1).

2.2. Treatments of Cultured Cells.

After 24 h, culturing cells were treated using cell culture media supplemented with 0 (control) or $10 \mu g/mL$ Salmonella enterica serovar. Typhimurium derived lipopolysaccharide (LPS) for 2 and 8 h incubation time. Further, in both of the control and LPS-challenged cultures, subgroups were prepared using 0.1% and 1% FWGE prepared from Immunovet®, silymarin ($50 \mu g/mL$), or ursodeoxycholic acid (UDCA, $200 \mu g/mL$) containing cell culture medium. In the latter two cases, cultures were treated with proved hepatoprotective and antioxidant substances.

To gain the FWGE working solutions (Immunovet®), 1 g of FWGE granules was homogenized using a mortar until a fine powder was received and dissolved in 10 mL sterile phosphate buffered saline (PBS) solution. The gained stock solution (100 mg/mL; 10%) was filtered in different steps, using gauze sheets (3 layers, 2 times filtering), a cell strainer ($70 \mu m$ pore size), and a sterile filter ($0.22 \mu m$ pore size) in the end (Merck Millipore, Burlington, MA, USA). Stock solution (10%) was diluted with PBS to 1% and 0.1% concentrations.

On both of the 96- and 6-well plates, 6 replicates were prepared per one treatment group ($n = 6$). In case of the 6-well plates, following either 2 or 8 h incubation, samples were taken from the cell culture media. Thereafter, wells were washed with PBS, and cells were lysed using Mammalian Protein Extraction Reagent (M-PER™, Thermo Fisher Scientific, Waltham, MA, USA). All of the collected samples were stored until further analysis at −80°C.

2.3. Measurements of Cellular Metabolic Activity, Extracellular H_2O_2 and Malondialdehyde Concentrations, and Glutathione Peroxidase Activity.

Following the treat-
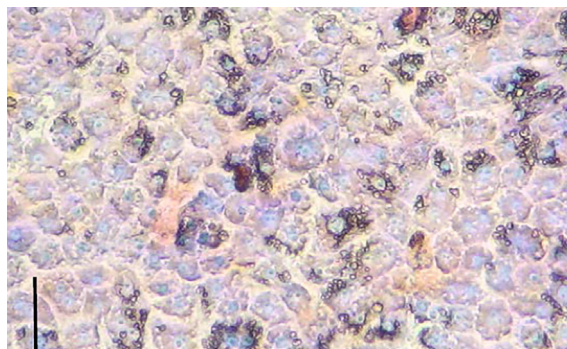
FIGURE 1: Primary hepatocyte cultures of rat origin after 24 h incubation. Giemsa staining, bar = 30 μm.

ments, metabolic activity of cells cultured on 96-well plates was checked using CCK-8 assay (Dojindo, Rockville, USA), monitoring the total amount of $NADH+H^+$ produced in the cellular catabolic reactions, successfully reflecting also to the potential cytotoxic effects. According to the manufacturer's instructions, $10 \mu L$ CCK-8 reagent and $100 \mu L$ Williams' Medium E were added to the cultured cells, and after 2 h of incubation at 37°C, the absorbance was measured at 450 nm with a Multiskan GO 3.2 reader (Thermo Fisher Scientific, Waltham, MA, USA).

Extracellular H_2O_2 concentration was detected in the culture medium using the fluorimetric Amplex Red method (Thermo Fisher Scientific, Waltham, MA, USA). After 30 min incubation of $50 \mu L$ freshly prepared, Amplex Red ($100 \mu M$) and HRP (0.2 U/mL) containing working solution with $50 \mu L$ culture medium at room temperature (21°C), fluorescence ($\lambda ex = 560$ nm; $\lambda em = 590$ nm) was detected using a Victor X2 2030 fluorometer (Perkin Elmer, Waltham, MA, USA).

Malondialdehyde (MDA) concentration as a marker of lipid peroxidation was monitored in cell culture media with a specific colorimetric test. According to the protocol, $300 \mu L$ freshly prepared thiobarbituric acid (TBA) stock solution was mixed with $100 \mu L$ cell culture media. Solutions were incubated at 95°C for 1 h followed by 10 min cooling on ice. Absorbance was measured at 532 nm with a Multiskan GO 3.2 reader (Thermo Fisher Scientific, Waltham, MA, USA).

As one of the most prominent members of the antioxidant defence system, activity of glutathione peroxidase enzyme of the cell lysates was also determined using a colorimetric kinetic assay. At first, GPx Assay Buffer was prepared according to the manufacturer's protocol, and $455 \mu L$ was mixed with $25 \mu L$ of NADPH Assay Reagent and $5 \mu L$ substrate solution (tert-butyl hyperoxide). The decrease of absorbance was continuously detected at 340 nm (initial delay: 15 sec; interval: 10 sec; number of readings: 6). Enzyme activity was calculated using the formula provided by the manufacturer.

2.4. Statistics.

All the data analysis was performed using the R 3.5.3. software (GNU General Public License, Free Software Foundation, Boston, MA, USA). On both of 96- and 6-well

plates, six wells were included in one treatment group. Normal distribution and homogeneity of variance were checked by Shapiro-Wilk test and Levene's test, respectively. Differences between various groups were assessed using one-way analysis of variance (ANOVA) and Tukey's post hoc tests for pairwise comparisons. Results were assessed as the mean ± standard error of the mean (SEM). Differences were assumed significant at $P < 0.05$. Results of the FWGE, silymarin, and UDCA treated groups were compared to the respective control groups (LPS free or LPS supplemented control groups). The effects of LPS supplementation were considered as main effect compared to the control groups without LPS treatment.

3. Results

3.1. Measurement of Cellular Metabolic Activity. Metabolic activity of the cultured cells was monitored using CCK-8 assay, indicating the cellular aerobe catabolic processes. According to our results, the majority of the applied treatments were not able to affect the metabolic activity of the cultures, except the observed significant decrease in case of the 2 h long 0.1% FWGE ($P = 0.016$; Figure 2(a)) exposure in the LPS challenged groups and the 8 h long silymarin and UDCA ($P = 0.029$ and $P < 0.001$; Figure 2(b)) treatments of LPS free control cells.

3.2. Measurement of H_2O_2 Production. The extracellular ROS production of the cells (H_2O_2 concentration in the cell culture media) was monitored with the Amplex Red method. ROS concentrations were elevated after both of the incubation times in the LPS treated groups (2 h incubation: $P = 0.0012$; 8 h incubation: $P = 0.036$; Figures 3(a) and 3(b)).

In cell cultures without LPS treatment, FWGE applied in 1% significantly increased ROS concentration of the cell culture media after both 2 h and 8 h incubation ($P < 0.001$ and $P = 0.007$, Figures 3(a) and 3(b)). Similarly to these findings, ROS production was significantly and tendentiously increased as a result of 2 h silymarin and UDCA treatments without LPS application (silymarin: $P = 0.014$; UDCA: $P = 0.058$; Figure 3(a)).

On the other hand, LPS triggered elevation of the ROS levels was significantly decreased applying both FWGE and silymarin supplementation after 8 h incubation (0.1% FWGE: $P = 0.020$; 1% FWGE: $P = 0.027$; silymarin: $P = 0.006$; Figure 3(b)).

3.3. Determination of Malondialdehyde Concentration. In order to monitor the lipid peroxidation processes in the cell cultures, MDA concentration was measured in the media after both incubation times. In the cells with no LPS treatment, FWGE applied in 1% concentration caused significantly higher MDA level after 2 h as well as 8 h incubation time (2 h: $P < 0.001$; 8 h: $P = 0.003$; Figures 4(a) and 4(b)). However, together with LPS treatment, 1% FWGE significantly decreased the production of MDA after both incubation times (2 h: $P < 0.001$; 8 h: $P = 0.044$; Figures 4(a) and 4(b)). Similarly to these findings, following 2 h of LPS exposure, FWGE applied in lower concentration as well as sily-

marin and UDCA treatment significantly decreased the MDA concentration of the cell culture supernatants (0.1% FWGE: $P = 0.018$, silymarin: $P = 0.004$, UDCA: $P < 0.001$; Figure 4(a)).

3.4. Measurement of Glutathione Peroxidase Activity. The activity of glutathione peroxidase enzyme of the lysed cells was monitored after 8 h incubation. As the effect of LPS challenge, enzyme activity was significantly elevated ($P < 0.001$; Figure 5.). Both of the applied FWGE concentrations along with the silymarin and UDCA incubation decreased the activity of glutathione peroxidase in the cell cultures without LPS treatment (0.1% FWGE, silymarin, and UDCA: $P < 0.001$; 1% FWGE: $P = 0.004$; Figure 5). In LPS exposed cells, only the UDCA treatment was able to decrease the activity of glutathione peroxidase enzyme in a significant manner ($P = 0.002$; Figure 5).

4. Discussion

In the present study, cellular effects of FWGE applied at different concentrations were investigated in cultured primary rat hepatocytes. FWGE is a standardized extract fermented by *Saccharomyces cerevisiae*, adjusted to a yield of 0.4 mg/g 2,6-dimethoxy-p-benzoquinone. The impact of FWGE on metabolic activity and redox homeostasis of cell cultures was monitored and analyzed in comparison with the potent hepatoprotective agents silymarin and UDCA. Applied concentrations of FWGE were set up based on the available literature data. In other studies, 1% FWGE (10 mg/mL) showed cytotoxic and cytostatic activity after 24 h incubation, while in case of pancreas and mammary tumors, it had cytotoxic effects already at 0.5% [4]. Further, higher sensitivity of tumorigenic cells does not necessarily correspond with the potential cytotoxic effects of FWGE in healthy, nontumorigenic cell types. However, considering the relatively higher vulnerability of primary hepatocyte cultures towards different toxic effects, in our study, FWGE was applied at 0.1% and 1% (1 and 10 mg/mL) concentrations. Dose of LPS (10 μg/mL) was determined previously in our studies regarding inflammatory processes using primary hepatocyte models [16], mimicking a severe inflammatory response. Incubation times (2 and 8 h) were also chosen in accordance with the similar investigations carried out in hepatocyte cell cultures, mimicking an acute and a subacute hepatic inflammation.

Cellular metabolic activity was monitored with the CCK-8 method. With the help of the assay, information can be gained regarding aerobe catabolic processes of biological oxidation by screening cellular NADH+H+ production. Based on our results, in case of LPS challenged cell cultures, a slightly but significantly decreased catabolic activity was detected in the samples treated with 0.1% FWGE (Figure 2(a)). This slight decrease presumably does not mean an intense cytotoxic effect but can refer to a rearrangement in the activity of different metabolic processes. Therefore, according to our findings, FWGE did not cause cytotoxic effects at 0.1 and 1% concentrations after 2 and 8 h
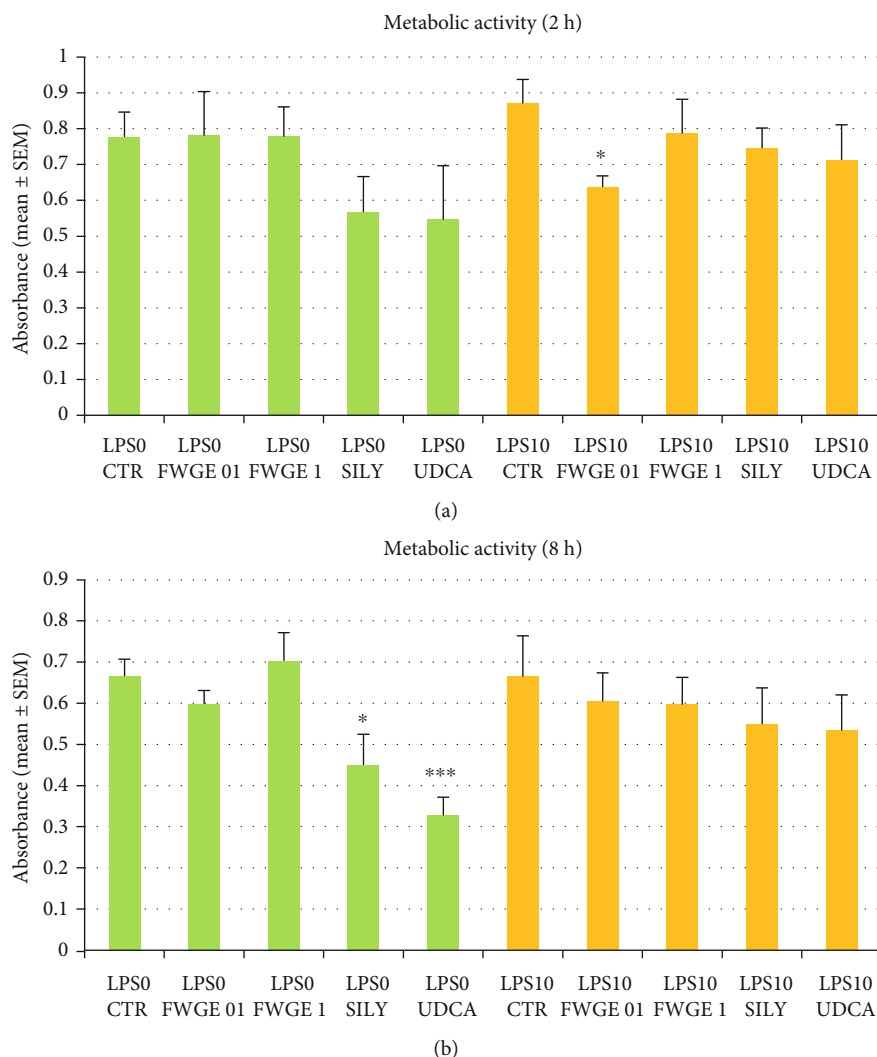
Figure 2: Metabolic activity of cultured cells after 2 h (a) and 8 h (b) incubation measured with the CCK-8 assay. LPS 0: cultures with no LPS exposure; LPS 10: LPS treated cultures ($10\,\mu g/mL$); FWGE 01: 0.1% FWGE; FWGE 1: 1% FWGE; SILY: silymarin ($50\,\mu g/mL$); UDCA: ursodeoxycholic acid ($200\,\mu g/mL$). Mean ± SEM, $^*P < 0.05$, $^{***}P < 0.001$.

incubation time in hepatocytes under normal physiological circumstances.

ROS production, as a key indicator of oxidative stress, was monitored by the determination of H_2O_2 concentration of the cell culture media. ROS production of LPS nontreated cultures was significantly elevated as the effect of 1% FWGE application after both 2 h and 8 h incubation (Figures 3(a) and 3(b)). This finding suggests that the application of FWGE at elevated concentrations may lead to oxidative stress in healthy hepatocytes not affected by inflammation. In contrast to these effects, in case of LPS challenged cultures, similarly to silymarin treatment, FWGE was capable to decrease the intensity of oxidative stress (Figure 3(b)). For this reason, based on our results, it can be stated that FWGE can show different effects on ROS production of healthy cells and cultures affected by severe inflammatory processes. Presumably, in the first scenario, it may have a mild prooxidant activity at high doses, while in the latter case, it can serve with relevant antioxidant effects. Depending on the applied con-

centration and other different factors, numerous investigations can be found in the literature referring the possibility of prooxidant effects of molecules considered as antioxidants. As an example, both pro- and antioxidant activities of flavonoids [17] or pyrroloquinoline quinone, applied widely as farm animal feed additive and redox modulator [18], were described under *in vitro* as well as *in vivo* conditions.

H_2O_2, investigated in our study, plays a multifaceted role in the regulation of the cellular redox homeostasis [19]. According to our recent knowledge, similarly to Ca^{2+}, ATP, or cAMP, H_2O_2 belongs to the group of main secondary messenger molecules [20]. Its increased concentration can lead to alterations of the cellular morphology and metabolism, decreasing or increasing cell proliferation; further, it is also involved in the activation of immune cells. It is of great importance that normal, well-regulated production of H_2O_2 is necessary for the development and maintenance of the so called oxidative eustress, resulting in beneficial physiological effects and efficacious cellular adaptation to different external
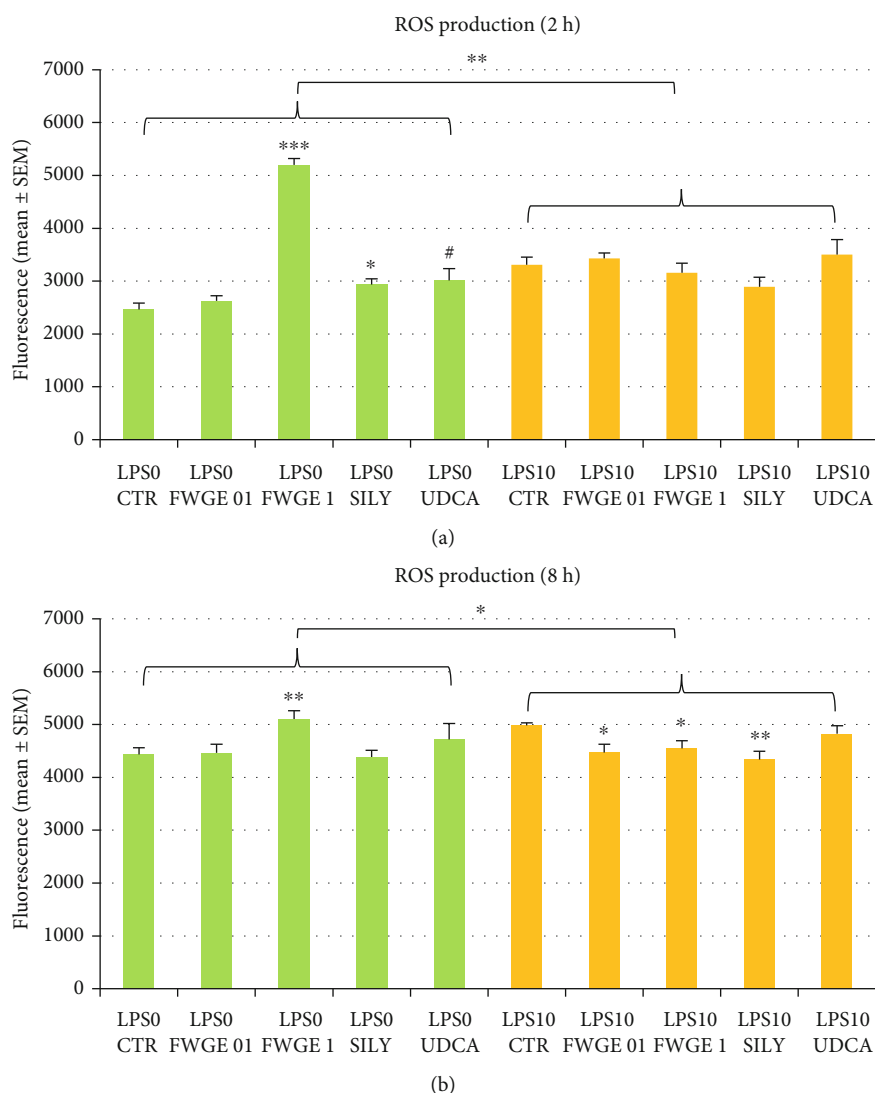
FIGURE 3: Extracellular ROS production of cell cultures after 2 h (a) and 8 h (b) incubation measured with the Amplex red method. LPS 0: cultures with no LPS exposure; LPS 10: LPS treated cultures ($10\,\mu$g/mL); FWGE 01: 0.1% FWGE; FWGE 1: 1% FWGE; SILY: silymarin ($50\,\mu$g/mL); UDCA: ursodeoxycholic acid ($200\,\mu$g/mL). Mean $\pm$ SEM, #$P < 0.10$, *$P < 0.05$, **$P < 0.01$, ***$P < 0.001$.

factors [19]. By this reason, elevated intensity of ROS production does not necessarily mean pathologic alterations of the cells as long as it is occurring within the confines of appropriately regulated and beneficial oxidative eustress. The presence of prooxidants can however contribute to the occurrence of oxidative distress, which can drive to cellular impairments such as the damage of DNA and proteins together with increased intensity of lipid peroxidation [19]. It is also an important aspect that the antitumor activity of FWGE is partially based on the prooxidant effect of the extract, since the increased H_2O_2 production and the therefore occurring oxidative distress entails the destruction of the cancer cells, resulting in slower growth and smaller tumor size [4].

Concerning the results of our study, FWGE administration in higher dose can supposedly increase ROS production of healthy liver cells; however, in case of inflammatory processes, application for a longer time, both in lower and higher

concentration, is able to decrease H_2O_2 production of cells, restoring the conditions of normal oxidative eustress. The presented data reminds to the importance of appropriate therapeutic dosage, avoiding the application of the antioxidants in too high concentration leading to prooxidant activity in healthy organisms.

One of the main consequences of the oxidative stress can be the increased cellular lipid peroxidation and the subsequent impairment of the cell membranes, resulting in the increment of membrane permeability. Lipid peroxidation was monitored by measuring the MDA concentration of cell culture media, which indicates the status of the cellular membranes. The FWGE administered in higher dose (1%) significantly increased MDA concentration, similarly to ROS production, in the LPS nontreated cultures mimicking healthy conditions after both incubation times (Figures 4(a) and 4(b)). In contrast, elevated MDA production in LPS triggered inflammation, in correlation with ROS production, was

Malondialdehyde concentration (2 h)

(a)

Malondialdehyde concentration (8 h)

(b)
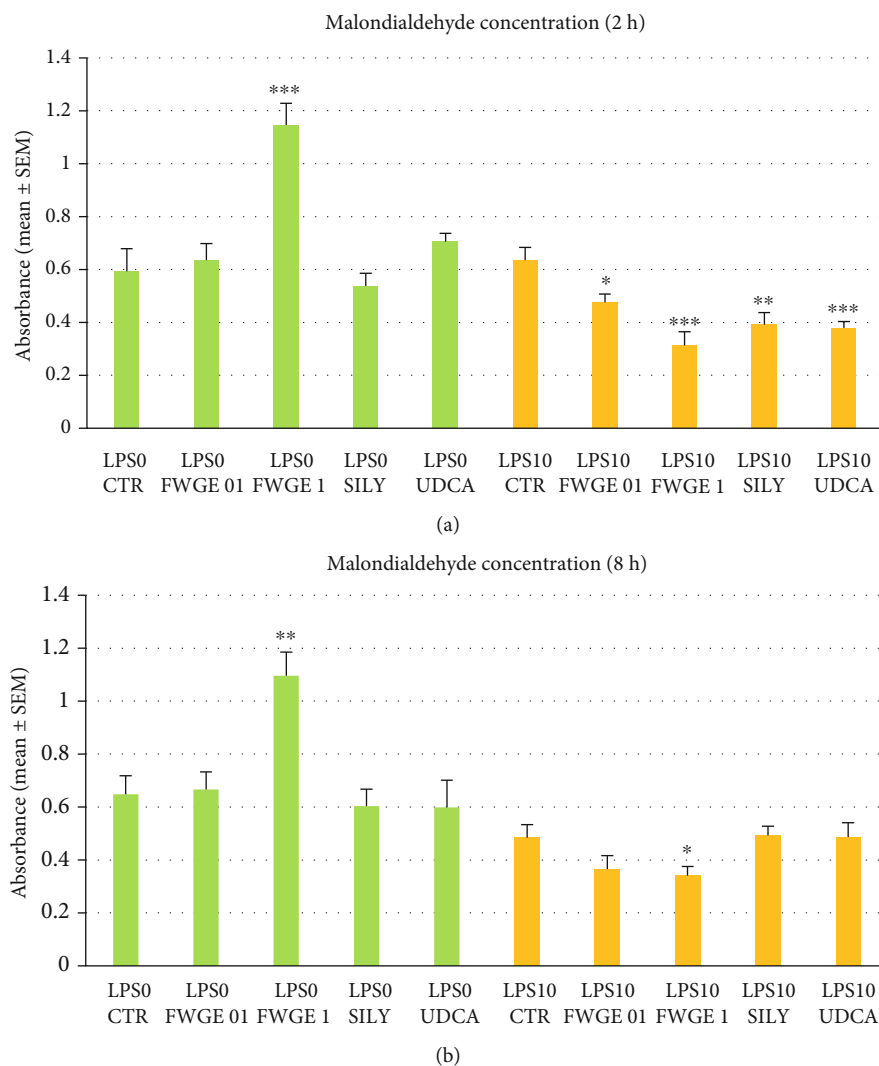
FIGURE 4: Malondialdehyde concentration measured in the cell culture media after 2 h (a) and 8 h (b) incubation. LPS 0: cultures with no LPS exposure; LPS 10: LPS treated cultures (10 μg/mL); FWGE 01: 0.1% FWGE; FWGE 1: 1% FWGE; SILY: silymarin (50 μg/mL); UDCA: ursodeoxycholic acid (200 μg/mL). Mean ± SEM, $^{*}P < 0.05$, $^{**}P < 0.01$, $^{***}P < 0.001$.

efficiently decreased when applying both FWGE concentrations after 2 h incubation and by 1% FWGE extract after 8 h incubation (Figures 4(a) and 4(b)). These results together with ROS production refer to the significance of appropriately chosen concentration of FWGE in order to avoid the adventitiously occurring prooxidant effects in normal, healthy circumstances. However, accordingly applied FWGE can serve as proper tool not only to remarkably decrease cellular free radical production but also to avoid the possible membrane damage caused by intense lipid peroxidation.

The function of the whole glutathione system was monitored with the applied glutathione peroxidase assay by assessing the NADPH+H^{+} amount needed for converting glutathione back to its reduced form by glutathione reductase. Glutathione is one of the most prominent antioxidants, oxidized by glutathione peroxidase enzyme, while taking part in the binding and inactivating of generated free radicals. With our measurements, we were able to achieve a more accurate picture regarding the function of the whole glutathione system, which—as a crucial intracellular antioxidant—refers to the oxidative status of the cells.

According to the present results, LPS treatment significantly increased the activity of the glutathione peroxidase (Figure 5), reflecting the more intense function and capacity of this antioxidant defence system due to the LPS provoked oxidative distress. Further, other studies showed similar results regarding the enhanced glutathione peroxidase enzyme activity observed in the liver of LPS challenged mice [21]. Similarly to silymarin and UDCA, FWGE was able to significantly reduce the activity of glutathione defence system in LPS nontreated cell cultures. The mildly decreased activity of the glutathione peroxidase caused by FWGE, indicating the overall oxidative status of the cells, suggests that the observed elevated ROS and MDA levels do not necessarily contribute to oxidative distress in noninflamed hepatocytes. In order to clarify possible species-specific differences,

Glutathione peroxidase activity (8 h)
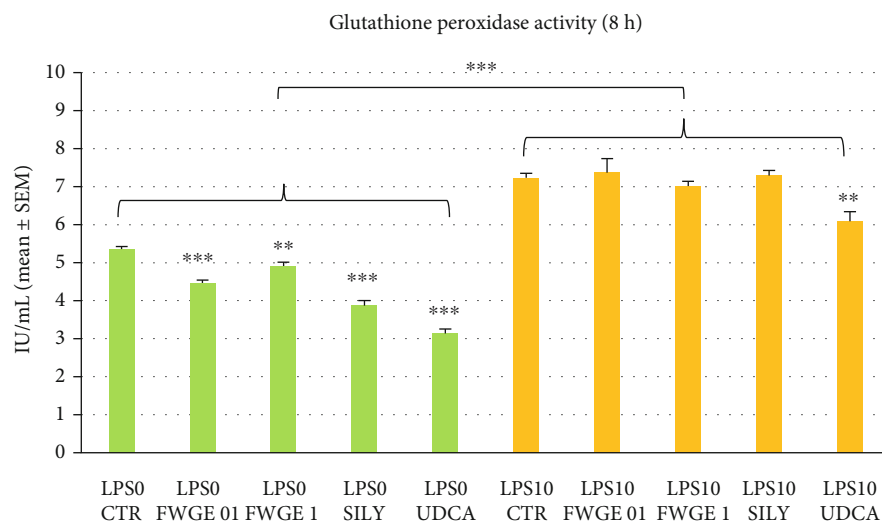
FIGURE 5: Glutathione peroxidase activity of the cultured cells after 8 h incubation. LPS 0: cultures with no LPS exposure; LPS 10: LPS treated cultures (10 μg/mL); FWGE 01: 0.1% FWGE; FWGE 1: 1% FWGE; SILY: silymarin (50 μg/mL); UDCA: ursodeoxycholic acid (200 μg/mL). Mean $\pm$ SEM, $^{**}P < 0.01$, $^{***}P < 0.001$.

further investigations using cell culture models of companion animal origin would be also beneficial in the future to observe the effects of FWGE in these target species.

5. Conclusions

Summarizing our results, it can be stated that the extract of FWGE containing Immunovet® product applied in well considered appropriate concentration did not possess cytotoxic effect in rat-derived primary hepatocyte cultures. The FWGE effectively decreased the ROS production of cultured cells and the consecutively occurring lipid peroxidation in case of LPS triggered inflammation in the applied *in vitro* hepatic model. Notwithstanding that the incidental prooxidant activity of FWGE in higher concentration is also remindful, it does not necessarily lead to oxidative distress. In conclusion, FWGE as a redox modulator can provide good possibilities in alleviating inflammation associated oxidative distress, preventing cell destruction and hence improving general health condition.

Data Availability

All relevant data analyzed during the current study are available from the corresponding author (mackei.mate@univet.hu) on request.

Conflicts of Interest

The authors declare that they have no conflict of interest.

Acknowledgments

References

[1] A. Iyer and L. Brown, "Fermented wheat germ extract (Avemar) in the treatment of cardiac remodeling and metabolic symptoms in rats," *Evidence-based Complementary and Alternative Medicine*, vol. 2011, Article ID 508957, 10 pages, 2011.

[2] T. Mueller and W. Voigt, "Fermented wheat germ extract - nutritional supplement or anticancer drug?," *Nutrition Journal*, vol. 10, no. 1, p. 89, 2011.

[3] A. Telekes, M. Hegedűs, C.-H. Chae, and K. Vékey, "Avemar (wheat germ extract) in cancer prevention and treatment," *Nutrition and Cancer*, vol. 61, no. 6, pp. 891–899, 2009.

[4] C. Otto, T. Hahlbrock, K. Eich et al., "Antiproliferative and antimetabolic effects behind the anticancer property of fermented wheat germ extract," *BMC Complementary and Alternative Medicine*, vol. 16, no. 1, 2016.

[5] L. G. Boros, K. Lapis, B. Szende et al., "Wheat germ extract decreases glucose uptake and RNA ribose formation but increases fatty acid synthesis in MIA pancreatic adenocarcinoma cells," *Pancreas*, vol. 23, no. 2, pp. 141–147, 2001.

[6] L. G. Boros, M. Nichelatti, and Y. Shoenfeld, "Fermented wheat germ extract (Avemar) in the treatment of cancer and autoimmune diseases," *Annals of the New York Academy of Sciences*, vol. 1051, no. 1, pp. 529–542, 2005.

[7] A. Telekes, A. Resetar, G. Balint et al., "Fermented wheat germ extract (Avemar) inhibits adjuvant arthritis," *Annals of the New York Academy of Sciences*, vol. 1110, no. 1, pp. 348–361, 2007.

[8] S. Patel, "Fermented wheat germ extract: a dietary supplement with anticancer efficacy," *Nutritional Therapy & Metabolism*, vol. 32, no. 2, pp. 61–67, 2014.

[9] M. Ehrenfeld, M. Blank, Y. Shoenfeld, and M. Hidvegi, "AVE-MAR (a new benzoquinone-containing natural product) administration interferes with the Th2 response in experimental SLE and promotes amelioration of the disease," *Lupus*, vol. 10, no. 9, pp. 622–627, 2016.

[10] M. Hidvégi, E. Rásó, R. Tömösközi-Farkas et al., "MSC, a new benzoquinone-containing natural product with antimetastatic effect," *Cancer Biotherapy and Radiopharmaceuticals*, vol. 14, no. 4, pp. 277–289, 1999.

[11] Á. Jerzsele, Z. Somogyi, M. Szalai, and D. A. Kovács, "Fermentált búzacsíra-kivonat hatása brojlercsirkék mesterséges Salmonella Typhimurium fertőzésére," Magyar Állatorvosok Lapja, 2020, accepted for publication.

[12] E. Kósa, G. Nagy, L. Jakab, M. Hidvégi, Á. Resetár, and I. Sári, "The effect of Immunovet-HBM® supplement on broiler turkey production results," in *Proceedings of the 15th European Symposium on Poultry Nutrition, Balatonfüred, Hungary, 25-29 September, 2005; World's Poultry Science Association (WPSA)*, pp. 408–410, Beekbergen, Netherlands, 2005.

[13] L. Stipkovits, K. Lapis, M. Hidvégi, E. Kósa, R. Glávits, and Á. Resetár, "Testing the efficacy of fermented wheat germ extract against Mycoplasma gallisepticum infection of chickens," *Poultry Science*, vol. 83, no. 11, pp. 1844–1848, 2004.

[14] E. A. Ferenczi, "Fermentált búzacsíra kivonat hatása a broilerek Salmonella Infantis ürítésére, termelési mutatóira és egyes vakcinák által kiváltott szerológiai áthangolódásra," Szent István University, Faculty of Veterinary Medicine, Budapest, 2011.

[15] G. Mátis, "Effects of butyrate on hepatic epigenetics and microsomal drug-metabolizing enzymes in chicken," Szent István University Postgraduate School of Veterinary Science, Budapest, Hungary, 2013.

[16] G. Mátis, A. Kulcsár, J. Petrilla, P. Talapka, and Z. Neogrády, "Porcine hepatocyte-Kupffer cell co-culture as an in vitro model for testing the efficacy of anti-inflammatory substances," *Journal of Animal Physiology and Animal Nutrition*, vol. 101, no. 2, pp. 201–207, 2016.

[17] D. Procházková, I. Boušová, and N. Wilhelmová, "Antioxidant and prooxidant properties of flavonoids," *Fitoterapia*, vol. 82, no. 4, pp. 513–523, 2011.

[18] T. Ishii, M. Akagawa, Y. Naito et al., "Pro-oxidant action of pyrroloquinoline quinone: characterization of protein oxidative modifications," *Bioscience, Biotechnology, and Biochemistry*, vol. 74, no. 3, pp. 663–666, 2014.

[19] H. Sies, "Hydrogen peroxide as a central redox signaling molecule in physiological oxidative stress: oxidative eustress," *Redox Biology*, vol. 11, pp. 613–619, 2017.

[20] A. van der Vliet and Y. M. W. Janssen-Heininger, "Hydrogen peroxide as a damage signal in tissue injury and inflammation: murderer, mediator, or messenger?," *Journal of Cellular Biochemistry*, vol. 115, no. 3, pp. 427–435, 2014.

[21] S. El Kamouni, R. El Kebbaj, P. Andreoletti et al., "Protective effect of argan and olive oils against LPS-induced oxidative stress and inflammation in mice livers," *International Journal of Molecular Sciences*, vol. 18, no. 10, p. 2181, 2017.

Research Article

Irvingia gabonensis Seed Extract: An Effective Attenuator of Doxorubicin-Mediated Cardiotoxicity in Wistar Rats

Olufunke Olorundare,[1] Adejuwon Adeneye [ID],[2] Akinyele Akinsola,[1] Phillip Kolo,[3] Olalekan Agede,[1] Sunday Soyemi,[4] Alban Mgbehoma,[5] Ikechukwu Okoye,[6] Ralph Albrecht,[7] and Hasan Mukhtar [ID][8]

[1]Department of Pharmacology and Therapeutics, Faculty of Basic Medical Sciences, College of Health Sciences, University of Ilorin, Ilorin, Kwara State, Nigeria
[2]Department of Pharmacology, Therapeutics and Toxicology, Faculty of Basic Clinical Sciences, Lagos State University College of Medicine, 1-5 Oba Akinjobi Way, G.R.A., Ikeja, Lagos State, Nigeria
[3]Department of Medicine, Faculty of Clinical, College of Health Sciences, University of Ilorin, Ilorin, Kwara State, Nigeria
[4]Department of Pathology and Forensic Medicine, Faculty of Basic Clinical Sciences, Lagos State University College of Medicine, 1-5 Oba Akinjobi Way, G.R.A., Ikeja, Lagos State, Nigeria
[5]Department of Pathology and Forensic Medicine, Lagos State University Teaching Hospital, 1-5 Oba Akinjobi Way, G.R.A., Ikeja, Lagos State, Nigeria
[6]Department of Oral Pathology and Medicine, Faculty of Dentistry, Lagos State University College of Medicine, 1-5 Oba Akinjobi Way, G.R.A., Ikeja, Lagos State, Nigeria
[7]Department of Animal Sciences, 1675 Observatory Drive, University of Wisconsin, Madison, WI 53706, USA
[8]Department of Dermatology, University of Wisconsin, Madison, Medical Science Center, 1300 University Avenue, Madison, WI 53706, USA

Correspondence should be addressed to Adejuwon Adeneye; adeneye2001@yahoo.com

Cardiotoxicity as an off-target effect of doxorubicin therapy is a major limiting factor for its clinical use as a choice cytotoxic agent. Seeds of *Irvingia gabonensis* have been reported to possess both nutritional and medicinal values which include antidiabetic, weight losing, antihyperlipidemic, and antioxidative effects. Protective effects of *Irvingia gabonensis* ethanol seed extract (*IGESE*) was investigated in doxorubicin (DOX)-mediated cardiotoxicity induced with single intraperitoneal injection of 15 mg/kg of DOX following the oral pretreatments of Wistar rats with 100-400 mg/kg/day of *IGESE* for 10 days, using serum cardiac enzyme markers (cardiac troponin I (cTI) and lactate dehydrogenase (LDH)), cardiac tissue oxidative stress markers (catalase (CAT), malonyldialdehyde (MDA), superoxide dismutase (SOD), glutathione-S-transferase (GST), glutathione peroxidase (GSH-Px), and reduced glutathione (GSH)), and cardiac histopathology endpoints. In addition, both qualitative and quantitative analyses to determine IGESE's secondary metabolites profile and its *in vitro* antioxidant activities were also conducted. Results revealed that serum cTnI and LDH were significantly elevated by the DOX treatment. Similarly, activities of tissue SOD, CAT, GST, and GSH levels were profoundly reduced, while GPx activity and MDA levels were profoundly increased by DOX treatment. These biochemical changes were associated with microthrombi formation in the DOX-treated cardiac tissues on histological examination. However, oral pretreatments with 100-400 mg/kg/day of *IGESE* dissolved in 5% DMSO in distilled water significantly attenuated increases in the serum cTnI and LDH, prevented significant alterations in the serum lipid profile and the tissue activities and levels of oxidative stress markers while improving cardiovascular disease risk indices and DOX-induced histopathological lesions. The *in vitro* antioxidant studies showed *IGESE* to have good antioxidant profile and contained 56 major secondary metabolites prominent among which are γ-sitosterol, Phytol, neophytadiene, stigmasterol, vitamin E, hexadecanoic acid and its ethyl ester, Phytyl palmitate, campesterol, lupeol, and squalene. Overall, both the *in vitro* and *in vivo* findings indicate that *IGESE* may be a promising prophylactic cardioprotective agent against DOX-induced cardiotoxicity, at least in part mediated via *IGESE*'s antioxidant and free radical scavenging and antithrombotic mechanisms.

1. Introduction

Doxorubicin (otherwise known as Adriamycin) is one of the antibiotic cytotoxic agent belonging to the anthracycline class of anticancer agents [1]. Doxorubicin is known to bind to and intercalate with DNA, thereby inhibiting the resealing action of topoisomerase II during normal DNA replication needed for cancer cell division and growth [2–5]. Doxorubicin is often used in clinical setting in combination with other classes of anticancer agents as "chemo cocktail" in the management of various types of solid and blood cancers such as breast and ovarian, leukemia (acute myelogenous leukemia (AML) and acute lymphoblastic leukemia), Hodgkin lymphoma, non-Hodgkin lymphoma, Wilm's tumor, neuroblastoma, and sarcoma [6–8]. For example, for breast cancer management, doxorubicin is typically combined and given with cyclophosphamide; for lymphomas and leukemias, it is combined with other cytotoxic agents to make regimens like CHOP (cyclophosphamide, doxorubicin hydrochloride, vincristine sulfate, and prednisone), R-CHOP (rituximab, cyclophosphamide, doxorubicin hydrochloride, vincristine sulfate, and prednisone), and ABVD (doxorubicin, bleomycin, vinblastine, dacarbazine) [9–12]. However, the clinical use of doxorubicin have been reported to be associated with major common side effects such as pain at the injection site, anorexia, fever, nausea and vomiting, stomatitis, dyspnea, nose bleeding, alopecia, immunosuppression, weight gain, hepatic and renal injuries, and severe cardiotoxicity [3, 13], while its occasional side effects include hyperuricemia, heart failure, pericardial effusion, cardiomyopathy, conjunctivitis, and skin rashes [14, 15]. Of these side effects, cumulative and dose-related cardiomyopathy and heart failure are of grave concerns to cancer patients and managing physicians alike, thus, limiting its clinical use [16–18]. Although the pathogenesis of doxorubicin-induced cardiotoxicity has been reported to be complex and fuzzy, the pivotal role of iron-mediated formation of reactive oxygen species (ROS) cannot be underscored [19].

In preventing the development of doxorubicin-induced cardiotoxicity, chemocurative and chemopreventive strategies involving the use of flavonoids, especially monoHER, have been advocated [20, 21]. MonoHER has been reported to elicit potent antioxidant, iron chelating, and carbonyl reductase inhibiting effects while still protecting the antitumor activity of anthracycline anticancer agents [22]. Similarly, the effectiveness of dexrazoxane (an iron chelating agent) [5, 23], dextromethionine [24, 25], and angiotensin-converting enzyme inhibitors—zofenopril and lisinopril [26, 27]—in ameliorating doxorubicin-related cardiotoxicity have also been reported. These agents, especially dexrazoxane, are known to mitigate oxidative stress by chelating iron and catalytically inhibiting topoisomerase II, thus preventing doxorubicin-induced double strand DNA breaks [28, 29]. However, these chemopreventive agents are expensive and not readily accessible to patients, therefore, necessitating the need for the discovery and development of more effective but cheaper and more readily accessible alternatives especially ones of medicinal plant origin. One of these is the *Irvingia gabonensis* seed extract.

Irvingia gabonensis (Aubry-Le Comte ex O'Rorke) Bail belonging to the family, Irvingiaceae, is known as African Mango (in English). Its other common names include bread tree, African wild mango, wild mango, and bush mango [30, 31], and its local names include *Apon* (in Yoruba, Southwest Nigeria), *Ogbono* (in Igbo, Southeast Nigeria), and *Goron* or *biri* (in Hausa, Northern Nigeria) [32, 33]. *Irvingia gabonensis* is widely cultivated in West African countries including southwest and southeast Nigeria, southern Cameroon, Côte d'Ivoire, Ghana, Togo, and Benin, to produce its edible fruit whose seed is used in the preparation of local delicious viscous soup for swallowing yam and cassava puddings [34]. Fat extracted from its seeds is commonly known as dika fat and majorly consists of C12 and C14 fatty acids, alongside with smaller quantities of C10, C16, and C18, glycerides and proteins [34]. *Irvingia gabonensis* seeds are also a good source of nutrients including a variety of vitamins and minerals such as sodium, calcium, magnesium, phosphorus, and iron. It is also a rich source of flavonoids (quercetin and kaempferol), ellagic acid, mono-, di-, and tri-O-methyl-ellagic acids, and their glycosides which are potent antioxidants [35, 36].

Phytochemical analysis of its seeds showed that it contains tannins, alkaloids, flavonoids, cardiac glycosides, steroids, carbohydrate, volatile oils, and terpenoids [33, 37, 38] and its proximate composition of moisture $1.4 \pm 0.11\%$, ash $6.8 \pm 0.12\%$, crude lipid $7.9 \pm 0.01\%$, crude fiber $21.6 \pm 0.45\%$, and crude protein $5.6 \pm 0.20\%$ [33]. Pure compounds already isolated from the seed extract of include: methyl 2-[2-formyl-5-(hydroxymethyl)-1   H-pyrrol1yl]-propanoate, kaempferol-3-0-β-D-6″ (p-coumaroyl) glucopyranoside and lupeol (3β-lup-20(29)-en-3-ol). Erstwhile, the antioxidant property of *Irvingia gabonensis* seed extract has been largely attributed to its high lupeol content [39].

In view of the above, the current study was designed at evaluating the possible protective effect of the crude non-defatted ethanol seed extract of *Irvingia gabonensis* against doxorubicin-mediated cardiotoxicity in rats using cardiac injury markers, oxidative stress markers, and histopathology results as endpoint outcomes.

2. Materials and Methods

2.1. Extraction Process and Calculation of Percentage Yield.

For *Irvingia gabonensis* seed extraction, 3 kg of pulverized *Irvingia gabonensis* dried seeds was macerated in 12 L of absolute ethanol for 72 hours after which it was continuously stirred for 1 hour before it was filtered using 180 mm of filter paper. The filtrate was then concentrated at 40°C to complete dryness using rotary evaporator. The dark-colored, oily paste-like residue left behind was weighed, stored in air- and water-proof container which was kept in a refrigerator at 4°C. This extraction process was repeated for two more times. From the stock, fresh solutions were made whenever required.

% yield was calculated as {weight of crude extract obtained (g) ÷ weight of pulverized dry seed extracted (g)} × 100.

2.2. Preliminary Qualitative Phytochemical Analysis of IGESE. The presence of saponins, tannins, alkaloids, flavonoids, anthraquinones, glycosides, and reducing sugars in IGESE was detected by the simple and standard qualitative methods described by Trease and Evans [40] and Sofowora [41].

2.3. Preliminary Quantitative Determination of Secondary Metabolites in and Phytoscan of IGESE. Preliminary quantitative analysis of the secondary metabolites (including phenol, flavonoids, tannin, terpenoids, steroids, reducing sugars, saponin, and phlobatannin) in IGESE was done using methods earlier described by Olorundare et al. [42]. Similarly, using gas chromatography-mass spectrophotometer (GC-MS) for phytoscan, the relative abundance of the secondary metabolites in IGESE was done using the procedures earlier described by Olorundare et al. [42].

2.4. In Vitro Antioxidant Studies of IGESE. DPPH scavenging activity, FRAP, and nitric oxide scavenging activities of IGESE were determined using the procedures earlier described by Olorundare et al. [42].

2.5. Experimental Animals. Young adult male Wistar Albino rats (aged 8-10 weeks old and body weight: 140-160 g) used in this study were obtained from the Animal House of the Lagos State University College of Medicine, Ikeja, Lagos State, Nigeria, after an ethical approval (UERC Approval number: UERC/ASN/2020/2022) was obtained from the University of Ilorin Ethical Review Committee for Postgraduate Research. The rats were handled in accordance with international principles guiding the Use and Handling of Experimental Animals [43]. The rats were maintained on standard rat feed (Ladokun Feeds, Ibadan, Oyo State, Nigeria) and potable water which were made available *ad libitum*. The rats were maintained at an ambient temperature between 28 and 30°C, humidity of $55 \pm 5\%$, and standard (natural) photoperiod of approximately 12/12 hours of alternating light and dark periodicity.

2.6. Measurement of Body Weight. The rat body weights were taken at the beginning and last of the experiment using a digital rodent weighing scale (®Virgo Electronic Compact Scale, New Delhi, India). The obtained values were expressed in grams (g).

2.7. Induction of DOX-Induced Cardiotoxicity and Treatment of Rats. Prior to commencement of the experiment, rats were randomly allotted into 7 groups of 7 rats per group such that the weight difference between and within groups was not more than ±20% of the average weight of the sample population of rats used for the study. However, the choice of the therapeutic dose range of 100, 200, and 400 mg/kg/day of IGESE was made based on the result of the orientation studies conducted.

Treatments of rats with distilled water, 100-400 mg/kg/day of IGESE in 5% DMSO distilled water, 20 mg/kg/day of vitamin C (standard antioxidant drug) for 10 days, and subsequent treatment with single intraperitoneal dose (15 mg/kg) doxorubicin in 0.9% normal saline on day 11 are as indicated in Table 1.

2.8. Collection of Blood Samples. 72 hours postdoxorubicin injection, overnight fasted rats were humanely sacrificed under light inhaled diethyl ether anesthesia, and whole blood samples were collected directly from the heart with fine 21G injectable needle and 5 ml syringe without causing damage to the heart tissues. The rat heart, liver, kidneys, and testes were carefully identified, harvested, and weighed.

2.9. Bioassays. Blood samples collected into 10 ml plain sample bottles were allowed to clot at room temperature for 6 hours and then centrifuged at 5000 rpm to separate clear sera from the clotted blood samples. The clear samples were obtained for assays of the following biochemical parameters: serum cardiac troponin I, LDH, TG, TC, and cholesterol fractions (HDL-c, LDL-c) using estimated standard bioassay procedures and commercial kits.

2.10. AI and CRI Calculation. AI was calculated as $LDL - c$ (mg/dl) $\div HDL - c$ (mg/dl) [44], while CRI was calculated as TC (mg/dl) $\div HDL - c$ (mg/dl) [45].

2.11. Determination of Cardiac Tissue Antioxidant Profile. After the rats were sacrificed humanely under inhaled diethyl ether, the heart was harvested *en bloc*. The heart was gently and carefully divided into two halves (each consisting of the atrium and ventricle) using a new surgical blade. The left half of the heart was briskly rinsed in ice-cold 1.15% KCl solution in order to preserve the oxidative enzyme activities of the heart before being placed in a clean sample bottle which itself was in an ice-pack filled cooler. This is to prevent the breakdown of the oxidative stress enzymes in these organs.

Activities of cardiac tissue oxidative stress markers such as SOD, CAT, MAD, GSH, GPx, and GST were assays using methods earlier described by Olorundare et al. [42].

2.12. Histopathological Studies. The right halves of the seven randomly selected rats from each treatment and control groups were subjected to histopathological examinations; the choice of the right ventricle was based on its reported most susceptibility to doxorubicin toxicity of the four heart chambers. The dissected right heart half was briskly rinsed in normal saline and then preserved in 10% formo-saline. It was then completely dehydrated in 100% ethanol before it was embedded in routine paraffin blocks. 4-5 μm thick sections of the cardiac tissue were prepared from these paraffin blocks and stained with hematoxylin-eosin. These were examined under a photomicroscope connected to a host computer for any associated histopathological lesions.

2.13. Statistical Analysis. Data were presented as mean ± S.E.M. of four observations for the *in vitro* studies and mean ± S.D. of seven observations for the *in vivo* studies, respectively. Statistical analysis was done using a two-way analysis of variance followed by the Student-Newman-Keuls test on GraphPad Prism Version 5. Statistical significance was considered at $p < 0.05$, $p < 0.001$, and $p < 0.0001$.

TABLE 1: Group treatment of rats.

Groups	Treatments
Group I	10 ml/kg of distilled water given *p.o.* for 10 days +1 ml/kg of 0.9% normal saline given *i.p.* on day 11
Group II	200 mg/kg/day of *IGESE* in 5% DMSO-distilled water given *p.o.* for 10 days +1 ml/kg of 0.9% normal saline given *i.p.* on day 11
Group III	10 ml/kg/day of distilled water given *p.o.* for 10 days +15 mg/kg of doxorubicin hydrochloride in 0.9% normal saline given *i.p.* on day 11
Group IV	20 mg/kg/day of Vit. C dissolved in 5% DMSO-distilled water given *p.o.* for 10 days +15 mg/kg of doxorubicin hydrochloride in 0.9% normal saline given *i.p.* on day 11
Group V	100 mg/kg/day of *IGESE* dissolved in 5% DMSO-distilled water given *p.o.* for 10 days +15 mg/kg of doxorubicin hydrochloride in 0.9% normal saline given *i.p.* on day 11
Group VI	200 mg/kg/day of *IGESE* dissolved in 5% DMSO-distilled water given *p.o.* for 10 days +15 mg/kg of doxorubicin hydrochloride in 0.9% normal saline given *i.p.* on day 11
Group VII	400 mg/kg/day of *IGESE* dissolved in 5% DMSO-distilled water given *p.o.* for 10 days +15 mg/kg of doxorubicin hydrochloride in 0.9% normal saline given *i.p.* on day 11

3. Results

3.1. % Yield.
Complete extraction of *Irvingia gabonensis* ethanol seed extract in absolute ethanol resulted in an average yield of 4.31%, which was a very dark brown, oily, and sweet-smelling paste-like residue that was soluble in methanol and ethanol but not in water.

3.2. Preliminary Qualitative Phytochemical Analysis of IGESE.
This shows the presence of phenol, flavonoids, tannin, terpenoids, steroids, and reducing sugars, while saponin and phlobatannin were absent.

3.3. Preliminary Quantification of the Secondary Metabolites in IGESE.
Preliminary quantitative analysis of *IGESE* showing the relative abundance and quantification of secondary metabolites (expressed in mg/100 g of dry *IGESE*) shows the presence of phenol (57.18 ± 0.05), flavonoids (18.19 ± 0.07), alkaloids (50.51 ± 0.17), steroids (47.47 ± 0.03), tannin (41.60 ± 0.03), and reducing sugars (65.64 ± 0.23) (Table 2).

3.4. Phytoscan for Secondary Metabolites in IGESE Using Gas Chromatography-Mass Spectrometry.
The presence and relative abundance of fifty-six (56) major secondary metabolites in *IGESE* obtained through gas chromatography-mass spectrometry and phytoscan based on CAS Library search included 4,6-di-O-methyl-alpha-d-galactose (27.08%), *n*-hexadecanoic acid (5.51%), undecanoic acid (5.08%), 9,12,15-octadecatrienoic acid, (Z,Z,Z) (4.84%), γ-sitosterol (4.18%), Phytol (3.84%), neophytadiene (3.77%), ethyl 9,12,15-octadecatrienoate (3.65%), stigmasterol (3.03%), vitamin E (2.91%), hexadecanoic acid, ethyl ester (2.51%), Phytyl palmitate (1.92%), campesterol (1.34%), lupeol (1.22%), 9,12-octadecadienoic acid (Z,Z) (0.96%), octadecanoic acid, ethyl ester (0.91%), lup-20(29)-en-3-one (0.84%), β-amyrone (0.82%), phenol (0.82%), 1-hexacosanol (0.77%), pyrrolidine, 1-(1-cyclohexen-1-yl)-(0.71%), triacontyl acetate (0.66%), octadecanoic acid, 2,3-dihydroxypropyl ester (0.59%), γ-tocopherol (0.35%), 1,2-bis(trimethylsilyl) benzene (0.34%), and squalene (0.26%) (Table 3 and Figure 1).

TABLE 2: Quantitative analysis of the secondary metabolites in *IGESE* (mg/100 g of dry extract sample).

Secondary metabolite	Quantity (mg/100 g of dry extract)
Flavonoids	18.19 ± 0.07
Alkaloids	50.51 ± 0.17
Reducing sugar	65.64 ± 0.23
Phenols	57.18 ± 0.05
Steroids	47.47 ± 0.03
Tannin	41.60 ± 0.03

3.5. In Vitro Antioxidant Profiling of IGESE

3.5.1. Determination of DPPH Scavenging Activity of IGESE.
Table 4 shows the *in vitro* DPPH scavenging activities of 25μg/ml, 50μg/ml, 75μg/ml, and 100μg/ml of *IGESE* in comparison with those of corresponding doses of the standard antioxidant drug (Vit. C) used. *IGESE*'s DPPH scavenging activities were significantly ($p < 0.001$ and $p < 0.0001$) dose related at 75μg/ml and 100μg/ml, and these were comparable to that of Vit. C (Table 4).

3.5.2. Determination of NO Scavenging Activity of IGESE.
Table 5 shows the *in vitro* NO scavenging activities of 25μg/ml, 50μg/ml, 75μg/ml, and 100μg/ml of *IGESE* in comparison with those of corresponding doses of the standard antioxidant drug (Vit. C). *IGESE*'s NO scavenging activities of the extract were significantly ($p < 0.001$, $p < 0.0001$) dose related and comparable to that of Vit. C at 75μg/ml and 100μg/ml of *IGESE* (Table 5).

3.5.3. Determination of FRAP of IGESE.
Table 6 shows *IGESE*'s *in vitro* ferric reducing activity power of 25μg/ml, 50μg/ml, 75μg/ml, and 100μg/ml in comparison with those of corresponding doses of the standard antioxidant drug. Again, *IGESE*'s FRAP activities were significantly ($p < 0.05$, $p < 0.001$, $p < 0.0001$) dose dependent and comparable to that of Vit. C especially at 50μg/ml, 75μg/ml, and 100μg/ml of *IGESE* (Table 6).

TABLE 3: Quantitative analysis of the secondary metabolites (PhytoScan) of *Irvingia gabonensis* ethanol seed extract (*IGESE*) using gas chromatography-mass spectrometry.

Pk#	RT	Area (%)	Library/IDRef#	CAS#	Quality (%)
1.	4.069	0.1378	Ethanol, 2-(ethylamino)-	000110-73-6	80
2.	4.906	0.0411	Oxime-, methoxy-phenyl-	1000222-86-6	91
3.	5.137	0.1764	1,2-Cyclopentanedione	003008-40-0	78
4.	5.455	0.0811	Cyclotetrasiloxane, octamethyl-	000556-67-2	83
5.	5.721	0.8170	Phenol	000108-95-2	90
6.	5.905	0.1070	Phenol	000108-95-2	60
7.	8.291	0.1399	Z,Z-7,11-Hexadecadien-1-ol	1000131-01-4	50
8.	8.458	0.0616	Cyclotetrasiloxane, octamethyl-	000556-67-2	64
9.	10.387	0.0843	Naphthalen-4a,8a-imine, octahydro-	005735-21-7	50
10.	10.503	0.7119	Pyrrolidine, 1-(1-cyclohexen-1-yl)-	001125-99-1	50
11.	11.288	0.1380	Cycloheptasiloxane, tetradecamethyl-	000107-50-6	60
12.	12.137	0.4489	4-Methyl-2,5-dimethoxybenzaldehyde	004925-88-6	60
13.	13.125	5.0814	Undecanoic acid	000112-37-8	53
14.	14.516	3.7713	Neophytadiene	000504-96-1	89
15.	15.088	27.0790	4,6-di-O-methyl-alpha-d-galactose	024462-98-4	52
16.	15.695	5.5072	n-Hexadecanoic acid	000057-10-3	99
17.	15.816	2.5123	Hexadecanoic acid, ethyl ester	000628-97-7	98
18.	16.116	0.0474	Heptadecanoic acid	000506-12-7	55
19.	16.595	0.1190	Heptadecanoic acid, ethyl ester	014010-23-2	60
20.	16.774	3.8358	Phytol	000150-86-7	91
21.	17.063	4.8375	9,12,15-Octadecatrienoic acid, (Z,Z,Z)-	000463-40-1	99
22.	17.185	3.6541	Ethyl 9,12,15-octadecatrienoate	1000336-77-4	99
23.	17.352	0.9067	Octadecanoic acid, ethyl ester	000111-61-5	98
24.	17.508	0.3478	14-Pentadecenoic acid	017351-34-7	86
25.	18.420	0.1330	Bicyclo[3.1.1]heptan-2-one, 6,6-dimethyl-	024903-95-5	55
26.	18.605	0.0633	Cis-vaccenic acid	000506-17-2	91
27.	18.761	0.1262	Heptadecanoic acid, ethyl ester	014010-23-2	70
28.	19.264	0.0555	Cyclopentadecanone, 2-hydroxy-	004727-18-8	90
29.	19.425	0.173	Ethyl 9-hexadecenoate	054546-22-4	58
30.	19.599	0.594	Octadecanoic acid, 2,3-dihydroxypropyl ester	000123-94-4	87
31.	19.818	0.0961	1,4-benzenedicarboxylic acid, mono(1-methylethyl) ester	1000400-56-6	52
32.	19.934	0.0379	Cis-9-tetradecenoic acid, heptyl ester	1000405-20-8	70
33.	20.078	0.1537	Docosanoic acid, ethyl ester	005908-87-2	93
34.	20.251	0.0452	18-nonadecenoic acid	076998-87-3	64
35.	20.742	0.3606	1,3,12-nonadecatriene	1000131-11-1	64
36.	20.887	0.1046	2-methyl-Z,Z-3,13-octadecadienol	1000130-90-5	55
37.	21.510	0.2565	Squalene	000111-02-4	90
38.	22.844	0.3462	γ-Tocopherol	007616-22-0	98
39.	23.052	0.6599	Triacontyl acetate	041755-58-2	95
40.	23.341	2.9085	Vitamin E	000059-02-9	99
41.	24.040	1.3362	Campesterol	000474-62-4	99
42.	24.277	3.0258	Stigmasterol	000083-48-7	99
43.	24.427	0.7673	1-hexacosanol	000506-52-5	91
44.	24.542	0.1545	Hexadecanoic acid, 2-hydroxy-,methyl ester	016742-51-1	59
45.	24.750	4.1775	γ-Sitosterol	000083-47-6	99
46.	24.843	0.8204	β-Amyrone	000638-97-1	94
47.	25.241	0.8408	Lup-20(29)-en-3-one	001617-70-5	97
48.	25.443	1.2194	Lupeol	000545-47-1	58

Pk#	RT	Area (%)	Library/IDRef#	CAS#	Quality (%)
49.	25.559	0.0751	Benz[b]-1,4-oxazepine-4(5H)-thione, 2,3-dihydro-2,8-dimethyl-	1000258-63-4	50
50.	25.969	0.3833	Stigmast-4-en-3-one	001058-61-3	87
51.	26.431	0.0624	2,4-Cyclohexadien-1-one, 3,5-bis(1,1-dimethylethyl)-4-hydroxy-	054965-43-4	50
52.	26.829	1.9166	Phytyl palmitate	1000413-67-8	96
53.	27.170	0.1216	1,4-Bis(trimethylsilyl)benzene	013183-70-5	78
54.	27.592	0.0250	2,4-Cyclohexadien-1-one, 3,5-bis(1,1-dimethylethyl)-4-hydroxy-	054965-43-4	50
55.	28.463	0.3430	1,2-Bis(trimethylsilyl)benzene	017151-09-6	76
56.	29.376	0.9577	9,12-Octadecadienoic acid (Z,Z)-	000060-33-3	50

Pk#: peak number; RT: retention time; Area%: percentage area covered; Library/ID Ref#: library/identification number; CAS#: chemical abstract scheme number.

FIGURE 1: GC-MS analysis showing the relative abundance of the secondary metabolites in *IGESE*.

TABLE 4: *In vitro* DPPH scavenging activity (% inhibition) of 25-100 μg/ml of *IGESE* and Vit. C.

Drug	Graded doses			
	25 μg/ml	50 μg/ml	75 μg/ml	100 μg/ml
IGESE	14.59 ± 0.31	43.53 ± 0.19	67.98 ± 0.38[b]	75.44 ± 0.51[c]
Vit. C	45.06 ± 0.28	56.55 ± 0.55[a]	76.92 ± 0.31[c]	89.83 ± 0.21[c]

[a], [b], and [c] represent significant increases at $p < 0.05$, $p < 0.001$, and $p < 0.0001$, respectively, when compared to the baseline value at 25 μg/ml.

TABLE 5: *In vitro* nitric oxide (NO) scavenging activity of 25-100 μg/ml of *IGESE* and Vit. C.

Drug	Graded doses			
	25 μg/ml	50 μg/ml	75 μg/ml	100 μg/ml
IGESE	13.55 ± 0.70	39.98 ± 0.70	68.39 ± 0.32[b]	77.09 ± 0.13[c]
Vit. C	47.89 ± 0.14	63.09 ± 0.24[b]	76.07 ± 0.47[c]	84.91 ± 0.31[c]

[a], [b], and [c] represent significant increases at $p < 0.05$, $p < 0.001$, and $p < 0.0001$, when compared to the baseline value at 25 μg/ml.

TABLE 6: *In vitro* FRAP activities of 25-100 μg/ml of *IGESE* and Vit. C.

Drug	Graded doses			
	25 μg/ml	50 μg/ml	75 μg/ml	100 μg/ml
IGESE	0.08 ± 0.00	0.13 ± 0.04[a]	0.28 ± 0.00[b]	0.48 ± 0.00[c]
Vit. C	0.24 ± 0.00	0.38 ± 0.00[b]	0.48 ± 0.00[c]	0.63 ± 0.00[c]

[a], [b], and [c] represent significant increases at $p < 0.05$, $p < 0.001$, and $p < 0.0001$, respectively, when compared to the baseline value at 25 μg/ml.

3.6. Effect of IGESE on the Cardiac Tissue Oxidative Stress Markers (GSH, GST, GPx, SOD, CAT, and MDA) of DOX-Treated Rats.

Intraperitoneal injection of DOX to rats resulted in significant ($p < 0.05$, $p < 0.001$, and $p < 0.0001$) decreased activities of SOD, CAT, GPx, GST, and GSH levels while significantly increasing ($p < 0.001$) MDA activities (Table 7). However, oral pretreatment with *IGESE* significantly ($p < 0.05$, $p < 0.001$, and $p < 0.0001$) attenuated the alterations in the activities of these cardiac tissue enzyme markers. Similarly, *IGESE* pretreatment significantly ($p < 0.001$ and $p < 0.0001$) and dose dependently reduced MDA levels (Table 7).
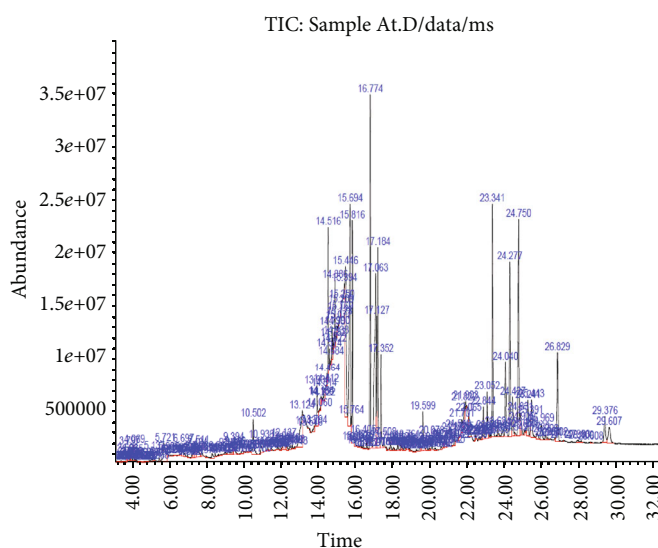
TABLE 7: Antioxidant enzyme activities of 100-400 mg/kg/day of *IGESE* in DOX-treated rat cardiac tissue.

Groups	Antioxidant parameters					
	GSH	GST	GPx	SOD	CAT	MDA
I	18.8 ± 1.6	1.6 ± 0.2	1.2 ± 0.1	9.5 ± 1.8	43.6 ± 4.7	4.3 ± 0.5
II	20.4 ± 0.6	$2.7 \pm 0.2^{b+}$	2.0 ± 0.2	10.4 ± 1.2	62.7 ± 4.4	6.0 ± 0.5
III	$14.8 \pm 0.8^{b-}$	$1.1 \pm 0.2^{a-}$	$1.0 \pm 0.1^{a-}$	$6.9 \pm 0.6^{b-}$	$16.7 \pm 2.3^{c-}$	$12.8 \pm 1.0^{c+}$
IV	$21.3 \pm 1.3^{e+,e}$	$2.6 \pm 0.3^{e+,e}$	$2.4 \pm 0.2^{e+,e}$	$11.5 \pm 1.5^{e+,e}$	$51.4 \pm 5.2^{d+,d}$	$5.2 \pm 0.5^{e-}$
V	17.0 ± 1.4^{d}	2.0 ± 0.2^{d}	1.3 ± 0.1	$11.1 \pm 1.5^{d+,d}$	$54.2 \pm 6.5^{d+,d}$	$5.3 \pm 0.6^{e-}$
VI	$19.6 \pm 1.8^{d+,d}$	$2.4 \pm 0.1^{e+,e}$	$2.3 \pm 0.3^{e+,e}$	$12.8 \pm 1.4^{e+,e}$	$56.6 \pm 4.3^{d+,d}$	$3.9 \pm 0.4^{f-}$
VII	$24.7 \pm 1.3^{e+,e}$	$3.0 \pm 0.4^{f+,f}$	$3.3 \pm 0.4^{f+,f}$	$15.4 \pm 1.6^{e+,e}$	$78.7 \pm 6.9^{f+,f}$	$3.5 \pm 0.4^{f-}$

[b+] represents a significant increase at $p < 0.001$ when compared to untreated negative (normal) control (Group I) values; [c+] represents a significant increase at $p < 0.0001$ when compared to *IGESE*-only treated (Group II) values; [a-,b-,] and [c-] represent significant decreases at $p < 0.05$, $p < 0.001$, and $p < 0.0001$, respectively, when compared to Groups I values; [d+] and [e+] represent significant increases at $p < 0.001$ and $p < 0.0001$, respectively, when compared to untreated positive control (DOX-only treated, Group III) values; while [e-] and [f] represent significant decreases at $p < 0.001$ and $p < 0.0001$, respectively, when compared to untreated positive control (DOX-treated only, Group III) values, respectively. [d, e,] and [f] represent significant increases at $p < 0.05$, $p < 0.001$, and $p < 0.0001$, respectively, when compared to untreated positive control (DOX-treated only, Group III).

3.7. Effect of IGESE on Cardiac Marker Enzymes (cTnI and LDH) of DOX-Treated Rats.

Single intraperitoneal injection of DOX resulted in significant ($p < 0.0001$) increases in the serum LDH and cTnI levels when compared to that of untreated negative control (Group I) values (Table 8). However, with oral pretreatments with 100-400 mg/kg/day of *IGESE* significantly attenuated ($p < 0.05$, $p < 0.001$, and $p < 0.0001$) increases in the serum cTnI and LDH levels dose dependently (Table 8), and these attenuations were comparable to that induced by oral pretreatment with 20 mg/kg/day of Vit. C (Table 8).

3.8. Effect of IGESE on the Serum Lipids (TG, TC, HDL-c, LDL-c) Level of DOX-Treated Rats.

Acute intraperitoneal DOX injection resulted in significant ($p < 0.05$) decreases in the serum TG, significantly ($p < 0.001$) increased serum TC and LDL-c while inducing insignificant ($p > 0.05$) alterations in the serum HDL-c level (Table 9). However, with 100-400 mg/kg/day of *IGESE* oral pretreatment, there were significant ($p < 0.05$ and p<0.0001) dose-related increases in the serum TG and HDL-c concentrations, while there were significant ($p > 0.05$ and $p < 0.001$) decreases in the serum TC and LDL-c concentrations when compared to DOX-only treated rats (Table 9). Oral pretreatment with 20 mg/kg/day of vitamin C elicited similar effects on the measured serum lipids parameters (Table 9).

3.9. Effect of Oral IGESE Pretreatment on Cardiovascular Risk Indices (AI and CRI) of DOX-Treated Rats.

Acute intraperitoneal injections with DOX resulted in significant ($p < 0.001$) increases in the AI and CRI values when compared to Groups I and II values (Table 10). However, with oral pretreatment with 100-400 mg/kg/day of *IGESE*, there were significant ($p < 0.05$, $p < 0.001$, and $p < 0.0001$) dose-related decreases in the AI and CRI values with similar effect induced by oral pretreatments with 20 mg/kg/day of Vit. C (Table 10).

3.10. Histopathological Studies of the Effect of IGESE Oral Pretreatment on DOX-Intoxicated Treated Heart.

Figure 2 is a photomicrograph of a cross-sectional representative of DOX-only treated heart showing myocyte congestion and

TABLE 8: Effect of 100-400 mg/kg/day of *IGESE* on serum LDH and cardiac troponin I (cTnI) levels in DOX-intoxicated rats.

Treatment groups	LDH (U/L)	cTnI (ng/ml)
I	4347 ± 596.4	3.4 ± 1.1
II	4338 ± 238.1	3.7 ± 1.1
III	$8151 \pm 441.0^{c+}$	$40.5 \pm 3.5^{c+}$
IV	$4887 \pm 217.5^{a-}$	$11.4 \pm 3.5^{c-}$
V	$4737 \pm 260.2^{a-}$	$25.5 \pm 3.3^{a-}$
VI	$4188 \pm 229.2^{b-}$	$19.8 \pm 2.4^{b-}$
VII	$3679 \pm 346.1^{c-}$	$14.8 \pm 1.1^{c-}$

[c+] represents a significant increase at $p < 0.0001$ when compared to untreated normal control (Group I) and *IGESE* only treated (Group II) values, while [a-,] [b-] and [c-] represent significant decreases at $p < 0.05$, $p < 0.001$, and $p < 0.0001$, respectively, when compared to DOX-only treated (Group III) values, respectively.

antemortem coronary microthrombi when compared to untreated normal (Figure 3) and *IGESE*-only treated heart tissues with normal cardiac architecture (Figure 4). However, pretreatment with varying doses of *IGESE* resulted in dose-related improvements in the histological distortions induced by DOX especially at 200 mg/kg/day (Figure 5) and 400 mg/kg/day of *IGESE* (Figure 6); although, histological features of vascular congestion were still seen with 100 mg/kg/day of *IGESE* oral pretreatment (Figure 7). On the contrary, there were histological features of persistent coronary microthrombi in rat heart pretreated with 20 mg/kg/day of Vit. C, indicating the lingering DOX-induced histological lesions, even with the standard antioxidant drug (Figure 8).

4. Discussion

The clinical use of doxorubicin in the management of solid and hematological cancers has been widely limited by its off-target severe cardiotoxicity which manifests biochemically by elevation of serum enzyme markers of cardiotoxicity. The diagnostic serum marker enzymes of cardiotoxicity are

TABLE 9: Effect of 100-400 mg/kg/day of *IGESE* on complete serum lipid profile.

Groups	Serum lipids			
	TG(mmol/l)	TC(mmol/l)	HDL-c(mmol/l)	LDL-c(mmol/l)
I	1.2 ± 0.1	2.0 ± 0.1	0.7 ± 0.0	0.7 ± 0.0
II	1.1 ± 0.1	1.8 ± 0.1	0.6 ± 0.0	0.6 ± 0.1
III	$0.9 \pm 0.1^{a-}$	$2.7 \pm 0.3^{c+}$	0.7 ± 0.0	$1.6 \pm 0.2^{c+}$
IV	$1.2 \pm 0.1^{d+}$	$1.4 \pm 0.2^{f-}$	$0.8 \pm 0.1^{a+}$	$0.4 \pm 0.2^{f-}$
V	1.0 ± 0.2	$2.4 \pm 0.2^{d-}$	$0.8 \pm 0.1^{a+}$	$1.2 \pm 0.1^{d-}$
VI	$1.3 \pm 0.2^{d+}$	$2.3 \pm 0.2^{d-}$	$0.9 \pm 0.1^{b+}$	$1.1 \pm 0.2^{d-}$
VII	$1.5 \pm 0.0^{e+}$	$1.6 \pm 0.1^{f-}$	0.6 ± 0.0	$0.6 \pm 0.1^{f-}$

[a-] represents a significant decrease at $p < 0.05$ when compared to (Groups I and II) values, while [c+] represents a significant increase at $p < 0.0001$ when compared to Groups I and II values; [d-] and [f-] represent significant decreases at $p < 0.05$ and $p < 0.0001$, respectively, when compared to DOX-only treated (Group III) values; [d+] and [e+] represent significant increases at $p < 0.05$ and $p < 0.001$, respectively, when compared to DOX-only treated (Group III) values.

TABLE 10: Effect of 100-400 mg/kg/day of *IGESE* on cardiovascular risk indices (atherogenic index (AI) and coronary risk index (CRI)) values in DOX-intoxicated rats.

Treatment groups	$TC \div HDL - c \, (AI)$	$LDL - c \div HDL - c \, (CRI)$
I	2.83 ± 0.05	1.05 ± 0.07
II	2.86 ± 0.12	1.11 ± 0.15
III	$3.85 \pm 0.19^{b+}$	$2.28 \pm 0.20^{c+}$
IV	$1.88 \pm 0.39^{a-}$	$0.64 \pm 0.33^{c-}$
V	$3.10 \pm 0.23^{a-}$	$1.51 \pm 0.16^{a-}$
VI	$2.56 \pm 0.27^{b-}$	$1.30 \pm 0.27^{b-}$
VII	$2.62 \pm 0.18^{b-}$	$0.98 \pm 0.16^{c-}$

[b+] and [c+] represent significant increases at $p < 0.001$ and $p < 0.0001$, respectively, when compared to Groups I and II values, respectively, while [a-], [b-], and [c-] represent significant decreases at $p < 0.05$, $p < 0.001$, and $p < 0.0001$, respectively, when compared to untreated positive control (DOX-only treated) (Group III) values, respectively.

FIGURE 2: A cross-sectional representative of 15 mg/kg of DOX-only intoxicated rat cardiac tissue showing antemortem coronary artery microthrombi and congested cardiomyocytes suggestive of coronary intravascular thrombosis (×400 magnification, Hematoxylin and Eosin stain).

AST, ALT, CK-MB, LDH, and cTnI which leak from cardiac tissue damage to the bloodstream due to their tissue specificity and serum catalytic activity [46]. DOX administration may result in the damage to the myocardial cell membrane or make myocytes more permeable, resulting in the leakage of the diagnostic cardiac enzyme markers cardiac AST, ALT, CK-MB, LDH, and cTnI into the bloodstream and their high circulating levels. In the present study, DOX-mediated cardiotoxicity was fully established as evidenced by the profound elevations in the serum cTnI and LDH levels which is in complete agreement with previous studies [47–52]. With oral *IGESE* pretreatments, the serum levels of cTnI and LDH were profoundly attenuated toward normal serum level indicating the ameliorative potential of *IGESE* in DOX-mediated cardiotoxicity. These effects were probably mediated through high antioxidant and/or free radical scavenging activities of *IGESE* on the myocardium, thus reducing the damaging effects of DOX to the cardiac muscle fibers, subsequently minimizing the leakage of such enzymes in the serum. Similarly, ROS-mediated mechanism is one of the proposed DOX-mediated cardiotoxicity mechanisms, leading to oxidative

stress that causes cardiomyopathy [53]. Oxidative stress has been reported to increase lipid peroxidation as indicated by an increase in MDA levels and altered enzymatic and nonenzymatic antioxidant systems [54, 55]. In this study, MDA level was profoundly increased by DOX treatment, while DOX treatment also suppressed the cardiac tissue activities of SOD, CAT, GPx, GST, and GSH levels in the treated rats in agreement with other studies. These altered biochemical alterations were supported by histological lesions characterized by myocyte congestion and coronary intravascular microthrombi formation. DOX has been previously reported to profoundly reduce vascular blood flow, disintegrate vascular endothelium, and promote GPIIb/IIIa-mediated platelet adhesion and aggregation, all resulting in microthrombi formation [56–58]. The fact that *IGESE* prevented microthrombi formation in DOX-treated coronary vasculature as evidenced by histopathological results of this study highlighted the possible inherent antithrombotic potential of *IGESE*; although, further studies are still needed in this respect in order to validate this hypothesis. However, *IGESE* profoundly attenuated
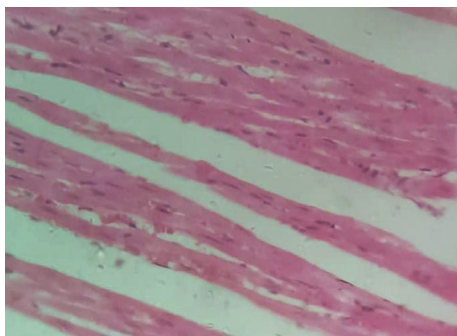
FIGURE 3: A cross-sectional representative of normal rat cardiac tissue showing normal cardiac histoarchitecture (×400 magnification, Hematoxylin and Eosin stain).
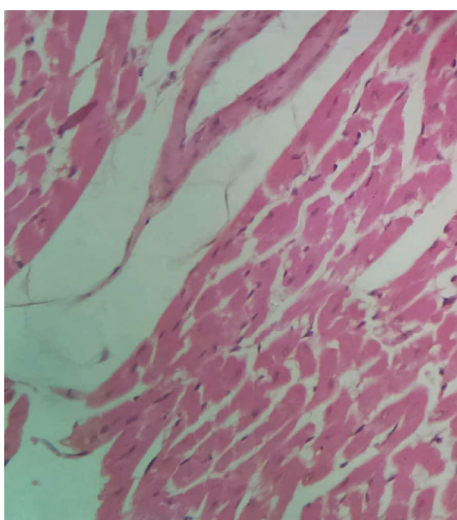
FIGURE 4: A cross-sectional representative of 200 mg/kg/day of *IGESE*-only pretreated rat cardiac tissue showing normal cardiac histoarchitecture (×400 magnification, Hematoxylin and Eosin stain).

FIGURE 5: A cross-sectional representative of 200 mg/kg of *IGESE* pretreated, DOX intoxicated rat cardiac tissue showing mildly congested cardiomyocytes (×400 magnification, Hematoxylin and Eosin stain).
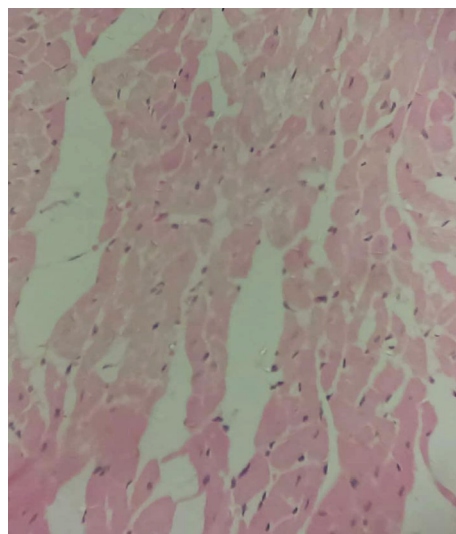
FIGURE 6: A cross-sectional representative of 400 mg/kg of *IGESE* pretreated, DOX intoxicated rat cardiac tissue showing normal cardiac histoarchitecture (×400 magnification, Hematoxylin and Eosin stain).

significant alterations in the cardiac tissue oxidative markers whose activities were significantly suppressed by DOX intoxication. *IGESE* has the tendency to neutralize ROS like superoxide radicals, singlet oxygen, nitric oxide, and peroxynitrite, thereby reducing the damage to lipid membranes [39]. Similarly, oral *IGESE* pretreatments profoundly improved and reversed the DOX-induced histological lesions especially at 200 mg/kg/day and 400 mg/kg/day of *IGESE* pretreatments.

The effects of DOX on serum lipids are also significant. DOX has been reported to cause hyperlipidemia (which include increased serum cholesterol, triglyceride, LDL-c, and FFAs) [59–64] and increases cardiovascular disease risk [65]. This hyperlipidemia is thought to be mediated via downregulation of PPAR-γ and subsequently affect GLUT4 and FAT/CD36 expression resulting in glucose and fatty acid transporters expression and causing hyperglycemia and hyperlipidemia [65]. *Irvingia gabonensis* seeds have been reported to induce weight loss, antihyperlipidemia, and reduced cardiovascular disease risk

factors in both animal [59–64] and human studies [66–72] which were reportedly mediated via downregulation of the PPAR-γ and leptin genes and upregulation of the adiponectin gene mechanisms [67]. Thus, the results of this study are in tandem with those of earlier studies.

The GC-MS analysis and phytoscan of *IGESE* are also notably significant. *IGESE* is shown to contain high contents of 4,6-di-O-methyl-alpha-d-galactose, *n*-hexadecanoic acid, undecanoic acid, 9,12,15-octadecatrienoic acid, γ-sitosterol, phytol, neophytadiene, ethyl 9,12,15-octadecatrienoate, stigmasterol, vitamin E, hexadecanoic acid ethyl ester, Phytyl palmitate, campesterol, and lupeol. Phytosterols such as sitosterol, stigmasterol, campesterol, and phytols have been reported to effectively mitigate lipid peroxidation through antioxidant and free radical scavenging mechanisms and physically stabilize cell membrane [73] as well as effectively
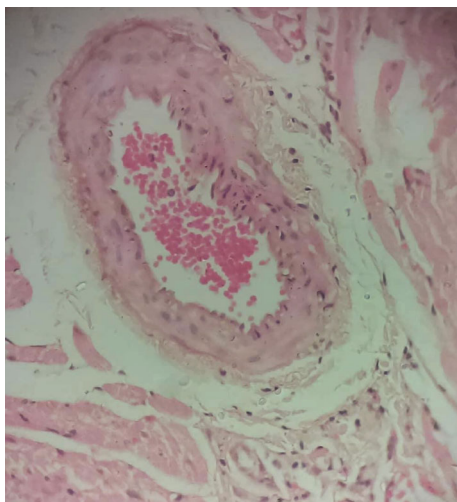
FIGURE 7: A cross-sectional representative of 100 mg/kg/day of IGESE-pretreated, DOX-intoxicated cardiac tissue showing mild-to-moderate vascular congestion but normal myocardiocytes (×400 magnification, Hematoxylin-Eosin stain).
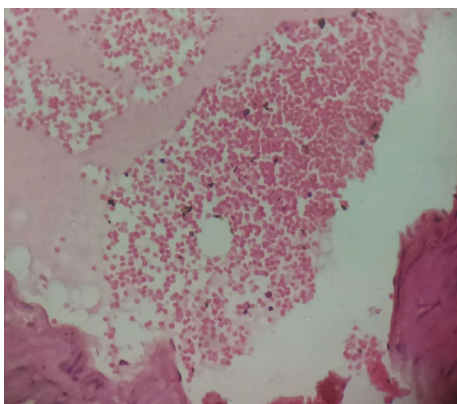
FIGURE 8: A cross-sectional representative of 20 mg/kg/day of vitamin C pretreated, DOX intoxicated rat cardiac tissue showing mild-to-moderate antemortem coronary artery thrombus and normal cardiomyocytes suggestive of coronary intravascular thrombosis (×400 magnification, Hematoxylin and Eosin stain).

lowered cholesterol especially the LDL-c fraction [74–78]. Similarly, stigmasterol, γ-sitosterol, lupeol, lupeol acetate, and α-amyrin are known to exhibit other important pharmacological activities such as anticancer, anti-inflammatory, and antibacterial activities [79]. Lupeol in particular is known to mediate anti-inflammatory, antimicrobial, anti-protozoal, antiproliferative, anti-invasive, antiangiogenic, and cholesterol-lowering activities [79, 80]. Phytol is an important diterpene that possesses antimicrobial, antioxidant, and anticancer activities [81, 82]. Hexadecanoic acid is known to exhibit strong antimicrobial and anti-inflammatory activity [83]. Squalene, a triterpene, is a natural antioxidant [84], possessing various other pharmacological properties including antimicrobial property [85, 86]. Neophytadiene is a good analgesic, antipyretic, anti-inflamma-

tory, antimicrobial, and antioxidant compound [87, 88]. Thus, the presence of stigmasterol, γ-sitosterol, lupeol, phytols, and neophytadiene in high amounts in IGESE could be responsible for the cholesterol-lowering, antioxidant, and antilipiperoxidation activities of IGESE in DOX-mediated cardiotoxic rats. Similarly, flavonoids, steroids, cardiac glycosides, tannin, and saponin have been reported to elicit antithrombotic activities [89–91], and more specifically, plant-derived sitosterol has been reported to have anticoagulant and thrombus-preventing activities in mice [78, 92, 93]. Thus, the presence of these phytochemicals especially steroids and tannin in high amounts in IGESE could be responsible for the observed antithrombotic action of IGESE in DOX-intoxicated rats.

5. Conclusion

Overall, results of this study showed that IGESE effectively attenuated DOX-mediated cardiotoxicity and its cardioprotective activities were mediated via antioxidant, free radical scavenging, antilipoperoxidation, and antithrombotic mechanisms.

Abbreviations

AI:	Atherogenic index
ALT:	Alanine transaminase
AST:	Aspartate transaminase
CAT:	Catalase
CK-MB:	Creatine kinase-MB
CRI:	Coronary artery index
DMSO:	Dimethyl sulfoxide
DNA:	Deoxyribonucleic acid
DOX:	Doxorubicin
DPPH:	1,1-diphenyl-2-picrylhydrazyl
FAT/CD36:	Fatty acid translocase
FFAs:	Free fatty acids
FRAP:	Ferric reducing activity power
GC-MS:	Gas chromatography mass spectrometer
GLUT4:	Glucose transporter member 4
GPIIb/IIIa:	Glycoprotein IIb/IIIa
GPx:	Glutathione peroxidase
GSH:	Reduced glutathione
GST:	Glutathione S-transferase
HDL-c:	High density lipoprotein cholesterol
i.p.:	Intraperitoneal
IGESE:	Irginvia gabonensis ethanol seed extract
KCl:	Potassium chloride
LDH:	Lactate dehydrogenase
LDL-c:	Low density lipoprotein cholesterol
MDA:	Malondialdehyde
NO:	Nitric oxide
p.o.:	Per os
PPARγ:	Peroxisome proliferator-activator receptor gamma
ROS:	Reactive oxygen species
rpm:	Revolution per minute
S.E.M.:	Standard error of the mean
SOD:	Superoxidase dismutase

TC: Total cholesterol
TG: Triglyceride
UERC: UNILORIN ethics and research committee
UNILORIN: University of Ilorin
Vit. C: Vitamin C.

Data Availability

Answer: Yes. Comment

Conflicts of Interest

The authors have none to declare.

Authors' Contributions

Olufunke Olorundare designed the experimental protocol for this study and was involved in the manuscript writing; Adejuwon Adeneye supervised the research, analyzed data, and wrote the manuscript; Akinyele Akinsola and Olalekan Agede are postgraduate students in Olufunke Olorundare's laboratory that performed the laboratory research under supervision; Phillip Kolo was part of the protocol design and read through the manuscript; Ikechukwu Okoye prepared the cardiac tissue slides; Sunday Soyemi and Alban Mgbehoma independently read and interpreted the cardiac tissue slides; Ralph Albrecht and Hasan Mukhtar are our collaborators in the U.S.A. who read through the manuscript.

Acknowledgments

References

[1] P. A. Henriksen, "Anthracycline cardiotoxicity: an update on mechanisms, monitoring and prevention," *Heart*, vol. 104, no. 12, pp. 971–977, 2018.

[2] Y. Pommier, E. Leo, H. Zhang, and C. Marchand, "DNA topoisomerases and their poisoning by anticancer and antibacterial drugs," *Chemistry & Biology*, vol. 17, no. 5, pp. 421–433, 2010.

[3] O. Tacar, P. Sriamornsak, and C. R. Dass, "Doxorubicin: an update on anticancer molecular action, toxicity and novel drug delivery systems," *The Journal of Pharmacy and Pharmacology*, vol. 65, no. 2, pp. 157–170, 2013.

[4] B. Pang, X. Qiao, L. Janssen et al., "Drug-induced histone eviction from open chromatin contributes to the chemotherapeutic effects of doxorubicin," *Nature Communications*, vol. 4, no. 1, article 1908, 2013.

[5] J. Kropp, E. C. Roti Roti, A. Ringelstetter, H. Khatib, D. H. Abbott, and S. M. Salih, "Dexrazoxane diminishes doxorubicin-induced acute ovarian damage and preserves ovarian function and fecundity in mice," *PLoS One*, vol. 10, no. 11, article e0142588, 2015.

[6] L. A. Smith, V. R. Cornelius, C. J. Plummer et al., "Cardiotoxicity of anthracycline agents for the treatment of cancer: systematic review and meta-analysis of randomised controlled trials," *BMC Cancer*, vol. 10, no. 1, p. 337, 2010.

[7] P. Spallarossa, N. Maurea, C. Cadeddu et al., "A recommended practical approach to the management of anthracycline-based chemotherapy cardiotoxicity: an opinion paper of the working group on drug cardiotoxicity and cardioprotection, Italian Society of Cardiology," *Journal of Cardiovascular Medicine*, vol. 17, Supplement 1, pp. e84–e92, 2016.

[8] P. Menna and E. Salvatorelli, "Primary prevention strategies for anthracycline cardiotoxicity: a brief overview," *Chemotherapy*, vol. 62, no. 3, pp. 159–168, 2017.

[9] A. Engert, J. Franklin, H. T. Eich et al., "Two cycles of doxorubicin, bleomycin, vinblastine, and dacarbazine plus extended-field radiotherapy is superior to radiotherapy alone in early favorable Hodgkin's lymphoma: final results of the GHSG HD7 trial," *Journal of Clinical Oncology*, vol. 25, no. 23, pp. 3495–3502, 2007.

[10] A. Brayfield, *Doxorubicin in: Martindale: The Complete Drug Reference*, Pharmaceutical Press, London, 2013.

[11] M. Zhao, X.-F. Ding, J.-Y. Shen, X. P. Zhang, X. W. Ding, and B. Xu, "Use of liposomal doxorubicin for adjuvant chemotherapy of breast cancer in clinical practice," *Journal of Zhejiang University. Science. B*, vol. 18, no. 1, pp. 15–26, 2017.

[12] M. Magni, G. Biancon, S. Rizzitano et al., "Tyrosine kinase inhibition to improve anthracycline-based chemotherapy efficacy in T-cell lymphoma," *British Journal of Cancer*, vol. 121, no. 7, pp. 567–577, 2019.

[13] A. Kaczmarek, B. M. Brinkman, L. Heyndrickx, P. Vandenabeele, and D. V. Krysko, "Severity of doxorubicin-induced small intestinal mucositis is regulated by the TLR-2 and TLR-9 pathways," *The Journal of Pathology*, vol. 226, no. 4, pp. 598–608, 2012.

[14] S. M. Swain, F. S. Whaley, and M. S. Ewer, "Congestive heart failure in patients treated with doxorubicin: a retrospective analysis of three trials," *Cancer*, vol. 97, no. 11, pp. 2869–2879, 2003.

[15] E. A. M. Feijen, W. M. Leisenring, K. L. Stratton et al., "Derivation of anthracycline and anthraquinone equivalence ratios to doxorubicin for late-onset cardiotoxicity," *JAMA Oncology*, vol. 5, no. 6, pp. 864–871, 2019.

[16] M. Theodoulou and C. Hudis, "Cardiac profiles of liposomal anthracyclines: greater cardiac safety versus conventional doxorubicin?," *Cancer*, vol. 100, no. 10, pp. 2052–2063, 2004.

[17] K. Chatterjee, J. Zhang, N. Honbo, and J. S. Karliner, "Doxorubicin cardiomyopathy," *Cardiology*, vol. 115, no. 2, pp. 155–162, 2010.

[18] J. V. McGowan, R. Chung, A. Maulik, I. Piotrowska, J. M. Walker, and D. M. Yellon, "Anthracycline chemotherapy and cardiotoxicity," *Cardiovascular Drugs and Therapy*, vol. 31, no. 1, pp. 63–75, 2017.

[19] M. Štěrba, O. Popelová, A. Vávrová et al., "Oxidative stress, redox signaling, and metal chelation in anthracycline cardiotoxicity and pharmacological cardioprotection," *Antioxidants & Redox Signaling*, vol. 18, no. 8, pp. 899–929, 2013.

[20] N. Kalay, E. Basar, I. Ozdogru et al., "Protective effects of carvedilol against anthracycline-induced cardiomyopathy," *Journal of the American College of Cardiology*, vol. 48, no. 11, pp. 2258–2262, 2006.

[21] F. Cai, M. Luis, X. Lin et al., "Anthracycline-induced cardiotoxicity in the chemotherapy treatment of breast cancer: preventive strategies and treatment (Review)," *Molecular and Clinical Oncology*, vol. 11, no. 1, pp. 15–23, 2019.

[22] H. Kaiserová, T. Šimůnek, W. J. F. van der Vijgh, A. Bast, and E. Kvasničková, "Flavonoids as protectors against doxorubicin cardiotoxicity: role of iron chelation, antioxidant activity and inhibition of carbonyl reductase," *Biochimica et Biophysica Acta (BBA) - Molecular Basis of DiseaseBiochimica et Biophysica Acta*, vol. 1772, no. 9, pp. 1065–1074, 2007.

[23] G. Minotti, P. Menna, E. Salvatorelli, G. Cairo, and L. Gianni, "Anthracyclines: molecular advances and pharmacologic developments in antitumor activity and cardiotoxicity," *Pharmacological Reviews*, vol. 56, no. 2, pp. 185–229, 2004.

[24] F. F. Che, Y. Liu, and C. G. Xu, "Study on the effect and mechanism of dextromethionine on cardiotoxicity induced by doxorubicin," *Journal of Sichuan University*, vol. 41, pp. 24–28, 2010.

[25] X. Gao, Z. Han, and X. Du, "Observation of the effects of dextromethine on cardiotoxicity induced by epirubicin," *Chinese Journal of Cancer Prevention and Treatment*, vol. 17, pp. 296–298, 2010.

[26] G. Sacco, M. Bigioni, S. Evangelista, C. Goso, S. Manzini, and C. A. Maggi, "Cardioprotective effects of zofenopril, a new angiotensin-converting enzyme inhibitor, on doxorubicin-induced cardiotoxicity in the rat," *European Journal of Pharmacology*, vol. 414, no. 1, pp. 71–78, 2001.

[27] G. Sacco, M. Bigioni, G. Lopez, S. Evangelista, S. Manzini, and C. A. Maggi, "ACE inhibition and protection from doxorubicin-induced cardiotoxicity in the rat," *Vascular Pharmacology*, vol. 50, no. 5-6, pp. 166–170, 2009.

[28] A. Vavrova, H. Jansova, E. Mackova et al., "Catalytic inhibitors of topoisomerase II differently modulate the toxicity of anthracyclines in cardiac and cancer cells," *PLoS One*, vol. 8, no. 10, article e76676, 2013.

[29] S. Deng, T. Yan, C. Jendrny et al., "Dexrazoxane may prevent doxorubicin-induced DNA damage via depleting both topoisomerase II isoforms," *BMC Cancer*, vol. 14, no. 1, p. 842, 2014.

[30] H. M. Burkill, *The Useful Plants of West Tropical Africa*, vol. 2, Royal Botanic Gardens, Kew, London, 1985.

[31] L. Karalliedde and I. Gawarammana, *Traditional Herbal Medicines - a Guide to the Safer Use of Herbal Medicines*, Hammersmith Press, London, 2008.

[32] B. C. Unaeze, C. E. Ilo, C. Egwuatu, I. Orabueze, and E. Obi, "Anti-diarrhoeal effects of three Nigerian medicinal plant extracts on *E.coli*-induced diarrhea," *International Journal of Biological and Chemical Sciences*, vol. 11, no. 1, pp. 414–419, 2017.

[33] G. K. Mahunu, L. Quansa, H. E. Tahir, and A. A. Mariod, "Irvingia gabonensis: phytochemical constituents, bioactive compounds, traditional and medicinal uses," in *Wild Fruits: Composition, Nutritional Value and Products*, A. Mariod, Ed., Springer Cham, New York, NY, USA, 2019.

[34] J. I. Okogun, "Drug discovery through ethnobotany in Nigeria: some results," in *Advances in Phytomedicine - Ethnomedicine and Drug Discovery*, M. M. Iwu and J. C. Wootton, Eds., vol. 1, pp. 145–154, Elsevier, London, 2002.

[35] J. Sun and P. Chen, "Ultra high-performance liquid chromatography with high-resolution mass spectrometry analysis of African mango (*Irvingia gabonensis*) seeds, extract, and related dietary supplements," *Journal of Agricultural and Food Chemistry*, vol. 60, no. 35, pp. 8703–8709, 2012.

[36] F. M. Awah, P. N. Uzoegwu, P. Ifeonu et al., "Free radical scavenging activity, phenolic contents and cytotoxicity of selected Nigerian medicinal plants," *Food Chemistry*, vol. 131, no. 4, pp. 1279–1286, 2012.

[37] O. A. Wolfe and U. F. Ijeoma, "Effects of aqueous extracts of *Irvingia gabonensis* seeds on the hormonal parameters of male Guinea pigs," *Asian Pacific Journal of Tropical Medicine*, vol. 3, no. 3, pp. 200–204, 2010.

[38] D. C. Don Lawson, "Proximate analysis and phytochemical screening of *Irvingia gabonensis* (Ogbono cotyledon)," *Biomedical Journal of Scientific & Technical Research*, vol. 5, no. 4, pp. 4643–4646, 2018.

[39] O. O. Ekpe, C. O. Nwaehujor, C. E. Ejiofor, W. Arikpo Peace, E. Woruji Eliezer, and T. Amor Emmanuel, "*Irvingia gabonensis* seeds extract fractionation, its antioxidant analyses and effects on red blood cell membrane stability," *PhOL*, vol. 1, pp. 337–353, 2019.

[40] G. E. Trease and W. C. Evans, *A Textbook of Pharmacognosy*, Bailliere Tindall Ltd, London, UK, 1989.

[41] A. Sofowora, *Medicinal Plants and Traditional Medicine in Africa*, Spectrum Books Ltd, Ibadan, Nigeria, 1993.

[42] O. E. Olorundare, A. A. Adeneye, A. O. Akinsola, D. A. Sanni, M. Koketsu, and H. Mukhtar, "*Clerodendrum* volubile ethanol leaf extract: a potential antidote to doxorubicin-induced cardiotoxicity in rats," *Journal of Toxicology*, vol. 2020, Article ID 8859716, 17 pages, 2020.

[43] National Research Council (US) Committee for the Update of the Guide for the Care and Use of Laboratory Animals, *Guide for the Care and Use of Laboratory Animals*, The National Academies Press, Washington, DC, USA, 2011.

[44] R. D. Abbott, P. W. Wilson, W. B. Kannel, and W. P. Castelli, "High density lipoprotein-cholesterol, total cholesterol screening and myocardial infarction: the Framingham study," *Arteriosclerosis*, vol. 8, no. 3, pp. 207–211, 1988.

[45] S. Alladi and K. R. Shanmugasundaram, "Induction of hypercholesterolemia by supplementing soy protein with acetate generating amino acids," *Nutrition Reports International*, vol. 40, pp. 893–899, 1989.

[46] J. Zheng, H. C. M. Lee, M. M. bin Sattar, Y. Huang, and J. S. Bian, "Cardioprotective effects of epigallocatechin-3-gallate against doxorubicin-induced cardiomyocyte injury," *European Journal of Pharmacology*, vol. 652, no. 1-3, pp. 82–88, 2011.

[47] S. Polena, M. Shikara, S. Naik et al., "Troponin I as a marker of doxorubicin induced cardiotoxicity," *Proceedings of the Western Pharmacology Society*, vol. 48, pp. 142–144, 2005.

[48] A. Shahzadi, I. Sonmez, O. Allahverdiyev et al., "Cardiac troponin-I (cTnI) a biomarker of cardiac injuries induced by doxorubicin alone and in combination with ciprofloxacin, following acute and chronic dose protocol in Sprague Dawley rats," *International Journal of Pharmacology*, vol. 10, no. 5, pp. 258–266, 2014.

[49] R. Simões, L. M. Silva, A. L. V. M. Cruz, V. G. Fraga, A. de Paula Sabino, and K. B. Gomes, "Troponin as a cardiotoxicity

marker in breast cancer patients receiving anthracycline-based chemotherapy: a narrative review," *Biomedicine & Pharmacotherapy*, vol. 107, pp. 989–996, 2018.

[50] R. Zilinyi, A. Czompa, A. Czegledi et al., "The cardioprotective effect of metformin in doxorubicin-induced cardiotoxicity: the role of autophagy," *Molecules*, vol. 23, no. 5, article 1184, 2018.

[51] M. F. Alam, G. Khan, M. M. Safhi et al., "Thymoquinone ameliorates doxorubicin-induced cardiotoxicity in Swiss albino mice by modulating oxidative damage and cellular inflammation," *Cardiology Research and Practice*, vol. 2018, Article ID 1483041, 6 pages, 2018.

[52] M. Adamcova, V. Skarkova, J. Seifertova, and E. Rudolf, "Cardiac troponins are among targets of doxorubicin-induced cardiotoxicity in hiPCS-CMs," *International Journal of Molecular Sciences*, vol. 20, no. 11, article 2638, 2019.

[53] E. K. C. Kong, S. Yu, J. E. Sanderson, K. B. Chen, Y. Huang, and C. M. Yu, "A novel anti-fibrotic agent, baicalein for the treatment of myocardial fibrosis in spontaneously hypertensive rats," *European Journal of Pharmacology*, vol. 658, no. 2-3, pp. 175–181, 2011.

[54] B. A. Freeman and J. D. Crapo, "Biology of disease free radicals and tissue injury," *Laboratory Investigation*, vol. 47, no. 5, pp. 412–426, 1982.

[55] S. Gaweł, M. Wardas, E. Niedwork, and P. Wardas, "Malondialdehyde (MDA) as a lipid peroxidation marker," *Wiadomosci Lekarskie*, vol. 57, no. 9-10, pp. 453–455, 2004.

[56] S. H. Kim, K. M. Lim, J. Y. Noh et al., "Doxorubicin-induced platelet procoagulant activities: an important clue for chemotherapy-associated thrombosis," *Toxicological Sciences*, vol. 124, no. 1, pp. 215–224, 2011.

[57] I. Ben Aharon, H. Bar Joseph, M. Tzabari et al., "Doxorubicin-induced vascular toxicity – targeting potential pathways may reduce procoagulant activity," *PLoS One*, vol. 8, no. 9, article e75157, 2013.

[58] H. Lv, R. Tan, J. Liao et al., "Doxorubicin contributes to thrombus formation and vascular injury by interfering with platelet function," *American Journal of Physiology-Heart and Circulatory Physiology*, vol. 319, no. 1, pp. H133–H143, 2020.

[59] G. F. Samelis, G. P. Stathopoulos, D. Kotsarelis, I. Dontas, C. Frangia, and P. E. Karayannacos, "Doxorubicin cardiotoxicity and serum lipid increase is prevented by dextrazoxane (ICRF-187)," *Anticancer Research*, vol. 18, no. 5A, pp. 3305–3309, 1998.

[60] Y. M. Hong, H. S. Kim, and H.-R. Yoon, "Serum lipid and fatty acid profiles in adriamycin-treated rats after administration of L-carnitine," *Pediatric Research*, vol. 51, no. 2, pp. 249–255, 2002.

[61] J. Lee, M. Chung, Z. Fu, J. Choi, and H. J. Lee, "The effects of *Irvingia gabonensis* seed extract supplementation on anthropometric and cardiovascular outcomes: a systematic review and meta-analysis," *Journal of the American College of Nutrition*, vol. 39, no. 5, pp. 388–396, 2020.

[62] S. E. Kuyooro, E. O. Abam, and E. B. Agbede, "Hypolipidemic effects of *Irvingia gabonensis* - supplemented diets in male Albino rats," *Biochemistry & Analytical Biochemistry*, vol. 6, no. 2, article 1000316, 2017.

[63] J. O. Fatoki, O. T. Adedosu, O. K. Afolabi et al., "Dyslipidemic effect of doxorubicin and etoposide: a predisposing factor for the antineoplastic drugs-induced cardiovascular diseases,"

Research & Reviews: Journal of Pharmacology and Toxicological Studies, vol. 6, no. 1, pp. 34–42, 2018.

[64] I. Mentoor, T. Nell, Z. Emjedi, P. J. van Jaarsveld, L. de Jager, and A. M. Engelbrecht, "Decreased efficacy of doxorubicin corresponds with modifications in lipid metabolism markers and fatty acid profiles in breast tumors from obese vs. lean mice," *Frontiers in Oncology*, vol. 10, p. 306, 2020.

[65] S. Arunachalam, P. B. Tirupathi Pichiah, and S. Achiraman, "Doxorubicin treatment inhibits PPARγ and may induce lipotoxicity by mimicking a type 2 diabetes-like condition in rodent models," *FEBS Letters*, vol. 587, no. 2, pp. 105–110, 2013.

[66] J. L. Ngondi, J. E. Oben, and S. R. Minka, "The effect of *Irvingia gabonensis* seeds on body weight and blood lipids of obese subjects in Cameroon," *Lipids in Health and Disease*, vol. 4, no. 1, p. 12, 2005.

[67] J. E. Oben, J. L. Ngondi, and K. Blum, "Inhibition of *Irvingia gabonensis* seed extract (OB131) on adipogenesis as mediated via down regulation of the PPARgamma and leptin genes and up-regulation of the adiponectin gene," *Lipids in Health and Disease*, vol. 7, no. 1, p. 44, 2008.

[68] J. L. Ngondi, B. C. Etoundi, C. B. Nyangono, C. M. F. Mbofung, and J. E. Oben, "IGOB131, a novel seed extract of the West African plant *Irvingia gabonensis*, significantly reduces body weight and improves metabolic parameters in overweight humans in a randomized double-blind placebo controlled investigation," *Lipids in Health and Disease*, vol. 8, no. 1, p. 7, 2009.

[69] I. Onakpoya, L. Davies, P. Posadzki, and E. Ernst, "The efficacy of *Irvingia gabonensis* supplementation in the management of overweight and obesity: a systematic review of randomized controlled trials," *Journal of Dietary Supplements*, vol. 10, no. 1, pp. 29–38, 2013.

[70] M. Lee, D. E. Nam, O. K. Kim, T. J. Shim, J. H. Kim, and J. Lee, "Anti-obesity effects of African mango (*Irvingia gabonesis*, IGOB 131TM) extract in leptin-deficient obese mice," *Journal of the Korean Society of Food Science and Nutrition*, vol. 43, no. 10, pp. 1477–1483, 2014.

[71] B. Azantsa, D. Kuate, R. Chakokam, G. Paka, B. Bartholomew, and R. Nash, "The effect of extracts of *Irvingia gabonensis* (IGOB131) and *Dichrostachys glomerata* (Dyglomera™) on body weight and lipid parameters of healthy overweight participants," *Functional Foods in Health and Disease*, vol. 5, no. 6, pp. 200–208, 2015.

[72] S. Patra, S. Nithya, B. Srinithya, and S. M. Meenakshi, "Review of medicinal plants for anti-obesity activity," *Translational Biomedicine*, vol. 6, no. 3, 2015.

[73] Y. Yoshida and E. Niki, "Antioxidant effects of phytosterol and its components," *Journal of Nutritional Science and Vitaminology*, vol. 49, no. 4, pp. 277–280, 2003.

[74] S. Meguro, K. Higashi, T. Hase et al., "Solubilization of phytosterols in diacylglycerol versus triacylglycerol improves the serum cholesterol-lowering effect," *European Journal of Clinical Nutrition*, vol. 55, no. 7, pp. 513–517, 2001.

[75] I. Demonty, R. T. Ras, H. C. M. van der Knaap et al., "Continuous dose-response relationship of the LDL-cholesterol-lowering effect of phytosterol intake," *The Journal of Nutrition*, vol. 139, no. 2, pp. 271–284, 2009.

[76] R. T. Ras, J. M. Geleijnse, and E. A. Trautwein, "LDL-cholesterol-lowering effect of plant sterols and stanols across different dose ranges: a meta-analysis of randomised controlled studies," *The British Journal of Nutrition*, vol. 112, no. 2, pp. 214–219, 2014.

[77] E. Trautwein, M. Vermeer, H. Hiemstra, and R. Ras, "LDL-cholesterol lowering of plant sterols and stanols - which factors influence their efficacy?," *Nutrients*, vol. 10, no. 9, article 1262, 2018.

[78] C. Yuan, X. Zhang, X. Long, J. Jin, and R. Jin, "Effect of β-sitosterol self-microemulsion and β-sitosterol ester with linoleic acid on lipid-lowering in hyperlipidemic mice," *Lipids in Health and Disease*, vol. 18, no. 1, p. 157, 2019.

[79] S. Abu-Lafi, M. Rayan, M. Masalha et al., "Phytochemical composition and biological activities of wild *Scolymus maculatus* L.," *Medicine*, vol. 6, no. 2, p. 53, 2019.

[80] M. Saleem, I. Murtaza, R. S. Tarapore et al., "Lupeol inhibits proliferation of human prostate cancer cells by targeting beta-catenin signaling," *Carcinogenesis*, vol. 30, no. 5, pp. 808–817, 2009.

[81] L. S. Wei, W. Wee, J. Y. F. Siong, and D. F. Syamsumir, "Characterization of anticancer, antimicrobial, antioxidant properties and chemical compositions of *Peperomia pellucida* leaf extract," *Acta Medica Iranica*, vol. 49, no. 10, pp. 670–674, 2011.

[82] Y. Song and S. K. Cho, "Phytol induces apoptosis and ROS mediated protective autophagy in human gastric adenocarcinoma AGS cells," *Biochemistry and Analytical Biochemistry*, vol. 4, p. 211, 2015.

[83] R. Amarowicz, "Squalene: a natural antioxidant?," *European Journal of Lipid Science and Technology*, vol. 111, no. 5, pp. 411-412, 2009.

[84] S.-K. Kim and F. Karadeniz, "Biological importance and applications of squalene and squalane," *Advances in Food and Nutrition Research*, vol. 65, pp. 223–233, 2012.

[85] A. Ben Arfa, S. Combes, L. Preziosi-Belloy, N. Gontard, and P. Chalier, "Antimicrobial activity of carvacrol related to its chemical structure," *Letters in Applied Microbiology*, vol. 43, no. 2, pp. 149–154, 2006.

[86] E. N. Muzalevskaya, L. A. Miroshnichenko, V. A. Nikolaevskii et al., "Squalene: physiological and pharmacological properties," *Eksperimental'naia i Klinicheskaia Farmakologiia*, vol. 78, no. 6, pp. 30–36, 2015.

[87] B. Venkata Raman, L. A. Samuel, M. P. Saradhi et al., "Antibacterial, antioxidant activity and GC-MS analysis of *Eupatorium odoratum*," *Asian Journal of Pharmaceutical and Clinical Research*, vol. 5, no. 2, pp. 99–106, 2012.

[88] M. K. Swamy, G. Arumugam, R. Kaur, A. Ghasemzadeh, M. M. Yusoff, and U. R. Sinniah, "GC-MS based metabolite profiling, antioxidant and antimicrobial properties of different solvent extracts of MalaysianPlectranthus amboinicusLeaves," *Evidence-Based Complementary and Alternative Medicine*, vol. 2017, Article ID 1517683, 10 pages, 2017.

[89] W. Cordier and V. Steenkamp, "Herbal remedies affecting coagulation: a review," *Pharmaceutical Biology*, vol. 50, no. 4, pp. 443–452, 2012.

[90] S. Mahmud, S. Akhter, M. A. Rahman et al., "Antithrombotic effects of five organic extracts of Bangladeshi plants in vitro and mechanisms in in silico models," *eCAM*, vol. 2015, article 782742, pp. 1–8, 2015.

[91] V. T. Thom, N. H. Tung, D. van Diep et al., "Antithrombotic activity and saponin composition of the roots of Panax *bipinnatifidus Seem.* growing in Vietnam," *Pharmacognosy Research*, vol. 10, no. 4, pp. 333–338, 2018.

[92] D. Gogoi, A. Pal, P. Chattopadhyay, S. Paul, R. C. Deka, and A. K. Mukherjee, "First report of plant-derived β-sitosterol with antithrombotic, *in vivo* anticoagulant, and thrombus-preventing activities in a mouse model," *Journal of Natural Products*, vol. 81, no. 11, pp. 2521–2530, 2018.

[93] P. S. Salunkhe, S. D. Patil, and S. R. Dhande, "Anti-thrombotic activity of isolated β-sitosterol from roots of *Hemidesmus indicus* Linn. in rat model," *Journal of Pharmacognosy and Phytochemistry*, vol. 7, no. SP6, pp. 10–14, 2018.

Research Article

Amelioration of Cigarette Smoke-Induced Mucus Hypersecretion and Viscosity by *Dendrobium officinale* Polysaccharides *In Vitro* and *In Vivo*

Rui Chen [iD],[1] **Yingmin Liang** [iD],[1] **Mary Sau Man Ip** [iD],[1] **Kalin Yanbo Zhang** [iD],[2] **and Judith Choi Wo Mak** [iD][1,3]

[1]*Department of Medicine, The University of Hong Kong, Hong Kong*
[2]*School of Chinese Medicine, Li Ka Shing Faculty of Medicine, The University of Hong Kong, Hong Kong*
[3]*Department of Pharmacology & Pharmacy, The University of Hong Kong, Hong Kong*

Correspondence should be addressed to Judith Choi Wo Mak; judithmak@hku.hk

Chronic obstructive pulmonary disease (COPD), characterized by oxidative stress and inflammation, is one of the leading causes of death worldwide, in which cigarette smoke (CS) is the major risk factor. *Dendrobium officinale* polysaccharides (DOPs) are the main active ingredients extracted from *Dendrobium officinale*, which have been reported to have antioxidant and anti-inflammatory activity as well as inhibition of mucin gene expression. This study is aimed at investigating the effect of DOPs on CS-induced mucus hypersecretion and viscosity *in vitro* and *in vivo*. For *in vitro* study, primary normal human bronchial epithelial cells (HBECs) differentiated at the air-liquid interface (ALI) culture for 28 days were stimulated with cigarette smoke medium (CSM) in the absence or presence of various concentrations of DOPs or N-acetylcysteine (NAC) for 24 hours. For *in vivo* study, male Sprague-Dawley rats were randomized to sham air (SA) as control group or CS group for 56 days. At day 29, rats were subdivided and given water as control, DOPs, or NAC as positive control as a mucolytic drug via oral gavage for the remaining duration. Samples collected from apical washing, cell lysates, bronchoalveolar lavage (BAL), and lung tissues were evaluated for mucin gene expression, mucus secretion, and viscosity. DOPs ameliorated the CS-induced mucus hypersecretion and viscosity as shown by the downregulation of MUC5AC mRNA, MUC5AC secretary protein, and mucus viscosity via inhibition of mucus secretory granules in both *in vitro* and *in vivo* models. DOPs produced its effective effects on the CS-induced mucus hypersecretion and viscosity via the inhibition of the mucus secretory granules. These findings could be a starting point for considering the potential role of DOPs in the management of the smoking-mediated COPD. However, further research is needed.

1. Introduction

Chronic obstructive pulmonary disease (COPD), which is characterized by persistent airflow limitation and airway inflammation, is the third leading cause of death globally [1]. Cigarette smoke (CS), as the major risk factor for COPD, has been reported to be associated with chronic airway inflammation, airway epithelium impairment, and mucus hypersecretion [2–4]. Traditional pathogenetic theory is linking COPD with inflammatory process; however, recent finding revealed the significant role of chronic mucus hypersecretion in the pathogenesis of COPD [5]. Therefore, new treatment should be developed targeting on mucus hypersecretion.

The airway epithelial surface is covered by mucus, which is an extracellular gel with two major components, water and mucins, protecting the lung from continuous environmental exposure [6]. Under healthy condition, the sputum mucus solid concentration is 1.7% (by weight), which is increased to 3.7% in COPD patients [7]. The viscosity of mucus is determined by mucus solid concentration, increased mucus viscosity led to disability of cilia clearance [8]. Mucus is

mainly secreted by epithelial surface goblet cells and secretory cells from submucosal glands in large airways [6]. Mucin-5AC (MUC5AC) is the major gel-forming mucin in proximal airways by surface goblet cells, which are the predominant subtype found in COPD patients [9]. Moreover, CS could also induce MUC5AC mucin overexpression, and the increased MUC5AC is correlated with smoking history [3, 10]. Epidermal growth factor receptor (EGFR) might play a crucial role in the regulatory mechanism of CS-induced mucus hypersecretion [11]. Cigarette smoke activates EGFRs which activate mitogen-activated protein (MAP) kinases and cause upregulation of mucin MUC5AC in airway epithelial cells and led to mucus hypersecretion [12]. Due to the increased synthesis and secretion of mucins, mucus is usually dehydrated and more viscous, impeding mucus clearance in COPD airways [13]. N-Acetylcysteine (NAC) has been widely used as a mucolytic drug; however, its efficacy is limited [14]. Therefore, more effective mucolytic drugs should be developed.

The genus *Dendrobium* is one of the largest groups of the family *Orchidaceae*. In China, more than fifty *Dendrobium*-based health food products for promoting body fluid production have been approved by the State Food and Drug Administration (see Supplementary Table (available here)). Polysaccharides are considered as one of the main active ingredients *in Dendrobium* plants [15]. *Dendrobium officinale* polysaccharides (DOPs) have been reported to possess multiple pharmacological activities including antioxidant, anti-inflammatory, antiapoptotic, and hypoglycemic activities [16]. Recent findings demonstrated that DOPs inhibited MUC5AC expression, leading to amelioration of airway inflammation in a rat model of COPD as well as improvement of vital capacity in COPD patients [17]. However, insight into the mechanism of DOPs on inhibiting the CS-indussssced MUC5AC overproduction in relation to viscosity of mucus in the airways is lacking. This study is aimed at investigating the effects of DOPs on CS-induced mucus hypersecretion and viscosity.

2. Materials and Methods

2.1. Cigarette Smoke Medium (CSM) Preparation. Cigarette smoke (CS) generated from two cigarettes in the same packet with the mouthpiece filters removed (Camel (11 mg tar, 0.8 mg nicotine); R.J. Reynolds, Winston-Salem, NC, USA) was drawn into a syringe before bubbling in 20 ml phosphate-buffered saline (PBS). The solution was filter-sterilized through a 0.22 μm membrane filter and regarded as 100% CSM. The CSM was standardized by measuring absorbance (OD = 1.1) at 320 nM wavelength using a spectrophotometer CLARIOstar (BMG Labtech; Ortenberg, Germany) and was stored in aliquots at -80°C.

2.2. Preparation of DOPs. DOPs were extracted by Hong Kong GMP Pharmaceutical Factory (Bright Future Pharmaceutical Laboratories Ltd.). High-performance liquid chromatography (HPLC) was performed to fingerprint total DOPs (see Supplementary Figure).

2.3. DOP Treatment in CSM-Exposed Air-Liquid Interface (ALI) Culture of Primary Human Bronchial Epithelial Cells. Well-differentiated normal primary human bronchial epithelial cells (HBECs; $n = 5$) were prepared using a previously described protocol [18]. HBECs from 2 different donors (Lonza, Walkersville, MD, USA; American Type Culture Collection (ATCC), Rockville, MD, USA) were seeded onto collagen-coated 12 mm transwell inserts with 0.4 μm pore size (2.5×10^5 cells per well; Corning Life Sciences, MA). After 100% confluent, medium was removed from the apical side of transwell and left to 28-day differentiation in an ALI medium with 1 : 1 mixture of BEBM (Lonza, Walkersville, MD, USA) and DMEM (Gibco, Carlsbad, CA) supplemented with 52 μg/ml bovine pituitary extract (BPE), 5 μg/ml insulin, 0.5 μg/ml hydrocortisone, 10 μg/ml transferrin, 0.5 μg/ml epinephrine, 0.5 ng/ml human epidermal growth factor (hEGF), 1.5 μg/ml bovine serum albumin (BSA), and 15 ng/ml retinoic acid. After 18 h starvation, cells were treated with 4% CSM in the absence or presence of various concentrations of DOPs (0.01, 0.1, or 1 μg/ml) or N-acetylcysteine (NAC; 10 nM, as positive control) for 24 hours (Figure 1(a)). Apical washing (350 μl) from ALI cultures of well-differentiated HBECs was collected and frozen in aliquots for further analysis.

2.4. DOP Treatment in CS-Exposed Rats. Equal numbers ($n = 8$) of male Sprague-Dawley (SD) rats were randomly divided into sham air (SA) as control group or CS group for 56 days. Rats in the CS group were exposed to CS using the computer-controlled whole body inExpose smoking system (SCIREQ, Montreal, Canada) at a total particulate matter (TPM) of 2000 mg/m³ for 1 hour (20 cigarettes) daily, while rats in the SA group were subjected to the same procedure in another ventilated chamber but exposed to fresh air. Cigarettes (10 mg TAR and 0.8 mg nicotine, Camel, R.J. Reynolds, Winston-Salem, NC, USA) were obtained from local commercial retailers. At day 29, rats were subdivided and given water as control, two doses of DOPs (50 mg/kg and 200 mg/kg b.wt.), or NAC (300 mg/kg b.wt., as positive control) daily via oral gavage for the remaining duration (Figure 1(b)). On day 57, rats were sacrificed 24 h after last exposure with overdose of pentobarbital (100 mg/kg; i.p.). Bronchoalveolar lavage (BAL) was obtained through washing with 1.5 ml ice-cold PBS for three times in total. After centrifugation at 1000 rpm for 10 min at 4°C to remove cellular debris, the supernatant was frozen in aliquots for further use. The largest lobe of the left lung tissue was fixed in 4% formalin solution and embedded in paraffin for sectioning. The remaining lung tissues were collected and frozen for further analysis. All animal procedures were performed in strict accordance with the guidelines from ARRIVE and Directive 2010/63/EU of the European Parliament, and the animal protocols were approved by the Committee on the Use of Live Animals in Teaching and Research (CULATR) of The University of Hong Kong (No. 4538-17).

2.5. RNA Extraction and RT-PCR for MUC5AC mRNA. Well-differentiated HBECs and lung tissues were harvested for RNA extraction using TRIzol reagent (Invitrogen, USA).
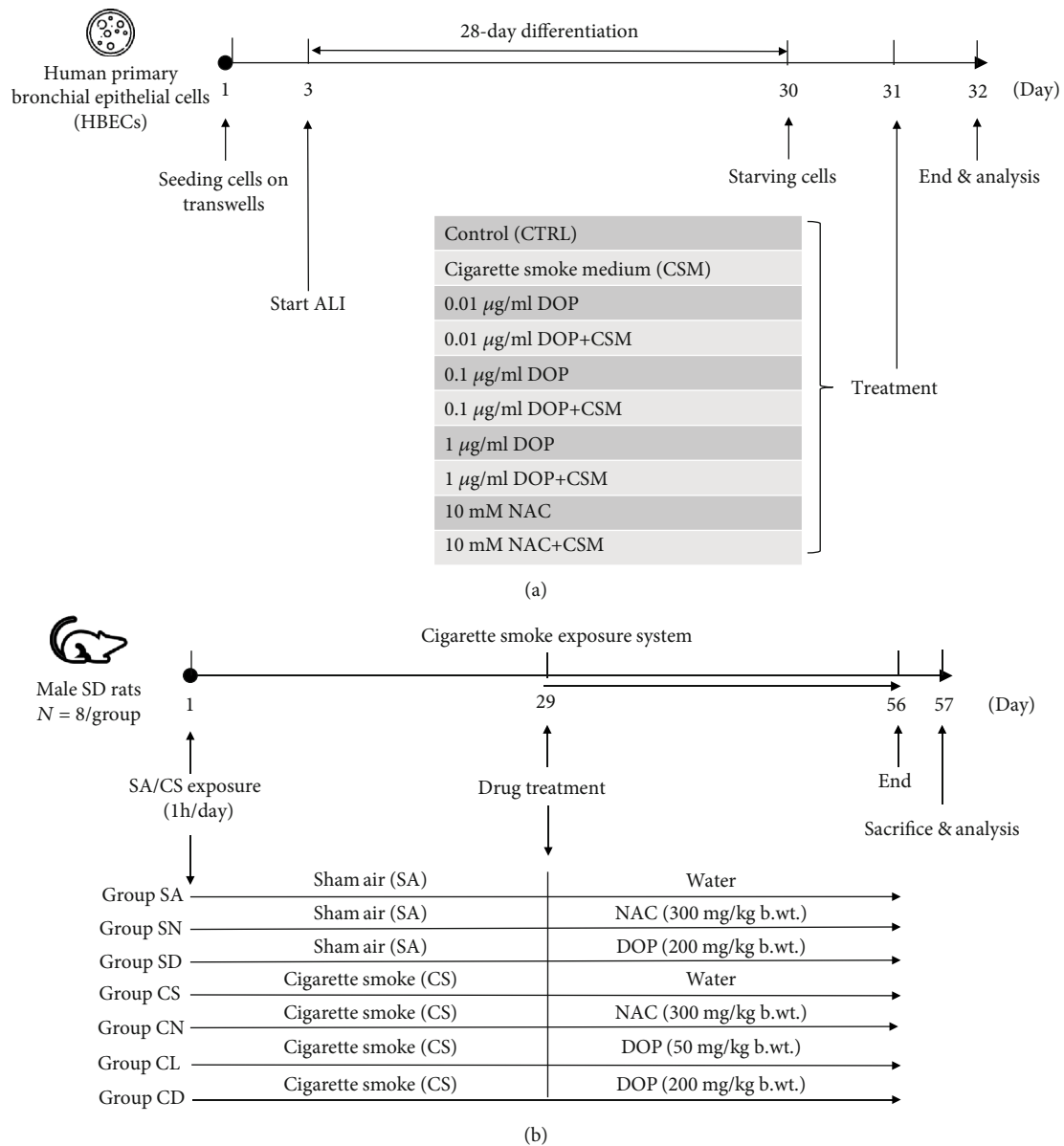
Figure 1: Experimental protocols for *in vitro* and *in vivo* models. (a) Schematic overview of air-liquid interface (ALI) culture of well-differentiated HBEC model with different treatments ($n = 5$). (b) Schematic overview of male Sprague-Dawley (SD) rat model with different treatment groups ($n = 8$).

Total RNA was DNase treated (Invitrogen, USA) before cDNA synthesis. Reverse transcription of RNA was conducted with EvoScript Universal cDNA Master kit (Roche, Basel, Switzerland) following the manufacturer's instruction. Quantitative RT-PCR assay was performed using SYBR Green Real-Time Master Mix (Applied Biosystems, Lithuania) based on the manufacturer's protocol. Relative quantity of mRNA was obtained by using the comparative Ct method and normalized by housekeeping genes such as human ribosomal protein S13 (RPS13) or rat glyceraldehyde 3-phosphate dehydrogenase (GAPDH). The primer for human MUC5AC is as follows: 5$'$-CTT TGG CAT CTG TGA GGA GC-3$'$ (forward primer) and 5$'$-CAC AGA AGC AGA GGT CTT GC-3$'$ (reverse primer). The primer for rat MUC5AC is

as follows: 5$'$-AAC TCT GCC CAC CAC AAG C-3$'$ (forward primer) and 5$'$-TGC CAT CTA TCC AAT CAG TCC AAT-3$'$ (reverse primer).

2.6. MUC5AC ELISA.
The method of MUC5AC ELISA was adapted from Parker et al.'s previous report [18]. Apical washing from the well-differentiated HBECs and BAL from rats was diluted (1 : 5 and 1 : 10, respectively) in carbonate-bicarbonate coating buffer (Sigma-Aldrich, St. Louis, MO, USA) and incubated at 37°C for 18 h. After washing with PBS/Tween-20 (0.05%), the plate was blocked with 2% BSA (Sigma-Aldrich) for 1 h at room temperature. After washing, a 1 : 200 dilution of MUC5AC mouse Mab (45M1; Thermo Fisher Scientific, Carlsbad, CA, USA) was added and

(a) (b) (c) (d)
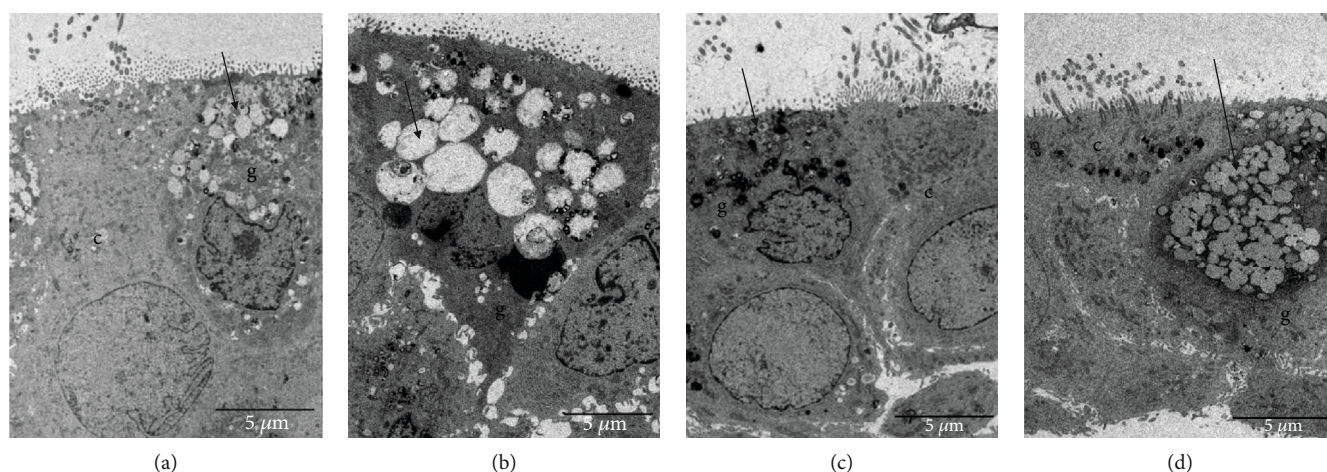
FIGURE 2: Transmission electron microscopy (TEM) images of *in vitro* model. Primary normal human bronchial epithelial cells (HBECs) after 28-day air-liquid interface (ALI) culture were stimulated with (a) control medium, (b) 4% cigarette smoke medium (CSM), (c) 4% CSM with *Dendrobium officinale* polysaccharides (DOPs) (1 μg/ml), and (d) 4% CSM with N-acetylcysteine (NAC) (10 mM). c: ciliated cells; g: goblet cells; arrow: secretory vesicles. Scale bar: 5 μm.

(a) (b) (c)
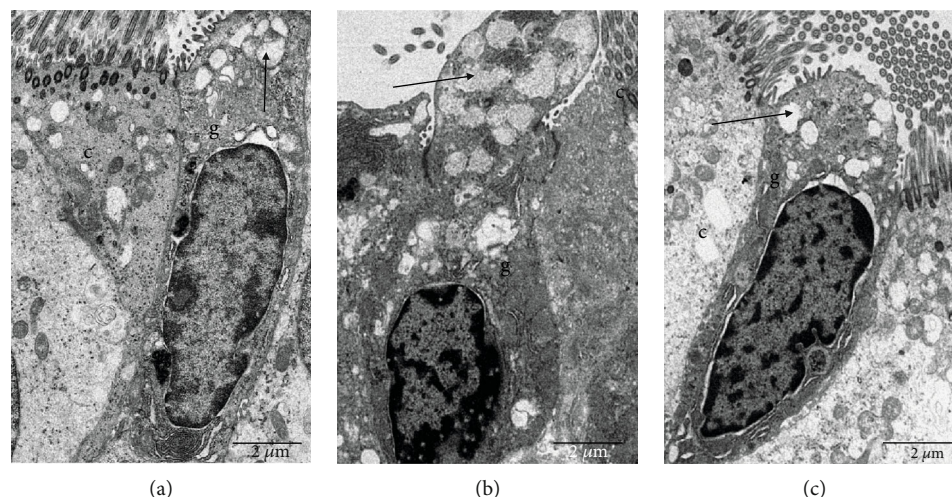
FIGURE 3: Transmission electron microscopy (TEM) images of airway epithelium of rat trachea. Male Sprague-Dawley (SD) rats were exposed to sham air (as control) or cigarette smoke for 56 days. At day 29, rats were subdivided as (a) sham air with water (as control), (b) cigarette smoke with water, and (c) cigarette smoke with DOPs (200 mg/kg b.wt.) via oral gavage for the remaining duration. c: ciliated cells; g: goblet cells; arrow: secretory vesicles. Scale bar: 2 μm.

incubated for 1 h at room temperature. A 1 : 2000 dilution of rabbit anti-mouse IgG antibody conjugated to HRP (Novus Biologicals, Littleton, CO, USA) was added after washing and incubated for 1 h at room temperature. After washing, tetramethylbenzidine (TMB) substrate solution (BD Biosciences, San Diego, CA, USA) was added and developed in the dark for 15 min. The reaction was stopped by adding 2N H_2SO_4, and the plate was read at 450 nm with 570 nm for wavelength correction using a spectrophotometer (CLARIOstar®, BMG Labtech, Ortenberg, Germany).

2.7. Mucus Viscosity. Apical washing from well-differentiated HBECs and BAL from rat was measured using a Brookfield LVDV-II+Pro cone and plate digital viscometer with CP-40 spindle (Brookfield AMETEK, MA, USA). The measurements were carried out at 25°C using a water bath with tem-

perature controller. Viscosity measured at a speed of 40 rpm and shear rate of 300 1/s was used to compare the groups after normalizing to relevant control, adapted from Sánchez-Véliz et al.'s previous report [19]. Data were collected from the first 30 s of the experiments.

2.8. Transmission Electron Microscopy (TEM). Selected ALI cultures of well-differentiated HBECs and rat trachea were fixed in 2.5% glutaraldehyde (Electron Microscopy Sciences, Ft. Washington, PA, USA) and sent to Electron Microscope Unit (EMU) of The University of Hong Kong for further processes. The samples were observed under a Philips CM 100 transmission electron microscope.

2.9. Histopathology. Alcian Blue/Periodic Acid-Schiff (AB/PAS) staining was applied to identify goblet cells in the
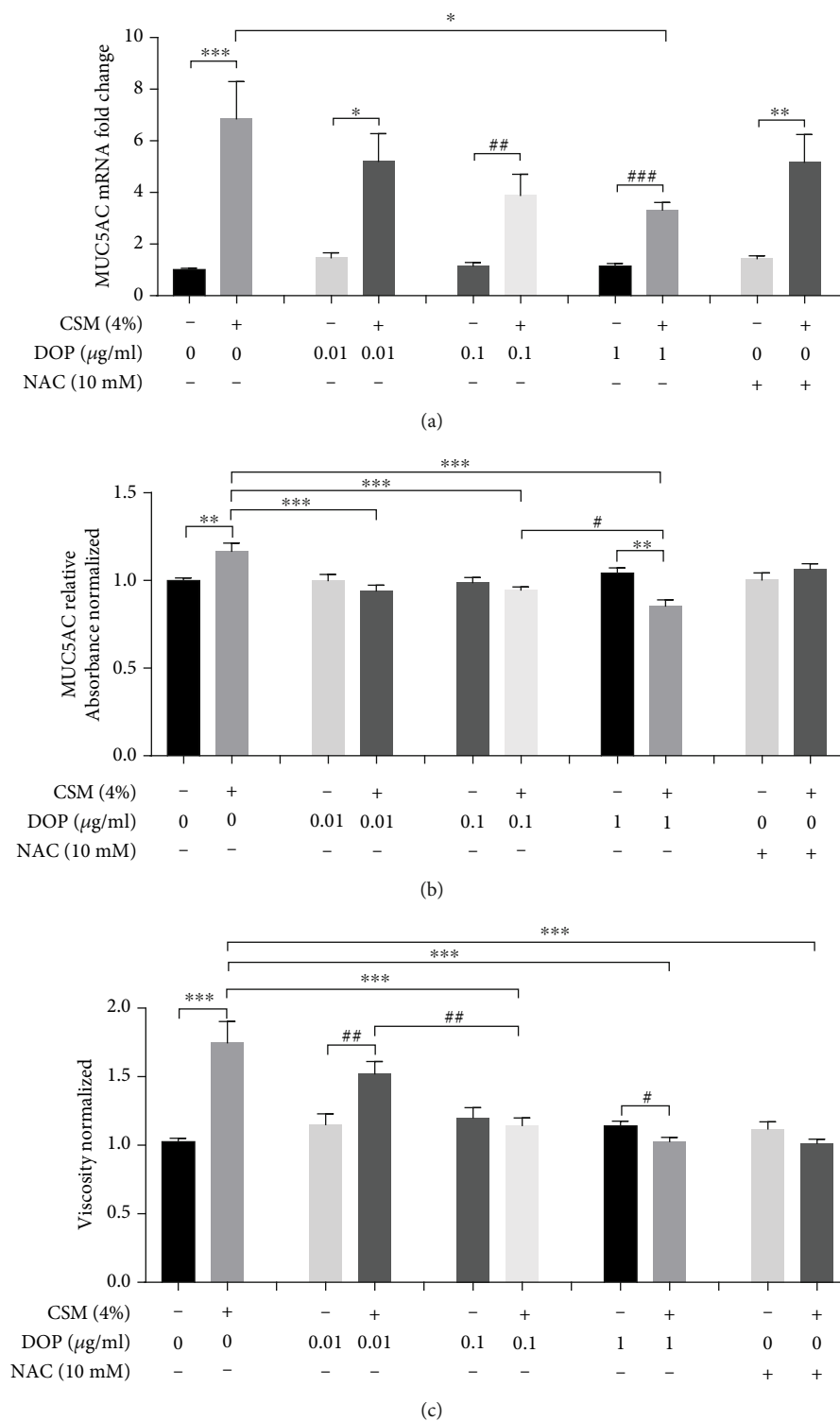
Figure 4: Effect of DOPs on CS-induced mucus secretion and viscosity in *in vitro* model. Primary normal human bronchial epithelial cells (HBECs) after 28-day air-liquid interface (ALI) culture were treated with DOPs or N-acetylcysteine (NAC) and then 4% cigarette smoke medium (CSM) for 24 hours. (a) Analysis of MUC5AC mRNA expression was carried out by real-time qPCR. (b) MUC5AC protein was quantitated by ELISA in apical washing. (c) Mucus viscosity was measured using a Brookfield LVDV-II+Pro cone and plate digital viscometer with CP-40 spindle in apical washing. Values are expressed as mean ± SEM ($n = 5$). $^*p < 0.05$, $^{**}p < 0.01$, and $^{***}p < 0.001$ for one-way ANOVA test with post hoc analysis (Bonferroni). $^\#p < 0.05$, $^{\#\#}p < 0.01$, and $^{\#\#\#}p < 0.001$ for Student's *t*-test.

(a)

(b)

(c)
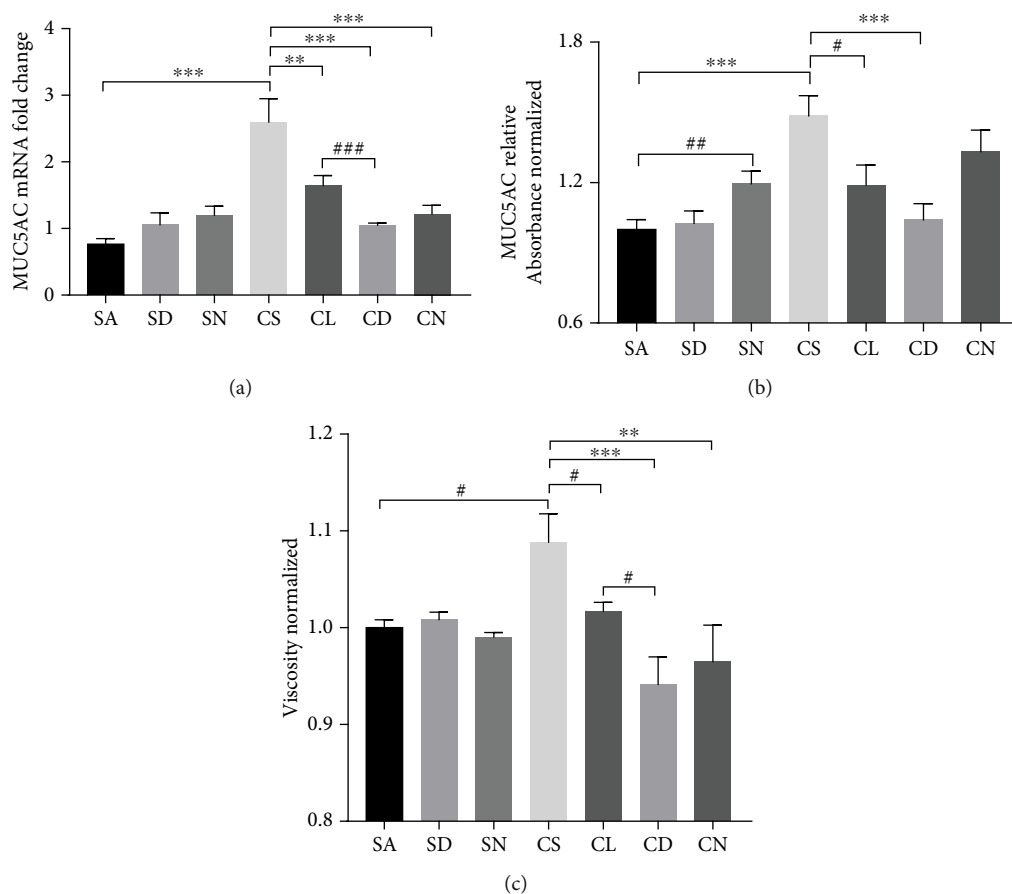
FIGURE 5: Effect of DOPs on CS-induced mucus secretion and viscosity in rat lungs. Male Sprague-Dawley rats were randomized to sham air (SA) (as control) or cigarette smoke (CS) group for 56 days. At day 29, rats were subdivided and given water as control (SA and CS groups), two doses of DOPs (100 mg/kg b.wt. and 200 mg/kg b.wt.) (SD, CL, and CD groups), or N-acetylcysteine (NAC; 500 mg/kg b.wt. as positive control) (SN and CN groups) daily via oral gavage for the remaining duration. (a) Analysis of lung MUC5AC mRNA expression was carried out by real-time qPCR. (b) MUC5AC protein was quantitated by ELISA in bronchoalveolar lavage (BAL). (c) Mucus viscosity was measured using a Brookfield LVDV-II+Pro cone and plate digital viscometer with CP-40 spindle in BAL. Values are expressed as mean ± SEM ($n = 8$). $**p < 0.01$ and $***p < 0.001$ for one-way ANOVA test with post hoc analysis (Bonferroni). $^{\#}p < 0.05$, $^{\#\#}p < 0.01$, and $^{\#\#\#}p < 0.001$ for Student's t-test.

airways. Images of 5 fields for epithelium in rat cartilaginous airways were captured randomly at ×40 magnifications by using a Nikon microscope (Nikon Instruments Inc., Tokyo, Japan) with a Nikon DS-Ri2 Digital Camera. The PAS-positive cells were measured using the software Nikon NIS-Elements BR.

2.10. Western Blot Analysis. Total protein of rat lung homogenate was separated in SDS-polyacrylamide gel and transferred onto a nitrocellulose membrane (GE Healthcare, Germany). After blocking, target protein was detected using specified antibody for analysis of phospho-EGFR (T678; ImmunoWay Biotechnology, Plano, TX, USA; 1 : 1000 dilution). Protein expression levels were normalized with α-tubulin.

2.11. Statistical Analysis. Data were presented as mean ± SEM. One-way ANOVA test with post hoc analysis (Bonferroni) was applied to compare multiple groups. Student's t-test was also carried out for variables measured at a single

time point where appropriate. All the statistical analyses were performed using GraphPad Prism 7 (GraphPad Software Inc., San Diego, CA, USA). Significance was achieved if p value < 0.05.

3. Results and Discussion

Under TEM, CSM or CS exposure caused an increase in the number of secretory vesicles and enlargement of the secretory vesicles associated with mucus secretion in the goblet cells *in vitro* (Figures 2(a) and 2(b)) and *in vivo* (Figures 3(a) and 3(b)), respectively, which were reversed by DOP treatment (Figures 2(c) and 3(c)). However, NAC treatment attenuated only the CSM-induced swollen secretory vesicles and caused no effect on the number of secretory vesicles (Figure 2(d)). The enlargement of secretory vesicles might lead to increased mucus secretion and viscosity. Treatment of DOPs diminished the number and the size of the secretory vesicles in both CS-exposed cell and rat models. As a mucolytic drug, NAC ameliorated only CS-induced

(a)   (b)   (c)   (d)

(e)
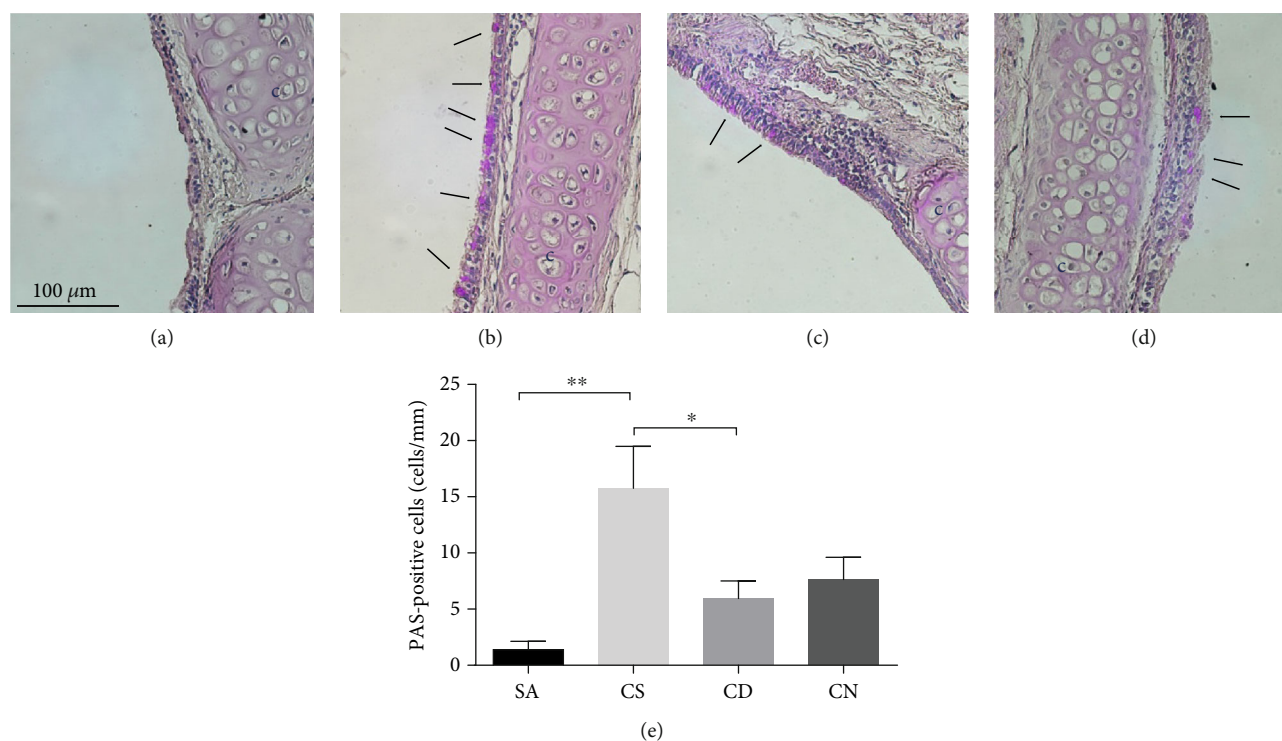
FIGURE 6: Effect of DOPs on CS-induced goblet cell hyperplasia in rat lungs. Male Sprague-Dawley (SD) rats were exposed to sham air (as control) or cigarette smoke for 56 days. At day 29, rats were subdivided as (a) SA: sham air with water (as control); (b) CS: cigarette smoke with water; (c) CD: cigarette smoke with DOPs (200 mg/kg b.wt.); and (d) CN: cigarette smoke with NAC (500 mg/kg b.wt.) via oral gavage daily for the remaining duration. (a–d) Representative images of cartilaginous airways in the rat lung sections stained with Alcian Blue/Periodic Acid-Schiff (AB/PAS). Scale bar = 100 μm. Goblet cells appear as purple staining (arrows) over epithelium. AB/PAS staining revealed increased goblet cell hyperplasia after CS exposure and DOPs or NAC reduced the CS-induced goblet cell hyperplasia. (e) Quantification of AB/PAS-positive cells per length of epithelium for goblet cells of different groups. Values are expressed as mean ± SEM ($n = 8$). $^{*}p < 0.05$ and $^{**}p < 0.01$ for one-way ANOVA test with post hoc analysis (Bonferroni).

swollen secretary vesicles in the goblet cells with no reduction in the number of secretory vesicles, suggesting the differential mucolytic effect between DOPs and NAC.

CSM or CS exposure caused significant upregulation of MUC5AC mRNA expression in well-differentiated HBECs under ALI culture (Figure 4(a)) and in rat lung (Figure 5(a)), which was attenuated by DOPs in a dose-dependent manner. However, NAC had no attenuation of CSM-induced MUC5AC mRNA *in vitro* (Figure 4(a)) but caused significant reduction in CS-induced MUC5AC mRNA in rat lung (Figure 5(a)). Following a similar trend to gene expression, CSM or CS stimulated mucus hypersecretion in apical washing of well-differentiated HBECs under ALI culture (Figure 4(b)) and in rat BAL (Figure 5(b)) by MUC5AC ELISA, which was effectively reversed by DOPs dose dependently (Figures 4(b) and 5(b)). NAC had no effect on CSM- or CS-induced mucus hypersecretion *in vitro* and *in vivo*. CSM or CS induced significant elevation of mucus viscosity in apical washing (Figure 4(c)) and in rat BAL (Figure 5(c)), respectively, which was ameliorated by DOPs and NAC (Figures 4(c) and 5(c)). In line with the *in vivo* findings, CS exposure caused a significant increase in the number of goblet cells containing mucus in the epithelium of the cartilaginous airways, which was reduced by the treatment with DOPs using PAS staining (Figure 6). Furthermore, previous findings suggested that epidermal growth factor receptor

(EGFR) is essential to mucin synthesis in response to CS stimulation [12, 20]. CS exposure caused significant upregulation of phospho-EGFR protein expression in rat lung, which was not reversed by either DOPs or NAC (Figure 7). However, NAC alone caused elevation of phospho-EGFR protein expression in rat lung (Figure 7).

The findings of the present study for the first time showed that DOPs could ameliorate mucus hypersecretion and mucus viscosity via inhibition of swollen secretory vehicles in the airway epithelium in both CSM- or CS-exposed models *in vitro* and *in vivo*. Mucus is essential for its role in protecting the airways. However, chronic inflammatory lung diseases, such as COPD, are often associated with excessive mucus production, especially in chronic bronchitis. Smoking is a common stimulus to promote mucus secretion via synthesis and secretion of MUC5AC [21]. MUC5AC has been recognized as the predominant secretary mucin in human airway epithelial cells, and its expression increases in smokers and COPD patients [22]. In this study, CS exposure caused upregulation of mucin MUC5AC in both *in vitro* and *in vivo* models, in agreement with previous studies [11, 23]. DOPs inhibited CS-induced MUC5AC overproduction in *in vitro* and *in vivo* models, in line with Song et al.'s previous report [17]. However, NAC had no significant effect on CS-induced MUC5AC overproduction *in vitro* and *in vivo*. The mechanism of NAC as a mucolytic drug might work through
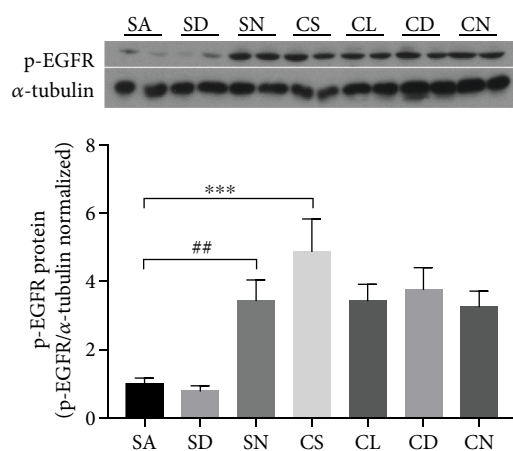
Figure 7: Effect of DOPs on CS-induced activation of epidermal growth factor receptor (EGFR) in rat lungs. Total protein from rat lungs was extracted. Phospho-EGFR was normalized by α-tubulin (housekeeping). Values are expressed as mean $\pm$ SEM ($n = 8$). ***p < 0.001 for one-way ANOVA test with post hoc analysis (Bonferroni). ##p < 0.01 for Student's t-test.

depolymerization of the mucin glycoprotein oligomer by hydrolyzing the mucin disulfide bonds and led to lessening of mucus viscosity [14, 24]. Although previous findings suggested that NAC could reduce mucin MUCA5C expression [25], the current data provided evidence for the insufficiency of NAC as a mucolytic drug especially under healthy condition [26]. The present findings on DOPs suggest a potential effective drug for amelioration of mucus hypersecretion. It is well recognized that CS induces mucus viscosity, which is consistent with the current findings in both *in vitro* and *in vivo* models [27]. DOPs attenuated CS-induced mucus viscosity dose dependently in both cultured cells and rat models, while NAC effectively reduced CS-induced mucus viscosity only.

To further study the mechanism of cigarette smoke-induced MUC5AC overexpression in airway epithelium, the expression of EGFR, which plays a crucial role in mucin production [28], was investigated. Oxidant stimuli such as CS exposure activate the expression of EGFR, which leads to activation of MAP kinases resulting in mucin gene (MUC5AC) transcription and induces mucus hypersecretion [12, 28]. Consistent to the previous findings, CS caused elevation of activated EGFR expression in rat lung [20, 23]. However, DOP had no significant effect on the inhibition of CS-induced EGFR activation, indicating that the alternative pathways might be involved in manipulating mucin MUC5AC overproduction. Unexpectedly, NAC alone caused upregulation of activated EGFR in rat lung of the sham air-exposed group. Except as a mucolytic drug, NAC also acts as an antioxidant to overcome oxidant-antioxidant imbalance in the inflammatory airways [29, 30], suggesting that NAC may serve as an oxidant under healthy condition.

Nevertheless, the present study has certain limitations. Firstly, direct CS exposure was not applied on the apical side of the epithelium in the *in vitro* study to mimic the human settings. Secondly, a passive smoking rat model was used *in vivo*, which might not exactly reflect the condition of

COPD patients who have actively smoked for a long time. Lastly, consolidating evidence for the mechanism of action of DOPs on viscosity is still lacking, which warrants further study.

In summary, DOPs produced its effective effects on CS-induced mucus hypersecretion and viscosity via the inhibition of the mucus secretory granules. These findings could be a starting point for considering the potential role of DOPs in the management of the smoking-mediated COPD. However, further research is needed.

Abbreviations

AB/PAS:	Alcian Blue/Periodic Acid-Schiff
ALI:	Air-liquid interface
BAL:	Bronchoalveolar lavage
BPE:	Bovine pituitary extract
BSA:	Bovine serum albumin
COPD:	Chronic obstructive pulmonary disease
CS:	Cigarette smoke
CSM:	Cigarette smoke medium
CULATR:	Committee on the Use of Live Animals in Teaching and Research
DOPs:	*Dendrobium officinale* polysaccharides
EGFR:	Epidermal growth factor receptor
EMU:	Electron Microscope Unit
GAPDH:	Glyceraldehyde 3-phosphate dehydrogenase
HBECs:	Human bronchial epithelial cells
hEGF:	Human epidermal growth factor
HPLC:	High-performance liquid chromatography
MAP:	Mitogen-activated protein
MUC5AC:	Mucin-5AC
NAC:	N-Acetylcysteine
PBS:	Phosphate-buffered saline
RT-PCR:	Real-time polymerase chain reaction
RPS13:	Ribosomal protein S13
SA:	Sham air
SD:	Sprague-Dawley
SEM:	Standard error of the mean
TEM:	Transmission electron microscopy
TMB:	Tetramethylbenzidine
TPM:	Total particulate matter.

Data Availability

Data will be available on request (judithmak@hku.hk).

Conflicts of Interest

The authors have no conflict of interest to declare.

Authors' Contributions

RC, YL, MSMI, KYZ, and JCWM designed the study. RC performed the experiments, collected and analyzed the data, and drafted the manuscript. YL assisted in the experiments, provided technical guidance, and analyzed the data. YL, KYZ, and JCWM secured the funding and edited the manuscript. All authors read and approved the final manuscript.

Acknowledgments

Supplementary Materials

Supplementary Table: examples of *Dendrobium*-based drugs and health food products approved by the State Food and Drug Administration in China. Supplementary Figure: HPLC fingerprint for total *Dendrobium officinale* polysaccharides (DOPs) used in this study. (*Supplementary Materials*)

References

[1] J. Vestbo, S. S. Hurd, A. G. Agustí et al., "Global strategy for the diagnosis, management, and prevention of chronic obstructive pulmonary disease: GOLD executive summary," *American Journal of Respiratory and Critical Care Medicine*, vol. 187, no. 4, pp. 347–365, 2013.

[2] J. Lee, V. Taneja, and R. Vassallo, "Cigarette smoking and inflammation: cellular and molecular mechanisms," *Journal of Dental Research*, vol. 91, no. 2, pp. 142–149, 2012.

[3] M. X. Shao, T. Nakanaga, and J. A. Nadel, "Cigarette smoke induces MUC5AC mucin overproduction via tumor necrosis factor-α-converting enzyme in human airway epithelial (NCI-H292) cells," *American Journal of Physiology-Lung Cellular and Molecular Physiology*, vol. 287, no. 2, pp. L420–L427, 2004.

[4] A. C. Schamberger, C. A. Staab-Weijnitz, N. Mise-Racek, and O. Eickelberg, "Cigarette smoke alters primary human bronchial epithelial cell differentiation at the air-liquid interface," *Scientific Reports*, vol. 5, no. 1, article 8163, 2015.

[5] I. Cerveri and V. Brusasco, "Revisited role for mucus hypersecretion in the pathogenesis of COPD," *European Respiratory Review*, vol. 19, no. 116, pp. 109–112, 2010.

[6] J. V. Fahy and B. F. Dickey, "Airway mucus function and dysfunction," *The New England Journal of Medicine*, vol. 363, no. 23, pp. 2233–2247, 2010.

[7] D. B. Hill, P. A. Vasquez, J. Mellnik et al., "A biophysical basis for mucus solids concentration as a candidate biomarker for airways disease," *PLoS One*, vol. 9, no. 2, article e87681, 2014.

[8] R. A. Cone, "Barrier properties of mucus," *Advanced Drug Delivery Reviews*, vol. 61, no. 2, pp. 75–85, 2009.

[9] G. Caramori, C. di Gregorio, I. Carlstedt et al., "Mucin expression in peripheral airways of patients with chronic obstructive pulmonary disease," *Histopathology*, vol. 45, no. 5, pp. 477–484, 2004.

[10] G. Caramori, P. Casolari, C. di Gregorio et al., "MUC5AC expression is increased in bronchial submucosal glands of stable COPD patients," *Histopathology*, vol. 55, no. 3, pp. 321–331, 2009.

[11] Y. Liang, K. W. K. Liu, S. C. Yeung, X. Li, M. S. M. Ip, and J. C. W. Mak, "(-)-Epigallocatechin-3-gallate reduces cigarette smoke-induced airway neutrophilic inflammation and mucin hypersecretion in rats," *Frontiers in Pharmacology*, vol. 8, p. 618, 2017.

[12] P. J. Barnes, "Inflammatory mechanisms in patients with chronic obstructive pulmonary disease," *Journal of Allergy and Clinical Immunology*, vol. 138, no. 1, pp. 16–27, 2016.

[13] G. D. Leikauf, M. T. Borchers, D. R. Prows, and L. G. Simpson, "Mucin apoprotein expression in COPD," *Chest*, vol. 121, no. 5, pp. 166S–182S, 2002.

[14] C. Ehre, Z. L. Rushton, B. Wang et al., "An improved inhaled mucolytic to treat airway muco-obstructive diseases," *American Journal of Respiratory and Critical Care Medicine*, vol. 199, no. 2, pp. 171–180, 2019.

[15] T. B. Ng, J. Liu, J. H. Wong et al., "Review of research on *Dendrobium*, a prized folk medicine," *Applied Microbiology and Biotechnology*, vol. 93, no. 5, pp. 1795–1803, 2012.

[16] Y. Lam, T. B. Ng, R. M. Yao et al., "Evaluation of chemical constituents and important mechanism of pharmacological biology in *Dendrobium* Plants," *Evidence-Based Complementary and Alternative Medicine*, vol. 2015, Article ID 841752, 25 pages, 2015.

[17] T.-H. Song, X.-X. Chen, S. C. W. Tang et al., "*Dendrobium officinale* polysaccharides ameliorated pulmonary function while inhibiting mucin-5AC and stimulating aquaporin-5 expression," *Journal of Functional Foods*, vol. 21, pp. 359–371, 2016.

[18] J. Parker, S. Sarlang, S. Thavagnanam et al., "A 3-D well-differentiated model of pediatric bronchial epithelium demonstrates unstimulated morphological differences between asthmatic and nonasthmatic cells," *Pediatric Research*, vol. 67, no. 1, pp. 17–22, 2010.

[19] R. Sánchez-Véliz, M. J. Carmona, D. A. Otsuki et al., "Impact of cardiopulmonary bypass on respiratory mucociliary function in an experimental porcine model," *PLoS One*, vol. 10, no. 8, article e0135564, 2015.

[20] L. Zhang, J. Li, J. Hu et al., "Cigarette smoke extract induces EGFR-TKI resistance via promoting EGFR signaling pathway and ROS generation in NSCLC cell lines," *Lung Cancer*, vol. 109, pp. 109–116, 2017.

[21] L. E. Haswell, K. Hewitt, D. Thorne, A. Richter, and M. D. Gaça, "Cigarette smoke total particulate matter increases mucous secreting cell numbers in vitro: a potential model of goblet cell hyperplasia," *Toxicology In Vitro*, vol. 24, no. 3, pp. 981–987, 2010.

[22] Y. P. Di, J. Zhao, and R. Harper, "Cigarette smoke induces MUC5AC protein expression through the activation of Sp1," *Journal of Biological Chemistry*, vol. 287, no. 33, pp. 27948–27958, 2012.

[23] K. Kanai, A. Koarai, Y. Shishikura et al., "Cigarette smoke augments MUC5AC production via the TLR3-EGFR pathway in airway epithelial cells," *Respiratory Investigation*, vol. 53, no. 4, pp. 137–148, 2015.

[24] A. M. Sadowska, "N-Acetylcysteine mucolysis in the management of chronic obstructive pulmonary disease," *Therapeutic Advances in Respiratory Disease*, vol. 6, no. 3, pp. 127–135, 2012.

[25] M. Mata, A. Ruiz, M. Cerda et al., "Oral N-acetylcysteine reduces bleomycin-induced lung damage and mucin Muc5ac expression in rats," *European Respiratory Journal*, vol. 22, no. 6, pp. 900–905, 2003.

[26] M. Decramer, M. Rutten-van Mölken, P. R. Dekhuijzen et al., "Effects of N-acetylcysteine on outcomes in chronic obstructive pulmonary disease (Bronchitis Randomized on NAC Cost-Utility Study, BRONCUS): a randomised placebo-controlled trial," *The Lancet*, vol. 365, no. 9470, pp. 1552–1560, 2005.

[27] V. Y. Lin, N. Kaza, S. E. Birket et al., "Excess mucus viscosity and airway dehydration impact COPD airway clearance,"

European Respiratory Journal, vol. 55, no. 1, article 1900419, 2020.

[28] P. Burgel and J. Nadel, "Roles of epidermal growth factor receptor activation in epithelial cell repair and mucin production in airway epithelium," *Thorax*, vol. 59, no. 11, pp. 992–996, 2004.

[29] M. G. Matera, L. Calzetta, and M. Cazzola, "Oxidation pathway and exacerbations in COPD: the role of NAC," *Expert Review of Respiratory Medicine*, vol. 10, no. 1, pp. 89–97, 2015.

[30] P. Santus, A. Corsico, P. Solidoro, F. Braido, F. di Marco, and N. Scichilone, "Oxidative stress and respiratory system: pharmacological and clinical reappraisal of N-acetylcysteine," *COPD: Journal of Chronic Obstructive Pulmonary Disease*, vol. 11, no. 6, pp. 705–717, 2014.

Review Article

The Great Healing Potential Hidden in Plant Preparations of Antioxidant Properties: A Return to Nature?

Małgorzata Kiełczykowska and **Irena Musik**

Chair and Department of Medical Chemistry, Medical University of Lublin, 4A Chodźki Street, 20-093 Lublin, Poland

Correspondence should be addressed to Małgorzata Kiełczykowska; malgorzata.kielczykowska@umlub.pl

The application of chemicals in industry and agriculture has contributed to environmental pollution and exposure of living organisms to harmful factors. The development of new pharmaceutical agents enabled successful therapy of various diseases, but their administration may be connected with side effects. Oxidative stress has been found to be involved into etiology of numerous diseases as well as harmful action of drugs and chemicals. For some time, plant origin substances have been studied as potential protective agents alleviating toxicity of various substances and symptoms of diseases. The aim of the current review was to present the diversity of the research performed during the last five years on animal models. The outcomes showed a huge protective potential inherent in plant preparations, including alleviating prooxidative processes, strengthening antioxidant defence, ameliorating immune parameters, and reversing histopathological changes. In many cases, plant origin substances were proved to be comparable or even better than standard drugs. Such findings let us suggest that in the future the plant preparations could make adjuvants or a replacement for pharmaceutical agents. However, the detailed research regarding dose and way of administration as well as the *per se* effects needs to be performed. In many studies, the last issue was not studied, and in some cases, the deleterious effects have been observed.

1. Introduction

In the recent centuries, a great change of the conditions of the human life has taken place, due to the development of industry, agriculture, medicine, and pharmacy. The new synthetic substances were applied to protection of crops as well as successful therapy of various diseases. However, except for beneficial influence, consisting in numerous facilitations of human existence and extending human life span, negative effects have also occurred [1, 2]. A growing pollution of natural environment, resulting from the industry development, has been observed for many years [3–5]. Despite the efforts aiming at alleviating and preventing this phenomenon, it still belongs to the most important problems to be solved by the mankind. The application of plant protection products has made another contribution to environmental contamination [6–9]. As it is not possible to improve the situation immediately, many people, i.e., industrial workers or farmers are still exposed to harmful substances like heavy metals [4, 10–12], organic chemicals (e.g., CCl_4) [13, 14], or pesticides and plant growth regulators [8, 15]. Another problem results from introducing plenty of new pharmaceutical agents. They allowed to relieve suffering of many subject and successive treatment in cases of mortal diseases. However, on the other hand, plenty of side effects have also been observed [16, 17]. Analgesic and antipyretic drugs like acetaminophen or aspirin can induce liver and kidney damage [18–22]. The antineoplastic agents can cause severe disturbances like testicular damage [23], nephrotoxic [16, 24], cardiotoxic [25, 26], and hepatotoxic [27] effects. Antibiotics have also proved to show side effects including liver and kidney damage [28, 29]. The widespread practice of using different additives to preserve and improve the taste of food makes another source of toxic action on human organisms [30]. The growing life span is connected with an increase in incidence of neurodegenerative disorders like Parkinson' disease [31] or

Alzheimer's disease [32]. Furthermore, in the recent decades, obesity, hyperlipidemia, and connected disturbances have become a significant worldwide problem [33, 34].

All the presented facts have made the scientists search for any agents which could exert protective effects against toxic environmental pollutants and chemicals used in industry and agriculture and replace the standard drugs or make beneficial adjuvants. The return to natural products, sometimes used for thousands years in traditional medicine, has become one of the significant directions of this research [35–39]. It could be stated, without any exaggeration, that "a great return to nature" is recently being observed. Plant extracts and plant origin substances *per se* do not show so many side effects as pharmacological substances. On the other hand, they contain numerous compounds of anti-inflammatory and antioxidative properties like polyphenolic derivatives and flavonoids [40–42]. The presented facts prompted large-scale research on possibilities of application of plant preparations as protective agents against toxicity of various substances as well as adjuvants alleviating the symptoms of diseases, obesity, and traumata [6, 25, 38, 43–49]. A great quantity of plant species have been investigated, and the obtained results seem to be very promising. Some studies have included the comparison of the investigated materials with standard drugs, and the outcomes suggest that in many cases the replacement would be possible [20, 31, 35, 50–53]. However, many questions remain to be solved as to the best way of treatment and the most beneficial dose.

Oxidative stress—the disturbed balance between generation of reactive oxygen species (ROS) and antioxidants' level in an organism—has been found to be involved, less or more, into the etiology of most diseases [54–56]. This process involves the generation of ROS, active particles capable of injuring all bioactive compounds—protein, lipids, and nucleic acids in an organism. Lipid peroxidation caused by ROS may lead to damage of membrane lipids. Living organisms developed a wide range of endogenous substances, both enzymatic and low-molecular ones, which can neutralize ROS. Negative effects resulting from stress, exposure to toxic substances, side effects of the standard drugs, or even food supplements have also been proved connected with prooxidative processes and deterioration of antioxidant defence [13, 30, 40, 57, 58]. Plant origin preparations, in turn, have been found to exert a strong antioxidant action due to high content of components of antioxidative properties. Numerous studies have revealed their direct influence on oxidative processes by reducing lipid peroxidation or protein carbonylation as well as increase in antioxidant enzymes' activities and low-molecular antioxidant concentrations [34, 43, 59, 60].

Different pathways involved in oxidative and inflammatory processes have been found to be affected in the course of protective action of plant preparations.

The studies have shown the involvement of Nrf2 and Keap1 proteins. Nrf2 is regarded as a key transcription factor mediating the endogenous antioxidant response, and Keap1 is its negative regulator. Under oxidative stress conditions, Nrf2 is released and translocated to the nucleus where it binds to ARE regions in DNA and stimulates antioxidant enzyme gene expression. Both Nrf2 and Keap1 as well proteins regulated by Nrf2, responsible for defence against antioxidant stress like HO-1 and γ-GCS, have been found to be disturbed by harmful factors (cadmium or high-fat diet) and regulated by plant preparations [12, 61]. Plant origin substances have been reported to cause upregulation of Nrf2, HO-1, and γ-GCS in both nonexposed and Pb-exposed rats [62].

Another pathway connected with oxidative and inflammatory processes which have been proved involved into protective properties of plant preparations is NF-κB pathway. NF-κB is a transcription factor responsible for expression of proinflammatory cytokines [56]. Its activation can be triggered by TLR receptors, belonging to pattern recognition receptors. The inflammation and redox balance have been found to be strongly connected with each other [63]. Interleukins, γ-interferon and tumour necrosis factor, have been found to affect ROS production [64]. The involvement of the LPS-TLR4-NF-κB pathway into protective action of plant materials has been reported [56, 65]. Other authors have stated that a protective effect of a plant extract, resulting from antioxidative and anti-inflammatory influence observed in diabetes animal model, could be attributed to inhibition of NF-κB activation [66].

Mitogen-activated protein kinases (MAPK) belong to enzymes which make mediators of various processes occurring in cells like death, proliferation, or differentiation. The MAPK pathway begins from a signal from an extracellular receptor and through a cascade of subsequent protein phosphorylation leads to activation of different proteins including transcription factors (e.g., p53 protein) and finally to the expression of genes. ROS have been proven to be connected with particular steps of the MAPK pathway. There are three kinds of MAPK in mammals: p38 MAPK, ERK1 (extracellular signal-regulated kinase 1), and JNK (c-Jun N-terminal kinase) [64, 67]. The studies on plant revealed the influence of the studied plant materials on some elements of the MAPK pathway [42].

The next pathway connected with oxidative stress which has been found affected by plant preparations is the JAK/STAT pathway. An outside signal, usually being a cytokine, binds to a membrane receptor resulting in its dimerization. The next stage is the activation of JAK which renders possible phosphorylation of receptor, which in turn enables STAT binding and phosphorylation. Activated by phosphorylation STAT is then translocated into the nucleus where it acts as a transcription factor [68]. The relationships between this pathway and ROS have been reported [69]. In the current study, disturbances of oxidative balance as well as bone marrow damage and reduction in pJAK2/JAK2 and pSTAT5a/STAT5a, caused by radiation exposure, have been found to be improved by a plant preparation, which made the authors suggest that the studied material can stimulate the JAK2/STAT5a signal pathway [70].

The aim of the current review is to present the results of the studies performed in the last five years regarding the protective and medicinal properties of plant origin preparations with particular emphasis on their antioxidant action.

2. The Protective Properties of Plant Preparations against Toxicity of Various Factors

2.1. The Protective Influence of Plant Preparations against Chemicals Applied in Agriculture. The use of different chemicals in food production has been growing dramatically in the recent years, causing the contamination of the natural environment and increasing thread to human health. Neurotoxicity, hepatotoxicity, reproductive disturbances, and cancerogenesis belong to the negative effects exerted on organisms [6, 8, 15, 71]. Moreover, chemicals of lipophilic character can be accumulated in membranes [9]. Enhanced generation of ROS was proved involved into their harmful influence [6, 9, 71]. Plant origin materials were revealed to show protective properties not only by strengthening the antioxidant barrier but also by reversing histopathological changes. A wide range of different materials was studied, including simple extracts [2, 6, 7] as well as commercial products [9, 15]. The saponins from *Tribulus terrestris*, which were reported to possess antiaging action, were found to exert protective effects against rotenone-induced parkinsonism [15].

The details concerning the above mentioned studies are presented in Table 1.

2.2. The Protective Influence of Plant Preparations against Toxic Effects of Heavy Metals. Environmental pollution with heavy metals makes a great global problem. The most toxic ones are lead, cadmium, and mercury. Even low concentrations can cause severe disturbances of organism, including brain, hepatic, renal, and reproductive damage [10]. As their harmful action is connected with oxidative stress induction, plant extracts showing antioxidant properties were studied as possible protective agents and the obtained results were found to be promising [10, 11], although the accumulation of a toxic metal could not be prevented in every case [62].

The ability of plant origin substances proanthocyanidins to prevent lead-induced hepatotoxicity was suggested to be connected with the Nrf2/ARE pathway (as an increase of mRNA expression levels of Nrf2 in the liver of mice administrated with proanthocyanidins and/or lead was observed) as well as with the reduction of endoplasmatic reticulum stress *via* a decrease in stress-related proteins GRP78 and CHOP [62].

In the experiments concerning the toxicity of mercury, plant extracts relieved the negative effects in the case of both an inorganic form (mercury (II) chloride) and organic one (dimethylmercury); at the same time, the beneficial influence included not only oxidant and immunological parameters but also histopathological changes [4, 72, 73].

Plant extracts were also found to exert wide protective effects against the third most dangerous heavy metal cadmium, with the results being confirmed by *in vitro* studies with using murine hepatocytes [3]. Additionally, an animal study showed the involvement of the Nrf2/Keap1 pathway into the protective action of *Pyrantha fortuneana* extract as the plant material, given both alone and coadministered with cadmium caused a significant increase in expression of Nrf2

and decrease in expression of Keap1 in the kidneys of rats vs. the control and Cd-exposed group, respectively [12].

Apart from lead, mercury, and cadmium the research concerning metals' toxicity included also liver injury caused by iron overload. 70% methanol extract of *Drosera burmannii* Vahl. showed a distinct, dose-dependent efficacy against iron-induced hepatoxicity. This effect, particularly in case of the highest dose, was comparable with that exerted by a standard drug desirox—an iron chelator. Additionally, the studied extract studied *in vitro* showed the ability to chelate Fe^{2+} ions. Such findings made the authors suggest that the studied preparation might be used as a medicine in cure of iron overload-induced diseases [50].

The details concerning the above-mentioned studies are presented in Table 2.

2.3. The Protective Influence of Plant Preparations against Various Chemicals. Plant origin substances, extracts and their particular fractions, essential oils, and seed powders were found to reverse or alleviate disturbances of organism resulting from exposure to different chemicals. The resent research included various compounds, e.g., hepatotoxic tetrachloromethane (CCl_4) used for years as a solvent and now regarded as an environmental pollutant [14], aluminium known for its neurotoxicity [74], aflatoxins produced by toxigenic fungi which made food contaminants [75], and chemicals used in industry and laboratory experiments like thioacetamide [76] or 1-chloro-2,4-dinitrobenzene [77]. Additionally, plant origin substances were proved to decrease mouse mortality resulting from the acute CCl_4 toxicity [78] as well as from Concanavalin A exposure [79]. Furthermore, several studies included the influence of plant materials alone, and generally, no harmful effects were observed [14, 54, 74, 75, 78, 80, 81].

The details of the performed studies are presented in Table 3.

2.4. The Protective Influence of Plant Preparations against Carcinogens. Plant extracts were studied using animal model as for their possible application in tumour therapy due to the presence of anticancer and antioxidant components. The necessity of searching for new agents, suitable for tumour treatment, was challenged by the lack of effective chemotherapy and severe side effects associated with the used medicines. The obtained results seem to be promising as the studied materials alleviated carcinogen-induced oxidative stress as well as disturbances of immunological parameters [47, 88, 89]. Histolopathological studies confirmed the beneficial effects of the investigated preparations [46, 89].

The detailed results of the performed studies are presented in Table 4.

2.5. The Protective Influence of Plant Preparations against Ethanol. Alcohol excessive consumption and addiction leads to different negative effects: liver injuries including steatosis [56, 91], brain damage [92], and reproductive system damage [93]. The disturbances of oxidative balance were suggested to be one of the factors underlying alcohol toxicity, which was confirmed by intensification of lipid peroxidation as well as

TABLE 1: The protective properties of plant extracts against toxicity of substances applied in agriculture.

Reference	Plant preparation, dose, way and time of treatment, animals	The toxic substance, dose, way and time of exposure, and negative effects	Protective effects of plant preparation	Effects of plant *per se*
Chaâbane et al. [6]	*Nitraria retusa* fruit aqueous extract Pretreatment for 6 days and treatment during penconazole exposure 300 mg/kg b.w., p.o., daily Male Wistar rats about 250 g	A fungicide penconazole-induced kidney injury 67 mg/kg b.w. (1/30 LD50) i.p., every 2 days from 7th until 15th day Plasma: GGT, ALP ↓; CR, urea, UA, LDH ↑ Urine: volume ↑, CR, urea, UA ↓ Kidney: LDH, MDA, H_2O_2, PC, AOPP, NP-SH, GSH, MT, CAT, SOD, GPx ↑ Kidney: enlarged Bowman's space, necrosis of the epithelial cells lining the tubules, infiltration of leucocytes, glomeruli fragmentation ↑	Plasma: ALP (+), urea, LDH, GGT (++), CR, UA (+++) Urea: UA (+), volume, CR, urea (++) Kidney: LDH, MDA, H_2O_2, PC, AOPP, NP-SH, GSH, CAT, SOD, GPx (++), MT (+++) Kidney: necrosis of the epithelial cells lining the tubules (++), enlarged Bowman's space, infiltration of leucocytes, glomeruli fragmentation (+++)	Plasma: urea, LDH ↑ Urine: volume ↑, CR, urea ↓
Alzahrani et al. [15]	Standardized *Tribulus Terrestris* extract tablets 1000 mg (min. 45% saponins) Now Sports Co. (USA) 5 or 10 mg/kg daily, p.o., for 17 days Male Swiss albino mice, 20-28 g	A pesticide rotenone-induced parkinsonism, nine doses of 1 mg/kg given each 48 ± 2 h, s.c. Activity index (18th day) ↓ Substantia nigra: % of pycnotic neurons ↑, % of viable neurons ↓ Striatum: relative expression of iNOS, COX-2 and MTH 1, MDA, 8-OH-dG ↑, dopamine, GSH, SOD, CAT ↓	Activity index (18th day) (+ 5, +++ 10) Substantia nigra: % of viable neurons (+ 50, +++ 10), % of pycnotic neurons (++ 5, +++ 10) Striatum: GSH, SOD, MDA (0 5, ++ 10), CAT (0 5, +++ 10), dopamine (+ 5, ++ 10), relative expression of COX-2 and iNOS (++ both doses), 8-OH-dG and relative expression of MTH 1 (++ 5, +++ 10)	None
Selmi et al. [71]	*Lavandula stoechas* essential oils 50 mg/kg b.w., p.o., for 30 days Male mice, 8-week old, 25-30 g	Malathion (a pesticide) 200 mg/kg b.w./day for 30 days, p.o. Serum: T ↓ Testis: relative weight, MDA, H_2O_2 ↑, -SH groups, GPx, CAT, SOD total, Cu/Zn-SOD, Mn-SOD ↓ Epididymis: relative weight, MDA, H_2O_2 ↑, -SH groups, GPx, CAT,	Serum: T (+++) Testis: Mn-SOD (0), -SH groups, SOD total (++), relative weight, MDA, H_2O_2, GPx, Cu/Zn-SOD, CAT (+++) Epididymis: CAT and H_2O_2 (++), relative weight, MDA, -SH groups, GPx, SOD total, Cu/Zn-SOD, Mn-SOD (+++)	Testis: CAT ↑

TABLE 1: Continued.

Reference	Plant preparation, dose, way and time of treatment, animals	The toxic substance, dose, way and time of exposure, and negative effects	Protective effects of plant preparation	Effects of plant per se
El Arem et al. [7]	*Phoenix dactylifera* L. date palm fruit aqueous extract 4 mL/kg daily, p.o., for 2 months Male Wistar rats 180–200 g	SOD total, Cu/Zn-SOD, Mn-SOD ↓ Dichloroacetic acid (a fungicide) 0.5 g/L or 2 g/L as drinking water, for 2 months 0.5 g/L: Weight: testes, epididymis ↓ Plasma: T, FSH, LH ↓ Testes: CAT, SOD, LPO ↑, GSH ↓ 2 g/L: Weight: testes, epididymis ↓ Plasma: T, FSH, LH ↓ Testes: CAT, SOD, LPO ↑, GSH, GPx ↓	0.5 g/L of dichloroacetic acid: Weight: testes, epididymis (+++) Plasma: T, FSH, LH (+++) Testes: CAT, SOD, LPO, GSH (+++) 2 g/L of dichloroacetic acid: Weight: testes (++), epididymis (+++) Plasma: T, FSH, LH (++) Testes: CAT, SOD, GSH, LPO (++), GPx (+++)	None
Mossa et al. [9]	*Vitis vinifera* grape pomace (El Kroom Company, Alexandria, Egypt) 80% ethanolic extract 100 or 200 mg/kg b.w., p.o., 28 consecutive days Weanling female rats about 50 g	Cypermethrin (an insecticide) 25 mg/kg b.w. (1/10 of LD50), p.o., for 28 consecutive days Relative weight: liver ↓, kidney ↑ Serum: TP, ALB ↓, AST, ALT, ALP, GGT, urea nitrogen, CR ↑ Liver: Kupffer cell activation, portal infiltration with inflammatory cells, hyperplasia of bile duct, congestion of central vein and hepatic sinusoids ↑ Kidney: vacuolization of endothelial lining glomerular tuft, vacuolization of epithelial lining renal tubules, necrosis of epithelial ↑	Relative weight: liver, kidney (+++ both doses); Serum: ALT, CR (++ both doses), AST, ALP, GGT, TP (++ 100, +++ 200), ALB, urea nitrogen (+++ both doses) Liver: Kupffer cell activation (+ 100, ++ 200), portal infiltration with inflammatory cells, hyperplasia of bile duct, congestion of central vein and hepatic sinusoids (+++ both doses) Kidney: vacuolization of endothelial lining glomerular tuft (++ 100, +++ 200), vacuolization of epithelial lining renal tubules, necrosis of epithelial (+++ both doses)	Both doses: Liver: Kupffer cell activation ↑
Mirzaei et al. [2]	*Quercus brantii* 70% ethanol extract of internal layer of the fruit 500 mg/kg, p.o., for 9 days Male Wistar albino rats, 150–200 g	Carbendazim: methyl-2-benzimidazole carbamate (a fungicide agent), 50 mg/kg p.o., for 9 days Serum: ALT, AST, ALP, urea nitrogen, CR ↑ Liver: MDA ↑, GSH ↓ Kidney: MDA ↑, GSH ↓	Serum: ALT, AST, ALP, urea nitrogen, CR (++) Liver: MDA (+), GSH (++) Kidney: MDA, GSH (++)	Not studied

TABLE 1: Continued.

Reference	Plant preparation, dose, way and time of treatment, animals	The toxic substance, dose, way and time of exposure, and negative effects	Protective effects of plant preparation	Effects of plant *per se*
Khalaf et al. [8]	*Punica granatum* L. pomegranate peel methanol extract 250 mg/kg daily, i.g., for 4 weeks Male Wistar rats, 140-160 g	Gibberellic acid-3 (a plant growth regulator) 20 mg/kg i.g, daily for 4 weeks Testes: area percent of androgen receptor immunoreaction, SOD, CAT ↓	Testes: area percent of androgen receptor immunoreaction, SOD, CAT (+++)	None

↓: a decrease vs. control; ↑: an increase vs. control; (+): a slight beneficial effect; (++): a distinct beneficial effect; (+++): a complete beneficial effect; (0): no beneficial effect.

Table 2: The protective effects of plant origin substances against toxicity of heavy metals.

Reference	Plant preparation, dose, way and time of treatment, animals	The toxic substance, dose, way and time of exposure, and negative effects	Protective effects of plant preparation	Effects of plant *per se*
Abdel Moneim [10]	*Indigofera oblongifolia* leaves water-methanol (1 : 2) extract 100 mg/kg b.w. p.o. daily, 1 h before Pb for 5 days Male Wistar rats, 8-week-old, 150–180 g	Pb lead acetate acute toxicity, 20 mg/kg b.w. daily for 5 days, i.p. Serum: AST, ALT, ALP, total bilirubin, TC, TG, LDL-c ↑, HDL-c ↓ Liver: relative weight, Pb accumulation, LPO, NO and H_2O_2 ↑, GSH, SOD, CAT, GPx, GR ↓ Liver: expression of mRNA of SOD2, CAT, GPx and Bcl-2↓, Bax and HO-1↑	Serum: ALP, total bilirubin, TG, HDL-c (++), AST, ALT, TC, LDL-c (+++) Liver: relative weight, Pb accumulation, NO, H_2O_2, SOD, CAT, GR (++), LPO, GSH, GPx (+++) Liver: HO-1(-), expression of mRNA of SOD2, CAT, GPx, Bax, Bcl-2 (++)	Liver: GSH, GPx ↑
Long et al. [62]	Proanthocyanidins extracted from grape seeds (Zelang Medical Technology Company, Nanjing, China) 100 mg/kg b.w., p.o., six days every week for 6 weeks Male Kunming mice, 3-week-old	Pb lead acetate 0.2% in drinking water for 6 weeks Blood: Pb ↑ Serum: ALT, AST, ALP ↑ Liver: GSH, GPx and SOD ↓, relative mRNA expression of Nrf2, γ-GCS, HO-1 slightly ↑, Pb and MDA as well as relative mRNA expression of Bax, GRP78 and CHOP ↑, relative mRNA expression of Bcl-2 ↓	Blood: Pb (0) Serum: ALT, AST, ALP (++) Liver: Pb (+), GPx, SOD, relative mRNA expression of Bax, Bcl-2 GRP78, CHOP (++), MDA, GSH (+++), relative mRNA expression of Nrf2, γ-GCS, HO-1 ↑	Liver: relative mRNA expression of Nrf2, γ-GCS, HO-1 ↑
El-Boshy et al. [11]	*Thymus vulgaris* leaf ethanol extract 500 mg/kg/day, p.o. for 6 weeks Sprague-Dawley male rats, about 150 g	Pb lead acetate 500 mg/L in drinking water, for 6 weeks Serum: TNF-α, IL-1β, IL-6 ↑, INF-γ, IL-10 ↓ Liver: Pb, MDA ↑, GSH, GPx, CAT ↓ Kidney: Pb, MDA↑, GSH, GPx, CAT↓	Serum: IL-1β, IL-6 (++), INF-γ and IL-10 (+++) Liver: Pb (++), MDA, GSH, GPx, CAT (+++) Kidney: Pb (++), MDA, GSH, GPx, CAT (+++)	Serum: IL-10 ↑ Liver: GSH, GPx ↑ Kidney: GSH, GPx ↑
Dua et al. [3]	*Ipomoea aquatica* and *Enhydra fluctuans* aerial parts aqueous extracts Pretreatment 100 mg/kg b.w., p.o., for 5 days followed by cadmium chloride Swiss male albino mice, 1-2 months, 20-30 g	Cd cadmium chloride, 4 mg/kg b.w., for 6 days, once daily, p.o. Blood: RBC, HGB ↓ Serum: ALT, AST, urea, TC, TG ↑, HDL-c ↓ Liver: cadmium, ROS, LPO, NADH oxidase, protein carbonylation ↑, total coenzymes Q9 and Q10, CAT, SOD, GST, GPx, GR, G6PD, GSH ↓ Kidney: cadmium, ROS, LPO, NADH oxidase, protein carbonylation ↑, total coenzymes Q9 and Q10, CAT, SOD, GST, GPx, GR, G6PD, GSH ↓ Heart: cadmium, ROS, LPO, NADH oxidase, protein carbonylation ↑, total coenzymes Q9 and Q10, CAT, SOD, GST, GPx, GR, G6PD, GSH ↓ Brain: cadmium, ROS, LPO, NADH oxidase, protein carbonylation ↑, total coenzymes Q9 and Q10, CAT, SOD, GST, GPx, GR, G6PD, GSH ↓ Testes: cadmium, ROS, LPO, NADH oxidase, protein carbonylation ↑, total coenzymes Q9 and Q10, CAT, SOD, GST, GPx, GR, G6PD, GSH ↓	Both extracts: Blood: RBC, HGB (++) Serum: ALT AST, urea, TC, TG, HDL-c (++) Both extracts: Cadmium burden, ROS, G6PD, NADPH oxidase: liver, kidney, heart, brain, testes (++) LPO: liver, kidney, heart, brain, testes (+++); Protein carbonylation: liver, kidney, heart, testes (++), brain (+++) Total coenzyme Q9: liver, brain, heart, testes (++), kidney (+++) Total coenzyme Q10: kidney, brain, testes (++), liver, heart (+++) CAT: liver, brain, heart (++), kidney, testes (+++) SOD, GST: liver, kidney, heart, brain, testes (+++) GPx: liver, heart, testes (++), brain, kidney (+++) GR: heart, testes, brain (++), liver, kidney (+++) GSH: heart, kidney, brain (++), liver, testes (+++)	Not studied

TABLE 2: Continued.

Reference	Plant preparation, dose, way and time of treatment, animals	The toxic substance, dose, way and time of exposure, and negative effects	Protective effects of plant preparation	Effects of plant per se
Olaniyan et al. [1]	Plukenetia conophora seeds methanol extract 100 or 200 mg/kg b.w., p.o., for 54 days after CdCl$_2$ treatment Male Wistar rats, 150-190 g	Cd cadmium chloride, a single dose 2 mg/kg b.w., i.p. Serum: T, LH, FSH ↓ Epididymal semen: count of cells, motility, viability ↓ Testis: MDA and NO ↑, SOD, CAT, GPx, GST, Na$^+$/K$^+$ ATPase, Ca^{2+} ATPase, Mg^{2+} ATPase ↓ Epididymis: MDA and NO ↑, SOD, CAT, GPx, GST ↓	Serum: LH (0 100, + 200), FSH (+ both doses), testosterone (++ 100, +++ 200) Epididymal semen: count of cells, motility, viability (++ both doses) Testis: Mg^{2+} ATPase (++ both doses), Na$^+$/K$^+$ ATPase (++ 100, +++ 200), MDA, NO, SOD, CAT, GST (+++ both doses), Ca^{2+} ATPase (+++ 100, ↑ 200), GPx (↑ both doses) Epididymis: GPx (+ both doses), SOD, GST, Na$^+$/K$^+$ ATPase and Ca^{2+} ATPase (++ both doses), CAT (++ 100, +++ 200), MDA, Mg^{2+} ATPase (+++ both doses), NO (+++ 100, ↓ 200)	Not studied
Mężyńska et al. [5]	Aronia melanocarpa L. berries extract (Adamed Consumer Healthcare, Tuszyn, Poland) 0.1% aqueous solution in form of the only drinking fluid for 3, 10, 17 or 24 months Female Wistar rats, 3-4-week-old	Cd cadmium chloride in diet 1 mg/kg (Cd$_1$) or 5 mg/kg (Cd$_5$) for 3, 10, 17 or 24 months Liver: SOD (Cd$_1$ 3, 10, 17 m) and (Cd$_5$ 17 m) ↓; CAT (Cd$_5$ 17 m) ↓; GPx (Cd$_1$ 3,10,17,24m), (Cd$_5$ 3, 10, 17, 24 m) ↓; GR (Cd$_1$ 10, 24 m), (Cd$_5$ 10, 17 m) ↓; GST (Cd$_1$ 3, 10, 17 m), (Cd$_5$ 3, 10, 17 m) ↓; GSH/GSSG (Cd$_1$ 17 m) (Cd$_5$ 10, 17 m) ↓; H$_2$O$_2$ (Cd$_1$ 10, 17, 24m), (Cd$_5$ 10, 17, 24 m) ↑; OSI (Cd$_1$ 10, 17 m), (Cd$_5$ 3, 10, 17, 24 m) ↑; MDA (Cd$_1$ 10, 17, 24 m), (Cd$_5$ 10, 17, 24m) ↑	Liver: SOD: Cd$_1$ (+ 3 m, 0 10 m, +++ 17 m), Cd$_5$ (+++ 17 m) CAT: Cd$_5$ (++ 17 m) GPx: Cd$_1$ (+++ 3, 10 m, ++ 17, 24 m), Cd$_5$ (0 3 m, ++ 10 and 17 m, +++ 24 m) ↓ GR: Cd$_1$ (+++ 10 m, ↑ 24m), Cd$_5$ (++ 1 m, - 17 m) GST: Cd$_1$ (+++ 3, 10, 17 m), Cd$_5$ (++ 3 m, 0 10 m, +++ 17 m) GSH/GSSG: Cd$_1$ (+++ 1 m), Cd$_5$ (+++ 10 m, ↑ 17 m) H$_2$O$_2$; Cd$_1$ (+++ 10, 17, 24 m), Cd$_5$ (+++ 10, 17, 24 m) OSI: Cd$_1$ (+++ 10, 17m), Cd$_5$ (+++ 3, 10, 17, 24 m) MDA: Cd$_1$ (+++ 10, 17, 24 m), Cd$_5$ (+++ 10, 17, 24m)	Liver: CAT10m ↓, GR 3 m ↓, GSH/GSSG 24m ↑
Ke et al. [12]	Pyracantha fortuneana fruits 60% ethanol extract Pretreatment, 1 h before cadmium, 250 mg/kg, p.o., for 5 days Male Wistar rats, 7-8-week-old, 150-170 g	Cd cadmium chloride, 6.5 mg/kg daily for 5 days, i.p. Body weight gain ↓ Kidney weight ↑ Plasma: UA, urea and CR ↑ Kidney: Cd accumulation, MDA, NO, expression of Keap1, Bax and TNF-α protein ↑, CAT, GPx, GSH, SOD, GR, expression of Bcl-2, HO-1, γ-GCS, NQO1 and Nrf2 protein ↓	Body weight gain (++) Kidney weight: (++) Plasma: urea, UA and CR (++) Kidney: Cd accumulation, MDA, NO, CAT, GPx, GSH, SOD, GR (++), expression of Bcl-2, Bax and TNF-α protein (++), expression of Keap1, HO-1, γ-GCS, NQO1 and Nrf2 protein ↑	Kidney: expression of Keap1, HO-1, γ-GCS, NQO1, Nrf2 ↑
Kim et al. [73]	Dendropanax morbifera leaf 80% ethanol extract 100 mg/kg, p.o., daily for 4 weeks Male Sprague-Dawley rats, 7-week-old	Hg dimethylmercury daily 5 μg/kg, i.p., for 4 weeks Hippocampus: Hg concentration, ROS production, GST, MDA ↑, SOD1, total sulfhydryl content, CAT, GPx, GR ↓	Hippocampus: CAT, total sulfhydryl content (+), Hg concentration, ROS production, MDA, SOD1, GST, GPx, GR (++)	None

TABLE 2: Continued.

Reference	Plant preparation, dose, way and time of treatment, animals	The toxic substance, dose, way and time of exposure, and negative effects	Protective effects of plant preparation	Effects of plant per se
Jahan et al. [72]	*Chenopodium album* Linn. seed ethanol extract 200 mg/kg b.w., p.o., for 30 days Sprague-Dawley male rats, about 240 g	Hg mercury(II) chloride, 0.15 mg/kg b.w. for 30 days, i.p. Body weight ↓ Plasma: BUN, CR, cholesterol, TG, LDL ↑, HDL, T ↓ Testicular tissue: TP, CAT, SOD, GST ↓, ROS and TBARS ↑ Daily sperm production: ↓	Body weight (+++) Plasma: cholesterol, TG (-), LDL, CR and HDL (++), BUN and T (+++) Testicular tissue: TP, CAT, SOD, GST, ROS and TBARS (++) Daily sperm production: (+++)	None
Gao et al. [4]	*Rheum palmatum* L. dried root and Rhizoma (Lixian Pharmaceuticals Company, Longnan, China) 60% ethanol extract 1200 mg/kg, i.g., daily for 7 days Sprague-Dawley male rats, 140–160 g	Hg mercury(II) chloride, a single dose of 2 mg/kg, s.c., on the 5th day Body weight: ↓ Serum: TP, ALB ↓ BUN, CR ↑ Kidney: GSH, GPx and CAT ↓ Renal tubule epithelial cells: swelling, necrosis, granular degeneration, interstitial vascular congestion ↑	Body weight: (++) Serum: ALB, CR, BUN (++); TP (+++) Kidney: GPx, CAT (0), GSH (+) Renal tubule epithelial cells: swelling (+), necrosis granular degeneration, interstitial vascular congestion (++)	Not studied
Ghate et al. [50]	*Drosera burmannii* Vahl. 70% methanol extract 50, 100, or 200 mg/kg b.w., p.o., for 21 days from the next day after first injection of iron dextran Male Swiss mice, 20 g	Iron-dextran 100 mg/kg b.w., i.p., five doses (one dose every two days) Serum: ALT, AST, ALP, bilirubin, ferritin ↑ Liver: SOD, CAT, GST, GSH ↓, LPO ↑	Serum: bilirubin (+ 50, ++ 100 +++ 200), ALT and AST (++ all doses), ALP and ferritin (++ 50 and 100, +++ 200) Liver: SOD (0 50, ++ 100, +++ 200); CAT, GST, and LPO (+++ all doses); GSH (0 50, ++ 100 and 200)	Not studied

↓: a decrease vs. control; ↑: an increase vs. control; (+): a slight beneficial effect; (++): a distinct beneficial effect; (+++): a complete beneficial effect; (0): no beneficial effect; (-): intensification of the harmful effect.

TABLE 3: The protective effects of plant preparations against toxicity of different chemicals.

Reference	Plant preparation, dose, way and time of treatment, and animals	The toxic substance, dose, way and time of exposure, and negative effects	Protective effects of plant preparation	Effects of plant per se
AlSaid et al. [13]	Piper cubeba fruits 70% ethanol extract Pretreatment 250 or 500 mg/kg for 7 days, p.o. Male Wistar albino rats 180–200 g	CCl$_4$-induced hepatotoxicity, a single dose of 0.4 mL/kg, i.p. Serum: ALT, AST, GGT, ALP, bilirubin, LDH ↑ Liver: MDA ↑, NP-SH, CAT, TP ↓ Liver: mRNA expression of TNF-α, IL-6, IL-10, HO-1, iNOS ↑	Serum: ALT, AST, LDH (0 250, ++ 500), GGT (+ 250, ++ 500), ALP, bilirubin (++ both doses) Liver: TP (0 250, ++ 500), MDA, CAT (+ 250, ++ 500), NP-SH (++ 250, +++ 500) Liver: mRNA expression of IL-10 (↑ both doses), TNF-α, IL-6, HO-1, iNOS (++)	Not studied
Bellassoued et al. [14]	Mentha piperita L. leaf essential oil Pretreatment 5, 15, and 40 mg/kg b.w., daily for 7 days, p.o. Male Wistar rats 200–220 g	CCl$_4$; 1 mL/kg b.w. on the 7th day, i.p. Serum: ALT, AST, ALP, LDH, GGT, TC, TG, LDL, urea, CR ↑, HDL ↓ Liver: LPO, inflammatory cells and cellular necrosis ↑, SOD, CAT, GPx ↓ Kidney: LPO, glomerular and epithelial cells of the proximal tubules necrosis ↑, SOD, CAT, GPx ↓	Serum: ALT, AST, ALP, LDH, GGT, TC, TG, HDL, LDL, urea, CR (+ 5, ++ 15, 40) Liver: inflammatory cells and cellular necrosis, LPO, SOD, CAT, GPx (+ 5, ++ 15, and 40) Kidney: LPO, SOD, CAT, GPx, glomerular and epithelial cells of the proximal tubules necrosis (+ 5, ++ 15, and 40)	40 mg/kg b.w. only studied: none
Simeonova et al. [54]	Astragalus monspessulanus L. n-butanolic extract—obtained by successive extraction of 80% methanol extract with CH$_2$Cl$_2$, ethyl acetate, and n-butanol Pretreatment 100 mg/kg, for 7 days, p.o. Male Wistar rats 200–220 g	CCl$_4$-induced hepatotoxicity a single dose 1.25 mL/kg of 10% CCl$_4$ in olive oil Serum: ALT, AST, ALP ↑ Liver: MDA ↑, GSH, CAT, SOD, GPx, GR, GST ↓	Serum: ALT, AST, ALP (+++) Liver: GR, GSH, CAT, GPx, GST (++), MDA, SOD (+++)	None
Shah et al. [80]	Commelina nudiflora L. methanol extract Pretreatment for 12 days and 2-day-treatment 150, 300, 450 mg/kg b.w., p.o. Male Sprague Dawley rats, 150–250 g	CCl$_4$ 1.0 mL/kg b.w, two doses on 13th and 14th days Serum: ALT, AST ↑ Liver: GSH, GST, GPx, GR, CAT, G6PD, QR ↓, LPO, HNE-modified protein adducts, 8-OHdG, TNF-α, IL-6, PGE$_2$ ↑	Serum: ALT, AST (++ all doses) Liver: GSH, GST, GR, CAT, G6PD, QR, LPO, HNE-modified protein adducts, 8-OHdG, TNF-α, IL-6, PGE$_2$ (++ all doses), GPx (++ 150, +++ 300, 450)	450 mg/kg b.w. only studied: none
Yoshioka et al. [78]	Sasa veitchii leaf extract Pretreatment 0.2 mL (1 mL made from 2.82 g of leaves) for 7 days once per day, p.o. Male ddY mice, 7 weeks	CCl$_4$ 3 g/kg a single injection, i.p. Plasma: ALT, AST, BUN, CR ↑ Liver: MDA, Ca ↑ Kidney: MDA ↑	Plasma: ALT, AST, BUN (++), CR (+++) Liver: MDA, Ca (++) Kidney: MDA (+)	None

TABLE 3: Continued.

Reference	Plant preparation, dose, way and time of treatment, and animals	The toxic substance, dose, way and time of exposure, and negative effects	Protective effects of plant preparation	Effects of plant *per se*
Lin et al. [82]	*Chenopodium formosanum* Koidz (red quinoa): whole seed powder, 50% ethanolic bran extract, aqueous bran extract 5.13 g/kg of red quinoa whole seed powder (rutin 8.46 mg/kg/day), p.o. 1.54 g/kg of red quinoa bran 50% ethanol extract (rutin 16.4 mg/kg/day), p.o. 1.54 g/kg of red quinoa bran water extract (rutin 3.92 mg/kg/day), p.o. Male BALB/c mice	CCl_4 0.5 mL/kg b.w, two times weekly (Thursday and Sunday) for 6 weeks, i.p. Serum: AST, ALT, TP, ALB, globulins, bilirubin, CR, BUN ↑, ALP ↓ Liver: TBARS, ROS, TNF-α, TGF-β1, IL-6 ↑, SOD, CAT ↓	Whole seed powder: Serum: ALP (0), CR, BUN, ALB, globulins (+), ALT, TP, bilirubin (++), AST (+++) Liver: TBARS, ROS, TNF-α, TGF-β1, IL-6, SOD, CAT (+++) Ethanol bran extract: Serum: ALP (↓), ALB, globulins, BUN (+), CR, ALT, AST, TP, bilirubin (++) Liver: TGF-β1 (+), ROS (++), TBARS, TNF-α, IL-6, CAT (+++), SOD (↑) Water bran extract: Serum: BUN, ALP (0), CR, bilirubin, ALB, globulins (+), ALT, AST, TP (++) Liver: CAT, TGF-β1, ROS (+), IL-6 (++), TBARS, TNF-α (+++), SOD (↑)	Not studied
Parvez et al. [83]	*Solanum surattense* leaves 70% ethanol extract 100 and 200 mg/kg b.w., p.o, for 3 weeks Male Wistar rats, 8-9-week-old, 200-220 g	CCl_4 in liquid paraffin (1: 1) 1.25 mL/kg b.w., i.p. Serum: AST, ALT, ALP, GGT, bilirubin, TC, TG, LDL, VLDL ↑; TP and HDL ↓ Liver: MDA ↑, NP-SH ↓	Serum: AST (0 100, + 200), TP, HDL (0 100, ++ 200), GGT, LDL, VLDL (+ 100, ++ 200) ALT, ALP, bilirubin, TC, TG (++ both doses) Liver: MDA (0 110, ++ 200), NP-SH (++ both doses)	Not studied
Bahcecioglu et al. [76]	*Pistacia terebinthus* coffee (coffee branded "Harput Çedene Coffee") Freshly prepared coffee in drinking water (the content increased by 25% during each preparation, reaching up to 100% at the end of 7 days), for 8 weeks Male Sprague-Dawley rats about 250 g	Thioacetamide-induced chronic liver injury, 100 mg/kg b.w., i.p., three times weekly for 8 weeks Plasma: MDA↑ Liver: TNF-α, NF-κB, TGF-β ↑ Liver: inflammation, necrosis, fibrosis ↑	Plasma: MDA (+) Liver: TNF-α, NF-κB, TGF-β (++) Liver: inflammation, necrosis, fibrosis (++)	Liver: TGF-β ↓
Thomaz al. [84]	*Eugenia dysenterica* leaf hydroalcoholic extract 10, 100, 300 mg/kg/day, p.o., for 45 days starting from the 45th day of $AlCl_3$ administration Male Swiss mice, 25-30 g	$AlCl_3$-induced neurotoxicity 100 mg/kg/day p.o., for 90 days Brain cortex: MDA ↑, SOD ↓ Hippocampus: MDA ↑, CAT, SOD ↓ Hippocampus CA1 area: % of viable neurons ↓, % of necrotic neurons ↑	Brain cortex: MDA and SOD (+++) all doses Hippocampus: CAT (0 10, +++ 100 and 300), MDA and SOD (+++ all doses) Hippocampus CA1 area: % of viable neurons (+++ 10, ++ 100, and 300), % of necrotic neurons (0 10, ++ 100, and 300)	Not studied
Feng et al. [74]	Defatted walnut meal (Shaanxi Sea Ecological Agriculture Co., Ltd, Shangluo, China) protein hydrolysates 1 g/kg per day, for 90 days, i.g., Male wild-type Kunming mice, 8 weeks	Neurotoxicity induced by D-galactose 200 mg/kg/day, s.c. (6 hours after plant material), and $AlCl_3$ (100 mg/kg in the drinking water) for 90 days Brain: SOD, GPx, ChAT ↓, MDA, AchE, TNF-α, IL-1β ↑	Brain: SOD, GPx, ChAT (++), MDA, AchE, TNF-α, IL-1β (+++)	None

TABLE 3: Continued.

Reference	Plant preparation, dose, way and time of treatment, and animals	The toxic substance, dose, way and time of exposure, and negative effects	Protective effects of plant preparation	Effects of plant *per se*
Kukongviriyapan et al. [81]	*Antidesma thwaitesianum* 95% ethanolic extract of the fruits pomace 100 or 300 mg/kg once daily, p.o. Male Sprague-Dawley rats, 200-220 g	N^{ω}-nitro-L-arginine methyl ester-induced nitric oxide deficiency, 50 mg/kg/day in drinking water, for 3 weeks Blood pressure: SBP, DBP↑ Plasma: MDA, PC↑, NO_3^-/NO_2^- level↓ Carotid artery: superoxide formation↑ Aortic tissue: eNOS protein expression↓	Blood pressure: SBP, DBP (++ both doses) Plasma: PC (0 100, +++ 200), MDA, NO_3^-/NO_2^- level (++ 100, +++ 200) Carotid artery: superoxide formation (++ 100, +++ 200) Aortic tissue: eNOS (+ 100, +++ 200)	None
Yang et al. [77]	*Rumex japonicus* Houtt. roots 95% ethanolic extract 4 mg/mL and 8 mg/mL, topically to the skin and ears, daily for 3 weeks Female Balb/c mice, 5-week-old	DNCB- (1-chloro-2,4-dinitrobenzene-) induced atopic dermatitis 200 μL of 0.5% DNCB (in acetone-olive oil mixture) to the dorsal skin and ear, on days 1-3 Ear thickness↑ Lymph nodes and spleen weights↑ Skin: mast cell number↑	Ear thickness: (++ both doses, a better effect for a higher dose) Weight of lymph nodes: (+ 4, ++ 8) Weight of spleen: (++ both doses) Skin: mast cell number (++ both doses, a better effect for a higher dose)	Not studied
Zheng et al. [85]	*Dracocephalum heterophyllum* 95% ethanol extract Pretreatment 2 h before Concanavalin A 20 mg/kg b.w., i.p. Female BALB/c mice, 6-8-week-old	Concanavalin A-induced hepatitis sublethal dose 15 mg/kg b.w., i.v. Serum 8, 16, and 24 hours after Concanavalin A: ALT, AST, IFN-γ, TNF-α↑ Liver: MDSCs↓, Kupffer cells↑	Serum 8, 16, and 24 hours after Concanavalin A: ALT, AST, IFN-γ, TNF-α (++) Liver: Kupffer cells (+++), MDSCs↑	Liver: Kupffer cells↑
Badr and Naeem [75]	*Physalis peruviana* cape goldenberry fruit powder 20% (w/w) fruit powder addition to diet, for 35 days Male albino rats, 1 month, 140-150 g	Aflatoxins B_1 and G_1 850 ng/kg b.w./day for 35 days Weight gain, food intake↓ Blood: HGB, RBC, PLT↓, HCT, WBC↑ Serum: Fe, T-AOC, cholesterol↓, TG, LDL-c, HDL-c, ALT, AST, ALP, MDA↑ Liver: SOD, CAT↓, MDA↑	AFB_1 Weight gain (++), food intake (+++) Blood: PLT, HCT, WBC, HGB (++), RBC (+++) Serum: MDA (+), LDL-c, HDL-c, Fe, cholesterol, T-AOC, TG, ALT, AST, ALP (++) Liver: SOD, MDA (++), CAT (+++) AFG_1 Weight gain (++), food intake (+++) Blood: PLT, HCT, WBC, HGB (++), RBC (+++) Serum: LDL-c, HDL-c, Fe, cholesterol, TG, ALT, AST, ALP, MDA (++), T-AOC (+++) Liver: SOD, MDA (++), CAT (+++)	None
Xu et al. [79]	Polysaccharides from *Morinda officinalis* processed root (processed root by Beijing Sanhe Pharmaceutical Co., Ltd.) 500 mg/kg i.g., once a day for 18 days Female Balb/c mice	Concanavalin A-induced liver damage 10 mg/kg i.v., once a week Weight index: liver and kidney↑, thymus↓ Serum: ALT and AST↑ Liver: CAT↓, MDA↑	Weight index: kidney (0), liver (+), thymus (+++) Serum: ALT and AST (+++) Liver: CAT, MDA (+)	Not studied

TABLE 3: Continued.

Reference	Plant preparation, dose, way and time of treatment, and animals	The toxic substance, dose, way and time of exposure, and negative effects	Protective effects of plant preparation	Effects of plant *per se*
Ahmed et al. [86]	*Pulicaria petiolaris* aerial part methanol extract Pretreatment 50 or 100 mg/kg, p.o., for 5 days Male Swiss albino mice, 25-27 g	LPS-induced hepato- and cardiotoxicity, a single dose 10 mg/kg i.p. Serum: ALT, AST, ALP, LDH, CK-MB, cTnI ↑ Liver: GSH, SOD ↓, MDA, NF-κB, TNF-α, IL-6, average severity of histopathological lesions ↑ Heart: GSH, SOD ↓, MDA, NF-κB, TNF-α, IL-6, average severity of histopathological lesions ↑	Serum: ALT, AST, ALP, CK-MB, cTnI (++ both doses), LDH (++ 50, +++ 100) Liver: average severity of histopathological lesions (+ 50, ++ 100), NF-κB, (++ both doses), MDA, IL-6, TNF-α, GSH (++ 50, +++ 100), SOD (+++ both doses) Heart: IL-6, NF-κB, TNF-α, GSH, SOD (++ both doses), average severity of histopathological lesions and MDA (++ 50, +++ 100)	100 mg/kg only studied: Serum: LDH ↓
Raish et al. [87]	*Lepidium sativum* seed ethanol extract Pretreatment 150 and 300 mg/kg p.o., for 14 days Male Wistar rats, 2-month-old, 180-205 g	D-Galactosamine+LPS-induced hepatotoxicity 400 mg/kg and 30 μg/kg, respectively, i.p., on the 15th day Serum: ALT, ALP, AST, bilirubin, GGT ↑ Liver: CAT, GSH, SOD ↓, MDA, MPO, NF-κB9 (p65) DNA binding activity, mRNA expression of TNF-α, IL-6, IL-10, HO-1, iNOS ↑	Serum: ALT, ALP, AST, GGT (++ both doses), bilirubin (++ 150, +++ 300) Liver: CAT (+ 150, ++ 300), GSH, SOD, MDA, MPO, NF-κB9(p65) DNA binding activity, mRNA expression of TNF-α, IL-6, HO-1, iNOS (++ both doses) Liver: expression of IL-10 (+ 150, ↑ 300) The greater the dose the more distinct the effect	Not studied
Albrahim and Binobead [30]	*Moringa oleifera* leaf water extract 200 mg/kg b.w., i.g., for 4 weeks Male albino rats, 9-10 weeks, 110-130 g	Monosodium glutamate-induced hepatotoxicity, 5 mg/kg b.w., i.g., for 4 weeks Serum: TP, globulins ↓, ALT, AST ↑ Liver: CAT, SOD, GST, GSH ↓, MDA, DNA damage, expression of PCNA and P53 proteins ↑	Serum: globulins (+), TP (++), ALT, AST (+++) Liver: CAT, SOD, GST, GSH, MDA (++); DNA damage (++), expression of PCNA and P53 proteins (++)	None

↓: a decrease vs. control; ↑: an increase vs. control; (+): a slight beneficial effect; (++): a distinct beneficial effect; (+++): a complete beneficial effect; (0): no beneficial effect.

TABLE 4: The protective effects of plant preparations against carcinogens.

Reference	Plant preparation, dose, way and time of treatment, and animals	The carcinogen, dose, way and time of exposure, and negative effects	Protective effects of plant preparation	Effects of plant per se
Bingül et al. [89]	Vaccinium corymbosum L. blueberries homogenate added to diet 8% (w/w) and given to rats for 16 weeks. Male Wistar rats, 200–250 g	Diethylnitrosamine 200 mg/kg, i.p., at 4th, 6th and 8th week of the experiment. Serum: ALT, AST, LDH ↑. Liver: MDA, DC, PC, GSH, GST ↑, SOD, CAT, GPx ↓. Liver: relative mRNA expression of SOD, CAT, GPx ↓, of GST-pi ↑	Serum: ALT (++), AST (+++), LDH (↓). Liver: GPx, GSH, GST, SOD, CAT (+), PC (++), MDA (+++), DC (↓). Liver: relative mRNA expression of SOD, CAT, GPx (0), of GST-pi (++)	None
Khan et al. [88]	Phoenix dactylifera L. (Aiwa dates) water extract 0.5 or 1.0 g/kg b.w., daily for 10 weeks, starting on the next day after diethylnitrosamine. Male Wistar rats, 5-6-week-old, 100-120 g	Diethylnitrosamine-induced hepatocellular carcinoma, two doses 180 mg/kg b.w. at 15 days interval, p.o. Serum: ALT, AST, ALP, IL-1α, IL-1β, GM-CSF, MDA ↑, SOD, GR, GPx, CAT, IL-2, IL-12, IL-4 ↓	0.5 g/kg b.w.: Serum: CAT, MDA, IL-1β (-), IL-4 (0), IL-2 (+), SOD, GR, GM-CSF, ALP (++), ALT, AST, GPx, IL-1α, IL-12 (+++) 1.0 g/kg b.w.: Serum: IL-4, CAT (0), ALP, MDA, AST, IL-1α (↓), SOD, GR, IL-β, GM-CSF, IL-2 (++), ALT (+++), GPx, IL-12 (↑)	Not studied
Choi et al. [46]	Centella asiatica leaf (Martin Bauer GmbH & Co. KG, Vestenbergsgreuth, Germany) 75% ethanol extract 100 or 200 mg/kg, p.o., daily for 5 days following carcinogen. Male Sprague-Dawley rats, 6-week-old, 180-200 g	Dimethylnitrosamine-induced liver injury 30 mg/kg, i.p. Serum: AST, ALT, ALP, total bilirubin, TNF-α, IL-1β, IL-6, INF-γ, IL-10, IL-12, IL-2, GM-CSF ↑. Liver: fibrosis, intralobular degeneration, focal necrosis, MDA ↑, GPx, SOD, CAT ↓	Serum: AST, INF-γ (↓ both doses), IL-10 (++ 100, 0 200), IL-12 (++ 100, + 200), total bilirubin, ALT (+ 100, ++ 200), ALP (++ 100, +++ 200), IL-12 (+++ 100, ++ 200), TNF-α, IL-1β, IL-6, GM-CSF (+++ both doses). Liver: SOD, CAT and fibrosis (+ 100, ++ 200), GPx (++ 100, +++ 200), intralobular degeneration and focal necrosis (++ both doses), MDA (+++ 100, ↓ 200)	Not studied
Kiziltas et al. [47]	Ferulago angulata flowers 80% methanol extract 150 or 300 mg/kg b.w., p.o., daily, for 21 days. Male Wistar rats, 4-week-old, about 200 g	N-Nitrosodimethylamine (dimethylnitrosamine)-induced oxidative stress, 10 mg/kg b.w., i.p., for the first 7 days. Liver: SOD, GPx, CAT ↓	Liver: SOD (+ 150, ++ 300), GPx, CAT (++ both doses)	Both doses: Liver: CAT ↓
Rouhollahi et al. [90]	Curcuma purpurascens Bl. rhizome dichloromethane extract 250 or 500 mg/kg, p.o., once a day for 2 months, after azoxymethane. Male Sprague-Dawley rats, 6 weeks, 200–220 g	Azoxymethane-induced aberrant crypt foci 15 mg/kg, s.c., once a week for 2 consecutive weeks. Colon: CAT, GPx, SOD ↓, aberrant crypt foci formation and MDA ↑	Colon: aberrant crypt foci formation, MDA, CAT (++ both doses), GPx and SOD (++ 250, +++ 500)	Not studied

↓: a decrease vs. control; ↑: an increase vs. control; (+): a slight beneficial effect; (++): a distinct beneficial effect; (+++): a complete beneficial effect; (0): no beneficial effect; (-): intensification of the harmful effect.

deterioration of antioxidant barrier, observed in animals exposed to ethanol [44, 56, 91]. The involvement of oxidant stress into ethanol toxicity was also showed by Phunchago et al. [92] who observed the protective influence of antioxidant vitamin C. The studies presented in the current review proved that plant materials showed a wide range of protective actions including ameliorating of liver markers, oxidative parameters, and alleviation of histopathological changes [56, 91, 92]. The involvement of LPS-TRL4-NF-κB pathway was also been proved [56, 65].

The detailed results of the performed studies are presented in Table 5.

2.6. The Protective Influence of Plant Preparations against Toxic Effects of Antipyretic and Analgesic Drugs.
The application of antipyretic and analgesic drugs has been growing rapidly in recent years. Acetaminophen, known also as paracetamol, N-acetyl-p-aminophenol or APAP, a substitute of aspirin, is one of the most often used over-the-counter medicines. However, its application can cause severe hepatotoxicity, and this fact is all the more dangerous because of possible overdose resulting from self-administration [18, 22, 40, 95]. Another side effect, connected with paracetamol application, is nephrotoxicity [22, 40]. The harmful action of acetaminophen includes oxidative stress, particularly the depletion of GSH and protein sulfhydryl groups blocking [96]. Several studies revealed the possibility of plant extract application as protective adjuvants, wherein *Moringa peregrine*, *Genista quadriflora*, *Teucrium polium geyrii*, and *Cassia surattensis* showed the best influence which included not only amelioration of liver damage markers but also improvement of antioxidant parameters and reduction of the lipid peroxidation process [19, 20, 96].

The details concerning the mentioned investigations are presented in Table 6.

2.7. The Protective Influence of Plant Preparations against Toxic Effects of Antibiotics.
Not only are antibiotics used for the treatment of Gram-negative bacterial infection, but they also can cause side effects to occur [98, 99]. Gentamycin belongs to those which are used in case of strains resistant to other antibiotics, but its application can lead to hepato and nephrotoxicity [28]. The similar properties are shown by an antibiotic polymyxin, whose application was ceased because of its nephrotoxicity, but an increased drug resistance of Gram-negative strains has rendered it being used again [99]. Oxidative stress as well as inflammation processes was suggested to take part in the development of the mentioned negative effects [29, 98, 99]. Materials obtained from plants containing antioxidant components and affecting immune functions were investigated as to their possible protecting application, and the results seem to be promising although they also pointed to the necessity of taking proper precautions and precise choosing the dose as in some cases the higher dose showed a better influence [29, 98], while other authors reported quite opposite results [28].

The details concerning the above mentioned issues are presented in Table 7.

2.8. The Protective Influence of Plant Preparations against Toxic Effects of Anticancer Drugs.
Cancer successful therapy is often a great problem because of the side effects of the applied agents which include deterioration of reproductive proficiency [23], nephrotoxicity [16, 100], and hepatotoxicity [37] and cardiotoxicity [26]. The results of the studies presented below clearly show that the toxic action of anticancer drugs is strongly connected with the prooxidative processes, deterioration of antioxidant barrier, and histopathological changes. The extracts of different plants, used as spices and drugs in traditional medicine for centuries, were studied for their protective potential [101]. Both simple extracts and particular fractions [25, 26] proved their protective properties which included the amelioration of the disturbed oxidant parameters. Antioxidant and antiapoptotic properties of plant extracts were confirmed by *in vitro* investigations performed on renal tubular epithelia cells [100] and cardiomyocytes [25]. Histopathological changes were also found to be relieved by plant materials [16, 23, 24, 26, 102].

The details concerning the above mentioned issues are presented in Table 8.

2.9. The Protective Influence of Plant Preparations against Side Effects of Various Drugs.
Many drugs' administration is accompanied with numerous side effects which cause life complication and may negatively influence patients' compliance. These facts prompted the searching for any adjuvants reversing or at least alleviating side effects. Recently, a growing interest in plant origin substances, often those used in traditional medicine, is being observed [104, 105]. The studies presented below revealed the effectiveness of plant extracts against toxicity of diverse drugs: psychiatric (lithium carbonate), thyrostatic (Propylthiouracil), and cardiac activity stimulators (Isoproterenol), a contrast medium (Iodixanol), and dermatological medicine (Triamcinolone acetonide). The negative influence of the studied drugs often included deterioration of antioxidant barrier [105, 106]. The studied preparations showed beneficial effects, and *in vitro* studies confirmed their antioxidant potential [104, 107].

The details concerning the above mentioned issues are presented in Table 9.

2.10. The Protective Effects of Plant Preparations Observed in Animal Models of Different Disorders

2.10.1. The Protective Effects of Plant Preparations Observed in Arthritis.
Arthritis has recently become a serious, worldwide problem as this disease is related with pain and physical disability, and no effective therapy except for a surgery can be applied [49]. As the risk of it increases with age, the growing spam life contributes to the still enhancing incidence. Plant substances were found to prevent enhancement of the proinflammatory cytokines like IL-1β, IL-6, and TNF-α, involved into osteoarthritis pathogenesis of OA. Additionally, the reduction of metalloproteinases responsible for joint damage as well as upregulation of their inhibitors—TIMPs and extracellular matrix components—was observed [48, 49]. Furthermore, plant origin substances were reported to reverse

oxidative parameters' disturbances, also taking part in osteo-arthritis development [55].

The detailed outcomes of the performed studies are collected in Table 10.

2.10.2. The Protective Effects of Plant Origin Materials in Cases of Neurodegenerative Disorders. The next type of disorders studied with using an animal model was neurodegenerative diseases. ROS have been reported to be involved in the development of Alzheimer's, Huntington's, and Parkinson's diseases. Extracts obtained from plants used in traditional Chinese and Ayurveda medicine, possessing numerous therapeutic properties and containing antioxidant components, were shown to exert a considerable beneficial influence [31, 32, 39].

Traumatic brain injury, regarded as a worldwide grave challenge being a cause of many death and disability cases, is considered to need an effective therapy. Water extracts of plant commercial products were revealed to show a beneficial influence on immunological and oxidative parameters [38, 60].

Psychiatric disorders like anxiety or depression were also proved to be connected with neurodegenerative disturbances as well as changes of immunological and oxidative parameters which were alleviated by plant extracts [111, 112].

The detailed outcomes of the performed studies are collected in Table 11.

2.10.3. The Protective Effects of Plant Origin Materials in Cases of Animal Menopause Model. In menopausal women, the deficiency of sex hormones can lead to various disturbances of organism. The research concerning hormone replacement therapy showed that it can cause different side effects, so the attention was paid to nonpharmaceutical agents, all the more because plant flavonoids were proved to possess phytoestrogen properties [114]. In the performed studies, plant origin materials improved some elements of lipid profile and oxidative parameters deteriorated by ovariectomy [115]. Bone mineral density in rats was also ameliorated, although this effect became less distinct along with lengthening of the experiment [114]. However, in some cases, the obtained results were not so distinctly beneficial [116].

The details of the performed studies are collected in Table 12.

2.10.4. The Protective Effects of Plant Origin Materials in Lung Disorders. Plant origin substances were shown to possess some efficacy against lung disorders, and the beneficial effect included the improvement of oxidative and inflammatory parameters, morphological disturbances, and factors controlling extracellular matrix functions and vascular homeostasis [117–119].

The details of the performed studies are collected in Table 13.

2.10.5. The Protective Effects of Plant Origin Materials in Lipid Profile Disturbances. Lipid profile disturbance is associated with severe diseases like diabetes as well as hepatic and cardiovascular disorders [120]. It is rated among the main factors causing disability and death [34]. Factors which were

used to induce such a condition were also found to cause intensification of prooxidative processes connected with deterioration of antioxidant defence and DNA damage. Plant preparations proved to display beneficial effects, although only in one case *per se* influence was studied [120].

The detailed results of the performed studies are collected in Table 14.

2.10.6. The Protective Effects of Plant Origin Materials in Ischaemia/Reperfusion Model. Ischaemia/reperfusion damage is a serious problem which can occur as a consequence of surgery, e.g., transplantation or coronary bypass, and may lead to severe injuries, resulting among other things from increase in ROS generation. Pretreatment with plant materials, obtained from species used in traditional medicine, was found to be effective against prooxidative processes and histopathological changes observed in ischaemia/reperfusion animal model [123–126].

The detailed results of the performed studies are collected in Table 15.

2.10.7. The Protective Effects of Plant Origin Materials in Animal Model Diabetes. Plant origin substances were observed to be effective at reversing disturbances observed in the course of diabetes. A wide range of agents was studied, simple extracts, combinations of two extracts as well as an oil, banana pasta or substances separated from plant material. A great variety of species was investigated, including herbs, fruits, or vegetables. Many of them had been known as being useful in different fields of medicine, sometimes from ancient times [66, 127–129]. In several studies, biochemical, oxidant, and inflammatory parameters in the blood and organs including the lens, brain, liver, pancreas, kidney, and heart were found considerably improved or restored by different materials [42, 57, 66, 128, 129]. Histopathological investigation revealed that plant preparations showed a considerable ability to attenuate pancreas, kidney, and liver damage observed in the animal model of diabetes [127, 128, 130]. The beneficial influence of plant extracts on the deterioration of sperm quality [131], diabetes-associated cataract, and retinopathy and an ability to suppress MAPK signal transduction [42] and the amyloidogenic pathway [57] were reported. However, there are limitations of these investigations as in most of them the effect of the applied plant substance was not studied.

The detailed results of the performed studies are collected in Table 16.

2.10.8. The Protective Effects of Plant Origin Materials in Animal Model of Obesity. Plant origin preparations were also investigated as to their potential to prevent pathological processes connected with obesity. This direction seems to be of great importance as obesity and related disturbances, resulting from sedentary lifestyle as well as excessive consumption, are becoming more and more serious world problem [132, 133]. Diet-induced obesity was found to be connected with different disturbances of various parameters including liver markers and lipid profile as well as inflammation, lipogenesis, and oxidative balance. The performed research revealed

TABLE 5: The protective effects of plant origin substances against toxicity of ethanol.

Reference	Plant preparation, dose, way and time of treatment, and animals	The dose, way and time of exposure, and negative effects	Protective effects of plant preparation	Effects of plant per se
Akbari et al. [93]	Zingiber officinale Roscoe (ginger) rhizome hydroalcoholic extract 1 g/kg of b.w./d, p.o., for 28 days Sprague-Dawley male rats, about 220 g	Ethanol 4 g/kg of b.w./d, p.o., for 28 days Serum: T, SHBG, DHEAs ↓ Testes: weight, Zn, Mg, Fe, Cu ↓; SOD, GPx, CAT ↓, MDA, tHcy ↑	Serum: T (++), SHBG, DHEAs (+++) Testes: Zn (-), Cu (+), Mg, weight, SOD, GPx, CAT, MDA, tHcy (+++), Fe (↑)	Serum: T ↓ Testes: Fe ↑, Zn, Mg, Cu ↓
Phunchago et al. [92]	Tiliacora triandra aerial parts aqueous extract, 100, 200 or 400 mg/kg b.w., p.o., for 14 days after developing ethanol dependence by15-week alcohol treatment Male Wistar rats, 8 weeks	Ethanol-dependence caused by a gradual increase of ethanol content in drinking fluid from 5% up to 30%, a 15-week alcohol treatment Hippocampus: AChE, MDA ↑, SOD, CAT, GPx ↓, neuron density in subregions CA1, CA2, CA3 and dentate gyrus ↓	Hippocampus: AChE (+ 100, ++ 200, 0 400), CAT (+++ 100 and 200, ++ 400), GPx (↑ 100 and 200, +++ 400), MDA, SOD (++ all doses), neuron density in subregions CA1, CA2, and CA3 and dentate gyrus (++ all doses)	Not studied
Liu et al. [91]	Ginseng oligopeptides extracted from roots of Panax ginseng C.A. Meyer (Jilin Taigu Biological Engineering Co., Ltd, China) Pretreatment: 0.0625, 0.125, 0.25, and 0.5 g/kg b.w., for 30 days, p.o., Sprague-Dawley male rats, 180–220 g	One dose of 50% ethanol 7 g (17.5 mL)/kg b.w., i.g. Serum: ALT, AST, TG, ALP, TNF-α, IL-6, IL-1β and LPS ↑, TC, HDL-c, LDL-c, TP ↓ Liver: steatosis and MDA ↑, SOD, GSH, GPx ↓	Serum: ALP (- lower doses, 0 the highest one); LDL-c, TP (0 all doses), HDL-c (0 the lowest dose, + other ones), TC (++ all doses), TG (++ lower doses, +++ higher ones), LPS (+++ except for 0.25 mg/kg ++), ALT, AST, (+++ all doses), TNF-α, IL-6 and IL-1β (↓ all doses) Liver: steatosis (++ all doses), GPx (+ lower doses, +++ 0.25, ↑ 0.5), GSH (+ lower doses, +++ higher ones), MDA (+++ all doses), SOD (+ lower doses, ++ highest one)	Not studied
Jung et al. [94]	Glycyrrhiza uralensis Fisher root 70% ethanol extract 100 mg/kg b.w., p.o., for 4 weeks Male C57BL/6 mice	Dietary ethanol Lieber–DeCarli liquid diet—36% of energy from ethanol, for 4 weeks Serum: TNF-α, ALT, AST ↑ Liver: GSH ↓, TG and mRNA expression of Srebf1, Cd36, Lpl, Fatp4 ↑	Serum: TNF-α, ALT, AST (++) Liver: TG, mRNA expression of Srebf1, Cd36 and Lpl (++), GSH and mRNA expression of Fatp4 (+++)	Not studied
Lou et al. [65]	Linderae radix (prepared slices, Zhejiang Tiantaishan Wuyao Biological Engineering Co., Ltd., China) extracted from tubers of Lindera aggregata (Sims) Kostern, 75% ethanol extract 1, 2 or 4 g/kg, i.g, for 20 days Male Sprague-Dawley rats, 160–180 g	50% alcohol 10 mL/kg b.w., once a day for 20 days, i.g. Serum: ALT, total bilirubin, IL-6, IL-8, TNF-α, NF-κB ↑ Portal vein: LPS ↑ Small intestine: expression of tight junction proteins claudin-1 and occludin ↓	Serum: IL-6 (+ 1 and 2, ++ 4), TNF-α (+++ 1, ++ 2, 0 4), NF-κB (++ 1, +++ 2, and 4), ALT, total bilirubin, IL-8 (+++ all doses) Portal vein: LPS (+++ all doses) Small intestine: expression of tight junction proteins claudin-1 (+ all doses) and occludin (+++ 1, ++ 2, 0 4)	Not studied

TABLE 5: Continued.

Reference	Plant preparation, dose, way and time of treatment, and animals	The dose, way and time of exposure, and negative effects	Protective effects of plant preparation	Effects of plant *per se*
Tang et al. [56]	*Cynara scolymus* L. (artichoke) in freeze-dried powder (Huimei Agricultural Science and Technology Co., Ltd., China) Pretreatment, 1 hour before alcohol 0.4, 0.8 or 1.6 g/kg b.w., p.o., daily for 10 days Male Institute of Cancer Research, mice, 7-week-old about 25 g	Ethanol 12 mL/kg b.w., p.o., daily for 10 days Liver index: ↑ Serum: ALT, AST, TG, TC ↑ Liver: SOD, GSH ↓, MDA↑, expression level of TLR4 and NF-κB p50 ↑, score of steatosis, inflammation and necrosis ↑	Liver index: (++ all doses) Serum: ALT (0 0.4, + 0.8, +++ 1.6),TG (0 0.4, ++ 0.8 and 1.6), AST (+ 0.4 and 0.8, ++ 1.6), TC (+ 0.4, ++ 0.8 and 1.6) Liver: SOD, GSH (++ 0.4 and 0.8, +++ 1.6), MDA (+ 0.4, +++ 0.8, and 1.6), score of steatosis (+ 0.4, ++ 0.8, and 1.6), score of inflammation (+ 0.4, ++ 0.8, and 1.6), score of necrosis (++ all doses), expression of TLR4 (+ 0.4, ++ 0.8, +++ 1.6), expression of NF-κB p50 (++ 0.4, +++ 0.8 and 1.6)	Not studied
Dogan and Anuk [44]	*Platanus orientalis* L. leas water extract 20 or 60 mg/mL leaf infusion *ad libitum*, for 28 days Male Wistar rats, 2 months aged, about 200 g	20% ethanol water *ad libitum* for 28 days Serum: AST, ALT, LDH, GGT, UA, urea ↑, cholesterol, HDL-c ↓ Liver: GSH ↓, GST, MDA ↑ Erythrocytes: GST, MDA ↑ Kidney: MDA ↑, SOD, GPx, CAT ↓	Serum: GGT (– 20, ++ 60), ALT, urea (+ 20, 0 60), HDL-c (+ both doses), LDH (++ 20, +++ 60), cholesterol (++ 20, + 60), AST, UA (+++ both doses) Liver: GSH and GST (+ both doses), MDA (++ both doses) Erythrocytes: GST (0 both doses), MDA (++ 20, +++ 60) Kidney: SOD (– 20, + 60), CAT (– 20, ++ 60), MDA (+++ both doses), GPx (+++ 20, ↑ 60)	Not studied

↓: a decrease vs. control; ↑: an increase vs. control; (+): a slight beneficial effect; (++): a distinct beneficial effect; (+++): a complete beneficial effect; (0): no beneficial effect; (-): intensification of the harmful effect.

TABLE 6: The protective effects of plant substances against toxicity of antipyretic and analgesic drugs.

Reference	Plant preparation, dose, way and time of treatment, and animals	The name of drug, dose, way and time of exposure, and negative effects	Protective effects of plant preparation	Effects of plant *per se*
Bouzenna et al. [21]	*Pinus halepensis* L. needles essential oil Pretreatment, 1% (*w/w*), with a dose of 1 mL/kg p.o., for 56 days Female Wistar rats, 150-200 g	Aspirin-induced liver and kidney damage 600 mg/kg thrice a day for 4 days, p.o. Weight: body, liver, kidney↓ Serum: glucose, TC, AST, ALT, LDH, CR, urea ↑ Liver: TBARS ↑, SOD, CAT, GPx ↓ Kidney: TBARS ↑, SOD, CAT, GPx ↓	Weight: body, liver, kidney (+++) Serum: glucose, TC, AST, ALT, LDH, CR, urea (+++) Liver: TBARS, SOD, CAT, GPx (+++) Kidney: TBARS, SOD, CAT, GPx (+++)	None
Ahmad and Zeb [18]	*Trifolium repens* leaf water extract 11 mg of solid weight/mL; 1, 2, or 3 mL of extract per day for 2 weeks Male albino mice about 28.6 g	Acetaminophen-induced hepatotoxicity 300 mg/kg for 2 weeks Serum: TC, TG, LDL-c, ALT, AST, ALP, glucose ↑, HDL-c ↓ Blood: RBC, HGB, HCT, PLT ↓, WBC ↑ Liver: TBARS ↑, GSH ↓	1 mL: Serum: ALP, glucose (0), TC, TG (+), HDL-c, ALT, AST (++), LDL-c (+++) Blood: PLT (0), HCT (+), WBC (++), RBC, HGB (+++) Liver: GSH (+), TBARS (++) 2 mL: Serum: TC (+), ALT, AST, ALP, TG, HDL-c, glucose (++), LDL-cholesterol (+++) Blood: PLT (+), RBC, HGB, HCT, WBC (+++) Liver: GSH, TBARS (++) 3 mL: Serum: HDL-c (0), TC, AST, ALT, AST (++), glucose, LDL-c (+++) Blood: PLT, RBC, HGB, HCT, WBC (++) Liver: TBARS, GSH (++)	Studied only for the 1 mL dose Serum: TC ↓, HDL-c ↑
Azim et al. [19]	*Moringa peregrina* leaves 70% ethanol extract 200 mg/kg b.w. p.o., one hour prior to acetaminophen, for 4 weeks Female albino rats, about 160 g	Acetaminophen-induced hepatotoxicity 750 mg/kg b.w., p.o. Serum: ALT, AST, ALP, GGT ↑ Blood: GSH, CAT, SOD ↓, MDA ↑ Liver: GSH, CAT, SOD ↓, GPx, MDA ↑ Brain: GSH, SOD ↓, GPx and MDA ↑	Serum: ALT, ALP (++), AST, GGT (+++) Blood: GSH, CAT, SOD, MDA (+++) Liver: GSH, CAT, SOD, GPx, MDA (+++) Brain: GPx, MDA (++), GSH, SOD (+++)	Not studied
Mishra et al. [97]	*Pandanus odoratissimus* root ethanolic extract 200 or 400 mg/kg b.w, p.o., once a day for 7 days Wistar rats 180-200 g	Paracetamol-induced hepatotoxicity 2 g/kg b.w., p.o., on the 5th day Serum: AST, ALT, ALP, direct bilirubin, total bilirubin, TG ↑	Serum: ALT, AST, ALP, direct bilirubin, total bilirubin, TG (++); The protective effect was better for the higher dose.	Not studied
Rashid et al. [40]	*Fagonia olivieri* DC. aerial parts 95% methanolic extract 200 and 400 mg/kg, i.g, for 7 days Male Sprague-Dawley rats, 6-week-old, 180-200 g	Acetaminophen-induced toxicity 750 mg/kg b.w, i.g. Serum: AST, ALT, ALP, LDH, total bilirubin, cholesterol, TG, HDL, LDL ↑ Blood: HGB, WBC ↓, PLT ↑ Liver: weight, CAT, SOD, GPx, GR, GSH and TP ↓, DNA fragmentation and TBARS ↑	Serum: AST, ALT, ALT, LDH, LDL (++) both doses, ALP, total bilirubin, TG, HDL (++ 200, +++ 400), cholesterol (+++ 200, 400 ↓) Blood: HGB (++ both doses), WBC (+++ both doses), PLT (+++ 200, ↑ 400) Liver: TP (0 200, ++ 400), DNA fragmentation, SOD, GR, GSH, TBARS (++ both doses), weight, CAT, GPx (++ 200, +++ 400)	400 mg/kg studied only Serum: TG, HDL, cholesterol ↓ Blood: WBC ↑, HGB ↓ Liver: TBARS ↓

TABLE 6: Continued.

Reference	Plant preparation, dose, way and time of treatment, and animals	The name of drug, dose, way and time of exposure, and negative effects	Protective effects of plant preparation	Effects of plant per se
Ebada [95]	Chamomilla recutita L. (chamomile) and Cuminum cyminum L. (green cumin) essential oils (Hashem Brothers for Essential Oils and Aromatic products) Pretreatment p.o., for 14 days, 400 mg/kg/day (cumin), 250 mg/kg/day (chamomile) Male Wistar rats, 180-200 g	Acetaminophen-induced hepatotoxicity 1 g/kg p.o., a single dose on the 14th day Serum: ALT and AST ↑ Liver: GSH ↓, MDA and SOD ↑ Liver histopathology: hepatocyte necrosis, inflammation, degeneration, dilated central vein, hemorrhage ↑	Cumin essential oil: Serum: ALT and AST (+++) Liver: GSH (0), MDA (-) and SOD (0) Liver histopathology: hepatocyte necrosis, inflammation, degeneration, dilated central vein, hemorrhage (++) Chamomile essential oil: Serum: ALT (++) and AST (0) Liver: MDA (-), GSH, SOD (++) Liver histopathology: hepatocyte necrosis, hemorrhage inflammation, dilated central vein, degeneration (+)	Not studied
Baali et al. [20]	Rich-polyphenol (n-butanol) fractions of 80% methanolic extract of Genista quadriflora Munby and 70% methanolic extract of Teucrium polium geyrii Maire Pretreatment 300 mg/kg daily, p.o., for 10 days Male Wistar rats, about 142 g	Acetaminophen-induced hepatotoxicity A single dose of 1 g/kg, p.o. Plasma: AST, ALT ↑ Liver: SOD, GPx, GR, GSH, GST, CYP2E1, TBARS and mRNA of TNF-α expression ↑ Liver mitochondria: CS and respiratory chain complexes I and II ↓	Genista quadriflora Plasma: AST, ALT (+++) Liver: SOD, GPx, GSH, GST, TBARS, CYP2E1 and mRNA of TNF-α expression (+++), GR ↑ Liver mitochondria: CS and respiratory chain complex I (+++), respiratory chain complex II ↑ Teucrium polium geyrii Plasma: AST, ALT (+++) Liver: SOD, GPx, GSH, GST, TBARS, CYP2E1 and mRNA of TNF-α expression (+++), GR ↑ Liver mitochondria: CS (+++), respiratory chain complexes I and II ↑	Not studied
Uthaya Kumar et al. [96]	Cassia surattensis seed methanol extract Pretreatment 250 or 500 mg/kg b.w., p.o., once daily for 7 days Male Swiss albino mice, 6-8-week-old, 25-30 g	Paracetamol-induced hepatotoxicity A single dose of 1 g/kg b.w., p.o. Relative liver weight: ↑ Serum: ALT, AST, ALP ↑ Liver: GSH, SOD ↓, MDA ↑	Relative liver weight: (+++ both doses) Serum: ALT, AST, ALP (++ both doses) Liver: MDA and GSH (++ 250, +++ 500), SOD (++ 250, ↑ 500)	Not studied
Chinnappan et al. [22]	Eurycoma longifolia root water extract Physta® (Biotropics Malaysia) 100, 200 or 400 mg/kg, p.o., 1 hour before paracetamol, for 14 days Male Wistar rats, 12-week-old, 120-150 g	Paracetamol-induced nephrotoxicity 200 mg/kg daily for 14 days, i.p. Serum: TP, ALB ↓, creatinine ↑ Blood: urea ↑ Creatinine clearance: ↓	100 mg/kg: Serum: ALB, creatinine (0), TP (+) Blood: urea and (0) Creatinine clearance: (0) 200 and 400 mg/kg: Serum: TP, ALB, creatinine (+++) Blood: urea (+++) Creatinine clearance: (+++)	Not studied

↓: a decrease vs. control; ↑: an increase vs. control; (+): a slight beneficial effect; (++): a distinct beneficial effect; (+++): a complete beneficial effect; (0): no beneficial effect; (-): intensification of the harmful effect.

TABLE 7: The protective properties of plant extracts against side effects of antibiotics.

Reference	Plant preparation, dose, treatment way and time, and animals	The name of drug, dose, exposure way and time, and negative effects	Protective effects of plant preparation	Effects of plant *per se*
Valipour et al. [98]	*Ferulago angulata* Ethanol : water (70 : 30, *v/v*) extract 200, 400, or 800 mg/kg b.w., p.o., for 7 days Male Wistar rats, about 200 g	Gentamicin 120 mg/kg b.w., daily for 7 consecutive days, i.p. Serum: HDL ↓; TG, TC, LDL, UA, urea, CR, PC, TNF-α, MDA ↑ Kidney: CAT, SOD and AA ↓, MDA and relative expression of TNF-α ↑	Serum: HDL (0 200 and 400, +++ 800), CR (+ 200, ++ 400 and 800), PC (+ 200, ++ 400, +++ 800), UA and urea (++ all doses), TC, LDL, TNF-α and MDA (++ 200 and 400, +++ 800), TG (++ 200, +++ 400 and 800) Kidney: SOD (0 200, ++ 400 and 800), relative expression of TNF-α (0 200, ++ 400, +++ 800), AA (0 200, +++ 400 and 800), CAT (++ 200 and 400, +++ 800), MDA (+++ 200, +++ 400 and 800)	Not studied
Boroushaki et al. [29]	*Rheum turkestanicum* root 70% ethanol extract 100 or 200 mg/kg, for 6 days, i.p., 1 hour before gentamycin Male Wistar rats, 250-300 g	Gentamycin 80 mg/kg/day, for 6 days, i.p. Serum: CR and urea ↑ Kidney: MDA ↑, total SH content ↓ Urine: protein and glucose ↑	Serum: CR, urea (++ both doses) Kidney: MDA, total SH content (++ both doses) Urine: protein (0 100, ++ 200), glucose (+ 100, ++200)	Not studied
Apaydin Yildirim et al. [28]	*Helichrysum plicatum* DC. subsp. *plicatum* aerial parts ethanol extract 100 or 200 mg/(kg·d) i.p., for 8 days Male Sprague-Dawley rats	Gentamicin 80 mg/(kg·d) i.p., for 8 days Serum: BUN and creatinine ↑ Liver: CAT and SOD ↓; MDA, degeneration, necrosis, inflammatory cells, biliary hyperplasia ↑ Kidney: SOD, CAT, GPx ↓, MDA, inflammatory cells, degeneration, necrosis ↑	Serum: BUN and creatinine (++ both doses) Liver: SOD (++ 100, 0 200), MDA (++ 100, +++ 200), CAT (+++ 100, ++ 200), necrosis, degeneration (++ 100, + 200), inflammatory cells (+++ 100, + 200), biliary hyperplasia (++ both doses) Kidney: GPx (both doses), SOD (+++ 100, 0 200), MDA, CAT (+++ 100, ++ 200) Kidney: degeneration and inflammatory cells (++ 100, + 200), necrosis (++ both doses)	Serum: BUN (↓100, ↑ 200) Liver: CAT (↓ 200), inflammatory cells, biliary hyperplasia and necrosis (↑ 200), degeneration (↑ both) Kidney: CAT (↑ both doses), inflammatory cells and necrosis (↑ 200), degeneration (↑ both)
Zhang et al. [99]	*Panax notoginseng* saponins (Guangxi Wuzhou Pharmaceutical Co., Ltd. Hangzhou, China) 10 mg/kg, twice a day for 14 days, i.m. Female ICR mice, 18-20 g	Polymyxin-induced nephrotoxicity 15 mg/kg twice a day for 14 days, i.m. Kidney weight: body weight ratio: ↑ Serum: BUN, CR ↑ Kidney: SOD ↓, MDA and number of apoptotic cells ↑	Kidney weight: body weight ratio: (++) Serum: BUN, CR (+++) Kidney: number of apoptotic cells (++), SOD and MDA (+++)	None

↓: a decrease vs. control; ↑: an increase vs. control; (+): a slight beneficial effect; (++): a distinct beneficial effect; (+++): a complete beneficial effect; (0): no beneficial effect; (-): intensification of the harmful effect.

TABLE 8: The protective effects of plant preparations against side effects of anticancer agents.

Reference	Plant preparation, dose, treatment way and time, and animals	The name of drug, dose, exposure way and time, and negative effects	Protective effects of plant preparation	Effects of plant *per se*
Kim et al. [100]	*Dendropanax morbifera* The $CHCl_3$ fraction of 70% methanol leaf extract 25 mg/kg once at 24 h before cisplatin and once a day for 5 days after, i.p. Sprague Dawley male rats, 8 weeks, about 200 g	Cisplatin, a single administration of 6 mg/kg, i.p. Body weight: ↓ Kidney/body weight ratio: ↑ Serum: BUN, CR ↑ Kidney: SOD ↓, cleaved caspase-3 and acute tubular necrosis score ↑	Body weight: (++) Kidney/body weight ratio: (+++) Serum: CR (++), BUN (+++) Kidney: acute tubular necrosis score (++), SOD and cleaved caspase-3 (+++)	Not studied
Kpemissi et al. [102]	*Combretum micranthum* leaf ethanol-water (8:2) extract 200 or 400 mg/kg/day p.o, for 10 days Male Wistar rats, 6-8-week-aged, 200-250 g	Cisplatin 7.5 mg/kg, i.p., a single injection on the 5th day Body weight: ↓ Relative kidney weight: ↑ Serum: CR, urea, UA, ALT, AST, GGT, ALP ↑, TP, ALB, Ca, Mg, P, NO, FRAP ↓ Urine: CR, urea, UA, P ↓, TP, ALB, Ca, Mg, ↑ Kidney: MDA ↑, FRAP, NO, GSH ↓	Body weight (++ both doses) Relative kidney weight: (+++ 200, ++ 400) Serum: urea (+++ 200, ++ 400), CR, UA TP, ALB, Ca, Mg, P, ALT, AST, ALP, NO, FRAP (+++ both doses), GGT (↓ both doses) Urine: CR, urea, UA TP, (+++ 200, ++ 400), ALB, Ca, Mg, P (+++ both doses) Kidney: NO, GSH (++ both doses), FRAP (+++ 200, ++ 400), MDA (+++ both doses)	Not studied
Hosseinian et al. [16]	*Nigella sativa* seeds 70% ethanol extract 100 or 200 mg/kg, i.p. (i) Pretreatment (6 days)+saline for 5 days after cisplatin (ii) Pretreatment (6 days)+extract for 5 days after cisplatin Male Wistar rats, 230-300 g	Cisplatin 6 mg/kg on the 6th day of the experiment, i.p. Serum: total SH ↓, MDA ↑ Kidney: total SH ↓, MDA ↑ slightly Renal tissue damage: ↑	(i) Serum: MDA (+++ both doses), total SH (+++100, ↑200) Kidney: MDA (- both doses), total SH (+++ both) Renal tissue damage: (++ both doses) (ii) Serum: MDA (+++ both doses), total SH (↑ both) Kidney: MDA (- 100, +++ 200), total SH (+++ both) Renal tissue damage: (++ both doses)	Not studied
Chen et al. [25]	Total flavonoids from *Clinopodium chinense* (Benth.) Pretreatment 20, 40, or 80 mg/kg, i.g, for 15 days Male Sprague-Dawley rats, 220-250 g	Doxorubicin-induced cardiotoxicity 3 mg/kg, i.p., every two days for a total of three injections Body and heart weight: ↓ Serum: AST, LDH, CK ↑ Heart: SOD, CAT, GPx ↓, MDA ↑	Body and heart weight: (++ 20, +++ 40 and 80) Serum: CK, LDH (++ 20, +++ 40 and 80), AST (+++ all doses) Heart: GPx (+ 20, ++ 40 and 80), CAT (++ all doses), MDA, SOD (++ 20, +++ 40 and 80)	80 mg/kg only studied: none

Table 8: Continued.

Reference	Plant preparation, dose, treatment way and time, and animals	The name of drug, dose, exposure way and time, and negative effects	Protective effects of plant preparation	Effects of plant per se
Ahmed et al. [24]	Allium sativum (garlic) aqueous extract 1 mL/100 g b.w., p.o., daily for 7 days before and 7 days after methotrexate Male Wistar rats, 100–120 g	Methotrexate-induced nephrotoxicity 20 mg/kg, a single injection, i.p. Serum: urea, CR, K, P ↑, Na ↓ Kidney: GSH, CAT ↓, MDA, ADA, NO ↑	Serum: urea (↓), P (+), CR, K, Na (+++) Kidney: MDA, NO (++), GSH, CAT, ADA (+++)	None
Tag et al. [37]	Morus nigra (mulberry) leaves 50% ethanol extract 500 mg/kg, i.g., daily for 14 days Male albino rats, 180–200 g	Methotrexate-induced hepatotoxicity, a single dose, 20 mg/kg, on 4th day, i.p. Liver weight/body weight: ↑ Serum: AST, ALT, ALP, LDH ↑ Liver: total pathological score ↑, mean score of hepatocyte degeneration, congestion, cellular infiltration, fibrosis ↑	Liver weight/body weight: (++) Serum: ALP (++), AST, ALT, LDH ↓ Liver: total pathological score (++), mean score of hepatocyte degeneration, congestion, cellular infiltration and fibrosis (++)	Serum: AST, ALT, ALP, LDH ↓
Moghadam et al. [103]	Curcuma longa L., ethanol extract 100 or 200 mg/kg, p.o., for 30 days Male Wistar rats, 220–280 g	Methotrexate-induced hepatotoxicity, a single dose 20 mg/kg i.p., on day 30th Body weight: ↓ Liver weight: ↑ Serum: ALB, TP ↓, ALT, AST, ALP, bilirubin ↑ Plasma: TAS ↓ Liver: SOD, GPx, CAT ↓, MDA, number of neutrophils, degree of injury ↑	Body weight: (++ both doses) Liver weight ratio: (++ both doses) Serum: AST, ALP (++ both doses), ALB, ALT, bilirubin, TP (++ 100, +++ 200) Plasma: TAS (++100, +++200) Liver: MDA, number of neutrophils (+ 100, ++ 200), degree of injury (++ both doses), SOD, CAT, GPx (++ 100, +++ 200)	The higher dose: Liver: CAT ↑ Plasma: TAS ↑
Omole et al. [26]	Kolaviron—a mixture of flavonoids obtained from Garcinia kola seeds Pretreatment 200 or 400 mg/kg/d, p.o., for 14 days Male Wistar rats, 120–150 g	Cyclophosphamide 50 mg/kg/d, i.p., 24 hours after the last dose of kolaviron, for 3 days Relative heart weight: ↑ Heart: SOD, CAT, GPx, GSH ↓, LDH, CK, MDA, H_2O_2, MPO and cTn I ↑	Relative heart weight: (+++ 200, ++ 400) Heart: LDH, CK, cTn I, MPO, and GSH (++ both doses), GPx, CAT, MDA, H_2O_2 (+++ 200, ++ 400), SOD (+++) both doses	None

TABLE 8: Continued.

Reference	Plant preparation, dose, treatment way and time, and animals	The name of drug, dose, exposure way and time, and negative effects	Protective effects of plant preparation	Effects of plant *per se*
Sheweita et al. [101]	Essential oils of *Foeniculum vulgare* Miller (fennel) seeds, *Cuminum cyminum* L. (cumin) seeds, and *Syzygium aromaticum* L. (clove) flower buds (0.12 mL/kg b.w., 0.10 mL/kg b.w., and 0.106 mL/kg b.w., (1/50 LD$_{50}$ doses), respectively), p.o. for 28 days Male Swiss albino mice, about 25 g	Cyclophosphamide 2.5 mg/kg b.w. for 28 days, p.o. Serum: ALT, AST, ALP ↑ Liver (S9 fraction): TBARS ↑; GSH, GPx, GR, GST, SOD, CAT ↓ Hepatic microsomal fraction: NADPH-cytochrome c reductase ↑	Serum: ALT, AST, ALP (++ all oils) Liver (S9 fraction): TBARS (++ clove oil, +++ fennel and cumin oils); GPx, GSH, GR, SOD, CAT (+++ all oils); GST ↑ all oils Hepatic microsomal fraction: NADPH-cytochrome c reductase (0 all oils)	Liver: TBARS ↓, GPx, CAT, GST ↑ (all oils), GR ↑ (cumin and clove), GSH, SOD ↑ (cumin), NADPH-cytochrome c reductase ↑ (all)
Rahate and Rajasekaran [27]	*Desmostachya bipinnata* Stapf (L.) roots—the polyphenolic fraction of 70% methanol *extract* 100 or 200 mg/kg b.w., p.o., 21 days Sprague-Dawley female rats, 150–200 g	Tamoxifen citrate 45 mg/kg b.w, p.o., 10th–21st days Serum: protein ↓, AST, ALT, ALP, cholesterol, TG, urea, CR, UA, bilirubin ↑ Liver: LPO↑, GSH, GPx, SOD, CAT ↓	Serum: protein, AST, ALT, cholesterol, TG, urea, UA (++ both doses), CR, bilirubin (++ 100, +++ 200), ALP (++ 100, ↓ 200) Liver: CAT (+ 100, ++ 200),LPO, GSH, GPx, SOD, (++ both doses)	Not studied

↓: a decrease vs. control; ↑: an increase vs. control; (+): a slight beneficial effect; (++): a distinct beneficial effect; (+++): a complete beneficial effect; (0): no beneficial effect; (-): intensification of the harmful effect.

TABLE 9: The protective effects of plant preparations against side effects of various drugs.

Reference	Plant preparation, dose, treatment way and time, animals	The name of drug, dose, exposure way and time, negative effects	Protective effects of plant preparation	Effects of plant per se
Ben Saad et al. [104]	Opuntia ficus-indica cladode extract obtained by homogenization with 10 mM Tris HCl, pH 7.4, and subsequent centrifugation Pretreatment, 100 mg/kg b.w. 30-day pretreatment and then for 30 days together with lithium Male Wistar rats, 2 months	Li (lithium carbonate), 25 mg/kg b.w., i.p., twice daily for 30 days Serum: glucose, TC, TG, ALT, AST, LDH, ALP ↑ Blood: RBC, HGB, HCT ↓, WBC ↑ Liver: SOD, CAT, GPx ↓, MDA ↑	Serum: ALT, AST (++), glucose, TC, TG, ALP, LDH (+++) Blood: RBC, HGB, HCT, WBC (++) Liver: CAT (++), SOD, GPx, MDA (+++)	None
Khalil et al. [105]	Withania somnifera leaf 70% ethanol extract Pretreatment, 100 mg/kg b.w., for 4 weeks Male Wistar rats, 140-160 g	Isoproterenol 85 mg/kg b.w., s.c. on 29th and 30th days Serum: TC, TG, VLDL-c, cTnI, CK-MB, LDH, AST, ALT ↑, HDL-c ↓ Heart: SOD, GR, GPx, GST ↓, MDA, weight ↑	Serum: CK-MB (0), TC, TG, VLDL-c, cTnI, LDH (++), HDL-c, AST, ALT (+++) Heart: SOD, weight (++), GR, GPx, GST, MDA (+++)	Serum: HDL-c ↑ Heart: GPx, GST ↑
Dianita et al. [106]	Labisia pumila var. alata water and 80% ethanolic extracts 100, 200, or 400 mg/kg, p.o., for 28 days Male Wistar rats, 150-200 g	Isoproterenol, 85 mg/kg of s.c., on 29th and 30th day of the experiment Serum: cTnI, CK-MB, LDH, AST, ALT ↑, SOD, CAT, GPx ↓ Heart: SOD, CAT, GPx ↓	Serum: cTnI (water extract ++ all doses, ethanol extract ++ 100 and 200, +++ 400), CK-MB, LDH, AST, ALT, SOD, CAT, GPx (++ both extracts all doses) Heart: SOD, GPx (water extract + 100, ++200 and 400, ethanol extract ++ all doses), CAT (++ both extracts, all doses)	Not studied
Shahat et al. [107]	Rhus tripartita 80% methanol extract of the stem part of male genotype 250 or 500 mg/kg/day p.o., for 21 days (19-day-pretreatment) Male Wistar rats, about 180 g	Isoproterenol 85 mg/kg, s.c. on 20th and 21st days Serum: AST, ALT, GGT, ALP, LDH, CK, TC, TG, LDL-c, VLDL-c↑, HDL-c ↓ Heart: MDA ↑, NP-SH and TP ↓	Serum: LDH, HDL-c (+ 250, ++500), AST, ALT, GGT, ALP, CK, TC, TG, LDL-c and VLDL-c (++ both doses) Heart: MDA, NP-SH and TP (++ both doses)	Not studied
Kemka Nguimatio et al. [108]	Aframomum melegueta seed water and methanol extracts 20 or 100 mg/kg for 28 days Male Wistar rats, sexually experienced, 3-month-old, 200-250 g	Propylthiouracil-induced hypothyroidism causing ejaculatory complications 10 mg/[kg·day] for 28 days Plasma: T ↓, TSH and prolactin ↑ Proejaculatory activity (contractile activity of the striated bulbospongiosus muscles): number of contractions after tactile stimulation and pharmacological activation (dopamine) ↓, intraseminal pressure after tactile stimulation and pharmacological activation (dopamine) ↓	Water extract: Plasma: TSH (0 both doses), T (+ 20, +++ 100), prolactin (+ 20, ++ 100) Proejaculatory activity: contractions number after both stimuli (++ 20, ↑ 100), intraseminal pressure: tactile stimulation (↑ both doses), pharmacological activation (+++ both doses) Methanol extract: Plasma: TSH (0 20, +100), T (+ 20, ++ 100), prolactin (++ 20, +100) Proejaculatory activity: contractions number after both stimuli (↑ both doses), intraseminal pressure: tactile stimulation (↑ both doses), pharmacological activation (+++ 20, ↑100)	Not studied

TABLE 9: Continued.

Reference	Plant preparation, dose, treatment way and time, animals	The name of drug, dose, exposure way and time, negative effects	Protective effects of plant preparation	Effects of plant per se
Nasri et al. [109]	Green tea 70% ethanol extract Posttreatment: after iodixanol, 10 mg/kg/d, i.p., for 3 days Pretreatment 10 mg/kg/d, i.p., for 3 days and iodixanol on the 3rd day Male Wistar rats, 6-week-aged, 200-250 g	Iodixanol, a contrast medium 10 mL/kg, i.v., a single dose Renal tubular cells: dilatation, degeneration, vacuolization, debris ↑	Posttreatment: Renal tubular cells: dilatation, degeneration, vacuolization, debris (++) Pretreatment: Renal tubular cells: dilatation, degeneration, vacuolization, debris (++) Pretreatment showed a slightly better effect	Not studied
El-Rahman et al. [110]	Saussurea lappa roots 70% ethanol extract 600 mg/kg, p.o., daily Cotreatment for 2 weeks concurrently with the drug Pretreatment for 1 week and then for 2 weeks concurrently with the drug Male albino rats, 150–160 g	Triamcinolone acetonide 40 mg/kg, i.p., twice a week for 2 weeks Serum: TNF-α, CRP, IL-12, IgG, IgM ↓ Lung: GPx, SOD ↓, MDA ↑ Spleen: GPx, SOD ↓, MDA ↑ Histopathological lesion score: spleen and lung ↑	Cotreatment: Serum: TNF-α and CRP (0), IL-12 and IgG (+), IgM (++) Lung: GPx (+), SOD, MDA (++) Spleen: GPx, SOD, MDA (++) Histopathological lesion: spleen and lung (++) Pretreatment: Serum: TNF-α, IL-12, CRP (0), IgG, IgM (++) Lung: GPx, SOD, MDA (++) Spleen: GPx, SOD (++), MDA (+++) Histopathological lesion: spleen and lung (++)	Serum: TNF-α, CRP, IL-12, ↓, IgG, IgM ↑ Lung: GPx, SOD ↑, MDA ↓ Spleen: GPx, SOD ↑, MDA ↓

↓: a decrease vs. control; ↑: an increase vs. control; (+): a slight beneficial effect; (++): a distinct beneficial effect; (+++): a complete beneficial effect; (0): no beneficial effect.

TABLE 10: The protective effects of plant origin materials in the animal model of arthritis.

Reference	Plant extract, dose, way and time of treatment, and animals	Inducing factor and negative effects	Protective effects of plant material	Effects of plant *per se*
Choudhary et al. [49]	*Spinacia oleracea* leaf ethanol extract 250 or 500 mg/kg/day, for 28 days, p.o. Healthy and pathogen-free female Sprague-Dawley rats, 4–16 weeks, 180-200 g	Osteoarthritis, induced by monosodium iodoacetate, a single injection of 3 mg through the intra-articular joint of the left knee Serum: GST, COMP ↑ Urine: CTX-II ↑ Isolated bone region containing cartilage and sub-chondral bone: relative mRNA expression of IL-1β, TNF-α, COL10, MMP-1, MMP-3, MMP-13 ↑, relative mRNA expression of BMP2, COL2, AGGRECAN, TIMP1, TIMP2 ↓	Serum: COMP (+ 250, ++ 500), GST (++ both doses) Urine: CTX-II (+ 250, ++ 500) Isolated bone region containing cartilage and sub-chondral bone: relative mRNA expression of TNF-α and MMP-13 (+ 250, ++ 500); relative mRNA expression of IL-1β, COL10, MMP-1, MMP-3 (++ both doses); relative mRNA expression of BMP2, COL2 and TIMP1 (0 250, ++ 500), relative mRNA expression of TIMP2 and AGGRECAN (++ both doses)	Not studied
Jeong et al. [48]	*Morus alba* L. leaf water extract 100 mg/kg, p.o., once per day for 3 weeks Male Sprague Dawley rats, 180-240 g, 5-week-old	Osteoarthritis, induced by monosodium iodoacetate, a single injection 3 mg/kg into the right knee joint Serum: IL-1β, IL-6, TNF-α, INF-γ, NO, PGE₂, COMP, CTX-II ↑ Articular cartilage: expression of MMP-13 ↑	Serum: INF-γ (0), IL-1β, IL-6, TNF-α, NO, PGE₂, CTX-II, COMP (++) Articular cartilage: expression of MMP-13 (++)	Articular cartilage: a slight increase in MMP-13 expression
Sundaram et al. [55]	Guggulipid, an ethyl acetate extract rich in lipids from *Commiphora whighitii* gum resin, obtained by extraction of guggulu oleoresin (NKCA pharmacy, Musurum India) 50 or 100 mg/kg/day, for 15 days, p.o. Adult Wistar rats, 10-week-old	Experimental arthritis induced by 100 μL of FCA (Freund's complete adjuvant containing 10 mg/mL heat-killed *Mycobacterium tuberculosis*) injected at the back surface of right hind paw, s.c. Blood: WBC ↑, RBC, HGB, PLT ↓ Serum: expression of MMP-1, MMP-3, MMP-9, MMP-13 ↑ Serum: ALT AST, SOD, CAT and GST ↑ Liver and spleen: ROS, hydroperoxides, LPO, PC, NO₂⁻, GSSG, SOD, CAT, GST ↑, GSH, GPx, GR ↓ Ankle joint homogenate: ACP, ALP ↑	Blood: HGB (0 50, ++ 100), WBC, RBC (++ both doses), PLT (++ 50, +++ 100) Serum: MMP-1 (+ 50, +++ 100), MMP-3 (+ 50, ++ 100), MMP-9 (++ 50, +++ 100), MMP-13 (+++ both doses) Serum: ALT, AST, CAT (++ 50, +++ 100), SOD and GST (+++ both doses) Liver: ROS, hydroperoxides, GPx, CAT (++ both doses), LPO, PC, NO₂⁻, SOD, GSH, GSSG and GR (++ 50, +++ 100) Spleen: ROS, hydroperoxides (++ both doses), LPO, PC, NO₂⁻, GR, GSH, GSSG (++ 50, +++ 100), SOD, CAT, GST (+++ both doses) Ankle joint homogenate: ACP (+ 50, ++ 100), ALP (++ both doses)	Not studied

↓: a decrease vs. control; ↑: an increase vs. control; (+): a slight beneficial effect; (++): a distinct beneficial effect; (+++): a complete beneficial effect; (0): no beneficial effect.

TABLE 11: The protective effects of plant origin materials in the animal model of neurodegenerative disorders.

Reference	Plant extract, dose, way and time of treatment, and animals	Disorder, inducing factor, and negative effects	Protective effects of plant material	Effects of plant per se
Hritcu et al. [32]	Piper nigrum fruits methanolic extract 50 or 100 mg/kg, p.o., daily, for 21 days. Male Wistar rats, 3 month-old, about 250 g	Animal model of Alzheimer's disease 400 pmol Aβ (1–42), i.c.v., 20 days prior to methanolic extract. Amygdala: GPx, GSH ↓, CAT, PC, MDA ↑	The lower dose: Bilateral amygdala: GPx ↑, GSH (0), PC and CAT ↓, MDA (++) The higher dose: MDA, PC, CAT ↓, GSH (++), GPx (+++)	Not studied
Malik et al. [39]	Celastrus paniculatus seed ethanol extract Pretreatment for 6 days 100 or 200 mg/kg, p.o., and then treatment concomitantly with 3-nitropropionic acid. Male Wistar rats, 220–250 g	3-Nitropropionic acid-induced Huntington's disease symptoms, 10 mg/kg, i.p., for 14 days. Body weight ↓ Striatum: MDA, NO_2^- ↑, CAT, SOD, GSH ↓ Cortex: MDA, NO_2^- ↑, CAT, SOD, GSH ↓	Body weight: (++ both doses) Striatum: MDA, NO_2^-, CAT, SOD, GSH (++ both doses) Cortex: MDA, NO_2^-, CAT, SOD, GSH (++ both doses)	Not studied
Chonpathompikunlert et al. [31]	Apium graveolens L., 70% methanolic extract 125, 250, and 375 mg/kg b.w., p.o., for 21 days. Male C57BL/6 mice, 25–30 g	Parkinson's disease induced by 1-methyl-4-phenyl-1,2,3,6-tetrahydropyridine, 15 mg/kg per day, i.p., divided into 4 injections at 2 h intervals on a single day. Cortex: MDA, MAO-A, MAO-B ↑, GPx ↓ Striatum: MDA, MAO-A, MAO-B ↑, GPx ↓	The lowest dose: Cortex and striatum: MAO-A, GPx (0), MDA, MAO-B (++). The middle dose: Cortex: MAO-B MAO-A, GPx (++), MDA (+++) Striatum: MAO-B MAO-A, GPx and MDA (++) The highest dose: Cortex: MDA, MAO-B, MAO-A and GPx (+++) Striatum: MDA ↓, MAO-B, MAO-A, GPx (+++)	Not studied
Wang et al. [38]	Rhizoma drynariae (a commercial product) made from dried roots of Drynaria fortunei water extract 20 mg/kg p.o., daily, for 14 or 28 days. Male Sprague-Dawley rats, about 250 g	Controlled cortical impact (CCI) model of traumatic brain injury Plasma: IL-6 after 1, 3, 7, 14, 21, and 28 days ↑ Brain: microglial activation after 1, 3, 7, and 14 days ↑	Plasma: IL-6 (0 after 3 and 7 days, ++ after 1 day, +++ after 14, 21, and 28 days) Brain: microglial activation (0 after 1 day, ++ after 3, 7, and 14 days)	Not studied
Xu et al. [60]	Rhubarb (three species are assigned as official Rhubarb, i.e., Rheum palmatum L., Rheum tanguticum Maxim. ex Balf., and Rheum officinale Baill), a commercial product, water extract 3, 6, 12 g/kg of Rhubarb p.o., after trauma Male Sprague-Dawley rats, 200-300 g sacrificed 8, 16, or 24 hours after Rhubarb	Controlled cortical impact (CCI) model of traumatic brain injury Brain 8 h after Rhubarb: MDA ↑, SOD, CAT, GSH/GSSG ↓ Brain 16 h after Rhubarb: MDA ↑, SOD, CAT, GSH/GSSG ↓ Brain 24 h after Rhubarb: MDA ↑, SOD, CAT, GSH/GSSG ↓	Brain 8 h after Rhubarb: MDA and CAT (0 3 and 6, ++ 12), SOD (0 3, + 6, ++ 12), GSH/GSSG (+3, ++ 6, +++12) Brain 16 h after Rhubarb: MDA (0 3, ++ 6 and 12), SOD (++3 and 6, +++ 12), CAT (0 3, ++ 6 and 12), GSH/GSSG (0 3, + 6, ++12) Brain 24 h after Rhubarb: MDA (++ 3 and 6, ++ + 12), SOD (+ 3, ++ 6, +++ 12), CAT (0 3, ++ 6 and 12), GSH/GSSG (+ 3, ++ 6, +++ 12)	Not studied

TABLE 11: Continued.

Reference	Plant extract, dose, way and time of treatment, and animals	Disorder, inducing factor, and negative effects	Protective effects of plant material	Effects of plant *per se*
Lin et al. [113]	*Uncaria hirsuta* 95% ethanol and water extracts of stems with hooks 80 mg/kg/day p.o. for 4 or 8 weeks Male BALB/c mice, 8 week-old	D-Galactose-induced neurotoxicity (12 g in 100 mL of normal saline) 0.1 mL per 10 g of weight, s.c. once a day, for 4 or 8 weeks Plasma 4 weeks: MDA ↑ Plasma 8 weeks: MDA ↑ Brain 8 weeks: MDA ↑	Ethanol extract: Plasma MDA: 4 weeks (++), 8 weeks (+++) Brain MDA: 8 weeks: (++) Water extract: Plasma MDA: 4 weeks (++); 8 weeks (+++) Brain MDA: 8 weeks (++)	Not studied
Mohale et al. [111]	*Nerium indicum* flowers ethyl acetate extract 200 and 400 mg/kg, once daily p.o. Male Sprague-Dawley rats, 200–250 g	Anxiety induced by 21-day isolation in dark room Blood: LPO ↑, SOD, CAT, GSH ↓ Brain: LPO ↑, SOD, CAT, GSH ↓	Blood: GSH (+ both doses), SOD (++ both doses), CAT (++ 200, +++ 400), LPO (+++ both doses); Brain: CAT (++) both doses, SOD and GSH (++ 200, +++ 400), LPO (+++ both doses)	Not studied
Wu et al. [112]	*Malva sylvestris* L. leaf and flower 95% methanol extract 250 mg/kg per day, i.g., for 7 days Adult SPF-grade mice	Lipopolysaccharide-induced depression 250 μg/kg i.p., a day before treatment (prior to injection sulindac sulfide 3.75 or 7.5 mg/kg for >3 weeks) Cortex: astrogliosis, IL-1, IL-6, TNF-α ↑, number of survival neurons ↓ Hippocampus: astrogliosis, IL-1, IL-6, TNF-α ↑, number of survival neurons ↓	Cortex: number of survival neurons, astrogliosis, IL-1, IL-6, TNF-α (++) Hippocampus: number of survival neurons, astrogliosis, IL-1, IL-6, TNF-α (++)	Not studied

↓: a decrease vs. control; ↑: an increase vs. control; (+): a slight beneficial effect; (++): a distinct beneficial effect; (+++): a complete beneficial effect; (0): no beneficial effect.

TABLE 12: The protective effects of plant origin materials in the animal model of menopause.

Reference	Plant extract, dose, way and time of treatment, and animals	Inducing factor and negative effects	Protective effects of plant material	Effects of plant *per se*
Leung et al. [115]	*Camellia sinensis* O. Ktze (black tea) extract (QP-lack tea extract, Quality Phytochemicals LLC) 15 mg/kg/day, i.g., for 4 weeks, 3 months after ovariectomy Female Sprague-Dawley rats, 3 months, 200–230 g	Ovariectomy Body weight: ↑ Serum: 17β-estradiol, cGMP ↓, non-HDL-c, HDL-c, TC, TG ↑ Aorta: peNOS ↓, NOX2, NOX4 ↑ Endothelium of aorta: ROS ↑	Body weight: (0) Serum: TG ↓, 17β-estradiol, non-HDL-c (0), HDL-c, TC (++), cGMP (+++) Aorta: peNOS, NOX2, NOX4 (+++) Endothelium of aorta: ROS (+++)	Not studied
Galanis et al. [114]	*Glycyrrhiza glabra* root methanol extract, in the form of drinking water at such a volume so as to obtain the upper threshold of glycyrrhizin (the main active component) of 12.4 mg/kg/rat per day, a day after surgery, for 3 or 6 months Female intact mature Wistar rats, 10 months	Ovariectomy Total tibia bone mineral density: after 3 and 6 months ↓ Proximal tibia bone mineral density: after both 3 and 6 months ↓ Uterine weight: after 6 months ↓	Total tibia bone mineral density: (+++ after 3 months, ++ after 6 months) Proximal tibia bone mineral density: after 3 months (+++), after 6 months (++) Uterine weight: (++)	Not studied
Hamm et al. [116]	*Humulus lupulus* L., hops flavonoid-rich extract (MetaGenics, Aliso Viejo, CA, USA) 400 mg/kg in food, daily, for 11 weeks Female C57BL/6 mice, 7 months	Ovariectomy Uterus weight ↓ Visceral adipose tissue weight ↑ Liver: TG ↑ Ileum: ALP ↑	Uterus weight (0) Visceral adipose tissue weight (+) Liver triglycerides (+++) Ileum: ALP (0)	Uterus weight ↓ Ileum: ALP ↑

↓: a decrease vs. control; ↑: an increase vs. control; (+): a slight beneficial effect; (++): a distinct beneficial effect; (+++): a complete beneficial effect; (0): no beneficial effect.

TABLE 13: The protective effects of plant origin materials in lung disorders.

Reference	Plant extract, dose, way and time of treatment, and animals	Inducing factor and negative effects	Protective effects of plant material	Effects of plant *per se*
Taguchi et al. [118]	Sakuranetin, a flavonoid obtained from methanol extract of aerial portions of *Baccharis retusa* by successive extraction and separation from CH_2Cl_2 phase. Posttreatment -20 mg/kg *via* intranasal instillation on days 0, 7, 14, and 28 (the end of the experiment) C57BL6 male mice, 7-9-week-old, 25 g	Emphysema induced by elastase, 50 μL (6.6 units/mg), an intranasal drop (0.667 IU) BALF: macrophages, lymphocytes, neutrophils, eosinophils, total cells ↑ Lung: NF-κB, M-CSF, IL-1β, MCP-1, TNF-α ↑, expression of TIMP-1, MMP-9, MMP-12 ↑ Lung: collagen and elastic fiber deposition ↑	BALF: eosinophils (-), macrophages, lymphocytes, neutrophils, total cells (++) Lung: MCP-1 (+), M-CSF, IL-1β, TNF-α, NF-κB (+++), expression of TIMP-1 ↑, expression of MMP-9, MMP-12 (++) Lung: collagen and elastic fiber deposition (++)	BALF: eosinophils ↑
Kaveh et al. [117]	*Portulaca oleracea* leaves, 70% ethanol extract 1, 2 and 4 mg/mL in drinking water for 21 days Male Wistar rats, about 220 g	Asthma rats sensitized on days 1, 2, and 3 by 1 mg/kg of ovalbumin (OVA)+100 mg Al(OH)$_3$, i.p., and exposed to 1% OVA aerosol for 20 min on days 6, 9, 12, 15, 18, and 21 Serum: thiol, SOD, CAT ↓, NO$_2^-$, NO$_3^-$, MDA ↑ Blood: lymphocytes ↓, total WBC, eosinophils, neutrophils ↑	Serum: thiol and MDA (0 1, + 2, ++ 4), SOD (0 1, + 2, +++ 4), CAT (0 1, ++ 2 and 4), NO$_2^-$ (++ 1, +++ 2 and 4), NO$_3^-$ (++ all doses) Blood: neutrophils and lymphocytes (0 1, ++ 2, +++ 4), eosinophils (0 1, +++ 2 and 4), total WBC (+++ all doses)	Not studied
Wang et al. [119]	Salvia miltiorrhiza Bge. f. alba root aqueous extract 4.6 or 14 g/kg b.w. daily in the drinking water, 21 days after MCT Male Sprague-Dawley rats, 200-220 g	Pulmonary hypertension animal model caused by monocrotaline (MCT)—a single dose of 60 mg/kg b.w., s.c. Mean pulmonary artery pressure, right ventricular systolic pressure ↑ Plasma: NO, 6-Keto-PGF1α ↓, ET-1 and TXB$_2$ ↑ Lung: TGF-β1 ↑	Mean pulmonary artery pressure and right ventricular systolic pressure (++ both doses) Plasma: 6-Keto-PGF1α and TXB$_2$ (++ both doses), NO, ET-1 (++ 4.6, +++ 14) Lung: TGF-β1 (++ both doses)	Not studied

↓: a decrease vs. control; ↑: an increase vs. control; (+): a slight beneficial effect; (++): a distinct beneficial effect; (+++): a complete beneficial effect; (0): no beneficial effect; (-): intensification of the harmful effect.

TABLE 14: The protective effects of plant origin materials in lipid profile disturbances.

Reference	Plant extract, dose, way and time of treatment, and animals	Inducing factor and negative effects	Protective effects of plant material	Effects of plant per se
de Toledo Espindola et al. [121]	Campomanesia adamantium root aqueous extract 200 mg/kg b.w, p.o., 8 weeks after hyperlipidemia Wistar rats, 140-150 g	Hyperlipidemia induced by high fructose diet for 16 weeks Body weight gain: ↑ Serum: TC, TG ↑	Body weight gain: (++ during the experiment, + in the end) Serum: TC, TG (+++)	Not studied
Veber et al. [34]	Brassica oleracea L. red cabbage aqueous extract 125 or 250 mg/kg, p.o., twice a day, for 3 days Male Wistar rats, 200-300 g	Hyperlipidemia induced by a single administration of Triton WR-1339 400 mg/kg, i.p. Serum: MDA, PC ↑ RBC: SOD ↑, CAT ↓ Liver: MDA, PC, SOD, GPx ↑, CAT ↓ Kidney: MDA, PC, GPx ↑, SOD, CAT ↓ Cerebral cortex: SOD ↓, MDA, PC ↑ Hippocampus: SOD, CAT ↓, GPx, MDA ↑	Serum: MDA (0 both doses), PC (0 125, +++ 250) RBC: CAT (0 125, +++ 250), SOD (+++ both doses) Liver: CAT (0 125, +++ 250), PC (+++ 125, ++ 250), MDA, SOD, GPx (+++ both doses) Kidney: MDA(0 both doses), GPx (0 125, +++ 250), PC, SOD, CAT (+++ both doses) Cerebral cortex: SOD (0 125, +++ 250), PC (++ 125, +++ 250), MDA (+++ both doses) Hippocampus: SOD (0 125, +++ 250),MDA (++ 125, +++ 250), CAT and GPx (+++ both doses)	Not studied
Khlifi et al. [120]	Erica multiflora L. leaf methanolic extract Pretreatment 150 or 250mg/kg, i.g., 1 hour before Triton WR-1339 Male Wistar rats, 150-200 g	Triton WR-1339-induced hyperlipidemia, a single dose 300 mg/kg, i.p. Serum: HDL-c ↓, TC, TG, VLDL-c, LDL-c↑ Plasma: ALT, AST ↑ Liver: SOD, GPx, CAT ↓, MDA ↑ Liver: total DNA damage ↑	Serum: HDL-c (0 150, ++ 250), TG, VLDL-c, LDL-c (++ both doses), TC (++ 150, +++ 250) Plasma: ALT (++ 150, +++ 250), AST (+++ both doses) Liver: SOD (+ 150, ++ 250), MDA (++ both doses), GPx (+ 150, +++ 250), CAT (++ 150, ++ 250) Liver: total DNA damage (++ both doses)	250 mg/kg only studied: Serum: VLDL-c, TG ↑ Liver: SOD ↑
Onyenibe et al. [122]	Monodora myristica fruit aqueous extract 100 or 200mg/kg b.w., p.o., five times a week for 8 weeks Male Wistar albino rats, 120-140 g	Hypercholesterolemia induced by cholesterol, p.o. 40 mg/kg/0.3 mL, five times a week for 8 weeks Serum: HDL-c ↓, LDL-c, TC, TG, AST, ALT ↑ Liver: SOD, CAT, GSH ↓, MDA ↑ Heart: SOD, CAT ↓, MDA ↑	Serum: LDL-c (0 100, + 200), AST, TC (++ both doses), TG, ALT (+++ both doses), HDL-c (↑ both doses) Liver: MDA (++ both doses), SOD, CAT, GSH (+++) both doses Heart: MDA (++ 100, +++ 200), SOD (+++) both doses, CAT (↑ both doses)	Not studied

↓: a decrease vs. control; ↑: an increase vs. control; (+): a slight beneficial effect; (++): a distinct beneficial effect; (+++): a complete beneficial effect; (0): no beneficial effect.

TABLE 15: The protective effects of plant origin materials in an ischaemia/reperfusion model.

Reference	Plant extract, dose, way and time of treatment, and animals	Inducing factor and negative effects	Protective effects of plant material	Effects of plant *per se*
Caskurlu et al. [124]	*Nigella Sativa* seeds oil Pretreatment, a single dose of 400 mg/kg p.o., 3 days before reperfusion Male Sprague-Dawley rats, 250-300 g, 10-12 weeks	Renal reperfusion injury 45 min occlusion of the bilateral renal pedicles + reperfusion (24 h) Kidney: tubulointerstitial damage ↑, glomerular injury score ↑, GPx, CAT ↓, MDA ↑	Kidney: tubulointerstitial damage (++), glomerular injury score (++), GPx, CAT, MDA (++)	Not studied
Sravanthi and Rao [126]	*Pentapetes phoenicea* methanolic extract Pretreatment, for 10 days 100, 200 or 400 mg/kg/day Male Wistar rats, 300–350 g	Global cerebral ischemia induced by temporary bilateral carotid artery occlusion (30 min) and subsequent 4 h reperfusion Brain: weight, water and protein content, infarct volume and LPO ↑, SOD, CAT, GSH, GPx, GR, GST ↓	Brain: weight, water and protein content, infarct volume, MDA, SOD, CAT, GSH, GPx, GR, GST (++ all doses) The greater the dose the better the effect	Not studied
Cakir et al. [123]	*Hypericum perforatum* 80% ethanol extract 50 mg/kg, i.p., at the beginning of ischemia Male Sprague-Dawley rats, 300–350 g	Right nephrectomy and subsequent ischaemia (45 min)/reperfusion (3 h) of the left kidney Serum: BUN and creatinine ↑ Kidney: CAT, SOD, GPx ↓, MDA ↑ Kidney: hydropic changes, tubular dilation, tubular desquamation congestion ↑	Serum: BUN and creatinine (-) Kidney: CAT, SOD, GPx and MDA (+++) Kidney: tubular desquamation congestion, hydropic changes, tubular dilation (++)	Not studied
Godinho et al. [125]	*Trichilia catigua* ethyl-acetate fraction of acetone-water (7:3) extract 200 mg/kg, 0.5 h before and 1 h after surgery (total dose 400 mg/kg), p.o. Male Wistar rats, 3-month-old	Cerebral ischaemia-reperfusion 4-VO model of transient global cerebral ischaemia, 15 min ischaemia Brain: GSH, GSH/GSSG, CAT, SOD ↓, GSSG, PCG, MDA ↑	Brain: CAT (0), GSH, GSSG, GSH/GSSG, SOD, PCG, MDA (+++)	Not studied

↓: a decrease vs. control; ↑: an increase vs. control; (++): a distinct beneficial effect; (+++): a complete beneficial effect; (0): no beneficial effect; (-): intensification of the harmful effect.

TABLE 16: The protective effects of plant origin materials in animal models of diabetes.

Reference	Plant extract, dose, way and time of treatment, and animals	Inducing factor and negative effects	Protective effects of plant material	Effects of plant per se
Ben Salem et al. [128]	Cynara scolymus leaves 75% ethanol extract 200 or 400 mg/kg b.w. daily, p.o., for 28 days Male Wistar rats, 10-12-week-old, 160-200 g	Alloxan monohydrate-induced diabetes, a single dose 150 mg/kg b.w., i.p. Body weight gain: ↓ Blood glucose: ↑ Serum: α-amylase, pancreatic lipase, ALT, AST, ALP, urea, CR ↑ Plasma: TG, TC, LDL-c ↑, HDL-c ↓ Blood: RBC, WBC, HGB, PLT ↓ Liver: SOD, CAT, GSH ↓, MDA, AOPP ↑ Pancreas: SOD, CAT, GSH ↓, MDA, AOPP ↑ Kidney: SOD, CAT, GSH ↓, MDA, AOPP ↑	Body weight gain: (+++ both doses) Blood glucose: (+++ 200, ++ 400) Serum: ALP (++ both doses), urea (++ 200, +++ 400), CR (+++ 200, ++ 400), ALT, AST, α-amylase, pancreatic lipase (+++ both doses) Plasma: TG, TC, LDL-c, HDL-c (+++ both doses) Blood: WBC (0 200, ++ 400), PLT (++ both doses), RBC and HGB (+++ both doses) Liver: MDA, SOD, CAT, AOPP (+++ both doses), GSH (+++ 200, ↑ 400) Pancreas: SOD (++ both doses), MDA, CAT (+++ 200, ++ 400), GSH, AOPP (+++ both doses) Kidney: SOD (+ 200, ++ 400), CAT (+++ 200, ++ 400), GSH, MDA, AOPP (+++ both doses)	Not studied
Dra et al. [127]	Caralluma europaea aerial part extract obtained by successive extraction with dichloromethane and methanol 250 or 500 mg/kg b.w, p.o., a single dose, followed for 10h Swiss albino mice, 8 weeks	Alloxan monohydrate-induced diabetes type 1, a single dose of 200 mg/kg b.w., i.p. Blood: glucose ↑ Islets diameter: ↓	The lower dose: Blood glucose: after 2, 4, and 6 h (++), after8 h (+++) and after 10 h (↓); islet diameter (++) The higher dose: Blood glucose: after 2 (++), after 4 and 6 h (+++), after 8 and 10h (↓)	Not studied
Silva et al. [59]	Musa × paradisiaca L. green banana pasta Commercial feed containing 25, 50, or 75% of green banana pasta, for 12 weeks Male Wistar rats, 6-8 weeks old, 180-300 g	Alloxan-induced diabetes, type 1, i.p., a single dose of 150 mg/kg Serum: glucose, ALT, AST, TC, TG, fructosamine ↑ Liver: total lipids, LPO and PC ↑ Kidney: PC ↑	Serum: AST (0 all doses), glucose, fructosamine (+ 25 and 50, +++ 75), TC (0 25, +++ 50, 0 75), ALT (0 25, +++ 50 and 75), TG (+++ all doses) Liver: total lipids (+ 25 and 50, +++ 75), LPO (0 25, +++ 50, ↓75), PC (0 25, ++ 50, +++ 75) Kidney: PC (0 25, +++ 50, ↓75)	Not studied
Du et al. [66]	Polysaccharide separated from Lycium barbarum 100, 250, or 500 mg/kg, p.o., for 4 weeks Male Sprague Dawley rats 8 weeks old, 180-220 g	High-fat diet for 8 weeks and then diabetes induced by streptozotocin injection, 30 mg/kg for a week Fasting blood glucose: ↑ Serum: insulin, SOD, GPx ↓, BUN, IL-2, IL-6, TNF-α, INF-α, MCP-1, ICAM-1 ↑ Urine: ALB ↑	Fasting blood glucose: (+ 100, ++ 250, and 500) Serum: INF-α (0 100 and 250, ++ 500), insulin, IL-2, ICAM-1 (0 100, + 250, ++ 500), SOD, TNF-α, BUN (0 100, + 250, +++ 500), GPx, IL-6 (0 100, +++ 250 and 500), MCP-1 (+ 250, +++ 250 and 500) Urine: ALB (+ 250, ++ 250 and 500)	Not studied
Wattanathorn et al. [42]	The combination of 50% hydroalcoholic extracts of Mangifera indica L. seeds and Polygonum odoratum L. aerial parts prepared at a ratio 1:5 2, 10, or 50 mg/kg b.w, daily, for 10 weeks Male Wistar rats, 180-220 g	Diabetes cataract and retinopathy induced by a single injection of streptozotocin 55 mg/kg b.w. Blood glucose after 5 and 10 weeks ↑ Grade of cataract severity ↓ Total retinal thickness ↓ Lens: SOD, CAT, GPx ↓, MDA, VEGF, ERK1/2, p38MAPK, AR ↑ Lens: opacity index ↑	Blood glucose after 5 weeks: (+ 2 and 50, ++ 10) Blood glucose after 10 weeks: (+ 2, 0 10, - 50) Total retinal thickness: (++ 2 and 10, 0 50) Grade of cataract severity: (++ all doses) Lens: SOD (++ 2, + 10, - 50), MDA (++ 2 and 10, 0 50), GPx (+ 2 and 50, ++ 10), CAT, AR, ERK1/2, p38MAPK (++ all doses), VEGF (+ 2, ++ 10, +++ 50) Lens: opacity index (++ all doses)	Not studied

TABLE 16: Continued.

Reference	Plant extract, dose, way and time of treatment, and animals	Inducing factor and negative effects	Protective effects of plant material	Effects of plant per se
Balbaa et al. [57]	Nigella sativa seed oil 2.0 mL/kg b.w., i.g., for 21 days after diabetes development Male Wistar rats, about 125 g	Type 2 diabetes induced by a high-fat diet for 2 weeks, followed by a single injection of streptozotocin 35 mg/kg, i.p. Serum: TNF-α, IL-6, AGE ↑ Brain: TBARS, XO, NO, TNF-α, IL-6, IL-1β, iNOS, AGE, AChE, Aβ-42, IDE ↑, GSH, GPx, GST, SOD, glucose ↓	Serum: TNF-α, IL-6 (+++), AGE ↓ Brain: AChE (↓), TBARS, XO, IL-6, IL-1β (++), NO, TNF-α, iNOS, GSH, GST, SOD, AGE, Aβ-42, IDE, glucose (+++), GPx (↑)	Serum: IL-6 and AGE ↓ Brain: AChE and Aβ-42 ↓, TBARS, NO, IDE, GPx, GST, SOD ↑
Fajri et al. [131]	Equisetum arvense aerial parts, methanolic extract 250 or 500 mg/kg b.w., daily p.o., for 45 days after diabetes inducing Male mice, 6-8 weeks	Streptozotocin-induced diabetes, 50 mg/kg b.w. i.p., for 5 days Sperm: viability, motility ↓, percentage of morphological abnormalities, DNA damage and nuclear immaturity ↑	The lower dose: viability, percentage of morphological abnormalities and DNA damage (++), motility and percentage of nuclear immaturity (+++) The higher dose: viability, motility (++), percentage of morphological abnormalities, DNA damage and nuclear immaturity (+++)	Not studied
Khanra et al. [129]	Abroma augusta L. leaf methanol extract 100 or 200 mg/kg, p.o., daily for 4 weeks Male Wistar rats, 2–3-month-old, about 180 g	Type 2 diabetes induced by a single injection of streptozotocin 65 mg/kg i.p, 15 min later nicotinamide 110 mg/kg, i. p. Fasting blood glucose: ↑ Serum: HDL-c, insulin ↓, TC, TG, HbA1c, ALT, AST, urea, LDH, CK, CRP ↑ Kidney: DNA fragmentation, ROS, TBARS, PC, IL-1β, IL-6, TNF-α, ↑, total coenzymes Q9 and Q10, GSH, CAT, SOD, GST, GPx, GR, G6PD, ATP, Bcl-2/Bax ↓ Kidney: expression of NF-κB, PKC (α, β, δ, ε), caspase 3, caspase 9 ↑ Heart: ROS, TBARS, PC, IL-1β, IL-6, TNF-α, GPx, GR, DNA fragmentation ↑, total coenzymes Q9 and Q10, GSH, CAT, SOD, GST, G6PD, ATP, Bcl-2/Bax ↓ Heart: expression of NF-κB, caspase 3, caspase 9, PKC (α, β, δ, ε) ↑	Fasting blood glucose: (++ both doses) Serum: TC, TG, HbA1c, ALT, AST, urea, LDH, CK, CRP, insulin (++ both doses), HDL-c (++ 100, +++ 200) Kidney: ROS, TBARS, PC, total coenzyme Q9, SOD, IL-1β, IL-6, TNF-α, DNA fragmentation, ATP and Bcl-2/Bax (++ both doses), total coenzyme Q10, GSH, GST, GPx, GR, G6PD (++ 100, +++ 200), CAT (+++ both doses) Kidney: expression of NF-κB, PKC (α, β, δ, ε), caspase 3, caspase 9 (++ both doses) Heart: ROS, TBARS, PC, GSH, CAT, SOD, IL-1β, IL-6, TNF-α, ATP, Bcl-2/Bax, DNA fragmentation (++ both doses), GST, G6PD (++ 100, +++ 200), total coenzymes Q9 and Q10 (+++ both doses), GPx, GR (↑ both doses) Heart: expression of PKC (α, β, δ, ε), caspase 3, caspase 9 (++ both doses), NF-κB (+++ both doses)	Not studied
Omodanisi et al. [130]	Moringa oleifera leaf extract obtained by successive extraction with n-hexane and 80% methanol, 250 mg/kg b.w., p.o., for 6 weeks Male Wistar rats, 10 weeks	Streptozotocin-induced diabetes, a single dose of 55 mg/kg, i.p. Plasma: glucose ↑ Serum: TP, ALB ↓ Kidney: weight and relative weight ↑ Kidney: GPx, SOD slightly ↓, CAT ↓, TNF-α slightly↑, MDA, IL-6 ↑	Plasma: glucose (++) Serum: ALB (+), TP (+++) Kidney: weight and relative weight (++) Kidney: GPx (-), CAT (0), TNF-α, IL-6 (+), SOD (++), MDA (+++)	Plasma: glucose ↓ Serum: TP, ALB ↑ Kidney: SOD ↑, GPx, IL-6, TNF-α ↓

↓: a decrease vs. control; ↑: an increase vs. control; (+): a slight beneficial effect; (++): a distinct beneficial effect; (+++): a complete beneficial effect; (0): no beneficial effect; (-): intensification of the harmful effect.

the protective effect of plant preparations which involved improvement of oxidative balance by activation of the Nrf2/HO-1 antioxidant pathway [61] and the ameliorating effect on lipid status [132, 133]. The latter was also confirmed *in vitro* as the lipolysis-promoting influence in 3T3-L1 cells was observed [61]. In mice fed a high-fat diet, coadministration of *Euterpe oleracea* extract reversed the changes of lipogenic proteins expression in the liver. Additionally, the investigated preparation increased hepatic expression of ABCG5 and ABCG8 transporters responsible for removing excess of cholesterol by secretion into bile [43].

The detailed results of the performed studies are collected in Table 17.

2.10.9. The Protective Influence of Plant Preparations against Gastric Ulcer-Inducing Factors. The gastric ulcers are regarded as the most common disease of gastrointestinal tract, but they can be caused by many various factors. Therapy of different disorders with using nonsteroidal anti-inflammatory drugs like indomethacin and excessive consumption of alcohol belong to important ones [45, 134]. As pharmaceutical agents are not fully effective and their application may also be connected with development of side effects, an alternative ways of treatment became the subject of research. Plant origin substances showed a wide range of beneficial effects, including alleviated or reversed oxidative stress which was found to be involved into gastric ulcer etiology as well as mechanism of indomethacin toxicity [135–137].

The detailed results of the performed studies are presented in Table 18.

2.10.10. The Protective Effects of Plant Origin Materials in Animal Model of Different Disorders. The symptoms of many other various disturbances were affected in a positive way by using plant materials of experimentally confirmed antioxidant properties and containing acknowledged antioxidants like phenolic acids and flavonoids [36, 41, 138]. A wide range of diseases: lithiasis, thyroid disorders, retinal degeneration, irritable bowel syndrome, hyperthyroidism, periodontitis, and mammary gland hyperplasia, were studied, pointing to great possibilities "hidden" in plant origin agents.

The details of the performed studies are presented in Table 19.

2.11. The Protective Effects of Plant Origin Materials against Radiation. Plant extracts also showed some efficacy against radiation-induced damage. The research revealed the involvement of JAK-STAT pathway into the mechanism of the protective influence on the hematopoietic system [70]. Animal studies also showed the reversing effect of plant material on the disturbances of antioxidant defence caused by γ-radiation in blood and organs [145, 146]. One of the recent *in vitro* investigations, performed on keratinocyte cells, confirmed the antioxidant action of a plant preparation against UVB radiation, which could contribute to development of new skin protective strategies [147].

The details of the performed studies are presented in Table 20.

3. The Comparison of Plant Preparations with Standard Drugs and Supplements: The Dependence of Effects on Treatment Way and Doses

The effects of plant origin materials were often investigated in comparison with those shown by standard drugs. The results clearly show that there may be a possibility to replace different medicines with plant preparations which do not cause so many severe side effects, but the detailed research must be performed before the final conclusions can be made.

The question of advantage of plant origin extracts over any standard drug is complicated, and a univocal answer is very difficult as in some cases the differences in the influence of the compared agents were strongly dependent on the applied dose [45, 135] and studied parameters [115, 129].

Hamm et al. [116] found that hops (*Humulus lupus* L.) flavonoid-rich extract protected against ovariectomy-induced visceral adiposity and increase in liver triglycerides observed in 7-month-old retired breeder C57BL/6 mice. However, particularly in case of the former parameter, the observed effect was not so distinct as that noted in animals receiving 17-β-estradiol. Additionally, hops extract could not prevent the loss of uterus weight caused by the surgery while estrogen showed quite a considerable reversing effect.

Leung et al. compared the effect of black tea extract with that exerted by estrogen in ovariectomized rats. The results were characterized by a considerable diversity. In case of body weight reduction, estradiol's benefit influence was much better. In contrast, aortic cGMP and serum TC and peNOS, NOX2, NOX4, and ROS generation in the aorta were affected in similar or even entirely the same way by both agents. Additionally, in case of serum TG the plant materials proved to possess much better ability to restore the values observed in sham-operated control animals [115].

3.1. The Comparison of Crude Extracts and the Particular Substances Separated from Plant Materials. The plant extract can show better properties than particular compounds administered alone as there may occur some synergistic effects among its components. Such an assumption could be supported by the results reported by He et al. [148] who compared the influence of *Paeonia suffruticosa* seed extract and 10 compounds (oligostilbenes) isolated from it with using an *in vitro* IL-1β-induced osteoarthritis model. In the study performed on rabbit chondrocytes, IL-1β caused a significant decrease in viability and 10 studied components used alone showed an improving effect, but the intensity of this effect was markedly different, depending on the structure. However, the application of the extract containing all the oligostilbenes showed the best effect, comparable with that observed for diacerein—a drug of IL-1β-inhibition action, used in osteoarthritis therapy. Such results made the authors suggest the possibility of synergism among the particular oligostilbenes.

3.2. Plant Preparations as Lipid Profile Regulating Agents – The Comparison with Standard Drugs. Plan preparations were studied in regard to the possibility of their application

TABLE 17: The protective effects of plant origin materials in animal models of obesity.

Reference	Plant extract, dose, way and time of treatment, and animals	Inducing factor and negative effects	Protective effects of plant material	Effects of plant *per se*
de Oliveira et al. [43]	Euterpe oleracea Mart. (açaí) seed hydroalcoholic extract 300 mg/kg/d, i.g., for 12 weeks Male mice C57BL/6, 4 weeks	Diet-induced obesity 60% fat diet for 12 weeks Epididymal and retroperitoneal fat mass ↑ Body weight gain↑ Liver/body weight↑ Glikaemia: ↑ Plasma: adiponectin ↓, leptin ↑ Serum: TC, TG, LDL, VLDL ↑ Liver: SOD, CAT, GPx ↓, cholesterol, TG, MDA, PC ↑ Liver expression of lipogenic proteins: pAMPK, pACC/ACC ↓, SREBP-1c, HMG-CoA-R ↑	Epididymal and retroperitoneal fat mass (++) Body weight gain (++) Liver/body weight: (+++) Glikaemia: (++) Plasma: leptin, adiponectin (+++) Serum: TC, TG, LDL, VLDL (++) Liver: cholesterol, TG (++), SOD, CAT, GPx, PC (+++), MDA (↓), CAT (↑) Liver expression of lipogenic proteins: pAMPK, SREBP-1c, HMG-CoA-R, pACC/ACC (+++)	Liver: TG ↓, SOD ↑
Budriesi et al. [133]	Castanea sativa Mill bark extract (ENC®, SilvaTeam S.p.a., San Michele Mondovì, Italy) 20 mg/kg, p.o., for 21 days Male Sprague-Dawley rats, 9-week-old, 270-300 g	High-fat diet for 10 weeks and then during extract administration Body weight gain: ↑ Serum: TC, LDL-c, TG ↑, HDL-c ↓ Plasma: IL-1α, IL-1β, IL-2, IL-5, IL-6, IL-7, IL-12p70, IL-17A, IL-18, TNF-α ↑, IL-4, IL-10, IL-13 ↓ Liver: SOD, GSSG-red, UDPGT ↓ Ileum: MDA ↑ Colon: MDA ↑	Body weight gain: (++) Serum: TG (++), TC, LDL-c, HDL-c (+++) Plasma: IL-1β (-), IL-5, IL-18 (0), IL-7, TNF-α (+), IL-1α, IL-2, IL-6, IL-12pro70, IL-4, IL-10 (++), IL-17A, IL-13 (+++) Liver: UDPGT (++), SOD, GSSG-red (↑) Ileum: MDA (++) Colon: MDA (++)	Liver: SOD ↑ Ileum: MDA ↑
El Ayed et al. [132]	10% ethanol extract of Vitis vinifera grape seed (50%) and skin (50%) 500 mg/kg b.w., i.p., daily for 6 weeks Male Wistar rats, 210-230 g	High-fat diet (40% fat, 45% carbohydrate, 15% protein) for 6 weeks Body and lung weight: ↑ Lung lipid content: ↑ Plasma: adiponectin, HDL-c ↓, CRP, TG, TC, VLDL-c, LDL-c/HDL-c, LDL-c ↑ Lung: CAT, SOD, Zn, Mg ↓, MDA, lipase, Ca, Fe ↑	Body and lung weight: (+++) Lung lipid content: (+++) Plasma: CRP and adiponectin (++), TG, TC, VLDL-c, LDL-c, LDL-c/HDL-c, HDL-c (+++) Lung: MDA (++), CAT, SOD, lipase, Mg, Zn, Ca, Fe (+++)	Plasma: TG, TC, VLDL-c, LDL-c, HDL-c, LDL-c/HDL-c ↓ Lung: Zn ↑, MDA, Mg ↓
Qiu et al. [61]	Hedansanqi Tiaozhi Tang (a Chinese herbal prescription) contains four traditional Chinese herbal medicines: Panax notoginseng dry root, Salvia miltiorrhiza Bunge dry root, Crataegus pinnatifida Bge. fruit, Nelumbo nucifera Gaertn leaf 350, 700, 1400 mg/kg/day, i.g., once a day, for 4 weeks Male Sprague-Dawley rats, 180-190 g	Hyperlipidaemia induced by high-fat diet (2% cholesterol, 10% lard, 10% egg yolk, 0.5% bile sodium, 77.5% standard diet (w/w), for 4 weeks Body weight ↑ Serum: TC, TG, LDL-c, AST, ALT, MDA ↑, HDL-c, SOD, CAT, GPx, T-AOC↓ Liver: T-AOC, SOD, CAT and GPx ↓, TC, TG, MDA ↑ Liver: steatosis, lobular inflammation, hepatocellular ballooning ↑	Body weight: (+ 350, ++ 700 and 1400) Serum: LDL-c, TC, (+ 350, ++ 700 and 1400), CAT (+ 350, +++ 700 and 1400), TG, GPx (++ 350 and 700, +++ 1400), T-AOC, MDA, SOD (++ 350, +++ 700 and 1400), HDL-c, ALT, AST, (+++ all doses) Liver: MDA (+ 350, ++ 700 and 1400), TC, TG, GPx (++ 350 and 700, +++ 1400), T-AOC, CAT (++ 350, +++ 700 and 1400), SOD (+++ all doses) Liver: steatosis (+ all doses), lobular inflammation (++ all doses), hepatocellular ballooning (++ 350 and 700, +++ 1400)	4200 mg/kg studied: none

TABLE 17: Continued.

Reference	Plant extract, dose, way and time of treatment, and animals	Inducing factor and negative effects	Protective effects of plant material	Effects of plant *per se*
Sheng et al. [33]	*Morus alba* var. *multicaulis (Perrott.) Loud.* (mulberry) leaves 20% mulberry leaf powder addition to high fat diet, 13 weeks Male C57BL/6J mice, 4-week-old, 15-20 g	Obesity caused by high fat diet (60% calories from fat), provided before (around 8 weeks) and during mulberry administration Body weight, fat mass ↑ BAT: body weight ratio ↓ Fasting blood glucose and plasma insulin ↑ HOMA-IR ↑ Serum: AST, CR↑	Body weight: (++ beginning from 6th week of treatment) Fat mass and BAT: body weight ratio (++), fasting blood glucose and plasma insulin (++), HOMA-IR (+++) Serum: AST, CR (+++)	Not studied

↓: a decrease vs. control; ↑: an increase vs. control; (+): a slight beneficial effect; (++): a distinct beneficial effect; (+++): a complete beneficial effect; (0): no beneficial effect; (-): intensification of the harmful effect.

TABLE 18: The protective effects of plant origin materials in animal models of gastric ulcers.

Reference	Plant preparation, dose, way, time of treatment, and animals	Inducing factor and negative effects	Protective effects of plant preparation	Effects of plant per se
Rtibi et al. [135]	*Ceratonia siliqua* L. pod aqueous extract Pretreatment, 500, 1000, and 2000 mg/kg. b.w., p.o., during 15 days Male Wistar rats, 220–250 g	Ethanol 4 g/kg, b.w., p.o., one dose Ulcer index ↑ Ulcer mucus volume ↓ Stomach mucosa: MDA, H_2O_2 ↑, -SH groups, SOD, CAT, GPx ↓	Ulcer index: (++ all doses, a decrease along with an increased dose) Ulcer mucus volume: (++ 500 and 1000, +++ 2000) Stomach mucosa: SOD, CAT (++ 500 and 1000, +++ 2000); MDA (++ 500 and 1000, +++ 2000); H_2O_2 -SH groups, GPx (0 500, ++ 1000, +++ 2000)	Not studied
Chanda et al. [45]	*Paederia foetida* L. leaf methanol extract 100, 200 mg/kg b.w./day, for 4 days Wistar rats, 150-180 g	Indomethacin-pylorus ligation induced ulcer Indomethacin 25 mg/kg, s.c., once daily for 4 days + surgical procedure on the 4th day Gastric secretion: volume, acid output ↑, pH ↓ Ulcer index: ↑	Gastric secretion: volume and acid output (++ both doses), pH (++ 100, +++ 200) Ulcer index: (++ both doses)	Not studied
Sabiu et al. [136]	*Spondias mombin* and *Ficus exasperata* leaf aqueous extracts Pretreatment 100 or 200 mg/kg b.w., p.o., for 21 days Wistar rats, about 180 g	Indomethacin-induced gastric ulceration, a single dose of 30 mg/kg b.w., p.o. Ulcer index: ↑ Gastric secretion: acid output ↑, pH ↓ Stomach: MDA ↑, SOD ↓ Gastric juice: pepsin activity ↑, mucin content ↓	Ulcer index: (++ both doses of both extracts) % ulcer inhibition: (++ both doses of both extracts) Gastric secretion: acid output and pH (++ both doses of both extracts) *Ficus exasperata* Stomach: MDA, SOD (++ both doses) Gastric juice: pepsin, mucin (++ both doses) *Spondias mombin* Stomach: MDA, SOD (++ both doses) Gastric juice: pepsin, mucin (++ both doses) The higher doses showed better beneficial effects	200 mg/kg b.w. only studied, slight effects Gastric secretion: acid output ↑, pH ↓ Gastric juice: mucin content ↓
Sattar et al. [137]	*Myristica fragrans* seeds 70% ethanol extract 200 mg/kg, an hour before ethanol, once a day for 15 days Wistar rats, 150-300 g	90% ethanol-induced gastric ulcers 5 mL/kg for 15 days, once a day Gastric contents: pH ↓, total acidity ↑; average number of ulcers per animal ↑ Ulcer index: ↑	Gastric contents: pH ↑, total acidity (++) Average number of ulcers per animal (++) Ulcer index: (++) % ulcer inhibition: (++)	Not studied
Raeesi et al. [134]	*Biebersteinia multifida* root 70% methanol extract Pretreatment 150 or 300 mg/kg, p.o., 1 h before ulcer induction Male Wistar rats, 200-250 g	75% ethanol-induced gastric ulcer 4 mL/kg, p.o. Ulcer area/stomach ↑; Number of ulcers/stomach ↑; Gastric mucosa: T-AOC ↓	Ulcer area/stomach: (+++ both doses) Number of ulcers/stomach: (++ both doses) Gastric mucosa: T-AOC (↑ both doses)	Not studied

↓: a decrease vs. control; ↑: an increase vs. control; (++): a distinct beneficial effect; (+++): a complete beneficial effect.

TABLE 19: The protective effects of plant origin materials in animal models of various diseases.

Reference	Plant extract, dose, way and time of treatment, and animals	Disorder, inducing factor, and negative effects	Protective effects of plant material	Effects of plant per se
Benhelima et al. [139]	Nigella sativa L. seeds essential oil, 5 mL/kg b.w. from 1st to 28th or from 15th to 28th days, p.o. Male Wistar rats, 120-130 g	Lithiasis induced by 0.75% ethylene glycol (EG) and 1.0% ammonium chloride in drinking water for 28 days, first 3 days both, then only EG, for 25 days. Body weight: ↓ Urine: Mg, Ca ↓, oxalate, UA, phosphate ↑ Serum: CR, UA, BUN ↑ Kidney: oxalate, Ca, phosphate ↑	From 1st to 28th. Body weight: (++). Urine: Ca, Mg, oxalate, UA, phosphate (++). Serum: CR, UA, BUN (++). Kidney: oxalate, Ca, phosphate (++). From 15th to 28th. Body weight: (++). Urine: Ca, Mg, oxalate, UA, phosphate (++). Serum: CR (+), UA, BUN (++). Kidney: oxalate, Ca, phosphate (++). The latter treatment showed worse effects	Not studied
Chang et al. [140]	Lycium barbarum fruit water extracts. Blended: particles 3.58 ± 3.8 µm. Submicron: particles 100 ± 70nm. Dietary pretreatment: 250 mg/kg for 54 days, p.o. Male Sprague-Dawley rats, 8-10 week, 200-300 g	Retinal degeneration induced by white cool light, the intensity 1,400–1,500 lux for 2 days, 12 h light/12 h dark cycle. Retinal thickness: ↓ Retina: GSSG+GSH ↓, MDA↑	Submicron extract: retinal thickness (++). Retina: GSSG+GSH ↑, MDA (+++). Blended extract: retinal thickness (+). Retina: GSSG+GSH (++), MDA (+++)	Not studied
Cojocariu et al. [141]	Chrysanthellum americanum polyphenolic (butanol) fraction of 80% ethanolic extract 100 mg/kg b.w., i.g., 2 days during and 4 days after stress paradigm. Female Wistar rats about 200 g	Irritable bowel syndrome animal model induced by multifactorial stress exposure paradigm for 7 days. Temporal lobe: SOD and GPx ↓, MDA ↑	Temporal lobe: SOD and GPx, MDA (++)	None
Sdayria et al. [41]	Euphorbia retusa leaf methanol extract. Pretreatment 200 mg/kg, p.o. Swiss albino mice, 20–30 g	Inflammation, induced by 1% carrageenan (in 0.9%NaCl) injection of 100 µL into the subplantar region of the right hind paw. Hind paw: MDA↑, SOD, CAT, GPx ↓ Liver: SOD, CAT, GPx ↓	Hind paw: MDA, CAT, GPx, SOD (++). Liver: SOD, CAT, GPx (++)	Not studied
Hatipoğlu et al. [142]	Crataegus orientalis M Bieber. fruit 70% ethanol extract 100 mg/kg/day, orogastrically, at placement of the ligature, for 11 days. Male Wistar rats, aged 4 months, about 340 g	Periodontitis caused by submerging a 4/0 silk ligature in the sulcus of the mandibular right first molars of rats, kept subgingivally for a period of 11 days. Serum: TOS, OSI ↑, TAS ↓ Interdental area between first and second molars: inflammatory cells, osteoclasts, osteoblasts ↑	Serum: TOS, OSI, TAS (+++). Interdental area between first and second molars: osteoblasts (0), inflammatory cells and osteoclasts (++)	Not studied

TABLE 19: Continued.

Reference	Plant extract, dose, way and time of treatment, and animals	Disorder, inducing factor, and negative effects	Protective effects of plant material	Effects of plant *per se*
Konda et al. [138]	*Azima tetracantha* root 95% ethanol extract Pretreatment 250 or 500 mg/kg, p.o., 60 min prior to glycerol Male Wistar albino rats, 150-250 g	Acute renal failure caused by hypertonic glycerol, a single dose of 8 mL/kg, i.m., into both hind limbs Serum: CR, BUN ↑, TP, ALB ↓ Urine output: ↓ Kidney: SOD, GSH, GR, GPx, CAT ↓	The lower dose: Serum: TP, CR, BUN, ALB (++) Urine output: (++) Kidney: GPx (0), CAT (+), SOD, GR (++), GSH (+++) The higher dose: Serum: TP, ALB (++), BUN, CR, (+++) Urine output: (+++) Kidney: SOD, GSH, GR, GPx, CAT (+++)	Only 500 mg/kg studied Urinary output: ↑ Kidney: SOD ↓
Panth et al. [36]	*Salicornia europaea* water extract 1400 mg/kg/day p.o., for 6 weeks Male rats: spontaneous hypertensive (SHR) rats and Sprague-Dawley, 6 weeks, about 200 g	Vascular dysfunction and hypertension, NaCl-induced, 800 mg/kg/day, p.o. for 6 weeks SD rats: systolic and diastolic pressure ↑ SHR rats: systolic and diastolic pressure ↑	SD rats: systolic pressure (+++), diastolic pressure (++) SHR rats: systolic pressure (++), diastolic pressure (+)	Not studied
El-Kashlan et al. [143]	*Phoenix dactylifera* L. date palm pollen (commercial product) 80% ethanol extract 150 mg/kg, p.o., every day for 56 days Male Wistar rats, about 250 g	L-thyroxine-induced hyperthyroidism 300 µg/kg, i.p., every day for 56 days Weight: final body, testes, epididymis, prostate gland, seminal vesicle↓ Serum: fT3, fT4, E2 ↑, LH, FSH, T, TSH ↓ Testis: SDH, LDH, ALP, ACP, G6PD, CAT, SOD, GPx, GR, GSH ↓, MDA, NO, AST, ALT ↑ 6-N-propyl-2-thiouracil-induced hypothyroidism 10 mg/kg, i.p., every day for 56 days Weight: final body, testes, epididymis, prostate gland, seminal vesicle↓ Serum: fT3, fT4, LH, FSH, T ↓, E2, TSH ↑ Testis: SDH, LDH, ALP, ACP, G6PD, CAT, SOD, GPx, GR, GSH ↓, MDA, NO, AST, ALT ↑	Hyperthyroidism Weight: final body, testes, epididymis, prostate gland, seminal vesicle (++) Serum: fT3, TSH, E2 (++), fT4, LH, FSH, T (+++) Testis: ALP (++), SDH, LDH, ACP, G6PD, GR, GSH, MDA, NO, AST, ALT, GPx (+++), CAT, SOD ↑ Hypothyroidism Weight: final body, testes (0), epididymis, prostate gland, seminal vesicle (++) Serum: TSH, fT3, fT4 (0), E2 (++), LH, FSH, T (+++) Testis: ALP, NO (++), SDH, LDH, ACP, G6PD, GR, GSH, MDA, AST, ALT (+++), GPx, CAT, SOD ↑	Weight: prostate gland, epididymis, seminal vesicle ↑ Serum: fT3, fT4 ↓, LH, T, E2 ↑ Testis: SDH, LDH, GR, CAT, SOD, GPx, GSH ↑, MDA, NO ↓
You et al. [144]	Fermented papaya extracts (obtained by fermentation of papaya through *Aspergillus oryzae* for 3 months and then for 3 months using *Saccharomyces cerevisiae* yeasts) 30, 15 or 5 mL/kg, p.o., days 1–30 Female SPF Sprague-Dawley rats, 180–200 g, 7-8 weeks	Mammary gland hyperplasia induced by estrogen and progestin, 0.5 mg/kg of estradiol benzoate Days 1-25 and 4 mg/kg of progestin days 26 – 30, i.m. Serum: E2, progesterone, LH, FSH, MDA, AST, total bilirubin ↑; GPx, SOD, ALT ↓ Liver: MDA ↑; GPx, SOD ↓ Mammary gland: GPx, SOD ↓, hyperplasia, MDA ↑	Serum: MDA (0 5, ++ 15 and 30), progesterone (+ 5 and 15, ++ 30), total bilirubin (0 5, ++ 5, +++ 30), E2 (++ all doses), LH (+ 5, ++ 5, +++ 30), FSH, ALT, AST (++ 5 and 15, +++ 30); GPx and SOD (0 5, +++ 15 and 30) Liver: MDA (0 5, ++ 15 and 30), GPx, SOD (0 5, ++ 15, +++ 30) Mammary gland: hyperplasia (0 5, + 15, ++ 30), MDA, GPx (0 5, ++ 15 and 30), SOD (0 5, +++ 15 and 30)	Only 30 mL/kg studied Serum: SOD ↑ Liver: SOD ↑

↓: a decrease vs. control; ↑: an increase vs. control; (+): a slight beneficial effect; (++): a distinct beneficial effect; (+++): a complete beneficial effect; (0): no beneficial effect.

TABLE 20: The protective effects of plant preparations against radiation.

Reference	Plant preparation, dose, way and time of treatment, animals	The dose and negative effects	Protective effects of plant preparation	Effects of plant *per se*
Dong et al. [70]	*Spatholobus suberectus* Dunn (Ji-Xue-Teng Beijing Lvye Pharmaceutical Co. Ltd., China) 75% ethanol extract 40 g/kg, p.o., for 21 consecutive days after irradiation Chinese Kun Ming (KM) mice, 6–8 week aged	^{60}Co γ-radiation, a dose of 6 Gy Body weight: ↓ Blood: WBC, RBC, PLT, HGB ↓ Bone marrow tissue: Bcl-2 expression, phosphorylation of JAK2 and STAT5a ↓ Liver: ROS, MDA↑, SOD, GPx ↓ Femur: bone marrow cells ↓	Body weight: (+++) Blood: WBC, PLT, HGB (++), RBC (+++) Bone marrow tissue: phosphorylation of JAK2 (++), phosphorylation of STAT5a and Bcl-2 expression (+++) Liver: ROS, MDA (++), SOD, GPx (+++) Femur: bone marrow cells (++)	Not studied
Jeena et al. [145]	*Zingiber officinale* R (ginger) essential oil (Kancore Ingredients Limited, Angamali, Kerala, India) 100 or 500 mg/kg b.w. p.o., 5-day pretreatment and then for 14 days Male Balb/C mice, 6-8 week	γ-Radiation, 6 Gy, whole body exposure Blood: WBC, HGB ↓ Intestinal mucosa: SOD, CAT, GPx, GSH ↓	Blood: WBC (++), HGB (+++) Intestinal mucosa: SOD CAT, GPx and GSH (++ 100, +++ 500)	Not studied
Khattab et al. [146]	*Borago officinalis* L. seeds oil Posttreatment: 50 mg/kg b.w./day, p.o., 3 hours after irradiation and for 2 weeks Pretreatment: 50 mg/kg b.w./day, p.o., one week before irradiation and for 2 weeks Male albino rats, 160-180 g	γ-Radiation a single sublethal dose of 6.5 Gy of whole body Serum: GSH, HDL-c ↓, AST, ALT, GGT, MDA, TG, TC, LDL-c ↑ Liver: GSH ↓, MDA ↑	Posttreatment: Serum: AST, ALT (++), GGT, MDA, TG, TC, GSH, LDL-c, HDL-c (+++) Liver: GSH (++), MDA (+++) Pretreatment: Serum: AST, ALT (++), GGT, MDA, TG, TC, GSH, LDL-c, HDL-c (+++) Liver: GSH (++), MDA (+++)	None
Wang et al. [147]	*Rubus idaeus* red raspberry ethanolic extract 750 μg/mL applied on the dorsal region of the nude mice 1 day before UVB and then for 5 days Female nude mice (ICR-Foxn/nu strain)	UVB 30 mJ/cm^2 in the dorsal region, once a day for 5 days Total dose of 150 mJ/cm^2 per mouse Skin epidermal thickness: ↑ Transepidermal water loss ↑ Erythema ↑ Skin: COX-2, DNA oxidation and protein carbonylation ↑	Skin epidermal thickness: (+++) Transepidermal water loss (++) Erythema (++) Skin: COX-2, DNA oxidation (++), protein carbonylation (+++)	Not studied

↓: a decrease vs. control; ↑: an increase vs. control; (++): a distinct beneficial effect; (+++): a complete beneficial effect.

as lipid profile normalizing agents, and the results seem to be auspicious [120–122]. Additionally, the researchers performed comparisons with standard drugs. The outcomes showed that the efficacy of plant material needs not be worse than that showed by acknowledged pharmaceutical agents. However, it should be emphasized that the final effects may be different, depending on the applied dose.

Veber et al. [34] compared the effects of two doses (125 or 250 mg/kg) of aqueous extract of red cabbage with that showed by fenofibrate, a drug used in therapy of abnormal lipids in the blood, on oxidative stress parameters in rats with hyperlipidemia caused by Triton WR-1339. Although the higher dose proved to possess protective properties generally comparable with the drug, the lower one in some cases showed no efficiency.

Erica multiflora L. leaf methanolic extract (150 or 250 mg/kg) effect was studied in rats with Triton WR-1339-induced hyperlipidemia in comparison with fenofibrate taking into account chosen lipid and antioxidant parameters. The higher dose showed comparable or even better protective action than the medicine. In contrast, total DNA damage was alleviated much better by the used drug [120].

Onyenibe et al. [122] investigated the efficiency of two doses of *Monodora myristica* aqueous extract as a protective agent in case of deterioration of lipid profile and oxidative parameters in hypercholesterolemic rats and compared the obtained results with those noted for a standard drug Questran. The authors found that generally two doses of plant preparation, namely, 100 and 200 mg/kg b.w., showed a better influence.

The effects of lipid-lowering drugs simvastatin and ciprofibrate as well as aqueous extract of *Campomanesia adamantium* O. Berg root were compared in rats with high-fructose diet-induced hyperlipidemia. The plant material exerted the entirely comparable influence in case of lipid parameters and even better as regards body weight gain lowering [121].

3.3. The Comparison of Plant Extracts of Hepatoprotective Properties with Pharmaceutical Agents.
Liu et al. [51] compared the protective action of pretreatment with *Sonneratia apetala* fruit water extract (100, 200, and 400 mg/kg) against hepatic damage caused by acetaminophen in mice with the effect of an acknowledged antidote NAC (N-acetyl-L-cysteine). The scientists observed the protective influence of plant preparation, which was not only comparable but in some cases better—particularly for serum ALT and AST as well as hepatic lipid peroxidation, antioxidant enzymes, TNF-α, and IL-6.

Similarly, the rich polyphenol fractions of methanolic extracts of *Genista quadriflora* Munby and *Teucrium polium geyrii* Maire showed a protective effect against hepatoxicity of acetaminophen (APAP) and the comparison with *N*-acetylcysteine showed their comparable properties with the drug, except for histological changes where *Teucrium polium geyrii* Maire exerted a better influence than two other studied agents [20].

3.4. The Comparison of Plant Extracts with Silymarin, an Acknowledged Dietary Supplement of Hepatoprotective Properties.
Many drugs and chemicals are distinguished by their hepatoxic effects. In view of the increasing environmental pollution as well as more and more common application of different drugs, often over-the-counter ones, the protective agents are highly desirable [18]. Silymarin, a preparation obtained from *Silybum marianum* L., has been used as a hepatoprotective adjuvant for years. Currently, the attention has been pointed to other plants, often those used since antiquity in traditional medicine [44]. Different hepatotoxicity animal models were used to perform comparison with silymarin.

The possibility of replacing silymarin by an extract of *Cassia fistula* L. leaves was studied by Kaur et al. [35] in rats exposed to thioacetamide. The studied extract was applied at three doses (50, 100, and 200 mg/kg b.w.), and beneficial effects of the two higher ones were not worse than those observed in rats receiving silymarin.

The similar observations were reported by Fahmi et al. [53] who compared the protective properties of dietary ginger against diethylnitrosamine hepatotoxicity in rats with those showed by silymarin and found that the studied material in the form of ginger powder or essential oil exerted the same or even better beneficial action.

Choi et al. [46] studied the possibility of *Centella asiatica* leaf ethanol extract (100 or 200 mg/kg) using as a protective agent against dimethylnitrosamine-induced hepatotoxicity in rats. The authors determined different inflammatory cytokines and mediators, liver injury markers, oxidant parameters, and histophological changes. In some cases (liver histology, serum IL-1β, TNF-α, and IL-2), both doses of the extract showed a better action than silymarin. In case of AST, ALP, IL-6, and INF-γ or liver MDA, both agents displayed the similarly significant properties. Furthermore, liver antioxidant enzymes were best ameliorated by the higher dose of plant preparation.

El-Hadary and Ramadan [52] in turn stated that *Moringa oleifera* leaf extract displayed protective properties against hepatotoxic action of diclofenac sodium. The comparison with silymarin proved that the plant preparation exerted comparable or even better effect.

Ahmad and Zeb [18] in turn compared an effectiveness of silymarin and different doses of water extract of *Trifolium repens* leaves against acetaminophen-induced hepatoxicity in mice. The authors reported that in case of most studied hematological, serum biochemical, and liver oxidative parameters, the effect of the highest dose was not worse than that shown by silymarin.

However, the comparison of protective action of leaf extract of *Solanum surattense* with that observed for silymarin in CCl$_4$-exposed rats revealed that the latter had entirely better effect regarding liver injury markers and lipid profile in serum as well as lipid peroxidation process in the liver [83].

On the other hand, Dogan and Anuk [44] observed that in ethanol-exposed rats water extract of leaves of *Platantus orientalis* L. generally showed the protective effects comparable or even better than those observed in silymarin-given animals. Interestingly, in case of some parameters, both silymarin and extracts showed insufficient effectiveness.

The possibility of applying a plant extract as an adjuvant which could augment an action of an acknowledged agent was also studied on an example of silymarin. Azim et al. [19] investigated effects of silymarin alone, *Moringa peregrina* leaf extract alone, and coadministration of those substances in rats subjected to acetaminophen. Generally, as regards plasma liver injury markers and oxidative parameters, the protective influence of all three treatments was found to be practically complete, but in some cases, the combination of both agents exerted the best effect. Interestingly, DNA damage was most markedly alleviated by plant extract alone while silymarin showed the slightest efficacy.

3.5. Immunosuppressive and Anti-Inflammatory Drugs vs. Plant Preparations.

Pistacia weinmannifolia root extract was compared regarding anti-inflammatory effects with roflumilast—a drug used in the therapy of lung inflammatory disorders, in mice with pulmonary inflammation induced by cigarette smoke and lipopolysaccharide. The results of the experiment showed that the studied preparation possessed protective properties absolutely comparable with the applied medicine [149].

Sundaram et al. [55] studied the protective effect of guggulipid (an extract from *Commiphora whighitii* gum resin) against morphology changes, cartilage degradation, and pro-oxidative processes in rats with experimental arthritis. Along with the evaluation of the plant preparation properties, the authors performed the comparison with a standard nonsteroidal anti-inflammatory drug ibuprofen. The influence of the studied extract proved to be comparable or even much more effective, particularly in cases of hematological and oxidative parameters.

In a study performed on mice subjected to 1-chloro-2,4-dinitrobenzene with the aim of inducing atopic dermatitis-like skin lesion, the effect of *Rumex japonicus* Houtt. root extract was compared with the efficacy of a synthetic glucocorticoid dexamethasone. The alleviation of the disease severity caused by the topical application of the plant extract was not much worse (particularly in the case of the higher dose) than that observed in animals treated intraperitoneally with dexamethasone [77].

Kaveh et al. [117] in turn compared the influence of different doses of hydroethanolic extract of *Portulaca oleracea* with that exerted by dexamethasone in rats with experimental asthma. According the authors, the effect of the highest dose (4 mg/mL in drinking water) was comparable with the drug. However, the lowest dose (1 mg/mL in drinking water) in some cases showed no beneficial influence.

In some cases, the pharmaceutical agents showed a better effect. Sdayria et al. [41] reported that in mice with carrageenan-induced paw edema pretreatment with a nonsteroidal anti-inflammatory drug indomethacin or *Euphorbia retusa* methanol extract showed comparable effects concerning % edema inhibition, although indomethacin displayed a little better properties. However, in case of oxidant parameters in the liver and paw, the drug exerted more distinct beneficial influence.

In the experiment performed by Jeong et al. [48], a nonsteroidal anti-inflammatory drug celecoxib proved to be much better in reversing the changes of biochemical parameters observed in rats with monosodium iodoacetate-induced osteoarthritis than a water extract of leaves of *Morus alba* L. Histological examinations confirmed the drug advantage.

3.6. Standard Drugs vs. Plant Preparations in Stomach Ulcer Animal Model.

Sattar et al. [137] performed a comparison of protective action of *Myristica fragrans* extract and sucralfate (a drug used for stomach ulcer treatment) in rats with ethanol-induced gastric ulcers. Although the plant preparation was not so effective with regard to amelioration of total acidity of stomach contents as well as macroscopic evaluation of gastric mucosa, ulcer index, and percentage of protection, its application did not cause serious increase in pH of stomach content as sulfacrate (4.25 vs. 5.0).

On the other hand, *Biebersteinia multifida* hydromethanolic extract showed a quite comparable or better protective effect than another drug—namely, omeprazole—in cases of gastric ulcers caused by 75% ethanol in rats. This effect included a decrease in ulcer area and number as well as enhancement of total antioxidant capacity in gastric mucosa [134].

Ateufack et al. [150] compared the effect of *Piptadeniastrum africanum* stem bark aqueous and methanol extracts (125, 250, or 500 mg/kg) in rat gastric ulcer induced by the HCl/ethanol mixture, indomethacin, and acetic acid with that showed by standard drugs (Maalox, Misoprostol, or Ranitidine). Plant extracts, particularly aqueous one when applied in the highest dose, displayed the protective action even better than the investigated drugs in case of animals exposed to HCl/ethanol mixture or indomethacin, but not in those treated with acetic acid.

Rtibi et al. [135] reported that in rats exposed to ethanol, pretreatment with *Ceratonia siliqua* L. aqueous extract (500, 1000, and 2000 mg/kg b.w.) showed a better or comparable effect with the standard drug famotidine when applied at the highest dose, while the lowest one was found to be either less effective or even ineffective at all.

The interesting results were reported by Chanda et al. [45]. The scientists studied the possibility of using *Paederia foetida* Linn. leaf methanol extract (100 and 200 mg/kg b.w.) as a gastroprotective agent in rats with gastric ulcers induced by indomethacin-pylorus ligation, alcohol, or water immersion stress. The effects were compared with those obtained for standard drugs ranitidine, sucralfate, and lansoprazole, respectively. As concerns ulcer protection, in the first and third models, there were no distinct differences between the plant material (particularly the higher dose) and the applied drug. In contrast, in the second model, the higher dose of extract showed much better effectiveness than the lower one, but nonetheless not so high as sucralfate.

3.7. The Comparison of Plant Preparations with Cytoprotective Adjuvants Used in Radio and Chemotherapy.

The advantage of plant origin substances over drugs was also shown by Dong et al. [70]. Ethanol extract of JXT (a traditional herb obtained from the *Spatholobus suberectus* Dunn dry rattan) given orally to mice caused a significant improvement of the biochemical parameters previously disturbed by

^{60}Co γ-radiation, i.e., morphology, bone marrow cell number, and liver lipid peroxidation level as well as activity of antioxidant enzymes. This effect was comparable or better than that exerted by amifostine, an agent applied in cases of radiation syndrome during radiotherapy.

3.8. Plant Preparations vs. Drugs and Supplements Applied in Neurological and Psychiatric Disorders. Pharmaceutical agents used for the treatment of psychiatric and neurodegenerative disorders may cause side effects worsening the condition of patients. Plant preparations, often used for centuries in traditional medicine, have been found to possess anxiolytic and antistress properties, and the comparison with acknowledged drugs and supplements showed their comparable efficacy [17, 58].

Plant materials, namely, extracts from two *Hypericum* species, were studied with regard to their effect on oxidative stress and inflammatory cytokines in an experimental anxiety animal model. The comparison with pure quercetin and a control drug alprazolam was also performed. In most cases, the disturbed brain parameters were positively influenced in a comparable or more distinct way by plant materials than by two other studied substances. It should be emphasized that in some cases the worst effect was observed in animals treated with alprazolam [17].

Almeida et al. [58] compared the protective effect of *Clitoria ternatea* extract with that shown by cotreatment with dietary supplements choline and docosahexanoic acid against brain oxidative stress caused by separation from mothers in rat pups. During 30-day experiment including the stressing factor and treatments as well as during the subsequent 330-day follow-up, both agents revealed comparable properties regarding the prevention of lipid peroxidation increase and thiol group content depletion.

Chonpathompikunlert et al. [31] compared the neuroprotective effect of *Apium graveolens* L. extract with that showed by a standard drug Tidomet Plus in an animal model of Parkinson disease. The efficacy of two doses (250 and 375 mg/kg b.w.) proved to be quite comparable (the lower one) or even better (the higher one) with the medicine as regards improvement of behavioral performance, oxidative parameters, and activities of monoamine oxidases A and B.

3.9. Antidiabetic Drugs vs. Plant Preparations. The possibility of plant preparations application in diabetic subjects was also studied. It was prompted by side effects occurring in patients treated by pharmacological agents. The outcomes seem to be promising although in view of the reported results the accurate research is needed to determine mechanism of action and the most beneficial dose [66, 127].

Khanra et al. [129] stated that *Abroma augusta* L. leaf methanol extract (100 or 200 mg/kg) was not so efficient at reversing the serum parameters disturbed in rats by type 2 diabetes course, particularly in the case of the lower dose, as a standard drug glibenclamide. However, in the case of alleviating DNA fragmentation, ATP level, chosen oxidant parameters, and expression of NF-κB in the kidney and heart, the prevalence of the drug was not so distinct.

The comparison of glibenclamide and methanolic extract of *Caralluma europaea* was performed by Dra et al. [127] on diabetic mice. The higher dose of plant material (500 mg/kg b.w.) was better effective in the reduction of blood glucose than a drug, beginning from the 4th hour after administration, while a lower one (250 mg/kg b.w.) showed a comparable effect. Additionally, according to the authors, the lower dose showed a more distinct beneficial influence in case of histopathological damage observed in diabetic animals.

The similar results were obtained by Du et al. [66] who compared the protective properties of a standard drug metformin hydrochloride and different doses (100, 250, and 500 mg/kg) of polysaccharide separated from *Lycium barbarum* in the rat model of diabetes induced by high-fat diet +streptozotocin. Metformin showed a better effect in case of fasting blood glucose and INF-α. As for insulin and ICAM-1, the highest dose of plant origin material proved to possess better ameliorating properties, while serum GPx was more improved by two higher doses.

Balbaa et al. [57] investigated the differences in effects of administration of *Nigella sativa* seeds oil, standard drugs metformin and glimepiride, and their combinations to diabetic rats. The oil had a better protective action when administrated alone than in combination with metformin or glimepiride against oxidative stress and neuroinflammatory cytokines' increase. When the results of administration of those three agents alone to diabetic rats were compared, the best properties of a plant material were also confirmed.

3.10. Plant Extract or a Single Substance of Antioxidant Properties? As beneficial effects of plant preparations were attributed to their antioxidative properties, some researches performed the comparisons with simple substances of acknowledged antioxidant character. The results showed that plant materials could exert a better influence due to the presence of many component which might cooperate with one another.

Jahan et al. [72] studied the possibility of application of *Chenopodium album* Linn. seed extract as a protective agent against the damage of reproductive functions caused by mercury exposure. They compared the effect of the plant extract with that showed by a known antioxidant vitamin C which was reported to exert beneficial influence on male fertility. Except for plasma cholesterol and triglycerides as well as GST and TBARS in testicular tissue, the benefit influence of the studied plant material was comparable or even better. The similar observations were reported as regards the testicular morphometric parameters.

The comparison of the protective influence of *Nigella sativa* extract and vitamin E against cisplatin nephrotoxicity was performed by Hosseinian et al. [16]. The cisplatin-induced negative changes, i.e., renal damage and thiol group decrease, and lipid peroxidation enhancement in the serum and kidney, were alleviated in a rather comparable way, except for serum thiols, where the prevalence of plant extract was indisputable.

The effects of two *Hypericum* (*H. maculatum* and *H. perforatum*) species extracts on oxidative stress and

inflammatory cytokines were studied in an experimental anxiety animal model and compared with pure quercetin. The beneficial influence of plant extracts was mostly comparable and in many cases better, particularly in the case of *Hypericum maculatum* [17]. Such results could point to synergistic action of various components of extracts, acting as confirmation of the conclusions made by He et al. [148].

3.11. The Action of a Plant Preparation Depending on Its Dose, Time and Form of Treatment

3.11.1. The Relationships between the Dose and the Effects. In many studies, the protective effects of plant extracts and constituents showed a direct dependency on the used dose [15, 29, 31, 56, 80, 107, 117].

However, sometimes, the similar effects were observed for a considerable wide range of the applied doses. Liu et al. [91] studied an effect of various doses (0.0625, 0.125, 0.25, 0.5 g/kg b.w.) of ginseng oligopeptides against ethanol toxicity, and the observed differences were quite slight considering the size of the applied range.

Malik et al. [39] performed a study on animals with Huntington's disease like symptoms and observed practically the same influence of two different doses (100 and 200 mg/kg) of *Celastrus paniculatus* seed ethanol extract on memory functions, locomotor activity, and oxidative parameters in the brain parts.

The relationships between used doses and an exerted influence were also studied in the experiment concerning the protective properties of water extract of *Sonneratia apetala* fruit against liver damage caused by acetaminophen exposure in mice. The effects of pretreatment with different doses (100, 200 and 400 mg/kg) were very interesting as in the case of some parameters a strong dose dependency was observed (e.g., liver GSH and MDA), while some other ones were affected in the same way, regardless of the applied dose (liver GSH, T-AOC, and TNF-α) [51].

In another study, Wang et al. [119] investigated the protective properties of two doses (4.6 or 14 g/kg b.w.) of aqueous extract of Salvia Miltiorrhiza Bge. f. alba in the monocrotaline-induced animal model of pulmonary hypertension. Various parameters were studied: mean pulmonary artery pressure, right ventricular systolic pressure, pulmonary artery remodelling, plasma vasoactive factors NO, 6-Keto-PGF1α, ET-1, and TXB$_2$, and lung TGF-β1, but the observed differences were not as considerable as one could expect taking into account the difference between the applied doses.

The similar observations were reported by El-Hadary and Ramadan [52] who studied two doses of *Moringa oleifera* leaf extract (150 and 300 mg/kg b.w.) against hepatotoxicity of diclofenac sodium. Both doses displayed protective properties, but again, the difference between them was not so great as one could predict considering their range.

Onyenibe et al. [122] studied the efficacy of two doses of *Monodora myristica* aqueous extract at preventing impairment of lipid profile and oxidative parameters in hypercholesterolemic rats and generally found no difference between 100 mg/kg b.w. and 200 mg/kg b.w.

Such results point to the necessity of complex research of any possible protective agent with using a wide range of doses. The issue of dependency between the used dose and its effects proved to be additionally complicated as not always a direct relationship was found. The effects of different doses were sometimes divergent as in the experiment performed by Khan et al. [88], who studied the influence of two doses 0.5 g/kg b.w. and 1.0 g/kg b.w. of ajwa dates (*Phoenix dactylifera* L.) water extract on the biochemical parameters in rats with diethylnitrosamine-induced liver cancer. The lower one in some cases showed even a harmful effect (potentializing the changes caused by the carcinogen), while the higher one showed considerable protective properties. Additionally, the lower dose effect was characterized by a significant diversity as apart from showing the above-mentioned harmful influence, it also exerted a beneficial action, ranging from slight to strong.

In some cases, the higher dose had the worse effect than a lower one. In the study performed by Omole et al. [26], concerning the possible use of pretreatment with kolaviron (a mixture of flavonoids obtained from *Garcinia kola* seeds, 200 or 400 mg/kg/d) against toxicity of cyclophosphamide, the higher dose proved to be less beneficial, not only exerting less protective properties but also causing a slight increase in lipid peroxidation in the heart tissue.

The similar observations were reported by Apaydin Yildirim et al. [28] who studied the influence of *Helichrysum plicatum* DC. subsp. *plicatum* extract (100 or 200 mg/(kg·d) against nephrotoxic as well as hepatotoxic effects of gentamicin in rats. The authors stated that the higher dose showed much less beneficial influence. Additionally, the higher dose exerted some harmful effects, particularly regarding histopahological changes, when administered alone.

In some studies, it would be really very difficult to decide which dose should be chosen for usage. In the experiment performed by Wattanathorn et al. [42], the beneficial influence of the combination of extracts of *Mangifera indica* L. and *Polygonum odoratum L.* against diabetes cataract and retinopathy was distinctly showed, but the effect of different doses (2, 10, or 50 mg/kg b.w.) was found to be highly diverse.

Phunchago et al. [92] studied the possible protective effect of *Tiliacora triandra* water extract against ethanol-induced hippocampus damage in rats. The authors compared three doses: 100, 200, and 400 mg/kg b.w., and found that the middle one showed the best influence in improving some studied parameters while in few cases the worst influence was found for the highest one.

3.11.2. The Relationships between the Period of Treatment and the Effects. The period of the treatment with the studied substances also proved to be a factor of importance. Xu et al. [60] investigated the effect of Rhubarb extract on the oxidative parameters in rats with traumatic brain injury. According to the reported results, the degree of improvement in lipid peroxidation intensity as well as antioxidants levels showed a dependency on the time of experiment. The animals sacrificed after a longer period, starting from surgery and plant material treatment, showed a better amelioration of the studied parameters.

3.11.3. The Relationships between the Way of Preparing Plant Materials and Their Effects. As plant extracts contain many active substances of different solubilities in various solvents, the way of the preparation of the used substances also proved to be an issue of importance.

Malik et al. [39] studied the fractions of *Celastrus paniculatus* seed ethanol extract, obtained by suspending it in water and sequential partitioning with using petroleum ether, ethyl acetate and n-butanol. These materials were investigated as to their ability to ameliorate the neurotoxic effect of 3-nitropropionic acid by reversing changes of oxidative parameters in striatum and cortex of experimental rats. In the case of improvement of enhanced MDA and nitrites as well as decreased CAT, SOD, and GSH, ethanol extract and aqueous fraction proved to be the most effective; the petroleum ether fraction showed much less efficacy while n-butanol and ethyl acetate ones practically none.

3.11.4. Treatment of Pretreatment? The way of treatment, i.e., pre or post, in some cases was shown to be a crucial factor influencing the observed effect to a considerable degree. Afsar et al. [23] studied the effects of ethyl acetate fraction of *Acacia hydaspica* methanol extract against cisplatin toxicity and observed that the protective influence observed in the case of posttreatment started concomitantly with cisplatin and continued for five days was decidedly less distinct than that of 15-day pretreatment combined with posttreatment.

On the other hand, some authors did not report any differences between the mentioned two ways. Khattab et al. [146] did not observe any differences between pre- and posttreatment with *Borago official* L. seed oil in rats exposed to γ-radiation.

The similar effects were observed by Nasri et al. [109] in rats subjected to a contrast medium iodixanol and 70% ethanol green tea extract. The plant agent alleviated iodixanol-induced histopathological kidney changes, but no significant differences between pre- and posttreatment were observed.

Hosseinian et al. [16] studied the possible protective effect against cisplatin nephrotoxicity of *Nigella sativa* extract (100 and 200 mg/kg) using the design, whereby two ways of administration were applied—pretreatment alone or with the addition of posttreatment. The outcomes were really interesting. In case of renal SH groups and tissue damage as well as serum SH groups and MDA plant material proved to possess beneficial effect, regardless of the way of administration.

4. The Effects of Plant Preparations Per Se

The fact that generally effects of plant preparations *per se* were observed occasionally makes the considerable limitation of the studies presented in the current review. Only a few scientists reported observations considering any influence of the studied materials. Sheweita et al., for instance, investigated the effects of application of essential oils of *Foeniculum vulgare* (fennel) Miller seeds, *Cuminum cyminum* L. (cumin) seeds, and *Syzygium aromaticum* L. (clove) flower and reported that the used oils themselves caused several beneficial effects like decrease in liver TBARS as well as enhancement of liver antioxidants [101].

El-Kashlan et al. [143] found the decrease in lipid peroxidation as well as reinforcement of antioxidant defence in rats receiving commercial date palm pollen.

El-Rahman et al. [110] reported alleviation of prooxidative processes as well as the increase in antioxidants in rats given *Saussurea lappa* root extract.

Furthermore, the beneficial influence of plant preparations included not only improvement in biochemical parameters. Sheng et al. [33] reported that, apart from positive effect on body and adipose tissue weight and insulin sensitivity, liver, and kidney functions, addition of mulberry leaves powder to diet also caused amelioration of microbiota community structure in gut of obese mice.

Balbaa et al. [57] investigated the differences in the effects of administration of *Nigella sativa* seeds oil, antidiabetic drugs metformin and glimepiride, and their combinations to rats. In some cases, the plant oil per se showed the least or no negative effect in nondiabetic rats when compared to medicines. The reduction of brain β-amyloid-42 as well as the increase in antioxidants' level was observed. On the other hand, brain lipid peroxidation was found to be enhanced.

However, some authors reported the negative effects of plant preparations on experimental animal organisms.

Apaydin Yildirim et al. [28] observed histopathological changes in organs of animals treated with *Helichrysum plicatum* DC. subsp. *plicatum* extract.

In one of the recently published articles, Nahdi et al. [151] observed that leaf *Hypericum humifusum* aqueous (200 or 400 mg/kg b.w.) and methanolic (10 or 20 mg/kg b.w.) extracts, given to rats, induced histopathological changes as well as impaired biochemical parameters including an increase in WBC, liver MDA, plasma ALT, AST, and LDH. Additionally, activities of hepatic antioxidant enzymes CAT and SOD were markedly decreased vs. control with no treatment. Interestingly, in case of the aqueous extract, the worse effect was exerted by the lower dose while the methanolic one was found to be more harmful when given in the higher dose.

5. Conclusions

The outcomes of the studies presented in the current review showed a huge potential inherent in plant preparations. They were revealed to reverse or alleviate toxicity of different factors, side effects of drugs, and symptoms of various diseases. In many cases, they were proved to be comparable or better than standard drugs which let us suggest that in future the plant origin substances could make a replacement for pharmaceutical agents. However, the presented above results of some experiments point to the fact that the proper precautions must be undertaken before applying any plant material. The detailed research regarding the *per se* effects, dose, and way of administration needs to be performed.

Abbreviations

AA:	Ascorbic acid
Aβ:	β-Amyloid peptide
ABCG:	ATP-biding cassette, subfamily G transporters
ACC:	Acetyl-CoA carboxylase
AChE:	Acetylcholine esterase
ACP:	Acid phosphatase
ADA:	Adenosine deaminase activity
AGE:	Advanced glycation end product
AGGRECAN:	Cartilage-specific proteoglycan core protein
ALB:	Albumin
AlCl$_3$:	Aluminium chloride
ALP:	Alkaline phosphatase
ALT:	Alanine aminotransferase
AOPP:	Advanced oxidation protein products
AR:	Aldose reductase
ARE:	Antioxidant-responsive element
AST:	Aspartate aminotransferase
ATP:	Adenosine triphosphate
BALF:	Bronchoalveolar lavage fluid
BAP:	Biological antioxidant power
BAT:	Brown adipose tissue
Bcl-2:	B-cell lymphoma 2
BMP2:	Bone morphogenetic protein 2
BUN:	Blood urea nitrogen
b.w.:	Body weight
Ca:	Calcium
Ca^{2+}ATPase:	Calcium-activated adenosine 5′-triphosphatase
CAT:	Catalase
CCl$_4$:	Tetrachlorometan (carbon tetrachloride)
Cd:	Cadmium
Cd36:	Cluster of differentiation 36
cGMP:	Cyclic guanosine-3′,5′-monophosphate
ChAT:	Choline acetyltransferase
CHOP:	C/EBP homologous protein
CK-MB:	Creatinine kinase-MB
COL2:	Collagen type-II
COL10:	Collagen type 10
COMP:	Cartilage oligomeric matrix protein
COX-2:	Cyclooxygenase-2
CR:	Creatinine
CRP:	C-reactive protein
CS:	Citrate synthase
cTnI:	Cardiac troponin I
CTX-II:	C-telopeptide of type II collagen
Cu:	Copper
CYP2E1:	Cytochrome P450-2E1
DBP:	Diastolic blood pressure
DC:	Diene conjugate
DHEAs:	Dehydroepiandrosterone sulfate
DNA:	Deoxyribonucleic acid
E2:	Estradiol
eNOS:	Endothelial nitric oxide synthase
ERK1/2:	Extracellular signal-regulated kinase 1 and 2
ET-1:	Endothelin-1

Fatp4:	Fatty acid transport protein 4
Fe:	Iron
FFA:	Free fatty acids
FRAP:	Ferric reducing ability of plasma
FSH:	Follicle-stimulating hormone
fT3:	Free T3
fT4:	Free T4
γ-GCS:	γ-Glutamyl cysteine synthetase
GGT:	γ-Glutamyl transferase
GM-CSF:	Granulocyte-macrophage colony-stimulating factor
G6PD:	Glucose-6-phosphate dehydrogenase
GPx:	Glutathione peroxidase
GR:	Glutathione reductase
GRP78:	78 kDa glucose-regulated protein
GSH:	Reduced glutathione
GSSG:	The oxidized form of glutathione
GSSG-red:	Oxidized glutathione reductase
GSSP:	Glutationylated proteins
GST:	Glutathione-S-transferase
HA:	Hyaluronidase
HbA$_1$c:	Glycated hemoglobin
HCT:	Haematocrit
HDL:	High-density lipoprotein
HDL-c:	High-density lipoprotein cholesterol
Hg:	Mercury
HGB:	Haemoglobin
HMG-CoA-R:	3-Hydroxy-3-methylglutaryl CoA reductase
HNE:	4-Hydroxy-2-nonenal
HO-1:	Heme oxygenase 1
H$_2$O$_2$:	Hydrogen peroxide
HOMA-IR:	Homeostasis model assessment-insulin resistance
ICAM-1:	Intercellular adhesion molecule
i.c.v.:	Intracerebroventricular
IDE:	Insulin degradation enzyme
IFN-α:	Interferon-α
IFN-γ:	Interferon-γ
i.g.:	Intragastrically
IgG:	Immunoglobulina G
IgM:	Immunoglobulina M
IL:	Interleukin
i.m.:	Intramuscularly
iNOS:	Inducible nitric oxide synthase
i.p.:	Intraperitoneally
i.v.:	Intravenously
JAK:	Janus kinase
K:	Potassium
KEAP1:	Kelch-like ECH-associated protein 1
6-Keto-PGF1α:	6-Keto-prostaglandin F1 alpha
LDH:	Lactate dehydrogenase
LDL:	Low-density lipoprotein
LDL-c:	Low-density lipoprotein cholesterol
LH:	Luteinizing hormone
Lpl:	Lipoprotein lipase
LPO:	Lipid peroxidation
LPS:	Lipopolysaccharide

MAO-A: Monoamine oxidase type B
MAO-B: Monoamine oxidase type B
MCP-1: Monocyte chemoattractant protein 1
M-CSF: Macrophage colony-stimulating factor
MDA: Malondialdehyde
MDSCs: Myeloid suppressor cells
Mg: Magnesium
$Mg^{2+}ATPase$: Magnesium-activated adenosine $5'$-triphosphatase
MIP: Macrophage inflammatory protein
MMP-1: Matrix metalloproteinase-1, interstitial collagenase
MMP-3: Matrix metalloproteinase-3, stromelysin-1
MMP-13: Matrix metalloproteinase-13, collagenase 3
MMP: Matrix metalloproteinase
MPO: Myeloperoxidase
mRNA: Messenger ribonucleic acid
MT: Metallothionein
MTH 1: A gene encoding 8-oxo-7,8-dihydrodeoxyguanosine triphosphatase
Na: Sodium
NADH: Nicotinamide adenine dinucleotide reduced form
$Na^+/K^+ATPase$: Sodium- and potassium-activated adenosine $5'$-triphosphatase
NASH: Nonalcoholic steatohepatitis
NF-κB: Nuclear factor-kappa B
NO: Nitric oxide
NO_3: Nitrate
NO_2: Nitrite
NOX: NADPH oxidase
NP-SH: Nonprotein sulfhydryl groups
NQO1: NAD(P)H:quinone oxidoreductase 1
Nrf2: Nuclear erythroid 2-related factor 2
8-OHdG: 8-Hydroxy-$2'$deoxyguanosine
OSI: Oxidative stress index
P: Phosphorus
P53: p53 protein
pACC: Phosphorylated acetyl-CoA carboxylase
pAMPK: Phosphorilated adenosine-monophosphate-activated protein kinase
Pb: Lead
PC: Protein carbonyls
PCG: Protein carbonyl groups
PCNA: Proliferating cell nuclear antigen
peNOS: Phosphorylated eNOS
PGE_2: Prostaglandin E_2
PGI2: Prostacyclin
PHGPx: Phospholipid hydroxyperoxide GPx
PKC: Protein kinase C
PLT: Platelets
P38 MAPK: p38 mitogen-activated protein kinase
pNF-κB: Phospho-NF-κB
p.o.: Orally
QR: Quinone reductase
RANTES: Regulated on Activation, Normal T-cell Expressed and Secreted
RBC: Red blood cells
ROS: Reactive oxygen species
SBP: Systolic blood pressure
s.c.: Subcutaneously
SDH: Sorbitol dehydrogenase
SH: Thiol groups
SHBG: Sex hormone-binding globulin
SOD: Superoxide dismutase
SPF: Specific pathogen free
Srebf1: Sterol regulatory element-binding transcription factor 1
SREBP-1c: Sterol-regulatory-element binding protein-1c
STAT: Signal transducer and activator of transcription
T: Testosterone
T-AOC: Total antioxidant capacity
TAS: Total antioxidant status
TBARS: Thiobarbituric acid reactive substances
TC: Total cholesterol
TG: Triglycerides
TGF-β: Transforming growth factor beta
tHcy: Total homocysteine
TIMP: Tissue inhibitor of metalloproteinases
TLC: Total leukocytic count
TLR: Tall-like receptor
TNF-α: Tumor necrosis factor alpha
TOS: Total oxidant status
TP: Total protein
TSH: Thyroid-stimulating hormone
TXA_2: Thromboxane A2
TXB_2: Thromboxane B2
UA: Uric acid
UDPGT: UDP-glucuronosyl transferase
VEGF: Vascular endothelial growth factor
VLDL: Very low-density lipoprotein
VLDL-c: Very low-density lipoprotein cholesterol
WBC: White blood cells
XO: Xanthine oxidase
Zn: Zinc.

Conflicts of Interest

The authors declare that there is no conflict of interest regarding the publication of this article.

References

[1] O. T. Olaniyan, O. T. Kunle-Alabi, and Y. Raji, "Protective effects of methanol extract of Plukenetia conophora seeds and 4H-pyran-4-one 2, 3-dihydro-3, 5-dihydroxy-6-methyl on the reproductive function of male Wistar rats treated with cadmium chloride," *JBRA Assisted Reproduction*, vol. 22, no. 4, pp. 289–300, 2018.

[2] A. Mirzaei, S. Sepehri, H. Sadeghi, and A. Alamdari, "Protecting impact of Jaft against carbendazim induced biochemical changes in male Wistar rats," *Journal of Medicine and Life*, vol. 8, no. Spec Iss 3, pp. 96–100, 2015.

[3] T. K. Dua, S. Dewanjee, R. Khanra et al., "The effects of two common edible herbs, Ipomoea aquatica and Enhydra

fluctuans, on cadmium-induced pathophysiology: a focus on oxidative defence and anti-apoptotic mechanism," *Journal of Translational Medicine*, vol. 13, no. 1, article 245, 2015.

[4] D. Gao, L. N. Zeng, P. Zhang et al., "Rhubarb anthraquinones protect rats against mercuric chloride ($HgCl_2$)-induced acute renal failure," *Molecules*, vol. 21, no. 3, p. 298, 2016.

[5] M. Mężyńska, M. M. Brzóska, J. Rogalska, and B. Piłat-Marcinkiewicz, "Extract from Aronia melanocarpa L. berries prevents cadmium-induced oxidative stress in the liver: a study in a rat model of low-level and moderate lifetime human exposure to this toxic metal," *Nutrients*, vol. 11, no. 1, p. 21, 2019.

[6] M. Chaâbane, M. Koubaa, N. Soudani et al., "Nitraria retusa fruit prevents penconazole-induced kidney injury in adult rats through modulation of oxidative stress and histopathological changes," *Pharmaceutical Biology*, vol. 55, no. 1, pp. 1061–1073, 2017.

[7] A. El Arem, L. Lahouar, E. B. Saafi et al., "Dichloroacetic acid-induced testicular toxicity in male rats and the protective effect of date fruit extract," *BMC Pharmacology and Toxicology*, vol. 18, no. 1, article 17, 2017.

[8] H. A. Khalaf, E. A. Arafat, and F. M. Ghoneim, "A histological, immunohistochemical and biochemical study of the effects of pomegranate peel extracts on gibberellic acid induced oxidative stress in adult rat testes," *Biotechnic & Histochemistry*, vol. 94, no. 8, pp. 569–582, 2019.

[9] A. T. Mossa, F. M. Ibrahim, S. M. Mohafrash, D. H. Abou Baker, and S. El Gengaihi, "Protective effect of ethanolic extract of grape pomace against the adverse effects of cypermethrin on weanling female rats," *Evidence-based Complementary and Alternative Medicine*, vol. 2015, Article ID 381919, 10 pages, 2015.

[10] A. E. Abdel Moneim, "Indigofera oblongifolia prevents lead acetate-induced hepatotoxicity, oxidative stress, fibrosis and apoptosis in rats," *PLoS One*, vol. 11, no. 7, article e0158965, 2016.

[11] M. E. El-Boshy, B. Refaat, A. H. Qasem et al., "The remedial effect of Thymus vulgaris extract against lead toxicity-induced oxidative stress, hepatorenal damage, immunosuppression, and hematological disorders in rats," *Environmental Science and Pollution Research International*, vol. 26, no. 22, pp. 22736–22746, 2019.

[12] Y. Ke, K. Yu, W. Zeng, and G. Lian, "Protective roles of Pyracantha fortuneana extract on acute renal toxicity induced by cadmium chloride in rats," *Acta Cirúrgica Brasileira*, vol. 34, no. 7, article e201900706, 2019.

[13] M. AlSaid, R. Mothana, M. Raish et al., "Evaluation of the effectiveness of Piper cubeba extract in the amelioration of CCl4-induced liver injuries and oxidative damage in the rodent model," *BioMed Research International*, vol. 2015, Article ID 359358, 11 pages, 2015.

[14] K. Bellassoued, A. Ben Hsouna, K. Athmouni et al., "Protective effects of Mentha piperita L. leaf essential oil against CCl_4 induced hepatic oxidative damage and renal failure in rats," *Lipids in Health and Disease*, vol. 17, no. 1, article 9, 2018.

[15] S. Alzahrani, W. Ezzat, R. E. Elshaer et al., "Standarized Tribulus terrestris extract protects against rotenone-induced oxidative damage and nigral dopamine neuronal loss in mice," *Journal of Physiology and Pharmacology*, vol. 69, no. 6, 2018.

[16] S. Hosseinian, M. A. Hadjzadeh, N. M. Roshan et al., "Renoprotective effect of Nigella sativa against cisplatin-induced nephrotoxicity and oxidative stress in rat," *Saudi Journal of Kidney Diseases and Transplantation*, vol. 29, no. 1, pp. 19–29, 2018.

[17] A. C. Sevastre-Berghian, V. A. Toma, B. Sevastre et al., "Characterization and biological effects of Hypericum extracts on experimentally-induced - anxiety, oxidative stress and inflammation in rats," *Journal of Physiology and Pharmacology*, vol. 69, no. 5, 2018.

[18] S. Ahmad and A. Zeb, "Effects of phenolic compounds from aqueous extract of Trifolium repens against acetaminophen-induced hepatotoxicity in mice," *Journal of Food Biochemistry*, vol. 43, no. 9, article e12963, 2019.

[19] S. A. A. Azim, M. T. Abdelrahem, M. M. Said, and A. Khattab, "Protective effect of Moringa peregrina leaves extract on acetaminophen-induced liver toxicity in albino rats," *African Journal of Traditional, Complementary, and Alternative Medicines*, vol. 14, no. 2, pp. 206–216, 2017.

[20] N. Baali, Z. Belloum, S. Baali et al., "Protective activity of total polyphenols from Genista quadriflora Munby and Teucrium polium geyrii Maire in acetaminophen-induced hepatotoxicity in rats," *Nutrients*, vol. 8, no. 4, p. 193, 2016.

[21] H. Bouzenna, N. Samout, E. Amani et al., "Protective effects of Pinus halepensis L. essential oil on aspirin-induced acute liver and kidney damage in female Wistar albino rats," *Journal of Oleo Science*, vol. 65, no. 8, pp. 701–712, 2016.

[22] S. M. Chinnappan, A. George, P. Thaggikuppe et al., "Nephroprotective effect of herbal extract Eurycoma longifolia on paracetamol-induced nephrotoxicity in rats," *Evidence-based Complementary and Alternative Medicine*, vol. 2019, Article ID 4916519, 6 pages, 2019.

[23] T. Afsar, S. Razak, A. Almajwal, M. R. Khan, and R. Acacia hydaspica, "Acacia hydaspica R. Parker ameliorates cisplatin induced oxidative stress, DNA damage and morphological alterations in rat pulmonary tissue," *BMC Complementary and Alternative Medicine*, vol. 18, no. 1, p. 49, 2018.

[24] W. Ahmed, A. Zaki, and T. Nabil, "Prevention of methotrexate-induced nephrotoxicity by concomitant administration of garlic aqueous extract in rat," *Turkish Journal of Medical Sciences*, vol. 45, no. 3, pp. 507–516, 2015.

[25] R. C. Chen, X. D. Xu, X. Zhi Liu et al., "Total flavonoids from Clinopodium chinense (Benth.) O. Ktze protect against doxorubicin-induced cardiotoxicity in vitro and in vivo," *Evidence-based Complementary and Alternative Medicine*, vol. 2015, Article ID 472565, 17 pages, 2015.

[26] J. G. Omole, O. A. Ayoka, Q. K. Alabi et al., "Protective effect of kolaviron on cyclophosphamide-induced cardiac toxicity in rats," *Journal of Evidence-Based Integrative Medicine*, vol. 23, article 2156587218757649, 2018.

[27] K. P. Rahate and A. Rajasekaran, "Hepatoprotection by active fractions from Desmostachya bipinnata stapf (L.) against tamoxifen-induced hepatotoxicity," *Indian Journal of Pharmacology*, vol. 47, no. 3, pp. 311–315, 2015.

[28] B. Apaydin Yildirim, S. Kordali, K. A. Terim Kapakin, F. Yildirim, E. Aktas Senocak, and S. Altun, "Effect of Helichrysum plicatum DC. subsp. plicatum ethanol extract on gentamicin-induced nephrotoxicity in rats," *Journal of Zhejiang University. Science. B*, vol. 18, no. 6, pp. 501–511, 2017.

[29] M. T. Boroushaki, S. Fanoudi, H. Mollazadeh, S. Boroumand-Noughabi, and A. Hosseini, "Reno-protective effect of *Rheum turkestanicum* against gentamicin-induced nephrotoxicity,"

Iranian Journal of Basic Medical Sciences, vol. 22, no. 3, pp. 328–333, 2019.

[30] T. Albrahim and M. A. Binobead, "Roles of Moringa oleifera leaf extract in improving the impact of high dietary intake of monosodium glutamate-induced liver toxicity, oxidative stress, genotoxicity, DNA damage, and PCNA alterations in male rats," *Oxidative Medicine and Cellular Longevity*, vol. 2018, Article ID 4501097, 11 pages, 2018.

[31] P. Chonpathompikunlert, P. Boonruamkaew, W. Sukketsiri, P. Hutamekalin, and M. Sroyraya, "The antioxidant and neurochemical activity of Apium graveolens L. and its ameliorative effect on MPTP-induced Parkinson-like symptoms in mice," *BMC Complementary and Alternative Medicine*, vol. 18, no. 1, article 103, 2018.

[32] L. Hritcu, J. A. Noumedem, O. Cioanca, M. Hancianu, P. Postu, and M. Mihasan, "Anxiolytic and antidepressant profile of the methanolic extract of Piper nigrum fruits in beta-amyloid (1-42) rat model of Alzheimer's disease," *Behavioral and Brain Functions*, vol. 11, no. 1, article 13, 2015.

[33] Y. Sheng, J. Liu, S. Zheng et al., "Mulberry leaves ameliorate obesity through enhancing brown adipose tissue activity and modulating gut microbiota," *Food & Function*, vol. 10, no. 8, pp. 4771–4781, 2019.

[34] B. Veber, A. Camargo, A. P. Dalmagro et al., "Red cabbage (Brassica oleracea L.) extract reverses lipid oxidative stress in rats," *Anais da Academia Brasileira de Ciências*, vol. 92, no. 1, article e20180596, 2020.

[35] S. Kaur, D. Sharma, A. P. Singh, and S. Kaur, "Amelioration of hepatic function, oxidative stress, and histopathologic damages by Cassia fistula L. fraction in thioacetamide-induced liver toxicity," *Environmental Science and Pollution Research International*, vol. 26, no. 29, pp. 29930–29945, 2019.

[36] N. Panth, S. H. Park, H. J. Kim, D. H. Kim, and M. H. Oak, "Protective effect of Salicornia europaea extracts on high salt intake-induced vascular dysfunction and hypertension," *International Journal of Molecular Sciences*, vol. 17, no. 7, p. 1176, 2016.

[37] H. M. Tag, "Hepatoprotective effect of mulberry (Morus nigra) leaves extract against methotrexate induced hepatotoxicity in male albino rat," *BMC Complementary and Alternative Medicine*, vol. 15, no. 1, article 252, 2015.

[38] W. Wang, H. Li, J. Yu et al., "Protective effects of Chinese herbal medicine Rhizoma drynariae in rats after traumatic brain injury and identification of active compound," *Molecular Neurobiology*, vol. 53, no. 7, pp. 4809–4820, 2016.

[39] J. Malik, M. Karan, and R. Dogra, "Ameliorating effect of Celastrus paniculatus standardized extract and its fractions on 3-nitropropionic acid induced neuronal damage in rats: possible antioxidant mechanism," *Pharmaceutical Biology*, vol. 55, no. 1, pp. 980–990, 2017.

[40] U. Rashid, M. R. Khan, and M. Sajid, "Hepatoprotective potential of Fagonia olivieri DC. against acetaminophen induced toxicity in rat," *BMC Complementary and Alternative Medicine*, vol. 16, no. 1, article 449, 2016.

[41] J. Sdayria, I. Rjeibi, A. Feriani et al., "Chemical composition and antioxidant, analgesic, and anti-inflammatory effects of methanolic extract of Euphorbia retusa in mice," *Pain Research & Management*, vol. 2018, article 4838413, pp. 1–11, 2018.

[42] J. Wattanathorn, P. Thiraphatthanavong, W. Thukham-Mee, S. Muchimapura, P. Wannanond, and T. Tong-Un, "Anticataractogenesis and antiretinopathy effects of the novel protective agent containing the combined extract of mango and Vietnamese coriander in STZ-diabetic rats," *Oxidative Medicine and Cellular Longevity*, vol. 2017, Article ID 5290161, 13 pages, 2017.

[43] P. R. de Oliveira, C. A. da Costa, G. F. de Bem et al., "Euterpe oleracea Mart.-derived polyphenols protect mice from diet-induced obesity and fatty liver by regulating hepatic lipogenesis and cholesterol excretion," *PLoS One*, vol. 10, no. 12, article e0143721, 2015.

[44] A. Dogan and O. O. Anuk, "Investigation of the phytochemical composition and antioxidant properties of chinar (Platanus orientalis L.) leaf infusion against ethanol-induced oxidative stress in rats," *Molecular Biology Reports*, vol. 46, no. 3, pp. 3049–3061, 2019.

[45] S. Chanda, L. Deb, R. K. Tiwari, K. Singh, and S. Ahmad, "Gastroprotective mechanism of Paederia foetida Linn. (Rubiaceae) - a popular edible plant used by the tribal community of North-East India," *BMC Complementary and Alternative Medicine*, vol. 15, no. 1, article 304, 2015.

[46] M. J. Choi, H. M. Zheng, J. M. Kim, K. W. Lee, Y. H. Park, and D. H. Lee, "Protective effects of Centella asiatica leaf extract on dimethylnitrosamine-induced liver injury in rats," *Molecular Medicine Reports*, vol. 14, no. 5, pp. 4521–4528, 2016.

[47] H. Kiziltas, S. Ekin, M. Bayramoglu et al., "Antioxidant properties of Ferulago angulata and its hepatoprotective effect against N-nitrosodimethylamine-induced oxidative stress in rats," *Pharmaceutical Biology*, vol. 55, no. 1, pp. 888–897, 2017.

[48] J. W. Jeong, H. H. Lee, J. Kim et al., "Mori folium water extract alleviates articular cartilage damages and inflammatory responses in monosodium iodoacetate-induced osteoarthritis rats," *Molecular Medicine Reports*, vol. 16, no. 4, pp. 3841–3848, 2017.

[49] D. Choudhary, P. Kothari, A. K. Tripathi et al., "Spinacia oleracea extract attenuates disease progression and subchondral bone changes in monosodium iodoacetate-induced osteoarthritis in rats," *BMC Complementary and Alternative Medicine*, vol. 18, no. 1, article 69, 2018.

[50] N. B. Ghate, D. Chaudhuri, A. Das, S. Panja, and N. Mandal, "An antioxidant extract of the insectivorous plant Drosera burmannii Vahl. alleviates Iron-induced oxidative stress and hepatic injury in mice," *PLoS One*, vol. 10, no. 5, article e0128221, 2015.

[51] J. Liu, D. Luo, Y. Wu et al., "The protective effect of Sonneratia apetala fruit extract on acetaminophen-induced liver injury in mice," *Evidence-based Complementary and Alternative Medicine*, vol. 2019, Article ID 6919834, 12 pages, 2019.

[52] A. E. El-Hady and M. F. Ramadan, "Antioxidant traits and protective impact of Moringa oleifera leaf extract against diclofenac sodium-induced liver toxicity in rats," *Journal of Food Biochemistry*, vol. 43, no. 2, article e12704, 2019.

[53] A. Fahmi, N. Hassanen, M. Abdur-Rahman, and E. Shams-Eldin, "Phytochemicals, antioxidant activity and hepatoprotective effect of ginger (Zingiber officinale) on diethylnitrosamine toxicity in rats," *Biomarkers*, vol. 24, no. 5, pp. 436–447, 2019.

[54] R. Simeonova, V. M. Bratkov, M. Kondeva-Burdina, V. Vitcheva, V. Manov, and I. Krasteva, "Experimental liver protection of n-butanolic extract of Astragalus

monspessulanus L. on carbon tetrachloride model of toxicity in rat," *Redox Report*, vol. 20, no. 4, pp. 145–153, 2015.

[55] M. S. Sundaram, M. K. Neog, M. Rasool et al., "Guggulipid ameliorates adjuvant-induced arthritis and liver oxidative damage by suppressing inflammatory and oxidative stress mediators," *Phytomedicine*, vol. 64, article 152924, 2019.

[56] X. Tang, R. Wei, A. Deng, and T. Lei, "Protective effects of ethanolic extracts from artichoke, an edible herbal medicine, against acute alcohol-induced liver injury in mice," *Nutrients*, vol. 9, no. 9, p. 1000, 2017.

[57] M. Balbaa, S. A. Abdulmalek, and S. Khalil, "Oxidative stress and expression of insulin signaling proteins in the brain of diabetic rats: role of Nigella sativa oil and antidiabetic drugs," *PLoS One*, vol. 12, no. 5, article e0172429, 2017.

[58] P. M. D. Almeida, S. U. Kamath, P. R. Shenoy, L. K. Bernhardt, A. Kishore, and K. S. Rai, "Persistent attenuation of brain oxidative stress through aging in perinatal maternal separated rat pups supplemented with choline and docosahexaenoic acid or Clitoria ternatea aqueous root extract," *Folia Neuropathologica*, vol. 56, no. 3, pp. 206–214, 2018.

[59] A. R. Silva, C. D. Cerdeira, A. R. Brito et al., "Green banana pasta diet prevents oxidative damage in liver and kidney and improves biochemical parameters in type 1 diabetic rats," *Archives of Endocrinology and Metabolism*, vol. 60, no. 4, pp. 355–366, 2016.

[60] X. Xu, H. Lv, Z. Xia et al., "Rhein exhibits antioxidative effects similar to Rhubarb in a rat model of traumatic brain injury," *BMC Complementary and Alternative Medicine*, vol. 17, no. 1, article 140, 2017.

[61] M. Qiu, F. Xiao, T. Wang et al., "Protective effect of Hedansanqi Tiaozhi Tang against non-alcoholic fatty liver disease in vitro and in vivo through activating Nrf 2/HO-1 antioxidant signaling pathway," *Phytomedicine*, vol. 67, article 153140, 2020.

[62] M. Long, Y. Liu, Y. Cao, N. Wang, M. Dang, and J. He, "Proanthocyanidins attenuation of chronic lead-induced liver oxidative damage in Kunming mice via the Nrf 2/ARE pathway," *Nutrients*, vol. 8, no. 10, p. 656, 2016.

[63] M. Muriach, M. Flores-Bellver, F. J. Romero, and J. M. Barcia, "Diabetes and the brain: oxidative stress, inflammation, and autophagy," *Oxidative Medicine and Cellular Longevity*, vol. 2014, Article ID 102158, 9 pages, 2014.

[64] L. Behrend, G. Henderson, and R. M. Zwacka, "Reactive oxygen species in oncogenic transformation," *Biochemical Society Transactions*, vol. 31, no. 6, pp. 1441–1444, 2003.

[65] Z. Lou, J. Wang, Y. Chen et al., "Linderae radix ethanol extract attenuates alcoholic liver injury via attenuating inflammation and regulating gut microbiota in rats," *Brazilian Journal of Medical and Biological Research*, vol. 52, no. 6, article e7628, 2019.

[66] M. Du, X. Hu, L. Kou, B. Zhang, and C. Zhang, "Lycium barbarum polysaccharide mediated the antidiabetic and antinephritic effects in diet-streptozotocin-induced diabetic Sprague Dawley rats via regulation of NF-κB," *BioMed Research International*, vol. 2016, Article ID 3140290, 9 pages, 2016.

[67] D. K. Morrison, "MAP kinase pathways," *Cold Spring Harbor Perspectives in Biology*, vol. 4, no. 11, article a011254, 2012.

[68] J. Zhao, Y. F. Qi, and Y. R. Yu, "STAT3, a key regulator in liver fibrosis," *Annals of Hepatology*, vol. S1665-2681, no. 20, pp. 30071–30075, 2020.

[69] A. Charras, P. Arvaniti, C. Le Dantec et al., "JAK inhibitors and oxidative stress control," *Frontiers in Immunology*, vol. 10, p. 2814, 2019.

[70] X. Z. Dong, Y. N. Wang, X. Tan, P. Liu, D. H. Guo, and C. Yan, "Protective effect of JXT ethanol extract on radiation-induced hematopoietic alteration and oxidative stress in the liver," *Oxidative Medicine and Cellular Longevity*, vol. 2018, Article ID 9017835, 12 pages, 2018.

[71] S. Selmi, K. Rtibi, D. Grami, H. Sebai, and L. Marzouki, "Lavandula stoechas essential oils protect against malathion-induces reproductive disruptions in male mice," *Lipids in Health and Disease*, vol. 17, no. 1, article 253, 2018.

[72] S. Jahan, T. Azad, A. Ayub et al., "Ameliorating potency of Chenopodium album Linn. and vitamin C against mercuric chloride-induced oxidative stress in testes of Sprague Dawley rats," *Environmental Health and Preventive Medicine*, vol. 24, no. 1, article 62, 2019.

[73] W. Kim, D. W. Kim, D. Y. Yoo et al., "Antioxidant effects of Dendropanax morbifera Léveille extract in the hippocampus of mercury-exposed rats," *BMC Complementary and Alternative Medicine*, vol. 15, no. 1, article 247, 2015.

[74] L. Feng, X. Wang, F. Peng et al., "Walnut protein hydrolysates play a protective role on neurotoxicity induced by d-galactose and aluminum chloride in mice," *Molecules*, vol. 23, no. 9, p. 2308, 2018.

[75] A. N. Badr and M. A. Naeem, "Protective efficacy using capegolden berry against pre-carcinogenic aflatoxins induced in rats," *Toxicology Reports*, vol. 6, pp. 607–615, 2019.

[76] I. H. Bahcecioglu, M. Ispiroglu, M. Tuzcu et al., "Pistacia terebinthus coffee protects against thioacetamide-induced liver injury in rats," *Acta Medica (Hradec Králové)*, vol. 58, no. 2, pp. 56–61, 2015.

[77] H. R. Yang, H. Lee, J. H. Kim et al., "Therapeutic effect of Rumex japonicus Houtt. on DNCB-induced atopic dermatitis-like skin lesions in Balb/c mice and human keratinocyte HaCaT cells," *Nutrients*, vol. 11, no. 3, p. 573, 2019.

[78] H. Yoshioka, M. Tanaka, H. Fujii, and T. Nonogaki, "Sasa veitchii extract suppresses carbon tetrachloride-induced hepato- and nephrotoxicity in mice," *Environmental Health and Preventive Medicine*, vol. 21, no. 6, pp. 554–562, 2016.

[79] H. Xu, L. Liu, Y. Chen et al., "The chemical character of polysaccharides from processed Morindae officinalis and their effects on anti-liver damage," *International Journal of Biological Macromolecules*, vol. 141, pp. 410–421, 2019.

[80] M. D. Shah, U. J. A. D'Souza, and M. Iqbal, "The potential protective effect of Commelina nudiflora L. against carbon tetrachloride (CCl_4)-induced hepatotoxicity in rats, mediated by suppression of oxidative stress and inflammation," *Environmental Health and Preventive Medicine*, vol. 22, no. 1, article 66, 2017.

[81] U. Kukongviriyapan, V. Kukongviriyapan, P. Pannangpetch et al., "Mamao pomace extract alleviates hypertension and oxidative stress in nitric oxide deficient rats," *Nutrients*, vol. 7, no. 8, pp. 6179–6194, 2015.

[82] T. A. Lin, B. J. Ke, C. S. Cheng, J. J. Wang, B. L. Wei, and C. L. Lee, "Red quinoa bran extracts protects against carbon tetrachloride-induced liver injury and fibrosis in mice via activation of antioxidative enzyme systems and blocking TGF-β1 pathway," *Nutrients*, vol. 11, no. 2, p. 395, 2019.

[83] M. K. Parvez, M. S. Al-Dosari, A. H. Arbab, P. Alam, M. S. Alsaid, and A. A. Khan, "Hepatoprotective effect of Solanum

surattense leaf extract against chemical- induced oxidative and apoptotic injury in rats," *BMC Complementary and Alternative Medicine*, vol. 19, no. 1, article 154, 2019.

[84] D. V. Thomaz, L. F. Peixoto, T. S. de Oliveira et al., "Antioxidant and neuroprotective properties of Eugenia dysenterica leaves," *Oxidative Medicine and Cellular Longevity*, vol. 2018, Article ID 3250908, 9 pages, 2018.

[85] W. Zheng, Q. Wang, X. Lu et al., "Protective effects of Dracocephalum heterophyllumin ConA-induced acute hepatitis," *Mediators of Inflammation*, vol. 2016, Article ID 2684321, 8 pages, 2016.

[86] N. Ahmed, D. S. El-Agamy, G. A. Mohammed, H. Abo-Haded, M. Elkablawy, and S. R. M. Ibrahim, "Suppression of LPS-induced hepato- and cardiotoxic effects by Pulicaria petiolaris via NF-κB dependent mechanism," *Cardiovascular Toxicology*, vol. 20, no. 2, pp. 121–129, 2020.

[87] M. Raish, A. Ahmad, K. M. Alkharfy et al., "Hepatoprotective activity of Lepidium sativum seeds against D-galactosamine/lipopolysaccharide induced hepatotoxicity in animal model," *BMC Complementary and Alternative Medicine*, vol. 16, no. 1, article 501, 2016.

[88] F. Khan, T. J. Khan, G. Kalamegam et al., "Anti-cancer effects of Ajwa dates (Phoenix dactylifera L.) in diethylnitrosamine induced hepatocellular carcinoma in Wistar rats," *BMC Complementary and Alternative Medicine*, vol. 17, no. 1, article 418, 2017.

[89] İ. Bingül, C. Başaran-Küçükgergin, A. F. Aydın et al., "Blueberry treatment attenuated cirrhotic and preneoplastic lesions and oxidative stress in the liver of diethylnitrosamine-treated rats," *International Journal of Immunopathology and Pharmacology*, vol. 29, no. 3, pp. 426–437, 2016.

[90] E. Rouhollahi, S. Z. Moghadamtousi, N. Al-Henhena et al., "The chemopreventive potential of Curcuma purpurascens rhizome in reducing azoxymethane-induced aberrant crypt foci in rats," *Drug Design, Development and Therapy*, vol. 9, pp. 3911–3922, 2015.

[91] R. Liu, Q. H. Chen, J. W. Ren et al., "Ginseng (Panax ginseng Meyer) oligopeptides protect against binge drinking-induced liver damage through inhibiting oxidative stress and inflammation in rats," *Nutrients*, vol. 10, no. 11, p. 1665, 2018.

[92] N. Phunchago, J. Wattanathorn, and K. Chaisiwamongkol, "Tiliacora triandra, an anti-intoxication plant, improves memory impairment, neurodegeneration, cholinergic function, and oxidative stress in hippocampus of ethanol dependence rats," *Oxidative Medicine and Cellular Longevity*, vol. 2015, Article ID 918426, 9 pages, 2015.

[93] A. Akbari, K. Nasiri, M. Heydari, S. H. Mosavat, and A. Iraji, "The protective effect of hydroalcoholic extract of Zingiber officinale Roscoe (ginger) on ethanol-induced reproductive toxicity in male rats," *Journal of Evidence-Based Complementary & Alternative Medicine*, vol. 22, no. 4, pp. 609–617, 2017.

[94] J. C. Jung, Y. H. Lee, S. H. Kim et al., "Hepatoprotective effect of licorice, the root of Glycyrrhiza uralensis Fischer, in alcohol-induced fatty liver disease," *BMC Complementary and Alternative Medicine*, vol. 16, article 19, 2015.

[95] M. E. Ebada, "Essential oils of green cumin and chamomile partially protect against acute acetaminophen hepatotoxicity in rats," *Anais da Academia Brasileira de Ciências*, vol. 90, 2 suppl 1, pp. 2347–2358, 2018.

[96] U. S. Uthaya Kumar, Y. Chen, J. R. Kanwar, and S. Sasidharan, "Redox control of antioxidant and antihepato-

toxic activities of Cassia surattensis seed extract against paracetamol intoxication in mice: in vitro and in vivo studies of herbal green antioxidant," *Oxidative Medicine and Cellular Longevity*, vol. 2016, Article ID 6841348, 13 pages, 2016.

[97] G. Mishra, R. L. Khosa, P. Singh, and K. K. Jha, "Hepatoprotective potential of ethanolic extract of Pandanus odoratissimus root against paracetamol-induced hepatotoxicity in rats," *Journal of Pharmacy & Bioallied Sciences*, vol. 7, no. 1, pp. 45–48, 2015.

[98] P. Valipour, E. Heidarian, A. Khoshdel, and M. Gholami-Arjenaki, "Protective effects of hydroalcoholic extract of Ferulago angulata against gentamicin-induced nephrotoxicity in rats," *Iranian Journal of Kidney Diseases*, vol. 10, no. 4, pp. 189–196, 2016.

[99] Y. Zhang, X. Chi, Z. Wang et al., "Protective effects of Panax notoginseng saponins on PME-induced nephrotoxicity in mice," *Biomedicine & Pharmacotherapy*, vol. 116, article 108970, 2019.

[100] E. S. Kim, J. S. Lee, M. Akram et al., "Protective activity of Dendropanax morbifera against cisplatin-induced acute kidney injury," *Kidney & Blood Pressure Research*, vol. 40, no. 1, pp. 1–12, 2015.

[101] S. A. Sheweita, L. S. El-Hosseiny, and M. A. Nashashibi, "Protective effects of essential oils as natural antioxidants against hepatotoxicity induced by cyclophosphamide in mice," *PLoS One*, vol. 11, no. 11, article e0165667, 2016.

[102] M. Kpemissi, K. Eklu-Gadegbeku, V. P. Veerapur et al., "Nephroprotective activity of Combretum micranthum G. Don in cisplatin induced nephrotoxicity in rats: in-vitro, in-vivo and in-silico experiments," *Biomedicine & Pharmacotherapy*, vol. 116, article 108961, 2019.

[103] A. R. Moghadam, S. Tutunchi, A. Namvaran-Abbas-Abad et al., "Pre-administration of turmeric prevents methotrexate-induced liver toxicity and oxidative stress," *BMC Complementary and Alternative Medicine*, vol. 15, no. 1, article 246, 2015.

[104] A. Ben Saad, B. Dalel, I. Rjeibi et al., "Phytochemical, antioxidant and protective effect of cactus cladodes extract against lithium-induced liver injury in rats," *Pharmaceutical Biology*, vol. 55, no. 1, pp. 516–525, 2017.

[105] M. I. Khalil, I. Ahmmed, R. Ahmed et al., "Amelioration of isoproterenol-induced oxidative damage in rat myocardium by Withania somnifera leaf extract," *BioMed Research International*, vol. 2015, Article ID 624159, 10 pages, 2015.

[106] R. Dianita, I. Jantan, A. Z. Amran, and J. Jalil, "Protective effects of Labisia pumila var. alata on biochemical and histopathological alterations of cardiac muscle cells in isoproterenol-induced myocardial infarction rats," *Molecules*, vol. 20, no. 3, pp. 4746–4763, 2015.

[107] A. A. Shahat, M. S. Alsaid, S. Rafatullah et al., "Treatment with Rhus tripartita extract curtails isoproterenol-elicited cardiotoxicity and oxidative stress in rats," *BMC Complementary and Alternative Medicine*, vol. 16, no. 1, article 351, 2016.

[108] F. X. Kemka Nguimatio, P. B. Deeh Defo, M. Wankeu-Nya et al., "Aframomum melegueta prevents the ejaculatory complications of propylthiouracil-induced hypothyroidism in sexually experienced male rats: evidence from intravaginal and fictive ejaculations," *Journal of Integrative Medicine*, vol. 17, no. 5, pp. 359–365, 2019.

[109] H. Nasri, S. Hajian, A. Ahmadi et al., "Ameliorative effect of green tea against contrast-induced renal tubular cell injury,"

Iranian Journal of Kidney Diseases, vol. 9, no. 6, pp. 421–426, 2015.

[110] G. I. A. El-Rahman, A. Behairy, N. M. Elseddawy et al., "Saussurea lappa ethanolic extract attenuates triamcinolone acetonide-induced pulmonary and splenic tissue damage in rats via modulation of oxidative stress, inflammation, and apoptosis," *Antioxidants*, vol. 9, no. 5, p. 396, 2020.

[111] D. S. Mohale, A. S. Tripathi, A. V. Shrirao, A. G. Jawarkar, and A. V. Chandewar, "Evaluation of antioxidant effect of Nerium indicum in anxious rats," *Indian Journal of Pharmacology*, vol. 48, no. 4, pp. 430–433, 2016.

[112] Y. Wu, A. Qiu, Z. Yang et al., "Malva sylvestris extract alleviates the astrogliosis and inflammatory stress in LPS-induced depression mice," *Journal of Neuroimmunology*, vol. 336, article 577029, 2019.

[113] C. M. Lin, Y. T. Lin, T. L. Lee, Z. Imtiyaz, W. C. Hou, and M. H. Lee, "In vitro and in vivo evaluation of the neuroprotective activity of Uncaria hirsuta Haviland," *Journal of Food and Drug Analysis*, vol. 28, no. 1, pp. 147–158, 2020.

[114] D. Galanis, K. Soultanis, P. Lelovas et al., "Protective effect of Glycyrrhiza glabra roots extract on bone mineral density of ovariectomized rats," *Biomedicine*, vol. 9, no. 2, p. 8, 2019.

[115] F. P. Leung, L. M. Yung, C. Y. Ngai et al., "Chronic black tea extract consumption improves endothelial function in ovariectomized rats," *European Journal of Nutrition*, vol. 55, no. 5, pp. 1963–1972, 2016.

[116] A. K. Hamm, D. K. Manter, J. S. Kirkwood, L. M. Wolfe, K. Cox-York, and T. L. Weir, "The effect of hops (Humulus lupulus L.) extract supplementation on weight gain, adiposity and intestinal function in ovariectomized mice," *Nutrients*, vol. 11, no. 12, article E3004, 2019.

[117] M. Kaveh, A. Eidi, A. Nemati, and M. H. Boskabady, "The extract of Portulaca oleracea and its constituent, alpha linolenic acid affects serum oxidant levels and inflammatory cells in sensitized rats," *Iranian Journal of Allergy, Asthma, and Immunology*, vol. 16, no. 3, pp. 256–270, 2017.

[118] L. Taguchi, N. M. Pinheiro, C. R. Olivo et al., "A flavanone from Baccharis retusa (Asteraceae) prevents elastase-induced emphysema in mice by regulating NF-κB, oxidative stress and metalloproteinases," *Respiratory Research*, vol. 16, no. 1, p. 79, 2015.

[119] Y. Wang, S. H. Cao, Y. J. Cui et al., "Salvia miltiorrhiza Bge. f. alba ameliorates the progression of monocrotaline-induced pulmonary hypertension by protecting endothelial injury in rats," *The Tohoku Journal of Experimental Medicine*, vol. 236, no. 2, pp. 155–162, 2015.

[120] R. Khlifi, A. Lahmar, Z. Dhaouefi et al., "Assessment of hypolipidemic, anti-inflammatory and antioxidant properties of medicinal plant Erica multiflora in triton WR-1339-induced hyperlipidemia and liver function repair in rats: a comparison with fenofibrate," *Regulatory Toxicology and Pharmacology*, vol. 107, article 104404, 2019.

[121] P. P. de Toledo Espindola, S. da Rocha Pdos, C. A. Carollo et al., "Antioxidant and antihyperlipidemic effects of Campomanesia adamantium O. Berg root," *Oxidative Medicine and Cellular Longevity*, vol. 2016, Article ID 7910340, 8 pages, 2016.

[122] N. S. Onyenibe, K. T. Fowokemi, and O. B. Emmanuel, "African nutmeg (Monodora myristica) lowers cholesterol and modulates lipid peroxidation in experimentally induced hypercholesterolemic male Wistar rats," *International Journal of Biomedical Sciences*, vol. 11, no. 2, pp. 86–92, 2015.

[123] M. Cakir, H. Duzova, I. Baysal et al., "The effect of hypericum perforatum on kidney ischemia/reperfusion damage," *Renal Failure*, vol. 39, no. 1, pp. 385–391, 2017.

[124] T. Caskurlu, M. Kanter, M. Erboga, Z. F. Erboga, M. Ozgul, and G. Atis, "Protective effect of Nigella sativa on renal reperfusion injury in rat," *Iranian Journal of Kidney Diseases*, vol. 10, no. 3, pp. 135–143, 2016.

[125] J. Godinho, A. B. de Sa-Nakanishi, L. S. Moreira et al., "Ethyl-acetate fraction of Trichilia catigua protects against oxidative stress and neuroinflammation after cerebral ischemia/reperfusion," *Journal of Ethnopharmacology*, vol. 221, pp. 109–118, 2018.

[126] K. N. Sravanthi and N. R. Rao, "Cerebroprotective activity of Pentapetes phoenicea on global cerebral ischemia in rats," *Indian Journal of Pharmacology*, vol. 48, no. 6, pp. 694–700, 2016.

[127] L. A. Dra, S. Sellami, H. Rais et al., "Antidiabetic potential of Caralluma europaea against alloxan-induced diabetes in mice," *Saudi Journal of Biological Sciences*, vol. 26, no. 6, pp. 1171–1178, 2019.

[128] M. Ben Salem, R. Ben Abdallah Kolsi, R. Dhouibi et al., "Protective effects of Cynara scolymus leaves extract on metabolic disorders and oxidative stress in alloxan-diabetic rats," *BMC Complementary and Alternative Medicine*, vol. 17, no. 1, article 328, 2017.

[129] R. Khanra, S. Dewanjee, T. K Dua et al., "Abroma augusta L. (Malvaceae) leaf extract attenuates diabetes induced nephropathy and cardiomyopathy via inhibition of oxidative stress and inflammatory response," *Journal of Translational Medicine*, vol. 13, no. 1, p. 6, 2015.

[130] E. I. Omodanisi, Y. G. Aboua, and O. O. Oguntibeju, "Assessment of the anti-hyperglycaemic, anti-inflammatory and antioxidant activities of the methanol extract of Moringa oleifera in diabetes-induced nephrotoxic male Wistar rats," *Molecules*, vol. 22, no. 4, p. 439, 2017.

[131] M. Fajri, A. Ahmadi, and R. Sadrkhanlou, "Protective effects of Equisetum arvense methanolic extract on sperm characteristics and in vitro fertilization potential in experimental diabetic mice: an experimental study," *International Journal of Reproductive BioMedicine (IJRM)*, vol. 18, no. 2, pp. 93–104, 2020.

[132] M. El Ayed, S. Kadri, S. Smine, S. Elkahoui, F. Limam, and E. Aouani, "Protective effects of grape seed and skin extract against high-fat-diet-induced lipotoxicity in rat lung," *Lipids in Health and Disease*, vol. 16, no. 1, article 174, 2017.

[133] R. Budriesi, F. Vivarelli, D. Canistro et al., "Liver and intestinal protective effects of Castanea sativa Mill. bark extract in high-fat diet rats," *PLoS One*, vol. 13, no. 8, article e0201540, 2018.

[134] M. Raeesi, N. Eskandari-Roozbahani, and T. Shomali, "Gastro-protective effect of *Biebersteinia multifida* root hydro-methanolic extract in rats with ethanol-induced peptic ulcer," *Avicenna journal of phytomedicine*, vol. 9, no. 5, pp. 410–418, 2019.

[135] K. Rtibi, M. A. Jabri, S. Selmi et al., "Gastroprotective effect of carob (Ceratonia siliqua L.) against ethanol-induced oxidative stress in rat," *BMC Complementary and Alternative Medicine*, vol. 15, no. 1, article 292, 2015.

[136] S. Sabiu, T. Garuba, T. Sunmonu et al., "Indomethacin-induced gastric ulceration in rats: protective roles of Spondias mombin a nd Ficus exasperata," *Toxicology Reports*, vol. 2, pp. 261–267, 2015.

[137] A. Sattar, A. Abdo, M. N. Mushtaq, I. Anjum, and A. Anjum, "Evaluation of gastro-protective activity of Myristica fragrans on ethanol-induced ulcer in albino rats," *Anais da Academia Brasileira de Ciências*, vol. 91, no. 2, article e20181044, 2019.

[138] V. R. Konda, R. Arunachalam, M. Eerike et al., "Nephroprotective effect of ethanolic extract of Azima tetracantha root in glycerol induced acute renal failure in Wistar albino rats," *Journal of Traditional and Complementary Medicine*, vol. 6, no. 4, pp. 347–354, 2016.

[139] A. Benhelima, Z. Kaid-Omar, H. Hemida, T. Benmahdi, and A. Addou, "Nephroprotective and diuretic effect of Nigella sativa L seeds oil on lithiasic Wistar rats," *African Journal of Traditional, Complementary, and Alternative Medicines*, vol. 13, no. 6, pp. 204–214, 2016.

[140] J. S. Chang, Y. J. Lee, D. A. Wilkie, and C. T. Lin, "The Neuroprotective and antioxidative effects of submicron and blended Lycium barbarum in experimental retinal degeneration in rats," *The Journal of Veterinary Medical Science*, vol. 80, no. 7, pp. 1108–1115, 2018.

[141] R. Cojocariu, A. Ciobica, I. M. Balmus et al., "Antioxidant capacity and behavioral relevance of a polyphenolic extract of Chrysanthellum americanum in a rat model of irritable bowel syndrome," *Oxidative Medicine and Cellular Longevity*, vol. 2019, Article ID 3492767, 13 pages, 2019.

[142] M. Hatipoğlu, M. Sağlam, S. Köseoğlu, E. Köksal, A. Keleş, and H. H. Esen, "The effectiveness of Crataegus orientalis M Bieber. (hawthorn) extract administration in preventing alveolar bone loss in rats with experimental periodontitis," *PLoS One*, vol. 10, no. 6, article e0128134, 2015.

[143] A. M. El-Kashlan, M. M. Nooh, W. A. Hassan, and S. M. Rizk, "Therapeutic potential of date palm pollen for testicular dysfunction induced by thyroid disorders in male rats," *PLoS One*, vol. 10, no. 10, article e0139493, 2015.

[144] Z. You, J. Sun, F. Xie et al., "Modulatory effect of fermented papaya extracts on mammary gland hyperplasia induced by estrogen and progestin in female rats," *Oxidative Medicine and Cellular Longevity*, vol. 2017, Article ID 8235069, 11 pages, 2017.

[145] K. Jeena, V. B. Liju, V. Ramanath, and R. Kuttan, "Protection against whole body γ-irradiation induced oxidative stress and clastogenic damage in mice by ginger essential oil," *Asian Pacific Journal of Cancer Prevention*, vol. 17, no. 3, pp. 1325–1332, 2016.

[146] H. A. H. Khattab, I. Z. A. Abdallah, F. M. Yousef, and E. A. Huwait, "Efficiency of borage seeds oil against gamma irradiation-induced hepatotoxicity in male rats: possible antioxidant activity," *African Journal of Traditional, Complementary, and Alternative Medicines*, vol. 14, no. 4, pp. 169–179, 2017.

[147] P. W. Wang, Y. C. Cheng, Y. C. Hung et al., "Red raspberry extract protects the skin against UVB-induced damage with antioxidative and anti-inflammatory properties," *Oxidative Medicine and Cellular Longevity*, vol. 2019, Article ID 9529676, 14 pages, 2019.

[148] Y. K. He, X. T. Cen, S. S. Liu, H. D. Lu, and C. N. He, "Protective effects of ten oligostilbenes from Paeonia suffruticosa seeds on interleukin-1β-induced rabbit osteoarthritis chondrocytes," *BMC Chemistry*, vol. 13, no. 1, article 72, 2019.

[149] J. W. Lee, H. W. Ryu, S. U. Lee et al., "Pistacia weinmannifolia ameliorates cigarette smoke and lipopolysaccharide-induced pulmonary inflammation by inhibiting interleukin-8 production and NF-κB activation," *International Journal of Molecular Medicine*, vol. 44, no. 3, pp. 949–959, 2019.

[150] G. Ateufack, E. C. Domgnim Mokam, M. Mbiantcha, R. B. Dongmo Feudjio, N. David, and A. Kamanyi, "Gastroprotective and ulcer healing effects of Piptadeniastrum africanum on experimentally induced gastric ulcers in rats," *BMC Complementary and Alternative Medicine*, vol. 15, no. 1, article 214, 2015.

[151] A. Nahdi, I. Hammami, R. B. Ali, O. Kallech-Ziri, A. El May, and M. V. El May, "Effect of Hypericum humifusum aqueous and methanolic leaf extracts on biochemical and histological parameters in adult rats," *Biomedicine & Pharmacotherapy*, vol. 108, pp. 144–152, 2018.

Research Article

Proanthocyanidins-Mediated Nrf2 Activation Ameliorates Glucocorticoid-Induced Oxidative Stress and Mitochondrial Dysfunction in Osteoblasts

Liang Chen,[1,2] **Sun-Li Hu,**[1,2] **Jun Xie,**[1,2] **De-Yi Yan,**[1,2] **She-Ji Weng,**[1] **Jia-Hao Tang,**[1,2] **Bing-Zhang Wang,**[1,2] **Zhong-Jie Xie,**[1] **Zong-Yi Wu,**[1] **and Lei Yang** ◉[1,2]

[1]*Department of Orthopaedic Surgery, The Second Affiliated Hospital and Yuying Childrens Hospital of Wenzhou Medical University, Wenzhou 325000, China*
[2]*Key Laboratory of Orthopaedics of Zhejiang Province, Wenzhou 325000, China*

Correspondence should be addressed to Lei Yang; wyey_yl@hotmail.com

The widespread use of therapeutic glucocorticoids has increased the frequency of glucocorticoid-induced osteoporosis (GIOP). One of the potential pathological processes of GIOP is an increased level of oxidative stress and mitochondrial dysfunction, which eventually leads to osteoblast apoptosis. Proanthocyanidins (PAC) are plant-derived antioxidants that have therapeutic potential against GIOP. In our study, a low dose of PAC was nontoxic to healthy osteoblasts and restored osteogenic function in dexamethasone- (Dex-) treated osteoblasts by suppressing oxidative stress, mitochondrial dysfunction, and apoptosis. Mechanistically, PAC neutralized Dex-induced damage in the osteoblasts by activating the Nrf2 pathway, since silencing Nrf2 partly eliminated the protective effects of PAC. Furthermore, PAC injection restored bone mass and promoted the expression of Nrf2 in the distal femur of Dex-treated osteoporotic rats. In summary, PAC protect osteoblasts against Dex-induced oxidative stress and mitochondrial dysfunction via the Nrf2 pathway activation and may be a promising drug for treating GIOP.

1. Introduction

Dexamethasone (Dex) is a synthetic glucocorticoid (GC) used widely for treating inflammatory and autoimmune diseases [1, 2]. However, chronic Dex treatment is associated with adverse effects, including decreased bone mineral density and microarchitecture porosity, eventually leading to glucocorticoid-induced osteoporosis (GIOP) and osteonecrosis [3–5]. Currently, therapeutics for GIOP are predominantly aimed to prevent excessive bone resorption; however, this therapy does not help to restore bone mass and bone microstructure. In addition, long-term use of antiresorptive drugs, such as bisphosphonates, may lead to a decrease in bone turnover. The development of GIOP is based on the disbalance between osteogenesis and osteoclastogenesis [6]. Therefore, preventing the deleterious effects on osteoblasts has become a major issue, and the underlying

mechanisms of Dex on osteoblasts remains to be unraveled. This is because endogenous GC activities are required for the maintenance of bone homeostasis [6]; however, excess GCs impede bone formation by impairing osteoblast differentiation, mineralization function, and survival [7]. The harmful effects of GC on osteoblasts are now considered as crucial factors in the development of GIOP [8, 9]. High-dose and long-term use of Dex leads to osteoblast apoptosis, which has been reported to be associated with the accumulation of reactive oxygen species (ROS) and the loss of mitochondrial membrane potential (MMP) [10, 11]. Furthermore, Dex-induced ROS accumulation and mitochondrial damage in osteoblasts exacerbate GIOP progression and bone mass loss through lipid peroxidation, inhibition of antioxidant enzymes, and increased osteoblast apoptosis [10, 11]. Moreover, an excess of oxidative stress induced by Dex has been reported to negatively impact the osteoblast

differentiation and mineralization function. Thus, key to the treatment of GIOP involves reducing intracellular oxidative stress in osteoblasts.

Nuclear factor erythroid 2-related factor 2 (Nrf2) is a vital transcription factor that is dysregulated in various oxidative stress-related pathologies [12]. Since ROS accumulation accelerates the development of GIOP [13, 14] and the activation of Nrf2 can effectively reduce oxidative stress and apoptosis [15], it is a promising therapeutic target for GIOP. In addition, Ibáñez et al. observed significant bone loss in ovariectomized Nrf2$^{-/-}$ compared to that in wild type controls [16], which points to an osteoprotective function of Nrf2 as well [17]. It combats intracellular oxidative stress by activating multiple downstream genes, such as heme oxygenase-1 (HO-1), superoxide dismutase (SOD), glutathione (GSH), and catalase (CAT) [18, 19], by binding to the upstream antioxidant response element (ARE) sequence [20].

Several plant-derived antioxidants can activate the Nrf2 pathway and protect cells against oxidative damage [21]. Proanthocyanidins (PAC) are a group of polyphenolic flavonoids present in many vegetables, flowers, fruits, and nuts [22] and exhibit antibacterial, antiviral, antioxidant, and other pharmaceutical effects [23]. In addition, several studies have shown that PAC can activate the Nrf2 pathway [24, 25]. However, their potential therapeutic effect in GIOP is still elusive. We demonstrated for the first time that PAC can suppress osteoblast apoptosis and dysfunction during the GIOP development by activating the Nrf2 pathway, indicating that PAC are a suitable therapeutic option for GIOP.

2. Materials and Methods

2.1. Reagents, Antibodies, and Media. PAC (≥96%) and Dex were purchased from Sigma-Aldrich (St. Louis, MO, USA). Primary antibodies against COL1A1, RUNX2, and OCN were from Abcam (Cambridge, UK), and those targeting Nrf2, HO-1, Bax, Bcl-2, cleaved caspase-3, β-actin, and lamin B were obtained from Cell Signaling Technology (Danver, MA, USA). Fetal bovine serum (FBS), Dulbecco's Modified Eagle Medium (DMEM), and penicillin/streptomycin were purchased from Gibco BRL (Thermo Fisher Scientific, Waltham, MA, USA). All other chemicals used were of analytical grade complying with tissue and cell culture standards.

2.2. Cell Culture. Primary osteoblasts were isolated from the calvarial bone of 1-day-old Sprague Dawley rats by continuous digestion with trypsin-collagenase [26] and cultured in complete DMEM supplemented with 1% (v/v) penicillin-streptomycin and 10% (v/v) FBS under 5% CO_2 at 37°C. Medium was changed every other day, and the cells were passaged when 80-90% confluent. In brief, cells received the following treatment: (1) Dex group: cells were treated with 5 μM Dex for 48 hours, then cultured in complete DMEM medium for another 48 hours; (2) Dex+PAC group: cells were treated with 5 μM Dex for 48 hours and then cocultured with 0.1 and 1 μM PAC for another 48 hours; and (3) control group: untreated osteoblasts were cultured for the same period of time as controls.

2.3. Cytotoxicity Assay. The effect of PAC and Dex on osteoblast viability was determined using the Cell Counting Kit-8 (CCK-8) assay (MedChemExpress LLC; Monmouth Junction, NJ, USA). The cells were seeded in a 96-well plate at the density of 5×10^3 cells per well and treated with varying doses of PAC (0.01, 0.1, 1, and 10 μM) with or without Dex pretreatment for 48 hours. After 48 hours, 10 μl of CCK8 reagent was added to each well, and the cells were incubated for another hour. The absorbance or optical density (OD) at 450 nm was measured using the Multiskan GO microdisk spectrophotometer (Thermo Fisher Science, Waltham, MA, USA).

2.4. Osteogenic Differentiation of Primary Calvarial Osteoblasts. The cells were seeded in a 24-well plate at the density of 5×10^4 cells per well. After having received the indicated treatment, osteoblasts were cultured in DMEM supplemented with 20 μM ascorbic acid and 10 mM β-glycerophosphate. The media was replaced every other day. The alkaline phosphatase (ALP) activity was measured after 7 days of differentiation using the ALP Staining Kit (Beyotime Institute of Biotechnology; Jiangsu, China). For mineralization and bone nodule formation, the cells were cultured under osteogenic conditions for 21 days, fixed, and stained with Alizarin Red S (ARS) (Solarbio Science & Technology; Beijing, China).

2.5. Western Blotting. Total protein was extracted from cultured cells using RIPA lysis buffer (Beyotime Institute of Biotechnology) containing protease and phosphatase inhibitors (Sigma-Aldrich) for 30 min at 4°C. The nuclear and cytoplasmic protein fractions were separated using a commercial kit according to the manufacturer's instructions (Beyotime Institute of Biotechnology). The cell lysates were centrifuged, and the protein concentration in the supernatant was determined by the BCA Protein Assay Kit (Beyotime Institute of Biotechnology) as per the manufacturer's protocol. An equal amount of protein (20 μg) per sample was denatured in SDS loading buffer by boiling for 5 mins and resolved on a 10-15% SDS–polyacrylamide gel. The protein bands were then transferred overnight to polyvinylidene difluoride (PVDF) membranes (Merck Millipore; Burlington, MA, USA) at 4°C. After blocking with 5% skim milk diluted in Tris-buffered saline with 0.1% Tween 20 (TBST) for 2 hours at room temperature, the blots were probed for 12 hours with the suitable primary antibodies at 4°C. The membranes were washed thrice with TBST and incubated with the corresponding HRP-conjugated secondary antibodies for 4 hours at room temperature. The positive bands were visualized by enhanced chemiluminescence on a ChemiDoc XRS+ imager (Bio-Rad; Hercules, CA, USA) and quantified by densitometry analysis using Image Lab V3.0 software (Bio-Rad). The experiment was repeated thrice.

2.6. Immunofluorescence. Primary calvarial osteoblasts were cultured on glass coverslips under suitable conditions, fixed with 4% paraformaldehyde (PFA) for 15 min at room temperature, and then permeabilized with 0.5% (v/v) Triton X-100 in PBS for 20 mins. Nonspecific antibody binding

was blocked with 1% (w/v) goat serum albumin for 1 hour at room temperature, followed by overnight incubation with primary antibodies in 0.2% BSA-PBS at 4°C with gentle shaking. The cells were washed with PBS and incubated with fluorescence-conjugated secondary antibodies for 1 hour at room temperature in the dark. After counterstaining with DAPI for 5 mins at room temperature, the cells were viewed under the Olympus BX53 fluorescence microscope (Olympus Life Science; Tokyo, Japan). Integrated optical density (IOD) of the positively stained samples was calculated using Image-Pro Plus software (Media Cybernetics, Inc; Rockville, MD, USA).

2.7. *Transfection.* The siRNA targeting Nrf2 was obtained from the RiboBio company. The osteoblasts were transfected with the Nrf2 or control siRNA according to the manufacturer's protocol.

2.8. *Caspase-3 Activity Assay.* The caspase-3 activity in the suitably treated cells was measured using a Caspase-3 Activity Assay Kit (Nanjing Jiancheng Bioengineering Institute, Nanjing, China) as per the manufacturer's instructions. In general, treated cells were washed 3 times with PBS and resuspended in lytic buffer and placed on ice for 20 minutes. The lysis solution was then added to the reaction buffer contaning Ac-DEVD-pNA and incubated at 37°C for 2 hours. Subsequently, the absorbance of yellow pNA from its corresponding precursor was measured by a spectrometer at 405 nm. The caspase-3 activity was calculated as the ratio of the value obtained from the treated cells to the value obtained from untreated control cells.

2.9. *TUNEL Assay.* Apoptosis was measured using an in situ Cell Death Detection Kit (Roche, South San Francisco, CA, USA) according to the instruction of the manufacturer. The number of the apoptotic cells was counted in three random fields under a fluorescence microscope (Olympus Life Science; Tokyo, Japan).

2.10. *Quantification of SOD, CAT, and GPx Activities.* The suitably treated cells were washed twice with PBS and lysed on ice for 30 minutes. The activities of SOD, CAT, and GPx in the lysates were detected using commercial assay kits (Jiancheng Biotechnology, Nanjing, China) as per the manufacturer's instructions.

2.11. *Intracellular ATP and ROS Assay.* Intracellular ATP and ROS levels were measured using the ATP Assay and Reactive Oxygen Species Assay Kits according to the manufacturer's instructions (Beyotime, Shanghai, China).

2.12. *Mitochondrial Function Assays.* The mitochondrial membrane potential (MMP) and superoxide ion levels in the suitably treated osteoblasts were determined by, respectively, staining with JC-1 and MitoSox as per the manufacturer's guidelines (Beyotime, Shanghai, China). Stained cells were observed under a fluorescence microscope (Olympus Life Science; Tokyo, Japan).

2.13. *Transmission Electron Microscopy (TEM).* Treated primary calvarial osteoblasts were fixed in 2.5% glutaraldehyde for 12 hours at 4°C, postfixed in 2% osmium tetroxide for 1 hour, and stained with 2% uranyl acetate for 1 hour at room temperature. Then, cells were dehydrated in cold graded ethanol series (30%, 50%, 70%, 80%, 90%, 100% ethanol; 10 mins each) and washed three times with 100% acetone (20 min each time with gentle rocking). Next, cells were embedded in araldite epoxy resin, and semithin sections were cut and stained with toluidine blue. TEM images were captured on a Hitachi Field Emission Transmission Electron Microscope (Hitachi High-Technologies Corp.; Tokyo, Japan).

2.14. *Establishment of a Rat Model of GIOP.* All animal experiments were approved by the Animal Ethics Committee of The Second Affiliated Hospital and Yuying Children's Hospital of Wenzhou Medical University (Wenzhou, China) and conducted pursuant to the criteria outlined in the Guide for the Care and Use of Laboratory Animals (NIH, Bethesda, MD, USA). Forty-five 3-month-old SD male rats were purchased from Shanghai Laboratory Animal Center (SLACCAS; Shanghai, China) and housed under SPF conditions at 22-25°C and 12 hours of the light/dark cycle. All animals had free access to tap water and a standard rodent diet consisting of 2.5% casein, 0.8% phosphorus, 1% calcium, 70-80% carbohydrates, and 5% fat (Provimi Kliba AG, Kaiseraugst, Switzerland). After one week of acclimatization, the rats were randomly divided into the vehicle control (sham group), untreated GIOP, and PAC-treated GIOP groups ($n = 15$ each). GIOP was induced by daily intraperitoneal injections of 5 mg/kg Dex for 4 weeks as previously described [4], and the rats in the sham group received daily injections of PBS during the same period. After 4 weeks of Dex treatment, the animals showing signs of osteoporosis as per X-ray radiograph imaging were treated with the vehicle or PAC (10 mg/kg) for another 8 weeks. The rats were sacrificed after the treatment regimen, and the bilateral femurs were removed and fixed in 4% paraformaldehyde. All procedures were conducted in strict accordance with the Animal Care and Use Committee of Wenzhou Medical University (Wenzhou, China).

2.15. *Micro-CT Analysis.* Microstructural analysis of the distal femoral bones was performed using a cabinet cone-beam micro-CT system and associated software (μCT 50, Scanco Medical; Brüttisellen, Switzerland). The images were acquired at 70 kV, 200 μA, and a spatial resolution of 14.8 mm in all directions. Three-dimensional reconstructed images were generated, and the volume of interest (VOI) included the trabecular compartment 2 mm below the highest point of the growth plate to the distal 100 CT slices. Quantitative bone parameters assessed within the VOI included the percentage bone volume to tissue volume (BV/TV), the mean trabecular thickness (Tb.Th, mm), the mean trabecular number (Tb.N, 1/mm), the mean trabecular separation (Tb.Sp, mm), and the mean connective density (Conn.D, $1/mm^3$).

2.16. *Histology, Immunohistochemistry (IHC), and Immunofluorescence.* The fixed femurs were decalcified in

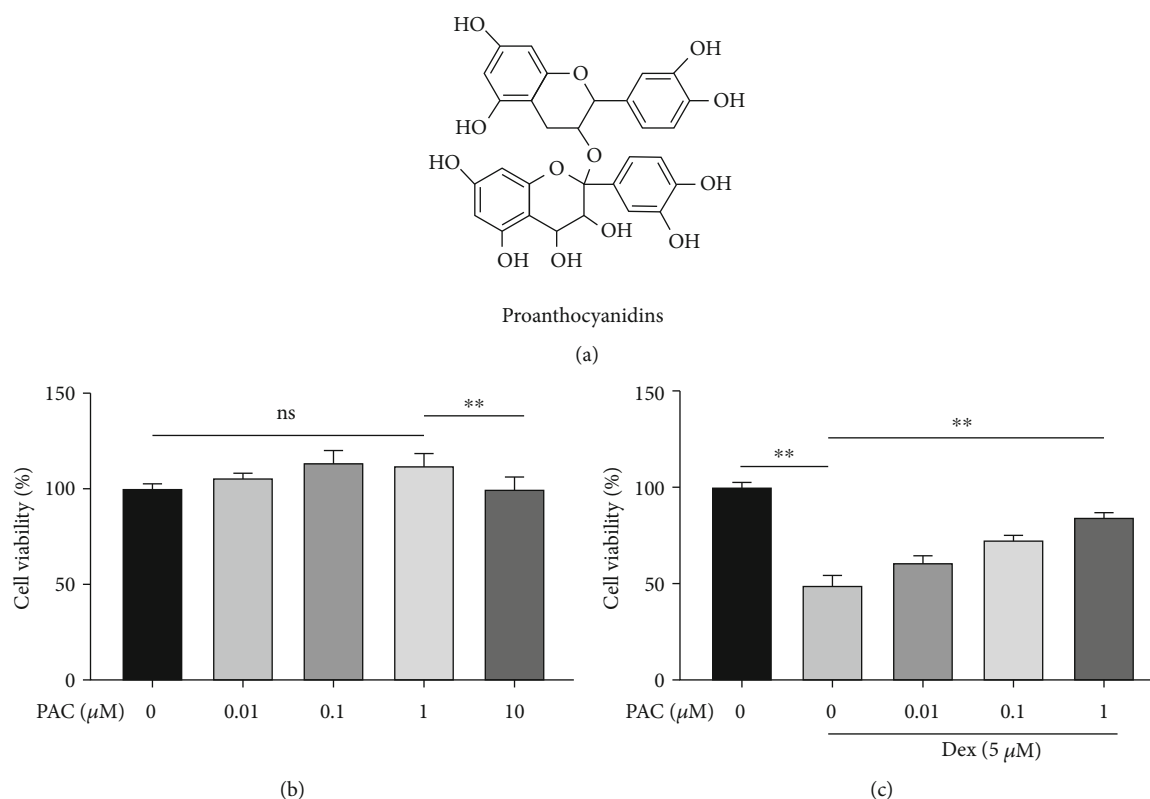Proanthocyanidins

(a)

(b)

(c)

FIGURE 1: Effects of PAC on osteoblast viability. (a) The chemical structure of PAC. (b) Percentage of viable cells receiving treatment with different PAC doses for 48 h. (c) Percentage of viable cells pretreated with Dex with/without different concentrations of PAC. The data in the figures represent the averages ± SEM of 5 times in duplicates. $^{**}p < 0.01$ versus the relative groups.

10% EDTA for 4 weeks, dehydrated through an ethanol gradient (70 to 100%), cleared with xylene, and embedded in paraffin. Hematoxylin-eosin and Mason trichrome staining were performed on longitudinal $4\,\mu$m-thick serial slices according to the manufacturer's instructions. For IHC, $6\,\mu$m-thick sections were incubated with the anti-Nrf2 primary antibody, followed by the horseradish peroxidase detection system according to the manufacturer's protocol (Vector Laboratories; Burlingame, CA, USA). For immuno-fluorescence staining, the sections were incubated overnight with the anti-Nrf2 antibody at 4°C, followed by the fluorochrome-conjugated secondary antibody at 37°C in the dark for 1 hour. After counterstaining with DAPI for 1 minute, the tissue sections were observed under a Olympus BX53 light/fluorescence microscope equipped with a Olympus DP71 digital camera (Olympus Life Science). The in situ Nrf2 expression was analyzed using Image-Pro Plus software.

2.17. Statistical Analyses. All statistical analyses were performed using the GraphPad Prism software (San Diego, CA, USA), and the data was presented as the mean ± standard error of mean (SEM) from at least three experimental repeats. Two-tailed Student's t-test was used to compare means between two groups, and one-way ANOVA with Bonferroni or Dunnett corrections was used for multiple comparisons. $p < 0.05$ was considered statistically significant.

3. Results

3.1. PAC Alleviated Dex-Induced Damage in Osteoblasts. PAC are electrophilic flavanols found predominantly in dark-colored plants (Figure 1(a)). We treated the primary osteoblasts with varying doses of PAC, and $1\,\mu$M was the highest nontoxic concentration (Figure 1(b)). Furthermore, PAC rescued the impaired viability of the Dex-treated cells in a dose-dependent manner (Figure 1(c)). Based on these results, 0.1 and $1\,\mu$M PAC were used for subsequent experiments. Dex treatment significantly increased the number of TUNEL positive apoptotic osteoblasts, which was alleviated by PAC (Figure 2(e)). Consistent with these findings, the proapoptotic caspase-3, cleaved caspase-3, and Bax were upregulated, the antiapoptotic Bcl-2 was downregulated in Dex-treated cells (Figures 2(a)–2(d), (f)), and these proteins returned to normal levels after PAC treatment. Taken together, our results indicated that PAC were able to ameliorate Dex-induced damage in osteoblasts.

3.2. PAC Neutralized Dex-Induced Oxidative Stress in Osteoblasts. The molecular basis of GIOP is the decreased osteogenic ability caused by high oxidative stress levels and mitochondrial dysfunction in the osteoblasts. Therefore, we also evaluated the effect of PAC on ROS production, mitochondrial dysfunction, and antioxidant enzyme activity in the Dex-treated osteoblasts. Compared to the untreated cells,
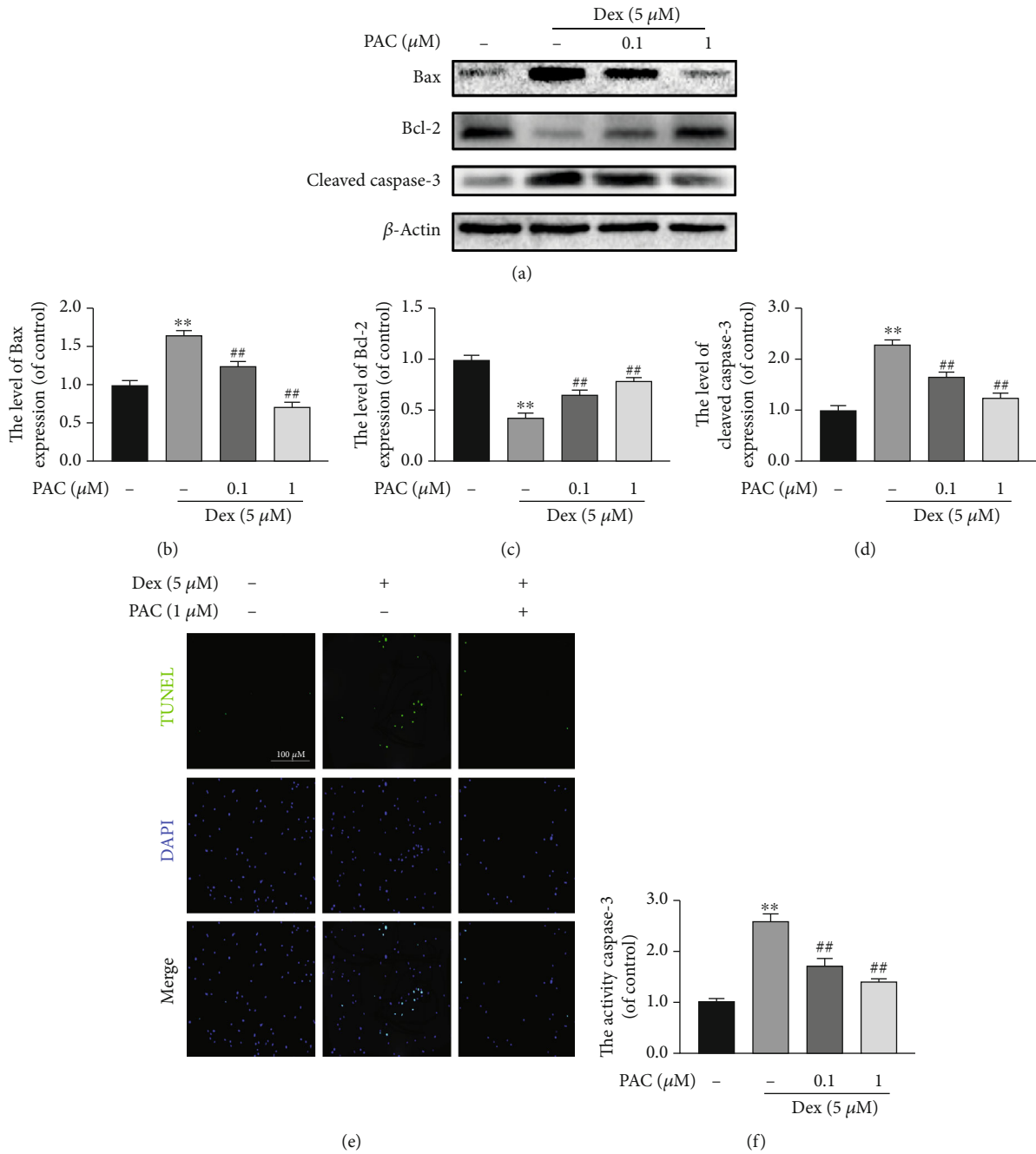
(a)

(b)

(c)

(d)

(e)

(f)

FIGURE 2: PAC suppressed Dex-induced apoptosis in osteoblasts. (a–d) Expression levels of cleaved caspase-3, Bcl-2, and Bax in the differentially treated osteoblasts. (e) Representative fluorescence images showing coculture with PAC (1 μM) reduced Dex-induced osteoblast apoptosis. (f) Caspase-3 activity in the differentially treated osteoblasts. The data in the figures represent the averages ± SEM of 5 times in duplicates. $^{**}p < 0.01$ versus the untreated group, $^{\#\#}p < 0.01$ versus the Dex group.

Dex exposure increased ROS accumulation, which was neutralized by PAC pretreatment (Figure 3(a)). The MMP and mitochondrial ROS were, respectively, detected using JC-1 and MitoSox probes. The Dex-treated cells had significantly lower MMP and elevated superoxide anion content compared to the control cells, and both were restored to near-physiological levels by PAC treatment (Figure 3(b)). This was further corroborated via TEM analysis, showing a deteriorating morphology of mitochondria after Dex exposure, which was restored by PAC treatment (Figure 3(c)).

In addition, Dex-treated osteoblasts, coculture with PAC, also restored the activities of SOD, CAT, and GPx (Figures 3(d)–3(f)), along with ATP levels (Figure 3(g)).

3.3. PAC Restored the Differentiation and Mineralization of Dex-Treated Osteoblasts. The osteogenic function of osteoblasts is inhibited by oxidative stress and mitochondrial dysfunction [4, 5]. Therefore, we next assessed the effect of PAC on the early differentiation and mineralization of the Dex-treated cells. Dex markedly reduced osteogenic
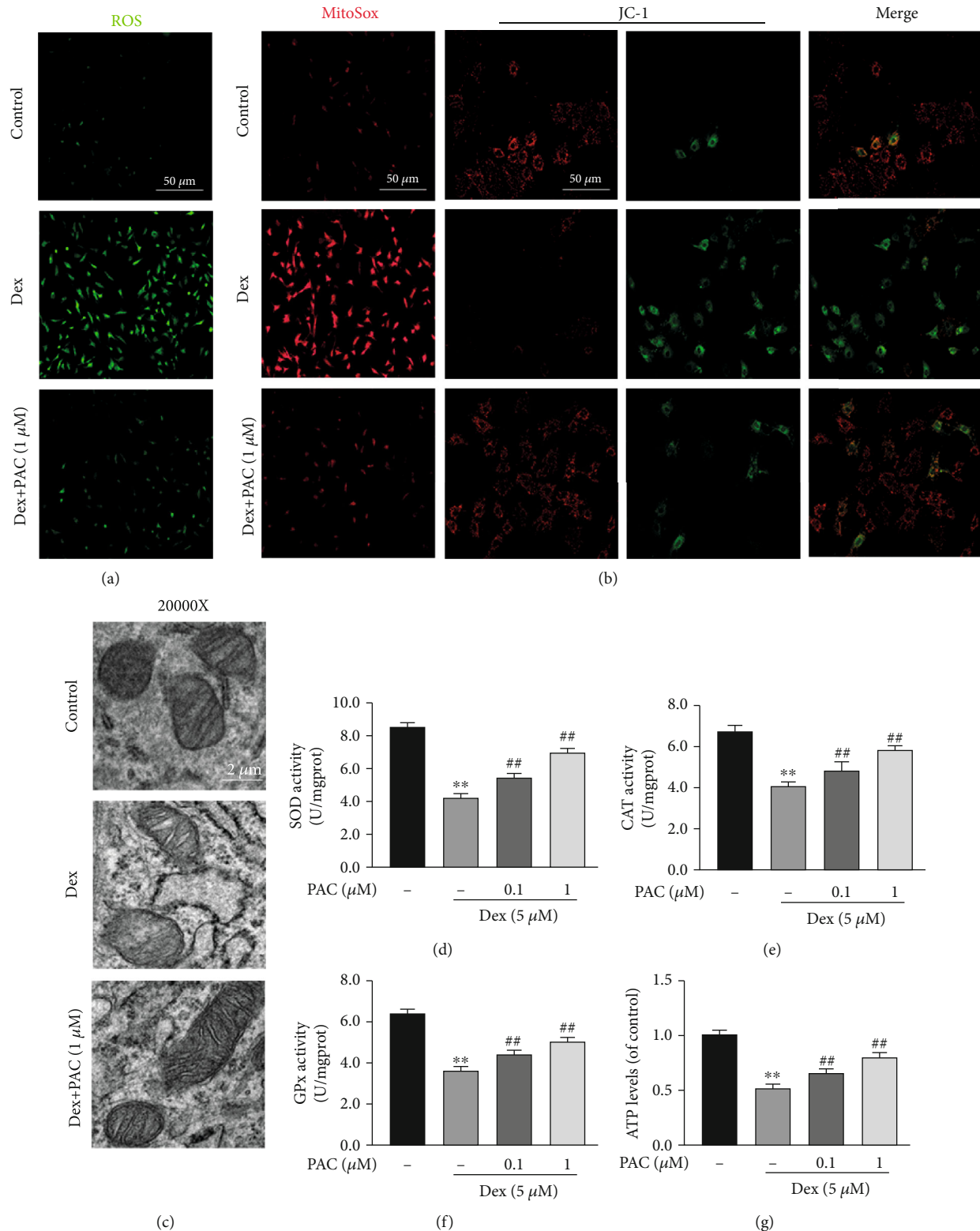
FIGURE 3: PAC neutralized Dex-induced oxidative stress and mitochondrial dysfunction in osteoblasts. (a) Representative images showing the ROS level in the differentially treated osteoblasts. (b) Representative images showing MitoSox and JC-1 intensities in the differentially treated osteoblasts. (c) Representative images showing mitochondrial morphology in the differentially treated osteoblasts. (d–f) The activities of SOD, CAT, and GPx in Dex-treated cells with/without PAC. (g) The ATP levels in the differentially treated osteoblasts. The data in the figures represent the averages ± SEM of 5 times in duplicates. $^{**}p < 0.01$ versus the untreated group, $^{\#\#}p < 0.01$ versus the Dex group.

differentiation, as measured by the ALP activity after 7 days of culture, and decreased the formation of calcium nodules by the 21st day (Figures 4(a) and 4(b)). However, cotreatment with PAC restored the ALP activity and the extent of mineralization in the Dex-treated osteoblasts, which also correlated with an upregulation of the osteogenic transcription factors RUNX2, COL1A1, and OCN after 7 days of osteogenic induction (Figures 4(c)–4(f)). Taken together, PAC protect osteoblasts against the inhibitory effects of Dex.

3.4. The Osteoprotective Effects of PAC Are Mediated by the Nrf2 Pathway. It was previously reported that PAC increased the nuclear translocation of Nrf2 in a lead-induced liver injury model, suggesting that the Nrf2 pathway likely mediates the protective effects of PAC [27]. As shown in Figures 5(a)–5(d), PAC treatment markedly reversed the inhibitory effect of Dex on the Nrf2 nuclear translocation and HO-1 expression and decreased the cytoplasmic Nrf2 levels in a dose-dependent manner (Figure 5(e)). Consistent with this, Nrf2 silencing abrogated the protective effects of PAC on the Dex-treated cells. Nrf2 knockdown partly decreased the expression levels of RUNX2, COL1A1, and OCN levels in the cells cotreated with PAC and Dex after 7 days of osteogenic induction (Figures 6(a)–6(d)) and reversed the beneficial effects of PAC on osteoblast differentiation and mineralization (Figures 6(e) and 6(f)). Taken together, PAC protect the osteoblast function by inducing the nuclear translocation of Nrf2 and activating its downstream pathway.

3.5. Pac Treatment Mitigated the Development of GIOP In Vivo. To further verify our assumption, the GIOP rat model was used in this study. The microstructure of the distal femur was determined by micro-CT scanning, and various parameters including BV/TV, Tb.Sp, Tb.Th, and Tb.N were calculated for each group (Figures 7(a)–7(e)). Compared to the untreated Dex-induced osteoporotic rats, 8 weeks of the PAC administration significantly increased BV/TV and Tb.N and decreased Tb.sp. Consistent with this, the histological examination of the distal femur sections indicated more numerous trabeculae in the PAC-treated versus untreated GIOP model. Moreover, the expression of Nrf2 in the distal femur was higher in the PAC-treated compared to the untreated animals (Figures 7(f)–7(i)). Taken together, PAC are potentially therapeutic against GIOP.

4. Discussion

In our study, we have proven for the first time that PAC can protect rat osteoblasts from oxidative stress, mitochondrial dysfunction, and osteogenic impairment induced by Dex. Mechanistically, as shown in Figure 8, PAC activated the antioxidant Nrf2 pathway and subsequently decreased ROS accumulation and mitochondrial superoxide levels in osteoblasts. In the in vivo GIOP model, PAC alleviated bone loss and upregulated the expression of Nrf2 in the distal femurs.

GCs are used to treat multiple inflammation-related diseases, and an estimated 1-2% of the population is currently receiving long-term GC treatment [28, 29]. Dex is a synthetic GC that accelerates osteoporosis and significantly increases the risk of fracture when used for an extended period of time [30]. Studies show that it can inhibit osteoblast proliferation and promote apoptosis [31, 32] by triggering oxidative stress and mitochondrial dysfunction. Li et al. found that Dex treatment increased intracellular ROS accumulation as well as the dissipation of MMP in MG63 cells [4]. The mitochondrial accumulation of ROS induced a vicious cycle of oxidative stress and mitochondrial dysfunction, which culminated in the activation of the apoptotic pathway [33]. Almeida et al. reported MMP loss and apoptosis in osteoblasts following Dex treatment [34]. Consistent with these studies, we found that Dex treatment led to osteoblast malfunction and apoptosis. Therefore, reducing the level of oxidative stress and mitochondrial dysfunction in osteoblasts is a potentially effective method for treating GIOP.

Proanthocyanidins (PAC) are a group of antioxidant polyphenolic flavonoids present in the dark pigmented fruits and vegetables [35]. Rodríguez-Pérez et al. reported that PAC prevent the H_2O_2-induced mitochondrial dysfunction and apoptosis in embryonic kidney cells [36]. In addition, the PAC administration protected against the iron overload-induced nephrotoxicity in rats [37]. Consistent with the above, we found that PAC significantly reduced Dex-induced oxidative stress and mitochondrial dysfunction in osteoblasts. Furthermore, PAC reduced the high rate of apoptosis in Dex-treated cells, downregulated the expression of apoptosis-associated protein Bax and cleaved caspase-3, and upregulated the anti-apoptosis protein Bcl-2. These results indicated that PAC may have an antiapoptosis effect to osteoblasts via attenuating the level of oxidative stress.

The major cause of bone loss in GIOP is the decrease in the osteoblast function. Dex inhibited osteoblast differentiation and accelerated the development of bone loss [4]. In addition, Dex disharmonizes organelle homeostasis within osteoblasts, thereby exacerbating its destiny of malfunction [32]. In the current study, we observed that Dex treatment reduced the expression of osteogenesis-related proteins RUNX2, COL1A1, and OCN, which was accompanied by the loss of osteogenic phenotype of ALP and ARS. Furthermore, coculture with PAC upregulated the expression of these proteins, which were suppressed by Dex and subsequently restored osteoblastogenesis in vitro. In vivo PAC treatment potently inhibited bone loss and microarchitechiture destruction induced by Dex. Therefore, PAC protect osteoblasts from Dex-induced oxidative stress and mitochondrial dysfunction and eventually restored osteoblastic function.

Nrf2 is considered an important transcription factor, and its activation can upregulate the expression of downstream genes of multiple antioxidant enzymes, such as HO-1, SOD, CAT, and GPx [5]. Consistent with previous reports that PAC activated the Nrf2 pathway, PAC facilitated the Nrf2 nuclear translocation and upregulated the expression of antioxidant enzymes in Dex-treated osteoblasts, which eventually lowered the level of oxidative stress and enhanced
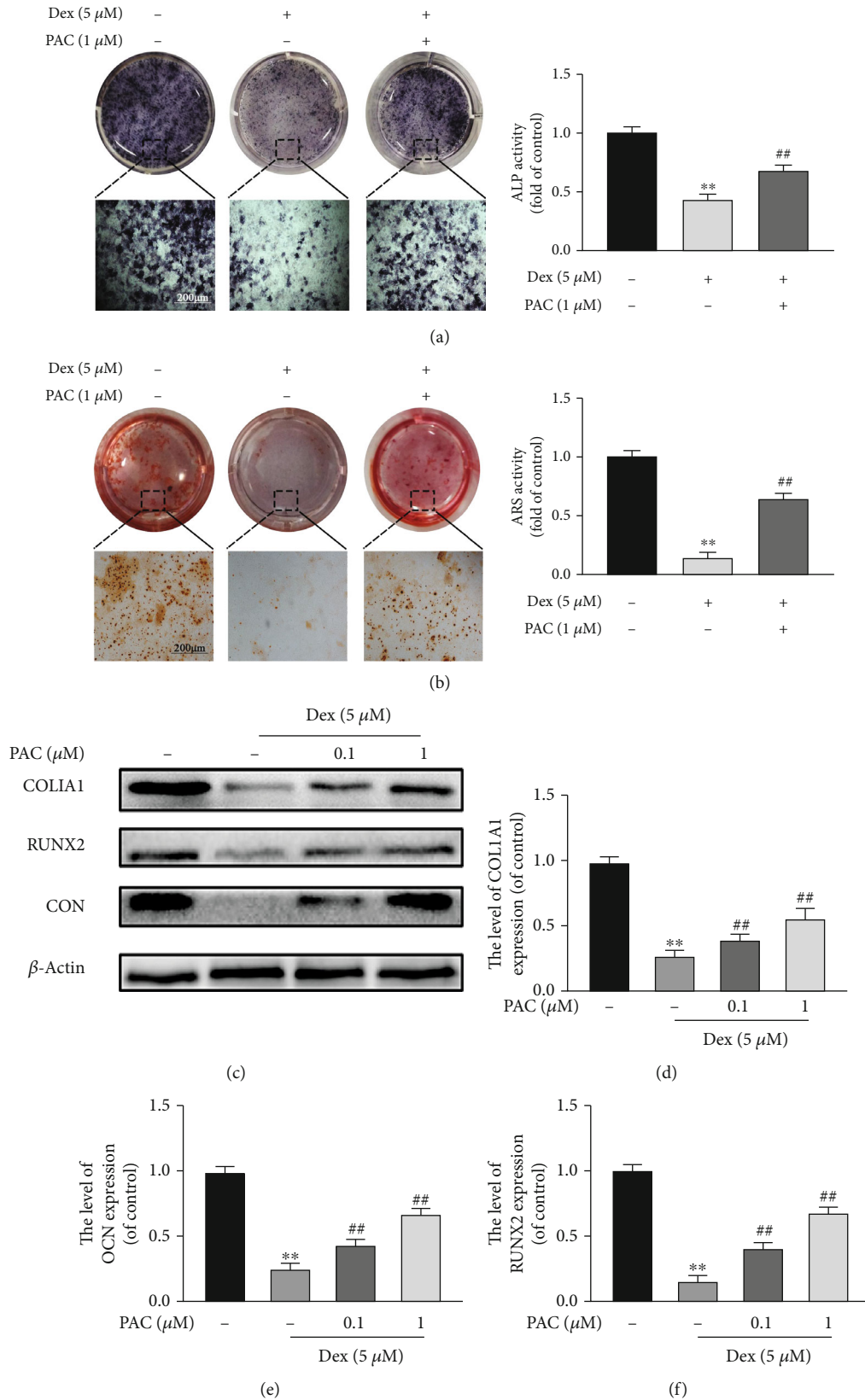
(a)

(b)

(c)

(d)

(e)

(f)

FIGURE 4: PAC restored differentiation and mineralization of Dex-treated osteoblast. Representative images showing (a) ALP staining on the 7th day and (b) ARS staining on the 21st day of osteogenic induction in differentially treated osteoblasts. (c–f) Expression levels of RUNX2, COL1A1, and OCN in the differentially treated osteoblasts. Data are the average ± SEM of 3 independent experiments. $^{**}p < 0.01$ versus the untreated group, $^{##}p < 0.01$ versus the Dex group.

(a)

(b)

(c)

(d)

(e)
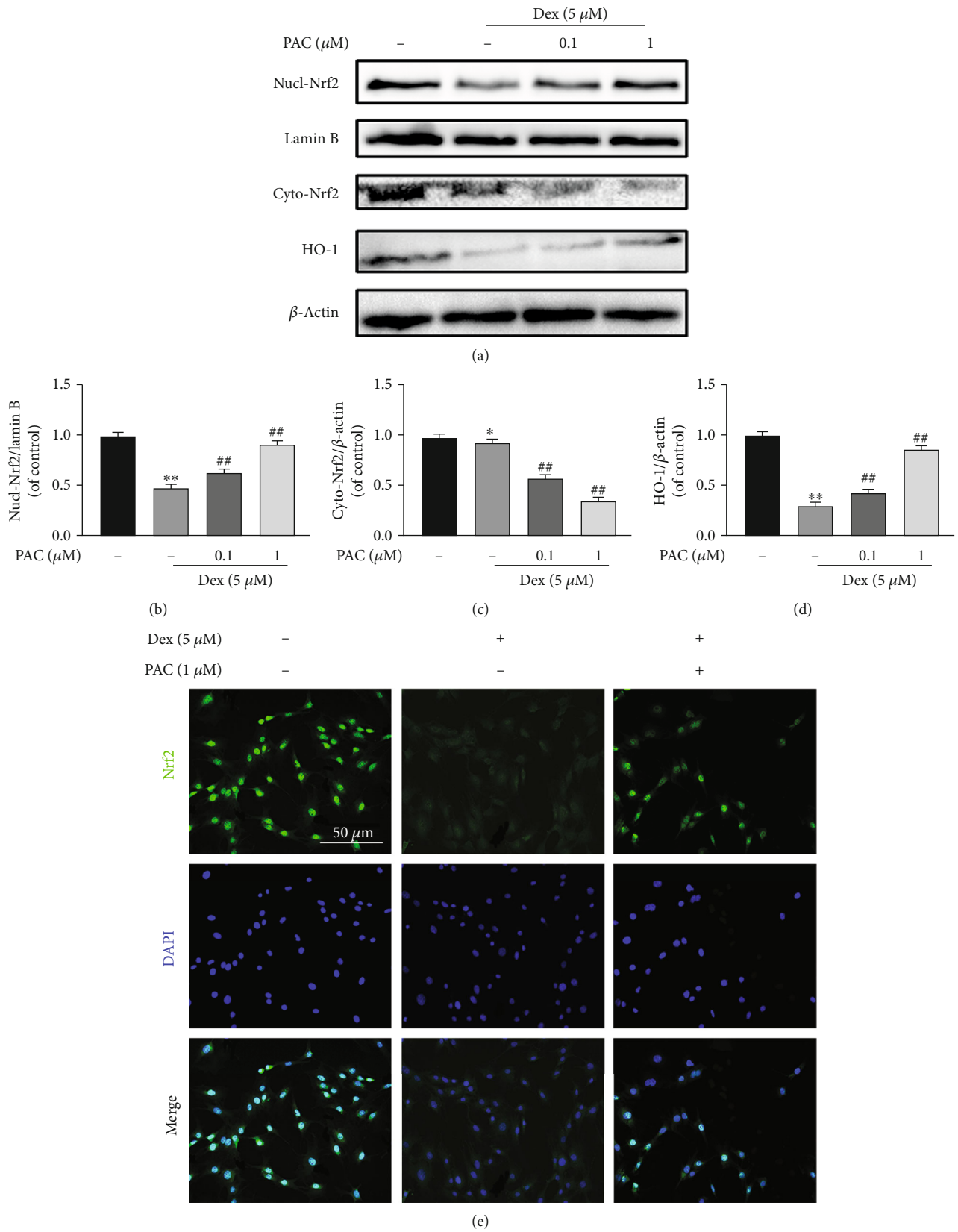
Figure 5: PAC activated the Nrf2 pathway in osteoblasts. (a–d) Immunoblot showing Nrf2 and HO-1 levels in the differentially treated osteoblasts. (e) Representative fluorescence images showing Nrf2 localization in the differentially treated cells. Data are the averages ± SEM of 3 independent experiments. $^*p < 0.05$, $^{**}p < 0.01$ versus the untreated group, $^{##}p < 0.01$ versus the Dex group.
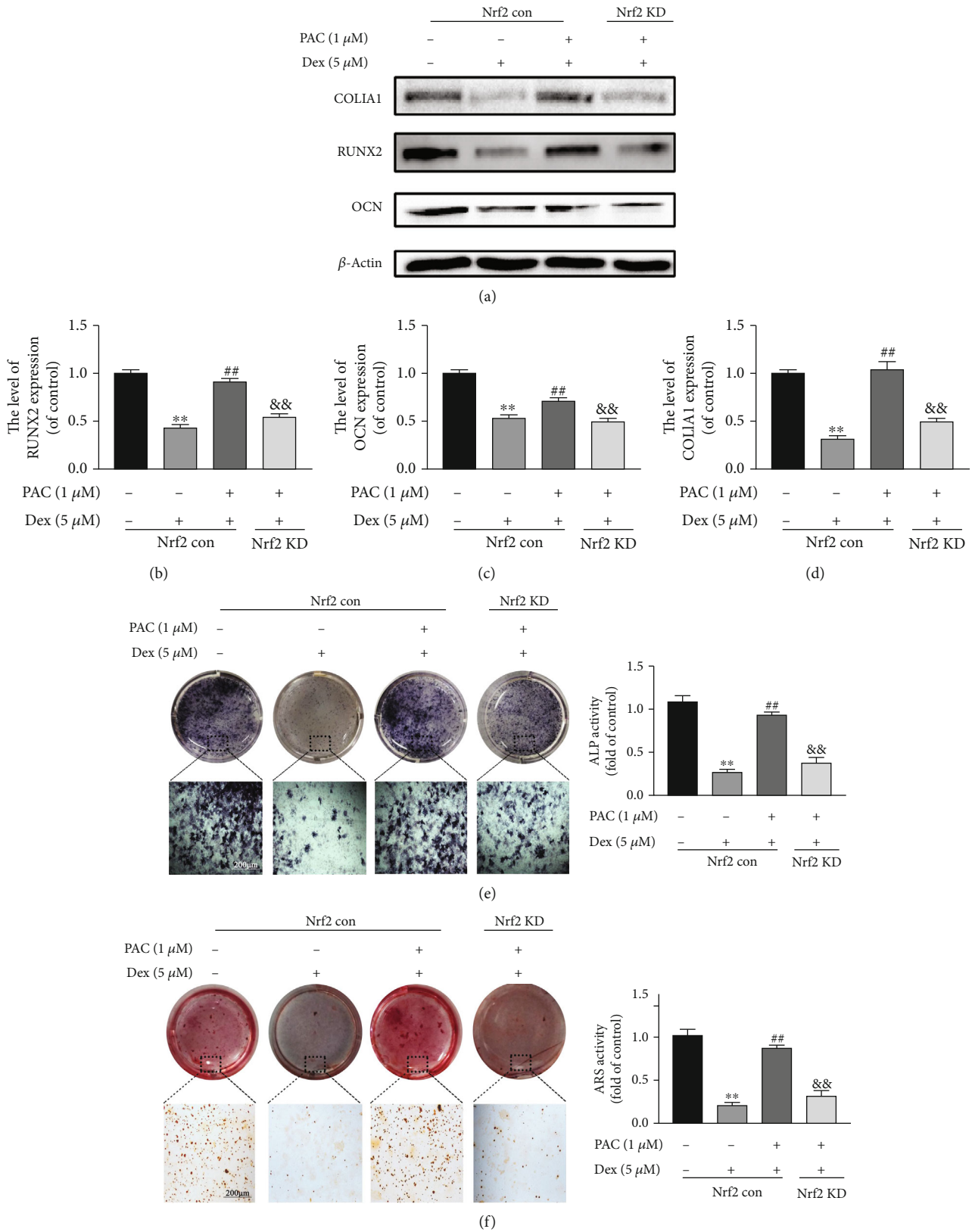
FIGURE 6: The Nrf2 pathway mediated the osteoprotective effects of PAC. Wild type (Nrf2 con) and Nrf2-knockdown osteoblasts were treated 1 μM PAC with/out 5 μM Dex pretreatment for 2 days. (a–d) Immunoblot showing RUNX2, COL1A1, and OCN in the differentially treated osteoblasts. Representative images showing ALP (e) staining on the 7th day and (f) ARS staining on the 21st day of osteogenic induction in differentially treated osteoblasts. Data are the averages $\pm$ SEM of 3 independent experiments. [**]$p < 0.01$ versus the untreated group, [##]$p < 0.01$ versus the Dex group, [&&]$p < 0.01$ versus the Dex+PAC group.
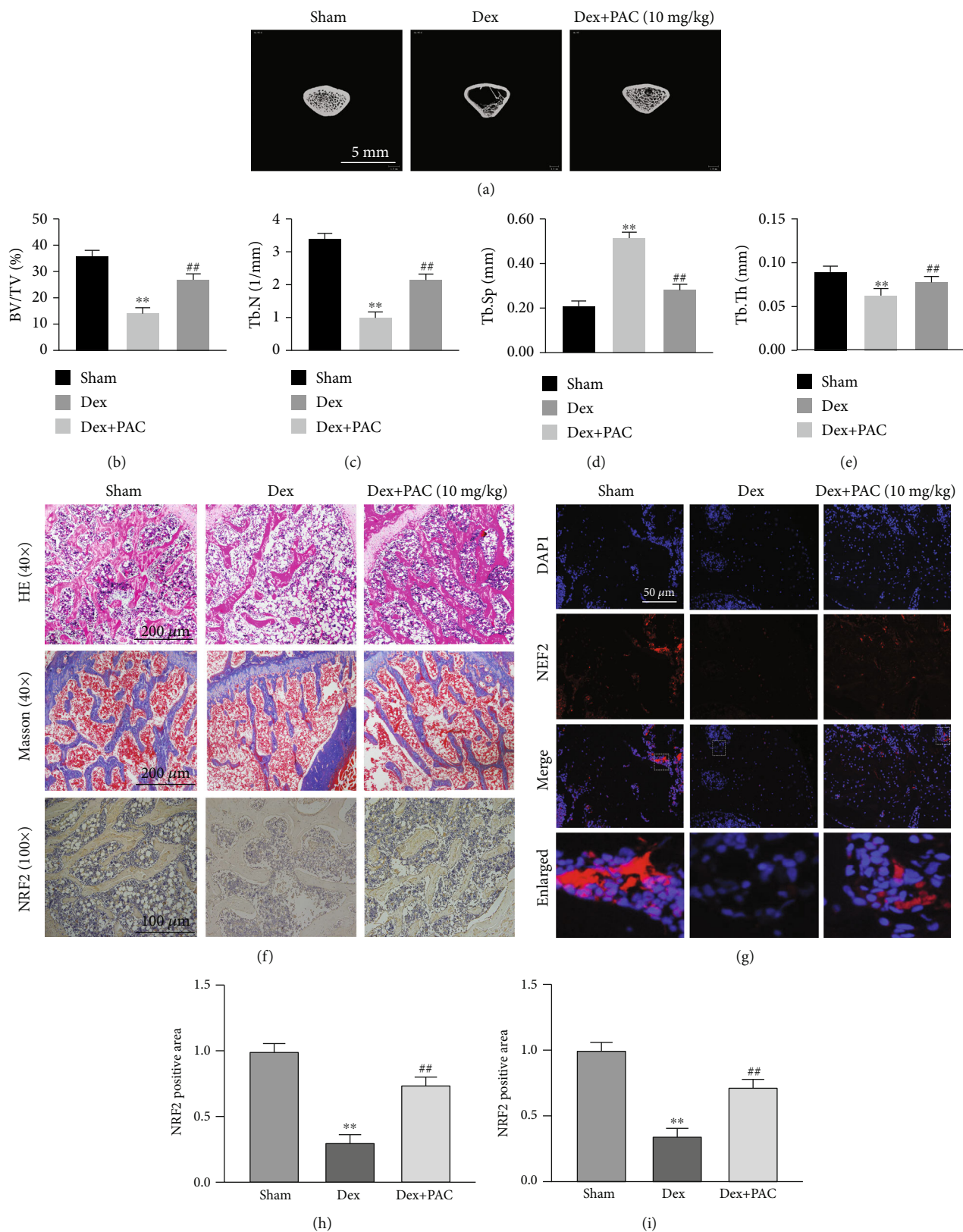
FIGURE 7: PAC treatment mitigated the development of GIOP in vivo. (a–e) Representative micro-CT images of the longitudinal and transverse sections of the distal femurs and the BV/TV, Tb.Sp, Tb.N, and Tb.Th values in the differentially treated animals. (f) Representative images of H&E staining, Masson's staining, and Nrf2 immunohistochemical (IHC) staining of the metaphyseal tissue of the thigh and (h) quantification of IHC. (g, i) Representative immunofluorescence image and quantification of the Nrf2 expression. Data are expressed as averages ± SEM of 3 times in duplicates. $^{**}p < 0.01$ vs the SHAM group, $^{##}p < 0.01$ vs. the DEX group.
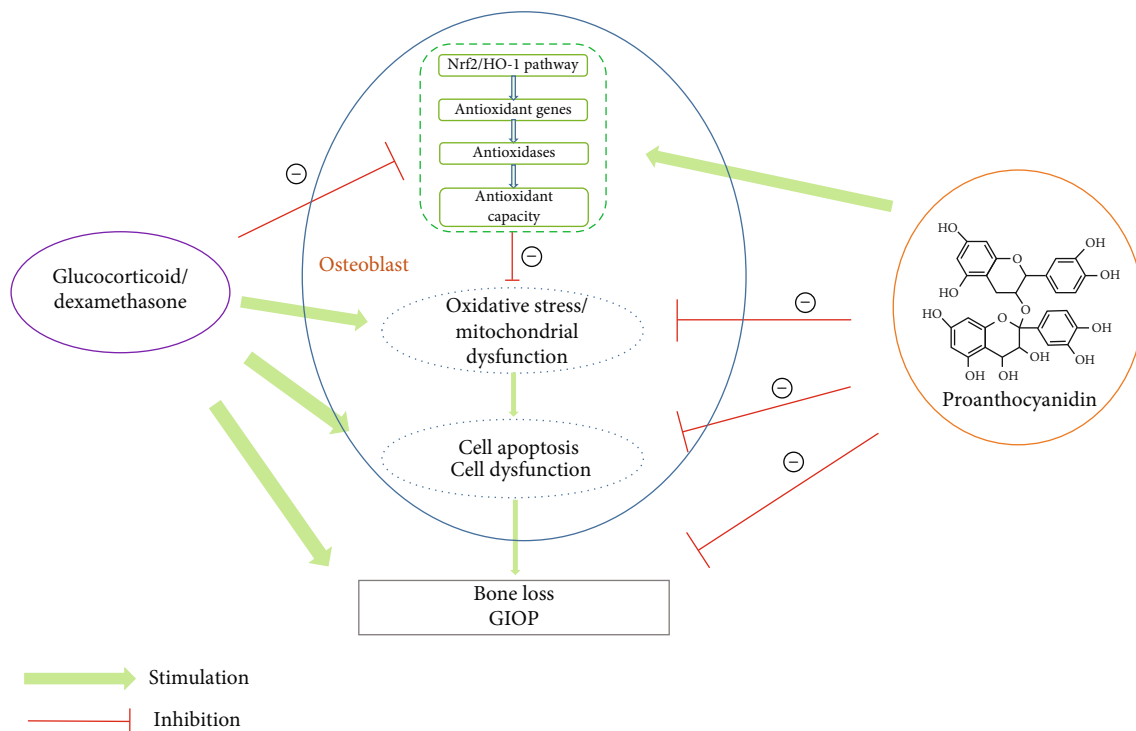
FIGURE 8: Mechanisms of the PAC action on GIOP. PAC reduces Dex-induced ROS accumulation and mitochondrial dysfunction in osteoblasts and prevents bone loss by activating the Nrf2 pathway.

osteogenic function. In addition, knocking down Nrf2 abrogated the osteoprotective effects of PAC, which further indicated that the Nrf2 pathway mediated the PAC action. Consistent with the in vitro experiments, PAC prevented GIOP progression and restored the Nrf2 in situ expression in a rat model.

5. Conclusion

To sum up, our study proved that PAC protected osteoblasts against Dex-induced oxidative stress, mitochondrial dysfunction, and osteogenic impairment by activating the Nrf2 pathway. In addition, the PAC administration suppresses the process of the GIOP development and mitigates the GIOP development in vivo. However, a potential limitation of our study is that we did not compare the effect of PAC to several clinical medications used for the treatment in GIOP patients, whereas this comparison could help us evaluate PAC as a remedy for GIOP. Thus, this needs to be proved in future studies. Despite this limitation, our study has shown that Dex-induced oxidative stress and mitochondrial dysfunction are deleterious for the osteoblast differentiation and mineralization function. Meanwhile, these results, PAC supplementation may significantly improve clinical outcomes of GIOP patients.

Data Availability

The data used to support the findings of this study are available from the corresponding author upon request.

Conflicts of Interest

The authors have no conflicts of interest.

Authors' Contributions

All authors that were listed made substantial contributions to the study. Lei Yang, Liang Chen, Sun-li Hu, Jun Xie, and De-Yi Yan participated in the experimental design and contributed to reagents, materials, and analytical tools. She-Ji Weng, Jia-Hao Tang, Zhong-Jie Xie, Zong-Yi Wu, and Bing-Zhang Wang were also involved in the experiments. Lei Yang and Liang Chen wrote the manuscript. Liang Chen, De-Yi Yan, and She-Ji Weng performed the data analysis. All authors read and approved the final version of the manuscript. All data shown in the figure are from the above authors' experiments.

Acknowledgments

Supplementary Materials

Figure 1: effects of PAC on cell viability. Osteoblasts received different concentrations of PAC for 48 hours. The data in the figure represent the averages ± SEM of 3 times in duplicates. $^{*}p < 0.01$, $^{**}p < 0.01$ versus the untreated group. Figure 2:

effects of different treating time of PAC on Dex-induced osteoblast viability. Percentage of viable cells received indicated treatment. The data in the figure represent the averages ± SEM of 3 times in duplicates. $**p < 0.01$ versus the untreated group, $\#p < 0.05$, $\#\#p < 0.01$ versus the Dex group. (Supplementary Materials)

References

[1] H. Schäcke, W. D. Döcke, and K. Asadullah, "Mechanisms involved in the side effects of glucocorticoids," *Pharmacology & therapeutics*, vol. 96, no. 1, pp. 23–43, 2002.

[2] Y. Xu, J. Mu, Z. Xu et al., "Modular acid-activatable acetone-based ketal-linked nanomedicine by dexamethasone prodrugs for enhanced anti-rheumatoid arthritis with low side effects," *Nano Letters*, vol. 20, no. 4, pp. 2558–2568, 2020.

[3] W. N. Xu, H. L. Zheng, R. Z. Yang, L. S. Jiang, and S. D. Jiang, "HIF-1α regulates glucocorticoid-induced osteoporosis through PDK1/AKT/mTOR signaling pathway," *Frontiers in Endocrinology*, vol. 10, 2020.

[4] Y. Li, Y. Zhang, X. Zhang et al., "Aucubin exerts anti-osteoporotic effects by promoting osteoblast differentiation," *Aging*, vol. 12, no. 3, pp. 2226–2245, 2020.

[5] D. Han, X. Gu, J. Gao et al., "Chlorogenic acid promotes the Nrf2/HO-1 anti-oxidative pathway by activating p21$^{Waf1/Cip1}$ to resist dexamethasone-induced apoptosis in osteoblastic cells," *Free radical biology & medicine*, vol. 137, pp. 1–12, 2019.

[6] J. Compston, "Glucocorticoid-induced osteoporosis: an update," *Endocrine*, vol. 61, no. 1, pp. 7–16, 2018.

[7] G. Shen, H. Ren, Q. Shang et al., "Autophagy as a target for glucocorticoid-induced osteoporosis therapy," *Cellular and Molecular Life Sciences*, vol. 75, no. 15, pp. 2683–2693, 2018.

[8] K. Hartmann, M. Koenen, S. Schauer et al., "Molecular actions of glucocorticoids in cartilage and bone during health, disease, and steroid therapy," *Physiological reviews*, vol. 96, no. 2, pp. 409–447, 2016.

[9] R. Rizzoli, "Towards a better management of glucocorticoid-induced osteoporosis?," *Nature Reviews Rheumatology*, vol. 13, no. 11, pp. 635-636, 2017.

[10] H. Li, W. Qian, X. Weng et al., "Glucocorticoid receptor and sequential P53 activation by dexamethasone mediates apoptosis and cell cycle arrest of osteoblastic MC3T3-E1 cells," *PLoS One*, vol. 7, no. 6, article e37030, 2012.

[11] Y. F. Zhen, G. D. Wang, L. Q. Zhu et al., "P53 dependent mitochondrial permeability transition pore opening is required for dexamethasone-induced death of osteoblasts," *Journal of cellular physiology*, vol. 229, no. 10, pp. 1475–1483, 2014.

[12] H. Kumar, I. S. Kim, S. V. More, B. W. Kim, and D. K. Choi, "Natural product-derived pharmacological modulators of Nrf2/ARE pathway for chronic diseases," *Natural product reports*, vol. 31, no. 1, pp. 109–139, 2014.

[13] R. H. Bhogal, C. J. Weston, S. M. Curbishley, D. H. Adams, and S. C. Afford, "Autophagy: a cyto-protective mechanism which prevents primary human hepatocyte apoptosis during oxidative stress," *Autophagy*, vol. 8, no. 4, pp. 545–558, 2012.

[14] R. Castellani, K. Hirai, G. Aliev et al., "Role of mitochondrial dysfunction in Alzheimer's disease," *Journal of neuroscience research*, vol. 70, no. 3, pp. 357–360, 2002.

[15] C. Zhao, D. D. Gillette, X. Li, Z. Zhang, and H. Wen, "Nuclear factor E2-related factor-2 (Nrf2) is required for NLRP3 and AIM2 inflammasome activation," *Journal of Biological Chemistry*, vol. 289, no. 24, pp. 17020–17029, 2014.

[16] L. Ibáñez, M. L. Ferrándiz, R. Brines, D. Guede, A. Cuadrado, and M. J. Alcaraz, "Effects of Nrf2 deficiency on bone microarchitecture in an experimental model of osteoporosis," *Oxidative medicine and cellular longevity*, vol. 2014, Article ID 726590, 9 pages, 2014.

[17] X. Sun, Z. Xie, B. Hu et al., "The Nrf2 activator RTA-408 attenuates osteoclastogenesis by inhibiting STING dependent NF-κb signaling," *Redox biology*, vol. 28, article 101309, 2020.

[18] T. W. Kensler, N. Wakabayashi, and S. Biswal, "Cell survival responses to environmental stresses via the Keap1-Nrf2-ARE pathway," *Annual review of pharmacology and toxicology*, vol. 47, no. 1, pp. 89–116, 2007.

[19] D. Malhotra, E. Portales-Casamar, A. Singh et al., "Global mapping of binding sites for Nrf2 identifies novel targets in cell survival response through ChIP-Seq profiling and network analysis," *Nucleic acids research*, vol. 38, no. 17, pp. 5718–5734, 2010.

[20] X. Shi and B. Zhou, "The role of Nrf2 and MAPK pathways in PFOS-induced oxidative stress in zebrafish Embryos," *Toxicology*, vol. 115, no. 2, pp. 391–400, 2010.

[21] S. K. Niture, J. W. Kaspar, J. Shen, and A. K. Jaiswal, "Nrf2 signaling and cell survival," *Toxicology and applied pharmacology*, vol. 244, no. 1, pp. 37–42, 2010.

[22] V. Nandakumar, T. Singh, and S. K. Katiyar, "Multi-targeted prevention and therapy of cancer by proanthocyanidins," *Cancer letters*, vol. 269, no. 2, pp. 378–387, 2008.

[23] Z. Ouyang, X. Guo, X. Chen et al., "Hypericin targets osteoclast and prevents breast cancer-induced bone metastasis via NFATc1 signaling pathway," *Oncotarget*, vol. 9, no. 2, pp. 1868–1884, 2018.

[24] M. Xu, Q. Niu, Y. Hu, G. Feng, H. Wang, and S. Li, "Proanthocyanidins antagonize arsenic-induced oxidative damage and promote arsenic methylation through activation of the Nrf2 signaling pathway," *Oxidative medicine and cellular longevity*, vol. 2019, Article ID 8549035, 19 pages, 2019.

[25] S. A. Rajput, L. Sun, N. Y. Zhang et al., "Grape seed proanthocyanidin extract alleviates aflatoxinB$_1$-induced immunotoxicity and oxidative stress via modulation of NF-κB and Nrf2 signaling pathways in broilers," *Toxins*, vol. 11, no. 1, 2019.

[26] A. D. Bakker and J. Klein-Nulend, "Osteoblast isolation from murine calvaria and long bones," *Methods in Molecular Biology*, vol. 816, pp. 19–29, 2012.

[27] B. Liu, H. Jiang, J. Lu et al., "Grape seed procyanidin extract ameliorates lead-induced liver injury via miRNA153 and AKT/GSK-3β/Fyn-mediated Nrf2 activation," *The Journal of nutritional biochemistry*, vol. 52, pp. 115–123, 2018.

[28] L. Fardet, I. Petersen, and I. Nazareth, "Prevalence of long-term oral glucocorticoid prescriptions in the UK over the past 20 years," *Rheumatology*, vol. 50, no. 11, pp. 1982–1990, 2011.

[29] R. A. Overman, J. Y. Yeh, and C. L. Deal, "Prevalence of oral glucocorticoid usage in the United States: a general population perspective," *Arthritis care & research*, vol. 65, no. 2, pp. 294–298, 2013.

[30] E. Hsu and M. Nanes, "Advances in treatment of glucocorticoid-induced osteoporosis," *Current opinion in endocrinology, diabetes, and obesity*, vol. 24, no. 6, pp. 411–417, 2017.

[31] S. Walsh, G. R. Jordan, C. Jefferiss, K. Stewart, and J. N. Beresford, "High concentrations of dexamethasone suppress

the proliferation but not the differentiation or further maturation of human osteoblast precursors *in vitro*: relevance to glucocorticoid-induced osteoporosis," *Rheumatology*, vol. 40, no. 1, pp. 74–83, 2001.

[32] H. Kang, H. Chen, P. Huang et al., "Glucocorticoids impair bone formation of bone marrow stromal stem cells by reciprocally regulating microRNA-34a-5p," *Osteoporosis International*, vol. 27, no. 4, pp. 1493–1505, 2016.

[33] J. F. Turrens, "Mitochondrial formation of reactive oxygen species," *The Journal of physiology*, vol. 552, no. 2, pp. 335–344, 2003.

[34] M. Almeida, L. Han, E. Ambrogini, R. S. Weinstein, and S. C. Manolagas, "Glucocorticoids and tumor necrosis factor α increase oxidative stress and suppress Wnt protein signaling in osteoblasts," *Journal of Biological Chemistry*, vol. 286, no. 52, pp. 44326–44335, 2011.

[35] Q. Sun, N. Jia, X. Li, J. Yang, and G. Chen, "Grape seed proanthocyanidins ameliorate neuronal oxidative damage by inhibiting GSK-3β-dependent mitochondrial permeability transition pore opening in an experimental model of sporadic Alzheimer's disease," *Aging*, vol. 11, no. 12, pp. 4107–4124, 2019.

[36] C. Rodríguez-Pérez, B. García-Villanova, E. Guerra-Hernández, and V. Verardo, "Grape seeds proanthocyanidins: an overview of in vivo bioactivity in animal models," *Nutrients*, vol. 11, no. 10, 2019.

[37] S. Yun, D. Chu, X. He, W. Zhang, and C. Feng, "Protective effects of grape seed proanthocyanidins against iron overload-induced renal oxidative damage in rats," *Journal of Trace Elements in Medicine and Biology*, vol. 57, article 126407, 2020.

Research Article

Pterostilbene Attenuates Cocultured BV-2 Microglial Inflammation-Mediated SH-SY5Y Neuronal Oxidative Injury via SIRT-1 Signalling

Qiang Zhu,[1,2] **Tao Tang,**[2] **Haixiao Liu,**[3] **Yinxue Sun** ⓘ**,**[4,5] **Xiaogang Wang,**[1] **Qiang Liu,**[1] **Long Yang,**[4] **Zhijie Lei,**[4] **Zhao Huang,**[4] **Zhao Chen,**[4] **Qiang Lei,**[4] **Mingyang Song,**[4] **and Bodong Wang** ⓘ[1]

[1]*Department of Neurosurgery, The 960th hospital, 25th Shifan Road, Jinan, 250031 Shandong, China*
[2]*Department of Neurosurgery, Yan'an University Affiliated Hospital, Yongxiang Road, Baota District, Yan'an, 716000 Shaanxi, China*
[3]*Department of Neurosurgery, Tangdu Hospital, The Fourth Military Medical University, 1st Xinsi Road, Xi'an, 710038 Shaanxi, China*
[4]*The 960th hospital, 25th Shifan Road, Jinan, 250031 Shandong, China*
[5]*Department of Traditional Chinese Medicine, Shandong University of Traditional Chinese Medicine, Jinan, Shandong 250355, China*

Correspondence should be addressed to Bodong Wang; wbd006@fmmu.edu.cn

Received 19 May 2020; Accepted 2 July 2020; Published 5 August 2020

Guest Editor: Marina Soković

Microglial inflammation plays an important part in the progression of multiple neurological diseases, including neurodegenerative diseases, stroke, depression, and traumatic encephalopathy. Here, we aimed to explore the role of pterostilbene (PTE) in the microglial inflammatory response and subsequent damage of cocultured neural cells and partially explain the underlying mechanisms. In the coculture system of lipopolysaccharide-activated BV-2 microglia and SH-SY5Y neuroblastoma, PTE (only given to BV-2) exhibited protection on SH-SY5Y cells, evidenced by improved SH-SY5Y morphology and viability and LDH release. It also attenuated SH-SY5Y apoptosis and oxidative stress, evidenced by TUNEL and DCFH-DA staining, as well as MDA, SOD, and GSH levels. Moreover, PTE upregulated SIRT-1 expression and suppressed acetylation of NF-κB p65 subunit in BV-2 microglia, thus decreasing the inflammatory factors, including TNF-α and IL-6. Furthermore, the effects above were reversed by SIRT-1 inhibitor EX527. These results suggest that PTE reduces the microglia-mediated inflammatory response and alleviates subsequent neuronal apoptosis and oxidative injury via increasing SIRT-1 expression and inhibiting the NF-κB signalling pathway.

1. Introduction

Inflammation is considered to play a pivotal part in diverse diseases, including neurodegenerative diseases [1, 2], brain trauma [3], stroke [4], infection [5], and even mental disorders [6], in the central nervous system (CNS). Accumulating evidences suggest that microglia, the resident innate immune cells, which accounts for 10% of CNS cells, are the active participants in the pathophysiological processes related to these neuroinflammatory diseases [7]. In physiological situations,

the microglia detect, transduce, integrate, and respond to extracellular signals, and participate in brain development and maintenance of CNS homeostasis by regulating programmed cell death, phagocytosis, and synaptic plasticity [7]. However, microglia dysfunction in pathological conditions and promote neurotoxicity through excessive inflammatory cytokine release [8]. Studies have shown that microglia-mediated inflammation and production of proinflammatory factors, including interleukins (ILs) and tumour necrosis factor (TNF) or noninflammatory factors, such as superoxide

ions, are important pathogenic bases of neurological diseases, such as intracranial infections, stroke, trauma, and Alzheimer's disease (AD) [1–6]. These overly released superoxide and cytokines trigger the oxidative injury and apoptosis of neurons. Therefore, targeting microglial functions and regulating microglia-mediated inflammatory processes and oxidative stress may yield potent paradigms for therapies of CNS disorders that were inconceivable under a neuron-centric view of the brain [7].

Pterostilbene (PTE), also known as trans-3,5-dimethoxy-4′-hydroxystilbene, is a natural stilbenoid in grapes, berries, and Chinese herbs. It belongs to the dimethylated analogs of resveratrol and is well known for its indisputable anti-inflammatory activity in vitro and in vivo [9, 10]. Moreover, PTE exhibit many pharmacological activities [11], including antiaging [12], anticancer [13, 14], antidiabetes [15], regulating fat metabolism [15–17], antioxidation [18–20], antidepression [10], and neuroprotection [10, 21]. Intriguingly, in the CNS, PTE are able to penetrate the blood brain barrier (BBB) and to modulate neural activity [22], which may exert protection against degenerative disorders [21], hyperprolactinemia [23], and stroke [18, 24, 25]. The biological effects of PTE on neural cells involve the regulation of neurogenesis [10], apoptosis [19], neuroinflammation [18, 24], and oxidative stress [19, 20]. Previously, we have found that PTE attenuates neural impairments in different neurological disorders, including glutamate or high-glucose-induced oxidative stress in neural cells [19, 20], inflammation and mitochondrial oxidative stress injury after cerebral ischemia reperfusion [18, 25], inflammation and oxidation-involved early brain injury following subarachnoid haemorrhage (SAH) [24]. Additionally, recent studies have shown that PTE inhibits the amyloid-β- and lipopolysaccharide- (LPS-) induced activation of microglia [26–28], whereas, it remains not fully clear whether PTE exerts neuronal protective effects by regulating microglia-mediated inflammatory and oxidative injury, as well as the molecular mechanisms.

Sirtuin 1 (SIRT-1), one of the seven mammalian homologues belonging to the silent mating type information regulation 2 family, is a regulator of proteins and genes involved in antioxidation, anti-inflammation, antiapoptosis, insulin response, metabolism, mitochondrial biogenesis, synaptic plasticity, stress resistance, and genomic stability, which is thus important in cell survival under stressful conditions [29, 30]. In the CNS, SIRT-1 plays an important role in promoting neurodevelopment, delaying brain senescence, maintaining homeostasis, and modulating circadian rhythm [30, 31] and has also been demonstrated as the neuroprotective roles under the condition of neurodegeneration and cerebral ischemia [30]. Furthermore, accumulating studies have suggested that SIRT-1 exhibits a key role in regulating neuroinflammation following CNS disturbances via inhibiting NACHT domain-, leucine-rich repeat-, and PYD-containing protein 3 (NLRP3) inflammasome activation, Toll-like receptor (TLR) 4 signalling, nuclear factor- (NF-) κB pathway, and IL-1β transcription, which may relate to the modulating of microglial function [32–35]. Previously, we have also found that SIRT-1/NF-κB signalling could attenuate inflammatory

injury in experimental SAH models [36]. Interestingly, PTE has been proved as a potent SIRT-1 activator in different cells, including hepatic cells [37], cardiomyocytes [38], and skeletal muscle cells [39]. However, the role of SIRT-1 signalling in microglia after PTE treatment and the relationship between microglial inflammation and neuronal oxidative injury in the PTE mediated neuroprotection have not been well investigated.

In view of the above, PTE presents the therapeutic potential to prevent or reduce microglial inflammation and neuronal oxidative stress injury in neurological disorders, such as neurodegenerative diseases, trauma, brain stroke, and infections. Therefore, in this study, we aimed to evaluate a possible modulating activity of PTE on the microglia-mediated inflammatory and neuronal oxidative injuries and to explore the underlying mechanisms mediated by SIRT-1signalling.

2. Material and Methods

2.1. Materials. PTE, EX527, and DCFH-DA and DAPI fluorescent probes were obtained from Sigma-Aldrich (St. Louis, MO, USA). Lactate dehydrogenase (LDH) cytotoxicity, Cell counting kit-8 (CCK-8), MDA, SOD, and GSH assay kits were obtained from Beyotime Biotechnology (Shanghai, China). TUNEL kit was obtained from Roche (Mannheim, Germany). TNF-α and IL-6 ELISA kits were obtained from Sangon Biotech (Shanghai, China). Antibodies against SIRT-1, p65, and acetylated p65 at Lys310 were obtained from Cell Signalling Technology (Danvers, MA, USA). Antibodies against β-actin, caspase 3, cleaved-caspase 3, Bax, Bcl-2, and secondary antibodies labelled by HRP were obtained from Wanleibio (Shenyang, China). Transwell Chamber was purchased from Corning (NY, USA). Cell culture reagents were obtained from Gibco (Grand Island, NY, USA). SH-SY5Y human neuroblastoma cell line and BV-2 mouse microglia cell line were obtained from the Neurological Lab of Tangdu Hospital.

2.2. Experimental Protocol

(i) Step 1. Evaluate the influences of PTE on the BV-2/SH-SY5Y cocultivation system, containing the effects on SH-SY5Y survival and SIRT-1 expression within BV-2 cells. The cells were randomly divided into the control and PTE (2.5, 5.0, or 10.0 μM) groups ($n = 6$). The groups were incubated with PTE or vehicle (0.01% DMSO) for 2 h and with FBS-free DMEM for another 24 h, followed by detections

(ii) Step 2. Investigate whether PTE treatment alleviates the injury of SH-SY5Y cells induced by LPS-activated BV-2 cells. Firstly, the damage effect on SH-SY5Y cells of LPS-activated BV-2 microglia was verified. The SH-SY5Y neuroblastomas were randomly divided into the control, BV-2 alone, LPS alone, and LPS-activated BV-2 groups ($n = 6$), which were separately incubated or cocultured with the vehicle, BV-2 cells, LPS (100 ng/mL), or BV-2 cells with LPS (100 ng/mL) stimulation for 24 h.

Secondly, the protective effects of PTE were tested. The SH-SY5Y cells were randomly divided into the control, LPS-activated BV-2 cocultured, LPS-activated BV-2 cocultured+PTE (2.5, 5.0, or, 10.0 μM)-treated groups ($n = 6$). In the experimental groups, the BV-2 microglia with the stimulation of LPS (100 ng/mL) were pretreated with PTE or vehicle for 2 h, followed by coculturing with SH-SY5Y cells for 24 h. The BV-2 microglia of the control group were treated with vehicle and without LPS stimulation. After interventions above, further detections were carried out, including cell survival, apoptosis, oxidative stress, and inflammatory factor.

(iii) Step 3. Explore the role of SIRT-1 in the protective effect of PTE against the injury induced by the LPS-activated BV-2 microglia. The SH-SY5Y cells were randomly divided into the control, LPS-activated BV-2 cocultured, LPS-activated BV-2 cocultured+5μM PTE, LPS-activated BV-2 cocultured+5 μM PTE+EX527 groups ($n = 6$). The BV-2 cells in the EX527-treated group were preincubated with 100 nM EX527 for 24 h, and other interventions of all groups were the same as step 2. After the interventions, further detections were carried out, including the expression of proteins, cell survival, apoptosis, oxidative stress, and inflammatory factor.

2.3. Cell Culture and Treatments. SH-SY5Y and BV-2 cells were cultured with Dulbecco's modified Eagle medium (DMEM) as previously described [18]. Culture media were changed every 2 days. PTE and EX527 were dissolved with dimethylsulfoxide (DMSO) and then diluted in DMEM before experiments (DMSO ≤ 0.1%). The coculture system was established as previously described [40]. In the coculture assay, BV-2 cells were cultured in a Transwell chamber (pore size 0.4 μm, polylysine-coated polycarbonate membrane) at a density of 2×10^5/well, and then treated with PTE or vehicle for 2 h, followed by LPS (diluted with phenol red-free DMEM at a final concentration of 100 ng/mL) stimulation and coculturing with SH-SY5Y cells for 24 h. In the inhibitory assay, BV-2 microglia were preincubated with EX527 at a final concentration of 100 nM.

2.4. Cell Viability and LDH Release Assay. The cell viability and LDH generation were measured using the CCK-8 and LDH release assay kits according to the manual. Briefly, following experimental intervention, cells were incubated with CCK-8 solution for 3 h at 37°C, and then the supernatants were transferred into a 96-well plate and detected at 450 nm. To detect LDH level, the culture media were transferred and incubated with 60 μL LDH detection buffer per well in a 96-well plate on a constant temperature (25°C) light-proof shaker for 30 min. Finally, the absorbance was detected using the microplate reader at 490 nm. The percentage of LDH release was then computed.

2.5. Western Blotting Assay. Cells were harvested after experimental intervention and lysed in 200 μL lysis buffer. Protein quantification and western blotting were conducted as previ-

ously described [18]. In short, the prepared samples were separated on the SDS-PAGE gel and then transferred onto a PVDF membrane, which was then cut into stripes according to the markers and incubated with different primary antibodies for 12 h at 4°C. Next, the stripes were washed and incubated with corresponding secondary antibodies for 2 h at 25°C. The concentrations of different antibodies were prepared as follows: anti-SIRT-1 (1 : 1000), anti-Ac-p65 (1 : 1000), anti-p65 (1 : 1000), anti-β-actin (1 : 2000), anti-Bcl-2 (1 : 1000), anti-Bax (1 : 1000), anti-cleaved-caspase 3 (1 : 500), anti-caspase 3 (1 : 500), and secondary HRP-labelled antibodies (1 : 20000). Finally, the stripes were reacted with a chemiluminescent reagent and then scanned under an imaging system (Bio-Rad, Hercules, CA), followed by analysis using ImageJ software (version 1.46).

2.6. TUNEL Staining. Cells were cultured in a special 24-well plate used for fluorescent detection. After the experimental intervention, cells were fixed in 4% paraformaldehyde for 30 min, and then reacted with a TUNEL solution for 1 h, and subsequently incubated with DAPI for 15 min at 37°C, followed by a fluorescence microscopy. Images were analysed using ImageJ software (version 1.46).

2.7. DCFH-DA Staining. The intracellular reactive oxygen species (ROS) were stained using fluorescent probe DCFH-DA as previously described. After the experimental intervention, the cells were treated with 10 μmol/L DCFH-DA in a lightproof place at 37°C for 30 min, followed by a fluorescence microscopy. Images were analysed using ImageJ software (version 1.46).

2.8. Measurement of MDA, SOD, GSH, TNF-α, and IL-6. Generally, after the experimental intervention, the cell samples were lysed and centrifuged to obtain intracellular supernatants. The MDA level, SOD activity, GSH level, and TNF-α and IL-6 levels in the supernatants were assessed using corresponding commercial detection kits, according to the manufacturer's instructions.

2.9. Statistical Analysis. All data were analysed using Graph-Pad Prism 5.0 (GraphPad Software Inc., La Jolla, CA) and are shown as mean ± standard error of mean (SEM). Group means were compared by one-way analysis of variance (ANOVA), and Tukey's post hoc tests were then performed for significant groups. It was considered significant when $p < 0.05$.

3. Results

3.1. The Effects of PTE on Cell Viability of SH-SY5Y, LDH Release, and SIRT-1 Expression in BV-2 Cells, in Coculture System. We first investigated the effects of PTE on the SH-SY5Y and BV-2 coculture systems without LPS stimulation at different concentrations. PTE (2.5, 5.0, or 10.0 μM) treatment had no effects on SH-SY5Y cell viability or LDH release in the cocultured system (Figures 1(a)–1(c)). Interestingly, PTE treatment (5.0 and 10.0 μM) significantly increased SIRT-1 expression in BV-2 cells to 1.29 ± 0.08- and 1.46 ± 0.01-fold, respectively (Figure 1(d)).

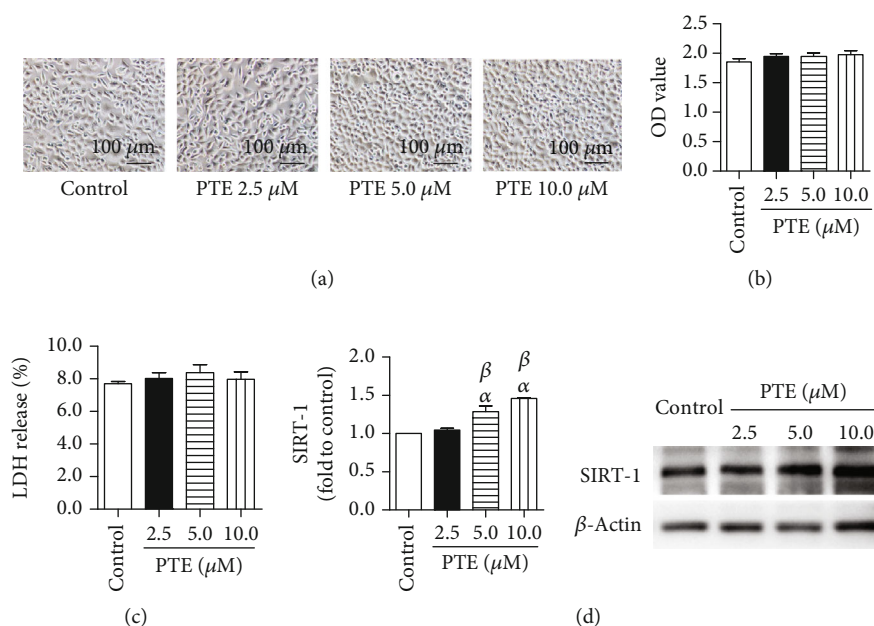FIGURE 1: Effects of PTE on the SH-SY5Y and BV-2 coculture systems. The BV-2 cells were incubated with vehicle control or PTE (2.5, 5.0, or 10.0 μM) for 2 h, followed by cocultivation with SH-SY5Y cells for 24 h. (a) The morphology of SH-SY5Y cells was photographed under an inverted/phase-contrast microscope, and (b) viability was quantified using a CCK-8 assay. (c) The LDH release in supernatants was determined using an LDH release assay and expressed as the percentage of maximum. (d) The expression of SIRT-1 in BV-2 cells was measured using western blot analysis and normalized to that of β-actin. Data are shown as mean $\pm$ SEM. $n = 6$. $^{\alpha}p < 0.05$, compared with the control. $^{\beta}p < 0.05$, compared with PTE 2.5 μM.

3.2. The Effects of PTE on Cell Viability, LDH Release, and Apoptotic Rate of SH-SY5Y in LPS-Activated BV-2 Coculture System. As shown in Figure 2(a), SH-SY5Y cells were cultured with the vehicle, BV-2 cells, LPS, and LPS-activated BV-2 cells for 24 h. Either BV-2 or LPS alone had no effect on cell morphology and viability of SH-SY5Y. Obviously, LPS-activated BV-2 microglia shrank and floated cocultured SH-SY5Y cells in morphology and weakened the viability of SH-SY5Y cells (OD value = 0.81 ± 0.03) compared with that of the control (OD value = 0.55 ± 0.03). In the cocultured system, the OD values of SH-SY5Y and BV-2 in the control group were 0.74 ± 0.02 and 0.99 ± 0.06, and LPS stimulation impaired SH-SY5Y viability (OD value = 0.50 ± 0.01) and promotes BV-2 viability (OD value = 1.88 ± 0.07). PTE (2.5, 5.0, or 10.0 μM) significantly increased OD values of SH-SY5Y to 0.65 ± 0.02, 0.76 ± 0.03, and 0.76 ± 0.04 and decreased those of BV-2 cells to 1.54 ± 0.03, 1.24 ± 0.08, and 1.07 ± 0.04, respectively (Figures 2(b) and 2(c)). Similarly, PTE (2.5, 5.0, or 10.0 μM) decreased LDH release in supernatant to 0.15 ± 0.01%, 0.12 ± 0.01%, and 0.09 ± 0.00% compared with 0.18 ± 0.01% of the LPS-activated BV-2 group (Figure 2(d)). In addition, apoptotic SH-SY5Y were stained with TUNEL. The apoptosis rate in LPS-activated BV-2 coculture group were 67.10 ± 6.08%, and PTE (2.5, 5.0, or 10.0 μM) treatment significantly decreased that to 38.6 ± 4.51%, 17.23 ± 6.96%, and 14.01 ± 3.83%, respectively (Figures 2(e) and 2(f)).

3.3. The Effects of PTE on Oxidative Stress of SH-SY5Y and Inflammatory Factors in Supernatant in LPS-Activated BV-2 Coculture System. DCFH-DA staining was used to mark oxidative SH-SY5Y cells, the average intracellular fluorescent

density were 29.48 ± 2.45 per pixel in the control group and significantly increased to 70.76 ± 1.03 per pixel in the LPS-activated BV-2 coculture group. PTE (2.5, 5.0, or 10.0 μM) treatment decreased the fluorescent density to 51.31 ± 0.85, 43.63 ± 1.43, and 37.81 ± 1.09 in a dose-dependent manner (Figures 3(a) and 3(b)). Similarly, PTE treatment decreased the MDA level, increased the SOD activity, and elevated the GSH level in SH-SY5Y cells, compared with those of the LPS-activated BV-2 coculture group (3.83 ± 0.19 mmol/mg, 22.84 ± 0.99 U/mg, and 2.23 ± 0.15 μM). These effects were significant with 5.0 μM and 10.0 μM PTE, which separately changed the MDA level, SOD activity, and GSH level to 2.51 ± 0.23 mmol/mg, 39.69 ± 3.33 U/mg, and 3.94 ± 0.39 μM at 5.0 μM and 2.10 ± 0.29 mmol/mg, 48.05 ± 3.65 U/mg, and 4.59 ± 0.37 μM at 10.0 μM, respectively (Figures 3(c)–3(e)).

The levels of inflammatory factors, TNF-α and IL-6, in the supernatant were 1.46 ± 0.09 ng/mL and 3.70 ± 0.16 ng/mL in the LPS-activated BV-2 coculture group, compared with 0.08 ± 0.00 ng/mL and 0.01 ± 0.01 ng/mL in the coculture group without LPS stimulation. PTE (2.5, 5.0, or 10.0 μM) separately decreased the levels of TNF-α to 1.07 ± 0.04 ng/mL, 0.61 ± 0.06 ng/mL, and 0.55 ± 0.04 ng/mL and those of IL-6 to 2.81 ± 0.20 ng/mL, 1.49 ± 0.07 ng/mL, and 0.95 ± 0.03 ng/mL, in a dose-dependent manner (Figures 3(f) and 3(g)).

3.4. The Effects of PTE and EX527 on Expression of SIRT-1 and Acetylated p65 in LPS-Activated BV-2 Microglia and Inflammatory Factors in Supernatant. We further estimated the expression of SIRT-1 and acetylated NF-κB subunit p65 in BV-2 microglia. LPS stimulation suppressed the expression of SIRT-1 and promoted the acetylation of p65, and
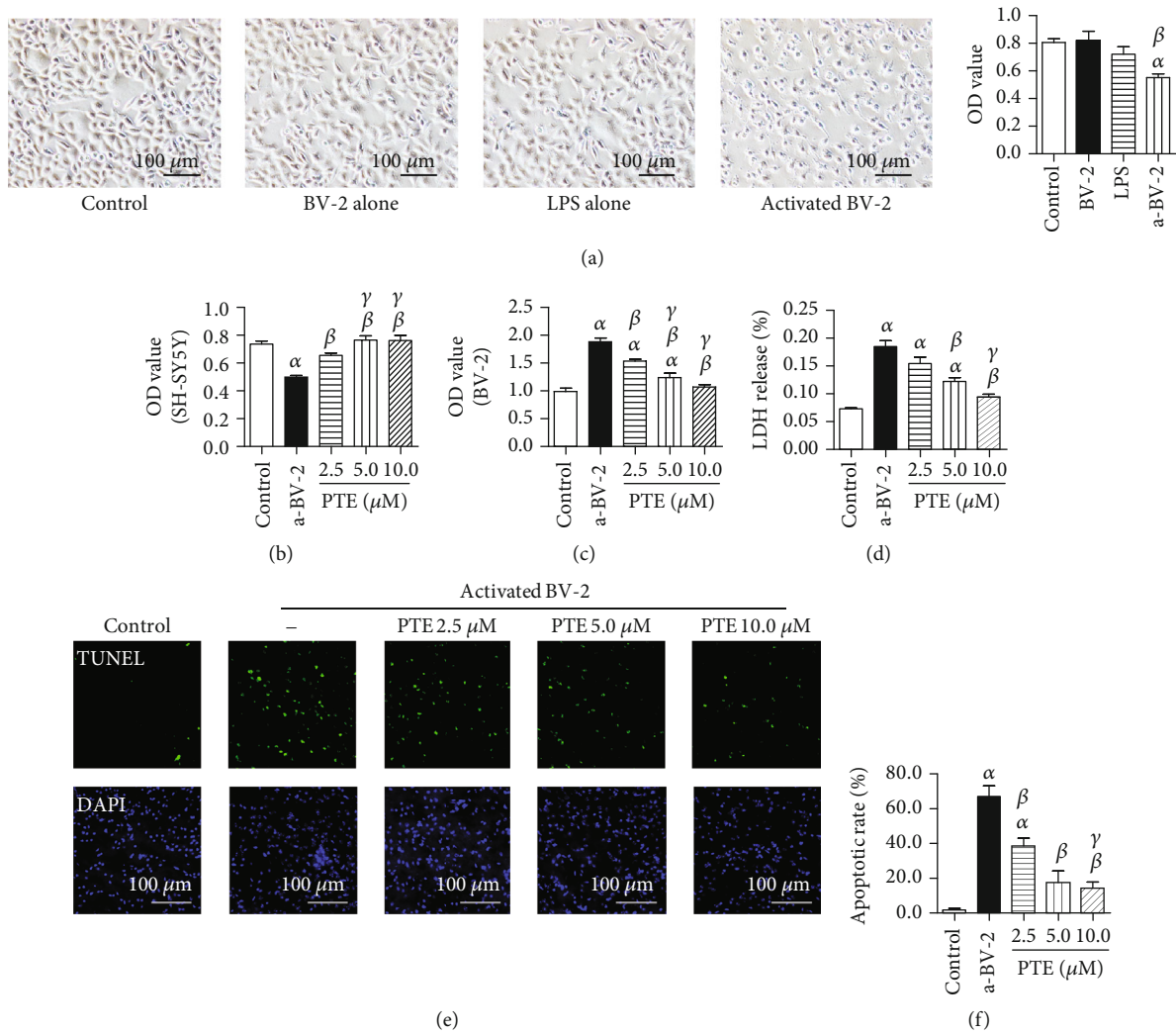
FIGURE 2: LPS induces BV-2 activation and SH-SY5Y injury in the coculture system, and PTE shows protective effects after LPS stimulation. SH-SY5Y cells were cocultured with BV-2 cells, LPS (100 ng/mL), or both BV-2 cells and LPS for 24 h, separately. (a) The morphology and viability of SH-SY5Y cells were observed under an inverted/phase-contrast microscope or using a CCK-8 assay, respectively. The BV-2 cells were preincubated with vehicle control or PTE (2.5, 5.0, or 10.0 μM) for 2 h, followed by LPS stimulation and coculturing with SH-SY5Y cells for 24 h. The viability of (b) SH-SY5Y and (c) BV-2 cells was measured using a CCK-8 assay. (d) The LDH release in supernatants was determined using an LDH release assay and expressed as the percentage of maximum. (e) The apoptosis of SH-SY5Y cells was assessed using a TUNEL assay. The apoptotic nuclei were stained with TUNEL (green), and all nuclei were stained with DAPI (blue). (f) Apoptotic rate was computed as a percentage of the TUNEL- to the DAPI-positive nuclei. Data are shown as mean ± SEM. $n = 6$. $^{\alpha}p < 0.05$, compared with the control. $^{\beta}p < 0.05$, compared with the a-BV-2. $^{\gamma}p < 0.05$, compared with the PTE 2.5 μM. LPS: lipopolysaccharide; a-BV-2: LPS-activated BV-2 coculture group.

PTE treatment significantly increased the level of SIRT-1 and decreased acetylated p65. However, EX527 treatment obviously reversed the effects of PTE (Figures 4(a) and 4(b)). In addition, The levels of TNF-α and IL-6 in the supernatant were increased in the LPS-activated BV-2 coculture group, and then those were decreased in 5.0 μM PTE-treated group, while the effects of PTE were significantly reversed in the EX527-treated group, which increased the levels of TNF-α and IL-6 to 2.07 ± 0.07 ng/mL and 5.28 ± 0.18 ng/mL (Figures 4(c) and 4(d)).

3.5. The Effects of PTE and EX527 on Apoptosis and Oxidative Stress of SH-SY5Y in LPS-Activated BV-2 Coculture System.

As shown in Figures 5(a) and 5(b), LPS stimulation on BV-2 cells significantly decreased the ratio of Bcl-2 to Bax and increased the percentage of cleaved-caspase 3 in cocultured SH-SY5Y cells, compared with those in the control group, and PTE (5.0 μM) treatment significantly reversed these effects. However, EX527 abolished the effects of PTE. PTE also decreased the fluorescent density of the DCFH-DA and MDA levels and increased the SOD activity and GSH level of SH-SY5Y cells, compared with those of the LPS-activated BV-2 coculture group. These effects of PTE were obviously abolished by EX527, which increased the fluorescent density of the DCFH-DA and MDA levels to 57.22 ± 1.28 per pixel and 3.72 ± 0.12
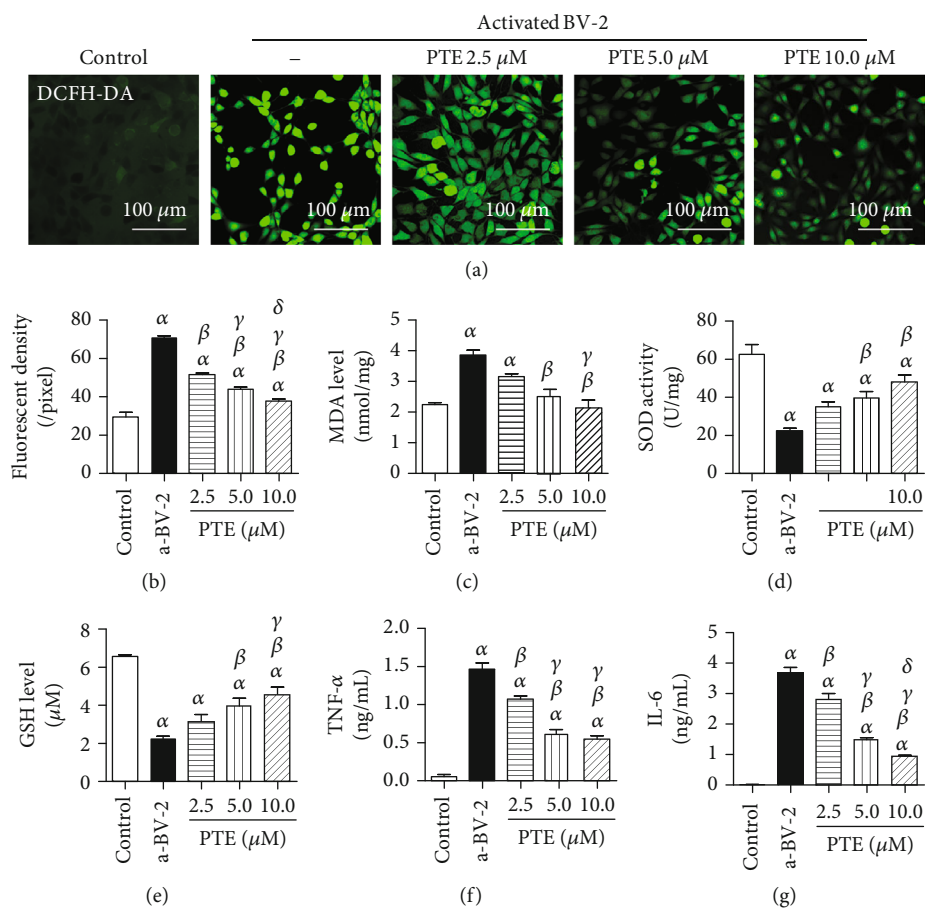
FIGURE 3: PTE reduces inflammatory factors released by LPS-activated BV-2 cells and attenuates the oxidative stress level of SH-SY5Y cells. BV-2 cells were pretreated with vehicle control or PTE (2.5, 5.0, or 10.0 μM) for 2 h, followed by LPS stimulation and coculturing with SH-SY5Y cells for 24 h. (a) The ROS in SH-SY5Y cells was stained with DCFH-DA (green), and (b) the level of ROS was computed as the average intracellular fluorescent density. (c) The MDA level, (d) SOD activity, and (e) GSH level in SH-SY5Y cells were assessed using standardized commercial kits, and the (f) TNF-α and (g) IL-6 in supernatants were determined using an ELISA assay. Data are shown as mean $\pm$ SEM. $n = 6$. $^{\alpha}p < 0.05$, compared with the control. $^{\beta}p < 0.05$, compared with the a-BV-2. $^{\gamma}p < 0.05$, compared with the PTE 2.5 μM. $^{\delta}p < 0.05$, compared with the PTE 5.0 μM. LPS: lipopolysaccharide; a-BV-2: LPS-activated BV-2 coculture group; ROS: reactive oxygen species; MDA: malondialdehyde; SOD: superoxide dismutase; GSH: glutathione.

nmol/mg and decreased the SOD activity and GSH level to 25.79 ± 2.48 U/mg and $2.36 \pm 0.23 \mu$M, respectively (Figures 5(c)–5(f)).

4. Discussion

PTE is a stilbenoid presenting in grapes and berries and also the biologically active compound of a Chinese herb, dragon's blood [10]. PTE has biological activities penetrating the BBB and shows no toxicity to neurons [22, 41]. Previously, we reported that PTE shows no toxic effect on HT22 neural cells at 10 μM in vitro [19]. In this study, 10.0 μM PTE treatment had no effects on SH-SY5Y cell viability or LDH release in the cocultured system, and this is consistent with the observation reported.

Recently, accumulating evidences have demonstrated the benefits of PTE and other analogue stilbenoids, including resveratrol, piceatannol, and gnetol, against inflammatory and oxidative processes in vitro and in vivo [9]. The anti-inflammatory effects of PTE involve many intra- and extra-

cellular signals, including nitric oxide (NO), inducible nitric oxide synthase (iNOS), NLRP3, NF-κB, TNF-α, and ILs [26–28, 42, 43]. We previously reported that PTE alleviates early inflammatory injury after SAH by inhibiting NLRP3 inflammasome and Nox2-related oxidative stress [24] and also attenuates the secondary astrocyte-induced inflammatory and oxidative stress after ischemia reperfusion injury by suppressing NF-κB signalling [18]. This anti-inflammatory activity together with the antioxidant activity of PTE is believed to stand behind the neuroprotective effects against neurological disorders, especially the neurodegenerative diseases [21, 26, 27, 41, 42, 44] and stroke [39]. However, the effector cells and the underlying mechanisms are not entirely elucidated.

Microglia were first properly visualized and described as a distinct cell population in 1919 and have been considered the resident phagocytes of the innate immune system in the CNS since 1924. It was until the 1980s did researchers found that the microglia act as the indicator of immune activation and are correlated with the amyloid plaques in AD [45].
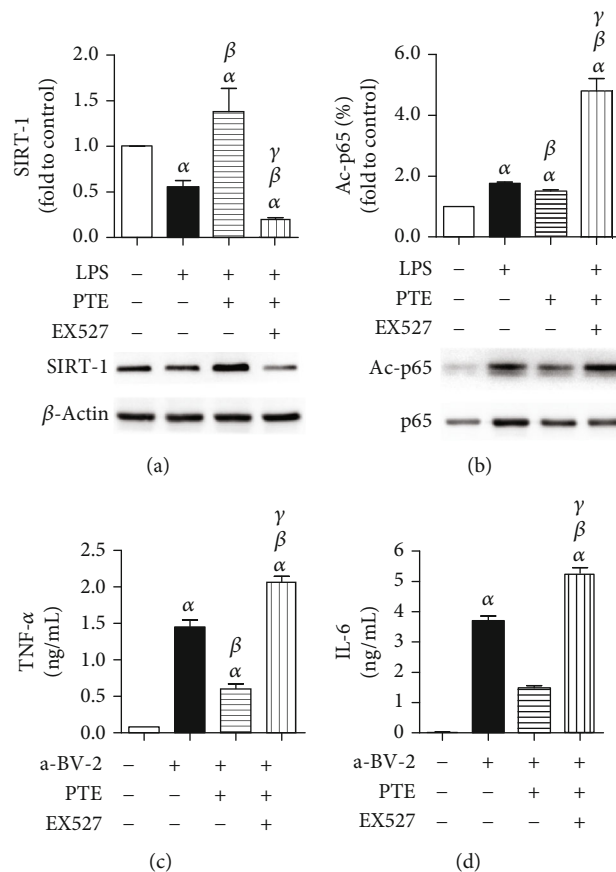
Figure 4: PTE promotes SIRT-1 expression, suppresses acetylation of p65 unit of NF-κB, and reduces inflammatory factor release in LPS-activated BV-2 cells, which can be abolished by EX527. BV-2 microglial cells were pretreated with vehicle or EX527 (100 nM) for 24 h and then incubated with vehicle or PTE (5.0 μM) for 2 h, followed by coculturing with SH-SY5Y cells with or without the presence of LPS (100 ng/mL) for 24 h. (a) The expression of SIRT-1 in BV-2 cells was measured using western blot analysis and normalized to that of β-actin. (b) The acetylated p65 (L310) in BV-2 cells was measured using western blot analysis and normalized to that of total p65. (c) The TNF-α and (d) IL-6 in supernatants were determined using an ELISA assay. Data are shown as mean ± SEM. $n = 6$. $^{\alpha}p < 0.05$, compared with the control. $^{\beta}p < 0.05$, compared with the a-BV-2. $^{\gamma}p < 0.05$, compared with the PTE 2.5 μM. LPS: lipopolysaccharide; a-BV-2: LPS-activated BV-2 coculture group.

Multiple studies suggested that the microglia play an important role in the CNS health and disease, involving the surveillance of local environment, phagocytosis, releases of cytokines, chemokines, and growth factors, as well as the interaction with infiltrating immune cells [46]. More recently, studies have indicated that the microglia drives programmed cell death by inducing apoptosis of neurons through the release of superoxide ions, nerve growth factor, or TNF, without provoking inflammation, as well as prune developing axons and synapses and regulates neuronal and synaptic plasticity [7]. With the technical advances, the proinflammatory M1-like and anti-inflammatory M2-like polarization phenotypes of the microglia were found, although some regarded them as a simplified interpretation of data when the microglial development and function had not been fully elucidated [47]. Interestingly, microglial polarization was observed in the cerebral haemorrhagic stroke, indicating an involvement of the microglia in producing proinflammatory or anti-inflammatory factors. Besides, the phagocytosis of cell debris and the potential crosstalk between microglia and T lymphocytes, neurons, astrocytes, and oligodendro-

cytes are also important pathologies after haemorrhagic stroke [48]. Additionally, in response to specific stimuli or with neuroinflammation, the microglia also have the capacity to damage and kill neurons. The uncontrolled microglial inflammatory response may result in the neuronal injury in neurodegenerative diseases, including Parkinson's disease (PD), Huntington's disease (HD), AD, and prion diseases, chronic traumatic encephalopathy, amyotrophic lateral sclerosis, and frontotemporal dementia [49]. Finally, although many mysteries exist regarding the effects and mechanisms of the microglia in neurological diseases, it shows the microglia as a promising future to treat neurological disorders, especially to cure neurodegeneration.

Increasing evidence has proved that PTE has regulatory effects on neurological disorders, especially neurodegeneration and stroke [18]. However, the modulatory roles of PTE in microglial activation and following injury have not been given enough attention. Neurodegenerative diseases have strong connections with microglial activation [50, 51]. A recent study compared the protective effects of PTE and its structural analogues on neurodegenerative diseases. It

(a)

(b)

(c)

(d)

(e)

(f)
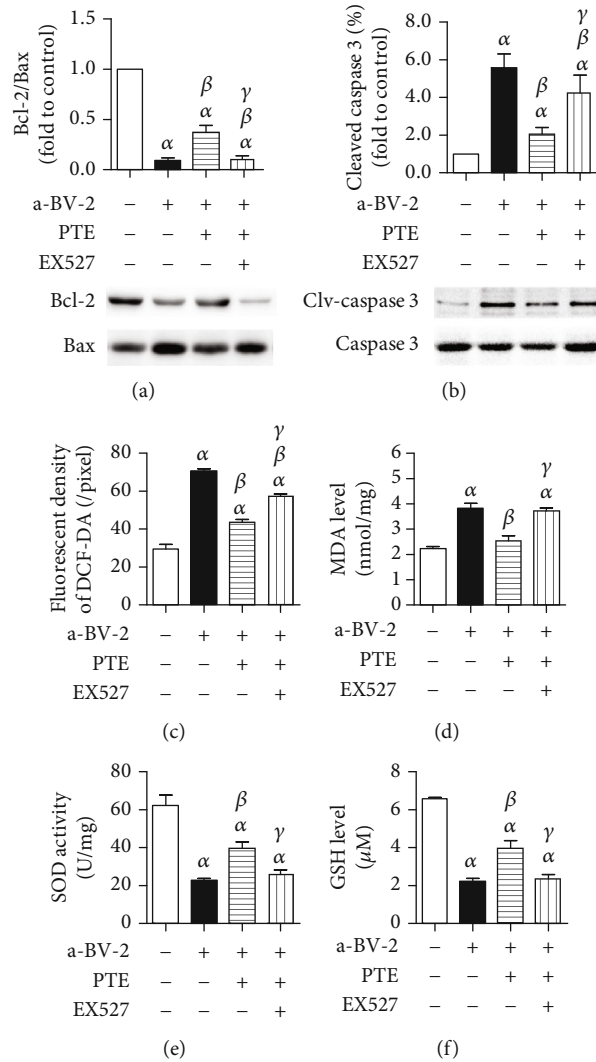
FIGURE 5: PTE attenuates apoptosis and oxidative stress of SH-SY5Y cells in the cocultured system with LPS-activated BV-2 cells, which can be abolished by EX527. BV-2 cells were pretreated with vehicle or EX527 (100 nM) for 24 h and then incubated with vehicle or PTE (5.0 μM) for 2 h, followed by coculturing with SH-SY5Y cells with or without the presence of LPS (100 ng/mL) for 24 h. (a) The expression of Bcl-2 and Bax in SH-SY5Y cells was measured using western blot analysis and was shown as the ratio of Bcl-2 to Bax. (b) The cleaved caspase 3 in SH-SY5Y cells was measured using western blot analysis and normalized to that of total caspase 3. (c) The level of ROS was measured using DCFH-DA staining and expressed as an average intracellular fluorescent density. (d) The MDA level, (d) SOD activity, and (e) GSH level in SH-SY5Y cells were measured using standardized commercial kits. Data are shown as mean ± SEM. $n = 6$. $^{\alpha}p < 0.05$, compared with the control. $^{\beta}p < 0.05$, compared with the a-BV-2. $^{\gamma}p < 0.05$, compared with the PTE 2.5 μM. LPS: lipopolysaccharide; a-BV-2: LPS-activated BV-2 coculture group; ROS: reactive oxygen species; MDA, malondialdehyde: SOD, superoxide dismutase: GSH; glutathione.

evaluates activities of these analogues on the LPS-induced release of proinflammatory factors, containing NO, iNOS, IL-6, IL-1β, and TNF-α, in BV-2 cells, and further involvement of the MAPKs (ERK1/2, JNK, and p38) and NF-κB signalling pathways [28]. Also, PTE was proved to attenuate the neuroinflammatory response induced by amyloid-β in BV-2 microglia through inhibiting the NLRP3/caspase-1 inflammasome pathway [26], indicating a therapeutic effect of PTE in AD. However, the interaction of microglia and released proinflammatory factors with neurons were not entirely elucidated. Consistent with the reported evidence, we found that LPS induced BV-2 activation, evidenced by the increased release of IL-6 and TNF-α, and further PTE treatment attenuated the level

of TNF-α and IL-6 in the media of BV-2 microglia in a dose-dependent manner. Besides, coculturing with LPS-activated BV-2 microglia cells, rather than BV-2 or LPS alone, induced the shrinkage, floating, and decreased viability of SH-SY5Y. Obviously, PTE treatment improved the SH-SY5Y viability, attenuated the BV-2 viability, and decreased LDH release in this coculture system. Similarly, PTE alleviated apoptosis and oxidative stress of SH-SY5Y cells induced by coculturing with LPS-activated BV-2 microglia. These may indicate an interaction between activated BV-2 and SH-SY5Y cells via proinflammatory factors, which induces apoptosis and oxidative injury of SH-SY5Y, and PTE could inhibit the activation of BV-2 microglia and subsequent generation of proinflammatory
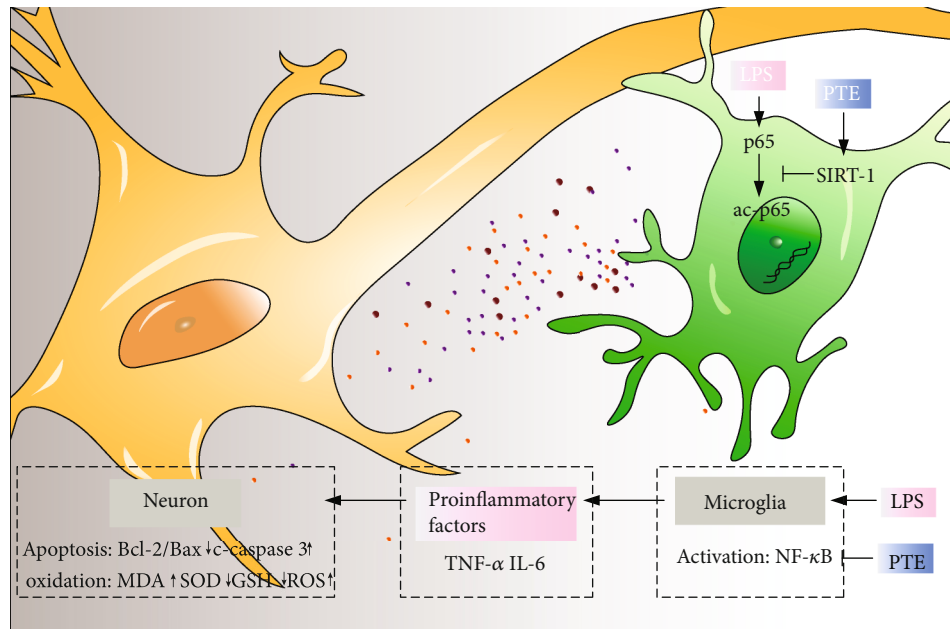
Figure 6: PTE attenuates microglial inflammation and neuronal apoptosis and oxidative stress via SIRT-1 pathway. PTE, pterostilbene. LPS, lipopolysaccharide. ROS, reactive oxygen species. MDA, malondialdehyde. SOD, superoxide dismutase. GSH, glutathione.

factors, thus presenting a neuronal protective effect in neurodegenerative diseases and stroke.

SIRT-1 is an evolutionarily conserved protein belonging to the sirtuin family of NAD (+)-dependent deacetylases [30]. For a long time, SIRT-1 has been considered to be correlated with neural development and antiaging in mammals, offering significant potential as an effective treatment strategy for neurodegenerative diseases [29, 31]. Recently, SIRT-1 has been reported to present protective effects on neurological diseases including AD, PD, motor neuron diseases, depression, cerebral ischemia, and SAH, which may relate to its regulatory functions in metabolism, stress resistance, inflammation, oxidative stress, and genomic stability [30, 31, 33, 36]. Besides, in the CNS, especially in the hypothalamus, SIRT-1 exerts pivotal roles in modulating the circadian rhythm and systemic energy homeostasis [30]. Importantly, accumulating evidences have shown that brain SIRT-1 plays neuroprotective roles in the context of neurodegenerative disorders and cerebral ischemia [30]. Studies have reported that increased SIRT-1 expression is related to reduced LPS-induced synaptic dysfunctions, suggesting a potential intervention for oxidative stress-related neurodegenerative diseases [52]. Also, studies have shown that activating SIRT-1 alleviated the SAH injury primarily by inhibiting the TLR4 [34] and NF-κB signalling pathway [36]. As to the relationship between microglia and SIRT-1, it was reported that SIRT-1 is decreased with the senescence of microglia and the SIRT-1 deficiency in microglia leads to memory deficits through IL-1β upregulation [32]. Another in vivo study showed that SIRT-1 promotes functional recovery and neuronal survival via attenuating microglial inflammation after spinal cord injury [35]. Therefore, it could be speculated that SIRT-1 is an intracellular modulator of microglia-mediated inflammation. Multiple studies have

revealed that PTE could activate SIRT-1 signalling in hepatic [37], myocardial [38], and skeletal muscle cells [39]. Interestingly, a study reported that a two-month diet of PTE or its analogue resveratrol did not increase SIRT-1 expression or the downstream signalling activation, whereas it increased peroxisome proliferator-activated receptor (PPAR) α expression, and thus modulated cellular stress, inflammation, and AD pathology [44]. However, another study suggested that resveratrol-related SIRT-1 activation alleviates cerebral ischemia reperfusion injury by inhibiting proinflammatory cytokine, reducing oxidative stress and apoptosis, and may protect against AD by inhibiting amyloid-β fibril formation, antiamyloidogenic effect, and delaying cognitive decline [12]. The effect of PTE on SIRT-1 activation in the neural cells is still undocumented. In this study, PTE treatment significantly increased the expression of SIRT-1, decreased the acetylation of NF-κB subunit p65 in BV-2 microglia, and thus alleviated LPS-induced release of TNF-α and IL-6, which further attenuated apoptosis and oxidative injury of cocultured SH-SY5Y neuronal cells. Furthermore, the regulatory effect on SIRT-1 and ac-p65 of PTE were reversed by SIRT-1 inhibitor EX527, as well as the neuroprotective effects, as indicated by the increased apoptosis and oxidative markers. These suggest that the effects of PTE on reducing microglial inflammation and subsequent neuronal oxidative stress and apoptosis are mediated by SIRT-1/NF-κB signalling pathways.

5. Conclusions

In summary, PTE reduced LPS-induced release of inflammatory factors, IL-6 and TNF-α, in BV-2 microglia, and thus attenuated oxidative stress and apoptosis in cocultured SH-SY5Y neural cells. Additionally, PTE mediated the

downregulation of NF-κB subunit p65 acetylation, which was likely due to increased SIRT-1 expression. This indicates that PTE treatment inhibited the NF-κB pathway and might induce direct interactions between SIRT-1 and NF-κB by stimulating SIRT-1 signalling, which then led to inhibition of LPS-induced microglial activation and subsequent inflammatory response, and thus attenuated the neuronal apoptosis and oxidative injury (Figure 6). These findings suggest PTE as a promising therapy of inflammation and oxidation-related diseases in the CNS, including neurodegenerative diseases and stroke, and provide a microglia-centric view of anti-inflammation and neuroprotection.

Data Availability

The data generated during the study are available from the corresponding author by request.

Conflicts of Interest

The authors declare no conflict of interest.

Authors' Contributions

B.W. conducted the study and refined the manuscript. Q.Z. and T.T. processed the data and wrote the initial manuscript. H.L., Y.S., X.W., Q.L.[1], L.Y., Z.L., Z.H., Z.C., Q.L.[3], and M.S. performed the main experiments. All authors reviewed and approved the final manuscript.

Acknowledgments

References

[1] F. Bright, E. L. Werry, C. Dobson-Stone et al., "Neuroinflammation in frontotemporal dementia," *Nature Reviews Neurology*, vol. 15, no. 9, pp. 540–555, 2019.

[2] M. T. Heneka, M. J. Carson, J. El Khoury et al., "Neuroinflammation in Alzheimer's disease," *The Lancet Neurology*, vol. 14, no. 4, pp. 388–405, 2015.

[3] M. C. Morganti-Kossmann, B. D. Semple, S. C. Hellewell, N. Bye, and J. M. Ziebell, "The complexity of neuroinflammation consequent to traumatic brain injury: from research evidence to potential treatments," *Acta Neuropathologica*, vol. 137, no. 5, pp. 731–755, 2019.

[4] L. Jackson, S. Dumanli, M. H. Johnson, S. C. Fagan, and A. Ergul, "Microglia knockdown reduces inflammation and preserves cognition in diabetic animals after experimental stroke," *Journal of Neuroinflammation*, vol. 17, no. 1, p. 137, 2020.

[5] R. A. Drummond, M. Swamydas, V. Oikonomou et al., "CARD9$^+$ microglia promote antifungal immunity via IL-1β- and CXCL1-mediated neutrophil recruitment," *Nature Immunology*, vol. 20, no. 5, pp. 559–570, 2019.

[6] Q. Q. Yang and J. W. Zhou, "Neuroinflammation in the central nervous system: symphony of glial cells," *Glia*, vol. 67, no. 6, pp. 1017–1035, 2019.

[7] M. W. Salter and B. Stevens, "Microglia emerge as central players in brain disease," *Nature Medicine*, vol. 23, no. 9, pp. 1018–1027, 2017.

[8] T. Wyss-Coray and J. Rogers, "Inflammation in Alzheimer disease—a brief review of the basic science and clinical literature," *Cold Spring Harbor Perspectives in Medicine*, vol. 2, no. 1, article a006346, 2012.

[9] M. Dvorakova and P. Landa, "Anti-inflammatory activity of natural stilbenoids: a review," *Pharmacological Research*, vol. 124, pp. 126–145, 2017.

[10] L. Yang, Y. Ran, Z. Quan et al., "Pterostilbene, an active component of the dragon's blood extract, acts as an antidepressant in adult rats," *Psychopharmacology*, vol. 236, no. 4, pp. 1323–1333, 2019.

[11] P. Wang and S. Sang, "Metabolism and pharmacokinetics of resveratrol and pterostilbene," *BioFactors*, vol. 44, no. 1, pp. 16–25, 2018.

[12] Y. R. Li, S. Li, and C. C. Lin, "Effect of resveratrol and pterostilbene on aging and longevity," *Biofactors*, vol. 44, no. 1, pp. 69–82, 2018.

[13] Z. Ma, X. Zhang, L. Xu et al., "Pterostilbene: Mechanisms of its action as oncostatic agent in cell models and *in vivo* studies," *Pharmacological Research*, vol. 145, article 104265, 2019.

[14] R. J. Chen, H. C. Kuo, L. H. Cheng et al., "Apoptotic and non-apoptotic activities of pterostilbene against cancer," *International Journal of Molecular Sciences*, vol. 19, no. 1, p. 287, 2018.

[15] S. Gomez-Zorita, I. Milton-Laskibar, L. Aguirre, A. Fernandez-Quintela, J. Xiao, and M. P. Portillo, "Effects of pterostilbene on diabetes, liver steatosis and serum lipids," *Current Medicinal Chemistry*, vol. 26, 2019.

[16] H. Kim, K. H. Seo, and W. Yokoyama, "Chemistry of pterostilbene and its metabolic effects," *Journal of Agricultural and Food Chemistry*, 2020.

[17] L. Aguirre, S. Palacios-Ortega, A. Fernandez-Quintela, E. Hijona, L. Bujanda, and M. P. Portillo, "Pterostilbene reduces liver steatosis and modifies hepatic fatty acid profile in obese rats," *Nutrients*, vol. 11, no. 5, p. 961, 2019.

[18] H. Liu, X. Wu, J. Luo et al., "Pterostilbene attenuates astrocytic inflammation and neuronal oxidative injury after ischemia-reperfusion by inhibiting NF-κB phosphorylation," *Frontiers in Immunology*, vol. 10, p. 2408, 2019.

[19] B. Wang, H. Liu, L. Yue et al., "Neuroprotective effects of pterostilbene against oxidative stress injury: involvement of nuclear factor erythroid 2-related factor 2 pathway," *Brain Research*, vol. 1643, pp. 70–79, 2016.

[20] Y. Yang, C. Fan, B. Wang et al., "Pterostilbene attenuates high glucose-induced oxidative injury in hippocampal neuronal cells by activating nuclear factor erythroid 2-related factor 2," *Biochimica et Biophysica Acta*, vol. 1863, no. 4, pp. 827–837, 2017.

[21] K. W. Lange and S. Li, "Resveratrol, pterostilbene, and dementia," *BioFactors*, vol. 44, no. 1, pp. 83–90, 2018.

[22] F. Xing, Y. Liu, S. Sharma et al., "Activation of the c-met pathway mobilizes an inflammatory network in the brain microenvironment to promote brain metastasis of breast cancer," *Cancer Research*, vol. 76, no. 17, pp. 4970–4980, 2016.

[23] H. Zhang, C. Wang, X. Li, and Y. Zhang, "Effects of pterostilbene on treating hyperprolactinemia and related

mechanisms," *American Journal of Translational Research*, vol. 8, no. 7, pp. 3049–3055, 2016.

[24] H. Liu, L. Zhao, L. Yue et al., "Pterostilbene attenuates early brain injury following subarachnoid hemorrhage via inhibition of the NLRP3 inflammasome and Nox2-related oxidative stress," *Molecular Neurobiology*, vol. 54, no. 8, pp. 5928–5940, 2017.

[25] Y. Yang, J. Wang, Y. Li et al., "HO-1 Signaling activation by pterostilbene treatment attenuates mitochondrial oxidative damage induced by cerebral ischemia reperfusion injury," *Molecular Neurobiology*, vol. 53, no. 4, pp. 2339–2353, 2016.

[26] Q. Li, L. Chen, X. Liu et al., "Pterostilbene inhibits amyloid-β-induced neuroinflammation in a microglia cell line by inactivating the NLRP3/caspase-1 inflammasome pathway," *Journal of Cellular Biochemistry*, vol. 119, no. 8, pp. 7053–7062, 2018.

[27] Y. Hou, G. Xie, F. Miao et al., "Pterostilbene attenuates lipopolysaccharide-induced learning and memory impairment possibly via inhibiting microglia activation and protecting neuronal injury in mice," *Progress in Neuro-Psychopharmacology & Biological Psychiatry*, vol. 54, pp. 92–102, 2014.

[28] L. Wang, H. Zhao, L. Wang et al., "Effects of selected resveratrol analogues on activation and polarization of lipopolysaccharide-stimulated BV-2 microglial cells," *Journal of Agricultural and Food Chemistry*, vol. 68, no. 12, pp. 3750–3757, 2020.

[29] D. J. Bonda, H. G. Lee, A. Camins et al., "The sirtuin pathway in ageing and Alzheimer disease: mechanistic and therapeutic considerations," *Lancet Neurology*, vol. 10, no. 3, pp. 275–279, 2011.

[30] J. Xu, C. W. Jackson, N. Khoury, I. Escobar, and M. A. Perez-Pinzon, "Brain SIRT1 mediates metabolic homeostasis and neuroprotection," *Frontiers in Endocrinology*, vol. 9, p. 702, 2018.

[31] A. Z. Herskovits and L. Guarente, "SIRT1 in neurodevelopment and brain senescence," *Neuron*, vol. 81, no. 3, pp. 471–483, 2014.

[32] S. H. Cho, J. A. Chen, F. Sayed et al., "SIRT1 deficiency in microglia contributes to cognitive decline in aging and neurodegeneration via epigenetic regulation of IL-1β," *The Journal of Neuroscience*, vol. 35, no. 2, pp. 807–818, 2015.

[33] B. I. Arioz, B. Tastan, E. Tarakcioglu et al., "Melatonin attenuates LPS-induced acute depressive-like behaviors and microglial NLRP3 inflammasome activation through the SIRT1/Nrf2 pathway," *Frontiers in Immunology*, vol. 10, p. 1511, 2019.

[34] X. Zhang, Y. Lu, Q. Wu et al., "Astaxanthin mitigates subarachnoid hemorrhage injury primarily by increasing sirtuin 1 and inhibiting the Toll-like receptor 4 signaling pathwa," *The FASEB Journal*, vol. 33, no. 1, pp. 722–737, 2019.

[35] H. Chen, H. Ji, M. Zhang et al., "An agonist of the protective factor SIRT1 improves functional recovery and promotes neuronal survival by attenuating inflammation after spinal cord injury," *The Journal of Neuroscience*, vol. 37, no. 11, pp. 2916–2930, 2017.

[36] L. Zhao, H. Liu, L. Yue et al., "Melatonin attenuates early brain injury via the melatonin receptor/Sirt1/NF-κB Signaling pathway following subarachnoid hemorrhage in mice," *Molecular Neurobiology*, vol. 54, no. 3, pp. 1612–1621, 2017.

[37] H. Zhang, Y. Chen, Y. Chen et al., "Comparison of the effects of resveratrol and its derivative pterostilbene on hepatic oxidative stress and mitochondrial dysfunction in piglets challenged with diquat," *Food & Function*, vol. 11, no. 5, pp. 4202–4215, 2020.

[38] D. Liu, Z. Ma, L. Xu, X. Zhang, S. Qiao, and J. Yuan, "PGC1alpha activation by pterostilbene ameliorates acute doxorubicin cardiotoxicity by reducing oxidative stress via enhancing AMPK and SIRT1 cascades," *Aging*, vol. 11, no. 22, pp. 10061–10073, 2019.

[39] Y. Cheng, S. Di, C. Fan et al., "SIRT1 activation by pterostilbene attenuates the skeletal muscle oxidative stress injury and mitochondrial dysfunction induced by ischemia reperfusion injury," *Apoptosis*, vol. 21, no. 8, pp. 905–916, 2016.

[40] B. Wang, H. Guo, X. Li et al., "Adiponectin attenuates oxygen–glucose deprivation-induced mitochondrial oxidative injury and apoptosis in hippocampal HT22 cells via the JAK2/STAT3 pathway," *Cell Transplantation*, vol. 27, no. 12, pp. 1731–1743, 2018.

[41] J. Meng, Y. Chen, F. Bi, H. Li, C. Chang, and W. Liu, "Pterostilbene attenuates amyloid-β induced neurotoxicity with regulating PDE4A-CREB-BDNF pathway," *American Journal of Translational Research*, vol. 11, no. 10, pp. 6356–6369, 2019.

[42] X. L. Meng, J. Y. Yang, G. L. Chen et al., "Effects of resveratrol and its derivatives on lipopolysaccharide-induced microglial activation and their structure-activity relationships," *Chemico-Biological Interactions*, vol. 174, no. 1, pp. 51–59, 2008.

[43] A. N. Carey, D. R. Fisher, A. M. Rimando, S. M. Gomes, D. F. Bielinski, and B. Shukitt-Hale, "Stilbenes and anthocyanins reduce stress signaling in BV-2 mouse microglia," *Journal of Agricultural and Food Chemistry*, vol. 61, no. 25, pp. 5979–5986, 2013.

[44] J. Chang, A. Rimando, M. Pallas et al., "Low-dose pterostilbene, but not resveratrol, is a potent neuromodulator in aging and Alzheimer's disease," *Neurobiology of Aging*, vol. 33, no. 9, pp. 2062–2071, 2012.

[45] M. Prinz, S. Jung, and J. Priller, "Microglia biology: one century of evolving concepts," *Cell*, vol. 179, no. 2, pp. 292–311, 2019.

[46] S. A. Wolf, H. W. Boddeke, and H. Kettenmann, "Microglia in physiology and disease," *Annual Review of Physiology*, vol. 79, no. 1, pp. 619–643, 2017.

[47] R. M. Ransohoff, "A polarizing question: do M1 and M2 microglia exist?," *Nature Neuroscience*, vol. 19, no. 8, pp. 987–991, 2016.

[48] X. Lan, X. Han, Q. Li, Q. W. Yang, and J. Wang, "Modulators of microglial activation and polarization after intracerebral haemorrhage," *Nature Reviews Neurology*, vol. 13, no. 7, pp. 420–433, 2017.

[49] S. Hickman, S. Izzy, P. Sen, L. Morsett, and J. El Khoury, "Microglia in neurodegeneration," *Nature Neuroscience*, vol. 21, no. 10, pp. 1359–1369, 2018.

[50] L. Yang, R. Zhou, Y. Tong et al., "Neuroprotection by dihydro-testosterone in LPS-induced neuroinflammation," *Neurobiology of Disease*, vol. 140, article 104814, 2020.

[51] Y. Liu, Y. Fu, Y. Zhang et al., "Butein attenuates the cytotoxic effects of LPS-stimulated microglia on the SH-SY5Y neuronal cell line," *European Journal of Pharmacology*, vol. 868, p. 172858, 2020.

[52] P. He, S. Yan, X. Wen et al., "Eriodictyol alleviates lipopolysaccharide-triggered oxidative stress and synaptic dysfunctions in BV-2 microglial cells and mouse brain," *Journal of Cellular Biochemistry*, vol. 120, no. 9, pp. 14756–14770, 2019.